A double edged sword:

Interferon-γ treatment worsens host outcomes in mouse models of pulmonary infection with *C. neoformans*

The University Of Sheffield.

Jacob Rudman

Department of Infection, Immunity & Cardiovascular Disease

School of Medicine

A thesis submitted in partial fulfilment of the requirements for the degree of Doctor of Philosophy

September 2021

Abstract

Cryptococcosis is a global opportunistic infection that can result in a fatal meningitis. Despite improved diagnostics, current treatments have issues including resistance, limited availability and toxicity, highlighting a need for new therapies. Interferon-γ has shown promise as an adjunctive treatment for cryptococcosis, but the mechanism of protection is not yet understood – a role of interleukin-1β has been proposed, but not validated. Therefore, I sought to determine the significance of interferon-γ and interleukin-1β in cryptococcosis. Firstly, I examined their effect on murine J774 cell interactions with *C. neoformans*, as immune responses in pulmonary cryptococcosis are macrophage-centric. Controversially, interferon-γ worsened J774 control of intracellular *C. neoformans*. I then established an inhalation infection mouse model of pulmonary cryptococcosis to confirm these findings *in vivo*. Using this model, I show that a single dose of interferon-γ at the time of infection failed to improve host outcomes while infection with an interferon-γ producing strain of *C. neoformans*, H99α IFNγ, significantly accelerated mouse mortality. However, infections of transgenic mice lacking interleukin-1β showed no differences in survival or fungal burden. However, as mice are not readily compatible with intravital imaging, the effect these cytokines on pulmonary host-pathogen interactions could not be assayed. Therefore, I also established a precision cut lung slice model of cryptococcosis so that live pulmonary immune responses to *C. neoformans* could be visualised *ex vivo*. Using this model to examine the first 24 hours of infection, I confirm that macrophages are the main cells to initially respond to inhaled *C. neoformans*, although do not appear to mediate early clearance – phagocytosis was limited and did not appear to inhibit fungal replication. In conclusion, I have provided evidence that interferon-γ may be dangerous if given to immunocompetent cryptococcosis patients, and present an *ex vivo* infection model that enables live pulmonary immune responses to be visualised.

Acknowledgements

I want to thank everyone who was kind enough to collaborate with me during this project to allow for the best science possible, and giving me the very best of the academic experience – Merete, Vikki Ridger, Leo Carlin, Claudia Tulotta, Penelope Ottewell, Sheila Francis and Alejandro Frangi.

In particular, a huge thank you to Dr Leo Carlin and his team for generously agreeing to share reagents and knowledge and training me in the PCLS methodology over 2 weeks where the bead data was generated. This was critical for the development of this model, and for that I am eternally grateful.

Another huge thank you to every member of BSU staff for all your hard work in ensuring that animal welfare was always a priority – Beka Armstrong, Anne Kimberly, Jane Cardwell, Joanne Bland, Lucy Whitfield and Michelle Bird. An extra special thank you to Carl Wright for all his hard work in the original *in vivo* work, and for always making time to help me whenever I pestered you with my stupid questions and annoying training needs.

In the lab, I want to thank everyone in D31 for their hospitality and making me feel like a part of the team. Special thank you to Kyle for giving me the role of Santa, Dave for putting up with my constant irritation, Stuart my fellow wellbeing wonder, Iwan Evans for fighting my corner, Phil Elks for many a pint, giggle and the occasional valid (non-fish) point, Topher my mosh mate, Anzar my other mosh mate, Amy for your diligence and support, Josie for such a kind introduction to the Johnston lab, Alfred for setting a flawless foundation with his hard work, Jess for hilarious outbursts of tear, Kate for being a fantastic friend and the voice of reason, Dan for being a great learner, Liv for robber running around Sheffield with me and Jelle for being too short and having poor tastes in music. Special thanks to my fellow starter Jaime for brightening every day with your purity and magic FITC beads, and Mahrukh, the most inspiring, hardworking and incredible colleague who is exemplary of what a postgraduate scientist should be. Another shout out to a pathogens best friend and my co-author Robbie, for all the training, all the laughs and all the mycoplasma.

A huge thank you to Steve Renshaw for taking a chance on me, and all the thank yous to Emily Goodall for being the literal best DTP manager ever and making DiMeN the best thing ever. Big love to my fellow DiMeN drinkers for some of the best memories – Jack, Blanca, Emily, Dheemanth, Chris, Katie, Tom and Lara.

A huge thank you to the greatest scientific mind I've ever met, attached to the man that is my supervisor Simon Johnston. Thank you for your contagious passion for knowledge

and somehow knowing everything. Thanks for being a fantastic colleague, an incredible scientist and a wonderful friend. And another huge thank you to Helen Marriott for all the *in vivo* support over the years, and for stepping in at the eleventh hour to support us over the finish line.

Thank you to Han for being the best lab sister, and to Mel for making my time in Sheffield so special and being the best friend I've ever had.

No thank yous to Edward, Chadwick or Rhogar who left me to die in Phalloidin, but big love to Harold, Chadders, Air and Quaf for the adventures, the laughs and the friendships I hope to never lose.

To the most elite of pharmacologists – Char Smalls, Queen Cindy, Dan Broom and Mabes – thank you for proving that friendships aren't just for university, and being among the kindest souls and brightest minds I know.

To TA, Philippe, Peter, Joe, Markos and Lewis for every single memory of us being awkward, sweaty, drunk and happy, I thank you. And for every Friday allowing me to be Mr Objective, and show you what real music is. Here's to all the gigs we'll get to experience after this. Little Cat.

Love to my Guildford friends – Steve, Amelia, George P, Adam, Rupert, Tommy, Tom, Simon and Horatio – for reminding me I always have a home when all else fails, and for being the best creative collaborators on the planet #splashzonegamers

And to mem and Gracie. There are no two more important people in history, who exemplify everything worth fighting for in life. You both made me the person I am today (for better or worse) and are a constant source of inspiration, admiration and adoration to me. You are the lights of my life and the support that keeps me standing.

And thank you to every single person that has tolerated me.

Support local music, fight intolerance and love yourself.

Contents

List of Abbreviations

2D – 2 Dimensional

3D – 3 Dimensional

5-FC – 5-fluorocytosine

α-MSH – α-Melanocyte-Stimulating Hormone

AF – Alexa Fluor

AIDS – Acquired Immune Deficiency Syndrome

AM – Alveolar Macrophage

AP-1 – Activator Protein 1

APC – Antigen-Presenting Cell

App1 – Anti-Phagocytic Protein 1

Arp2/3 – Actin Related Protein 2/3 Complex

ART – Antiretroviral Therapy

ASC – Apoptosis-Associated Speck-Like Protein Containing a CARD

BAL – Broncheoalveolar Lavage

BBB – Blood-Brain Barrier

BDG – β-d-Glucan

BSA – Bovine Serum Albumin

CARD – Caspase Recruitment Domain

CCR2 – C-C chemokine receptor type 2

cfu – Colony Forming Units

CNS – Central Nervous System

COMP – Competent

CR3 – Complement Receptor 3

CRZ1 – Calcineurin-Responsive Zinc Finger 1

CSF – Cerebrospinal Fluid

CXCR3 – C-X-C Motif Chemokine Receptor 3

CXCL11 - C-X-C motif chemokine 11

DC – Dendritic Cell

DIC – Differential Interference Contrast

DMEM – Dulbecco's Modified Eagle Media

DMSO – Dimethyl Sulfoxide

DNA – Deoxyribonucleic Acid

dpi – Days Post Infection

DPPC - Dipalmitoylphosphatidylcholine

ELISA – Enzyme-Linked Immunosorbent Assay

ERK – Extracellular Signal-Regulated Protein Kinase

FACS – Fluorescence-Activated Cell Sorting

FBS – Fetal Bovine Serum

Fc – Fragment Crystallisable

FcγRI – Fc γ Receptor 1

FcγRIIb – Fc γ Receptor 2b

FcGR3A – Fc γ Receptor 3A

flox – Flanking LoxP sites

GFP – Green Fluorescent Protein

gp – Glycoprotein

GPR1 – G Protein Coupled Receptor 1

GXM – Glucuronoxylomannan

GXMGal – Glucuronoxylomannogalactan

HAART – Highly Active Antiretroviral Therapy

HEPA – High-Efficiency Particulate Air

HIV – Human Immunodeficiency Virus

hpi – hours post infection

HPI – Animal was culled x number of hours post infection

ICP – Intracranial Pressure

ID – Identification

IFN – Interferon

IFNγ – Interferon-γ

IgG – Immunoglobulin G

IgM – Immunoglobulin M

IL- – Interleukin

IL-1R – IL-1 Receptor

iNOS – Inducible Nitric Oxide Synthase

IRF – Interferon Regulatory Factor

IRG-1 – Immune-Responsive Gene 1

IRIS – Immune Reconstitution Inflammatory Syndrome

IU – International Units

IV – Intravenous

kDa - kiloDaltons

L-DOPA – L-3,4-dihydroxyphenylalanine

LFA1 – Lymphocyte Function-Associated Antigen 1

LHC1 – Lactonohydrolase

loxP – Locus of X-over P1

LPS - Lipopolysaccharide

LRR – Leucine-Rich Repeat

mAb – Monoclonal Antibody

MALDI-TOF MS – Matrix Assisted Laser Desorption Ionisation-Time of Flight Mass Spectrometry

MAT – Mating Type

MBL – Mannose Binding Lectin

MCP-1 – Monocyte Chemoattractant Protein-1

mDC – Monocyte Derived Dendritic Cell

MDM – Monocyte Derived Macrophage

MHC – Major Histocompatibility Complex

MIC_{50} – Minimum Inhibiting Concentration required to inhibit the growth of 50% of organisms

MOI – Multiplicity of Infection

MyD88 – Myeloid Differentiation Primary Response 88

NA – Numerical Aperture

Neut – Neutrophil

NFκB – Nuclear Factor Kappa-Light-Chain-Enhancer of Activated B Cells

NHS – National Health Service

NLRP3 – NOD-, LRR- and pyrin domain-containing protein 3

NK – Natural Killer

NO – Nitric Oxide

NOD – Nucleotide Oligomerisation Domain

NSAID – Non-steroidal Anti-Inflammatory Drug

PAMP – Pathogen Associated Molecular Pattern

PBMC – Peripheral Blood Mononuclear Cell

PBS – Phosphate Buffered Saline

PCK1 – Phosphoenolpyruvate Carboxykinase 1

PCR – Polymerase Chain Reaction

PCLS – Precision Cut Lung Slices

PCR – Polymerase Chain Reaction

PGE_2 – Prostaglandin E_2

PFA – Paraformaldehyde

PGK – Phosphoglycerate Kinase

PI – Phagocytic Index

PI3K – Phosphoinositide 3-kinase

PKC – Protein Kinase C

PLA_2 – Phospholipase A2

Plb1 – Phospholipase B1

PMA – Phorbol 12-myristate-13-acetate

PRR – Pattern Recognition Receptor

RNA – Ribonucleic Acid

RNA-Seq – RNA Sequencing

RONS – Reactive Oxygen and Nitrogen Species

ROS – Reactive Oxygen Species

rpm – Rotations per minute

SDA – Sabourand Agar

SF – Serum free

siRNA – Small Interfering RNA

SP-A – Surfactant Protein A

SP-D – Surfactant Protein D

Sre1 – Sterol Regulatory Element-Binding Protein 1

STAT – Signal Transducer and Activator of Transcription

TGFβ – Transforming Growth Factor Beta

Th1 – Type I Helper T Cell

Th2 – Type II Helper T Cell

Th17 – Type 17 Helper T Cell

TLR – Toll-like Receptor

TNFα – Tumour Necrosis Factor α

Treg – Regulatory T Cell

UK – United Kingdom

USA – United States of America

UV – Ultraviolet

WT – Wild-type

YPD – Yeast Extract Peptone Dextrose

Figures

Tables

Chapter 1 – Introduction

1.1 – The burden of opportunistic infection

Infectious diseases remain a leading cause of death globally (*The top 10 causes of death*, 2017) and a major healthcare burden. In particular, opportunistic infections – infections characteristically avirulent in the immunocompetent population – are increasingly prevalent. One of the main reasons for this is a growing 'at risk' population. Susceptibility to opportunistic infection is a direct result of immunocompromise, which is affecting an increasing number of patients – either as a result of diseases that directly suppress immunity (e.g uncontrolled HIV/AIDS) or as a consequence of long term immunosuppressant therapy for autoimmune and inflammatory diseases (Lerner, Jeremias and Matthias, 2015). Another, more concerning observation, is that there are case reports emerging that describe dangerous incidences of opportunistic infections in apparently immunocompetent patients. This is either indicative of increasing pathogen virulence or that there are unidentified immunocompromising conditions that can result in an increased susceptibility to infection (Chen *et al.*, 2008; Pappas, 2013). An additional complication is that opportunistic pathogens are often ubiquitous in the environment (*Cryptococcus neoformans*) or can be part of the human microbiome (*Staphylococcus aureus, Streptococcus pneumoniae*; Nunes *et al.*, 2005; Krismer *et al.*, 2017) – making avoiding or eradicating these causative agents near impossible. When combined with the ongoing antimicrobial resistance crisis and a lack of new classes of antimicrobial therapy in drug discovery pipelines, opportunistic infections represent a clear and critical threat to human health. Of particular concern are invasive fungal infections. As these infections affect large patient groups, such as those suffering from cancer, transplant recipients and uncontrolled HIV, invasive fungal infections represent a significant healthcare burden (Person, Kontoyiannis and Alexander, 2010). Globally, one of the main fungi of concern are pathogenic *Cryptococcus* species.

In this chapter, I will first introduce the major pathogenic species of the *Cryptococcus* genus, *Cryptococcus neoformans* (*C. neoformans*) and *Cryptococcus gattii* (*C. gattii*). I will then describe the infections they cause – cryptococcosis – including the pathology, epidemiology, diagnosis and treatment. Subsequently, I will describe the rationale behind developing immunotherapy to treat these infections, and discuss our current understanding of the immune response and the nature of host-pathogen interactions that occur in cryptococcosis. I will also introduce the *in vivo* and *in vitro* systems used to model this infection. Finally, I will highlight the current gaps in knowledge and justify exploring these concepts experimentally.

1.2 – *Cryptococcus* genus

Fungi of the *Cryptococcus* genus are heterothallic yeasts, capable of producing spores and able to transition between either a hyphal or yeast form – the latter being how *Cryptococcus* is typically observed in the environment, in the laboratory and in the clinic (Casadevall and Perfect, 1998). The hyphal form, however, is still important in the life cycle of *Cryptococcus* species for the production of basidiospores (McClelland et al., 2004). *Cryptococcus* is able to reproduce sexually or asexually. Sexual reproduction, or mating, in *Cryptococcus* occurs when haploid cells of the two mating (MAT) types, **a** and α, undergo fusion (Kwon-Chung and Bennett, 1978). In the context of human disease, the α MAT type is most commonly isolated from patients. However, mating can also occur between cells of the same MAT type, described as monokaryotic fruiting (Wickes et al., 1996).

Of the >80 known cryptococcal species, there are several known to cause infections in humans. However, incidences of infections due to most of these species are relatively rare despite their widespread use as biological tools in agriculture and bioengineering. For example, *Cryptococcus curvatus* is currently being trialled for processing cocoa butter, but was first identified in sputum samples from a tuberculosis patient (Dromer *et al.*, 1995; Hassan *et al.*, 1995). Meanwhile, *Cryptococcus albidus* is reported to readily colonise human skin, yet as of 2017 only 24 human infections had been reported (Aghaei Gharehbolagh *et al.*, 2017). Finally, *Cryptococcus laurentii* is widely used as a biological deterrent against *Penicillum expansum* mould in apple orchards (Yu and Zheng, 2007). Despite this application, however, only 19 cases of *Cryptococcus laurentii* infection have been reported in the literature (Ben Abid *et al.*, 2020). Although infections due to these species should not be ignored, their global impact is significantly less than that of the two major pathogenic *Cryptococcus* species, *C. neoformans and C. gattii* (Figure 1). Therefore, these two species are the focus of my research.

It is important to note that the nomenclature and differentiation of *C. neoformans* and *C. gattii* are currently debated. Until 2015, pathogenic cryptococci were described as either *C. neoformans* or *C. gattii*, with four different serotypes (A-D) contained within these two terms (Kwon-Chung and Varma, 2006) – serotype A (*C. neoformans* var grubii) and serotype D (*C. neoformans* var neoformans) were labelled as *C. neoformans*, while both serotypes B and C were ascribed to *C. gattii* species.

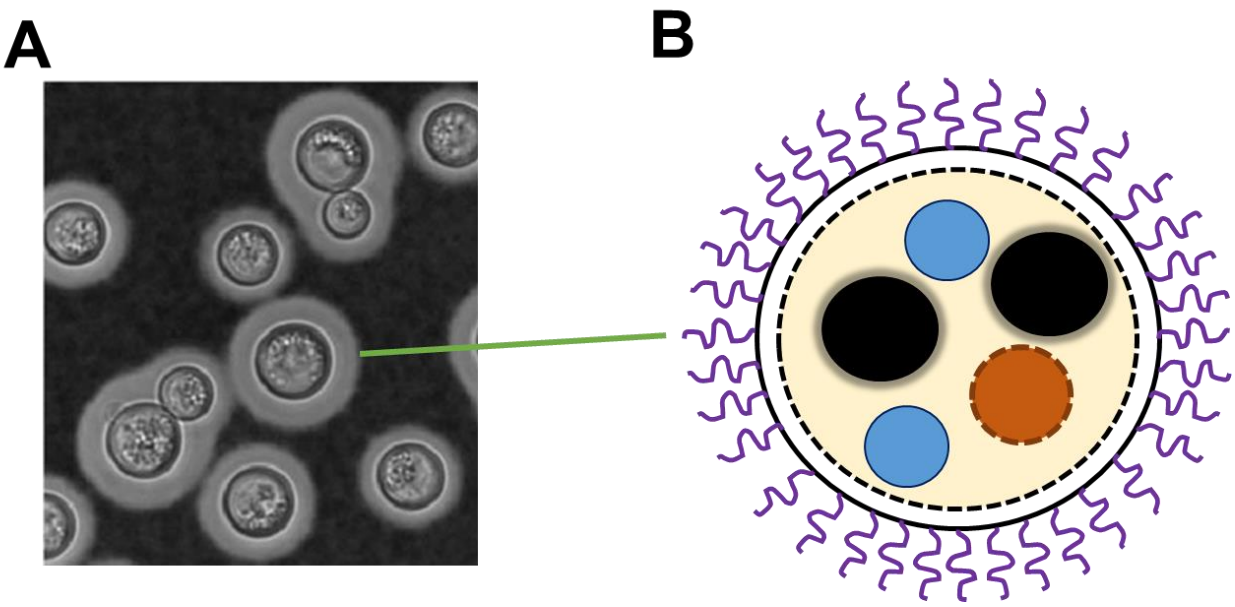

Figure 1 – Visual representation of *Cryptococcus neoformans*. (**A**) Representative image of *Cryptococcus neoformans* cells when negatively stained with India Ink. Image originally from (Wang, Li and Doering, 2018)*. (**B**) – Schematic highlighting the typical structure of a *Cryptococcus neoformans* cell based on observations using electron microscopy. **Purple lines at exterior** – Polysaccharide capsule (Wang, Li and Doering, 2018). **Solid black line** – cell wall. **Dashed black line** – cell membrane. **Pale yellow** – cytoplasm. **Solid black circles** – melanin (Mandal *et al.*, 2007). **Blue circle** – vacuole (Wanner and Baird, 1974). **Brown dashed circle** – nucleus.

* (**A**) is originally from Wang, Li and Doering, 2018. Unraveling synthesis of the cryptococcal cell wall and capsule. *Glycobiology,* 28 (10), 720. Reused here by permission of Oxford University Press.

However, an overhaul of this system was proposed in 2015 that would split *C. neoformans* and *C. gattii* isolates into seven new species (Hagen *et al.*, 2015): *C. neoformans* would become two species – *C. neoformans* (previously var grubii) and *Cryptococcus deneoformans* (previously var neoformans), while *C. gattii* would describe *gattii, bacillisporus, deuterogattii, tetragattii* and *decagattii* species.

This proposal was disputed by Kwon-Chung *et al.* on the basis that the genotyping methods that informed the proposed changes are ordinarily reserved for organisms that ordinarily undergo sexual reproduction (Kwon-Chung *et al.*, 2017). It was also noted that the 2,606 reference strains used to determine this differentiation also showed significant variation, and therefore seven species would complicate nomenclature without suitably encapsulating this deviation. However, it should be noted that *Cryptococcus* species can replicate sexually and this approach has been applied to differentiate other yeast genera.

Subsequently, Hagen *et al.* replied that rejecting this classification system actively encourages ignorance of *Cryptococcus* diversity, particularly with regard to clinical studies where species differences may significantly impact patient outcomes or treatment (Hagen *et al.*, 2017). They also highlighted that it is possible to robustly differentiate between the proposed species using Matrix Assisted Laser Desorption Ionisation-Time of Flight Mass Spectrometry (MALDI-TOF MS). Additionally, the seven species proposal was also refined in this rebuttal to instead describe ten species: *amylolentus, bacillisporus, decagattii, deneoformans, deuterogattii, neoformans, gattii, tetragattii* and two filamentous species, *depauperatus* and *luteus*.

At the time of writing, no consensus has been reached with regard to which system is most appropriate. Therefore, for the remainder of my thesis, I will use the original species complex nomenclature so as to remain consistent with the majority of previous research. However, I acknowledge and see the benefits to using the ten species system (Figure 2).

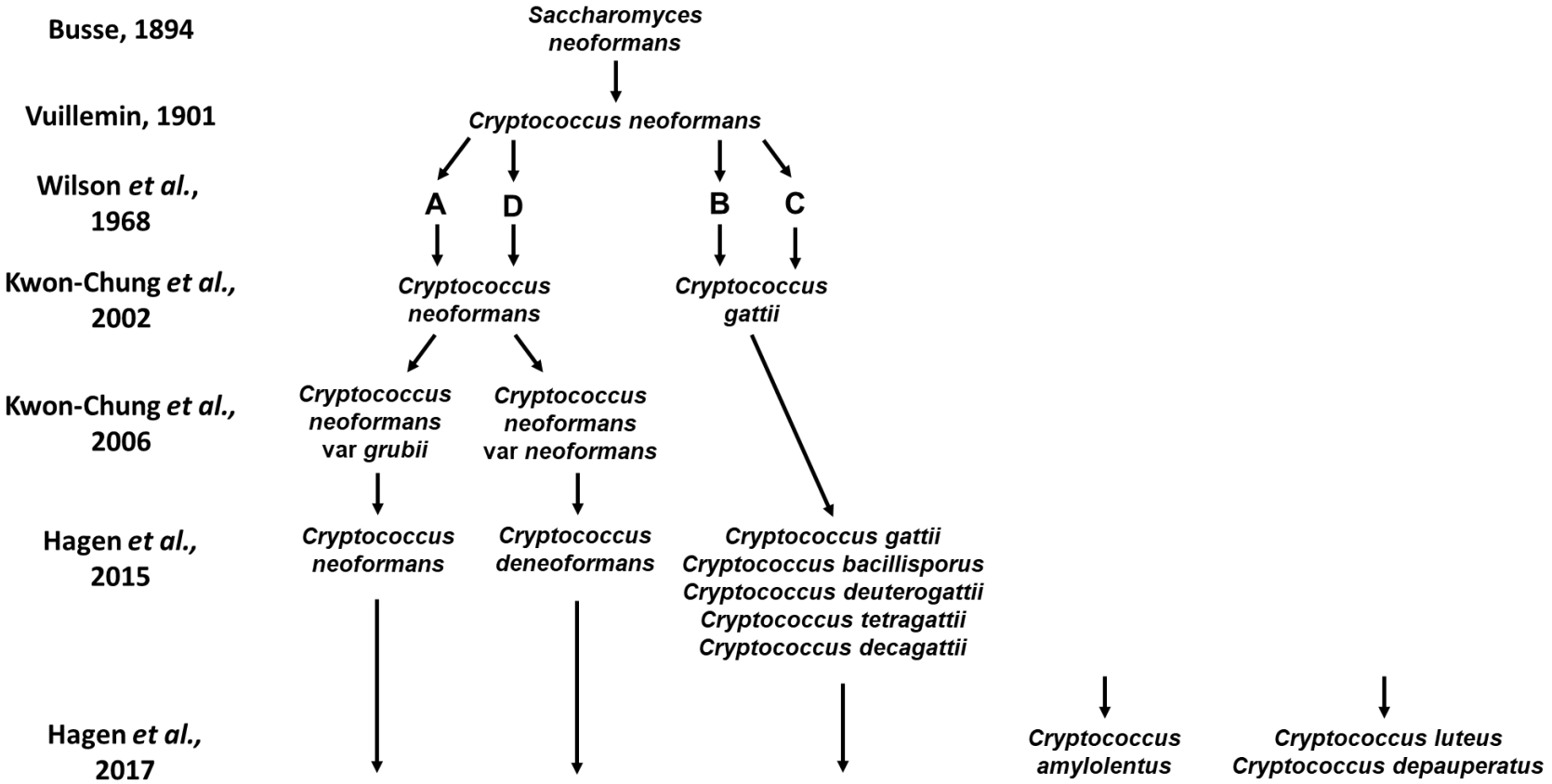

Figure 2 – History of the *Cryptococcus neoformans/Cryptococcus gattii* complex. A schematic showing how the nomenclature and differentiation of pathogenic *Cryptococcus* species changed over time. *Only one pathogenic species was described initially, named* Saccharomyces neoformans based on its appearance (Busse, 1894). This was renamed *Cryptococcus neoformans* (Barnett, 2010). Based on differential serological responses *in vivo*, four serotypes of *Cryptococcus neoformans* were then described (Wilson, Bennett and Bailey, 1968). After overwhelming evidence in the following years, *Cryptococcus gattii* was eventually recognised as a unique *Cryptococcus* species, accounting for serotypes B and C (Kwon-Chung *et al.*, 2002)**.** *Cryptococcus neoformans* was then split into two new variants (Kwon-Chung and Varma, 2006). However, these classifications have been suggested not to go far enough, and additional *Cryptococcus* species have been proposed to exist (Hagen *et al.*, 2015, 2017)**.**

1.2.1 – Cryptococcus neoformans

1.2.1.1 – History of *C. neoformans*

The most common causative agent of cryptococcosis is *C. neoformans* (Rajasingham *et al.*, 2017). *C. neoformans* was first isolated in 1894 from the infected bone of a female patient (Busse, 1894). However, the realised clinical burden of cryptococcosis then remained minimal over the next 50 years, with less than 300 cases reported during this period (Littman and Zimmerman, 1956). It wasn't until the HIV/AIDS pandemic was officially recognised in 1981 that *C. neoformans* became a pathogen of global significance (CDC, 1981). Uncontrolled HIV and a low CD4+ cell count remain the biggest risk factors for incidences of cryptococcosis (Lin, Shiau and Fang, 2015), with cryptococcal meningitis currently estimated to kill 181,000 patients worldwide every year (Rajasingham *et al.*, 2017).

1.2.1.2 – Ecology of *C. neoformans*

C. neoformans is a ubiquitous environmental pathogen found worldwide. It can be found in multiple environmental niches, including rotting tree matter (Randhawa *et al.*, 2008), soil (Litvintseva *et al.*, 2011) and bird excreta, primarily that of the pigeon (Hedayati *et al.*, 2011). A recent review of sources of *C. neoformans* isolates found that *Eucalyptus* trees are one of the most common reservoirs (Cogliati *et al.*, 2016).

1.2.1.3 – Identification of *C. neoformans*

The most widely utilised method to accurately identify *C. neoformans* is MALDI-TOF MS, which identifies samples based on their mass spectrometry spectra (McTaggart *et al.*, 2011). However, in resource limited settings, simpler methods are available. If incubated on SDA plates, *C. neoformans* cultures appear milky white and smooth. However, if cultured on niger seed agar plates, colonies appear brown in colour as the L-DOPA in niger seed is converted by *C. neoformans* cells into melanin – a dark pigment molecule that helps to differentiate isolates of *C. neoformans* from other pathogenic yeast (Staib and Bethauser, 1968; Denning, Stevens and Hamilton, 1990). Additionally, the dense polysaccharide capsule that surrounds *C. neoformans* cells exclude India ink, creating a 'halo' effect around fungal cells when treated with this compound and then visualised under a microscope (Casadevall *et al.*, 2019).

1.2.2 – Cryptococcus gattii

In comparison to *C. neoformans*, *C. gattii* infections are rarer. However, *C. gattii* infection is not associated with infections of the immunocompromised, instead appearing to more commonly affect immunocompetent individuals (Mitchell *et al.*, 1995).

1.2.2.1 – History of *C. gattii*

C. gattii was first described in 1970 after an atypical clinical isolate of *Cryptococcus* was identified in Africa (Vanbreuseghem and Takashio, 1970). However, it wasn't until 2002 that *C. gattii* was formally recognised as a separate species (Kwon-Chung *et al.*, 2002). Historical clinical isolates of *Cryptococcus* were then reanalysed, revealing that the first recorded case of *C. gattii* infection was actually in 1896 (Kwon-Chung *et al.*, 2002). Also around this time, the clinical significance of *C. gattii* was fully realised with the Vancouver Island outbreak, believed to have started in 1999 (Stephen *et al.*, 2002). This incident occurred in a region of Canada that typically reported an average number of 4-6 human cases of cryptococcosis a year. However, there were 50 cases in 2002 and 218 cases by 2007 (Galanis and MacDougall, 2010).

1.2.2.2 – Ecology of *C. gattii*

When it was first identified, *C. gattii* was thought to be found only in tropical and sub-tropical regions (Kwon-Chung and Bennett, 1984). However, since the aforementioned Vancouver Island outbreak (see 1.2.2.1), cases of *C. gattii* infection are reported globally, including in temperate regions (Cogliati, 2013). In the environment, *C. gattii* is found in similar niches to *C. neoformans*, including soil and *Eucalyptus* trees (Ellis, 1987; DeBess *et al.*, 2014). However, avian guana is not a common environmental niche for *C. gattii*, as it is for *C. neoformans* (Cogliati, 2013).

1.2.2.3 – Identification of *C. gattii*

C. gattii can be differentiated from other fungal genera the same was as *C. neoformans.* However, differentiating between *C. neoformans* and *C. gattii* is difficult, as both fungi show the same results for many laboratory tests – which likely contributed to the limited awareness of this pathogen throughout the late 20th century. MALDI-TOF MS can differentiate between the two species, although this technology is not available in all settings. Prior to the utilisation of MALDI-TOF, the gold standard test to differentiate *C. neoformans* and *C. gattii* was to incubate cultures on canavanine glycine bromothymol blue agar (Klein *et al.*, 2009). Resulting colonies of *C. gattii* on these plates will appear blue because *C. gattii* uniquely expresses a glycine decarboxylase which converts glycine to ammonia. This creates a more basic pH, which causes the bromothymol indicator to appear blue (Min and Kwon-Chung, 1986).

1.3 – Cryptococcosis

Cryptococcosis is the name given to infections caused by species of the *Cryptococcus* genus. In humans, cryptococcosis is hypothesised to most commonly start in the lungs, after patients inhale infectious basidiospores or desiccated yeast cells (Mitchell and

Perfect, 1995) – although it should be noted that it has yet to be determined which of these are the primary infectious propagules. Most cryptococcosis studies use yeast cells. While only a small selection of studies have investigated spores, it has been observed that *C. neoformans* spores can be germinated on minimal media, and infection with as few as 5 colony forming units (cfu) results in 100% lethality in invertebrate and mammalian models of infection (Velagapudi *et al.*, 2009). Additionally, a direct comparison of yeast and spore infections in mice revealed that spore infected animals exhibited higher fungal burdens, although delayed mortality. However, spores from *C. neoformans* strains that are reported to be avirulent in the yeast form, have been observed to be universally fatal in a mouse model of infection (Walsh *et al.*, 2019). These different infection phenotypes with spores and yeast warrants further investigation.

1.3.1 – Pathology

Regardless of the infectious propagule, to cause infection, inhaled *Cryptococcus* cells are thought to have to end up deposited in the alveoli and lower airways, primarily by sedimentation (Weibel, 1963; Casadevall and Perfect, 1998). If not rapidly cleared, deposited *Cryptococcus* is able to effectively adapt to the host environment, evade the subsequent host immune response and even survive intracellularly within leukocytes (Goldman *et al.*, 2000). During this pulmonary infection, patients are thought to be largely asymptomatic, potentially presenting with non-specific symptoms such as a dry chesty cough, chest pain and fever (Setianingrum, Rautemaa-Richardson and Denning, 2019). However, it is important to note that some cases pulmonary cryptococcosis can be serious, resulting in difficulty breathing and total respiratory failure (Shirley and Baddley, 2009).

Even though the lungs are thought to be the portal of entry for *Cryptococcus* in most cases, the most common clinical presentation of cryptococcosis is disseminated infection. It is not yet fully understood by what mechanisms cryptococci escape the lungs and infect other tissues. It is currently thought that cryptococci disseminate via patient circulation, as cryptococci are observed to survive in the bloodstream of patients (Chrétien *et al.*, 2002). Additionally, an *in vivo* study in mice found that in a tail vein infection model, the vascular fungal burden correlated with those in the spleen and brain – although this may have been the result of artificially initiating a bloodstream infection (Lortholary *et al.*, 1999). How cryptococci cross the air-blood barrier in the lung and cross into the bloodstream, however, is currently a major gap in knowledge – airway epithelial cells (A549) that internalise cryptococci are observed undergo cell death *in vitro* (Zhu *et al.*, 2007), although whether this occurs *in vivo* has yet to be confirmed.

In terms of dissemination, several tissues are common secondary sites of infection. Cutaneous cryptococcosis is one of the most common presentations, resulting in skin lesions. While by themselves these skin lesions are not life-threatening, because they indicate disseminated infection either has or may occur, cutaneous cryptococcosis is a major clinical concern. However, because the lesions are highly variable in appearance and can be indistinguishable from lesions due to other infectious agents, diagnosing cutaneous cryptococcosis can be difficult (Hayashida *et al.*, 2017). The prostate is another site of infection, reported to be a potential 'reservoir' in latent *Cryptococcus* infection, when a previously dormant infection can re-emerge later in life in response to changes in host immune status, concurrent infection or trauma (Shah *et al.*, 2017). As with pulmonary cryptococcosis, infection of the prostate is largely asymptomatic, but can be diagnosed by assaying seminal fluid (Staib, Seibold and L'Age, 1990). Ocular cryptococcosis became recognised during the HIV/AIDS epidemic (Kestelyn *et al.*, 1993) – symptoms include abnormal eye movements (ocular palsies), swelling of the optic nerve (papidilemma) and blindness (Kestelyn *et al.*, 1993). Finally, infection of bone despite being the first reported clinical presentation of cryptococcosis, is only estimated to have affected 89 patients between 1997 and 2013 (Zhou *et al.*, 2014). However, even in this low number of patients, multiple sites throughout the skeleton have been infected, although the vertebrae are reported to be the most common (Chleboun and Nade, 1977). However, cryptococcosis can occur in any tissue. In general, this results in pain and swelling in the affected area. Tissue-specific symptoms can occur, which aid diagnosis, although confirmation relies on aspiration or a biopsy of the affected tissue.

However, the most common complication of cryptococcosis is dissemination to the CNS and resulting cryptococcal meningitis. This remains the primary cause of mortality in cryptococcosis patients (Rajasingham *et al.*, 2017). Unlike is observed with other centrally invasive pathogens, initial *Cryptococcus* CNS infection does not result in a rapid pathological increase in intracranial pressure (ICP). Instead, the life-threatening increase in ICP only occurs with the continued presence of *Cryptococcus* in the CNS if it is not successfully cleared by the immune system, or treated (Loyse *et al.*, 2010). If a pathologically raised ICP does occur, neurotoxicity occurs and symptoms can include headaches, personality changes, ataxia and seizures (Kambugu *et al.*, 2008). If untreated, cryptococcal meningitis has an 100% mortality rate (Mwaba *et al.*, 2001). This dangerous clinical manifestation and associated healthcare burden has led to a significant amount of research into the mechanisms and pathophysiology of cryptococcal meningitis. However, despite this clinical significance it is still not understood how *Cryptococcus* typically cells enter the CNS. The CNS is protected by the blood-brain barrier (BBB), a protective structure that prevents the infiltration of pathogens and regulates immune cell recruitment. Both transcellular (Chang *et al.*, 2004) and

paracellular (Vu *et al.*, 2013) crossing the BBB by cryptococci have been observed in various models. However, the other theory of how cryptococci cross both the lung epithelium and BBB is via 'Trojan Horse' dissemination. Because cryptococci can parasitise leukocytes, specifically macrophages, it is hypothesised that these infected cells act as 'Trojan Horses', migrating across barriers in the lung and brain, whereupon intracellular cryptococci can escape (Casadevall, 2010).

Another complication that can occur in cryptococcosis patients is immune reconstitution syndrome (IRIS). IRIS describes a situation where the patient immune response becomes over activated either following or during infection, resulting in dangerous systemic inflammation (Wiesner and Boulware, 2011). In cryptococcosis, this pathology is associated with both the initiation of anti-retroviral therapy during acute infection in HIV positive patients, or up to a year following an initial cryptococcosis diagnosis (Lortholary *et al.*, 2005).

1.3.2 – Epidemiology

Exposure to *Cryptococcus* is thought to be ubiquitous and global. A study of 185 immunocompetent individuals aged 21 and younger in urban Canada, with no history of cryptococcosis or immunocompromise, found that 70% of the participants actually had positive cryptococcal serology, indicating a previous infection with *Cryptococcus* (Goldman, Khine, *et al.*, 2001). Although this study had a relatively low number of participants and was not multi-centre, it still provides important evidence of the opportunistic nature of cryptococcosis – while most individuals may be exposed to *Cryptococcus*, infections are largely cleared sub-clinically.

Clinically, it is estimated that there are 223,000 cases of cryptococcosis a year globally, with the majority of cases in sub-Saharan Africa (Rajasingham *et al.*, 2017). This region specificity is thought to be due to multiple factors – the tropical climate of this region associated with increased detection of environmental cryptococci (Cogliati, 2013) and higher rates of poorly or uncontrolled HIV/AIDS, the single biggest risk factor for the development of clinical cryptococcosis. In HIV/AIDS patients, cryptococcosis remains the second leading cause of death and is responsible for 15% of HIV/AIDS related deaths globally (Rajasingham *et al.*, 2017). Aside from HIV/AIDS, other at-risk populations for cryptococcosis include cancer patients receiving myeoabalative therapy (Reisfeld-Zadok *et al.*, 2009), solid organ transplant patients receiving triple therapy (Meier-Kriesche *et al.*, 1999; Husain, Wagener and Singh, 2001) and patients receiving long term glucocorticoid therapy for inflammatory diseases (True, Penmetcha and Peckham, 2002; Lionakis and Kontoyiannis, 2003). Worldwide, the mortality rate for cryptococcal meningitis remains as high as 70%, estimated to result in 181,000 deaths annually –

although mortality rates are known to be region specific based on socioeconomic factors (Rajasingham *et al.*, 2017).

1.3.3 – Diagnosis

The non-specific symptoms and sometimes chronic nature of cryptococcosis means there can be significant delays between a patient presenting with symptoms and the start of treatment. In a single centre in America, the average time to diagnosis for cryptococcosis patients with one known major risk factor was 2-3 weeks (Bratton *et al.*, 2012). However, a single centre study in Germany found HIV positive patients only waited an average of 2-3 days (Katchanov *et al.*, 2014). While this shows diagnosis times can be region-specific, both of these studies found that a diagnosis took twice as long on average for patients with no known risk factors, which is significant as delays in treatment are associated with poorer patient outcomes (Perfect and Bicanic, 2015).

Although there are delays in the diagnosis of cryptococcosis, this is not due to a lack of appropriate biochemical assays for clinical samples. Historically, identifying *Cryptococcus* in clinical samples relied on either microscopy of India ink stained patient fluids (cerebrospinal fluid, blood; Diamond and Bennett, 1974), histopathology of biopsied tissue (mucicarmine, Fontana-Masson staining; Gazzoni *et al.*, 2009), or culture in specific conditions (see 1.2.1.3, 1.2.2.3). However, false positives are common using these methods and fungal cultures take a relatively long time to grow, delaying treatment. More recently, ELISAs were developed to identify *Cryptococcus* in biological samples, which had an associated sensitivity and specificity of 93-98% (Tanner *et al.*, 1994). However, this approach is associated with false negatives when patients have low titres of *Cryptococcus*, limiting the utility of this test early in infection.

Therefore, the big diagnostic shift in the field has been towards semi-quantitative lateral flow assays to detect titres of *Cryptococcus* capsule. At the time of writing, this approach has only been approved for use with blood, but has also been trialled successfully with cerebrospinal fluid (CSF) and urine (Lourens *et al.*, 2014). Compared to other methods, lateral flow assays are rapid, can be used at the bedside, have a limited requirement for specialist equipment and are relatively low cost at $3.84-$6.03 per test (Perfect and Bicanic, 2015; Cassim *et al.*, 2017). This has enabled the uptake of lateral flow assays in low resource settings, where the burden of cryptococcosis is highest. This method may also be a useful tool for screening at-risk patients. In Brazil, >7% of HIV positive patients screened using the lateral flow assay tested positive (Borges *et al.*, 2019), while in the USA, screening HIV-positive blood samples identified 3% of the samples positive for cryptococcal antigenaemia (McKenney *et al.*, 2014). This suggests that implementation of screening programmes could significantly benefit the HIV positive

population globally. Additionally, the semi-quantitative nature of the lateral flow assay means that patient prognosis can also be predicted based on the titre for which a sample was identified as positive, which may inform patient treatment (Jarvis *et al.*, 2014).

However, the lateral flow assay is not thought to have much utility in monitoring treatment efficacy in patients (Perfect and Bicanic, 2015). Running multiple assays was found to be labour intensive and no longer cost-effective due to the high cost of additional reagents. Instead, the (1->3)-β-D-glucan (BDG) assay has been proposed as an alternative assay for the purpose of therapeutic monitoring (Rhein, Boulware and Bahr, 2015). While the BDG assay has been found to be no better than the lateral flow assay with regard to patient diagnosis, repeated BDG assays of the same cryptococcosis patients during treatment have found results correlate with falling fungal burdens, as confirmed by fungal culture. Additionally, the lateral flow assay is unable to differentiate between cases of *C. neoformans* and *C. gattii* (Kammalac Ngouana *et al.*, 2015).

Several other assays that provide additional information and a greater level of specificity have also been investigated for their utility in the clinic. PCR based approaches have received attention in recent years for their ability to track clinical isolates and their lineage. PCR methods also have unmatched specificity (100%), are able to differentiate between not only *C. gattii* and *C. neoformans,* but all ten of the species proposed (see 1.2; Gago *et al.*, 2014; Hagen *et al.*, 2017). Additionally, PCR based approach have been shown to be able to differentiate between IRIS and relapsing patients, informing the differential treatment of these patients (Kumari *et al.*, 2016). The other method is MALDI-TOF MS. This method is widely used in the research landscape and has superior specificity to the lateral flow assay. MALDI-TOF MS, once established, has a relatively low cost per sample ($0.50), although the high initial cost of $200,000 and need for expertise to maintain and operate the equipment currently limits the viability of this technology within the healthcare sector, particularly in low income settings (Zvezdanova *et al.*, 2020). Additionally, the recent uptake of the 'ideal' lateral flow assay also limits the uptake of these more advanced techniques.

Finally, IRIS diagnosis is also complicated, as the associated inflammation in the CNS and lungs results in symptoms that mimic cryptococcosis (Haddow *et al.*, 2010; Hu *et al.*, 2020). However, as IRIS requires differential treatment, prompt diagnosis is important (Wiesner and Boulware, 2011). Diagnostic criteria have been proposed, although this still relies on clinician intuition in the absence of definitive diagnostic assays (Haddow *et al.*, 2009).

1.3.4 – Treatment

The current gold standard treatment for diagnosed cryptococcosis is a combination of three antifungal medications – amphotericin B, 5-fluorocytosine (5-FC) and fluconazole (Figure 3; Perfect *et al.*, 2010). Once diagnosed, cryptococcal meningitis patients receive initially one week of intravenous (IV) amphotericin B and oral 5-FC, followed by one week of high dose fluconazole (induction phase). This is followed by fluconazole for a minimum of 8 weeks (consolidation phase; Boyer-Chammard *et al.*, 2019). During this phase of treatment, patient CSF is reanalysed – if high fungal burdens are detected, the patient re-enters the induction phase with a higher dose of amphotericin B. If the CSF is sterile, a patient then transitions into the maintenance phase, consisting of low dose fluconazole for at least twelve months – ensuring CNS sterility and for $CD4^+$ cell counts to be restored in HIV positive patients (Boyer-Chammard *et al.*, 2019). If *Cryptococcus* is found to be resistant to fluconazole, voriconazole may be given as an alternative during the consolidation or maintenance phase (Jeans *et al.*, 2011). A small clinical study (88 patients) also found that IFNγ adjunctive to amphotericin B and 5-FC during the induction phase improves HIV positive patient fungal clearance in cryptococcal meningitis (Jarvis *et al.*, 2012).

Although these treatment regiments have been optimised over time, there are still many issues. Amphotericin B, the only fungicidal antifungal of the three, has numerous side effects including anaemia, renal toxicity and phlebitis (Laniado-Laborín and Cabrales-Vargas, 2009). Plus, as amphotericin B has to be administered IV, patients require constant monitoring in a hospital setting, increasing treatment cost (Krysan, 2015). Meanwhile, 5-FC is only fungistatic and at the time of writing, one dose of 5-FC costs twice as much as two weeks of fluconazole treatment, limiting availability in low resource settings where the burden of cryptococcosis is highest (Kneale *et al.*, 2016; Merry and Boulware, 2016). Finally, resistance to fluconazole is observed globally, with MIC_{50} concentrations having doubled the past 10 years, owing to its widespread use as a broad spectrum antifungal (Naicker *et al.*, 2020). Additionally, fluconazole is only fungistatic rather than fungicidal.

Aside from pharmacotherapy, cryptococcal meningitis patients also require treatment to manage the pathological raised ICP in order to avoid neurotoxicity. However, the only approved treatment at the time of writing is repeated lumbar punctures to reduce the volume of CSF, consequently reducing ICP (Perfect *et al.*, 2010). The procedure, developed in 1891, involves inserting a syringe into the spinal column. This proximity to the spine of the patient can make this technique very dangerous, and is only a temporary measure that does not treat the underlying mechanism (Engelborghs *et al.*, 2017).

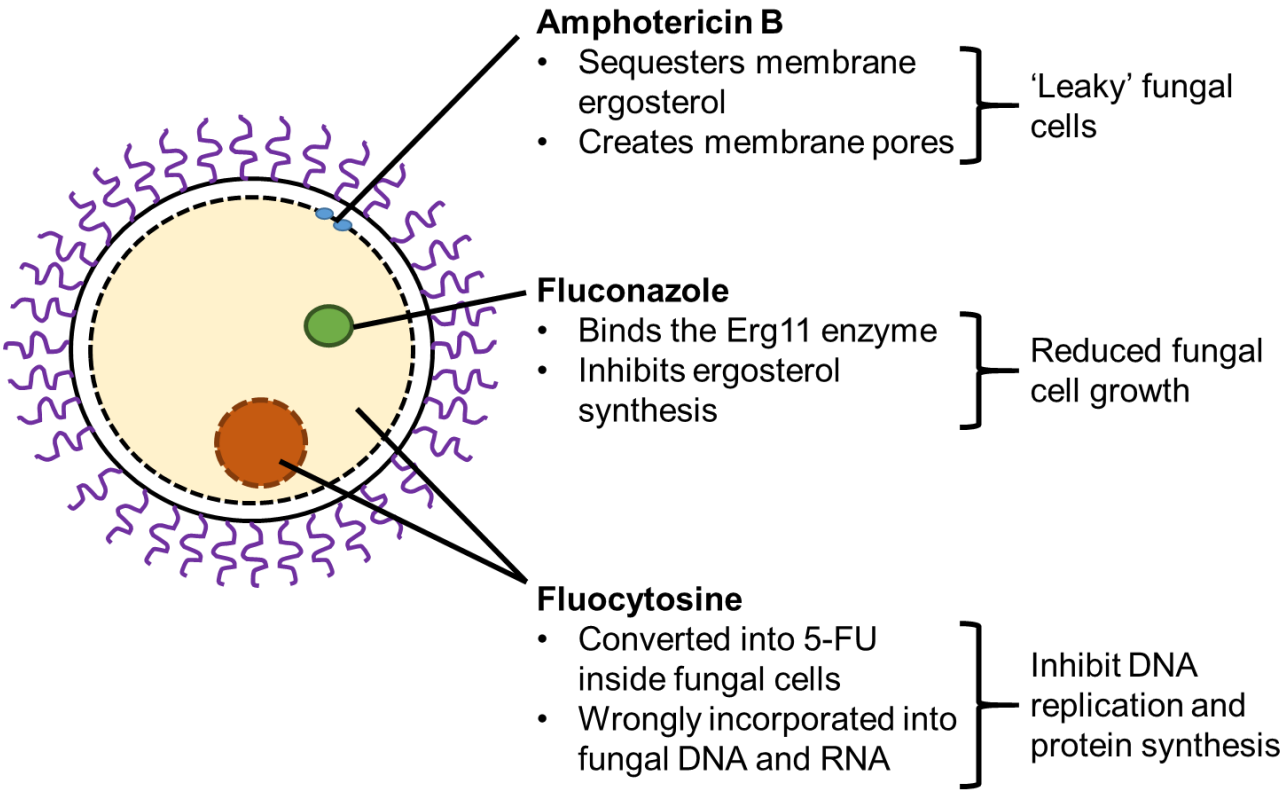

Figure 3 – Mechanism of action for antifungal therapies used in cryptococcosis. A summary of how the three classes of antifungal therapies inhibit or kill cryptococcal cells (Bermas and Geddes-McAlister, 2020)

In the case of IRIS, treatment is case specific at the time of writing, although clinical guidelines recommend that antifungal treatment is unchanged and the priority of the clinician is to reduce patient fungal burdens and manage the raised intracranial pressure (Perfect *et al.*, 2010). Additionally, there is currently no prognostic marker for IRIS to stratify patients. Immunomodulation to control the inflammation present in IRIS has been trialled in single cases or centres using corticosteroids (Musubire *et al.*, 2012), NSAIDs (Manfredi *et al.*, 2000) and thalidomide (Lortholary *et al.*, 2005). However, these have still yet to been licensed for IRIS. These highly circumstantial criteria surrounding IRIS treatment highlights a need for more specific treatment guidelines that maintain antifungal efficacy while reducing pathological inflammation.

Finally, it is important to note that even if successfully treated, cryptococcal meningitis can result in lifelong conditions that can significantly affect patient quality of life. A study by Aye *et al*. found that poorer outcomes for cryptococcal meningitis patients correlated with delays in diagnosis, and that ongoing conditions included incontinence, deafness, blindness, ataxia, seizures and cognitive impairment (2016). This highlights that current treatments can still be insufficient in many cases, and a greater understanding of cryptococcosis pathology is needed in order to develop novel antifungal therapies to improve patient outcomes.

1.4 – Host-pathogen interactions in cryptococcosis

The combination of universal exposure to *Cryptococcus*, an association of infection with immunocompromise and our lack of understanding regarding IRIS suggests that a better understanding of the immune response to this infection is key to better management and treatment. However, the immune system is multifaceted and complex, with mechanisms that vary from physical barriers to interconnected cellular networks. In this section, I will introduce and describe the interactions of *C. neoformans* with the immune system, how cryptococci evade these mechanisms and outline areas of potential therapeutic exploitation.

1.4.1 – Host immunity to *Cryptococcus*

Because of the clear relationship between incidences of cryptococcosis and immune function, understanding the host-pathogen interactions that occur during cryptococcosis may reveal novel targets for therapeutic exploitation. In this section, I introduce the human immune system and outline the current understanding of how these elements contribute to either cryptococcal clearance or cryptococcosis pathology.

1.4.1.1 – Humoral immunity

Although the immune system is largely characterised by the function and activity of specialised immune cells, some of the most important components of host defence are humoral. These elements of the immune system contribute to all stages of immune response, from preventing initial infection to the clearance of established infection, either directly or indirectly.

1.4.1.1.1 – Surfactant

Inhaled cryptococci that are deposited in the alveoli of the lung are likely to first encounter lung surfactant – a protein rich solution coating the lung epithelium that primarily functions to reduce surface tension and maintain lung structure during respiration (Schurch, Lee and Gehr, 1992). This solution is produced by secretory type II alveolar cells and features hydrophilic and hydrophobic components that enable adsorption to the air-liquid interface. The solution primarily consists of dipalmitoylphosphatidylcholine (DPPC), but also contains the C-type lectins SP-A and SP-D (Goerke, 1998). These hydrophilic proteins exist as multimers in physiological conditions and feature a carbohydrate recognition domain that is thought to allow surfactant proteins to bind pathogen oligosaccharides (Haczku, 2008). This is believed to have an opsonising effect that enhances the recognition and phagocytosis of pathogens by innate immune cells such as macrophages and neutrophils (Pikaar *et al.*, 1995; Hartshorn *et al.*, 1998). In the context of cryptococcosis, both SP-A and SP-D are reported to bind capsular to *C. neoformans*, yet with different results.

SP-A has yet to be observed to significantly impact cryptococcosis outcomes. One *in vitro* study revealed that SP-A can bind to thinly capsulated *C. neoformans* (Walenkamp *et al.*, 1999). However, when the experiment was repeated with the highly virulent H99α strain of *C. neoformans* – which has a significantly denser capsule – SP-A binding first required cells to be opsonised with IgG (Giles *et al.*, 2007). Even then, the consequence of SP-A binding to IgG was an inhibition of the opsonising action of IgG in relation to phagocytosis by macrophages, suggesting that the presence of bound SP-A disrupts the interaction of the Fc region of IgG molecules with macrophage Fc receptors. *In vivo*, SP-A knockout mice infected with *C. neoformans* showed no differences in infection outcomes, immune cell recruitment or fungal burdens compared to wild-type controls (Giles et al., 2007), however, implying that SP-A has a redundant role in cryptococcosis.

SP-D is reported to have a more significant impact on cryptococcosis outcomes in models of infection. *In vitro,* SP-D can bind both capsular and acapsular *C. neoformans* (Geunes-Boyer *et al.*, 2009), although SP-D binding increased the survival of cryptococci phagocytosed by macrophages. This negative role for SP-D was confirmed *in vivo*, with

SP-D knock out mice infected with *C. neoformans* surviving longer and exhibiting decreased fungal burdens. These differential outcomes were correlated with intracellular *C. neoformans* cell survival within macrophages, with SP-D opsonised cryptococci hypothesised to be more protected from macrophages derived reactive oxygen species (ROS), such as H_2O_2 (Geunes-Boyer *et al.*, 2012).

Aside from acting as opsonins, both SP-A and SP-D have also been observed to modulate cytokine signalling. For example, SP-A ordinarily inhibits rat alveolar macrophage nitric oxide (NO) production. However, in the presence of elevated IFNγ, SP-A actually enhances IFNγ stimulated NO production (Stamme, Walsh and Wright, 2000). This may have important consequence for the detrimental role of SPs observed in experimental models. However, this enhanced NO production in the presence of IFNγ with SP-A was not observed in human alveolar macrophages – highlighting significant differences between human patients and *in vivo* models (Minutti *et al.*, 2016). It is also important to note that surfactant is typically absent in most *in vitro* models, which may further limit translatability of findings using these approaches.

Combined, all the current evidence surrounding the role of SPs in cryptococcosis suggests their action is actually detrimental. However, as there are discrepancies in the effects of SPs between rodent and humans, these observations should be confirmed in humanised models.

1.4.1.1.2 – Complement

Another important humoral component of innate immunity is the complement pathway (Figure 4). This signalling cascade in response to pathogens leads to the production of both opsonising molecules (C3b) and directly antimicrobial membrane attack complexes (Ehlenberger and Nussenzweig, 1977; Guo and Ward, 2005; Tegla *et al.*, 2011). During homeostasis, complement proteins circulate as inactive pro-peptides that are activated by serine proteases by one of three pathways – depending on the antigen encountered (Gál *et al.*, 2013). The classical pathway is primarily activated by IgG/IgM-antigen complexes (Brown *et al.*, 1983), the alternative pathway is spontaneously activated in physiological conditions, as well as by non-opsonised antigen (Lachmann and Halbwachs, 1975; Law and Levine, 1977), while the lectin pathway utilises mannose binding lectin (MBL) to bind mannose residues (Noris and Remuzzi, 2013).

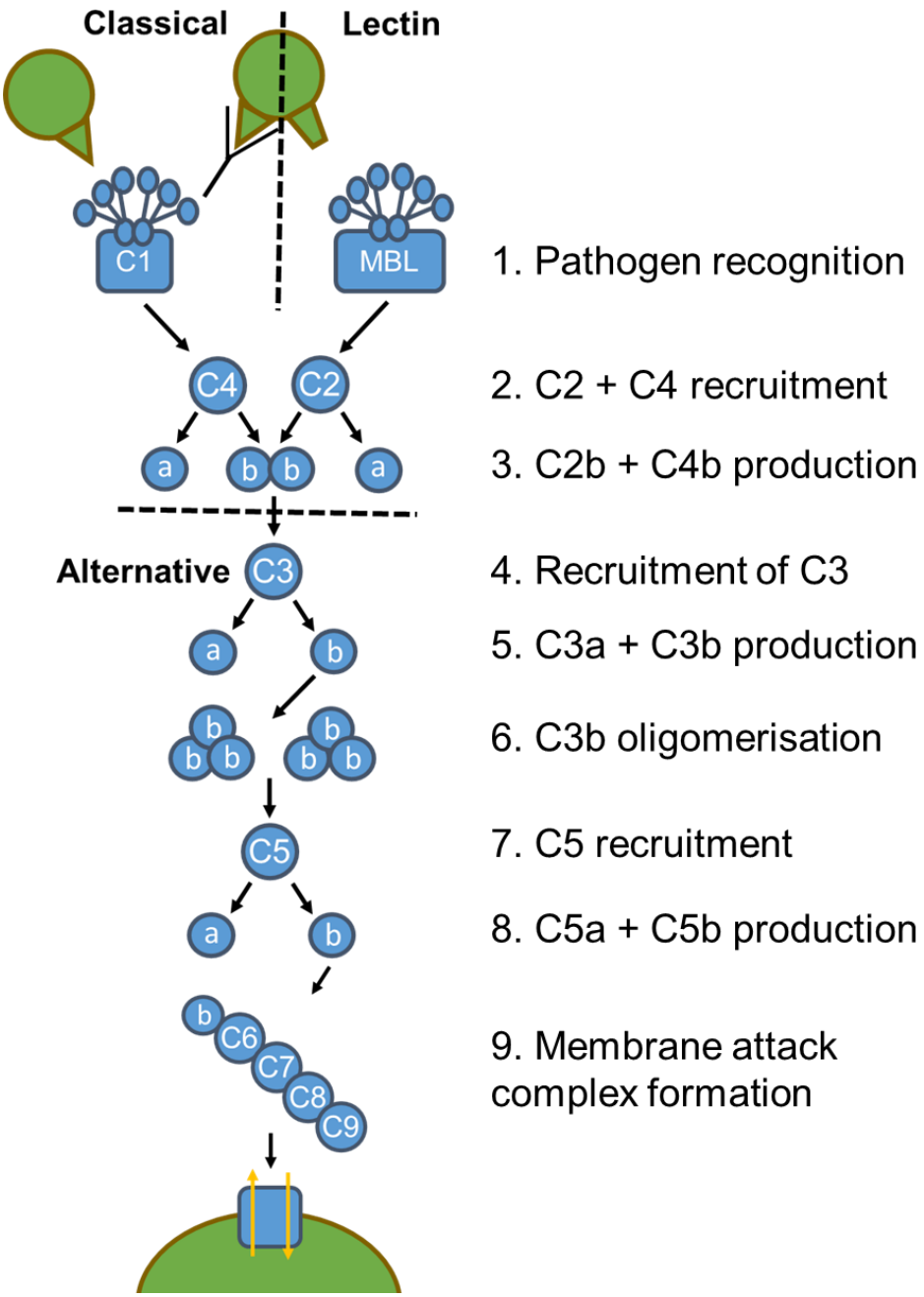

Figure 4 – The complement cascade. Schematic summarising the three complement pathways. Activation of either the classical or lectin pathways results in the recruitment of C2 and C4 proteins. The dimerisation of the b subunit of C2 and C4 leads to recruitment of C3 – the alternative pathway is independent of C2 or C4. The b subunit of multiple recruited C3 proteins then oligomerise, which enables the recruitment of C5. Finally, C5b is the first protein required for the formation of a membrane attack complex, following the recruitment and assembly of additional complement proteins (C6-9; Janeway Jr. *et al.,* 2001)

Complement is known to be important in immunity to cryptococcosis with encapsulated *C. neoformans* observed to robustly activate the alternative complement pathway (Kozel, Wilson and Murphy, 1991). Non-encapsulated *C. neoformans* is also able to also activate the classical complement pathway, providing more evidence that the cryptococcal capsule is important for masking immunogenic components of the *Cryptococcus* cell wall. However, a more recent study observed that *in vitro* activation of the alternative pathway by *C. neoformans* is dependent on the presence of MBL (Mershon-Shier *et al.*, 2011), suggesting this relationship may be more complex than first thought.

In response to complement signalling, *C. neoformans* is observed to be resistant to complement C3b opsonisation. In the case of the alternative pathway, *C. neoformans* produces additional GXM in response to C3b deposition on the cryptococcal capsule, masking bound C3b and preventing enhanced phagocytosis (Zaragoza, Taborda and Casadevall, 2003). Additionally, the cryptococcal hydrolytic enzyme LHC1 has been observed to alter the architecture of the cryptococcal capsule to decrease C3b deposition (Park *et al.*, 2014). Despite these adaptations by *C neoformans*, however, the complement pathway is still important for host defence *in vivo* – reported to aid the recognition and phagocytosis of *C. neoformans* by dendritic cells (Kelly *et al.*, 2005), while genetically ablating C5 in mice in experimental models of cryptococcosis increases mortality (Dromer *et al.*, 1989).

The complement pathway is also important in the case of *C. gattii* infection, although the alternative pathway is not as robustly activated by *C. gattii in vitro* compared to *C. neoformans* (Young and Kozel, 1993). C3b deposition on *C. gattii* cells *in vitro* is also less sensitive to changes in MBL levels (Mershon *et al.*, 2009). *In vivo*, C3 deficient mice infected with *C. gattii* show higher pulmonary burdens compared to wild-type controls (Mershon *et al.*, 2009), although pre-opsonising *C. gattii* with C3b does not rescue animal survival. This suggests that in the case of *C. gattii*, C3 downstream signalling is more important for host protection *in vivo* than C3b opsonisation (Mershon *et al.*, 2009). However, this highlights that host defence to cryptococcosis has a strong association with the complement system.

1.4.1.1.3 – Antibodies

Antibodies are proteins (~150kDa) that bind specific antigenic regions, which can have a multitude of effects including opsonisation, pathogen aggregation, neutralising extracellular molecules and interfering with pathogen receptor signalling. However, antibodies are best known for their role in immunological memory. This feature led to the aforementioned study (see 1.3.2), where healthy individuals aged 21 and younger were examined for anti-cryptococcal antibodies as evidence of previous exposure to

Cryptococcus (Goldman *et al.*, 2001). It was observed that ~70% of the individuals sampled were positive for antibodies against cryptococcal GXM. Not only does this study indicate that exposure to *Cryptococcus* is likely common, it also indicates that antibodies are produced as a part of the immunocompetent response to this pathogen that results in fungal clearance. Additionally, HIV patients have attenuated B cell responses, which may contribute to cryptococcosis susceptibility in this population (Pirofski, 2001).

When the classes of antibody produced in response to cryptococcosis were analysed, IgM antibodies – the first antibodies to be produced during the course of infection that have high avidity – were the most abundant (Goldman *et al.*, 2001). Higher affinity IgG and mucosal IgA molecules were also observed, although at relatively lower levels. However, in studies of HIV patients, lower circulating levels of IgM are observed (Pirofski, 2001), suggesting that this class of antibody specifically may be important in early infection. It is important to note that although anti-*Cryptococcus* antibodies in patient sera are typically against capsular GXM, likely due to its abundance on the surface of *Cryptococcus* cells, antibodies against melanin have also been observed in mouse models of infection (Nosanchuk, Rosas and Casadevall, 1998).

Aside from immunological memory, antibodies are also studied for their role as an opsonin as *Cryptococcus* cells are inherently resistant to phagocytosis. The binding of anti-capsular antibodies to cryptococci robustly enhances phagocytosis by macrophages and dendritic cells *in vitro*, presumably via Fc mediated phagocytosis (Casadevall *et al.*, 1998). So significant is this enhancement, that it was previously stated that phagocytosis of encapsulated *Cryptococcus in vitro* required cryptococci to be opsonised (Zaragoza et al., 2003). Aside from increasing recognition by immune cells, the binding of antibodies to *Cryptococcus* cells was also observed to increase capsule rigidity, an important physical change that increases the chances of successful phagocytosis (McLean *et al.*, 2002). Additionally, antibody binding to *Cryptococcus* is also reported to impair fungal budding (Cordero *et al.*, 2013). However, the pattern of antibody binding to fungal cells has been reported to affect whether this action is beneficial or detrimental, and so some antibodies generated during infection may not necessarily benefit the host (Cleare and Casadevall, 1998).

Despite this, antibodies have been repeatedly demonstrated *in vivo* to increase host protection. In mice, antibodies enabled the phagocytosis of large cryptococci ordinarily resistant to phagocytosis (Zaragoza, Taborda and Casadevall, 2003). Additionally, defects in antibody production were found to reduce protective responses to *C. neoformans in vivo*, with IgM shown to skew immune responses towards a more protective T helper 1 (Th1) phenotype (Subramaniam *et al.*, 2010). This was also seen when anti cryptococcal IgM were exogenously applied to infected mice, resulting in

significantly reduced fungal burdens in tissues (Subramaniam *et al.*, 2010). This strong association between antibodies and protective responses led to a clinical trial of an anti-GXM IgG antibody as a therapeutic in cryptococcal meningitis patients (Casadevall *et al.*, 1998). However, despite successful phase I/II clinical trials in 2005, no further trials took place (Larsen *et al.*, 2005). One explanation for this lack of translation identified during clinical trials was poor penetration of the antibody, 18B7, into patient CSF, which may have significantly limited treatment efficacy in cryptococcal meningitis. Limited CNS penetration of antibody therapies is commonplace, which has limited development of biological therapies for CNS conditions. However, novel approaches are being investigated to exploit endogenous transport mechanisms to cross these molecules across the BBB. One such example in clinical trials is an anti-insulin receptor monoclonal antibody (mAb) conjugated to the enzyme idursulfase for the treatment of Hunter syndrome, which is designed to exploit endogenous receptor mediated transcytosis (Freskgård and Urich, 2017). Approaches like this may overcome the pharmacokinetic limitations of a mAb therapy for cryptococcosis in the future.

1.4.1.1.4 – Cytokines

Co-ordination of immune responses is primarily mediated by cytokines – paracrine immune signalling molecules. These relatively small proteins (8-30kDa) affect all aspects of leukocyte biology, including recruitment, proliferation and function. This significant influence makes patient cytokine profiles during infection important determinants of clinical outcomes, a useful descriptor of immune responses and a potential target for therapeutic exploitation. Although actions of specific cytokines are discrete and context specific, they can be described based on the T helper (Th) cell phenotype they are typically associated with. Th1 cytokines are 'pro-inflammatory' – typically associated with increased antimicrobial activity against bacteria, viruses and some fungal and parasitic infections, as well as autoimmunity. Th2 cytokines, meanwhile, are associated with immunity to some fungal pathogens and wound healing, but generally are associated with reduced antimicrobial activity and allergy. Th17 cytokines were more recently described and are more akin in nature to Th1 responses than Th2, but have critical, distinct roles in both the clearance of certain fungal infections and the pathology of various autoimmune diseases (Damsker, Hansen and Caspi, 2010). Other Th subsets have been described (Th22, Th9), although their contribution to host defence during cryptococcosis have yet to be described (Cui, 2019).

In mouse models of cryptococcosis, cytokine profiles as early as one-week post infection can be used to identify resistant and susceptible individuals, while similarly surviving cryptococcal meningitis patients were found express higher levels of Th1 biomarkers (Hoag *et al.*, 1995; Siddiqui *et al.*, 2005; Jarvis *et al.*, 2013). This highlights the utility of

cytokines for both predicting host outcomes and their ability to influence fungal clearance. However, *C. neoformans* infection in both mouse models and patients typically induces a Th2 cytokine profile early in infection – associated with reduced cryptococcal clearance (Milam *et al.*, 2007). In animal models Th1 profiles are observed later in infection (3-5 weeks post infection), although this is believed to be a case of 'too little too late' and is usually insufficient to improve host outcomes due to *C. neoformans* infection (Arora *et al.*, 2005). From this, one can infer that a Th1 response early in infection is critical for host protection during cryptococcosis and understanding how cytokines affect these responses may yield opportunities for immunotherapeutics (Arora *et al.*, 2011).

1.4.1.1.4.1 – Interferon-γ

The cytokine most emblematic of Th1 immune responses is interferon-γ (IFNγ). In patients, elevated CSF levels of this cytokine are significantly correlated with positive host outcomes, supporting the notion of Th1 responses being of benefit to the host (Siddiqui *et al.*, 2005; Jarvis *et al.*, 2013). Additionally, IFNγ is primarily produced by the cells of the adaptive immune system – the response impaired in advanced HIV/AIDS, the largest risk factor for cryptococcal meningitis (Murray *et al.*, 2002). This strong association with improved patient outcomes therefore means IFNγ has been widely explored in the context of cryptococcosis. Reported effects of IFNγ include increased expression of MHC class II (Fulton *et al.*, 2004), complement proteins (C2 and C4; Lappin *et al.*, 1992) and inducible nitric oxide synthase (iNOS; Zhou *et al.*, 2007; Mosser and Edwards, 2008; Davis *et al.*, 2015). Additionally, there is a plethora of clinical evidence that patients that have deficiencies in IFNγ signalling, such as those with autoantibodies against IFNγ, have an increased risk of developing numerous infections, including those with invasive non-tuberculosis mycobacterial pathogens such as *Cryptococcus neoformans* (Barcenas-Morales, Cortes-Acevedo and Doffinger, 2019). Mutations in STAT1, a critical signalling molecule in the IFNγ pathway, have also been associated with increased incidences of cryptococcosis (Toubiana *et al.*, 2016). These significant associations between IFNγ and cryptococcosis provide overwhelming evidence of a protective role led to a clinical trial of IFNγ in cryptococcal meningitis patients. In this trial, cryptococcal meningitis patients received either gold standard induction therapy (amphotericin B and fluocytosine), or both induction therapy and adjunctive IFNγ. Additionally, IFNγ treated patients either received doses every day for 2 weeks, or only on days 1 and 3. This trial found that both treatment groups that received adjunctive IFNγ therapy had increased clearance of *C. neoformans* from CSF (Jarvis *et al.*, 2012). However, this clinical trial only examined IFNγ when given adjunctive to traditional antifungal therapy, and it is yet to be determined whether IFNγ treatment alone

would benefit patients. Additionally, guidance surrounding the use of IFNγ in cryptococcosis remains unclear

1.4.1.1.4.2 – Tumour Necrosis Factor-α

Another Th1-associated cytokine that has been historically associated with clearance in cryptococcosis is tumour necrosis factor-α (TNFα, Kawakami *et al.*, 1996). Like IFNγ, TNFα in patient CSF is also associated with survival in cryptococcal meningitis (Jarvis *et al.*, 2014), and patients receiving anti-TNFα therapy (adalimumab) are at a higher risk of cryptococcosis (Liao, Chen and Chen, 2016). Additionally, TNFα is reported to increase macrophage-mediated phagocytosis of cryptococcal cells (Cross and Bancroft, 1995) via complement based mechanisms (Collins and Bancroft, 1992) and inhibition of TNFα action in mice accelerated mortality in model of cryptococcosis (Rayhane *et al.*, 1999; Herring *et al.*, 2005). Despite this, TNFα has not received the same attention as IFNγ in terms of immunotherapeutic development because TNFα is also reported to be detrimental for host outcomes. In the context of HIV/AIDS, TNFα stimulates HIV viral transcription and so may further immunocompromise these patients (Israël *et al.*, 1989). Additionally, *in vivo* TNFα levels actually correlate with increased CNS dissemination via macrophage 'Trojan horse' mechanisms in mice, and so may actually increase CNS fungal burdens in cryptococcal meningitis patients (Santiago-Tirado *et al.*, 2017). This suggests that TNFα only has diagnostic and prognostic uses in cryptococcosis.

1.4.1.1.4.3 – Interleukin 12 and Interleukin 18

Other Th1 cytokines that have shown promise in improving host outcomes include interleukin (IL) 12 and IL-18. *In vitro,* virulent strains of *C. neoformans* abrogate the production of IL-12 by murine macrophages (Kawakami *et al.*, 1999) while *in vivo,* genetically ablating IL-12 in mice increased mortality (Decken *et al.*, 1998). Additionally, in a HIV positive mouse model of *C. neoformans* infection, treatment with exogenous IL-12 corrected defects in NK cell binding to *C. neoformans* (Kyei *et al.*, 2016).

However, it has been subsequently found that the main benefit of IL-12 is in stimulating the release of other cytokines. When IL-12 was administered to mice in combination with IL-18 – a cytokine structurally related to IL-1β – treatment increased Th1 marker expression and reduced fungal burdens. However, neither cytokine when administered alone protected animals, implying that IL-18 and IL-12 act synergistically (Zhang *et al.*, 1997). However, when IL-12 knockout animals were treated with IL-18, improved host outcomes were observed. This suggests a redundant role for IL-12, and that instead IL-18 is critical for host protection (Kawakami, Koguchi, Qureshi, Miyazato, *et al.*, 2000). In support of this, when transgenic mice lacking either the IL-1 or the IL-18 receptor were infected with *C. neoformans*, it was found that only loss of the IL-18 receptor impacted

survival (Wang *et al.*, 2011). However, mechanistic studies of both IL-12 and IL-18 have found they both act by stimulating the production of IFNγ (Hoag *et al.*, 1997; Kawakami *et al.*, 1997). Therefore, it is likely that IL-18 and IL-12 primarily mediate host protection via IFNγ, and so are not alternative targets for immune enhancement.

1.4.1.1.4.4 – Interleukin 1

Aside from IL-18, two other Th1 cytokines are the Th1 'sister' cytokines IL-1α and IL-1β. These cytokines, despite having distinct activity and functions, are both ligands of the same receptor (IL-1R), which along with the associated signal transduction protein, MyD88, have been shown to be indispensable for protection and survival in mouse models of cryptococcosis (Gasse *et al.*, 2007; Shourian *et al.*, 2018). Of the two cytokines, IL-1α is poorly understood in the context of protective immunity during cryptococcosis. Elevated IL-1α has been observed in infected mice, with increased expression in the CNS of animals as early as 1 day post infection (dpi; Maffei *et al.*, 2004; Aratani *et al.*, 2006). However, the biological significance of this finding has yet to be determined. IL-1β, on the other hand, has received relatively more attention with regard to its role in cryptococcosis. This is largely because it is one of the main cytokines produced by pro-inflammatory macrophages, along with TNFα and IL-6, and these cells feature heavily in the cellular response in cryptococcosis (Spinelle-Jaegle *et al.*, 2001). There is also evidence that *Cryptococcus* attempts to suppress IL-1β production. Acapsular cryptococci, which are avirulent in mouse inhalation infection models, readily activate the NLRP3 inflammasome, the post translational modification protein complex required for IL-1β production (Guo *et al.*, 2014). Additionally, cryptococcal polysaccharide has been shown to reduce human monocyte expression of IL-1β (Vecchiarelli *et al.*, 1995). This suggests that the virulence of *Cryptococcus* may be related to lower IL-1β expression. *In vivo*, mice infected with the mildly virulent *C. neoformans* strain, 52D, were found to require IL-1β for protection and animal survival (Shourian *et al.*, 2018). With strong evidence of a role for IL-1β in mediating protective immunity, potentially via macrophages, there is a justification for determining the significance of IL-1β in the protection (or pathology) of cryptococcal disease.

1.4.1.1.4.5 – Th17 cytokines

Th17 responses are less well understood in the context of cryptococcosis, but reports that do exist are already conflicted with regard to if these responses are beneficial to the host. Effects of the signature Th17 cytokine, IL-17A, include increased nuclear factor kappa-light-chain-enhancer of activated B cells (NFκB) signalling (Onishi and Gaffen, 2010) and NO production (Miljkovic and Trajkovic, 2004), which are associated with increased antimicrobial activity. Additionally, infection of IL-17A$^{-/-}$ mice with 52D *C.*

neoformans revealed that IL-17A was required for leukocyte recruitment, fungal clearance and lFNγ production by T cells (Murdock *et al.*, 2014). Similarly, both IL-23$^{-/-}$ and IL-17RA$^{-/-}$ mice inoculated with 52D *C. neoformans* were observed to have more Th2 skewed cytokine profiles (Szymczak, Sellers and Pirofski, 2012). However, tissue fungal burdens in all these transgenic animal *in vivo* studies were unaffected, suggesting Th17 responses are less important than Th1 responses for fungal clearance – a conclusion reached by several groups (Zhang *et al.*, 2009; Hardison *et al.*, 2010; Wozniak *et al.*, 2011; Valdez *et al.*, 2012).

Therefore, while cytokine profiles are often useful determinants of host outcomes in cryptococcosis, more work is needed to determine the biological significance of these profiles, and which cytokines and associated pathways may provide an opportunity for therapeutic opportunity.

1.4.1.2 – Innate immune cells

The innate immune phase of the immune response is rapid and non-specific, with an aim to contain and control pathogens while a more specific adaptive response is generated. The major cell populations that effect these responses include macrophages, dendritic cells (DCs), neutrophils (neuts), granulocytes (mast cells, eosinophils) and innate lymphoid cells. In order to quickly respond to pathogens, these cells possess a repertoire of extracellular and intracellular pattern recognition receptors (PRRs) that recognise a variety of common pathogen associated molecular patterns (PAMPs). Major classes of PRR include Toll-like receptors (TLRs), Nucleotide oligomerisation domain (NOD) like receptors, C-type lectin receptors and the mannose receptor (Figure 5). Additionally, innate leukocytes also possess well conserved antimicrobial mechanisms that vary between cell types. Below, the understanding of each cell type and its contribution to host-pathogen interactions in cryptococcosis are described.

1.4.1.2.1 – Alveolar epithelial cells

While humans possess multiple mechanisms of immune defence, it is always of benefit to the host to prevent infection occurring in the first place. To this end, epithelial layers, such as those of the skin and lungs, serve as important barriers to preventing pathogen from accessing and colonising deeper tissues. These barriers are especially important in the case of a disseminating pathogen such as *C. neoformans*, and therefore understanding these interactions of *Cryptococcus* with the epithelium is critical in order to prevent the spread of infection.

In the case of pulmonary infection, it is important to note that cryptococcosis is primarily associated with infection of the lower airways and alveoli. This means the interactions of

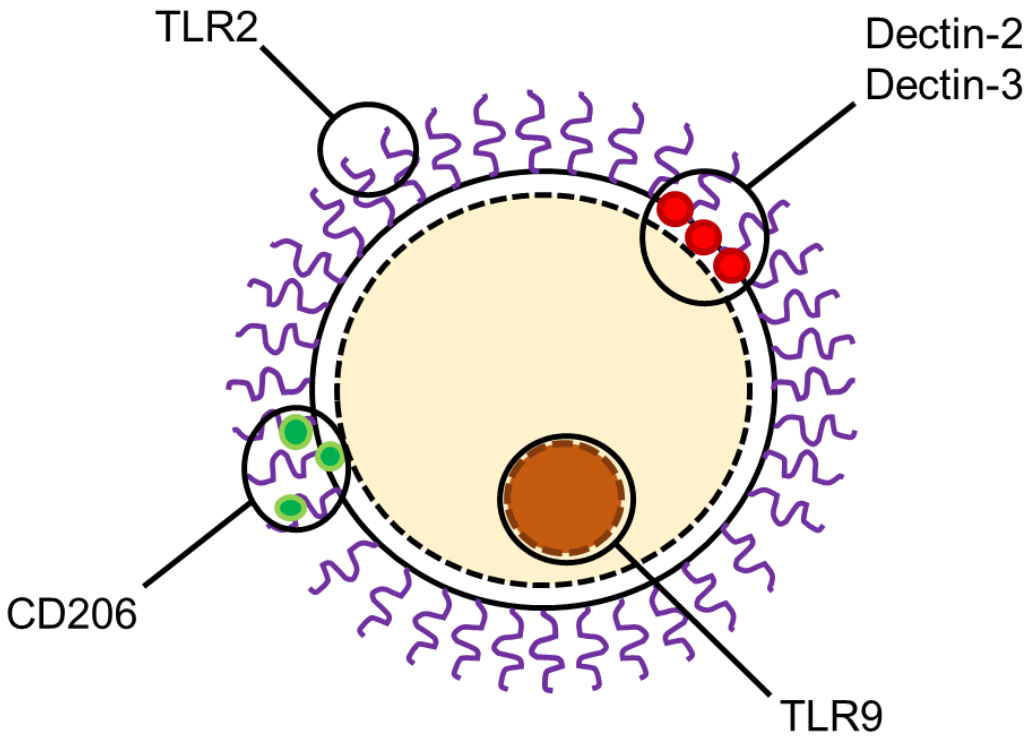

Figure 5 – Antigenic recognition of *Cryptococcus* by pattern recognition receptors. A diagram highlighting which components of the *Cryptococcus* cell can be recognised by specific pattern recognition receptors of the immune system. **TLR2 –** Recognises capsular GXM (purple lines; Yauch *et al.*, 2004). **Dectin-2 and Dectin-3 –** Recognises cell wall, capsular GXM and mannan (red circles; Huang *et al.*, 2018; Mansour, Latz and Levitz, 2006). **CD206 –** Recognises capsule and cell wall associated mannan (green circles; Mansour, Latz and Levitz, 2006). **TLR9 –** Recognises cryptococcal nuclear DNA (nucleus – brown circle; Nakamura *et al.*, 2008).

Cryptococcus with the cells of upper respiratory tract epithelium is poorly understood *in vivo*, as is the contribution of mucociliary clearance to host defence.

Although it is not known if *C. neoformans* directly kills epithelial cells *in vivo* to escape the lungs, *C. neoformans* has been observed to be internalised by A549 epithelial cells *in vitro*. Interestingly, this uptake was associated with increased epithelial cell death (Barbosa *et al.*, 2006), although a mechanism connecting these events has yet to be determined. However, the same increase in cell death was not observed when A549 cells were treated with GXM alone, suggesting this effect is dependent of active infection (Barbosa *et al.*, 2006).

Epithelial cells also have an important role in immune surveillance, evidenced by their expression of PRRs and their capacity to produce cytokines and alarmins. CD14 is one epithelial cell PRR that recognises cryptococcal GXM (Anas, Poll and de Vos, 2010). Activation of CD14 by capsulated and acapsular strains of *C. neoformans* in primary human bronchial epithelial cells is associated with production of IL-8, a cytokine that mediates neutrophil recruitment (Reddi *et al.*, 2003; Barbosa *et al.*, 2007). However, as cryptococcosis is associated with infection of the lower airways, these results may not be highly applicable to the clinical situation. Another epithelial derived factor with strong relevance to human infection is IL-33. IL-33 is a cytokine with numerous effects that are highly context dependent – although these effects are primarily associated with Th2 responses and are associated with poorer host outcomes in cryptococcosis (Flaczyk *et al.*, 2013). Specifically, Heyen *et al.* observed that IL-33 reduced E-cadherin expression, an adhesion molecule important for maintaining the integrity of the lung epithelium (Heyen *et al.*, 2016). However, the effect of this IL-33 mediated reduction in E-cadherin on dissemination and leukocyte recruitment in models of cryptococcosis has yet to be examined.

1.4.1.2.2 – Macrophages

The immune cells that have received the most attention in the context of cryptococcosis are macrophages. *In vivo* and *in vitro* studies have shown that macrophages significantly affect host outcomes, with genetic ablation of these cells in zebrafish significantly decreasing survival due to *C. neoformans* infection (Bojarczuk *et al.*, 2016). However, the capacity for macrophages to actually kill *Cryptococcus* cells is controversial, and appears to be model dependent. *In vitro, w*here macrophage antifungal activity is quantified by intracellular cfu counts at different time points post infection, macrophage killing is reported (Bulmer and Tacker, 1975; Granger, Perfect and Durack, 1986). However, there are issues with this experimental approach. Firstly, results are based on the assumption that all extracellular cryptococci are removed from cultures, so only

changes in intracellular fungal cell numbers are being reported, which has yet to be confirmed. Also, this approach is not compatible with repeated sampling of the same samples and fungal cell number can be affected by other processes such as vomocytosis, which may reduce intracellular cfu counts but be attributed to fungal killing rather than persistence of *Cryptococcus* cells. More recent studies have used live imaging methods to examine macrophage-*Cryptococcus* interactions *in vitro* to assess macrophage antifungal activity. However, studies that utilise this method do not observe fungal cell killing – instead intracellular *Cryptococcus* cells are observed to replicate intracellularly at different rates (Mitchell and Friedman, 1972; Steenbergen, Shuman and Casadevall, 2001). Furthermore, macrophages are hypothesised to aid cryptococcal dissemination via Trojan horse dissemination (Santiago-Tirado *et al.*, 2017). Therefore, the role of macrophages in host defence is still unclear (Rudman, Evans and Johnston, 2019).

Before proceeding, it is important to distinguish between the two major macrophage populations that exist *in vivo* – resident macrophages and interstitial macrophages (Byrne *et al.*, 2015). Although these cells have the same repertoire of antimicrobial mechanisms at their disposal, these cell types have distinct origins, differential surface molecule expression and have different roles in antifungal immunity. In the lung, tissue resident macrophages – alveolar macrophages – are distributed throughout alveoli at a relatively low density. These cells are derived from unique progenitors that are present in the foetal yolk sac during the early stages of organism development, differentiating them from other macrophage populations. Compared to other macrophages, alveolar macrophages have a relatively long life-span with limited regeneration (Tan and Krasnow, 2016). In the case of pulmonary infection, alveolar macrophages play a sentinel role in the lung – being among the first cells that respond to inhaled microbes and raising the immunological alarm following pathogen recognition (McQuiston and Williamson, 2012).

Monocyte-derived macrophages (MDMs), meanwhile, have to first be recruited to sites of infection. These cells are generated via haematopoiesis in the bone marrow and circulate around the body in the vasculature as monocytes. Once these cells infiltrate into the affected tissue, these cells differentiate into macrophages (Tan and Krasnow, 2016). However, this need to be recruited means interstitial macrophages appear in significant numbers later than alveolar macrophages. Furthermore, these cells also have a higher turnover and so remain at sites of infection for a shorter time. Despite these differences, the host-pathogen interactions of both cell populations are similar, with responses that range from phagocytosis, to cytokine production, to antigen presentation.

1.4.1.2.2.1 – Phagocytosis

The best-known response of macrophages to pathogens is phagocytosis. Cryptococci possess many adaptations to evade phagocytosis (see 1.4.1.1.3), such as the antiphagocytic capsule (see 1.4.2.1) and the ability to switch to the phagocytosis resistant titan cell morphology (see 1.4.2.8). This led to the theory that for the phagocytosis of cryptococci to occur, cryptococci were required to be opsonised. This theory has since been refined to phagocytosis does occur in the absence of opsonin, albeit at significantly lower levels (Mukherjee, Feldmesser and Casadevall, 1996). Nevertheless, the importance of cryptococcal cell opsonin status with regard to phagocytosis means that opsonins have been extensively studied in cryptococcosis models.

As described previously, antibodies against cryptococcal GXM have been shown to enhance the phagocytosis of cryptococci (see 1.4.1.1.3). The Fc region of IgG molecules that are bound to *C. neoformans* are recognised by Fc receptors on macrophages, which recognise and bind this domain and mediate the uptake of antibody opsonised cryptococci. Clinical observations of the Fc receptor have identified two polymorphisms that significantly affect cryptococcosis outcomes – FcGR3A and FcγRIIB. The FcGR3A polymorphism has been determined to be a risk factor for cryptococcosis in both HIV positive and negative patients (Rohatgi *et al.*, 2013). Interestingly, this polymorphism increases the binding affinity of the Fc receptor to the Fc region, although the mechanism behind this susceptibility has yet to be elucidated. On the other hand, the FcγRIIB polymorphism reduces the receptor binding affinity for the Fc region, which controversially increases macrophage phagocytosis of cryptococci (Surawut *et al.*, 2017). However, as this polymorphism increases patient susceptibility to cryptococcosis, this implies that phagocytosis of *Cryptococcus* is detrimental to the host. This was also the conclusion when J774 cells were infected with clinical isolates of *C. neoformans* of varying virulence. Again, clinical isolates that were phagocytosed more by J774 cells were associated with decreased patient survival and higher patient fungal burdens. This suggests that the phagocytosis of *Cryptococcus* by macrophages may actually be detrimental to the host during cryptococcosis (Sabiiti *et al.*, 2014). This indicates that the role of phagocytosis in host defence is unclear, and should be studied *in vivo* to understand in which contexts phagocytosis by macrophages is appropriate.

1.4.1.2.2.2 – Phagosomal processing

Following phagocytosis, internalised pathogens are contained within phagosomes – intracellular structures inside which host cells attempt to kill intracellular pathogens. Endosomes and lysosomes fuse to the infected phagosome over time, generating an

increasingly antimicrobial environment until the phagosome develops into a mature phagolysosome (Smith, Dixon and May, 2015). The antimicrobial environment within phagolysosomes is generated by multiple mechanisms – primarily the production of antimicrobial molecules, an acidic pH and nutrient starvation.

The major class of antimicrobial molecules produced by macrophages are reactive oxygen and nitrogen species (RONS) – highly reactive chemical species that are thought to damage pathogen DNA and RNA, as well as affect enzyme function (Li *et al.*, 2021). The melanin of *C. neoformans* is thought to be able to scavenge and neutralise RONS (see 1.4.2.2) – however, this can be overcome by stimulating macrophages with the appropriate cytokines to overwhelm this scavenging capacity.

C. neoformans also minimises RONS production. *In vitro, C. neoformans* infection fails to induce macrophage expression of iNOS – an enzyme critical for the production of NO, an antifungal reactive nitrogen species (Naslund, Miller and Granger, 1995; Wager *et al.*, 2015). In contrast, pro-inflammatory cytokines such as IL-17A, TNFα and IFNγ are all reported to increase macrophage iNOS expression (Miljkovic and Trajkovic, 2004; Zhang *et al.*, 2012; Salim, Sershen and May, 2016). However, it is worth noting that these studies used mice, a species that are reported to produce higher amounts of NO compared to humans. Therefore the results of these studies may not be representative of what happens in humans (Kmoníčková *et al.*, 2007).

The role of low pH in the killing of *Cryptococcus* is less clear. Unlike many other intracellular pathogens that rely on inhibiting phagosomal maturation to prevent acidification taking place, *C. neoformans* is also able to survive and replicate in the highly acidic environment (Johnston and May, 2013). This is evidenced by *C. neoformans* persisting in phagosomes positive for Lamp1 – a marker of acidic phagosomes that are ordinarily antimicrobial (Levitz *et al.*, 1999). To survive in this environment, many cryptococcal virulence factors become activated at a low pH, including Plb1 (see 1.4.2.4, Levitz *et al.*, 1999). However, there is no consensus in the literature as to which pH is optimal for cryptococcal growth. Pharmacologically raising the phagosomal pH above 7 *in vitro* decreases the survival of intracellular cryptococci (Levitz *et al.*, 1999), suggesting that an acidic pH is advantageous for cryptococcal growth (Smith, Dixon and May, 2015). More specifically, it has been previously proposed that a pH of 5 is ideal for fungal growth (Levitz *et al.*, 1997), which is slightly less acidic than mammalian lysosomes (Lodish *et al.*, 2000).

However, *C. neoformans* also does manipulate phagosomal pH. One of the ways *C. neoformans* achieves this is via the activity of urease, which produces ammonia from urea. This raises phagosomal pH, suggesting it is beneficial for *C. neoformans,* although

it results in slower *C. neoformans* intracellular growth (Fu *et al.*, 2018). Despite reduced growth though, urease is still required for virulence in mouse models of cryptococcal infection. This suggests that *C. neoformans* may have two distinct mechanisms of surviving phagosomal pH – either raising phagolysosomal pH via urease at the cost of lower rates of intracellular replication, or allowing acid activated virulence factors such as Plb1 to damage the phagolysosome and result in leakage and dilution of antimicrobial mediators. However, there is a need to better understand the relationship between phagosomal pH and *C. neoformans* survival in order to fully understand macrophage antifungal activity.

Nutrient starvation is the least studied of the three antifungal mechanisms in the context of host immunity to *Cryptococcus*. Continuous *Cryptococcus* production of GXM is required for intracellular survival. However, it is also known that macrophage phagosomes are low or devoid of metal ions that are critical for *C. neoformans* growth and survival (Ward, Uribe-Luna and Conneely, 2002; Cellier, Courville and Campion, 2007). Despite this, the size of the *C. neoformans* capsule is still observed to increase with intracellular fungal growth (Bojarczuk *et al.*, 2016). Several cellular sensors expressed by *Cryptococcus* have been identified to be critical for fungal cell survival and growth in these conditions, including PI3K, Pck1 and Sre1 (Panepinto *et al.*, 2005; Chun, Liu and Madhani, 2007; Hu *et al.*, 2008).

To acquire carbon sources, cryptococci are thought to damage phagolysosomal membranes and scavenge liberated phospholipids. One way that *Cryptococcus* may do this is via the action of extracellular phospholipases, such as Plb1 (see 1.4.2.4; Evans *et al.*, 2019) – an enzyme critical for the 'leaky' phagosome phenotype in infected macrophages. Additionally, this action may also enable the entry of cytosolic nutrients into the phagolysosome for utilisation by *C. neoformans*. However, this phenotype has been primarily studied in relation to phagosomal pH and antimicrobial species concentrations (De Leon-Rodriguez *et al.*, 2018), and this role of *Cryptococcus* Plb1 in nutrition has yet to be examined experimentally. Furthermore, host IFNγ has been shown to reduce phagolysosomal permeabilisation, indicating this may be part of the protective action of this cytokine – although it could just be the result of polarising macrophages towards a more pro-inflammatory phenotype, consequently reducing cryptococcal cell viability (De Leon-Rodriguez *et al.*, 2018). It is also important to note that *C. neoformans* phagolysosomal leakage activates macrophage inflammasomes, resulting in increased IL-1β (Chen *et al.*, 2015). This should be considered in *in vitro* studies of IL-1β production by macrophages, where during *C. neoformans* infection, IL-1β may be elevated in response to either a more protective pro-inflammatory macrophage phenotype indicative of host protection, or due to lysosomal damage and poor host responses.

1.4.1.2.2.3 – Vomocytosis

While cryptococci are observed to persist intracellularly within macrophages, *Cryptococcus* is also able to escape the out of the macrophage phagolysosome back into the extracellular environment. Vomocytosis, also known as non-lytic exocytosis, describes the release of intracellular pathogens from a macrophage, where both the pathogen and macrophage remain intact (Alvarez and Casadevall, 2006; Ma *et al.*, 2006). While this process is still under investigation, it is likely *Cryptococcus* evolved this mechanism in response to selection pressures from amoebae in the environment, where escaping back into the extracellular environment is likely to benefit fungal cells. Currently vomocytosis is relatively difficult to study and has yet to be observed in mammalian tissue. However, as more intravital and *ex vivo* imaging modalities become more widely available, the significance of this event may be better understood *in vivo*.

The significance of this process in the pathology of cryptococcosis is believed to primarily be in aiding cryptococcal dissemination to other tissues *in vivo* (Gilbert *et al.*, 2017; Seoane *et al.*, 2020). Vomocytosis only occurs with live *Cryptococcus* and not with heat killed cells, highlighting that vomocytosis requires the active involvement of phagocytosed *Cryptococcus*. Although, the exact mechanism of vomocytosis still remains unknown, the sequence of events that take place in vomocytosis have been described, as have a number of factors that influence incidences of vomocytosis. Cryptococcal factors known to influence vomocytosis include the presence of capsule, Plb1 and laccase, although it is important to note that these factors are also important for intracellular survival. Therefore, rather than directly influencing vomocytosis, these factors may just increase the survival of intracellular cryptococci, enabling vomocytosis to occur (Chayakulkeeree *et al.*, 2011; Gilbert, 2017; Frazão *et al.*, 2020).

Interestingly, several host factors have also been identified to affect the incidence of vomocytosis. Phagosomal pH was one such factor, with alkaline treatment of macrophages increasing vomocytosis while acidic phagosomes prevented vomocytosis (Ma *et al.*, 2006). Additionally, the sub-cellular localisation of the phagosome is important, and must be in close proximity to the macrophage cell membrane. Furthermore, a reduction in phagolysosomal membrane integrity is observed immediately prior to vomocytosis (Johnston and May, 2010). This association of vomocytosis with macrophage memebranes was examined in greater detail by Stukes *et al.*, who examined the contribution of the membrane binding protein, Annexin A2, to vomocytosis (Stukes *et al.*, 2016). Genetic ablation of Annexin A2 reduced both vomocytosis and the phagocytosis of *C. neoformans*. However, intracellular cryptococci in Annexin A2 deficient macrophages were observed to be larger in size. As capsule enlargement occurs prior to vomocytosis, it is hypothesised that capsular enlargement

continued for longer due to reduced fusion of the phagosomal to macrophage plasma membranes. In contrast, pharmacological inhibition of actin polymerisation enhanced vomocytosis (Johnston and May, 2010). When examined further, it was observed that transient 'cages' made of actin – described as actin flashes – form around phagosomes prior to vomocytosis. Through pharmacological inhibitors, it was found that actin flashes were dependent on Arp2/3. Consequently, inhibiting Arp2/3 both reduced actin flashes and increased vomocytosis, and vice-versa. This suggests that these actin cages function to physically contain phagosomal cargo and prevent their escape.

Finally, macrophage immunological status has also been observed to affect the occurrence of vomocytosis. Type I interferons are cytokines that skew macrophages towards a proinflammatory phenotype, and have been observed to increase the vomocytosis of *C. neoformans* (Seoane *et al.*, 2020). Significantly, expression of these cytokines are elevated in HIV/AIDS patients, suggesting this may contribute to the increased susceptibility in these patients (Hardy *et al.*, 2013). Conversely, the cytokines IL-4 and IL-13 which polarise macrophages towards a Th2 phenotype – a phenotype associated with poorer control of cryptococcosis – actually reduced vomocytosis (Voelz, Lammas and May, 2009). This implies that vomocytosis is beneficial to the host in some way. In the case of amoebae, these organisms are known to constitutively vomocytose indigestible cargo – suggesting that this process may be a conserved protective process for phagocytic cells. Either this may maintain macrophage viability during infection with pathogens, or prevents cells 'wasting resources' on resistant pathogens, and encouraging the phagocytosis of 'easier' targets (Watkins *et al.*, 2018). To this end, increasing vomocytosis in mice infected with *C. neoformans* with type I interferons actually resulted in lower fungal burdens in the brain (Sionov *et al.*, 2015). Therefore, while vomocytosis may be a way that *Cryptococcus* can escape from host immune cells and disseminate, excessive rates may result in *C. neoformans* being ejected before macrophages leave the site of initial infection, reducing dissemination.

This highlights how context specific the role of vomocytosis is in host-pathogen interactions *in vivo*, and contributes to the current confusion regarding whether enhancing or inhibiting macrophage activity is a benefit or a detriment to the host.

1.4.1.2.2.4 – Dragotcytosis

Dragotcytosis is a more controversial mechanism of cryptococcal escape. Originally called lateral transfer, dragotcytosis describes the process by which an intracellular cryptococcal cell disappears from one macrophage and appears in another, with all cells surviving the process (Ma *et al.*, 2007). Originally this process was hypothesised to be a single event – however, a recent study by Dragotakes *et al.* revealed the process is

instead likely the result of an incidence of vomocytosis followed by an incidence of phagocytosis by a different macrophage (Dragotakes, Fu and Casadevall, 2019). This finding has called into question other lateral transfer events that have been postulated to occur in the case of other intracellular pathogens (*Scedosporium apiospermum*, *Lomentospora prolificans* and *Aspergillus fumigatas*; Trzaska, 2019). Regardless, as dragotcytosis is even less frequent than vomocytosis, the *in vivo* significance of this event on infection outcomes has yet to be determined.

1.4.1.2.3 – Neutrophils

Being the most abundant circulating type of immune cell, neutrophils are involved in many innate immune responses (Rosales, 2018). Neutrophils are among the first cells typically recruited to sites of infection – with their numbers ordinarily peaking within 2-6 hours of an acute immune insult (Sapey and Stockley, 2019). However, at the time of writing, neutrophils have yet to be observed to have a significant role in the human immune response to cryptococcosis. Clinically, no association has been found between patients who have deficiencies in neutrophil number or function, and incidences of cryptococcosis (Gibson and Johnston, 2015). A single case report has concluded there may be a significant role of neutrophils, however, this study described an incidence of cryptococcosis in a B-cell lymphoma patient receiving chemotherapy and steroid therapy, and so many factors may have influenced infection susceptibility (Hirai *et al.*, 2011).

It is important to note that neutrophils are still observed to interact with cryptococci *in vivo*. Intravital imaging of the brains of mice infected with *C. neoformans* revealed that neutrophils that infiltrated the CNS are able to phagocytose disseminated cryptococci (Neumann *et al.*, 2018). It is also observed that neutrophil defensins can both inhibit the growth of, and kill cryptococci (Mambula *et al.*, 2000). Despite this potential for antifungal activity, however, animal studies have shown that depleting neutrophil numbers does not significantly affect fungal burdens, and in some cases actually improves animal survival (Mednick *et al.*, 2003; Osterholzer, Chen, *et al.*, 2009). In *C. gattii* infection, neutrophils may actually play a pathological role. Although increased neutrophil activity is associated with ordinarily protective Th1 responses, if neutrophils aren't significantly contributing to fungal clearance, their increased number and function will result in inappropriate inflammation and damage to host tissues due to their non-specific mechanisms of activity. In the case of *C. gattii* infection, compared to *C. neoformans* infection is associated with a greater degree of inflammation and immune mediated damage in the lungs (Krockenberger *et al.*, 2010). In a rat of model of *C. gattii* infection, even low inocula of *Cryptococcus* resulted in significantly elevated numbers of pulmonary neutrophils. Additionally, neutrophils are a key cell type in many autoimmune conditions for mediating

tissue damage (Hoenderdos and Condliffe, 2013; Tang *et al.*, 2019). This means that neutrophils may not be protective, and instead mediate tissue damage in *C. gattii* infection.

1.4.1.2.4 – Dendritic cells

Dendritic cells (DCs) are leukocytes best known for their role in antigen presentation – the critical process that links the innate and adaptive immune responses (Figure 6). Briefly, professional antigen-presenting cells (APCs) 'show' antigenic fragments of a pathogen on major histocompatibility complex (MHC) class II surface molecules. These antigens are then recognised by specific T helper cells. Following recognition, additional receptors are engaged on APCs and T cells, leading to the selection, expansion and activation of specific T cells, and the generation of an adaptive immune response. However, because of how complex this process is, these responses take days and any bottlenecks can delay this process even further. Therefore, DCs are critical cells in many infections.

In cryptococcosis, DCs have been observed to be critical for generating T cell responses to *C. neoformans*, both *in vitro* and *in vivo* (Bauman, Nichols and Murphy, 2000; Bauman, Huffnagle and Murphy, 2003). Specifically, the recruitment of DCs out of circulation is correlated with fungal clearance and improved host outcomes in a mouse model of cryptococcosis. Additionally, $CD11b^{+}$ DCs were observed to be critical for pulmonary clearance and protective immune responses in studies of experimental cryptococcal vaccines (Osterholzer, Chen, *et al.*, 2009). A role for DCs in immunity to *C. gattii* has also been observed, although *C. gattii* appears to be better adapted to resisting DC antifungal action – encapsulated *C. gattii* cells have been observed to inhibit both DC maturation and antigen presentation – a phenomenon not observed with *C. neoformans* (Huston *et al.*, 2013).

As DCs and macrophages are both able to perform phagocytosis and antigen presentation, the relationship between these two cell types has been studied. Firstly, the role of AMs in recruiting DCs has been investigated, as AMs are the most abundant myeloid cells in the lung prior to infection. AM expression of both MCP-1 and CCR2 were both shown to be critical for the recruitment of DCs into the lungs of mice (Osterholzer *et al.*, 2008). In terms of phagocytosis, opsonising cryptococci with both complement and antibody results in increased phagocytosis by DCs. Furthermore, anti-GXM antibodies have been shown to be important for DC induced T cell responses *in vitro* (Kelly *et al.*, 2005). Murine pulmonary DCs isolated from bone marrow are observed to kill *C. neoformans*, dependent on lysosomal ROS, and Dectin 3 and CXCR3 receptor engagement (Huang *et al.*, 2018). However, there are important differences in how

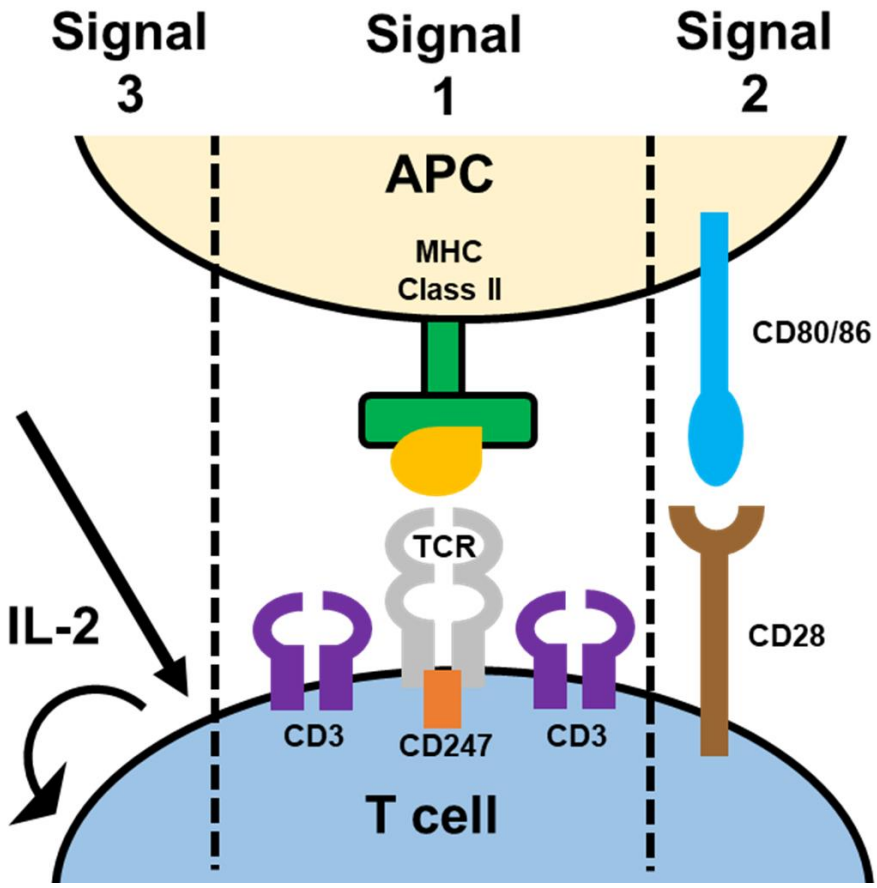

Figure 6 – Schematic of antigen presentation. Diagram describing the three main signals required for T cell activation via the process of antigen presentation. **Signal 1** – Foreign antigen presented on MHC class II molecules, and is recognised by the corresponding TCR receptor, with accompanying CD3 signals. **Signal 2** – CD80/86 ligand on APC then binds to the CD28 receptor. **Signal 3** – Autocrine and paracrine IL-2 then stimulates expansion of T cell populations.

phagocytosed cryptococci are processed intracellularly by AMs and DCs, as cathepsin B is an antimicrobial lysosomal protein specific to DCs that has dose dependent cryptocidal activity (Hole *et al.*, 2012). Finally, depleting both AMs and DCs in mice with diphtheria toxin results in rapid mortality due to cryptococcosis (Osterholzer, Milam, *et al.*, 2009).

As both AMs and DCs are present early in infection, it is unsurprising that depleting both cell types reduces survival. What is surprising, however, is that the increased mortality in treated animals was not the result of increased fungal burdens – rather increased inflammation and tissue damage. This implies an important regulatory role of AM/DC crosstalk, potentially through generating regulatory T cells (Tregs). However, there is overwhelming evidence that DCs are critical cells in protective immune responses in cryptococcosis, particularly within the lungs. This subject is reviewed in greater detail by Wozniak (Wozniak, 2018).

1.4.1.2.5 – Eosinophils

Eosinophils are granulocytes that degranulate in response to immune challenges – releasing intracellular granule contents, antimicrobial and inflammatory mediators, into the extracellular milieu. However, these cells are also phagocytic and able to act as APCs. Despite this multitude of roles, eosinophils are typically ineffectual or even pathological cells, except in the case of helminth and parasite infection (Huang and Appleton, 2016) – although even in these contexts their efficacy is disputed (Herndon and Kayes, 1992). This is hypothesised to be due to the degranulation response – the indiscriminate release of inflammatory mediators fails to generate a suitably antimicrobial mediator concentration, yet still results in tissue damage. Additionally, eosinophils are indicative of ineffectual Th2 immune responses and potentiate these responses via Th2 cytokine production (Osterholzer, Surana, *et al.*, 2009). This is evidenced by depleting eosinophils in mouse models of cryptococcosis, which was observed to reduce pathological inflammation in mouse models of cryptococcosis and skew cellular and cytokine profiles towards a more antifungal Th1/Th17 profile (Feldmesser *et al.*, 1997).

However, it is important to note that cytokine profiles in animal models are artificial, and may be the result of the relatively high inocula of *Cryptococcus* animals receive. Therefore, when larger animal models are used, such as rats, different *Cryptococcus* infection phenotypes can be observed. More specifically, it has been shown that eosinophils are instead associated with Th1 immune responses (Garro *et al.*, 2011). Additionally, rat eosinophils express MHC class II, which is hypothesised to contribute to the increased MHC class II expression observed in models of cryptococcosis. Complementary to this finding, eosinophils have been observed to migrate to the lymph

nodes and spleen in cryptococcosis models and stimulate the generation of specific B and T cells (Garro *et al.*, 2011). Furthermore, eosinophil longevity at sites of infection has been observed to inversely correlate with ROS production – lower eosinophil ROS production extends the lifespan of eosinophils and the time for antimicrobial activity (Wedi *et al.*, 1999). As *C. neoformans* is reported to inhibit ROS production, this would theoretically extend the amount of time that eosinophils remain at sites of infection and act as either APCs or phagocytes (Garro *et al.*, 2011). The model differences and conflicting data from these experimental model, however, highlights that further work is needed to characterise the role of eosinophils in cryptococcosis, as they may be an important cellular component of protective immune responses.

1.4.1.2.6 – Natural Killer Cells

NK cells are one of few classes of innate lymphocytes, and are typically associated with immune responses to viruses and tumours. However, NK cells also have significant roles in host defence in response to various fungal pathogens, including *Cryptococcus*, *Candida* and *Aspergillus* (Ma *et al.*, 2004; Bouzani *et al.*, 2011; Voigt *et al.*, 2014). In the case of cryptococcosis, the primary contribution of NK cells is thought to be direct fungicidal activity. *In vitro*, cryptocidal activity has been observed, found to be dependent on engagement of the NKp30 receptor with cryptococci – confirmed with greatly reduced fungal killing observed when NKp30 is inhibited using either immunologically (blocking antibodies) or genomically (siRNA; Li *et al.*, 2013). Clinically, HIV patients are reported to have reduced expression of NKp30, which may contribute to the increased risk of disseminated disease in this population. Importantly, treating HIV patient NK cells with IL-12 *in vitro* rescues NKp30 expression and may be another benefit of IL-12 treatment in animal models (Kyei *et al.*, 2016).

Once in contact with cryptococci, NK cell binding leads to the formation of an immunological synapse between the NK cell and target fungal cell. This is followed by the exocytosis of cytotoxic granules into the synaptic space between the two cells. The trafficking of cytotoxic granules within host cells prior to exocytosis have been shown to be reliant on host PI3K activity, and downstream ERK1/2 signalling (Wiseman *et al.*, 2007). However, cryptocidal activity due to signalling within the immunological synapse is not well understood. For example, the NK cell receptor LFA1 has been shown to not be important for NK cryptocidal activity (Jones *et al.*, 2009). However, an examination of NK cell cytotoxic granules, which contain a mixture of several antimicrobial mediators, has identified that the killing of *C. neoformans* appears to be entirely mediated by perforin (Ma *et al.*, 2004), which mediates cytotoxicity by forming pores within cell membranes, leading to osmotic lysis and cell death.

Although fungal killing is reported to be the largest contribution of NK cells, it has also been suggested that NK cells augment the antifungal activity of other leukocytes (Kawakami, Koguchi, Qureshi, Yara, *et al.*, 2000). NK cells are also known to be a source of IFNγ. Because of the previously described potential benefit to the host of IFNγ (see 1.4.1.1.4.1), NK cells may also provide an early source of this cytokine to enhance the antifungal activity of innate cells. This potential benefit of NK cells in cryptococcosis, despite less attention than macrophages, suggest these cells warrant further research to understand their exact role in host defence.

1.4.1.3 – Adaptive cells

Although the cells of the innate immune response are important for controlling fungal infections, and an important determinant of infection outcomes, the cells best known to have a role in host protection during cryptococcosis are those of the adaptive immune response – the response notably impaired in HIV/AIDS patients. However, because of time it takes for an adaptive immune response to be generated in the first instance, the significance of this response is only apparent later in infection. Below, the role and contribution of various adaptive cells to fungal clearance in cryptococcosis are discussed.

1.4.1.3.1 – T cells

T cells are the signature cells of the adaptive immune system. However, the term 'T cell' actually encompasses multiple distinct sub populations of cells, each with significantly different roles, functions and contributions to cryptococcosis immunity. The contribution of each of the major T cell subtypes in the immune response during cryptococcosis ($CD4^+$, $CD8^+$, Treg) are discussed.

1.4.1.3.1.1 – T helper cells

Th cells, also described as $CD4^+$ cells, are not known for their directly antimicrobial action. Instead, Th cells primarily co-ordinate and support immune responses via cytokine production. These cells are plastic, and can have a number of phenotypes, depending on the local cytokine profile – each differentially affecting the host immune response. Although Th cell polarisation states are plastic and discrete, the most commonly observed phenotypes are broadly described as Th1, Th2 or Th17, as described previously (see 1.4.1.1.4). Th1 phenotypes arise primarily due to IL-12, and subsequently can be characterised by IFNγ and IL-2 production. Meanwhile, a Th2 skewed phenotype is the result of IL-4 signalling and can be characterised by IL-5 and IL-10 production. Finally, the Th17 phenotype emerges in the presence of IL-6 and TGFβ, and is then characterised by IL-17, IL-21 and IL-22 production (Kaiko *et al.*, 2008).

Because of this central role of Th cells, they significantly affect infection outcomes regardless of phenotype. This is best evidenced in HIV/AIDS patients, characterised by low or absent Th cell numbers, who are more susceptible to many infections, opportunistic or not (Simon, Ho and Abdool Karim, 2006). However, in cryptococcosis the exact roles of Th cells in the host immune response have yet to be fully described, despite the clear association between HIV/AIDS and incidences of infection. This is potentially due to the difficulty in studying lymphocytes compared to innate immune cells as adaptive immunity is less well conserved across specie. Additionally, adaptive immune responses are more complex due to their specificity, and their presence only later in infection extends experiment time and makes their research less high throughput.

In the case of pulmonary cryptococcosis models, depleting Th cells *in vivo* reduces the recruitment of neutrophils, eosinophils and macrophages into the lungs (Huffnagle *et al.*, 1994). Additionally, this treatment reduces the expression of the Th2 cytokines IL-4, IL-5 and IL-10 *in vivo,* evidencing how central the role of Th cells are for defining cytokine profiles (Arora *et al.*, 2006). In the context of disseminated disease, the protective role of Th cells is less clear. Historically, Th cells have been assumed to benefit the host during cryptococcal meningitis. Additionally, a cryptococcal vaccine study found that Th cells crossed the blood brain barrier in immunised mice that were protected during secondary *C. neoformans* infection (Buchanan and Doyle, 2000). These Th cells were also Th1 skewed – a phenotype associated with protective responses, leukocyte recruitment, IFNγ production and increased iNOS expression.

However, more recent studies have suggested that Th cells may actually do more harm than good during infection. Neal *et al*. confirmed that the presence of Th1 IFNγ producing Th cells within the CNS of mice infected with *C. neoformans* had lower CNS fungal burdens. Despite this, ~50% of these mice had to be culled due to symptoms of neurological dysfunction (Neal *et al.*, 2017). Further analysis revealed that CNS fungal burdens plateaued at 7dpi, whereas leukocyte numbers peaked at 21dpi. As mouse mortality occurred between 21 and 35dpi, this suggests that the CNS pathology was due to the presence of Th cells rather than due to *C. neoformans* infection. When this experiment was repeated in Th cell depleted mice after $CD4^+$ cells were ablated, mouse survival was significantly higher and fewer animals presented with neurological symptoms (Neal *et al.*, 2017). This was despite impaired clearance of fungal cells from the CNS, lower IFNγ production and fewer cytotoxic T cells (Tc) and myeloid cells. It is important to note this study utilised a less virulent 52D *C. neoformans* strain, whereas the vaccine study where Th cells were observed to be protective utilised a highly virulent KN99α *C. neoformans* infection. Therefore, the work of Neal *et al.* should be repeated using KN99α *C. neoformans* infection, where impaired fungal clearance may instead

result in higher mortality than the neuroinflammation related to Th cell antifungal activity (Specht *et al.*, 2015). However, this may also provide a model of IRIS, which is known to be closely associated with Th cell numbers (Jarvis *et al.*, 2015).

Th cells are also observed to be directly cryptocidal – one study observed that Th cells have superior cryptocidal activity compared to Tc cells and NK cells when peripheral blood mononuclear cells (PBMCs) treated with IL-2 were assayed *in vitro* (Chun *et al.*, 2007). Unlike NK cells, Th cell cryptocidal activity was observed to be mediated by granulysin, not perforin – although this protein also creates leaky microbial membranes (Stenger *et al.*, 1998; Chun *et al.*, 2007). Th cells from HIV patients have also been reported to have defects in granulysin and perforin pathways (Chun *et al.*, 2007) which may contribute to the increased susceptibility of HIV patients to cryptococcosis. This may be particularly significant, as even if well managed with high-activity anti-retroviral therapy (HAART), Th cells may still have impaired cryptocidal activity.

Although the exact role of $CD4^+$ still remains to be elucidated, the high levels of antifungal activity and ability to control and dictate immune responses does highlight how important these cells are to the immune response to cryptococcosis. A better understanding of differences in immunity to cryptococcosis with and without Th cells may enable us to understand the susceptibility of HIV/AIDS patients, and develop specific therapeutics to protect this group.

1.4.1.3.1.2 – Cytotoxic T cells

Tc cells are typically described as more direct effectors of adaptive immune response, hence their label of 'killer' T cells. Typically, these cells are investigated in the context of viral infection and cancer, where they kill infected or damaged host cells. Like Th cells, however, these cells also can kill *Cryptococcus* cells by granulysin based mechanisms, albeit with less activity than Th cells *in vitro* (Andersson *et al.*, 2007; Chun *et al.*, 2007). Additionally, it has also been observed that Tc cell antifungal activity depends on the presence of both Th cells and IL-15 signalling in order for sufficient Tc cell granulysin expression to mediate fungal cell killing (Ma *et al.*, 2002).

However, even in the absence of Th cells, Tc cells are still observed to be important for host defence in the lungs of mice infected with *C. neoformans* in the absence of $CD4^+$ cells (Lindell *et al.*, 2005). Additionally, Tc cells can also recruit Th cells, and vice versa, suggesting the presence of a positive feedback loop that may be significant in uncontrolled HIV/AIDS where Th cell numbers are lower. Furthermore, Tc cells can also recruit macrophages and neutrophils to the lungs during infection, filling the role of Th cells. Although, unlike Th cells, Tc cells do not appear to be able to mediate the recruitment of eosinophils (Huffnagle *et al.*, 1994). However, as the benefit of eosinophils

are still debated and are associated with ineffective Th2 responses, Tc mediated recruitment may actually be of benefit – although as HIV/AIDS patients are susceptible to cryptococcosis despite reduced Th cell numbers, it suggests that the contributions of Tc cells to immune cell recruitment are not enough to compensate for low or absent Th cells.

Finally, Tc cells also have an important role in IFNγ production. Th cells are a major source of IFNγ, although in mice Tc cells are required for high concentrations of IFNγ at sites of infection and inducing sufficient macrophage antifungal activity – shown using neutralising antibodies (Lindell *et al.*, 2005). Therefore, in the absence of Tc cell derived IFNγ, fungal burdens in the lung were significantly higher, particularly intracellularly within macrophages. This, again, has important implications for HIV/AIDS patients, where Tc cells may offer a level of protection to the host in the absence of Th cells, particularly as the source of IFNγ is irrelevant to the protection it imparts (Jarvis *et al.*, 2012). Therefore, although Tc cells cannot entirely compensate for the absence of Th cells, these cells are still multifaceted and an important component of host defence.

1.4.1.3.1.3 – Regulatory T cells

The other major T cell subtype are regulatory T cells (Treg). As the name implies, Treg cells suppress effector responses of the immune system, either to minimise tissue damage, prevent autoimmunity and resolve immune responses after an infection is cleared.

In the lungs during cryptococcosis, Th2 responses are reported to be detrimental for host outcomes and immune mediated clearance of *Cryptococcus*. To this end, Treg cells are reported to specifically inhibit ineffectual Th2 responses during infection in mice, helping to skew immune responses towards a more antimicrobial phenotype (Wiesner et al., 2016). More specifically, Treg cells were observed to accumulate in the lungs of mice in an IRF4 dependent manner, which prevented the expansion of Th2 responses.

In the CNS, however, patient immune responses tend to be Th1 skewed. As mentioned previously, however, increased fungal clearance may be dangerous and induce neuroinflammation and mortality (see 1.4.1.3.1.1). Xu *et al.* therefore investigated the potential role for Treg cells in abrogating this pathological damage in a mouse model of cryptococcosis. Interestingly, Treg cells that were observed produced IFNγ, suggesting these cells might controversially contribute to neuroinflammation (Xu *et al.*, 2020). Instead, however, this IFNγ signal was found to be required for the recruitment of significant numbers of Treg cells into the CNS during infection. Consequently, preventing Treg recruitment by using anti-CD25 antibodies resulted in increased mouse mortality in this model, while selective expansion of Treg cells with low dose IL-2 treatment improved

mouse outcomes. Mechanistically, Treg cells generated during infection were observed to suppress monocyte-derived macrophage (MDM) function and number, and reduce Tc cell mediated inflammation *in vivo* – reducing neuroinflammation. Despite these potential benefit to the host of modulating host immunity in both the lungs and CNS, these cells are seldom the subject of cryptococcosis research.

1.4.1.3.2 – B cells

B cells are the antibody producing cells of the immune system, and as described previously, antibodies are important in host protection against cryptococcosis (1.4.1.1.3). Therefore, the function and phenotype of B cells are critical for successful host immunity during cryptococcosis. Interestingly, one study that examined B cell populations in a mouse model of cryptococcosis found that although B1a, B1b and B2 B cell numbers were elevated, there was no evidence of clonal expansion early in infection (3dpi; Rohatgi and Pirofski, 2012). However, adoptive transfer of B1a cells to mice depleted of B1a cells found these cells were important in the early immune response (Dufaud *et al.*, 2018) – their absence resulted in increased lung and serum fungal burdens, as well as reduced phagocytosis of *C. neoformans* by AMs. This suggests that there may be roles for B cells outside of antibody production, although this is likely still their primary function.

1.4.1.4 – CNS-specific immunity

Because of the predisposition of *C. neoformans* to disseminate to the CNS, it is important to acknowledge the unique immunology of this tissue. The CNS is regarded as an immune privileged site. This phenotype is defined by various criteria, including a lack of traditional lymphatics and professional APCs, and physical barriers to control the entry of circulating immune cells into the organ from the rest of the body – in this case the blood brain barrier (Carson *et al.*, 2006). This is thought to have evolved to protect the highly sensitive tissue of the brain from inflammation, although it also could be due to the metabolic requirements of the CNS and the immune system being too high to be maintained together. The result of this is that the CNS has a unique immune system during homeostasis, and if pathogens such as *C. neoformans* do cross the blood brain barrier, immune responses can be reliant on the relatively low numbers of immune cells resident in the CNS, or risk neuroinflammation by recruiting immune cells from the rest of the body.

The only specialised immune cell type present in the CNS during homeostasis are microglia (Rock *et al.*, 2004). Similar to AMs, these cells are the resident macrophages of the CNS – they play a sentinel role, phagocytose pathogens and efferocytose damaged or apoptotic cells. As maintaining a sterile environment in the CNS is very important for host survival, microglia express highly sensitive potassium channels that

assist in the detection of pathogens. However, unless exposed to *C. neoformans* or IFNγ, these cells are poor APCs, evidenced by low expression of MHC class II (Aguirre and Miller, 2002). Also similar to macrophages, activated microglia produce TNFα and IL-1β, the latter of which is associated with neuronal damage and death. This pathway may therefore significantly contribute to neurotoxicity bought about by IFNγ stimulation in mouse models (Brás *et al.*, 2020).

It is also important to note that other cells of the CNS which are not specialised immune cells also support immune responses. Pericytes, which primarily function to provide metabolic support to neuronal cells, also regulate leukocyte trafficking in the neuronal vasculature and produce TGFβ which is important for generating Treg cells (Domev *et al.*, 2014; Rudziak, Ellis and Kowalewska, 2019) – which may be important for controlling the neuroinflammation associated with cryptococcal meningitis. There is also evidence that DCs, previously thought to be absent in the CNS, are actually present in the CSF of cryptococcal meningitis patients – indicating a potential role for these cells in CNS immune mediated protection (Panackal *et al.*, 2015). However, despite the association of the CNS with cryptococcosis, the response of CNS resident immune cells is still poorly understood.

1.4.1.5 - Granulomas

The other important response of the immune system to cryptococcosis are thought to be granulomas, which are a common feature observed with cryptococcosis patients (Shibuya *et al.*, 2005). Granulomas are immune structures that can form in response to persistent infectious and non-infectious antigens (G. James, 2000). These structures are defined as a distinct collection of leukocytes at or around a specific point – most notably consisting of macrophages. Typically, granulomas appear as an often circular mass of immune cells with a border of adaptive immune cells, an outer layer of macrophages, described as epithelioid in appearance, and a central core that can be necrotic or non-necrotic – depending on the original cause.

In the case of cryptococcosis, these structures are hypothesised to be protective for the host (Farnoud *et al.*, 2015). By containing fungal cells within a central static core, this is thought to prevent dissemination. Additionally, the high density localisation of macrophages and adaptive lymphocytes ($CD4^+$ cells) allows for maximal stimulation of macrophages towards a Th1 like phenotype, increasing the antifungal capacity of these cells (G. James, 2000). However, because these structures are difficult to study in mice and take a long time to develop, the significance of these structures and more specific

detail about their formation and role in cryptococcosis have yet to be determined (Farnoud *et al.*, 2015).

1.4.2 – *Cryptococcus* virulence factors

Many pathogens of humans evolve virulence factors in response to selection pressures present during infection of a mammalian host. However, pathogenic *Cryptococcus* species are different in that they are hypothesised to instead be incidental pathogens of humans. Instead, *Cryptococcus* virulence factors are hypothesised to have evolved in response to selection pressures in the environmental niche that *Cryptococcus* inhabits - the soil (Casadevall, 2008). In the soil, the natural predators of *Cryptococcus* are amoebae such as *Acanthamoeba castellani*. Despite a great evolutionary distance between amoebae and mammalian macrophages, the two are not functionally dissimilar (phagocytosis, respiratory burst). As interactions between amoebae and *Cryptococcus* cells are similar to those observed between macrophages and *Cryptococcus*, many of the cryptococcal virulence factors related to evading and surviving phagocytosis are hypothesised to be adaptations to the predator-prey relationship with amoebae in the environment (Steenbergen, Shuman and Casadevall, 2001). Regardless, these adaptations have enabled *C. neoformans* and *C. gattii* to become successful pathogens of humans, and understanding these virulence factors is critical in order to understand cryptococcal host-pathogen interactions.

1.4.2.1 – Cryptococcal capsule

The signature virulence factor for pathogenic cryptococci is the large polysaccharide capsule located outside of the cell wall that gives cryptococci a ‘hairy ball’ like structure (Figure 1). The capsule is made of several components, although the primary constituents are the polysaccharides glucuronoxylomannan (GXM) and glucuronoxylomannogalactan (GXMGal; Bose *et al.*, 2003). of the major pathogenic cryptococcal species. Studies using acapsular mutants of *C. neoformans*, such as the Cap59 strain, have shown the capsule is integral to virulence *in vivo* in mouse models of infection, although still able to grow *in vitro* (Chang and Kwon-Chung, 1994; Feldmesser *et al.*, 2000).

One of the primary functions of the capsule with regard to host-pathogen interactions is thought to be as a steric hindrance – preventing or limiting interactions between host pattern recognition receptors (PRRs) and antigenic components of the cryptococcal cell wall (Levitz and DiBenedetto, 1989). Additionally, the capsule increases the size and diameter of cryptococcal cells – as phagocytosis is known to be dependent on target geometric properties, this increases *Cryptococcus* resistance to immune cell activity

(Champion, Walker and Mitragotri, 2008). Even if a cryptococcal cell is phagocytosed, however, the capsule is still thought to protect *Cryptococcus* cells from the antimicrobial environment of the phagosome, with capsular components thought to neutralise reactive oxygen species (ROS) and act as 'ablative armour' (Zaragoza *et al.*, 2008). Evidence of this protective role has been observed in *in vivo* and *in vitro* studies of acapsular *Cryptococcus* strains (Feldmesser *et al.*, 2000).

Because of this critical role of the capsule for virulence, synthesis of the cryptococcal capsule has been extensively investigated. Capsular components are synthesised intracellularly and can be exported to the cell wall in microvesicles (Rodrigues *et al.*, 2008). Interestingly, however, some of microvesicles have been observed to not associate with the cell wall, but rather are instead released into the extracellular milieu. This is thought to be another mechanism of virulence mechanism, as the major capsular component, GXM, has been observed to directly suppress host immunity, with specific effects that include inhibiting neutrophil recruitment by reducing chemotactic receptor expression (Ellerbroek *et al.*, 2004), inhibiting T cell proliferation (Yauch, Lam and Levitz, 2006) and inducing apoptosis in certain leukocyte populations (Chiapello *et al.*, 2003). Additionally, GXM is also thought to inhibit the agglutinating action of surfactant protein (SP)-D (Van De Wetering *et al.*, 2004).

1.4.2.2 – Melanin

Another virulence factor signature of pathogenic *Cryptococcus* species is melanin, the pigment molecule found in humans. As in animals and human, melanin is thought to protect cryptococci from environmental UV radiation (Wang and Casadevall, 1994). As with comparative studies of capsule, investigations of non-melanising cryptococcal strains, such as those lacking laccase expression, have been observed to be less virulent *in vivo* (Salas *et al.*, 1996). It is hypothesised that the anionic nature of melanin make it an important ROS scavenging molecule. Therefore, when cryptococci are phagocytosed, this enables the intracellular survival of *Cryptococcus* within the phagolysosome of immune cells (Casadevall, Rosas and Nosanchuk, 2000). Similarly, melanin is also thought to bind and neutralise the antifungal drug amphotericin B, conferring a level of antifungal resistance to *Cryptococcus* cells (Ikeda *et al.*, 2003).

However, melanin in *Cryptococcus* is only synthesised if cultured in the presence of suitable precursor compounds. In the case of human infection, L-DOPA, an important precursor for the synthesis of dopamine, adrenaline and melanin, is hypothesised to be one such source (Eisenman *et al.*, 2007). The enzyme responsible for this conversion is laccase, which has been shown to be critical for this biochemical pathway.

1.4.2.3 – Urease

Cryptococcal urease catalyses the conversion of urea into CO_2 and ammonia. This has been revealed to be important for *Cryptococcus* growth at an acidic pH, as evidenced by culture of knockout strains – an important characteristic of virulent cryptococci (Fu *et al.*, 2018). The high expression of urease by pathogenic *Cryptococcus* means that urease was originally investigated as a diagnostic biomarker of cryptococcosis (Canteros *et al.*, 1996).

Unlike many other human pathogens, *Cryptococcus* species have yet to be identified to produce any directly cytotoxic products. However, cryptococcosis still results in damage to and remodelling of human tissue (Casadevall, Coelho and Alanio, 2018). Urease is hypothesised to potentially enable indirect damage to host tissue, specifically in the context of dissemination. In mouse models *in vivo*, Olszewski et al. observed that urease activity was required for cryptococcal cell 'clumping' in microvessels in the vicinity of the BBB (2004). However, it has yet to be determined whether this was the result of urease mediated ammonia production, and whether this either increased local adhesin expression on the endothelium, or directly damaged BBB tight junctions, enabling paracellular dissemination (Olszewski *et al.*, 2004). However, as this role of urease was not observed in an immunosuppressed rabbit *in vivo* model of cryptococcosis, this role of urease requires further investigation (Cox *et al.*, 2000).

1.4.2.4 – Phospholipase B

C. neoformans phospholipase B (Plb1) is one of the most significant virulence factors. Plb1 is an enzyme that can be cell wall associated or extracellular (Siafakas *et al.*, 2007). The cell wall associated form of Plb1 is thought to have a role in maintaining the integrity of the cell wall at higher temperatures, as evidenced by increased expression *in vitro* (Siafakas *et al.*, 2007). This suggests Plb1 has an important role in thermotolerance – a critical characteristic required for the virulence of any human pathogen.

Plb1 has also been shown to be indispensable for *C. neoformans* survival inside the macrophage phagosome following phagocytosis. Plb1 has optimal activity at an acidic pH – as is found in the phagosome of immune cells (Chen *et al.*, 2000). Functionally, Plb1 liberates arachidonic acid from membrane phospholipids – similar to the human enzyme PLA_2 (Burke and Dennis, 2009). In the absence of glucose, as is found in the low nutrient environment of the phagosome, *C. neoformans* can sustain itself for 24 hours on host arachidonic acid, suggesting a role of Plb1 in protecting fungal cells from nutrient starvation due to phagocytosis (Wright *et al.*, 2007). Additionally, this metabolism of host phospholipids has been associated with the lysis of phagosomal membranes in macrophages *in vitro* (De Leon-Rodriguez, Fu, *et al.*, 2018). These 'leaky' phagosomes

were associated with reduced antifungal activity and macrophage apoptosis. This all suggests a critical, multifaceted role of Plb1 for intracellular survival within macrophages.

Another feature of *C. neoformans* host-pathogen interactions in experimental models is that cryptococcosis results in a phenotypic shift in the host immune response to a less antimicrobial state – suggesting *C. neoformans* can manipulate the host immune system to be more favourable for fungal growth. Aside from utilising liberated arachidonic acid for nutrition, *C. neoformans* Plb1 also can convert arachidonic acid into an analogue of PGE_2, a human prostaglandin. This *C. neoformans* derived PGE_2 is then further dehydrogenated to 15-keto-PGE_2 (Evans *et al.*, 2015, 2019) – a biologically active signalling molecule able to mimic human PGE_2 and manipulate host immunity. Comparative studies of transgenic Plb1 knockout strains of *C. neoformans* have identified that not only is *C. neoformans* Plb1 critical for intracellular growth within macrophages in both mouse and zebrafish *in vivo* models of infection (Evans *et al.*, 2015, 2019), but also prevents the development of T helper 17 (Th17) immune responses by inhibiting IL-17 expression (Valdez *et al.*, 2012). This suggests that Plb1 has important roles intracellularly and extracellularly for enabling *C. neoformans* survival and growth.

1.4.2.5 – Anti-phagocytic protein 1

Anti-phagocytic protein 1 (App1) is secreted by *C. neoformans* and can be observed in infected patient serum (Luberto *et al.*, 2003). The most significant effect of App1 on the host immune response is reduced phagocytosis of *C. neoformans* by macrophages. This effect is mediated by App1 binding to and inhibiting complement receptor 3 (CR3) on macrophages (Stano *et al.*, 2009). It has been observed that App1 secretion is upregulated in low glucose conditions, as is found in the lungs, suggesting that this response may be important for colonising host tissue during initial infection (Williams and del Poeta, 2011). Evidence of the contribution of App1 to virulence can be observed *in vivo*, where mortality in mouse models was delayed in animals infected with App1 knockout strains of *C. neoformans*. This suggests that while increased phagocytosis of *C. neoformans* did not make the strain avirulent, but a smaller extracellular population potentially slowed fungal growth *in vivo* (Luberto *et al.*, 2003).

Interestingly, when App1 knockout *C. neoformans* was inoculated into mice lacking natural killer (NK) cells and T cells, animal mortality occurred significantly earlier than with wild-type *C. neoformans* infection (Luberto *et al.*, 2003). A potential explanation for this controversial result is that although App1 deficient *C. neoformans* cells were phagocytosed more by macrophages, the lack of lymphocyte derived cytokines, such as IFNγ, meant that macrophages were not stimulated sufficiently to control intracellular

cryptococci, meaning that intracellular cryptococci grow uncontrolled (Fa *et al.*, 2017). However, this hypothesis still needs to be tested experimentally.

1.4.2.6 – Calcineurin

As fungi are eukaryotic organisms, many proteins are expressed by both *Cryptococcus* and humans. When Mody *et al*. attempted to establish an immunocompromised mouse model of cryptococcosis by treating mice with the calcineurin inhibitor, Cyclysporin A, as calcineurin is a calcium sensitive phosphatase that in humans has an important role in T cell activation (Bueno *et al.*, 2002). However, mouse mortality was surprisingly reduced in treated animals (Mody, Toews and Lipscomb, 1988). It has been subsequently determined that *C. neoformans* also expresses calcineurin. However, in *C. neoformans* this protein is instead implicated in several stress responses (Odom *et al.*, 1997), including thermotolerance (Chen *et al.*, 2013), crz1-mediated control of cell wall integrity and sexual development (Chow *et al.*, 2017).

Clinically, many organ transplant recipients are on calcineurin inhibitors as part of an immunosuppressive therapeutic regimen (Rush, 2013). Subsequent clinical studies have revealed that disseminated cryptococcosis has a lower incidence in calcineurin treated patients, despite solid organ transplant being a risk factor for cryptococcosis (Singh *et al.*, 2007). This is important, as it means many patients at-risk for cryptococcosis can be better protected with the appropriate immunosuppressive regimen. Therefore, a better understanding of the exact contribution of calcineurin to virulence is important to better understand how these drugs may help to balance therapeutic immune suppression and protection against infection.

1.4.2.7 – Hog1

Hog1 is a stress activated mitogen activated protein kinase found in yeast, akin to mammalian p38 MAPK, first identified in the model yeast organism *Saccharomyces Cerevisiae* (Posas, Takekawa and Saito, 1998). Since its expression by *C. neoformans* has been confirmed, transcriptomic analysis has identified that 545 genes are affected by Hog1 expression (Ko *et al.*, 2009). Such a central role for cryptococcal virulence and homeostasis means that Hog1 has been shown to be critical for both brain and lung colonisation in mice. To date, Hog1 has been shown to regulate *C. neoformans* ergosterol production, cell growth and several stress responses. It's role in ergosterol synthesis is of particular note, as this is the target for amphotericin B (Figure 3), and therefore may affect antifungal resistance or treatment efficacy in cryptococcosis (Kamiński, 2014).

Additionally, other virulence factors have also been identified to be dependent on Hog1. ENA1 is a Na+/ATPase efflux pump that has been identified to be regulated by Hog1, and is important for cryptococcal growth at a low pH, with ENA1 knockouts being avirulent *in vivo* (Jung *et al.*, 2012). Additionally, Hog1 modules expression of sulfiredoxin and peroxiredoxin, two ROS scavenger molecules expressed by *C. neoformans* in response to leukocyte hydrogen peroxide, suggesting a role for intracellular survival also (Upadhya *et al.*, 2013).

1.4.2.8 – Titan Cells

Another signature mechanism of *Cryptococcus* virulence is the titan cell morphology. Observations in mouse models of cryptococcosis have observed that up to 20% of cryptococcal cells undergo a significant phenotypic shift in the lungs *in vivo* and massively increase their cell body diameter from 5-7μm to ≥10μm, with some cells even observed to be ~100μm in diameter (Okagaki *et al.*, 2010). Aside from greatly increased cell size, other features of these cells include polyploidy, a large vacuole, and a thicker cell wall and capsule. This phenotypic shift greatly affects the host-pathogen interactions of *C. neoformans*, as titan cells are incredibly resistant to phagocytosis and host-derived antimicrobial ROS. In mouse models of infection, *Cryptococcus* cells of this phenotype are more virulent, although interestingly, at the cost of reduced dissemination to the CNS. Several cryptococcal regulators of the titan cell phenotype have been identified, including Gpr1, pkr1 and Rim101 (Hommel *et al.*, 2018), but exogenous factors can influence this phenotype too, such as bacterial muramyl dipeptide (Dambuza *et al.*, 2018).

1.5 – Experimental models of cryptococcosis

As evidenced during this chapter, there is a wealth of data currently available regarding the immune response during cryptococcosis. However, a multitude of different experimental approaches are used across these studies, with the choice of model able to significantly influence results important for the translatability of findings. Below, the models utilised in pre-clinical cryptococcosis research are described, along with the caveats that should be taken into account when interpreting studies of this type regarding host-pathogen interactions in cryptococcosis.

1.5.1 – *In vitro* models

One of the most fundamental approaches to study host-pathogen interactions is by assaying immune cells and *Cryptococcus* in isolated culture. This removes many of the confounding factors that affect host-pathogen interactions, enabling the contribution of specific pathways and proteins to be assessed. However, as this is not representative of ‘real-world’ biological systems, these studies often fail to recapitulate everything that

exists about phenomena *in vivo*. For example, *in vitro* studies often only utilise two dimensional cell culture, despite the three dimensions of *in vivo* systems. Additionally, tissues *in vivo* contain multiple cell types, which means observations in many monoculture systems lack the influence of these other cell types that may significantly affect results, and therefore limit translation if not supported by *in vivo* data.

It is also important to note that the cell lines used vary from study to study, and can have significantly different features, even if the same cell type. As the focus of my research is on the role of macrophages and their contribution to protective host immunity in cryptococcosis, I will detail the different *in vitro* models often used to model host-pathogen interactions, and the advantages and disadvantages associated with each.

1.5.1.1 – J774 cells

J774 cells are one of the most popular immortal cell lines used to model macrophage-*Cryptococcus* interactions *in vitro*. These cells were originally derived from a BALB/c mouse sarcoma (Ralph and Nakoinz, 1975) and perform many of the same functions as human macrophages. These include the phagocytosis of pathogens and expression of both C3 and Fc receptors, making them particularly suitable for studying the phagocytosis response of *Cryptococcus* (Mukherjee, Feldmesser and Casadevall, 1996). Although J774 cells can be polarised with cytokine treatment, it is important to note that J774 cells are inherently proinflammatory, evidenced by detectable constitutive levels of lysozyme and IL-1β production at baseline (Hirano *et al.*, 2017). This may limit the suitability of J774 cells to study macrophage polarisation or cytokine production in response to *Cryptococcus* infection. This may also mean that unstimulated J774 cells have a higher basal level of fungicidal activity compared to unstimulated primary cells. Finally, it is also important to remember that these cells are cancer derived. While this makes these cells easy to culture, it does mean that these cells have changed biology compared to wild-type primary macrophages, and so their behaviour may be significantly different than those *in vivo*.

1.5.1.2 – THP-1 cells

THP-1 cells are another cancer-derived immortal cell line, although originally isolated from a human acute monocytic leukaemia patient (Tsuchiya *et al.*, 1980). These cells serve as a self-replicating model of human macrophages. More specifically, THP-1s are a useful model of MDMs – THP-1 cells ordinarily exist as monocyte-like cells until differentiated into a macrophage-like phenotype. Once differentiated, resulting macrophages can be polarised through cytokine stimulation, using either IFNγ and LPS (proinflammatory) or IL-4, IL-13 and IL-10 (anti-inflammatory; Baxter *et al.*, 2020). THP-

1 cells also express CR3 and Fc receptors, making them a suitable model to study the effect of immunologically relevant opsonins (Tsuchiya *et al.*, 1980).

It is also possible to differentiate THP-1 cells into monocyte-derived DCs with the appropriate cytokine signals, meaning the THP-1 cell line is a versatile *in vitro* model that enables the study of host-pathogen interactions for multiple cell types (Berges *et al.*, 2005). Despite these benefits, it is also important to note that THP-1 cells constitutively express IL-1β, similar to J774 cells, and so may have higher baseline levels of antifungal activity compared to primary cells (Kahlenberg and Dubyak, 2004). Additionally, there is also the potential for significantly different biology because these cells are cancer derived.

1.5.1.3 – Primary alveolar macrophages

Because of the inherently low replication rate of AMs, there is, at the time of writing, no widely utilised immortal AM cell line (Maus *et al.*, 2006). This means that to study these cells, primary AMs have to be taken from live organisms of the species of interest, such as mice or humans, by the process of broncheoalveolar lavage (BAL). Briefly, BAL involves flushing the lungs of an animal with fluid and drawing it back out. The recovered BAL fluid will contain cells that were present in the airways at the time of sampling, which in healthy individuals, should be primarily AMs (Hussell and Bell, 2014). However, the relatively long lifespan of AMs does allow for relatively term studies compared to other cells such as neutrophils, if cultured appropriately. However, being primary cells, the phenotype of cells is donor dependent, making comparisons between studies difficult as cells will likely differ between and within studies. Additionally, the BAL process is very invasive and so is difficult to do with humans, meaning the majority of AM studies are done using mouse cells.

1.5.1.4 – Peripheral blood mononuclear cells

The term PBMC describes the subset of leukocytes in blood samples that have a rounded nucleus. This proportion includes monocytes, NK cells, T cells and B cells (Autissier *et al.*, 2010). These different cells can then be further purified by either FACS or selective culture (Dockrell *et al.*, 2001) – although the entire PBMC population can be assayed, allowing for the interactions between innate and adaptive cells (antigen presentation) to be interrogated in the context of *Cryptococcus* infection *in vitro* (Pline, 2019). However, analysis of these assays is difficult in the absence of specific markers for each cell type present, due to the number of cells present in these systems. Although due to their size, fluorescent tags such as GFP can affect protein function, significantly affecting host-pathogen interactions in this model. Additionally, as with primary alveolar macrophages, cells are donor specific, which makes comparisons between studies

difficult. Fortunately, however, blood sampling is simpler than the BAL process, and so studies on human PBMCs are more routinely conducted.

1.5.1.5 – 3D *in vitro* models

As all real world biology does not occur in 2D, there are also a number of 3D tissue culture systems that have been developed to allow for more translational research without the need for expensive *in vivo* studies.

The simplest example of this is to study phenomena in tissues removed from animals, such as in organ bath experiments (Collins *et al.*, 1996). In the case of modelling pulmonary infection and immunity, precision cut lung slices also offer an ability to study the immune response in the context of the live lung (Sanderson, 2011). This model – whereby live lung tissue is cut thin enough to allow for optical transparency and cellular responses to be studied in the context of lung tissue. However, this approach requires the use of animals to source tissues and there are more likely to be individual variation between studies. Other 3D models include organ-on-a-chip and organoid models. Organ-on-a-chip systems are microfluidics device in which the 3D microenvironment of tissue is captured within a small area in combination with traditional cell culture system. This small size and controllable environment makes this approach highly appropriate for high throughput screening (Q. Wu *et al.*, 2020). Alternatively, organoids utilise stem cells, co culture and bioengineering approaches to generate tissue similar in structure and function to that being modelled (Kim, Koo and Knoblich, 2020). Both of these approaches, while more expensive, do provide models that have the capacity to better represent the tissue system of interest. However, all of these approaches do still involve studying a tissue in isolation, limiting the complexity of organisms *in vivo.* Additionally, these approaches are all relatively more expensive than more simple 2D cell culture, limiting their uptake.

In the context of cryptococcosis, despite the power of these systems, they have yet to be properly utilised to study all aspects of this infection.

1.5.2 – Invertebrate models

Although *in vitro* models enable concepts to be studied in isolation, studies using this approach have limited translation due to their relative simplicity compared to *in vivo* models. These limitations include the lack of three dimensional structure that is found in tissues and the interactions of multiple cell types and tissues. Therefore, *in vivo* modelling is required to confirm the biological significance of any *in vitro* findings.

However, as with cell culture, the selection of the most appropriate model species for *in vivo* studies is critical for translatable results. Due to the ethical considerations of animal research, the animal model chosen should be done using the species with the lowest neuro-sensitivity possible, without sacrificing model relevance. Invertebrate models (excluding cephalopods) are important alternative animal models that when used appropriately reduce the number of regulated procedures that protected animals are subjected to (Kendall *et al.*, 2018). In the field of cryptococcosis, there are several examples of invertebrate model species that have been notably used to model cryptococcosis host-pathogen interactions *in vivo*.

1.5.2.1 – *Dictyostelium discoideum*

Dictyostelium discoideum are among the most basic *in vivo* model systems used to study cryptococcosis. These single cell organisms are social amoebae, found naturally in the soil – similar to natural predators of environmental *Cryptococcus* (Watkins *et al.*, 2018). When infected with *Cryptococcus*, *Dictyostelium discoideum* are a model of macrophages, able to phagocytose cryptococci and making them a model to study host-pathogen interactions. Additionally, the *Dictyostelium discoideum* genome is fully sequenced and have simple husbandry requirements, which makes them ideal for high-throughput screening methods to identify host or cryptococcal factors that are significant in phagocytosis or intracellular survival (Steenbergen *et al.*, 2003). They are also appropriate when studying the evolution of cryptococcal virulence in the environment. However, their relative simplicity compared to mammals and humans means they are not appropriate for modelling systemic cryptococcosis, although the virulence of strains in mammalian *in vivo* models do correlate with their virulence in *Dictyostelium discoideum* models, but only when differences in virulence are related to phagocytosis and evasion of host immunity (Steenbergen *et al.*, 2003).

1.5.2.2 – *Acanthamoeba castellanii*

Similar to *Dictyostelium discoideum*, *Acanthamoeba castellanii* are single celled social amoebae. However, this species is observed in the environment to be a natural predator of *Cryptococcus* and attempting to phagocytose *Cryptococcus* when co-cultured (Bunting, Neilson and Bulmer, 1979; Ruiz, Neilson and Bulmer, 1982). This natural predator-prey relationship makes *Acanthamoeba castellanii* a powerful *in vivo* system to model the evolution of *Cryptococcus* virulence (Steenbergen, Shuman and Casadevall, 2001). Additionally, they can act as a model of macrophages, with host-pathogen interactions with *Cryptococcus* including phagocytosis, intracellular replication and non-lytic exocytosis all observed when the two are cultured together (Chrisman, Alvarez and Casadevall, 2010). However, these organisms are less widely used than other

invertebrate models, and so are more poorly characterised. However, the biological relevance of *Acanthamoeba castellanii* to *Cryptococcus* means that uptake of this model should increase, particularly as a model species to study the evolution of cryptococcal virulence within its environmental niche.

1.5.2.3 – *Caenorhabditis elegans*

These nematodes are a species used to model many areas of biology, because of their simple husbandry, non-protected status and well characterised genetics (Apfeld and Alper, 2018). In the case of cryptococcosis, this species has only been infected via inoculating the bacteria on which *Caenorhabditis elegans* feeds with *Cryptococcus*. However, this method greatly limits dose accuracy and reliability as it is dependent on how much is ingested by individual nematodes. This also localises infection to the digestive tract, where it does not disseminate (Mylonakis *et al.*, 2002). Coupled with *Caenorhabditis elegans* lack of professional phagocytes, this means that there are limited instances where this model is suitable (Sabiiti, May and Pursall, 2012).

Although *Caenorhabditis elegans* are not suitable for modelling host-pathogen interactions or dissemination, the *in vivo* virulence of various *C. neoformans* strains in *Caenorhabditis elegans* has been observed to correlate with virulence in mammalian models (Lee *et al.*, 2010). This may mean this species is a suitable *in vivo* model for high throughput screens to identify *Cryptococcus* mutants with significant changed virulence. However, it is important to note that the capsule of *C. neoformans* is not critical for virulence in *Caenorhabditis elegans* (Mylonakis *et al.*, 2002). This is likely due to the absence of phagocytosis in this species, but does indicate that there are many limitations to using *Caenorhabditis elegans* to model human infection in *Caenorhabditis elegans*.

1.5.2.4 – *Drosophila melanogaster*

Also known as fruit flies, *Drosophila melanogaster* are another alternative animal model widely used in many areas of pre-clinical research (Jennings, 2011). As with all invertebrate models, fruit flies have relatively easy husbandry, short gestation periods and a well characterised genome. Also, unlike the other invertebrate models described up until this point (see 1.5.2.1-3), *Drosophila melanogaster* share multiple complex anatomical features with mammals, such as the eye.

In terms of routes of *Cryptococcus* infection in *Drosophila melanogaster*, infection of food, similar to *Caenorhabditis elegans*, has been trialled, as has systemic injection (Apidianakis *et al.*, 2004; Thompson *et al.*, 2014) - both of which are inconsistent with proposed natural routes of human infection. Despite this, when the virulence of various strains of *C. neoformans* were screened in *Drosophila melanogaster* via digestive tract

infection, it was found that the virulence of strains in *Drosophila melanogaster* correlated with their virulence in mouse models (Apidianakis *et al.*, 2004).

Additionally, the primary immune cells of *Drosophila melanogaster*, haemocytes, share many features with mammalian macrophages, potentially making *Drosophila melanogaster* a suitable model to study host-pathogen interactions (Roddie *et al.*, 2019). However, this has yet to be trialled.

1.5.2.5 – *Galleria mellonella*

The larvae of *Galleria mellonella* (greater wax moths), were proposed as a model organism to study cryptococcosis in 2005 (Mylonakis *et al.*, 2005). Compared to other invertebrates, *Galleria mellonella* are relatively large compared to other invertebrates (1.5-2.5cm in length), making working with them relatively easy. These organisms can be inoculated topically or via injection – in the case of injection, haemocol injection results in no skin damage or scar formation, minimising wound responses that may interfere with immune responses to inoculated *Cryptococcus* (Kavanagh and Fallon, 2010). Immunologically, *Galleria mellonella* are similar to *Drosophila melanogaster*, with macrophage-like haemocytes. This means that hypothetically *Galleria mallonella* can also be used to model macrophage-pathogen interactions *in vivo*.

However, when the virulence of *C. neoformans* strains were screened in *Galleria mallonella,* the virulence of these strains did not correlate with virulence in mammals – all examined strains of *C neoformans* in this study caused 100% mortality in larvae (Mylonakis *et al.*, 2005). Additionally, there was no correlation between the survival times of infected *Galleria mallonella* and infected mice with various strains (Bouklas *et al.*, 2015). This suggests that while this model may be suitable for studying host-pathogen interactions at a cellular level, there is likely little to no utility in using this model to study systemic cryptococcosis.

1.5.3 – Vertebrate models

Despite global efforts to find alternatives to animal testing, there are still many instances where appropriate alternatives that enable high levels of translation do not exist. In particular, animal models are still required to model multisystem diseases, the complexity of the adaptive immune system or tissue specific responses. When appropriately designed, *in vivo* findings can support the development of new therapeutics or help refine existing treatment guidelines for patients. In the case of cryptococcosis, the disseminating nature of infections and its association with the adaptive immune system means that vertebrate models are required in order for results to have relevance to human infection.

However, there are a variety of vertebrate species that can and have been used to model cryptococcosis *in vivo*, which can complicate study design and interpretation. Below, the major vertebrate models used to model cryptococcosis are described, with references to advantages and disadvantages associated with their use.

1.5.3.1 – Mouse (*Mus musculus*)

Mice are the archetypal pre-clinical *in vivo* model species and are the species of choice for the majority of *in vivo* cryptococcosis research. Their use throughout history means laboratory mice are well characterised, both genomically and phenotypically (Waterston *et al.*, 2002). Also, compared to other mammalian models mice are relatively cheap with simple husbandry requirements, enabling most groups to conduct large scale studies using these animals. The anatomy shared between mice and humans means that all of the major tissues affected in cryptococcosis (lungs, CNS) are compatible with model *Cryptococcus* infection. Additionally, the pathology of pulmonary cryptococcosis mouse models mirrors what is known about the human clinical situation, from pulmonary infection (Zaragoza *et al.*, 2007), to dissemination out of the lungs (Vanherp *et al.*, 2019) and also cryptococcal meningitis (M. Zhang *et al.*, 2016) – allowing for all these elements of infection to be modelled in mice. Finally, the mouse immune system consists of innate and adaptive responses, with all the major cell types present, including resident macrophage populations (Haley, 2003) – making mice suitable to study host-pathogen interactions *in vivo*.

However, when interpreting and designing mouse *in vivo* studies, it is important to appreciate that the term 'mouse' is non-specific – encompassing multiple animal 'strains', each with significant differences in their biology, including different lung architecture, differences in immunological pathways and differential susceptibilities to cryptococcosis (Zaragoza *et al.*, 2007). The inbred laboratory mouse strains most commonly used to study cryptococcosis are summarised in Table 1. The second important consideration when using mice is which route of infection to use. Many routes of infection can be used in mice, and each one greatly generates an infection with a unique progression, phenotype and time course. Therefore, the route used should be chosen depending on the hypothesis being tested (Zaragoza *et al.*, 2007). The routes of infection used to generate experimental models of cryptococcosis, and their associated infection characteristics, are summarised in Table 2. Although this many potential combinations of variables is complex, the widespread use of these models means understanding them is critical in order to appropriately design and interpret *in vivo* cryptococcosis models. A thorough understanding of mouse cryptococcosis models also can inform study design to refine and reduce *in vivo* studies, minimising the number of animals subjected to regulated procedures.

It also important to acknowledge significant limitations of mice as a model of human cryptococcosis. Firstly, the architecture of human and mouse lungs are different – both human lungs are multilobed, one with two lobes, one with three, while mice only have one multilobed lung, while the other does not have separate lobular components (Pan, Deutsch and Wert, 2019). Furthermore, human airways also feature additional tertiary bronchi that are absent in mice. These differences in lung structure may affect the distribution of an inoculum, resident leukocytes or affect the recruitment of circulating leukocytes. There are also significant differences in the immunology of mice compared to humans – summarised in Table 3 (Mestas and Hughes, 2004). Finally, *C. neoformans* infection in humans is associated with immunocompromise, resulting in sub-clinical infection in immunocompetent individuals. However, infection of mice, immunocompetent or not, results in a universally fatal infection, suggesting important model differences exist when examining host factors that impact host susceptibility to cryptococcosis (Zaragoza *et al.*, 2007).

Mouse strain	Appearance	Features	*C. neoformans* strain susceptibility	References
C57BL/6	Black	Reduced P_2X_7 signalling No expression of CXCL11 No expression of Ly49 Reduced Cathepsin E Impaired Nramp1 Th1 dominant immune responses No expression of IgG2A	KN99α WT – Resistant H99α – Resistant 52D – Susceptible	(Adriouch *et al.*, 2002), (Castro-Lopez *et al.*, 2018), (Mayer, Lilly and Duran-Reynals, 1980), (Tulone *et al.*, 2007), (Swihart *et al.*, 1995), (Nielsen *et al.*, 2005), (Carroll *et al.*, 2012), (Martin and Lew, 1998), (Caron *et al.*, 2002)
Balb/c	White	Impaired Nramp1 Th2 dominant immune responses	KN99α WT – Susceptible H99α – Susceptible 52D – Resistant	(Mattner *et al.*, 1996), (Nielsen *et al.*, 2005), (Caron *et al.*, 2002), (Carroll *et al.*, 2012)
A/JCR	White	No expression of C5 Absence of IL-3 receptor No expression of Naip5	KN99α WT – Susceptible H99α – Susceptible 52D – Resistant	(Gervais, Desforges and Skamene, 1989), (Lindemann and Mertelsmann, 1995), (Kang *et al.*, 2010), (Nielsen *et al.*, 2005), (Carroll *et al.*, 2012)
C3H/HeJ	Brown	Reduced TLR4 response to LPS Impaired Nramp1	52D – Susceptible	(Poltorak *et al.*, 1998), (Nowicki *et al.*, 1999), (O'Brien, Rosenstreich and Taylor, 1980), (Carroll *et al.*, 2012)

Table 1: Summary of differences in immunology between different inbred laboratory mouse strains

Route of infection	Protocol description	Pathology	Purpose	Examples
Intranasal (i.n.)	Light anaesthetic (gaseous) Inocula pipetted onto the naves and breathed in by the animal Significant portion is swallowed	Localised lung infection Rapid dissemination to the CNS Dissemination to other tissues, such as spleen and liver	Simple method Resulting infection follows human progression Can be used to study dissemination out of the lungs or into the CNS	(Coelho *et al.*, 2019)
Intratracheal (i.t.)	Deep anaesthesia Trachea exposed surgically Inocula pipetted directly into the lungs via small incision	Localised lung infection Dissemination to other tissues, such as CNS, spleen and liver	Highly efficient Resulting infection follows human progression Can be used to study dissemination out of the lungs or into the CNS	(Zaragoza *et al.*, 2007)
Intravenous (i.v.)	Animal restrained Inoculum is injected into the tail vein Systemic distribution of inocula	Rapid systemic dissemination	Rapidly dissemination Systemic infection Study vascular infection	(Aguirre, Gibson and Johnson, 1998)
Intraperitoneal (i.p.)	Animal restrained Inoculum is injected into the peritoneal cavity Localised infection	Localised peritoneal infection Eventual systemic dissemination	Simplest method Disseminating infection that does not originate in the lungs	(Bava, Iovannitti and Negroni, 1989)
Intracranial (i.c.)	Animal anaesthetised Inoculum injected into the CNS through the skull Localised infection	Localised CNS infection Rapid mortality	Specifically for rapidly generating a CNS infection only	(Mukherjee *et al.*, 1993)

Table 2: Summary of different routes of infection utilised to study cryptococcosis in mice

Zebrafish

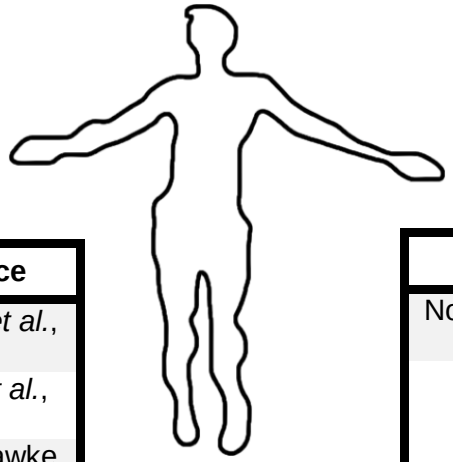

Mouse

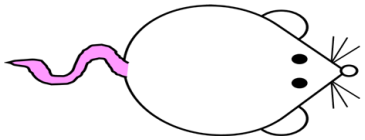

Difference	Reference
TLR4 does not respond to LPS	(Sepulcre *et al.*, 2009)
No resident macrophages have been described	(Martins *et al.*, 2019)
Significant differences in NK receptors	(Litman, Hawke and Yoder, 2001)
No adaptive immunity in zebrafish embryos until 4-6 weeks after hatching	(Lam *et al.*, 2004)
Only produce IgM and IgD classes of antibodies	(Wilson *et al.*, 1992)
No lymph nodes	(Trede *et al.*, 2004)
Different eosinophil morphology	(Crowhurst, Layton and Lieschke, 2002)
Haematopoiesis occurs in the kidney, not bone marrow	(Davidson and Zon, 2004)
28^{o}C body temperature, thermotolerance is absent	(Lam *et al.*, 2004)

Difference	Reference
No IL-8 expression, alternatives are KC, MIP-2, GCP-2	(Fan *et al.*, 2007)
Higher NO production	(Schneemann and Schoedon, 2002)
No CD89 (IgA receptor) expression	(Monteiro and Van De Winkel, 2003)
No FcγRIIA or FcγRIIA expression	(Daëron, 1997)
IL-13 does not induce IgE	(Lai and Mosmann, 1999)
IFNα does not induce Th1 phenotype in Th cells	(Farrar and Schreiber, 1993)
T cells do not express Kv1.3 K^{+} channels	(Koo *et al.*, 1997)
IL-10 not produced by Th1 cells	(Del Prete *et al.*, 1993)
Activated T cells do not express MHC class II	(Denton *et al.*, 1999)

Table 3: Description of immunological differences between humans and model species

1.5.3.2 – Zebrafish (*Danio rerio*)

Zebrafish have become an increasingly popular alternative vertebrate *in vivo* model species over the past decade. Part of the minnow family, zebrafish are typically found in tropical regions, in freshwater streams in South East Asia (Teame *et al.*, 2019). Compared to mice, zebrafish offer many attractive benefits to researchers compared to mice – smaller size, a shorter gestation period and high fecundity. This means that highly powered large scale *in vivo* studies can be generated relatively rapidly. Additionally, zebrafish are optically transparent which enables intravital imaging – a modality which is extremely difficult and expensive to do in mice (Keller, 2013). Furthermore, adult zebrafish (~three months old) possess both innate and adaptive leukocytes (Trede *et al.*, 2004). However, as the use of adult zebrafish is regulated, this means that the majority of *in vivo* zebrafish cryptococcosis studies utilise zebrafish embryos younger than 5.2 days post fertilisation, as in the UK can be used for research purposes without regulation (Teame *et al.*, 2019). Because zebrafish embryos develop outside of the mother, their use is relatively simple.

Zebrafish embryos can be infected with *Cryptococcus* in different ways to cause either a localised or infection that disseminates to the CNS, making them a suitable model of both early and late stage infections (Davis *et al.*, 2016). Additionally, these embryos possess macrophages and neutrophils which are observed to be functionally equivalent to those in humans, observed to undergo chemotaxis, phagocytosis, respiratory burst and antigen presentation (Gomes and Mostowy, 2020). However, prior to 5.2 days post fertilisation, the absence of adaptive cells does limit the contexts in which embryonic models of cryptococcosis are appropriate (Lam *et al.*, 2004). It has been suggested that the absence of adaptive cells in the zebrafish embryo makes them a suitable model of HIV associated cryptococcosis. However, it is important to note that HIV does not simply result in a loss of adaptive cells, but rather results in simultaneous immunosuppression and inflammation (Zicari *et al.*, 2019).

Similar to mice, the phenotype of zebrafish embryo infections is highly dependent on the route of inoculation, although the majority of infections are done via micro-injection with a glass needle. Inoculation into general circulation results in a systemic infection with brain involvement (Bojarczuk *et al.*, 2016). Alternatively, injection of the embryonic yolk sac results in a localised infection that has the potential to disseminate systemically. However, the yolk sac is a development specific structure that provides nutrition to the zebrafish embryo only up to 4dpf, limiting the relevance of findings generated by studying cryptococcal infection of this tissue (Kimmel *et al.*, 1995; Rosowski *et al.*, 2018). Injection into the zebrafish embryo hindbrain is also possible where rapidly generating cryptococcal meningitis is a benefit (Davis *et al.*, 2016).

There are several other important features of zebrafish embryo *Cryptococcus* infections that are significantly different from human infection. The biggest difference is that zebrafish lack lungs, meaning that the initial pulmonary infection cannot be suitably modelled. The gills, which are the zebrafish site of oxygenation, consist of a series of epithelial layers that enable oxygenation of blood via the counter current flow of water. However, these structures are not present until two weeks post fertilisation, so can only be studied in adult zebrafish (Kimmel *et al.*, 1995). Even then, the immunology of the gills significantly differs from that of the mammalian lungs. As described previously (see 1.4.2.2.2, see 1.4.2.2.4), the cell types present in the lungs prior to infection are AMs and DCs. Not only are these resident populations not observed in zebrafish, the gills of adult zebrafish are observed to primarily contain lymphocytes prior to infection, meaning that initial immune responses would be different to what happens in humans (Wan *et al.*, 2017). Other zebrafish tissues have been proposed as models of the mammalian lung – the swim bladder is a specialised air cavity that inflates and deflates to change the depth at which fish swim, and appears at three days post fertilisation. This tissue consists of a single layer of epithelial cells, similar to the lung (Y. Zhang *et al.*, 2016). However, these structures lack the specialised alveolar epithelium, complex 3D structure of the lungs and presence of lung surfactant, meaning this too is not a suitable model.

Another issue with zebrafish cryptococcosis models is that at the time of writing, no resident macrophage populations have been identified. Currently, all embryonic macrophages are observed to be generated by erythropoiesis, albeit in different tissues (Lin, Wen and Xu, 2019). The lack of these cells greatly affects the immunology of host-pathogen interactions, and is a significant difference compared to human infection. Additional differences in zebrafish immunology compared to humans are also summarised in Table 3. Finally, in the case of infection of the zebrafish embryo, it is important to note the developing nature of the organisms. Because the physiology and immunology of the embryo changes significantly during the first 5 days of development, from hour to hour, there are likely major focal points of apoptosis as tissues are remodelled that may significantly affect immune responses (Popgeorgiev *et al.*, 2018). Additionally, the rapid changes in biology may affect result variability when multiple embryos are inoculated, where there may be significant differences in the stage of development the first and last embryo inoculated are at.

1.5.3.3 – Rat (*Rattus rattus*)

The rat is the first mammalian species described here reported to acquire cryptococcosis in nature (Scrimgeour and Purohit, 1984). Compared to mice, rats are larger animals which enables more complex experimental manipulations – including intubation, repeated venous sampling and CSF sampling (Krockenberger *et al.*, 2010). Routes of

inoculation used in rats are similar to those used in mice, although intratracheal instillation to generate a respiratory infection with the potential to disseminate is the most common (Krockenberger *et al.*, 2010). Additionally, rat infections can have different outcomes, as established with *C. gattii* inoculation, including resolving, non-resolving and latent infection – the latter of which is a pathology seldom studied despite its clinical significance (Goldman *et al.*, 2000; Krockenberger *et al.*, 2010).

At the time of writing, granulomas in mice are only reported when animals are inoculated with specific transgenic strains of *C. neoformans* and under specific conditions (Farnoud *et al.*, 2015). As granuloma formation is thought to be associated with host protection, this greatly limits the utility of mice as an *in vivo* model of cryptococcosis (Ristow and Davis, 2021). These structures have been observed to form in response to experimental *Cryptococcus* infection, these potentially critical structures have yet to be studied in detail using this model (Krockenberger *et al.*, 2010). This makes rats well poised as a model species to study these potentially critical phenomena in further detail.

Overall, despite slightly more complex husbandry, rats are an important model species for cryptococcosis research that should be utilised more to confirm observations in mouse and zebrafish models of cryptococcosis.

1.5.3.4 – Guinea pig (*Cavia porcellus*)

Guinea pigs are another large rodent model, meaning their use as a model species is associated with many of the same advantages and disadvantages as rats. Historically, guinea pigs have been an important for modelling respiratory disease phenomena *in vivo*, offering researchers a balance between relatively simple husbandry and large mammals, with pulmonary biology that is observed to be highly representative of what occurs in humans (Adner *et al.*, 2020).

In the case of cryptococcosis, guinea pigs have to been reported to have particular utility for *in vivo* pharmacokinetic/pharmacodynamic modelling of antifungal therapeutics – size matched clinical doses of fluconazole, fluocytosine and amphotericin B when administered to guinea pigs with disseminated cryptococcosis found these drugs offered similar levels of protection observed in humans (Kirkpatrick *et al.*, 2007). This suggests that guinea pigs would be an important pre-clinical model for any potential immunotherapeutic, particularly with regard to establishing pharmacodynamic and pharmacokinetic parameters for first time in human trials.

Despite this, it is worth noting that compared to mice and rats, guinea pigs do have more complex husbandry requirements, particularly with regard to the amount of space animals require, makes guinea pig models a non-viable option for many groups

(Anderson, 1987). Additionally, there are fewer genetic and immunological tools available to use with these species which may greatly limit study design. However, cryptococcosis modelling in these animals should still have a role informing pre-clinical studies of new cryptococcosis therapeutics.

1.5.3.5 – Rabbit (*Oryctolagus cuniculus*)

In 2003 rabbits were proposed to be the 'gold standard' species in which to study cryptococcal meningitis *in vivo* (Steen *et al.*, 2003). This was due to their large size, allowing for repeated CSF sampling, enabling the design of *in vivo* experiments that study the development of cryptococcal meningitis. Additionally, rabbits are inherently resistant to cryptococcosis – immunocompetent rabbits intratracheally inoculated with *C. neoformans* experience a localised pulmonary infection that is contained by the host immune system (Perfect, Lang and Durack, 1980). However, pre-treating rabbits with corticosteroids – an immunosuppressant medication that is associated with cryptococcosis in humans – results in a *Cryptococcus* infection that disseminates to the CNS and causes animal mortality. This opportunistic nature of cryptococcosis in rabbits and human patients indicates that rabbits are a powerful *in vivo* model that may enable predictive and translatable research. However, as with guinea pigs, the use of rabbits in research is associated with high costs and complex husbandry, meaning these models are available only to a few groups. However, candidate therapies for clinical trials should first be trialled in these animals to confirm efficacy in a model with a high level of translation.

1.5.3.6 – Non-human primates

Non-human primates are the closest relatives of humans in the animal kingdom, and therefore results of *in vivo* studies that utilise these animals should be of the greatest relevance to human health. There is only one recent cryptococcosis study that used non-human primates (*Macaca fascicularis*) – a comparison of whole genome RNA-Seq data from mice and non-human primates following infection with *C. neoformans* at 7dpi (Li *et al.*, 2019). Importantly, this study revealed that only ~20% of the examined gene expression patterns overlapped between the two species, serving as a remind of how different responses in mice can be from those of non-human primates and humans.

However, non-human primates are not a suitable *in vivo* model species to study cryptococcosis. Because of their high neuro-sensitivity and similarity to humans, use of non-human primates is extremely controversial and their use is restricted to cases where no alternative exists. In the case of cryptococcosis, other mammalian species, such as rats, guinea pigs and rabbits, offer *in vivo* models of cryptococcosis with a high level of translatability to human infection, with no clear evidence that non-human primates would

offer any significant benefit over these models. Ethics aside, the extremely complex husbandry associated with their use makes nigh-impossible for most groups to utilise.

1.6 – Gap in knowledge

The cytokine IFNγ is well described to be associated with host immune responses to infectious disease. In the case of cryptococcosis, IFNγ has a well described protective role, as shown in both experimental models and even a successful clinical trial where it significantly improved fungal clearance when administered as an adjunctive therapy for HIV/AIDS associated cryptococcal meningitis. Despite this clinical potential, however, a biological mechanism that describes how IFNγ may enhance fungal clearance in cryptococcosis patients has yet to be described (Jarvis *et al.*, 2012). Previous work has associated IFNγ with Th1 skewed immune responses *in vivo* and enhanced macrophage control of *C. neoformans* (Hoag *et al.*, 1997; Chen *et al.*, 2005; Voelz, Lammas and May, 2009). Macrophages are involved at at all stages of cryptococcosis, from the initial immune responses to inhaled *Cryptococcus* in the lung through to their presence in potentially protective granulomas. Therefore, enhancing the activity of these cells with IFNγ treatment would explain the significant benefit seen in HIV positive cryptococcal meningitis patients who received adjunctive IFNγ therapy (Mansour *et al.*, 2014; Bojarczuk *et al.*, 2016).

To better understand the *in vivo* action of IFNγ on macrophages during early cryptococcosis, Kamuyango utilised a low inocula zebrafish embryo model of localised *C. neoformans* infection to examine how IFNγ treatment affected macrophage antifungal activity (Kamuyango, 2017). Even in the absence of adaptive immune cells, IFNγ treatment at the time of infection enhanced the clearance of cryptococci by the innate immune response in zebrafish embryos. This clearance was observed to be dependent on macrophages, with IFNγ treatment significantly reducing the intracellular replication of *C. neoformans* within zebrafish macrophages. Although an exact mechanism by which IFNγ treatment enhanced macrophage antifungal activity was not proposed, Kamuyango did observe that IFNγ treatment significantly increased zebrafish IL-1β expression within 12 hours of infection with *C. neoformans*, as observed using GFP tagged IL-1β transgenic zebrafish embryos.

IL-1β expression is associated with cryptococcosis *in vitro* (Retini *et al.*, 1996; Chen *et al.*, 2015). Additionally, the expression of IFNγ and IL-1β are known to be closely associated in the context of macrophage signalling, with IFNγ stimulation (and a concurrent TLR4 signal) known to stimulate macrophages to produce both IL-1β and TNFα by macrophages (Arango Duque and Descoteaux, 2014). IL-1β is also known to increase *in vitro* macrophage expression of iNOS – an important enzyme for the

production of NO, an antimicrobial mediator with antifungal activity (Carnovale *et al.*, 2001). Additionally, IL-1β is reported to increase the expression of IRF7, a IFNγ signalling protein, potentially indicating the presence of a positive feedback loop between IL-1β and IFNγ (Corr *et al.*, 2011). Furthermore, when the contribution of the IL-1β receptor was investigated, infecting IL-1R$^{-/-}$ mice with a relatively less virulent strain of *C. neoformans* (52D) resulted in reduced animal survival and increased fungal burdens compared to wild-type controls (Shourian *et al.*, 2018). However, when the same mice were inoculated with hypervirulent *C. neoformans* (H99α WT), the significant role of IL-1R was lost. Instead, IL-18, an IL-1 family cytokine, was instead found to be indispensable for survival (Wang *et al.*, 2011). However, as IL-18 is primarily monocyte derived, its significance in initial host-pathogen interactions is unlikely (Lee *et al.*, 2017). However, at the time of writing, the only clinical evidence of a role for IL-1β in cryptococcosis is a single case report of a 21-year-old female cryptococcosis patient identified to have low IL-1β production (Marroni *et al.*, 2007). However, the same patient also had abnormal levels of TNFα and NO, and so their susceptibility cannot be attributed solely to defects in IL-1β. However, none of this evidence confirms the significance of IL-1β in cryptococcosis.

Therefore, it is currently still not understood exactly how IFNγ treatment is protective in cryptococcosis, and in which contexts IFNγ treatment is appropriate. However, IFNγ does appear to significantly affect early expression of IL-1β during cryptococcosis. Additionally, it is not confirmed how, if at all, IL-1β contributes to host protection *in vivo*, particularly in the context of the macrophage response to cryptococcosis in the mammalian lung.

1.7 – Aims

Despite a reduction in cryptococcosis cases over the past decade, the proportion of HIV/AIDS patients that still die from fatal cryptococcal meningitis has remained constant (Park *et al.*, 2009; Rajasingham *et al.*, 2017). The current ‘gold standard’ antifungal treatments have not changed during this time, despite numerous issues including side effects, efficacy and resistance. As there are also increasing reports of infections in immunocompetent individuals, there a pressing need to develop alternative classes of cryptococcosis therapy that are better for patients and healthcare systems globally (Zhu *et al.*, 2010). Since cryptococcosis is associated with compromised immunity, and the immune system uses multiple mechanisms to control and clear infection, an immune enhancing treatment may confer protection to cryptococcosis patients. While IFNγ has been shown to potentially benefit HIV positive cryptococcal meningitis patients when administered adjunctive to standard antifungal therapy, a better understanding of IFNγ

mechanisms of protection are required before it can be routinely used in the clinic (Jarvis *et al.*, 2012). My research aims to confirm the protective role of IFNγ in cryptococcosis by examining the effect of IFNγ on macrophages *in vitro* and in mice *in vivo* to determine if any protection offered by IFNγ treatment is reliant on IL-1β.

The first section of my thesis examines how different reference strains of *C. neoformans* interact with murine J774 macrophage like cells, in order to characterise the host-pathogen interactions between *C. neoformans* and macrophages. Then, how IFNγ and IL-1β treatment affected the interactions of macrophages with *C. neoformans in vitro* was examined, to see how this affected previously characterised host-pathogen interactions. This section also informs the design of subsequent *in vivo* studies.

The second section outlines the development and characterisation of a murine intranasal infection model of cryptococcosis because zebrafish embryo models of infection utilised previously by Kamuyango are not appropriate for modelling the pulmonary immune response in cryptococcosis (Kamuyango, 2017). Using this model, the virulence of two strains of *C. gattii* are compared using survival analysis, bodyweight data and fungal burden analysis.

The third section describes how the intranasal infection mouse model of cryptococcosis, in combination with transgenic approaches, is used to determine the effect of IFNγ treatment on cryptococcosis outcomes and whether this action is dependent on IL-1β. By genetically ablating IL-1β signalling, the contribution of this cytokine is assessed, and how this affects tissue fungal burdens, bodyweight and mouse survival.

The fourth and final experimental section characterises a novel precision cut lung slice (PCLS) model of cryptococcosis. One of the largest issues with mammalian models is the inability to directly visualise host-pathogen interactions without expensive and complicated intravital imaging set ups. The PCLS methodology allows for immune cells and cryptococci to be visualised *ex vivo* in live tissue. The model is then used to characterise the macrophage response in the first 24 hours of cryptococcal intranasal infection.

Finally, the findings within the thesis are discussed, and future experiments that should be conducted in the future as a result of this work.

Chapter 2 – Methods

2.1 – Ethics statement

All animal work was carried out in accordance with both national and institutional ethical guidelines. All procedures were within the scope of an approved project license (40/3726 or P4802B8AC) and carried out by trained and competent individuals, as dictated by the 1986 Animal (Scientific Procedures) Act. For each protocol, individual study plans were assessed and approved by the Animal Care and Welfare Committee of the University of Sheffield.

2.2 – Animal husbandry

For experiments where beads were instilled into the lungs of mice *ex vivo* (see 6.4), C57BL/6 mice were bred and used within the Beatson Biological Research Unit, Glasgow, UK. All other housing, transgenic breeding and *in vivo* experimentation took place in The University of Sheffield Biological Services Unit, Sheffield (UK), while wild-type C57BL/6 mice were purchased from Charles River (UK). All experiments were conducted on animals that were aged between 6-13 weeks old, as mice of this age are observed to be immunologically mature (Holladay and Smialowicz, 2000). Animal ID numbers were assigned to individuals using a random number generator (Google Random Number Generator, tinyurl.com/2p66uw7d; Google, California, USA). Animals were then randomly assigned to treatment groups by using a random number generator on animal ID numbers (Google Random Number Generator, tinyurl.com/2p66uw7d; Google, California, USA). Once assigned to treatment groups, all animals were left alone for at least five days to allow animals to acclimatise to their new surroundings and cage mates – standard practice that improves animal welfare and minimises animal stress that may significantly impact *in vivo* studies (Obernier and Baldwin, 2006). For all experiments, female mice were used as there is a lower risk of aggressive behaviour with group housed female mice compared to males (Van Loo *et al.*, 2003). However, it should be noted that no *in vivo* study in this thesis was blinded. This was due to the health and safety and logistics associated with infection studies. Particularly due to subjective nature of assessing animal health status for all survival studies, this may have presented a significant source of bias.

Animals were housed at a density no greater than 6 animals per cage, in individually vented cages which received their own HEPA filtered air supply – this was in order to avoid contaminating animals via the external environment, and vice versa. All cages contained a red house (NKP Plastics, Coalville, UK), wool paper (Datesand Ltd,

Stockport) and sawdust bedding (Datesand Ltd, Stockport), with water and Tekland Global 18% Protein Rodent Diet (Envigo, Alconbury, UK) available *ad libitum*. For additional environmental enrichment, sunflower seeds (Cronston Corn Mill Ltd, Leyland) were mixed in with sawdust bedding. All holding and procedure rooms were maintained at 28^{o}C on a 12hr light-dark cycle, and kept at a negative pressure to reduce the risk of contaminating holding rooms.

All inoculated animals were weighed daily inside category 2 containment hoods to monitor health status. Additionally, animals were monitored daily using the GRIMACE scale to identify any animals that may have been showing signs of suffering or infection (Langford *et al.*, 2010). Symptoms that were commonplace in mice with cryptococcosis included open mouth breathing (Weisbroth and Freimer, 1969) – often associated with rodent pneumonia - and ataxia (Bauler *et al.*, 2017) – a common symptom of rodent meningitis.

2.3 – Breeding of transgenic animals

In order to knock out IL-1β from mice *in vivo* for experiments presented in chapter 5, the conditional cre/LoxP system was exploited (Sternberg and Hamilton, 1981). Originally observed in P1 bacteriophages, cre/LoxP describes the Cre recombinase enzyme (Cre) and two marker regions of DNA, 34 base pairs long (loxP). When expressed, Cre will recognise loxP sequences and excise any DNA contained between the two.

For survival experiments in chapter 5, two transgenic mouse strains were used (Figure 7). The first strain was the 'wild-type(IL1β$^{tm1c(EUCOMM)}$)' strain. This mouse line was originally developed as described by Helyes *et al* (Helyes *et al.*, 2019). Briefly, genetically modified embryonic mouse stem cells were purchased that contained loxP sites either side of the IL-1β gene. These cells were injected into 4-8 cell stage embryos from C57BL/6 mice that lacked black fur pigment. Offspring chimeric in appearance were screened to confirm that animals were positive for this modification, and these offspring were bred with C57BL/6 mice to confirm that the modifications was carried in the germline. Offspring from these crosses that had black fur were crossed with C57BL/6NTg(CAG-Flpo)1Afst/Mmucd mice, which resulted in offspring that were homozygous for loxP sites that flanked exons 4 and 5 of the IL-1β gene (Pinteaux *et al.*, 2020). In the absence of cre enzyme expression, these LoxP sites act as introns and so IL-1β expression is preserved. Therefore, wild-type(IL1β$^{tm1c(EUCOMM)}$) animals served as a control group.

The second transgenic mouse strain used for this work was the IL-1β KO(*pgk2-Cre-IL1β^{tm1d}*) strain, which were derived from breeding the previously generated wild-

type(IL1β$^{tm1c(EUCOMM)}$) mice with PGK:Cre mice, as described by Tulotta *et al.* (2021). PGK:Cre mice express Cre under the control of the PGK2 promoter – a promoter in all tissues in adult mice that becomes activated at 3.5dpf (McBurney *et al.*, 1994). This means that in these animals, Cre is expressed in all tissues from 3.5 days post fertilisation. When crossed with wild-type(IL1β$^{tm1c(EUCOMM)}$), offspring positive for both Cre and LoxP sites will have exons 4 and 5 of IL-1β excised by Cre from 3.5 days post fertilisation, meaning animals were unable to express IL-1β from this point forward. This genotype in IL-1β KO(*pgk2-Cre-IL1β^{tm1d}*) animals was confirmed by real-time PCR of the lungs (Tulotta *et al.*, 2021).

To maintain these transgenic colonies once they were established, breeding pairs were established. A single male and female of the same strain would be housed together in normal cages (see 2.2). If male numbers were low, two females would be housed together with a single male. Female mice were then checked daily for evidence of plugs – a whitish mass that can be observed in the vaginal opening of female mice following a successful mating. If only a single litter was required, males would be removed at this point. Otherwise, males were kept in the cage – even if a plug was found – so that mating could resume immediately following pregnancy.

Following a successful pregnancy, pups were kept in the same cage as the mother and father until nineteen days old. Litters were then segregated based on gender and put in new cages separate from the mother so that pups could be weaned. These new cages were setup as before (see 2.2) with no more than six animals per cage. If any animals appeared to be smaller than cage mates, this animal would receive additional food in the form of mashed diet supplement (normal diet mixed with water; see 2.2). Food was put in the appropriate cage and made available *ad libitum* until the smaller animal had gained enough weight to be similar in weight to cage mates. When animals reached six weeks old, female mice were randomised into treatment groups (see 2.2).

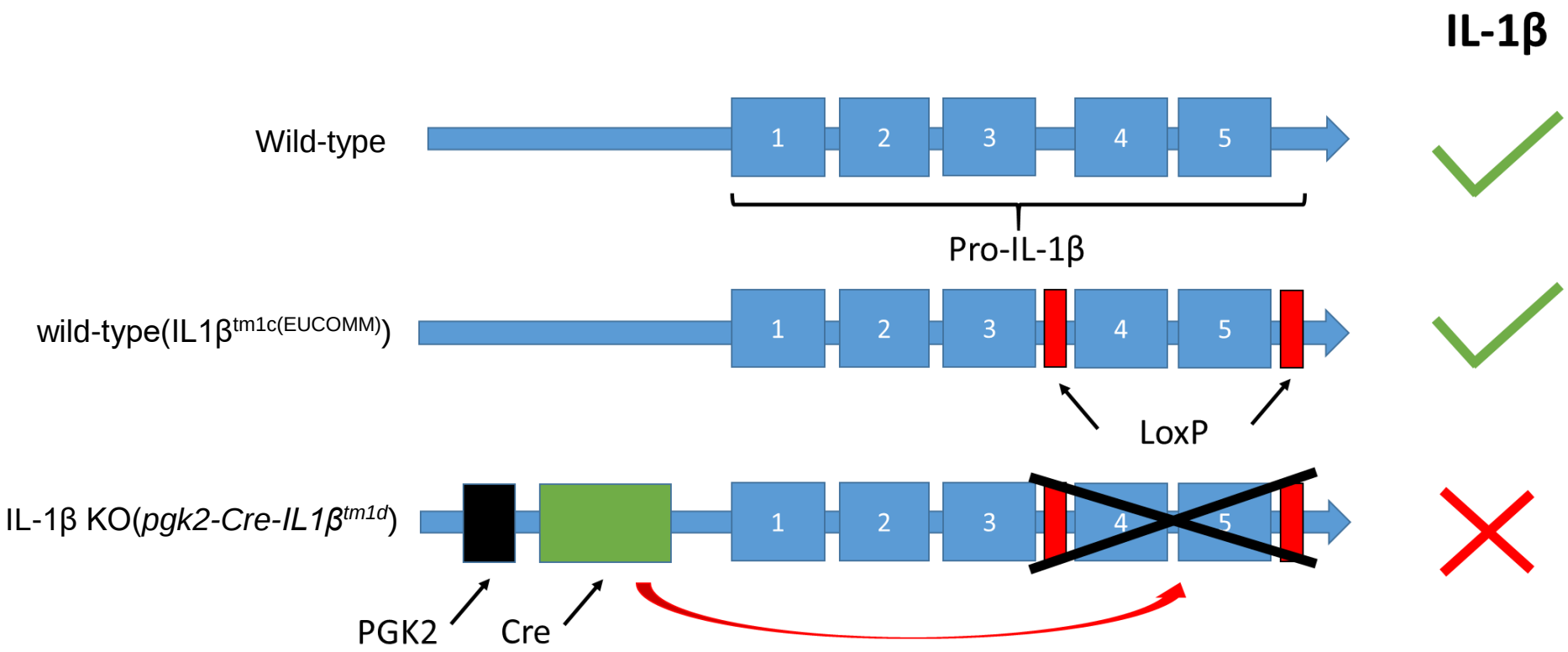

Figure 7 – IL-1β genomics of wild-type, wild-type(IL1β$^{tm1c(EUCOMM)}$) and IL-1β KO(*pgk2-Cre-IL1β*^{tm1d}) mice. Schematic describing the different genomics of wild-type and transgenic mouse strains, and how this affects expression of IL-1β. Wild-type mice express IL-1β, for which the gene features at least five exons. The wild-type(IL1β$^{tm1c(EUCOMM)}$) strain has LoxP sites flanking either side of exons 4 and 5 of the IL-1β gene. By themselves, these LoxP sites do not directly affect the IL-1β gene, and so wild-type(IL1β$^{tm1c(EUCOMM)}$) mice still express IL-1β. The IL-1β KO(*pgk2-Cre-IL1β*^{tm1d}) strain also contains the gene for Cre, under control of the universal promoter PGK2. When Cre is expressed, it recognises the LoxP sites and excises exons 4 and 5 of the IL-1β gene, effectively knocking out IL-1β (Helyes et al., 2019; Pinteaux et al., 2020; Tulotta et al., 2021).

2.4 – Culture of C. neoformans and C. gattii

All strains of *C. neoformans* and *C. gattii* used in this thesis are described in Table 4. *Cryptococcus* strains were stored at -80ºC using MicroBank™ beads (Pro-Lab Diagnostics, Birkenhead, UK), except for H99α IFNγ, which was stored on plastic beads that were kept in 500µl of 50% glycerol solution made up in distilled water. However, all working stocks were kept in or on YPD, as it is reported to provide the optimal conditions for maximal cryptococcal growth (Kraus *et al.*, 2004; Waterman *et al.*, 2012; Squizani *et al.*, 2018).

Cryptococcus working stocks were maintained on YPD agar plates (25% w/v YPD Broth (Fisher BioReagents, Pittsburgh, USA), 10% w/v agar (Sigma Aldrich, St Louis, USA), 25ml final volume in distilled water). YPD agar was first autoclaved and while warm (50ºC) was poured into sterile 9cm petri dishes and allowed to set (Scientific Laboratory Supplies, Nottingham, UK). A bead from frozen *Cryptococcus* stocks was agitated on a YPD agar plate, and the plate was then incubated for 48 hours (28ºC, 5% CO_2) to allow fungal growth. As some fungal cells did not survive being freeze thawed, a fresh working stock plate was made by streaking colonies from the original agitated plate in order to minimise the number of dead cells on plates, and this new plate was then cultured for 48 hours (28ºC, 5% CO_2).

Resulting working stock plates were stored at 4ºC for no longer than one month to minimise the chance of genetic drift occurring with fungal cells. After this time, working stock plates were discarded and new working stocks were made. Where antibiotic plates were required (see 3.2), YPD plates would be prepared as above. The antibiotic would then be applied at the appropriate concentration to specific petri dishes while the YPD agar was poured, when the solution was approximately 50ºC. Antibiotics were not added prior to microwaving or autoclaving to avoid thermal breakdown of agents.

Strain Name	Description	Reference
H99α WT (*C. neoformans*)	Highly virulent MAT-α reference strain, serotype A, first isolated from patient CSF in 1978, Duke University Medical Centre	(Janbon *et al.*, 2014)
H99α GFP (*C. neoformans*)	Biolistically transformed H99α strain to express GFP cytoplasmically, under the control of the *act1* promoter	(Voelz *et al.*, 2010)
H99α IFNγ (*C. neoformans*)	Biolistically transformed H99α strain to express murine IFNγ outside the capsule, under the control of the PLB1 promoter	(Wormley *et al.*, 2007)
KN99α WT (*C. neoformans*)	Highly virulent MAT-α reference strain, serotype A, produced by a sexual cross of H99 with intermediate MAT-a strain, KNA14	(Nielsen *et al.*, 2003)
KN99α GFP (*C. neoformans*)	Biolistically transformed KN99α strain to express GFP cytoplasmically, under the control of the *act1* promoter	(Voelz *et al.*, 2010)
52D (*C. neoformans*)	Moderately virulent MAT-α reference strain, serotype D, first isolated from patient CSF in 1968, Maryland	(Brandt, Bragg and Pinner, 1993; Gyetko *et al.*, 1996)
H99α PLB1 GFP (*C. neoformans*)	Biolistically transformed H99α strain to no longer produce PLB1, while expressing cytoplasmic GFP, less virulent than parent strain	(Cox *et al.*, 2001)
R265 WT (*C. gattii*)	Highly virulent MAT-α reference strain, serotype B, first isolated from patient bronchial washing from Vancouver Island outbreak	(Kidd *et al.*, 2004)
R265 GFP 14 (*C. gattii*)	Biolistically transformed R265 strain to express GFP cytoplasmically, under the control of the *act1* promoter	(Voelz *et al.*, 2010)

Table 4 – All strains of *Cryptococcus neoformans* and *Cryptococcus gattii* used for experiments

2.5 – Preparation of *C. neoformans* and *C. gattii* inocula

One day prior to inoculation, a streak of multiple colonies from 4°C working stock plates was taken (see 2.4) and suspended in 2ml autoclaved YPD broth (25% w/v in distilled water; Fisher BioReagents, Massachusetts, United States). These YPD suspensions of *Cryptococcus* were cultured overnight (28°C, 5% CO_2) whilst rotating at 20rpm – this was to ensure all yeast cells were exposed to nutrients and oxygen. This overnight culture was done to rescue cryptococci from their dormant state that was induced by storage at 4°C, and ensure all cryptococcal cells were in their logarithmic growth phase at the time of infection.

On the day of inoculation, to avoid YPD contaminating any assays, 1ml of the overnight *Cryptococcus* culture was washed in triplicate using sterile PBS. Washing was achieved by centrifuging the culture suspension (3300g, 1 minute), removing the supernatant and resuspending the resulting cryptococcal pellet in 1ml of sterile PBS (Oxoid, Cheshire, UK). An aliquot of the washed 1ml PBS/cryptococcal suspension was then diluted 1:100 so that fungal colonies could be counted on a haemocytometer (Hawksley, Sussex, UK) using an optical microscope (20x, Nikon Eclipse E100). After counting, the washed *Cryptococcus* culture was diluted in sterile PBS (except in IFNγ experiments; see 2.7) to the desired concentration according to the following equation:

$$\frac{Required\ concentration\ (cfu/ml) \times Required\ volume\ (ml)}{Count \times 100 \times 10^4 (cfu/ml)} = \begin{matrix} volume\ of\ overnight\ culture \\ to\ add\ to\ inoculum\ (ml) \end{matrix}$$

If antibody opsonised cryptococci were required, inocula were prepared as above. An anticapsular IgG antibody kindly provided by Arturo Casadevall, 18B7 (Casadevall *et al.*, 1998), was then added to prepared inocula at a concentration of 1:1000. This mixture was then rotated for an hour (20rpm) at room temperature (Johnston and May, 2010) to maximise opsonin binding.

2.6 – Preparation of bead inocula

Inert polystyrene Fluoresbrite® YG Microspheres labelled with FITC (Polysciences, Hamburg, Germany) were used as a negative control for infection experiments as their size could be controlled and they could be visualised by fluorescent imaging. Bead inocula were prepared almost identically to cryptococcal inocula (see 2.5). The only differences were that overnight culture was not required, and bead inocula could be prepared in advance of inoculation and stored at 4°C until required.

Beads could also be antibody opsonised prior to inoculation (Plested *et al.*, 2001). 10^8 beads of the appropriate size were incubated overnight at 4°C in PBS containing

10mg/ml bovine serum albumin (BSA; Sigma Aldrich, St Louis, USA) to allow for BSA to adhere to the surface of beads. Unbound BSA was removed by washing samples in triplicate with PBS (see 2.5). BSA-coated beads were then labelled with mouse anti-BSA IgG antibody (Invitrogen, California, USA), which was added bead inocula at a final concentration of 1µg/ml and was rotated at 20rpm for an hour at room temperature to allow for antibody binding. Opsonised bead preparations were also prepared ahead of time and stored out of direct sunlight at 4^{o}C until required.

2.7 – Cytokine preparation

Recombinant mouse IL-1β (25µg) and IFNγ (100µg) were purchased from Kingfisher Biotech (St Paul, USA). Each cytokine was resuspended in sterile PBS containing 0.1% BSA (Sigma Aldrich, St Louis, USA), which was split into multiple aliquots that were stored at -20^{o}C until required. Thawed aliquots would then be diluted as required using sterile PBS containing 0.1% BSA (Sigma Aldrich, St Louis, USA).

For *Cryptococcus* inocula that also contained IFNγ (50µg/ml), overnight cultures were washed in triplicate PBS containing 0.1% BSA (Sigma Aldrich, St Louis, USA). Following the counting of *Cryptococcus* cells, the final inocula was also prepared in PBS containing 0.1% BSA. Inocula were then centrifuged (3300g, 1min) and *Cryptococcus* were resuspended in PBS containing 0.1% BSA and 50µg/ml IFNγ.

2.8 – Intranasal inoculation of mice

All intranasal inocula for mouse infection experiments contained 50,000cfu of *Cryptococcus* in 50µl. This size of inocula was chosen as previous mouse infections at this dose resulted in systemic, disseminating infection that has an associated mortality rate of ~100% when untreated, as is observed with human infection (Wiesner *et al.*, 2015; Shourian *et al.*, 2018). For bead studies, various numbers of beads were used, although all inocula were in a total volume of 50µl PBS.

To intranasally inoculate mice, animals were firstly lightly anaesthetised using a mixture of isoflurane (Henry Schein Inc, New York, USA) and oxygen in an anaesthetic box (Vet-Tech UK, Congleton, UK) – a suitable level of anaesthesia was reached when respiration appeared to slow. Anaesthetised animals were then suspended by the head while the body was supported, and the inoculum was pipetted slowly onto the naves, where it was inhaled by the animal. Once inoculated, animals were weighed and then returned to their home cage, where they were monitored closely until they showed complete recovery.

2.9 – Euthanasia of mice

All mice were humanely euthanised using approved Schedule 1 methods by trained individuals. For all experiments, animals were sacrificed by an intraperitoneal overdose of sodium pentobarbital (20mg; Covetrus, Ohio, USA) – this was chosen over other methods to preserve the animal trachea for both PCLS (see 2.12) and for removing lung tissue (see 2.11). Injected animals were monitored until it was established that breathing has stopped, there was the absence of a heartbeat and there was no pedal pinch reflex in the hindleg (Buitrago *et al.*, 2008). Death was then confirmed by exsanguination – the femoral artery in the hindleg was exposed surgically and cut using scissors.

2.10 – Mouse survival analysis

In order to assess the virulence of *Cryptococcus* and determine the contribution of various cytokines to host protection, mouse survival analysis was carried out. For survival experiments, once infected with *Cryptococcus* (see 2.8), mice had their health status checked daily, consisting of daily weighing and observing animals for symptoms of lethal infection (see 2.2). To reduce animal suffering, humane end points were used in place of allowing mice to succumb to infection – if an animal met any one of the endpoint criteria, the animal was assumed to be in the late stages of lethal infection, and so was humanely euthanised (see 2.9). Humane endpoints for all survival experiments were weight loss no greater than 20% of their initial weight, or exhibiting symptoms not limited to hunched posture, continuous shivering, open mouth breathing and ataxia. Any animal that did not meet any of these criteria during the pre-determined study period were culled instead on the end date (see 2.9). Regardless of what time point animals were culled, in all cases the relevant tissues were taken from culled animals for analysis (see 2.11).

2.11 – Mouse tissue burden analysis

Tissue fungal burdens are useful measure for assessing pathogen virulence and the progression of infection *in vivo.* Therefore, assessing tissue burdens at pre-determined time points can provide an important insight into the virulence of many pathogens. For comparing fungal burdens at pre-determined time points, animals were inoculated with *Cryptococcus* (see 2.8) and monitored daily for health status using the same humane endpoint criteria as used in survival analysis (see 2.10). If any animals met any humane endpoints prior to the pre-determined time-point, the animal would be culled early for welfare reasons. Animals that survived to the pre-determined day of culling were culled (see 2.9) and the relevant tissues were taken for analysis. For all experiments, the brain

and lungs were removed, with trachea and spleen also taken for *C. gattii* experiments (Chapter 4).

Once removed, tissues were suspended in 500µl of sterile PBS – although larger tissues sometimes required an additional 500µl PBS (Oxoid, Cheshire, UK) in order to ensure tissues were submerged. Fungal cells were then liberated from tissues using a handheld tissue homogeniser (IKA t10 basic, Cole Parmer, Illinois, USA) to completely dissociate tissue. Between tissues, the homogeniser was washed in triplicate in 50ml distilled water and 70% IMS (Sigma Aldrich, St Louis, USA) to avoid cross contamination of samples.

Resulting tissue suspensions were diluted 1:2 in sterile PBS, and serially diluted 1:10 down to a dilution factor of $2x10^5$. 20µl of each dilution was then spread on YPD agar plates (see 2.3) and cultured for 48 hours (28ºC, 5% CO_2). Plates that yielded 10-300 colonies were then counted as these numbers allowed for a balance of accuracy and precision. Total tissue burdens were then calculated according to the following equation:

$$\frac{Plate\ count\ (cfu)\ \times Dilution\ Factor}{Original\ tissue\ suspension\ volume\ (ml)} = Total\ tissue\ burden\ (\frac{cfu}{tissue})$$

2.12 – Preparation of precision cut lung slices

PCLS are an *ex vivo* methodology where lung tissue from a recently culled animal is prepared and cultured in such a way that the tissue remains viable and elements of lung physiology and immunology are preserved (Sanderson, 2011).

Firstly, 2% low melting point agarose (Sigma Aldrich, St Louis, USA) was prepared in PBS – concentrations between 1-4% are suitable for PCLS, with a higher percentage making for easier cutting, at the expense of visibility, restricted cell migration and a reduced pore size. The agarose solution was heated to boiling point in a microwave when first made up to ensure the agarose had completely dissolved. The agarose was then left to cool and stored at 4ºC until required. On the day that animals would be culled and PCLS prepared, the agarose solution was reheated to boiling point in the microwave.

Immediately after animals had been culled and death confirmed (see 2.8), the trachea of the mouse was exposed by blunt dissection. A small incision was made in the trachea, a cannula (iv catheter 10G, Jelco, Leicester, UK) was inserted and tied in place with nylon thread. 1ml of the still warm agarose solution (~40ºC) was then instilled into the trachea using a 1ml syringe, inflating the lungs. The cannula was then removed while at the same time the nylon thread was tied tight to prevent agarose solution from leaking back out of the original incision. The agarose was then allowed to set into a gel by placing

the cadaver on ice for ~1 minute, before the lungs were carefully removed from the animal and suspended in 20ml PBS.

In a cateory 2 containment hood, the single lobe (left) and multilobe (right) lung were then seperated from each other using scissors. The single lobed lung was used for PCLS as the single lobe meant that cutting of the tissue was easier, while the multilobe lung was taken for tissue burden analysis (see 2.11). For PCLS, the single lobed lung was mounted to a rubber cutting block with tissue adhesive (Vetbond, IMS (Euro), Stockport, UK) so that the tissue could be attached to the vibratome (Vibratome Series 1500; Leica, London, UK). In the reservoir of the vibratome, the lung was bathed in high glucose DMEM (Thermo Fisher Scientific, Massachusetts, USA), supplemented with 10% fetal bovine serum (FBS; Sigma Aldrich, St Louis, USA) and 1% penicillin-streptomycin (5g; P4333, Sigma Aldrich, St Louis, USA) that had been heated to 37^{o}C in a water bath prior to use. The lung tissue was then cut longtudinally into 300µm thick slices, either until there was no tissue left or the quality of PCLS decreased – typically due larger airways deeper in the lung interfering with the cutting process. Slices of a high quality (based on their appearance) were then selected and taken for analysis by various means.

2.13 – Treatment of precision cut lung slices

Once PCLS were prepared (see 2.12), they were maintained in 1ml high glucose DMEM (Thermo Fisher Scientific, Massachusetts, USA) supplemented with 10% FBS (Sigma Aldrich, St Louis, USA) and 1% penicillin-streptomycin (5g; P4333, Sigma Aldrich, St Louis, USA). PCLS were kept in wells of a sterile 24 well plate (VWR International, Lutterfield, UK) in a cell culture incubator (37^{o}C, humidified, 5% CO_2; Sanyo, Osaka, Japan).

When fixed PCLS were required, slices were immersed in 1ml 4% paraformaldehyde (PFA; Sigma Aldrich, St Louis, USA) for 30 minutes at room temperature, or overnight at 4^{o}C. Slices were then transferred to PBS, and stored at 4^{o}C until required.

To visualise elements of the immune system and study host-pathogen intereactions, PCLS were treated with various dyes and antibody conjugates (Table 5), to identify

Cell surface marker	Conjugate	Expressed by	Amount in working stock	Concentration used	Reference
CD11c	AF647	AMs, MDMs, DCs	0.5mg/ml	1:200	(Lyons-Cohen *et al.*, 2017)
CD88	AF594	AMs, Neutrophils, MDMs	1mg/ml	1:100	(Lyons-Cohen *et al.*, 2017)
CD172α	AF555	MDMs, DCs	0.5mg/ml	1:100	(Lyons-Cohen *et al.*, 2017)
Isolectin GS-IB_4	AF647	AMs, endothelial cells	1mg/ml	1:200	(Sorokin and Hoyt, 1992)

Table 5 – Antibodies used for imaging of precision cut lung slices

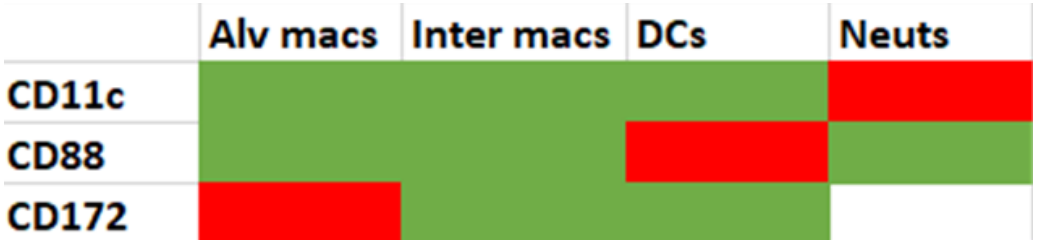

Figure 8 – Cell surface markers used to identify innate immune cells in precision cut lung slices. A figure showing which cell surface markers were used to identify which cell populations. Green – positive/high. Red – negative/low. White – not examined. (Sorokin and Hoyt, 1992; Lyons-Cohen *et al.*, 2017).

various immune cell populations (Figure 8). All antibodies and dyes were added directly to the media in which PCLS were suspended, immediately prior to imaging. It is important to note that the CD88 (BioRad, Kidlington, UK) and CD172α (Biolegend, London, UK) antibodies were both initially unconjugated. To make them compatible with fluorescent imaging, both of these antibodies were manually conjugated to fluorophores: Anti-CD88 was conjugated to Alexa Fluor 594 and anti-CD172α was conjugated to Alexa Fluor 555 according to kit instructions (Invitrogen, California, USA). Briefly, the antibody was suspended in a 1M sodium bicarbonate solution and the appropiate conjugate was added. These mixtures were left for one hour for conjugation to occur, before antibodies were purified by centrifugation (1,100g) on a resin bed.

2.14 – Brightfield imaging of precision cut lung slices

PCLS were imaged in glass bottom dishes (Thermo Fisher Scientific, Massachusetts, USA) for 20x brightfield imaging or 24 well plates (VWR International, Lutterfield, UK) for 2x brightfield imaging. Because of the buoyant nature of PCLS, PCLS were weighed down using stainless steel wire and bent into a horseshoe shape, with fishing wire tied across both sides of the metal structure.

All brightfield imaging was done using the Nikon Eclipse Ti (Tokyo, Japan). Live PCLS were imaged within the microscope sealed chamber (37^{o}C, 5% CO_2, 95% air) in order to maintain PCLS viability. Each PCLS would be imaged at 4-5 different XYZ positions where inoculated GFP-tagged particles could be seen. At each position, images were captured every 3.23µm in the Z axis over a range of 100µm, with the movement of the camera within the Z axis controlled by a custom piezo Z-stage (Mad City Labs, Madison, WI, USA). When PCLS were imaged over time, images were taken every 5 minutes for 12 hours, and then every 30 minutes for the subsequent 12 hours. All imaging was done using NIS Elements AR software (Tokyo, Japan) and files were captured in an .nd2 format.

Fixed PCLS were imaged at a magnification of 2x at a single time point and single Z position, without the need for CO_2 or heat.

2.15 – Confocal Imaging of PCLS

For all PCLS experiments where 1µm and 10µm beads were inoculated into mice *ex vivo* (see 6. REF), PCLS were imaged on a confocal system. PCLS were mounted in Ibidi 4 well mulitchambers (Glasgow, UK), weighed down (see 2.14) and kept in a sealed chamber (37^{o}C, 95% air and 5% CO_2) for the duration of imaging. The confocal microscope used was an LSMZeiss 880 Airyscan Fast microscope and PCLS were imaged with a 20x 0.8 N.A. air objective (Cambridge, UK). The microscope was setup in

Airyscan Fast mode and processed with default processing options in Zeiss Zen Black software.

2.16 – J774 cell culture

Murine J774 macrophage-like cells are an immortal cell line originally derived from a mouse sarcoma, and are a well characterised *in vitro* model of macrophages (see 1.5.1.1; Ralph, Moore and Nilsson, 1976; Lam *et al.*, 2009). Stocks of J774 cells were stored long-term in liquid nitrogen, suspended in 2ml low glucose - Dulbecco's Modified Eagle Media (DMEM; Sigma Aldrich, St Louis, USA) supplemented with 20% FBS (Sigma Aldrich, St Louis, USA), 1% penicillin-streptomycin (5g; P4333, Sigma Aldrich, St Louis, USA) and 10% DMSO (Sigma Aldrich, St Louis, USA).

When cells were required, an aliquot of stored cells were thawed at 37ºC in a water bath (Nickel-Electro Ltd., Weston-super-Mare, UK). Thawed cells were then transferred to T75 cell culture flasks (Grenier Bio-One, Kremsmünster, Austria) and resuspended in 10ml low glucose DMEM (Sigma Aldrich, St Louis, USA) supplemented with 10% FBS (Sigma Aldrich), 1% L-glutamine (Sigma Aldrich, St Louis, USA) and 1% penicillin-streptomycin (5g; P4333, Sigma Aldrich, St Louis, USA). This media is also known as COMP DMEM, and is reported to provide the optimal growth conditions for J774 cells (Lee, Nir and Papahadjopoulos, 1993; Szabó *et al.*, 1994; Vertut-Doï, Ishiwata and Miyajima, 1996).

T75 flasks containing J774 cells were cultured in a cell incubator (37ºC, humidified, 5% CO_2; Sanyo, Osaka, Japan). To maintain J774 cell growth, flasks were regularly passaged. Briefly, old media containing dead cells was removed from flasks and replaced with 10ml fresh COMP DMEM every few days. Then, as the density of J774 cells at this point was too high to support continued growth, J774 cells were diluted into a new flask. As J774 cells are adherent cells, cell scrapers (Corning, Amsterdam, The Netherlands) were employed to mechanically dislodge cells. J774 cells were not diluted more than 1:10 into new flasks to ensure that there was a sufficient cell density for optimal growth. J774 cells were discarded after 16 passages to minimise the chance of significant genetic drift.

2.17 – Preparing J774 cells for imaging

For imaging of host-pathogen interactions *in vitro*, J774 cells were transferred to plates appropriate for high-content imaging. Cell culture protocol (see 2.16) was followed until the day prior to imaging. J774 cells were then passaged as normal (see 2.16) until after J774 cells had been dislodged into solution. 14µl of the resulting J774 cell suspension was then counted using a haemocytometer (Hawksley, Sussex, UK) on an optical

microscope (20x, Nikon Eclipse E100, Tokyo, Japan). The scraped solution of J774 cells was then diluted to the desired concentration in COMP DMEM according to this equation:

$$\frac{Desired\ macrophage\ concentration\left(\frac{cells}{ml}\right) \times Required\ volume\ (ml)}{Cell\ count \times 10^4\left(\frac{cells}{ml}\right)} = Volume\ of\ J774\ cell\ solution\ in\ dilution\ (ml)$$

J774 cells were then transferred to a sterile 24 well plate, with 1ml of J774 cells per well. The 24 well plate containing J774 cells was cultured for 2-18 hours (37°C, humidified, 5% CO_2) to allow for J774 cells to adhere to the bottom of wells without allowing enough time for significant J774 replication. After this time had elapsed, COMP DMEM solution was replaced with 1ml serum free (SF) DMEM per well – COMP DMEM without 10% FBS (see 2.16; Sigma Aldrich, St Louis, USA). SF DMEM was used when assessing host-pathogen interactions as FBS can contain immunogenic components that could influence immune signalling.

2.18 – Infection of J774 cells with *C. neoformans*

For *in vitro* infections of J774 cells with *C. neoformans*, J774 cells were infected for 2 hours to allow for phagocytosis to occur. All *in vitro* inocula of *C. neoformans* were at a concentration of 10^7 cfu/ml in PBS (see 2.4 and 2.5). If required, cultures would be pre-opsonised with antibody (see 2.5). Infection of J774 cells was done after J774 cells had adhered to the bottom of 24 well plates (see 2.17), whereupon 100µl of SF DMEM was removed from each well and replaced with 100µl of *C. neoformans* inoculum (10^6 cfu). This inoculum created a multiplicity of infection (MOI) of 10:1, which used to maximise the number of *C. neoformans* cells that were phagocytosed and therefore the number of intracellular cryptococci for analysis. Infected J774 cells were incubated for 2 hours in a cell incubator (37°C, humidified, 5% CO_2) to allow for a significant number of phagocytosis events to occur (Mukherjee, Lee and Casadevall, 1995).

After 2 hours, infected J774 cells were washed in triplicate using PBS to remove as many extracellular cryptococci as possible, before infected J774 cells were imaged for 18 hours to assess antifungal activity. This washing step was done because extracellular cryptococci replicate at such a high rate *in vitro* that their numbers can saturate the field of view in 24 well plates, making analysis impossible.

2.19 – Treatment of J774 cells

Various treatments were also applied to J774 cells to determine how this affected phagocytosis and control of intracellular cryptococci. Phorbol 12-myristate-13-acetate (PMA) is a compound that readily activates protein kinase C and polarises macrophages towards a proinflammatory phenotype (Boneh, Mandla and Tenenhouse, 1989; Monick

et al., 1998; Qiao and May, 2009). Where pro-inflammatory polarised J774 cells were required, PMA (Sigma Aldrich, St Louis, USA) was prepared by making a 1:100 working stock in PBS. This solution was then further diluted 3:200 in SF DMEM and added to J774 cells 1 hour prior to *C. neoformans* infection (10ng). Wells were then washed in triplicate with SF DMEM to remove PMA from culture solution prior to *C. neoformans* infection.

For cytokine experiments, IFNγ and IL-1β were prepared (see 2.7) and administered to J774 cells at the time of *C. neoformans* infection, at a volume of 50µl. In order to maintain the presence of these cytokines in SF DMEM, following the two-hour infection period (see 2.18), cytokine treated media was removed from each well and transferred to labelled eppendorfs. These media were centrifuged (3300g, 1 minute) to pellet any extracellular cryptococci still in this solution, while the wells were washed with PBS in triplicate (see 2.18). The cytokine treated media, minus the cryptococcal pellet, was then readministered to the corresponding wells for the 18 hours of *in vitro* assay.

2.20 – Brightfield imaging of J774 cells

In order to assess J774 handling of intracellular *C. neoformans*, brightfield imaging of infected J774 cells was employed. Imaging was carried out in the same way as time lapse brightfield imaging of live PCLS (see 2.14) with a few differences. Z stacks were not captured as J774 cultures were 2D. Additionally, only three images were taken per condition. Finally, images were instead taken every 10 minutes for 18 hours. Images were taken based on where a significant number of intracellular *C. neoformans* cells could be observed.

2.21 – Image processing and analysis

All brightfield images were analysed in the .nd2 format in NIS Element Viewer (Kingston Upon Thames, UK) or ImageJ. Cell number, shape and size were calculated by manually segmenting cells of interest and using measure functions within NIS Elements AR software or ImageJ. GFP positive cell sizes were measured in the GFP channel. The growth equations for cryptococci in the PCLS work (see 6.20) were derived by manually tracking intracellular *C. neoformans* and noting the times that budding occurred. These times were then plotted into Graphpad Prism 7-8, and doubling times were derived from exponential growth curve equations.

Several measures were used to quantify macrophage-cryptococcal interactions. The intracellular fate of cryptococci was determined by manually tracking cells over the course of a time lapse, and noting when a cell showed evidence of a particular behaviour – although only cells that were visible from the start of the time lapse were quantified.

The percentage of phagocytic macrophages was used to estimate the phagocytic capacity of a macrophage population. Intracellular fold change was used to estimate intracellular replication of fungi within macrophages. Phagocytic index (PI) standardises the intracellular number of cryptococci to the number of infected macrophages. All three equations are described below:

$$\left(\frac{Number\ of\ macrophages\ containing\ cryptococci}{Total\ number\ of\ macrophages}\right) \times 100 = Percentage\ phagocytic\ macrophages$$

$$\frac{Number\ of\ intracellular\ cryptococci\ at\ the\ end\ of\ time\ lapse}{Number\ of\ intracellular\ cryptococci\ at\ the\ start\ of\ time\ lapse} = intracellular\ fold\ change$$

$$\frac{Number\ of\ intracellular\ cryptococci}{Number\ of\ infected\ macrophages} = Phagocytic\ index$$

Confocal images were visualised using Imaris software (Oxford Instruments, Oxford, UK). Images were masked using the inbuilt semi-automatic segmentation function, althoguh quantification was done manually.

2.22 – Statistical analysis

In all cases, significance was taken to be $p<0.05$ following adjustment for multiple comparisons. All statistical tests were carried out using GraphPad Prism 7 and 8 (GraphPad Software Inc, San Diego, USA). Normality for all datasets was determined by visual inspection of the data informed by normality testing, which determined whether parametric or non-parametric analysis was applied. However, it is acknowledged that this method can be subjective, and so could be differentially interpreted by other readers, and would be made more robust by formal normality testing (Ghasemi and Záhediasl, 2012). For parametric data, if two treatment groups were being compared, a t-test was conducted. In all cases, an F test was conducted to determine if the variance of the two datasets was significantly different – where this was the case, a Welch's t-test was conducted instead of a student's t-test (Ruxton, 2006). In the case that experiments had more than two treatment groups, with two different factors, an analysis of variance was first conducted to establish if any factor, or combination there of, significantly impacted the distribution of datasets, leading to inequalities or differences (Strasak *et al.*, 2007). In the case of parametric datasets, as established based on if the data was continuous, a one-way or two-ANOVA be applied. If a significant effect of any factor was established, appropiate *post-hoc* testing would be conducted to establish if specific differences between treatment groups could be established. In the case of data established to be non parametric (non-continuous, proportion data), multiple Kruskal-Wallis ANOVA tests would be applied, which allow for non-parametric analysis of variance, corrected for multiple comparisons. In the case of IL-1β analysis, non-linear regression was applied to non-parametric datasets to determine if there was a dose-response relationship based

on goodness of fit. Curves would then be compared to establish if the relationship was significantly different with or without IFNγ. Survival curves were first analysed with a Chi-squared, with *post-hoc* log-rank tests with corrections made for multiple comparisons. Growth equations were only determined for fungal cells where 3 or more incidences of replication were observed. Additionally, only growth characterisitcs were an R^2>0.7 were considered for analysis. For all *in vivo* work, each animal was considered a biological repeat, although all experiments were repeated on at least three separate days.

When reporting results, the relevant t and F values are reported for each test, so that results can be confirmed in t-value and F-value look up tables, to allow for the results of a statistical test to be confirmed (Weissgerber *et al.*, 2018). F-value tables and t-value tables can both be generated online using table generators, depending on the degrees of freedom and value for p determined to be significant (Fisher, 1918).

Chapter 3 – IFNγ and IL-1β do not enhance J774 control of *C. neoformans in vitro*

3.1 – Introduction

3.1.1 – Interferon-γ in cryptococcosis

The patient groups with the highest risk of invasive cryptococcosis are those with uncontrolled/advanced HIV/AIDS, solid organ transplant recipients or those on chronic immunosuppressive therapy (Maziarz and Perfect, 2016). This association between immune dysfunction and incidences of uncontrolled cryptococcosis has meant the immune response to *Cryptococcus* is the focus of much cryptococcosis research. More specifically, as HIV/AIDS is currently the largest risk factor for disseminated cryptococcosis, immune factors that are affected or made absent by this condition are investigated as potential therapeutic targets – theoretically correcting defects in this condition should improve cryptococcosis patient outcomes.

IFNγ is a cytokine primarily produced by $CD4^+$ cells – the cell type low or absent in advanced HIV/AIDS (Murray *et al.*, 2002) – and is known to be important for maintaining and effecting Th1 immune responses (Adams and Hamilton, 1984; Bradley, Dalton and Croft, 1996). In the context of cryptococcosis, Th1 responses are strongly associated with improved host outcomes in both *in vivo* models (Koguchi and Kawakami, 2002) and cryptococcosis patients (Jarvis *et al.*, 2013, 2015). This culminated in a small clinical trial of adjunctive IFNγ treatment in a clinical trial of HIV-positive cryptococcal meningitis patients, where two doses of IFNγ therapy adjunctive to antifungal therapy were found to significantly enhance fungal clearance in patients (Jarvis *et al.*, 2012). However, the mechanism by which IFNγ affords protection to cryptococcosis patients has yet to be determined.

Among the known effects of IFNγ, one that is thought to be especially significant in cryptococcosis is in enhancing the antifungal activity of innate immune cells, including macrophages. Macrophages highly feature at all stages of cryptococcosis, from the initial pulmonary infection (Bojarczuk *et al.*, 2016) to protective granuloma formation (Farnoud *et al.*, 2015) and in late-stage disseminated infection of the CNS (Lee *et al.*, 1995). IFNγ is reported to have a multitude of effects on macrophages which are observed to enhance the antimicrobial activity of these cells (Nathan *et al.*, 1983). Specific effects of IFNγ signalling in macrophages include increased expression of iNOS, an enzyme important for the production of antimicrobial mediators (Ding, Nathan and Stuehr, 1988), MHC class II, a surface molecule that is critical for antigen presentation. IFNγ has also been reported to increase macrophage expression of IL-2, a cytokine important for T-cell

clonal expansion, and expression of IFI44L, a protein known to result in increased NFκB expression – a protein associated with pro-inflammatory responses (Leopold Wager *et al.*, 2018; DeDiego, Martinez-Sobrido and Topham, 2019). These numerous changes in macrophage phenotype due to IFNγ, combined with the omnipresent nature of macrophages during the course of cryptococcal infection suggests that the action of IFNγ on macrophages is critical for host defence in cryptococcosis (King and Jones, 1983).

However, despite the wealth of literature regarding host-pathogen interactions between *C. neoformans* and macrophages, a significant role of IFNγ in these interactions has yet to be fully described. Currently, the lack of mechanistic understanding regarding IFNγ has limited its assimilation into clinical guidelines, as without a mechanism treatment efficacy cannot be ensured and side effect profiles cannot be accurately predicted. Additionally, a detailed mechanistic understanding of IFNγ may enable the development of more specific therapeutics that have better therapeutic profiles and fewer side effects than IFNγ. There is therefore a need to better characterise the effects of IFNγ on macrophage-*Cryptococcus* host pathogen interactions both *in vitro* and *in vivo*.

3.1.2 – Role of IFNγ in the immune response to C. neoformans in a zebrafish embryo in vivo infection model

To better understand the role of IFNγ and macrophage activity *in vivo*, it was previously examined in our lab how a single dose of IFNγ at the time of infection affected host outcomes in a low-dose localised *C. neoformans* infection in zebrafish embryos (Kamuyango, 2017). Because the zebrafish embryo only possesses innate immune cells and is compatible with intravital imaging, this model is an attractive modality for studying the interactions of IFNγ, macrophages and *C. neoformans in vivo*.

Using this model, it was observed that treating infected zebrafish embryos with 5μg/ml IFNγ at the time of infection significantly lowered burdens of highly virulent KN99α GFP *C. neoformans* at 48hpi compared to untreated controls (Kamuyango, 2017). IFNγ treatment also increased the number of animals that completely cleared infection. When immune responses in IFNγ treated and untreated zebrafish embryos were compared, it was observed that IFNγ treatment resulted in higher numbers of macrophages and neutrophils at the site of infection. However, specifically depleting macrophages with metronidazole revealed that it was macrophages, not neutrophils, that were critical for improved host outcomes.

Therefore, the antimicrobial activity of zebrafish embryo macrophages was examined *in vivo,* with and without IFNγ treatment (Kamuyango, 2017). While phagocytosis appeared to be unaffected, the fungistatic activity of infected macrophages was found to be

enhanced by IFNγ treatment – intracellular *C. neoformans* cells replicated ~50% slower with IFNγ treatment compared to untreated controls. All combined, this provides strong *in vivo* evidence that IFNγ imparts protection by enhancing the antifungal activity of macrophages during infection with *C. neoformans* which reduce intracellular replication.

3.1.3 – Linking the action of IFNγ, IL-1β and enhanced macrophage control of *C. neoformans*

Despite strong evidence of IFNγ treatment efficacy in the zebrafish embryo model, no mechanism was proposed that explained how IFNγ treatment enhanced macrophage control of intracellular *C. neoformans* in the zebrafish embryo (Kamuyango, 2017). However, an interesting observation was that IFNγ treatment increased infected zebrafish embryo expression of IL-1β at 12hpi. In the context of macrophage biology, IFNγ and IL-1β signalling are known to be closely linked – IFNγ and a concurrent TLR4 signal are observed to skew mammalian macrophages towards a pro-inflammatory phenotype, characterised by TNFα and IL-1β production (Crosby *et al.*, 2010; Qiao *et al.*, 2013). However, as TNFα expression in the zebrafish embryo model was not significantly affected by IFNγ, this specific increase in IL-1β expression early in infection suggests that IL-1β may be important for the protective action of IFNγ treatment in relation to macrophages.

Compared to IFNγ, the contribution of IL-1β to protective immunity in cryptococcosis is less clear. *In vivo*, intracellular *C. neoformans* and capsular GXM are observed to activate the NLRP3-ASC-capsase 8 inflammasome – an important protein complex in the secretion of active IL-1β (Chen *et al.*, 2015). Additionally, it has also been observed that the B3501 strain of *C. neoformans* produces small molecules – hydroxyphenyllactic acid and DL-Indole-3-lactic acid – which inhibit inflammasome activity and reduce levels of IL-1β (Bürgel *et al.*, 2020). Treating either amoebae (*Acanthamoeba castellanii*) or mice with conditioned media that contains these inhibitory small molecules results in higher *C. neoformans* burdens, providing evidence of a protective role for IL-1β. Additionally, Shourian *et al.* showed that the IL-1β receptor, IL-1RI, is indispensable for host protection in mice infected with the moderately virulent 52D strains of *C. neoformans* (2018). In the absence of this receptor, mice had lower expression of IL-1β and IFNγ in the lungs, higher fungal burdens and reduced survival. However, this study did not infect mice with more virulent strains of *C. neoformans* (KN99α WT, H99α WT) to confirm if this significant effect was strain specific. Additionally, IL-1RI is a receptor for not just IL-1β, but also IL-1α, and so the results of this study may have been due to the absence of signalling due to IL-1β, IL-1α or a combination of both. Finally, there is currently no clear clinical association between IL-1β levels and incidences of cryptococcosis. At the time

of writing, only a single case report has proposed a clinical link between defects in IL-1β and cryptococcosis, which describes a single patient found to also have defects in the TNFα and NO (Marroni *et al.*, 2007). Because of the multifaceted nature of the patients immunocompromise, it is tenuous to attribute their susceptibility to cryptococcosis solely to defects in IL-1β production.

This means that currently no study has specifically explored the connection between IFNγ and IL-1β in a mammalian model of cryptococcosis regarding macrophage antifungal activity. However, before studying anything *in vivo*, it is important to first examine host-pathogen interactions *in vitro* so as to inform and refine study design. Therefore, I first sought to characterise the host-pathogen interactions of four reference strains of *C. neoformans* using the widely utilised macrophage cell line, J774 cells. Having characterised this model, I then examined the effects of IFNγ and IL-1β treatment on these host-pathogen interactions, to determine if these cytokines improved macrophage control of intracellular *C. neoformans in vitro*.

3.2 – Results

3.2.1 – H99α IFNγ *C. neoformans* is resistant to the antibiotic nourseothricin

In order to establish the effects of IFNγ and IL-1β on J774 handling of intracellular *C. neoformans*, the host-pathogen interactions between J774 cells and various reference strains of *C. neoformans in vitro* were first characterised. For these experiments, the four reference strains used were KN99α WT (highly virulent), H99α WT (highly virulent), 52D (moderately virulent) and H99α IFNγ (low virulence; Table 4). Unlike the other investigated strains of *C. neoformans,* H99α IFNγ is a transgenic strain that produces murine IFNγ constitutively and has been shown to be hypovirulent in mouse models of infection (Wormley *et al.*, 2007; Castro-Lopez *et al.*, 2018). This makes this strain a useful tool for studying the role of IFNγ in cryptococcosis. However, despite being first generated in 2007, the host-pathogen interactions of this strain with J774 cells *in vitro* have yet to be described.

Before use, the H99α IFNγ strain (kindly provided by Floyd Wormley) was first confirmed to be resistant to nourseothricin. When the strain was first generated, an acetyltransferase gene selection marker was used to impart nourseothricin resistance to successfully transformed cells, as *C. neoformans* is inherently susceptible to this antibiotic *in vitro* (McDade and Cox, 2001; Wormley *et al.*, 2007). Therefore, to confirm the presence of the original construct and provide evidence that the H99α IFNγ strain had the genotype expected, H99α IFNγ and the parental strain, H99α WT, were cultured

for two days on YPD agar plates containing PBS or 100µg/ml nourseothricin to confirm the antibiotic resistance phenotype (Figure 9).

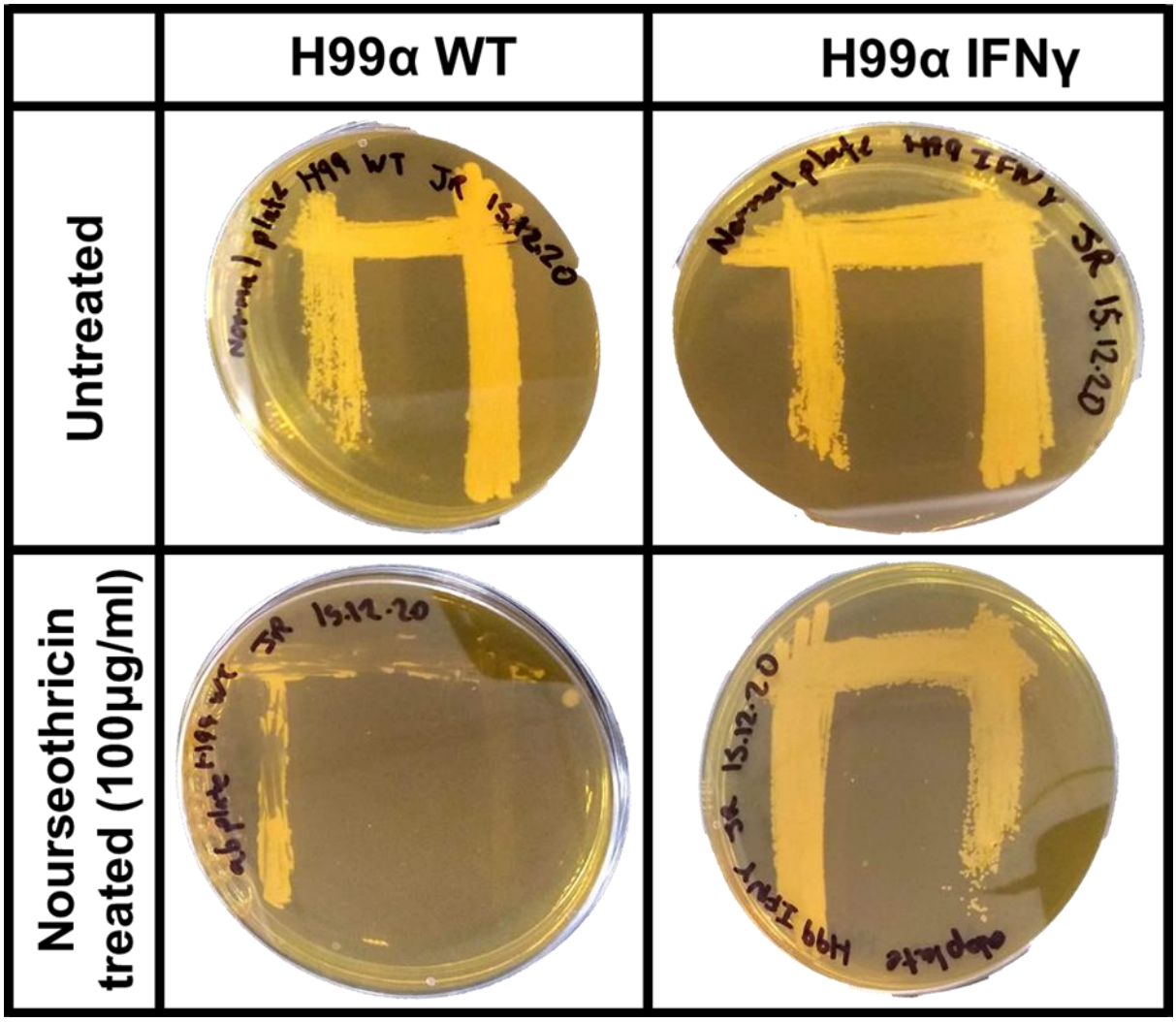

Figure 9 – H99α IFNγ *C. neoformans* is resistant to nourseothricin. Images showing the growth of H99α WT and H99α IFNγ *C. neoformans* on YPD plates, with and without 100µg/ml nourseothricin. The high growth of H99α IFNγ in the presence of nourseothricin compared to wild-type H99α WT provides strong evidence that the transgenic H99α IFNγ genome is as expected

The limited growth of H99α WT on antibiotic treated plates confirmed the susceptible phenotype of *C. neoformans in vitro* and confirmed that resistance had not emerged in this strain. Additionally, the unaffected growth of H99α IFNγ in the presence of nourseothricin provides evidence that the H99α IFNγ strain used in these experiments had expected phenotype (Wormley *et al.*, 2007).

3.2.2 – J774 cell intracellular burdens of *C. neoformans* after two hours of infection are strain dependent

Immortal J774 cells are a widely used *in vitro* model of macrophages and have been used historically to model cryptococcosis host-pathogen interactions (Mukherjee, Feldmesser and Casadevall, 1996). Therefore, the host-pathogen interactions between J774 cells and four reference strains of *C. neoformans* were first characterised, as the investigated strains all had differential virulence *in vivo* (Table 4). 100,000 J774 cells were infected with each strain of *C. neoformans* at an MOI of 10:1 in order to maximise the number of intracellular *C. neoformans* cells for analysis. In addition, some J774 cells were pre-treated with PMA to generate pro-inflammatory macrophages and determine if any of the investigated strains of *C. neoformans* were better handled by proinflammatory J774 cells (Qiao and May, 2009). The number of J774 cells and intracellular *C. neoformans* cells were then quantified per frame, with frames selected for comparable numbers of cells to quantify. The appearance of J774 cells and extracellular and intracellular *C. neoformans* cells can be observed in Figure 15A. The numbers of J774 cells for infections with different *C. neoformans* strains were found to be significantly different, although on average there were greater than 100 J774 cells for analysis per frame (Figure 10A).

Initially, host-pathogen interactions at 2hpi were analysed – after extracellular cryptococci had been removed. Despite this washing step, extracellular and intracellular *C. neoformans* cells were observed across all four strains. However, the presence of intracellular *C. neoformans* cells meant that host-pathogen interactions could be assessed. Initially, the number of phagocytosed *C. neoformans* cells per strain were compared to determine if any strain was more or less resistant to phagocytosis (Figure 10). No significant differences in the proportions of J774 cells that contained cryptococcal cells could be identified, regardless of strain or whether J774 cells were pre-treated with PMA (Figure 10B). Interestingly though, the mean number of 52D cells per infected J774 cell was significantly lower compared to H99α or KN99α cells (Figure 10C). This could mean that either fewer 52D *C. neoformans* cells were phagocytosed, or that comparatively less intracellular replication of 52D *C. neoformans* occurred in the first two hours of infection.

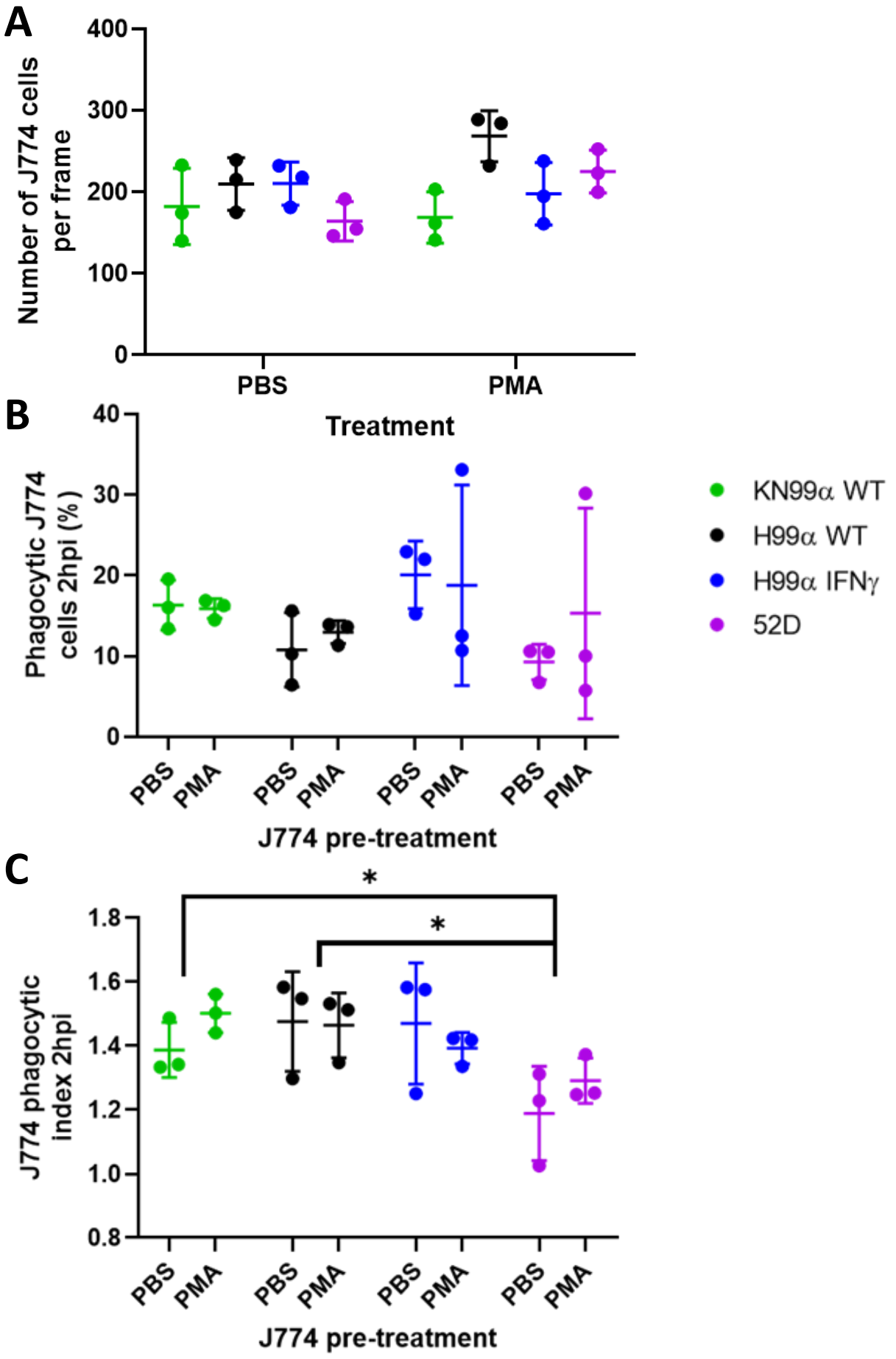
A
Number of J774 cells per frame
400
300
200
100
0
PBS
PMA
B
Treatment
Phagocytic J774 cells 2hpi (%)
40
30
20
10
0
PBS
PMA
J774 pre-treatment
KN99α WT
H99α WT
H99α IFNγ
52D
C
*
*
J774 phagocytic index 2hpi
1.8
1.6
1.4
1.2
1.0
0.8
PBS
PMA
J774 pre-treatment

Figure 10 - Infected J774 cell intracellular fungal burdens of *C. neoformans* 52D at 2hpi were significantly lower compared to other strains. Although there were no significant differences in the phagocytic proportions of J774 cells infected with different strains of *C. neoformans* at 2hpi *in vitro*, the mean number of intracellular 52D *C. neoformans* cells per infected J774 cell was significantly lower compared to other strains. (**A**) There were significant differences in the number of J774 cells per frame between strains of *C. neoformans* examined to analyse host-pathogen interactions. Interaction – $F(3, 16)=2.456$, $p=0.1005$. PMA – $F(1,16)=3.034$, $p=0.1007$. Strain – $F(3,16)=3.935$, $p=0.028$. (**B**) The proportion of phagocytic J774 cells after 2 hours of *in vitro* infection did not vary with *C. neoformans* strain or PMA pre-treatment. Untreated cells: Kruskal-Wallis statistic=6.897, number of groups=4, number of values=12, adjusted p value=0.1004. PMA treated cells: Kruskal-Wallis statistic=2.385, number of groups=4, number of values=12, adjusted p value>0.9999. (**C**) The mean number of intracellular 52D *C. neoformans* cells per infected J774 cell were significantly lower than was observed with the more virulent KN99α ($p=0.0372$) and H99α ($p=0.0139$) strains. Interaction – $F(3,16)=0.9249$, $p=0.4513$. PMA treatment – $F(1,16)=0.4438$, $p=0.5148$. Strain – $F(3,16)=4.845$, $p=0.0139$. Phagocytic J774 proportions were compared using Kruskal-Wallis tests, one for untreated cells and one for PMA cells, with *post hoc* Dunn's multiple comparisons. All presented p values for **A** were corrected for multiple comparisons (each p value was multiplied by two). The number of J774 cells per frame and the phagocytic index of infected J774 cells were compared using a two-way ANOVA with *post hoc* Tukey's multiple comparisons where appropriate. Data shown is mean ± SD. Each point represents the mean value of three fields of view from one experiment. * - $p<0.05$.

3.2.3 – J774 cell intracellular fungal burdens *C. neoformans* are affected by strain at 20hpi

One of the key pathological features of *C. neoformans* is the ability for phagocytosed cryptococci to survive and replicate inside macrophages (Goldman *et al.*, 2000). Therefore, intracellular fungal burdens after 20 hours of culture were compared between the examined strains of *C. neoformans*, 18 hours after extracellular cryptococci were removed.

As was observed in Figure 10, there were no significant differences in the proportion of J774 cells infected with *C. neoformans* after 20 hours, irrespective of strain or PMA treatment status (Figure 11A). However, the phagocytic index (PI) of J774 cells at 20hpi was found to be significantly affected by *C. neoformans* strain (Figure 11B). Although specific strain differences in PI values could not be identified, the PI of J774 cells infected with 52D *C. neoformans* was ~1.5, while for all other investigated strains these values were closer to 2.0-2.5.

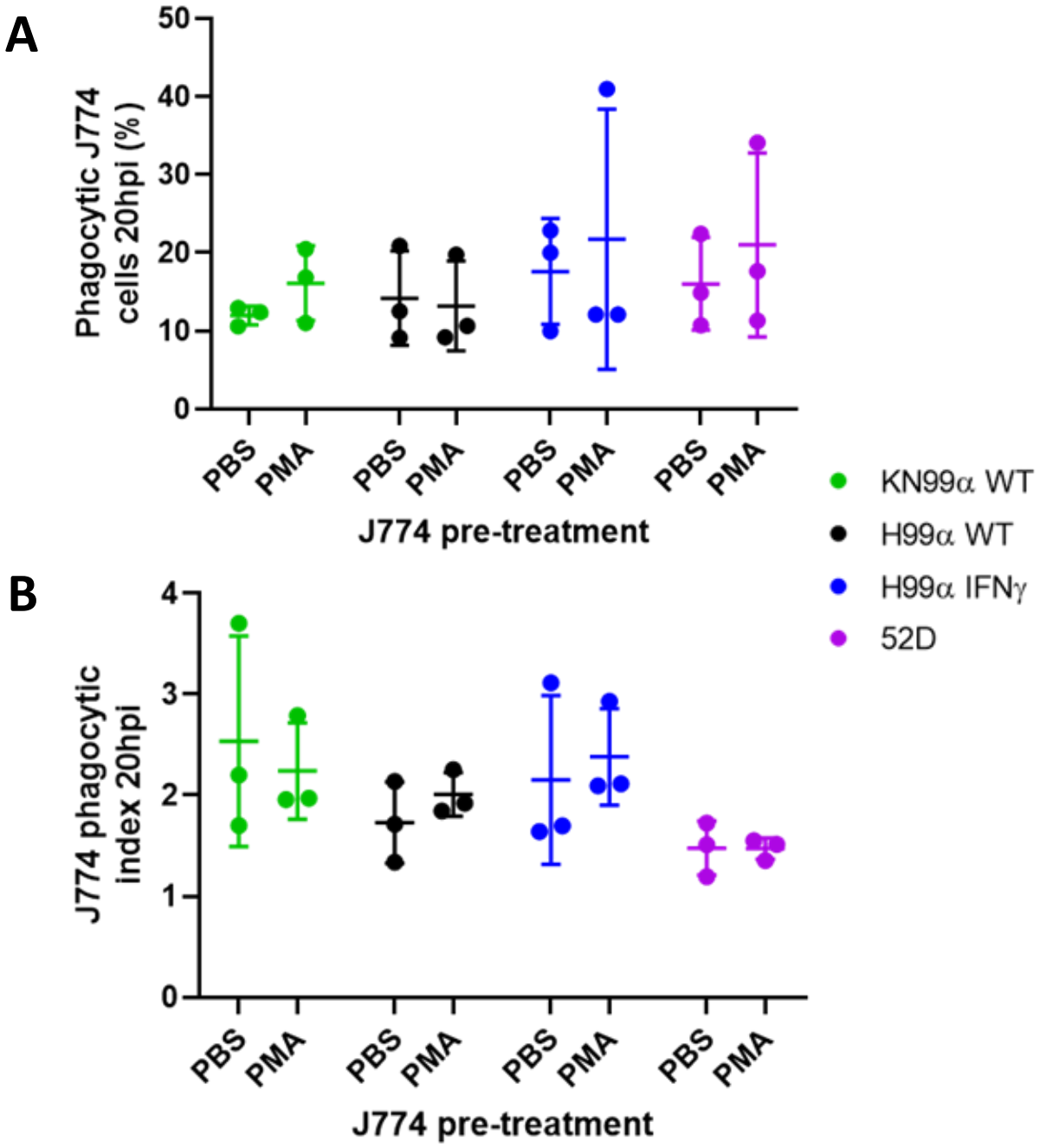
A
Phagocytic J774 cells 20hpi (%)
50
40
30
20
10
0
PBS
PMA
PBS
PMA
PBS
PMA
PBS
PMA
J774 pre-treatment
KN99α WT
H99α WT
H99α IFNγ
52D
B
J774 phagocytic index 20hpi
4
3
2
1
0
PBS
PMA
PBS
PMA
PBS
PMA
PBS
PMA
J774 pre-treatment

Figure 11 - Infected J774 cell intracellular fungal burdens at 20hpi were significantly different between strains of *C. neoformans*. At 20hpi, the proportion of infected J774 cells was the same across all treatment conditions, although the strain of *C. neoformans* that J774 cells were infected was found to significantly affect PI values. (**A**) The proportion of J774 cells infected with *C. neoformans* at 20hpi was not affected by strain or PMA pre-treatment. Untreated cells: Kruskal-Wallis statistic=1.308, number of groups=4, number of values=12, adjusted p value>0.9999. PMA treated cells: Kruskal-Wallis statistic=2.077, number of groups=4, number of values=12, adjusted p value>0.9999. (**B**) The phagocytic index of infected J774 cells at 20hpi was significantly affected by the strain of *C. neoformans*, although specific differences could not be identified. Interaction – F(3,16)=0.3264, p=0.8063. PMA treatment – F(1,16)=0.05056, p=0.8249. Strain – F(3,16)=3.25, p=0.0495. Phagocytic J774 cell proportions were compared using Kruskal-Wallis tests, one for untreated cells and one for PMA pre-treated cells, with *post hoc* Dunn's multiple comparisons where appropriate. All presented p values for **A** were corrected for multiple comparisons (each result was multiplied by two). The phagocytic index of infected J774 cells was compared using a two-way ANOVA with *post hoc* Tukey's multiple comparisons. Data shown is mean ± SD. Each point represents the mean value of three fields of view from one experiment.

3.2.4 – J774 replication was not affected by *C. neoformans* infection

Although significant differences in PI values were identified at both 2 and 20hpi, many processes can influence PI values, including intracellular replication, phagocytosis and vomocytosis. It can also be affected by the number of phagocytes. Being sarcoma derived, J774 cells replicate in culture. Therefore, the replication of J774 cells was assessed to see if either PMA pre-treatment or *C. neoformans* infection affected this process.

Therefore, to better understand how *C. neoformans* infection affects J774 cells, J774 cell numbers were compared over 18 hours – from 2 to 20hpi (Figure 12). No significant differences in J774 replication in any examined condition, despite a lower fold change in PMA pre-treated J774 cells infected with 52D *C. neoformans,* was observed.

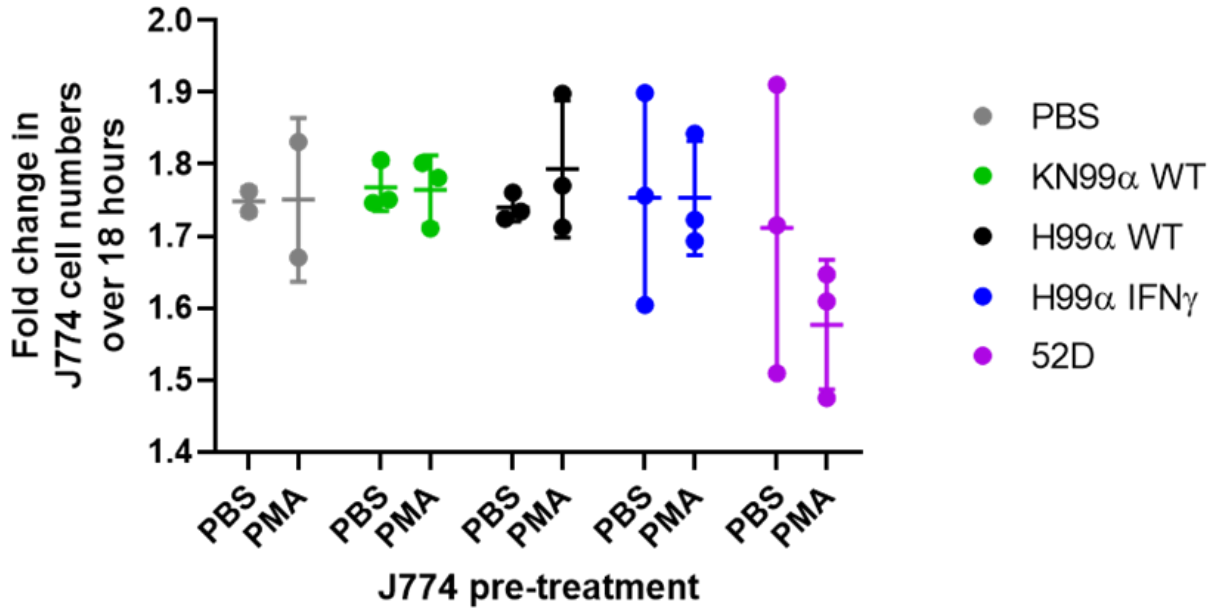

Figure 12 – J774 cell replication over 18 hours was not significantly affected by *C. neoformans* infection or PMA pre-treatment. Interaction – F(4,18)=0.6886, p=0.6092. PMA – F(1,18)=0.1736, p=0.6818. Strain – F(4,18)=1.498, p=0.2447. Fold changes in J774 cell numbers were compared using a two-way ANOVA. Data shown is mean ± SD. Each point represents the mean value of three fields of view from one experiment.

3.2.5 – Phagocytosis of 52D *C. neoformans* by J774 cells appears more frequent over 18 hours compared to other strains

Although there were significant differences in the host-pathogen interactions of 52D *C. neoformans* with J774 cells, it was unclear whether 52D *C. neoformans* cells were more susceptible to phagocytosis or replicated less intracellularly than other strains *in vitro*. Therefore, the intracellular numbers of *C. neoformans* were compared between 2 and 20hpi to better understand this difference (Figure 13A). Despite being relatively less virulent *in vivo*, the largest fold change in intracellular cell numbers during this time period were observed with the 52D and H99α IFNγ strains of *C. neoformans*, although this was not significant (p=0.17).

However, this value could be the result of additional phagocytosis occurring over 18 hours, as not all extracellular *C. neoformans* cells could be removed at 2hpi. Therefore, the fold change in the number of infected J774 cells, rather than the change in the number of intracellular *C. neoformans* cells, were assessed over 18 hours (Figure 13B) – an increase in the number of infected J774 cells is indicative of increased phagocytosis rather than intracellular replication. Importantly, there was a significantly higher fold change in the number of J774 cells that contained 52D *C. neoformans* over 18 hours compared to those that contained the highly virulent H99α WT and KN99α WT strains of *C. neoformans*. This difference therefore supports the notion that 52D *C. neoformans* is not better at replicating inside J774 cells, but rather is more susceptible to being phagocytosed compared to other strains. However, the H99α IFNγ strain did not appear to be phagocytosed more, and so appears to replicate intracellularly as much as the highly virulent strains of *C. neoformans* (KN99α WT, H99α WT).

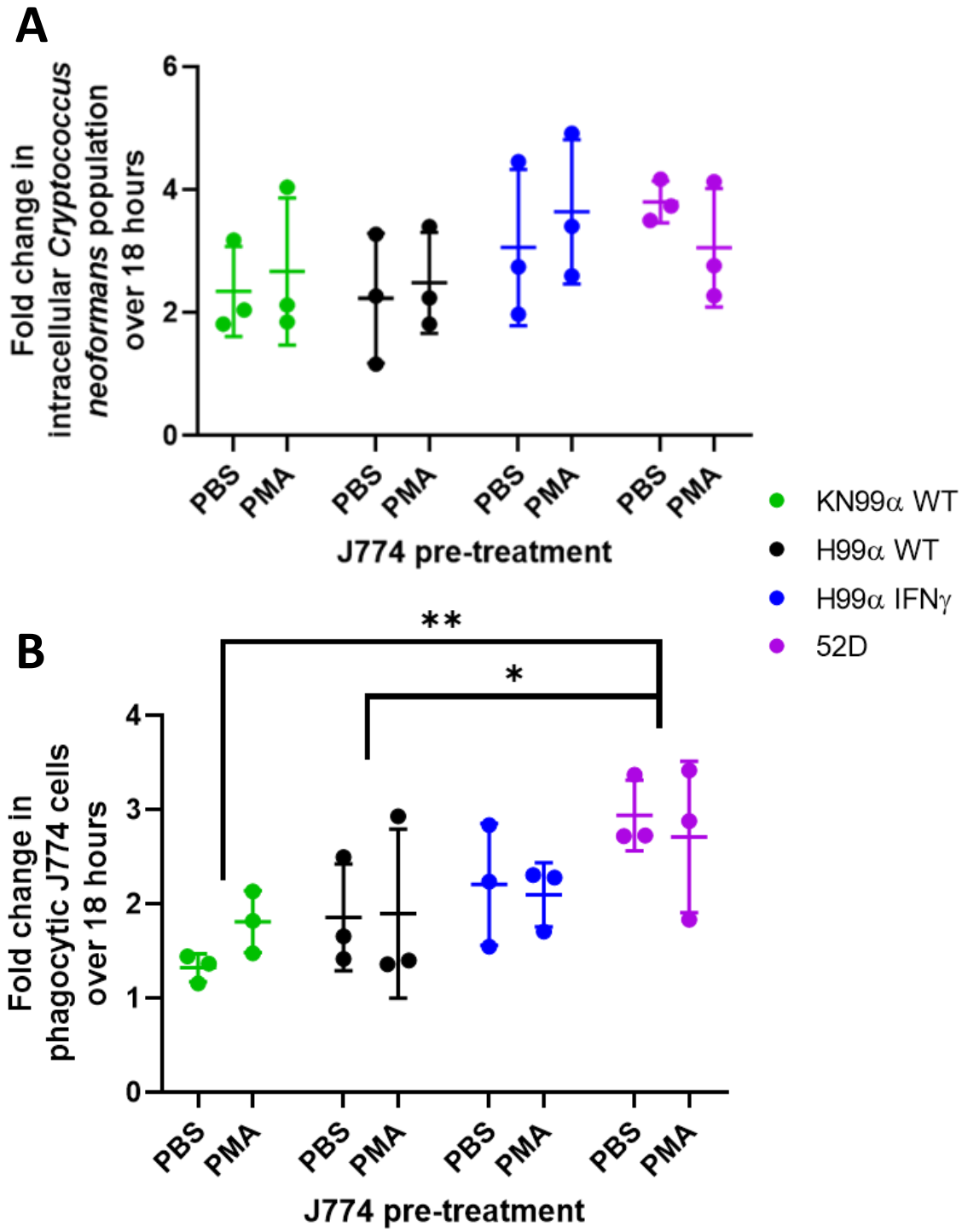
A
Fold change in intracellular *Cryptococcus neoformans* population over 18 hours
0
2
4
6
PBS
PMA
PBS
PMA
PBS
PMA
PBS
PMA
J774 pre-treatment
KN99α WT
H99α WT
H99α IFNγ
52D
B
Fold change in phagocytic J774 cells over 18 hours
**
*
0
1
2
3
4
PBS
PMA
PBS
PMA
PBS
PMA
PBS
PMA
J774 pre-treatment

Figure 13 - Significantly more J774 cells become infected with 52D *C. neoformans in vitro* over 18 hours compared to other strains. The fold change in the number of intracellular *C. neoformans* cells within J774 cells over 18 hours did not vary significantly between strains, but there was a significant increase in the number of J774 cells infected with 52D *C. neoformans* compared to other strains during this time period. (**A**) There was no significant difference in the fold change in intracellular *C. neoformans* cells over 18 hours of *in vitro* infection regardless of treatment. Interaction – $F(3,16)=0.5239$, $p=0.6720$. PMA treatment – $F(1,16)=0.06519$, $p=0.8017$. Strain – $F(3,16)=1.902$, $p=0.17$. (**B**) The increase in the number of J774 cells infected with 52D *C. neoformans* over 18 hours was significantly higher than the increase in infected J774 cells with either KN99α WT ($p=0.0071$) or H99α WT ($p=0.0471$) strains of *C. neoformans*. Interaction – $F(3,16)=0.4596$, $p=0.7143$. PMA treatment – $F(1,16)=0.04233$, $p=0.8396$. Strain – $F(3,16)=5.358$, $p=0.0095$. Fold changes in both the number of intracellular *C. neoformans* cells and phagocytic J774 cells were compared using a two-way ANOVA with *post hoc* Tukey's multiple comparisons where appropriate. Data shown is mean ± SD. Each point represents the mean value of three fields of view from one experiment. * - $p<0.05$, ** - $p<0.01$.

3.2.6 – Significantly fewer 52D *C. neoformans* cells replicate inside PMA treated J774 cells compared to other strains

It was clear that there was significant difference in the *in vitro* host-pathogen interactions of J774 cells with 52D *C. neoformans* compared to other strains – specifically that the 52D strain appeared to be phagocytosed significantly more over 18 hours. However, the ability for 52D *C. neoformans* cells to replicate intracellularly within J774 cells had yet to be directly measured. Additionally, there had been no evidence of avirulence in the interactions of the H99α IFNγ strain with J774 cells, despite being less virulent *in vivo*.

All readouts up until this point had been the product of comparing single images at 2 and 20hpi. Therefore, intracellular *C. neoformans* cells were manually tracked over 18 hours and the number of cells of each strain observed to replicate intracellularly were quantified. Only replication events of intracellular *C. neoformans* cells that were present in the first frame of the time lapse were counted, and for a cell to count as non-replicating it had to be visible and remain intracellular for the entire 18 hours. The proportion of intracellular *C. neoformans* cells that replicated were then compared.

Contrary to intracellular fold change data (Figure 13A), a significant effect of PMA pre-treatment on the proportion of *C. neoformans* cells that replicated inside J774 cells was observed (Figure 14). Although specific differences could not be identified, the proportion

of 52D *C. neoformans* cells that replicated was lower compared to other strains – potentially providing further evidence that 52D *C. neoformans* is less well adapted to the intracellular environment of macrophages. However, the proportion of other *C. neoformans* strains that replicated intracellularly appeared to be similar. However, this data suggests that the hypovirulence of the H99α IFNγ strain is not due to an increased susceptibility to macrophage responses.

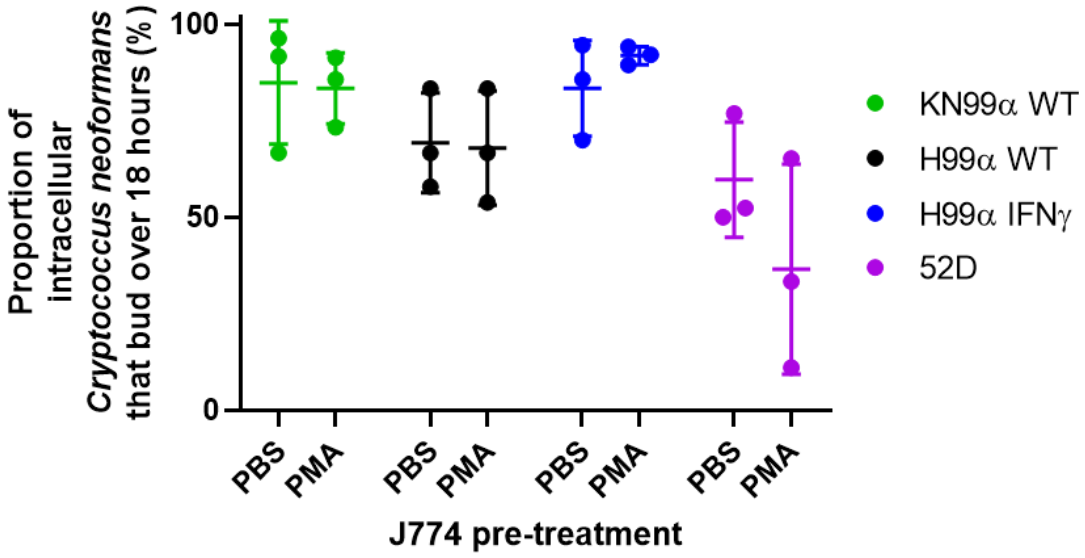

Figure 14 – PMA pre-treatment significantly affects the proportion of *C. neoformans* cells that replicate intracellularly within J774 cells. Although specific differences could not be determined, PMA pre-treatment was observed to significantly affect the proportion of intracellular *C. neoformans* cells that replicated within J774 cells *in vitro* over 18 hours. Untreated cells: Kruskal-Wallis statistic=5.082, number of groups=4, number of values=12, adjusted p value=0.3402. PMA treated cells: Kruskal-Wallis statistic=9.051, number of groups=4, number of values=12, adjusted p value=0.0064. Proportions of intracellular *C. neoformans* cells that replicated were compared using Kruskal-Wallis tests, one for untreated cells and one for PMA pre-treated cells, with *post hoc* Dunn's multiple comparisons where appropriate. All presented p values are corrected for multiple comparisons (each result was multiplied by two). Data shown is mean ± SD. Each point represents the mean value of three fields of view from one experiment. ** - p<0.01.

3.2.7 – Unique host-pathogen interactions can be observed between *C. neoformans* and J774 cells *in vitro*

While manually tracking intracellular *C. neoformans* cells to quantify intracellular replication, additional host-pathogen interactions were also observed (Figure 15).

The first of these is vomocytosis, also known as non-lytic exocytosis (Figure 15A) – the process by which intracellular *C. neoformans* cells are expelled from macrophages back into the extracellular environment without the death of either cell. This process could have substantially reduced the number of intracellular *C. neoformans* cells and led to lower fold changes in intracellular cell numbers despite increased fungal cell survival. Therefore, vomocytosis is an important mechanism of virulence that should be quantified.

A second behaviour that some intracellular fungal cells were observed to exhibit was a large increase in cell size – a phenotype described a 'big' (Figure 15B). Titan cells are a unique phenotype that *C. neoformans* cells can have characterised by cell sizes larger than 10μm, increased capsule production and polyploidy (Dambuza *et al.*, 2018). Titan cells have been observed in cryptococcosis patient biopsies and are observed to be associated with virulence (Setianingrum, Rautemaa-Richardson and Denning, 2019). For this study, intracellular *C. neoformans* cells observed to be greater than 8μm is diameter were defined as 'big'. This size was chosen as *in vitro* protocols for generating titan cells are currently 72 hours long, so in 18 hours it was assumed cells >8μm in diameter may be indicative of early titan cell formation (Dambuza *et al.*, 2018).

The final phenomena that was also observed is described as 'disappearing' (Figure 15C). While some intracellular *C. neoformans* cells were vomocytosed, some intracellular cells disappeared from the intracellular environment whilst showing no evidence of vomocytosis. This 'disappearing' behaviour could therefore have been indicative of fungicidal activity and the destruction of *C. neoformans* cells – although this could not be determined with certainty in the absence of an appropriate live/dead stain.

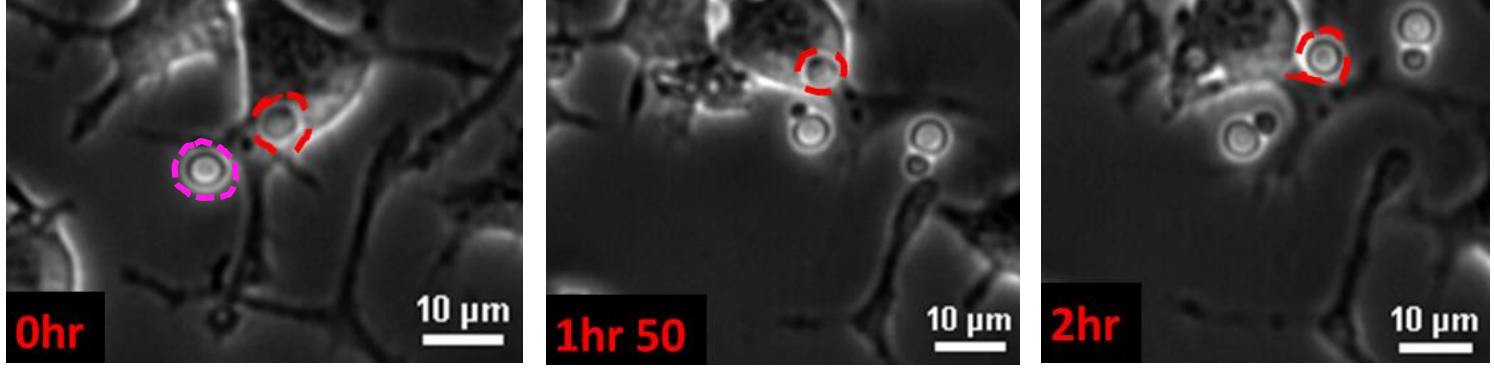
0hr
10 µm
1hr 50
10 µm
2hr
10 µm

B

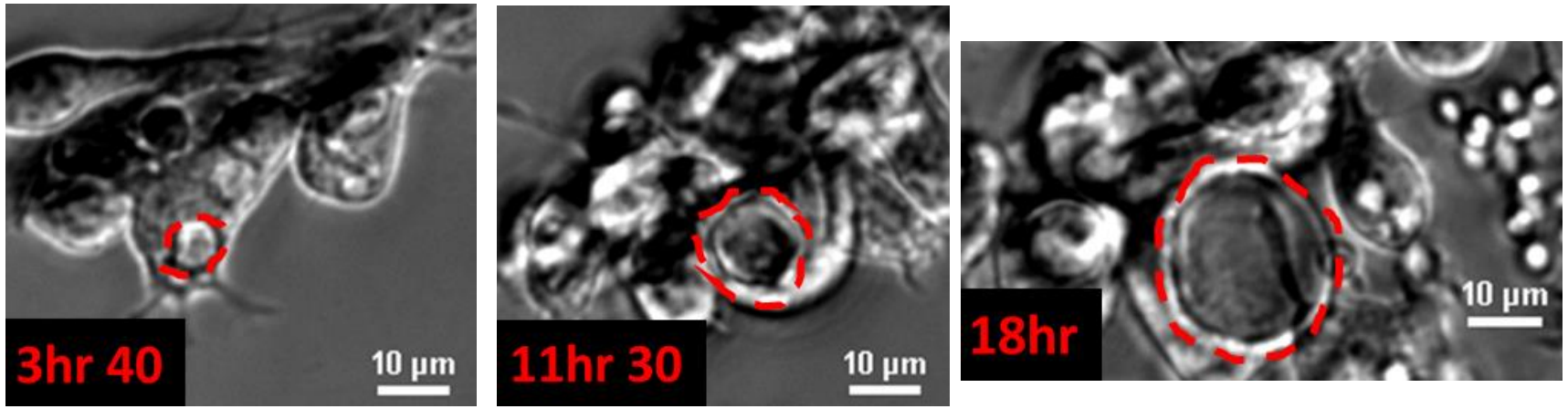
3hr 40
10 µm
11hr 30
10 µm
18hr
10 µm

C

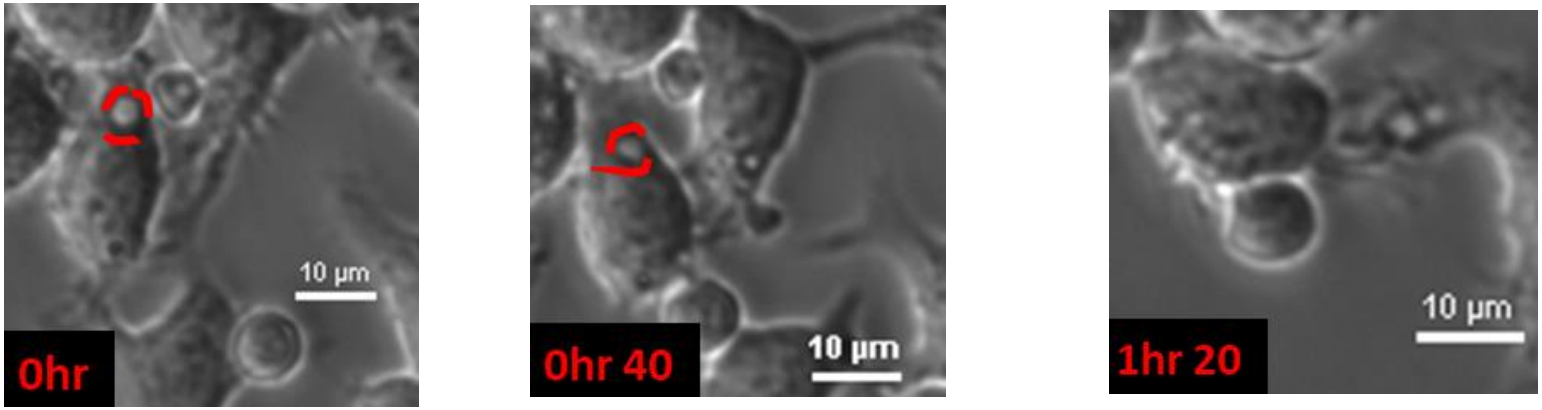
0hr
10 µm
0hr 40
10 µm
1hr 20
10 µm

Figure 15 – Intracellular *C. neoformans* cells and J774 cells exhibit unique host-pathogen interactions *in vitro*. (**A**) Example widefield images (20x) of a *C. neoformans* cell (red dashed line) being vomocytosed from a J774 cell. Also an example of an extracellular *C. neoformans* cell (purple dashed line). (**B**) Example widefield images (20x) of a 'big' *C. neoformans* cell (red dashed line) that grew in size while remaining intracellular. Diameter of cell from left to right - 6.72µm, 13.43µm, 21.83µm. (**C**) Example widefield images (20x) of an intracellular cryptococci (red line) that 'disappeared'.

3.2.8 – Proportions of intracellular *C. neoformans* that exhibited unique host-pathogen interactions were not significantly different between strains

Having identified vomocytosis, 'big' and 'disappeared' behaviours (see 3.2.7), the proportions of intracellular *C. neoformans* cells that exhibited these behaviours following phagocytosis by J774 cells were compared between strains, with and without PMA pre-treatment. Proportions were determined by manually tracking intracellular *C. neoformans* cells over 18 hours – any intracellular *C. neoformans* cells that did not exhibit these any of these behaviours were described as 'normal'.

Despite the association of these behaviours with intracellular survival, there were no significant differences in the proportion of intracellular cells that exhibited these behaviours, regardless of strain or PMA pre-treatment status (Figure 16). This suggests that incidences of these behaviours did not differentially affect intracellular *C. neoformans* cell numbers between strains.

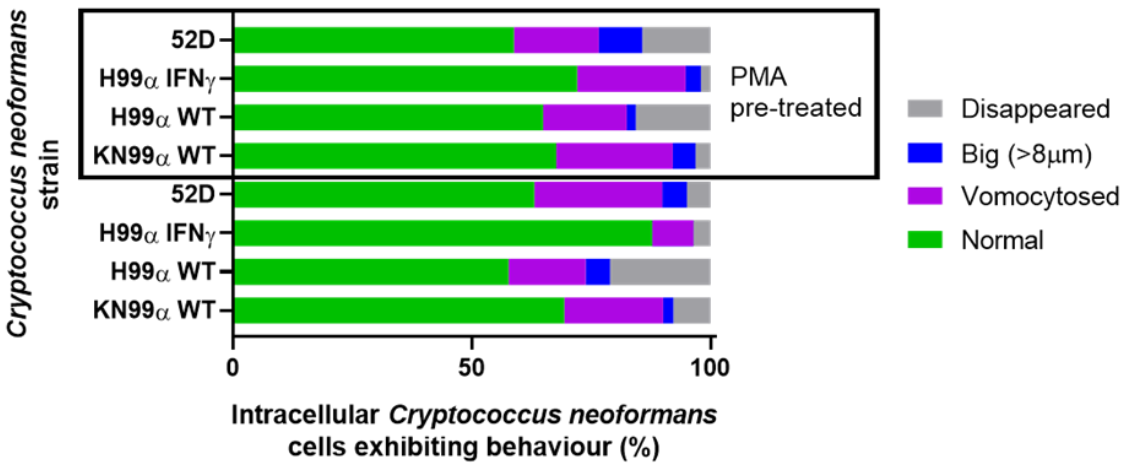

Figure 16 – The proportions of intracellular *C. neoformans* cells that exhibited unique behaviours inside J774 cells were consistent between strains and treatments. No investigated strain of *C. neoformans* showed significant differences in the proportion of intracellular fungal cells that exhibited vomocytosis, 'big', 'disappeared' or 'normal' behaviours, regardless of PMA pre-treatment status. **Normal.** Untreated cells: Kruskal-Wallis statistic=6.59, number of groups=4, number of values=12, adjusted p value=0.1362. PMA treated cells: Kruskal-Wallis statistic=2.084, number of groups=4, number of values=12, adjusted p value>0.9999. **Vomocytosis.** Untreated cells: Kruskal-Wallis statistic=2.282, number of groups=4, number of values=12, adjusted p value>0.9999. PMA treated cells: Kruskal-Wallis statistic=1.769, number of groups=4, number of values=12, adjusted p value>0.9999. **Big.** Untreated cells: Kruskal-Wallis statistic=1.97, number of groups=4, number of values=12, adjusted p value>0.9999. PMA treated cells: Kruskal-Wallis statistic=1.01, number of groups=4, number of values=12, adjusted p value>0.9999. **Disappeared.** Untreated cells: Kruskal-Wallis statistic=4.185, number of groups=4, number of values=12, adjusted p value=0.518. PMA treated cells: Kruskal-Wallis statistic=4.655, number of groups=4, number of values=12, adjusted p value=0.4412. Proportions of *C. neoformans* cells positive for each behaviour were treated as independent, as proportions for different behaviours were not compared to each other. Proportions of intracellular *C. neoformans* cells positive for a unique behaviour were compared using Kruskal-Wallis tests, one for untreated cells and one for PMA pre-treated cells, with *post hoc* Dunn's multiple comparisons where appropriate. All presented p values were corrected for multiple comparisons (each result was multiplied by two). Data shown is mean proportion across three experiments.

3.2.9 – IFNγ treatment of J774 cells does not enhance the early phagocytosis of KN99α GFP

Analysing the host-pathogen interactions of *C. neoformans* reference strains with J774 cells revealed that the moderately virulent 52D strain of *C. neoformans* was relatively less well suited to handling the antifungal activity of J774 cells. However, the less virulent H99α IFNγ strain instead showed comparative intracellular survival to highly virulent strains (H99α WT and KN99α WT) – despite producing murine IFNγ constitutively which is reported to enhance macrophage antifungal activity (Hardison *et al.*, 2010; Jarvis *et al.*, 2012; Kamuyango, 2017). However, due to the intracellular localisation of the majority of *C. neoformans* cells in this assay, it may have been that the IFNγ was not able to interact with the IFNγ receptor on the membrane, the interferon gamma receptor (IFNGR).

Therefore, it was investigated whether exogenous IFNγ improved murine J774 cell handling of intracellular *C. neoformans.* J774 cells were therefore infected with highly virulent KN99α GFP *C. neoformans* in the same assay as above, with some differences. Firstly, previous *in vivo* infections of zebrafish embryo used a GFP expressing transgenic strain of KN99α WT, KN99α GFP (Table 4). Therefore, to recapitulate more elements of previous *in vivo* infections, for these experiments J774 cells were infected with KN99α GFP *C. neoformans* (Kamuyango, 2017). Additionally, the GFP signal would enable *C. neoformans* cells to be more confidently identified *in vitro* rather than just relying on fungal cell morphology, as can be seen in Figure 17A (Voelz *et al.*, 2010). A further difference was the different treatments that were applied to J774 cells. Instead of PMA pre-treatment, J774 cells were instead treated at the time of infection with 100ng/ml of exogenous IFNγ, various concentrations of IL-1β (1, 5, 25, 100ng/ml) or a combination of both. The concentration of IFNγ used was chosen as it was estimated to be the same used in previous studies of IFNγ and J774 cells – as the majority of studies report cytokine treatments in international units rather than concentrations, this makes it impossible to compared amounts between studies without a validation assay (Voelz, Lammas and May, 2009). On the other hand, a variety of IL-1β concentrations were used to determine if there was a dose-response relationship with host-pathogen interactions. Additionally, cytokines were administered at the time of infection to further recapitulate the experimental set up used in the previous *in vivo* zebrafish embryo experiments (Kamuyango, 2017). The final difference was that KN99α GFP cells were opsonised prior to infection with anti-capsular 18B7 IgG, which is well established to increase the phagocytosis of *C. neoformans* by J774 cells (Casadevall *et al.*, 1998). This increased the number of intracellular *C. neoformans* cells, and therefore increased the number of observable intracellular events.

Initially, it was determined whether IFNγ or IL-1β affected the phagocytosis of opsonised *C. neoformans* by J774 cells at 2hpi (Figure 17A). No relationship between IL-1β concentration and the phagocytic proportion of J774 cells was observed, nor was an effect of IFNγ. However, the proportion of phagocytic J774 cells in these experiments (~50%) were higher than was observed with non-opsonised experiments (~20%; Figure 10A) – probably due to *C. neoformans* cells being pre-opsonised with 18B7 IgG for these experiments. Also, no effect of either cytokine was observed on PI values at 2hpi (Figure 16B), suggesting that in the first two hours of *in vitro* infection, neither cytokine significantly affects the recognition or phagocytosis of *C. neoformans* by J774 cells.

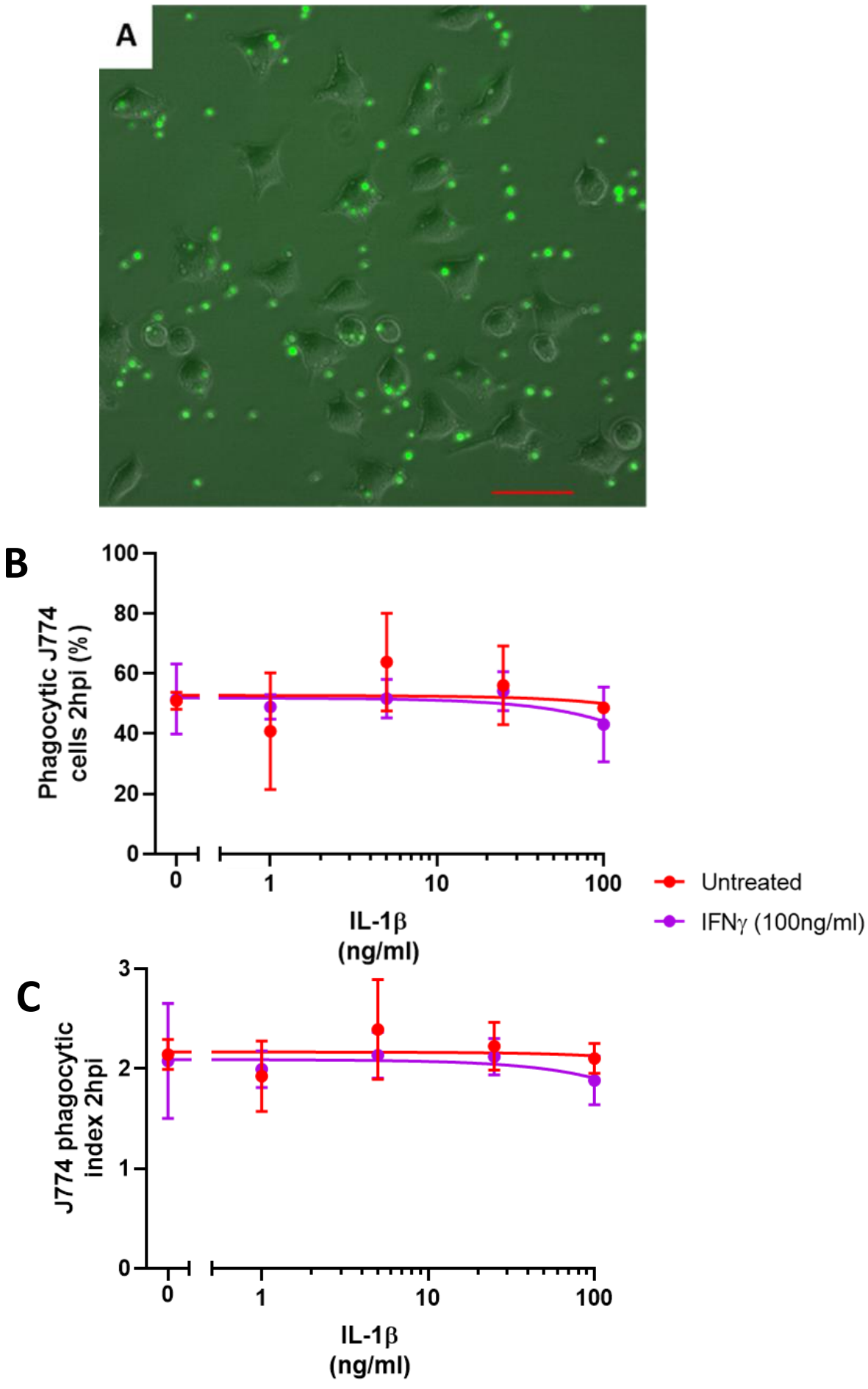
A
B
Phagocytic J774 cells 2hpi (%)
100
80
60
40
20
0
0
1
10
100
IL-1β (ng/ml)
Untreated
IFNγ (100ng/ml)
C
J774 phagocytic index 2hpi
3
2
1
0
0
1
10
100
IL-1β (ng/ml)

Figure 17 – Neither IFNγ or IL-1β significantly affect the phagocytosis of KN99α GFP *C. neoformans* by J774 cells over two hours *in vitro*. There was no clear relationship between cytokine treatment and both the proportion of J774 cells that phagocytosed KN99α GFP cells, or the mean fungal burden of infected J774 cells. (**A**) Representative 20x widefield image showing J774 cells infected with GFP expressing KN99α GFP *C. neoformans* cells (red scale bar - 50μm). (**B**) There was no significant effect of IL-1β treatment on the proportion of J774 cells that phagocytosed KN99α GFP *C. neoformans* cells at 2hpi with untreated (Kruskal-Wallis statistic=2.762, number of groups=5, adjusted p value>0.9999) or IFNγ treated (Kruskal-Wallis statistic=2.433, number of groups=5, adjusted p value>0.9999) J774 cells. Untreated (degrees of freedom=9, R^2=0.1149, sum of squares=2234, Sy.x=15.76) and IFNγ treated (degrees of freedom=10, R^2=0.1727, sum of squares=827.1, Sy.x=9.094) dose-response curves could not be compared due to the weakness of the curve fitting, suggesting that IFNγ also did not affect phagocytic J774 cell proportions. (**C**) IL-1β and IFNγ treatment did not significantly affect infected J774 fungal burdens at 2hpi. Interaction – F(4,19)=0.2462, p=0.9084. IFNγ treatment – F(1,19)=0.9196, p=0.3496. IL-1β treatment – F(4,19)=0.9151, p=0.4754. Additionally, there was a poor fit for untreated (degrees of freedom=9, R^2=0.1109, sum of squares=1.139, Sy.x=0.3558) and IFNγ treated (degrees of freedom=10, R^2=0.07802, sum of squares=1.06, Sy.x=0.3256) dose response curves. Phagocytic J774 proportions at 2hpi were compared using two Kruskal-Wallis tests, one for untreated J774 cells and one for IFNγ treated J774 cells to determine if there was an effect of IL-1β in either treatment condition. Non-linear regression was then used to generate dose-response curves, with a 5-parameter fit, one for untreated J774 cells, and one for IFNγ treated J774 cells, and curves were compared using a sum of squares F-test to determine if there was an effect of IFNγ treatment. All p values for **A** were corrected for multiple comparisons by multiplying by two. The PI values of infected J774 cells at 2hpi was compared using a two-way ANOVA. Non-linear regression with a 5-parameter fit was used to generate dose response curves for both untreated and IFNγ treated cells. Data shown is mean ± SD. Each point represents the mean value of three fields of view from one experiment.

3.2.10 – IFNγ significantly increases the intracellular fungal burden of J774 cells infected with KN99α GFP *C. neoformans* at 20hpi

Next, the intracellular handling of KN99α GFP *C. neoformans* cells by J774 cells was then examined at 20hpi – 18 hours after extracellular cryptococci had been washed away, and there had been more time for changes in J774 expression due to IFNγ and IL-1β.

As was observed at 2hpi, neither IFNγ or IL-1β significantly affected the proportion of J774 cells infected with KN99α GFP *C. neoformans* at 20hpi (Figure 18A). A significant effect of IFNγ was observed on the PI of infected J774 cell at 20hpi (Figure 18B). However, controversially it was observed that there was a significant effect of IFNγ treatment, resulting in increased the mean number of KN99α GFP *C. neoformans* cells per infected J774 cell at all – suggesting increased intracellular fungal replication (Figure 10B). However, there was no significant change in the PI of infected J774 cells with increasing concentrations of IL-1β.

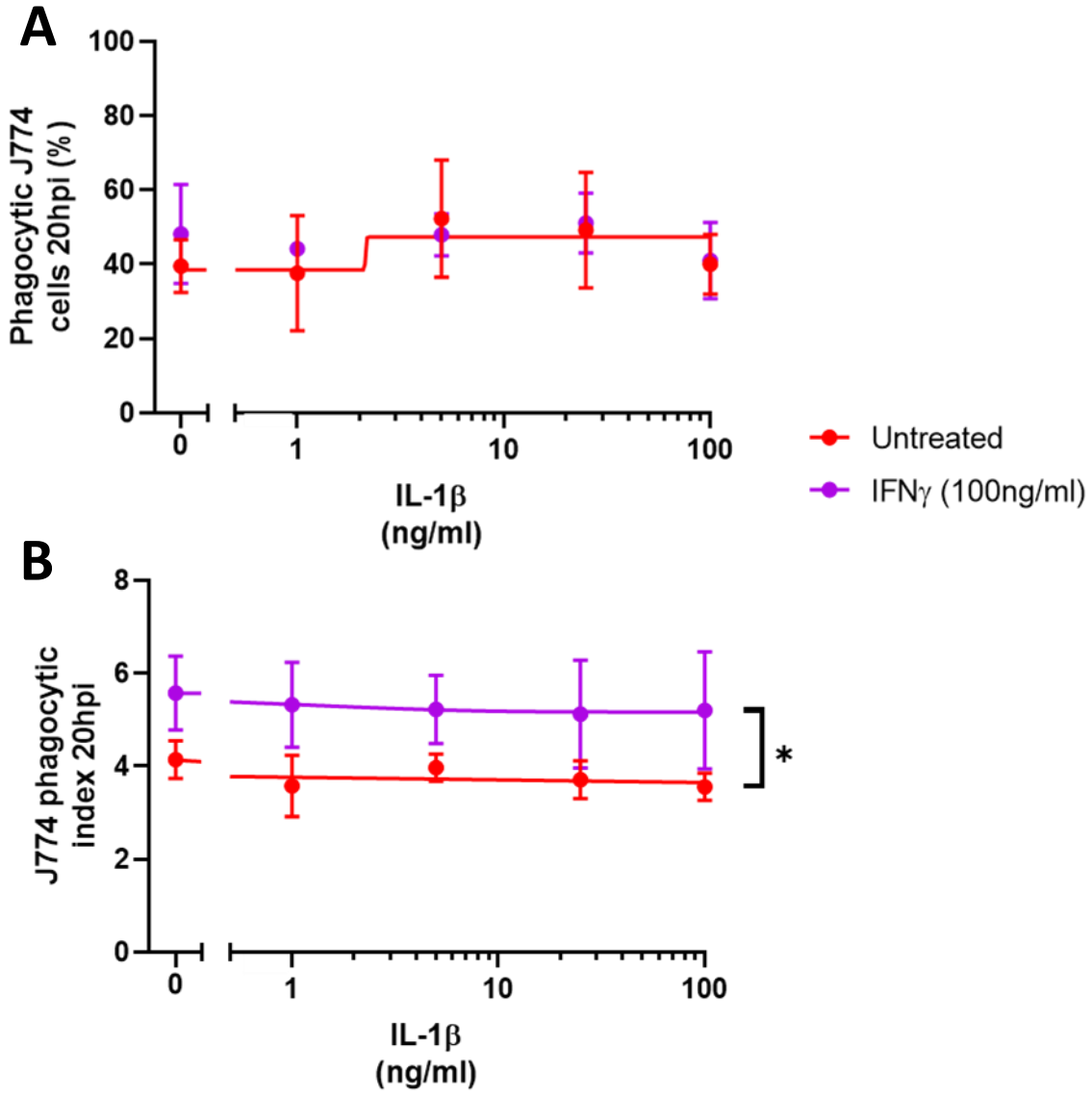

Figure 18 – IFNγ treatment significantly affects the mean J774 cell intracellular burden of KN99α GFP *C. neoformans* cells at 20hpi. IFNγ treatment significantly increased the mean infected J774 intracellular fungal burden at 20hpi, but did not affect the phagocytic proportion of J774 cells. No significant effect of IL-1β was observed on either measure. (**A**) There was no significant effect of IL-1β on the phagocytic proportion of J774 cells at 20hpi with untreated (Kruskal-Wallis statistic=4.010, number of groups=5, adjusted p value=0.9094) or IFNγ treated (Kruskal-Wallis statistic=1.3, number of groups=5, adjusted p value>0.9999) J774 cells. The untreated (degrees of freedom=9, R^2=0.1154, sum of squares=1888, Sy.x=14.48) and IFNγ treated IL-1β dose response curves could not be compared due to the lack of a line of best bit for IFNγ treated J774 cells. (**B**) The PI of infected J774 cells at 20hpi was significantly increased by IFNγ treatment at all concentrations of IL-1β, although there was no significant effect of IL-1β. Interaction – F(4,19)=0.09651, p=0.9823. IFNγ treatment – F(1,19)=0.9196, p<0.0001. IL-1β treatment – F(4,19)=0.3249, p=0.8578. There was no significant effect of IL-1β treatment with both untreated (degrees of freedom=9, R^2=0.1453, sum of squares=2.039, Sy.x=0.476) and IFNγ treated (degrees of freedom=10, R^2=0.03434, sum of squares=9.898, Sy.x=0.9949) cells on PI values at 20hpi. The phagocytic proportions of J774 cells at 20hpi were analysed using non-linear regression to generate dose-response curves for untreated and IFNγ treated datasets with a 5-parameter fit. Two Kruskal-Wallis tests were conducted, one on untreated data and one on IFNγ treated data. All p values from analysis of **A** were corrected for multiple comparisons by multiplying by two. The PI of infected J774 cells at 20hpi were compared using a two-way ANOVA with *post hoc* Sidak multiple comparisons where appropriate. Non-linear regression with a 5-parameter fit was used to generate dose response curves for both untreated and IFNγ treated J774 cells. Data shown is mean ± SD. Each point represents the mean value of three fields of view from one experiment. * - p<0.05, **** - p<0.0001

3.2.11 – IFNγ reduces the total and infected numbers of J774 cells over 18 hours

The significant increase in the mean fungal burden of infected J774 cells due to IFNγ treatment either meant that IFNγ decreased J774 antifungal activity or increased J774 phagocytosis of KN99α GFP *C. neoformans* cells. However, it could also have been due to changes in J774 cell numbers. Therefore, the effect of cytokine treatment on the change in J774 cells between 2 and 20hpi was assessed. Additionally, the change in the numbers of phagocytic J774 cells in this same period were also examined in the context of IL-1β and IFNγ treatment.

Interestingly, IFNγ was observed to significantly reduce the replication of J774 cells, although specific differences could not be identified, nor did there appear to be a significant effect of IL-1β (Figure 19A). IFNγ treatment was also observed to significantly decrease the number of infected J774 cells over 18 hours compared to untreated controls (Figure 19B). These findings provide evidence that IFNγ impairs J774 cell replication, although controversially also decreased the number of infected J774 cells. Importantly, this provides evidence that the increased intracellular burden of infected J774 cells (Figure 18B) was not the result of increased phagocytosis.

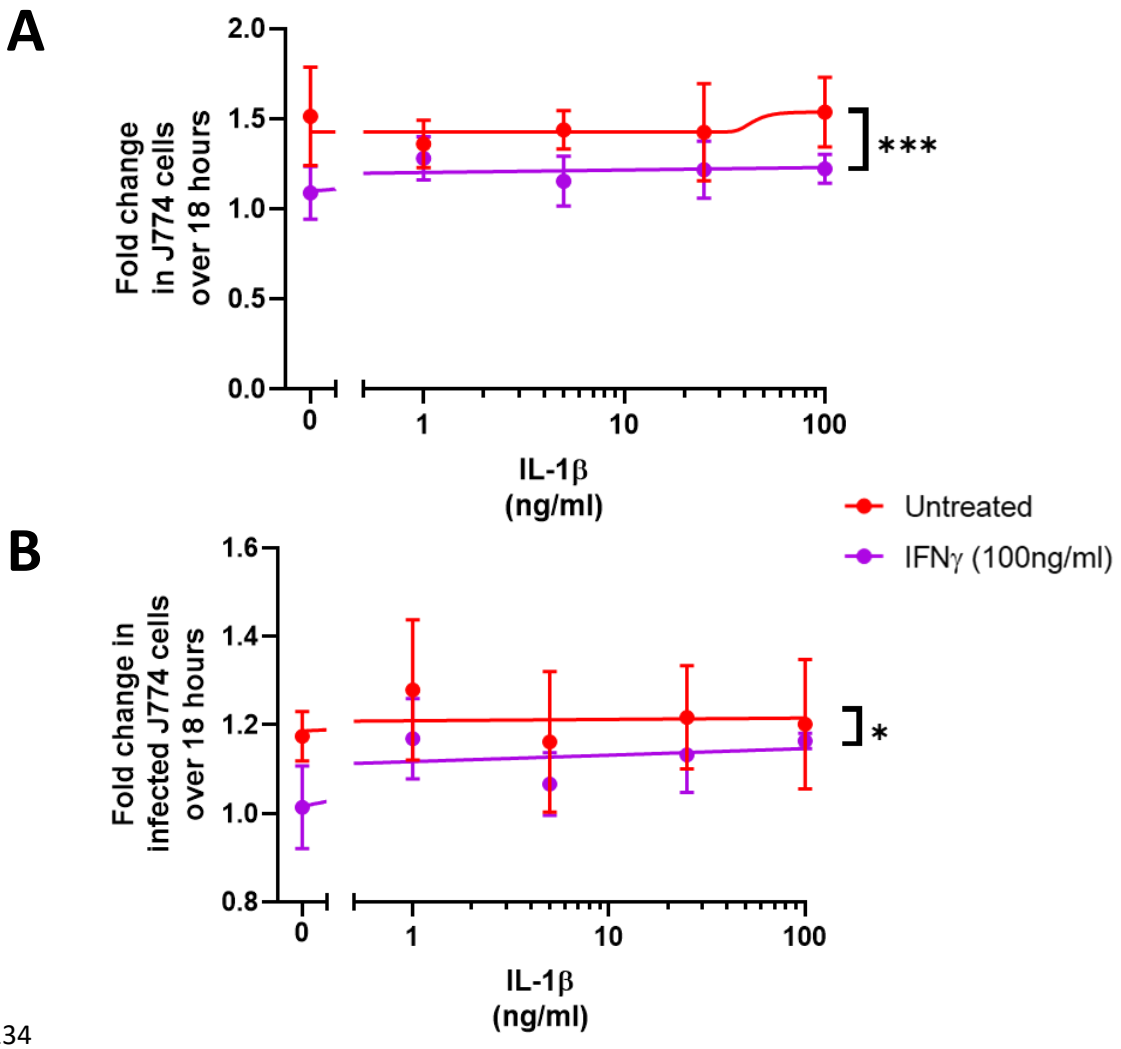

Figure 19 – IFNγ significantly reduced the change in total and infected J774 cell numbers over 18 hours *in vitro*. 100ng/ml IFNγ reduced the proliferation of J774 cells in the presence of KN99α GFP, and resulted in a smaller increase in the fold change in infected J774 cell numbers over 18 hours *in vitro*. (**A**) The replication of J774 cells between 2 and 20hpi was reduced by IFNγ. Interaction – $F(4,19)=0.8151$, $p=0.5312$. IFNγ treatment – $F(1,19)=17.8$, $p=0.0005$. IL-1β treatment – $F(4,19)=0.2288$, $p=0.9188$. There appeared to be no clear relationship between IL-1β concentration and the replication of both untreated (degrees of freedom=9, $R^2=0.0686$, sum of squares=0.3824, Sy.x=0.2061) and IFNγ treated (degrees of freedom=10, $R^2=0.1683$, sum of squares=0.1977, Sy.x=0.1406) J774 cells. (**B**) IFNγ significantly lowered the fold change in the number of J774 cells infected with KN99α GFP *C. neoformans* cells between 2 and 20hpi *in vitro*. Interaction – $F(4,19)=0.2149$, $p=0.9269$. IFNγ treatment – $F(1,19)=5.597$, $p=0.0288$. IL-1β treatment – $F(4,19)=1.275$, $p=0.3145$. There was no clear relationship between IL-1β and fold changes in infected macrophages with untreated (degrees of freedom=9, $R^2=0.01227$, sum of squares=0.1953, Sy.x=0.1473) and IFNγ treated (degrees of freedom=10, $R^2=0.3037$, sum of squares=0.07863, Sy.x=0.08867) J774 cells. The fold changes in total and infected J774 cell numbers were compared using a two-way ANOVA with *post hoc* Sidak multiple comparisons where appropriate. Non-linear regression with a 5-parameter fit was used to generate all dose response curves for both untreated and IFNγ treated J774 cells. Data shown is mean ± SD. Each point represents the mean value of three fields of view from one experiment. * - $p<0.05$, *** - $p<0.001$

3.2.12 – IFNγ increased KN99α GFP *C. neoformans* replication within J774 cells

Knowing that IFNγ significantly affected the replication of J774 cells, it was also established whether IFNγ affected the replication of intracellular KN99α GFP *C. neoformans* cells. Therefore, the fold change in the number of intracellular KN99α GFP *C. neoformans* cells between 2 and 20hpi was determined in the presence of cytokine treatment. Treating J774 cells at the time of infection with IFNγ resulted in significantly higher fold changes in the number of intracellular KN99α GFP *C. neoformans* cells (Figure 20). This suggests that controversially, in this model, IFNγ actually decreased the antifungal activity of J774 cells, reducing their ability to inhibit intracellular fungal replication. Again, individual differences could not be identified, but higher fold changes in intracellular numbers of KN99α GFP cell numbers were observed with IFNγ at all tested concentrations of IL-1β. Additionally, there was no clear relationship between IL-1β concentration and the fold change in the number of intracellular KN99α GFP *C. neoformans* cells over 18 hours, suggesting that this cytokine had no significant effect.

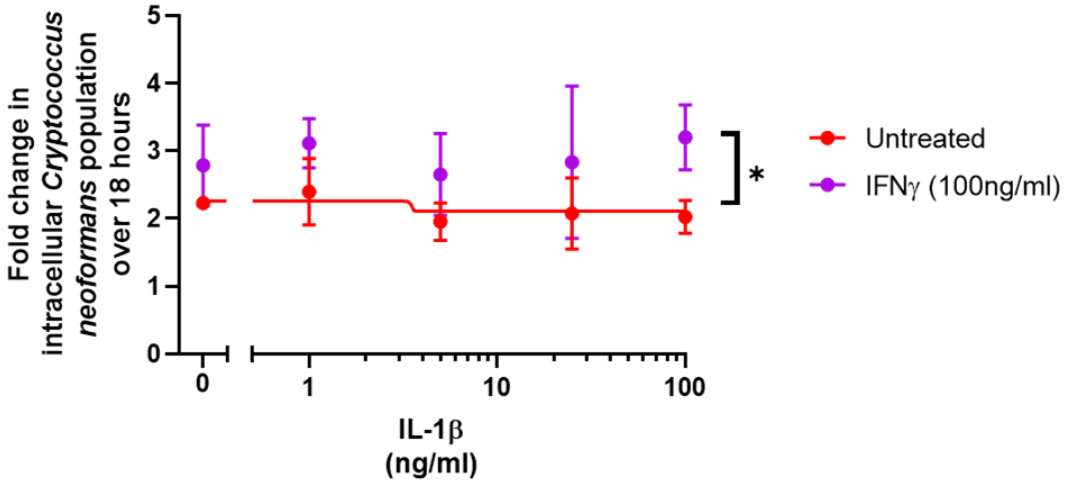

Figure 20 – IFNγ increased the fold change in intracellular KN99α GFP *C. neoformans* cells within J774 cells over 18 hours. Administered at the time of infection, IFNγ results in significantly increased numbers of intracellular *C. neoformans* KN99α GFP cells between 2 and 20hpi within J774 cells. Interaction – F(4,19)=0.2463, p=0.9084. IFNγ treatment – F(1,19)=13.81, p=0.0015. IL-1β treatment – F(4,19)=0.5453, p=0.7046. There was no evidence of a clear dose-response relationship for untreated (degrees of freedom=9, R^2=0.1616, sum of squares=1.417, Sy.x=0.3968) J774 cells, and a dose-response curve could not be fit for IFNγ treated J774 cell data. Fold changes in intracellular KN99α GFP *C. neoformans* cell numbers were compared using a two-way ANOVA with *post hoc* Sidak multiple comparisons where appropriate. Non-linear regression with a 5-parameter fit was used to model dose-response relationships. Data shown is mean ± SD. Each point represents the mean value of three fields of view from one experiment. * - p<0.05.

3.2.13 – Treating J774 cells with IFNγ increased the proportion of intracellular KN99α GFP *C. neoformans* cells that replicated inside J774 cells

Although there was strong evidence that IFNγ enabled increased the replication of intracellular KN99α GFP *C. neoformans* cells within J774 cells over 18 hours, it had yet to be determined whether this was the result of increased replication by either a few intracellular *C. neoformans* cells or the general intracellular *C. neoformans* population. Therefore, the proportion of intracellular KN99α GFP *C. neoformans* cells that replicated over 18 hours were quantified. Due to the high amount of phagocytosis as a result of intracellular cells as a result of pre-opsonising KN99α GFP cells with 18B7 IgG, only 25 intracellular KN99α GFP cells were tracked per field of view. Additionally, only the fate of intracellular KN99α GFP *C. neoformans* cells that were contained in J774 cells that only contained one fungal cell at 2hpi were analysed for ease of tracking.

The presence of IFNγ significantly increased the proportion of intracellular KN99α GFP *C. neoformans* cells that replicated, although specific differences could not be determined (Figure 21). Additionally, although there was no significant effect of IL-1β on intracellular KN99α GFP *C. neoformans* cell replication, non-linear regression of untreated J774 cells showed evidence of an inverse relationship between IL-1β concentration and intracellular replication. This suggests that higher concentrations of IL-1β may result in lower numbers of intracellular KN99α GFP *C. neoformans* cells that replicate. Interestingly, evidence of this relationship was lost in the presence of IFNγ, suggesting the two cytokines may have had opposing actions *in vitro*.

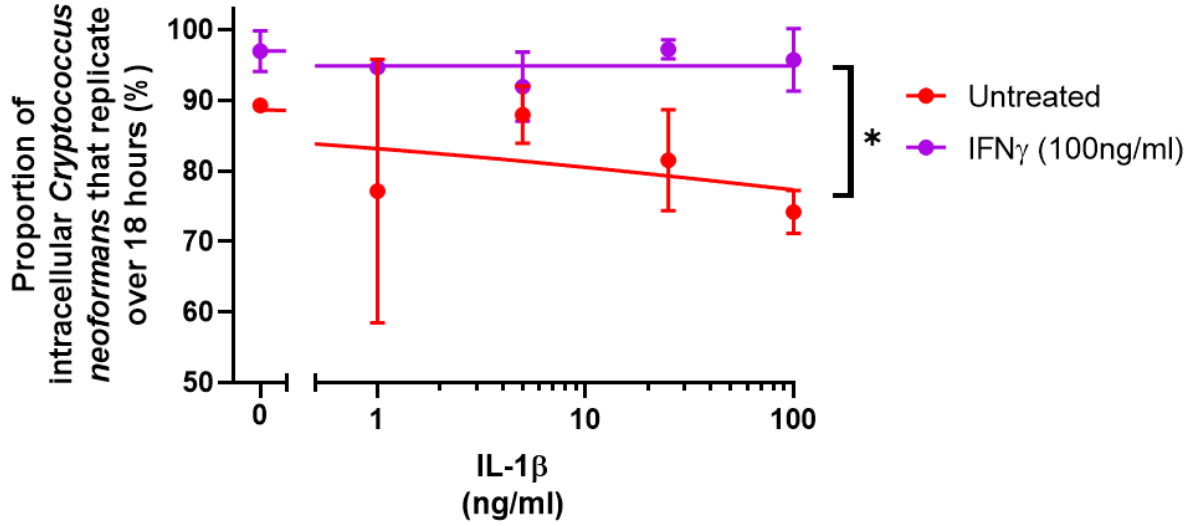

Figure 21 – A higher proportion of intracellular KN99α GFP *C. neoformans* cells replicate within J774 cells treated with IFNγ. The proportion of the intracellular KN99α GFP *C. neoformans* cell population that replicated was significantly larger in the presence of IFNγ (F=4.829 (5, 19), adjusted p value=0.0153). No significant effect of IL-1β treatment was observed with untreated (Kruskal-Wallis statistic=5.889, number of groups=5, adjusted p value=0.6321) or IFNγ treated (Kruskal-Wallis statistic=5.289, number of groups=5, adjusted p value=0.8283) J774 cells. However, non-linear regression did show evidence of a dose-response relationship between IL-1β concentration and the proportion of *C. neoformans* cells that replicated intracellularly with untreated J774 cells (degrees of freedom=9, R^2=0.1674, sum of squares=1095, Sy.x=11.03), with an EC_{50} of 41.86ng/ml and a Hill value of 1.498. This relationship, however, appeared to be lost in the presence of IFNγ (degrees of freedom=10, R^2=0, sum of squares=164.4, Sy.x=4.055). Replicating intracellular KN99α GFP *C. neoformans* cell populations were analysed using non-linear regression with a 5-parameter fit to generate dose-response curves, one for untreated and one for IFNγ treated J774 cells. The resulting curves were compared using a sum of squares F-test. Then, Kruskal-Wallis tests were conducted, one on untreated data and one on IFNγ treated data, to determine if IL-1β treatment resulted in significant differences. All p values are corrected for multiple comparisons by multiplying by three. Data shown is mean ± SD. Each point represents the mean value of three fields of view from one experiment. * - $p<0.05$.

3.2.14 – Neither IFNγ or IL-1β affected the incidence of unique host-pathogen interactions between intracellular KN99α GFP *C. neoformans* and J774 cells

In addition to assessing the proportion of intracellular KN99α GFP *C. neoformans* cells that replicated intracellularly, the proportion of intracellular fungal cells that exhibited other host-pathogen interactions were compared to see if they were also affected by cytokine treatment (see 3.2.7, Figure 15 and 16).

Figure 22 shows that all the intracellular *C. neoformans* behaviours previously described were also observed with intracellular KN99α GFP *C. neoformans* (Figure 15 and 16). However, no significant differences in the proportion of intracellular KN99α GFP *C. neoformans* cells that exhibited these behaviours were identified due to either IFNγ or IL-1β treatment. Importantly, this suggests that differences in KN99α GFP *C. neoformans* replication are likely not due to other behaviours, such as vomocytosis.

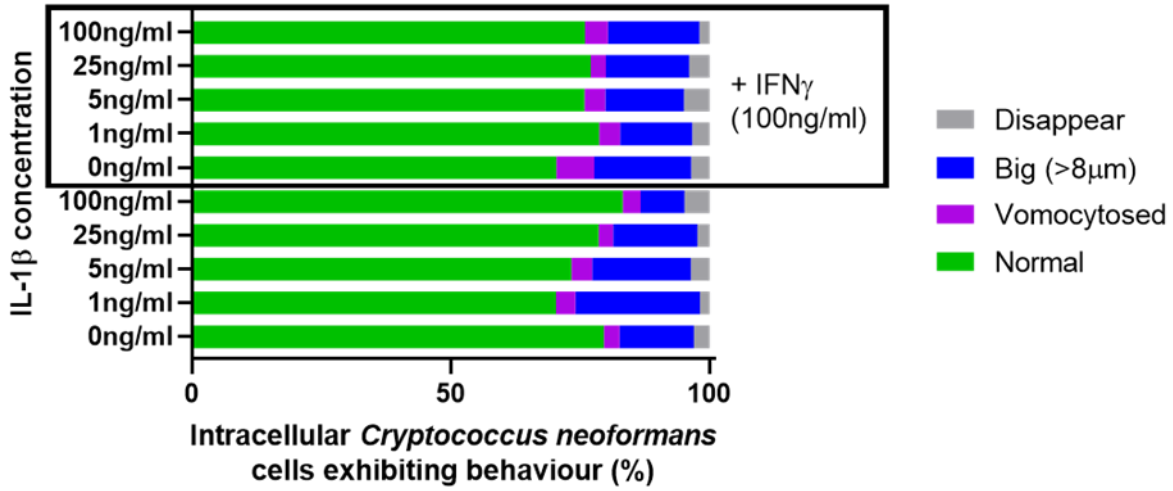
IL-1β concentration
100ng/ml
25ng/ml
5ng/ml
1ng/ml
0ng/ml
+ IFNγ
(100ng/ml)
100ng/ml
25ng/ml
5ng/ml
1ng/ml
0ng/ml
0
50
100
Intracellular Cryptococcus neoformans
cells exhibiting behaviour (%)
Disappear
Big (>8μm)
Vomocytosed
Normal

Figure 22 – Proportions of intracellular KN99α GFP *C. neoformans* cells that exhibited unique intracellular behaviours were not significantly affected by IFNγ or IL-1β. Proportions of intracellular KN99α GFP *C. neoformans* cells that were vomocytosed, 'big' or 'disappeared' behaviours were not significantly different between treatment groups. **Normal.** There was no significant difference in the proportion of 'normal' intracellular KN99α GFP *C. neoformans* cells in J774 cells treated with IFNγ compared to those that weren't (F=0.5933 (5, 19), adjusted p value>0.9999). Additionally, 'normal' proportions were not affected by IL-1β. Untreated: Kruskal-Wallis statistic=3.029, number of groups=5, number of values=14, adjusted p value>0.9999. IFNγ treated: Kruskal-Wallis statistic=2.367, number of groups=5, number of values=15, adjusted p value>0.9999. **Vomocytosed.** There was no significant difference in the proportion of intracellular KN99α GFP *C. neoformans* cells that were vomocytosed by J774 cells treated with IFNγ compared to those that weren't (F=0.4554 (5, 19), adjusted p value>0.9999). Additionally, vomocytosis was not significantly affected by IL-1β. Untreated: Kruskal-Wallis statistic=0.3955, number of groups=5, number of values=14, adjusted p value>0.9999. IFNγ treated: Kruskal-Wallis statistic=2.033, number of groups=5, number of values=15, adjusted p value>0.9999. **Big.** There was no significant difference in the proportion of 'big' intracellular KN99α GFP *C. neoformans* cells within J774 cells treated with IFNγ compared to those that weren't (F=1.026 (5, 19), adjusted p value>0.9999). Additionally, 'big' proportions were not affected by IL-1β. Untreated: Kruskal-Wallis statistic=5.886, number of groups=5, number of values=14, adjusted p value=0.6372. IFNγ treated: Kruskal-Wallis statistic=2.262, number of groups=5, number of values=15, adjusted p value>0.9999. **Disappeared.** There was no significant difference in the proportion of intracellular KN99α GFP *C. neoformans* cells that disappeared from J774 cells treated with IFNγ compared to those that weren't (F=0.461 (5, 19), adjusted p value>0.9999). Additionally, 'disappeared' proportions were not affected by IL-1β. Untreated: Kruskal-Wallis statistic=1.895, number of groups=5, number of values=14, adjusted p value>0.9999. IFNγ treated: Kruskal-Wallis statistic=5.3, number of groups=5, number of values=15, adjusted p value=0.8301. Proportions of *C. neoformans* cells positive for each behaviour were treated as independent and proportions of different behaviours were not compared to each oth34. Intracellular KN99α GFP *C. neoformans* cell proportions were analysed using non-linear regression with a 5-parameter fit, one for untreated J774 cells, and one for IFNγ treated J774 cells. Dose-response curves were then compared using a sum of squares F-test. To assess the effect of IL-1β treatment on the examined behaviours, Kruskal-Wallis tests were conducted, one on untreated data and one on IFNγ treated data. All p values were corrected for multiple comparisons by multiplying by three.

3.3 – Discussion

Here, I present an *in vitro* J774 cell model that enables the *in vitro* interactions of *C. neoformans* and J774 cells to be modelled and quantified. Using this model, I show that the moderately virulent 52D *C. neoformans* strain is less well adapted to the intracellular fungal environment compared to more highly virulent strains, while the H99α IFNγ strain is well adapted to surviving J774 cell antifungal activity, despite low virulence *in vivo*. Additionally, treatment of J774 cells with IFNγ appears to reduce the ability of J774 cells to control *C. neoformans* infection *in vitro*, with minimal effects of IL-1β treatment observed.

3.3.1 – Interactions of J774 cells and *C. neoformans*

J774 cells are a popular cell line for modelling macrophage behaviours *in vitro*, particularly in cryptococcosis research. This means that the host-pathogen interactions of J774 cells and *C. neoformans* are well characterised. In this study, all non-opsonised strains of *C. neoformans* were phagocytosed at relatively low levels – in agreement with previous observations (Mukherjee, Feldmesser and Casadevall, 1996). However, there is a large difference in PI values at 2hpi between this study and those reported by Mukherjee *et al.* – this is because PI values were calculated differently between studies. Mukherjee *et al*. calculated PI by dividing the intracellular number of *C. neoformans* cells by the total number of macrophages per frame. However, this approach means that PI values in that study were not only affected by the phagocytic capacity of macrophages, but is also affected by the number of macrophages in frame. However, in my study PI values were calculated by dividing the intracellular numbers of *C. neoformans* cells by only the number of infected macrophages – standardising the intracellular fungal burden of infected J774 cells based on the number of J774 cells per frame. Therefore, although the measures used here differ from previously reported studies, both PI and phagocytic proportions when used in combination a useful descriptor of macrophage behaviour.

Another observation was that fold changes in the intracellular number of *C. neoformans* cells between 2 and 20hpi did not always match the proportions of intracellular *C. neoformans* cells that replicated inside J774 cells. Fold changes in the number of intracellular pathogens within macrophages are a higher throughput measure of *in vitro* host-pathogen interactions as intracellular fungal burdens only have to be determined at two time points. However, there are some potential issues with this value. Although extracellular *C. neoformans* were washed off after 2 hours, this process is not 100% efficient and extracellular cells are still present in these assays and additional phagocytosis can occur between 2 and 20hpi. This can result in higher number of intracellular fungal cells – the resulting higher fold changes in intracellular *C. neoformans*

cell numbers may be misinterpreted as increased fungal replication and lower J774 antifungal activity. Additionally, fold changes in intracellular numbers of *C. neoformans* may mean that actually phagocytosis of 52D was just significantly slower – also explaining the significantly higher fold change. In this instance, although uptake was slower, this could still mean that phagocytosis eventually caught up. However, in the case of infection, this could still have significant effects on virulence and pathology. Given more time to evade immune cell activity, this may allow for more adaptation to the host environment, such as more increased GXM production or larger cell size.

Additionally, both non-lytic exocytosis and J774 cell death result in *C. neoformans* cells being released into the extracellular environment. In contrast, this would result in lower fold changes in intracellular *C. neoformans* numbers, which could be wrongly interpreted as increased J774 antifungal activity despite increased fungal cell escape. Although vomocytosed cells could be phagocytosed again, this is unlikely to occur, as in response to being phagocytosed, *C. neoformans* cells increase their capsule size, making vomocytosis a second time less likely (Bojarczuk *et al.*, 2016). Therefore, while fold change in intracellular *C. neoformans* cell numbers are a useful descriptor of host-pathogen interactions, this measure can be misinterpreted. Therefore, the proportion of intracellular *C. neoformans* cells that replicate, which involves manually tracking cells, is a more direct measure that is less affected by confounding factors or opposing processes. On the down side, as this analysis produces a proportion (% intracellular cells that replicate), non-parametric statistical tests are required (Warton and Hui, 2011) – these tests have lower power which can increase the number of repeats required for sufficient power. Additionally, this analysis can be time consuming. This highlights the importance of selecting readouts during the design of a study, as well as what to consider when interpreting these metrics.

All the strains of *C. neoformans* that were compared in this study were phagocytosed by J774 cells in equal measure regardless of their virulence *in vivo* – implying that the early uptake of *C. neoformans* by J774 cells does not correlate with improved infection outcomes. However, the idea that phagocytosis is not correlated with improved host outcomes is not controversial – other studies have observed that the phagocytosis of clinical isolates of *C. neoformans* by J774 cells over 2 hours instead inversely correlates with virulence in patients (Sabiiti *et al.*, 2014). This provides evidence that macrophages are not sufficient for host protection and fail to control intracellular *C. neoformans* replication. *In vivo*, phagocytosis by macrophages that then fail to control intracellular replication may instead contribute to the pathology of cryptococcosis, providing an environment permissive for fungal growth that is protected from extracellular mechanisms of host defence (Kechichian, Shea and Del Poeta, 2007; Charlier *et al.*,

2009). Even when macrophage antifungal activity was observed *in vivo*, this has been found to be independent of phagocytosis – we previously showed in our lab that while treating zebrafish embryos with IFNγ enhanced clearance of *C. neoformans* via the action of macrophages, this enhanced fungal clearance was found to be independent of macrophage phagocytosis (Kamuyango, 2017). Therefore, assessing the intracellular survival of *C. neoformans* cells within macrophages is likely to be a more translatable measures of macrophage antifungal activity.

The intracellular growth of *C. neoformans* within macrophages is a signature host-pathogen interaction that has been observed both *in vitro* and *in vivo* (Tucker and Casadevall, 2002; Bojarczuk *et al.*, 2016). Many *Cryptococcus* virulence factors, that are critical for virulence *in vivo*, have been identified to play a role in intracellular survival – including PLB1 (Evans *et al.*, 2015), laccase (Sabiiti *et al.*, 2014; Hansakon, Ngamskulrungroj and Angkasekwinai, 2020), urease (Fu *et al.*, 2018) and the *Cryptococcus* capsule (Feldmesser *et al.*, 2000; Bojarczuk *et al.*, 2016). In this study, all four of the reference strains of *C. neoformans* investigated were observed to replicate inside J774 cells, highlighting how well conserved this ability is by pathogenic cryptococci. Additionally, higher levels of intracellular replication observed with KN99α WT and H99α WT *C. neoformans* cells is unsurprising given that both of these strains are the most virulent in mouse models of infection (Nielsen *et al.*, 2003). Furthermore, reduced intracellular replication was observed with 52D *C. neoformans* when J774 cells were pre-treated with PMA. This strain is comparatively less virulent *in vivo,* suggesting that this lower virulence may be due to an increased susceptibility to pro-inflammatory macrophages – providing further evidence of an association between the intracellular replication of *C. neoformans* in macrophages *in vitro* and virulence *in vivo* (Zaragoza *et al.*, 2007).

3.3.2 – IFNγ fails to enhance J774 control of intracellular *C. neoformans*

However, the H99α IFNγ strain of *C. neoformans* was an exception to this trend. In this study, the proportions of H99α IFNγ cells that replicated intracellularly were as high as was observed with H99α WT and KN99α WT strains, despite H99α IFNγ *C. neoformans* being comparatively the least virulent strain *in vivo* (Wormley *et al.*, 2007; Castro-Lopez *et al.*, 2018). Pulmonary infection with H99α IFNγ *C. neoformans* infection resulted in 0% mortality in BALB/c mice (Wormley *et al.*, 2007) and although there was mortality when this was repeated with C57BL/6 mice (~40%), this was still significantly less than the mortality that was observed when the same animals were infected with the parental H99α WT strain (100%, Castro-Lopez *et al.*, 2018). This disconnect between the hypovirulence of H99α IFNγ infection *in vivo* and the high levels of intracellular replication of H99α IFNγ

cells *in vitro* suggests that the hypovirulence of this strain is independent of macrophages. However, despite the association of macrophages with cryptococcosis host immunity, this is not the first time macrophages and IFNγ have been proposed to be independent. IFNγ is associated with Th1 responses, which are associated with improved host outcomes and fungal clearance in cryptococcosis models and patients (Arora *et al.*, 2011; Jarvis *et al.*, 2012). *In vivo* mouse studies have revealed that H99α IFNγ infection resulted in a Th1 skewed immune response, characterised by increased Th1 marker expression (iNOS) and decreased expression of Th2 markers (IL-4, arginine), resulting in lower fungal burdens (Hardison *et al.*, 2010). However, Hardison *et al.* noted that fungal clearance in the lungs of these animals did not correlate with macrophage numbers in the lung – also suggesting that the improved control and clearance of H99α IFNγ is not dependent on macrophages.

Instead, it may be that the protective action of IFNγ is by enhancing the antifungal activity of cell types other than macrophages. Other cells known to significantly interact with *C. neoformans* include NK cells, T cells and DCs; all three of these cell types are known to have antifungal activity against *C. neoformans* and be affected by IFNγ (Kawakami, Koguchi, Qureshi, Yara, *et al.*, 2000; Uicker, McCracken and Buchanan, 2006; Wozniak *et al.*, 2009). Therefore, the interactions of these cell types with H99α IFNγ and H99α WT *C. neoformans* should be assessed *in vitro* to determine whether the antifungal activity of these cells were significantly enhanced by IFNγ.

It is also possible that the H99α IFNγ strain of *C. neoformans* used for these experiments was significantly different from the H99α IFNγ strain originally described (Wormley *et al.*, 2007). Although the originally described antibiotic resistance phenotype of the H99α IFNγ strain was confirmed (Figure 9), neither the IFNγ producing phenotype or genotype were confirmed. An attempt was made to confirm IFNγ production in these cells by ELISA (Invitrogen, California, USA; item number 88-7314), although this data was lost due to files becoming corrupted during the backup process and therefore cannot be shown. Overnight cultures of H99α IFNγ *C. neoformans* were grown at 37ºC, in multiple media (COMP DMEM, SF DMEM, YPD or PBS) to control for culture media affecting the detection of IFNγ in samples. Furthermore, each media was spiked with IFNγ at the concentration reported to be produced by H99α IFNγ (50pg/ml) to ensure this concentration could be detected by ELISA. Both non-centrifuged and centrifuged cultures (3300g, 1 minute) were analysed. The assay was run twice, and both times the IFNγ standard curve developed as expected (R^2>0.99) and ~50pg/ml of IFNγ was detected in all spiked samples. However, no fluorescence was observed in any of the H99α WT or H99α IFNγ cultures. This may mean that although the nourseothricin antibiotic resistance selection marker (acetyltransferase) was present in the genome of

H99α IFNγ strain used in this study, the murine IFNγ gene may have been significantly changed.

However, the results seen with exogenous IFNγ treatment in this study provides evidence that IFNγ controversially worsened mammalian macrophage control of intracellular *C. neoformans*. Historically, IFNγ has been reported to enhance various macrophage antimicrobial activity and superoxide production (Goldberg, Belkowski and Bloom, 1990). However, it is important to note that most *in vitro* protocols that use IFNγ to skew macrophages towards a pro-inflammatory phenotype use IFNγ in combination with a TLR4 agonist (Crosby *et al.*, 2010; Qiao *et al.*, 2013). Activation of TLR4 and downstream MyD88 signalling is reported to enhance IFNγ receptor signalling and inhibit interferon regulatory factors (Müller *et al.*, 2017; Piaszyk-Borychowska *et al.*, 2019). However, as no exogenous TLR4 signal was provided in this study, it may have been that IFNγ treatment alone not only failed to induce a sufficiently pro-inflammatory phenotype, but in the case of infected J774 cells, may have actually skewed J774 cells towards a less antimicrobial phenotype. In the absence of a TLR4 signal, IFNγ can negatively impact iron homeostasis. Iron is an important cofactor in the Fenton reaction – an important step in RONS production in macrophages, particularly the production of NO (Gutteridge, 1989; Weiss *et al.*, 1994). *In vitro,* stimulating J774 cells with IFNγ and a concurrent TLR4 signal increases iron uptake via J774 transferrin, increasing NO production (Mulero and Brock, 1999). However, in the absence of a concurrent TLR4 signal, IFNγ actually inhibited iron uptake, reducing J774 cell production of antimicrobial NO. In this study, this may have significantly impeded the antimicrobial capacity of IFNγ treated J774 cells, resulting in the poorer control of intracellular *C. neoformans* over 18 hours that was observed.

However, IFNγ treatment alone was enough to induce host protection by skewing macrophages towards a more pro-inflammatory phenotype in zebrafish embryos *in vivo* (Kamuyango, 2017). There are several model differences that may explain this discrepancy. Firstly, during *in vivo* zebrafish embryo experiments, animals were not kept in sterile water. Therefore, the intramuscular injection may have enabled contamination of the infection site and inadvertently provided a concurrent TLR signal. Alternatively, zebrafish TLR4 signalling is significantly different compared to mammals, known to be non-responsive to LPS (Sepulcre *et al.*, 2009). Therefore, IFNγ signalling may be different in this species and not require a concurrent TLR4 signal to sufficiently enhance macrophage antifungal activity. Also, all mammalian TLRs are reported to recruit MyD88 and zebrafish are known to express eight unique TLRs, it might be that these zebrafish TLRs can recognise and be activated by *C. neoformans* (Quiniou, Boudinot and Bengtén, 2013; Kawasaki and Kawai, 2014).

It is also possible that the TLR4 signal is not required for IFNγ signalling. In the context of other infections, IFNγ treatment alone has been shown to enhance macrophage antimicrobial activity. In the context of *Salmonella enterica* infection, IFNγ pre-treatment of MDMs enhanced non-opsonic uptake and reduced bacterial replication (Gordon *et al.*, 2005) – the latter believed to be due to the increased localisation of ROS to the phagolysosome (Bewley *et al.*, 2017), which has also been observed with MDM interactions with *Streptococcus pneumoniae* (Morris, 2017). It is therefore possible that in my J774 experiments, internalised *C. neoformans* cells were resistant to ROS dependent killing mechanisms, or that this process was different in some way. Confirming ROS levels and their sub cellular localisation would enable this to be examined further.

It is also possible that this experimental approach was not appropriate for modelling IFNγ and J774 cell interactions in the context of *C. neoformans* infection. Firstly, J774 cells are observed to have a pro-inflammatory phenotype even in the absence of stimulation cytokine treatment. Pro-inflammatory macrophages are characterised by production of TNFα and IL-1β (Arango Duque and Descoteaux, 2014). However, unstimulated J774 cells are observed to produce IL-1β constitutively, meaning that these cells may already have a pro-inflammatory phenotype (Hirano *et al.*, 2017). As a result, exogenous IFNγ treatment may have instead induced negative feedback responses, such as via anti-inflammatory IL-10 production. Cytokine levels were not analysed in this experiment but quantifying IL-1β and IL-10 levels would enable this mechanism to be studied further.

Another potential issue with the J774 cell model is their cancerous nature. Being sarcoma derived, J774 cells are able to replicate indefinitely (Ralph and Nakoinz, 1975). While this is a useful feature that makes them a convenient cell line to use, this changed biology means various pathways may be significantly changed compared to *in vivo* experiments. In the case of IFNγ, this cytokine is reported to arrest the cell cycle of cancer cells (Hobeika *et al.*, 1999), which has been previously reported to occur in J774 cells (Goldberg, Nagata and Bloom, 1985) and was observed in this study (Figure 19). It is worth noting that reduced J774 cell replication was not observed with H99α IFNγ experiments, but this is likely because the majority of H99α IFNγ cells were intracellular, whereas the receptor for IFNγ, IFNγ receptor, is only found to signal extracellularly (Marchetti *et al.*, 2006). However, in the case of exogenous IFNγ treatment, inadvertently 'treating' the cancerous nature of J774 cells in this study may have affected additional pathways related to antifungal immunity. However, it is worth noting that even if J774 cell replication was inhibited, IFNγ is still reported to skew macrophages towards a pro-inflammatory phenotype, evidenced by increased iNOS expression (Miyakawa *et al.*, 1989; Blanchette, Jaramillo and Olivier, 2003). However, this study should be repeated

with primary cells, where this cancerous nature is absent, either using mouse AMs or MDMs. However, it is important to note that *C. neoformans* has been observed to also affect J774 cell replication and viability. A study found that *C. neoformans* is able to significantly affect J774 cell numbers (Ben-Abdalleh *et al.*, 2012), both through impairment of the cell cycle and a capsule dependent induction of apoptosis. In this study, this phenotype was only observed at 40hpi – however, was found to be dependent on NFκB. As NFκB is known to induced by pro-inflammatory stimuli, this may have been the mechanism by which IFNγ signalling resulted in reduced J774 replication. However, this would need confirming using a NFκB reporter line.

Other issues with this approach relate to the *in vitro* nature of the experiments*. In vivo*, Th1 T cells are a major source of IFNγ, although T cells also release a substantial number of other mediators that may modulate IFNγ signalling. For example, granulocyte macrophage-colony stimulating factor is released by activated T cells and induces the growth of macrophages (Shi *et al.*, 2006). In J774 cells, the growth stimulating effect of granulocyte macrophage-colony stimulating factor may have protected J774 cells from the cell cycle arrest induced by IFN-γ (Goldberg, Nagata and Bloom, 1985). Therefore, by having other T cell derived signals absent in my J774 model, IFNγ may only have been 'treating' the cancerous nature of J774 cells without skewing cells towards a pro-inflammatory phenotype.

Finally, the lack of increased antifungal activity may be the result of the timing of treatment. In zebrafish embryo *in vivo* experiments, significant fungal clearance due to IFNγ treatment was observed at 48hpi (Kamuyango, 2017). However, in this J774 cell study, fungal burdens were only examined at 20hpi, which may not have been enough time for functional changes in J774 cells due to IFNγ to significantly affect numbers of intracellular *C. neoformans* cells. In support of this, previous *in vitro* studies of IFNγ typically pre-treat J774 cells for >18 hours prior to starting the assay (Miyakawa *et al.*, 1989; Mukherjee *et al.*, 1994). This suggests that this study should be repeated using J774 cells pre-treated with IFNγ. However, it can still be concluded that any beneficial effects of IFNγ on antifungal activity likely require more than 18 hours of treatment. This is because the effects of IFNγ stimulation are primarily mediated by transcription and changes in gene expression. As these changes take time to mediate, it may have been that beneficial changes of IFNγ treatment were not observed. With pre-treatment, these changes may have become apparent, and significantly reduced intracellular *C. neoformans* cell replication. Alternatively, the dose of IFNγ may have been too high or too low. If too high, exogenous IFNγ may have resulted in receptor desensitisation and internalisation, leading to a reflex suppression of inflammation (Farrar and Schreiber, 1993). Alternatively, too low a dose may have failed to sufficient skew J774 cells towards

a pro-inflammatory phenotype that significantly affected host-pathogen interactions (Kamuyango, 2017). This should have been confirmed with a positive control, using a fluorescent reporter line or cytokine assay to establish that IFNγ was having an effect on these cells. Additionally, repeating this study in primary cells, such as mouse BMDMs or human MDMs, which may not be negatively impacted by IFNγ treatment, would also be beneficial.

3.3.3 – IL-1β did not significantly affect the host-pathogen interactions of J774 cells with *C. neoformans*

While IFNγ appeared to worsen J774 cell control of intracellular *C. neoformans*, IL-1β treatment had no significant effect on J774 cell host-pathogen interactions with *C. neoformans* at any investigated concentration. This is interesting as macrophage IL-1β is a marker of pro-inflammatory macrophages and therefore could be assumed to be associated with increased antimicrobial activity (Lin and Hu, 2017). However, there is only minimal evidence for an important role of IL-1β to date in the context of cryptococcosis, both clinically and *in vivo* (see 3.1.3, Marroni *et al.*, 2007; Shourian *et al.*, 2018; Bürgel *et al.*, 2020). Otherwise, the role of IL-1β in cryptococcosis has yet to be fully described, particularly with reference to macrophage responses. This is unlike other infections with an important role for macrophages, where the role of IL-1β is better described – including *Candida albicans* (Vonk *et al.*, 2006; Wellington, Koselny and Krysan, 2013), *Mycobacterium marinum* (as a natural fish pathogen related to *Mycobacterium tuberculosis;* Ogryzko *et al.*, 2019) and the encapsulated bacterial pathogens *Staphylcoccus aureus* (Ali *et al.*, 2017) and *Steptococcus pneumoniae* (Lemon, Miller and Weiser, 2015).

Although not statistically significant, there was evidence of a dose-response relationship between IL-1β and reduced proportions of *C. neoformans* cells that replicate intracellularly (Figure 21). While the effects of IL-1β on macrophages in relation to cryptococcosis have yet to be determined, other IL-1 family cytokines have been shown to have a significant role in cryptococcosis. The IL-1 family cytokine IL-18, also produced by macrophages in response to pro-inflammatory stimuli, has been shown *in vivo* to be important for generating IFNγ responses (Kawakami *et al.*, 1997; Tsutsui *et al.*, 1999; Kawakami, Koguchi, Qureshi, Miyazato, *et al.*, 2000). Importantly, this cytokine is not thought to be expressed by zebrafish, and therefore the elevated IL-1β observed in zebrafish embryo *in vivo* experiments may have been a compensatory function that is fulfilled by IL-18 in mammals (Meijer *et al.*, 2004). The lack of a significant change may also have been the result of a short treatment time as with IFNγ, with previous studies of IL-1β and J774 cells pre-treating cells for days prior to analysis (Jayaraman *et al.*, 2013).

However, it is important to note that the range of IL-1β concentrations used in the Jayaraman *et al*. study are comparable to those used in my experiments, suggesting that dose selection was not the issue in this instance.

It is also important to note that there were no significant effects observed when IFNγ and IL-1β were administered together. However, there did appear to be a loss of an IL-1β dose-response with regard to the proportion of *C. neoformans* cells that replicate inside J774 cells in the presence of IFNγ (Figure 21). This suggests that IFNγ may be antagonistic with regard to any antifungal action of IL-1β, although this has yet to be determined (Goldberg, Nagata and Bloom, 1985; Goldberg, Belkowski and Bloom, 1990). It should also be noted that the number of variables in the IL-1β experiments may have meant statistical analysis was not as powerful as it could have been, particularly given the low n numbers. Instead an IL-1β dose response experiment should have been carried out firstly, in the absence of IFNγ, to establish if there was a clear effect of IL-1β, analysed by non-linear regression. There then should have been second experiment where the effects of a single dose of IFNγ, a single dose of IL-1β, and a combination of both were assessed, which could be analysed by two-way ANOVA. This would have better answered the question if there was an effect of IL-1β, and then separately examined whether IFNγ and IL-1β had significant effects in combination.

3.3.4 – *C. neoformans* exhibits unique interactions with J774 cells *in vitro*

One behaviour that intracellular *C. neoformans* cells exhibited was hugely increased cell size, or 'big' behaviour. Changes in cell size are a well-known aspect of cryptococcal virulence so it is not surprising that this behaviour was observed with all examined strains (Crabtree *et al.*, 2012). Recently, a reliable *in vitro* protocol to generate *C. neoformans* titan cell cultures *in vitro* was published (Dambuza *et al.*, 2018). Interestingly, some of these culture conditions were recapitulated in this J774 cell assay, including temperature (37ºC) and CO_2 (5%). However, other conditions, such as FBS and 72 hours of culture were both absent during the infection *in vitro* study. Despite this, cells approaching or larger than 10μm in diameter were observed in all examined conditions. It is important to note that although some intracellular *C. neoformans* cells met the size requirements to be classified as titan cells, polyploidy could not be confirmed meaning these cells cannot be confirmed to be titan cells. However, the significance of the titan cell morphology has only been studied with regard to virulence *in vivo* (Crabtree *et al.*, 2012), dissemination (Dambuza *et al.*, 2018) and preventing phagocytosis (Okagaki and Nielsen, 2012), with little attention given to their formation intracellularly. However, this phenotypic shift likely important implications for *C. neoformans* intracellular survival and escape from the macrophage intracellular environment. The large increase in capsular content

associated with the titan cell phenotype may increase the intracellular survival of *C. neoformans* cells (Okagaki *et al.*, 2010; Trevijano-Contador *et al.*, 2017). Additionally, the largely increased cell size may result in the lysis of macrophages. However, this requires further investigation.

The other host-pathogen interaction that was observed in all cases and is signature to cryptococcosis was the vomocytosis of *C. neoformans* cells from J774 cells. This process by which intracellular fungal cells can escape back into the extracellular environment is the subject of much research as to its significance in Trojan horse mechanisms of dissemination (Sionov *et al.*, 2015; Gilbert *et al.*, 2017; Santiago-Tirado *et al.*, 2017; Seoane *et al.*, 2020). A surprising finding in this study was that J774 cell treatments did not affect vomocytosis. PMA is known to activate mammalian PKC (Boneh, Mandla and Tenenhouse, 1989), an enzyme also expressed by *C. neoformans*. In fungal cells, PKC is associated with increased Plb1 secretion – a virulence factor strongly associated with vomocytosis (Chayakulkeeree *et al.*, 2008). Therefore, a lack of an effect with PMA pre-treatment suggests that either cryptococcal and mammalian PKC differ enough in structure, or that PMA is not retained intracellularly within J774 cells. However, Plb1 has optimal activity at an acidic pH, and therefore more vomocytosis was anticipated with PMA, IFNγ and IL-1β treatment, as pro-inflammatory macrophages have more acidic phagolysosomes (Evans *et al.*, 2015). Therefore, with this strong association between macrophage inflammatory phenotype and vomocytosis, it is surprising that no significant differences in vomocytosis were observed in any treatment condition.

The final behaviour that was described here was ‘disappearing’ – intracellular *C. neoformans* cells that disappeared from view without evidence of vomocytosis. This behaviour may have been indicative of cell death. However, in the absence of an appropriate live/dead stain compatible with *C. neoformans*, this cannot be confirmed. In this study, this behaviour was rare with KN99α GFP *C. neoformans* cells (<5%; Figure 22), yet appeared to be more common and variable with non-GFP strains of *C. neoformans* (5-25%, Figure 16). This discrepancy with GFP and non-GFP isolates is likely the result of human error – the lack of a fluorophore may have led to various J774 cell intracellular structures being misinterpreted as *C. neoformans* cells. This highlights the importance of fluorophores in image analysis for minimising subjective readouts.

In summary, while the host-pathogen interactions of J774 cells with various reference strains of *C. neoformans* correlate with their virulence *in vivo*, this was not observed when the relationship between intracellular *C. neoformans* and pro-inflammatory cytokines were investigated. While the model was need to be optimised, it does highlight the large difference between *in vitro* and *in vivo* models. These differences may be due to differences in the signals present in the two model systems, the cancer biology of J774

cells or may highlight that enhanced macrophage activity are not critical to host protection in cryptococcosis as first hypothesised. There is also the potential that IFNγ may actually have a detrimental role in host immune responses. There was also minimal evidence of a significant role for IL-1β and no evidence of co-operative action with IFNγ and IL-1β.

Chapter 4 – Establishing an *in vivo* mouse inhalation model of cryptococcosis

4.1 – Introduction

4.1.1 - Issues with non-mammalian *in vivo* models of cryptococcosis

Exposure to *C. neoformans* is thought to be global and ubiquitous (May *et al.*, 2016) – a small clinical study of healthy <21 year olds in an urban environment (Ontario, Canada) found serological evidence of cryptococcal infection in the majority of sampled individuals despite no clinical history (Goldman *et al.*, 2001). Although infection of the CNS is dangerous and often symptomatic (Parikh, Tucci and Galwankar, 2012), cryptococcal meningitis patients are reported to also present with pulmonary colonisation as well (Maziarz and Perfect, 2016). It is therefore assumed that infection with *Cryptococcus neoformans* starts in the lungs, where fungal cells are inhaled into the lower airways and alveoli. There, infection can either be cleared asymptomatically, become latent or grow uncontrolled and eventually disseminate to the CNS. If true, this will mean that the outcome of infection is highly dependent on the pulmonary immune response. Therefore, understanding host-pathogen interactions in this tissue during these earlier stages of cryptococcosis is critical in order to reveal opportunities for new therapies.

Even though pulmonary cryptococcosis is estimated to be common place, there is a distinct lack of clinical data available regarding protective immunity in the lung. This is because in most individuals infection is thought to be asymptomatic, with only susceptible patients presenting to the clinic, and typically for treatment during symptomatic cryptococcal meningitis after dissemination has occurred (Bratton *et al.*, 2012). Therefore, understanding early stage pulmonary cryptococcosis relies almost exclusively on animal models, where predictive power is dependent on the suitability of the model for the hypothesis being tested. For example, invertebrate animal models such as *Galleria* (Mylonakis *et al.*, 2005), *Dictostyllium* (Watkins *et al.*, 2018) and *Drosophila* (Apidianakis *et al.*, 2004) are ideal for high throughput screening or interrogating a conserved biochemical pathway with known disease relevance. However, their significantly different biology and anatomy from humans, however, can greatly limit the translation of findings in these models. Non mammalian vertebrate models, in particular zebrafish, offer a greater level of similarity to human biology, while still being compatible with intravital imaging. This makes them a powerful tool for studying host-pathogen interactions *in vivo*, though again major anatomical and physiological differences between zebrafish and humans, in particular the lack of lungs, still limit the utility of this

model outside of screening compounds for their effects on biochemical pathways with known disease relevance.

4.1.2 – *In vivo* mouse models of cryptococcosis

This means that mammalian models are more appropriate for exploratory studies of the pulmonary immune response to cryptococcosis. Although several mammalian species have been utilised for cryptococcosis research (rats, guinea pigs, rabbits), the most commonly used species is the laboratory mouse. Mice offer many of the same benefits as zebrafish, such as genetic tractability and relatively cheap husbandry. Additionally, mice have more similar anatomy to humans, possess a respiratory system similar to humans and have a core body temperature of 37^{o}C, recapitulating several additional biological elements of human infection. Additionally, the advent of more powerful imaging technologies now mean that mice are also compatible to be used with various intravital and *ex vivo* imaging modalities (Sanderson, 2011; Vanherp *et al.*, 2019).

In the context of cryptococcosis, there are several possible routes of inoculation available to researchers – each of which generates a unique infection phenotype (Table 2). Due to the clinical burden of disseminated disease, intravenous inoculation of *Cryptococcus* is commonplace as this leads to a rapidly disseminating infection (Vu *et al.*, 2014). However, bloodbourne transmission of cryptococcosis is not widely reported, lessening the relevance of this route of infection to human disease. Therefore, pulmonary inoculation is the most akin to real world infection. However, there are several methods by which to generate a pulmonary infection – intratracheal instillation, oropharyngeal aspiration and intranasal inoculation. Intratracheal aspiration involves surgically anaesthetising the animal, and instilling the inoculum directly into the trachea (Shourian *et al.*, 2018). This route of administration has the highest efficiency as there is no swallowing of the dose by the animal. However, this is the most invasive method of the three, with risks of post-surgical infection at the site of inoculation and toxicity due to the deep level of anaesthesia. A non-invasive alternative to this method is where a lightly anaesthetised animal is intubated via the mouth and an inoculum is pipetted directly into the lungs (Das *et al.*, 2013). While this avoids the risk of post-surgical infection, this approach requires a high level of training and there is the chance of the inocula being pipetted into the stomach instead of the lungs. Alternatively, oropharyngeal aspiration involves instilling the inoculum into the back of the throat (Nielsen *et al.*, 2018). As mice are obligate nose breather, the nose and tongue are then restrained manually until the animal is forced to breathe using its mouth, resulting in the inoculum being inhaled into the lungs rather than swallowed. This method is less invasive than intratracheal instillation and still results in a high dosing efficiency. However, this technique does

require either specialist equipment or two investigators for the manual handling of the animal. Intranasal dosing is the simplest but least efficient methodology of the three (Thuang, Murphy and Cauley, 1980). For this approach, the animal is lightly anaesthetised, as with oropharyngeal aspiration, although the inoculum is simply pipetted onto the mouse naves to be inhaled by the animal. This method is the least efficient as a significant portion of the inoculum is swallowed or coughed up.

For this research, establishing as simple and non-invasive a methodology as possible was paramount, and so the intranasal infection methodology was chosen. For the following experiments, all *in vivo* procedures were handled by Carl Wright, Jessica Willis and Dr Helen Marriott, while *ex vivo* processing of tissue was handled by me.

4.1.3 – A GFP tagged strain of R265 *C. gattii* shows evidence of avirulence *in vivo*

As mentioned previously (see 3.3.4), fluorescent tagged pathogens are key tools for studying infection. The expression of fluorescence enables the easy identification of pathogens and their proteins in samples. In the case of *Cryptococcus*, the method of choice for generating GFP expressing fungal strains is biolistic transformation (Voelz *et al.*, 2010) – whereby GFP constructs are inserted into *Cryptococcus* cells mechanically for the construct to be integrated into the fungal genome. However, despite numerous published protocols and the identification of genomic 'safe havens', genetic manipulation can still result in unintended alterations to the *Cryptococcus* genotype or phenotype.

Due to the ongoing outbreak of *C. gattii,* there has been great interest in generating fluorescent clinical and laboratory strains for use in research (Datta *et al.*, 2009). Therefore, Voelz *et al*. generated several GFP tagged variants of the highly virulent reference *C. gattii* strain, R265 (2010). Aside from confirming GFP expression, all generated transgenic strains were screened for functional defects *in vitro* – no differences in growth or stress tolerance were identified.

Recently, however, our lab observed one of these GFP-R265 constructs had significantly attenuated virulence in a zebrafish *in vivo* model of cryptococcosis compared to wild-type R265 (WT-R265; Bojarczuk, 2020). However, it had yet to be determined if this avirulence was specific to the zebrafish model. Therefore, there was a need to determine if the GFP-R265 *C. gattii* strain was avirulent in a mammalian model of infection.

Therefore, this provided an opportunity to develop an *in vivo* mouse inhalation model of cryptococcosis while confirming whether the GFP-R265 strain of *C. gattii* was also avirulent in a mammalian model of cryptococcosis. In this chapter, I sought to compare the virulence of WT-R265 and GFP-R265 strains of *C. gattii* in a mouse model of intranasal infection.

4.2 – Results

4.2.1 – Intranasal inocula of WT-R265 and GFP-R265 did not significantly differ

Before the virulence of the two *C. gattii* strains (WT-R265 and GFP-R265) could be compared, successful inoculation of mice was first confirmed, as was the reliability of the inoculum preparation protocol. Prepared inocula were quantified by culture on YPD plates (Figure 23A). Despite variability, the inoculum for both strains was approximately $5x10^4$cfu, with no significant difference (p=0.5613).

Next, the efficiency and reliability of the intranasal dosing protocol was determined. Animals intranasally dosed with $5x10^4$ cfu/50µl of either WT-R265 or GFP-R265 *C. gattii* and then immediately culled. Lung homogenates were then analysed to determine how much of the inoculum could be recovered from the lungs (Figure 23B). This confirmed that animals were successfully inoculated with *Cryptococcus* by this method, with an efficiency of ~20%. Again, despite variation from animal to animal, there was no difference in the initial lung fungal burdens of WT-R265 and GFP-R265 infected animals.

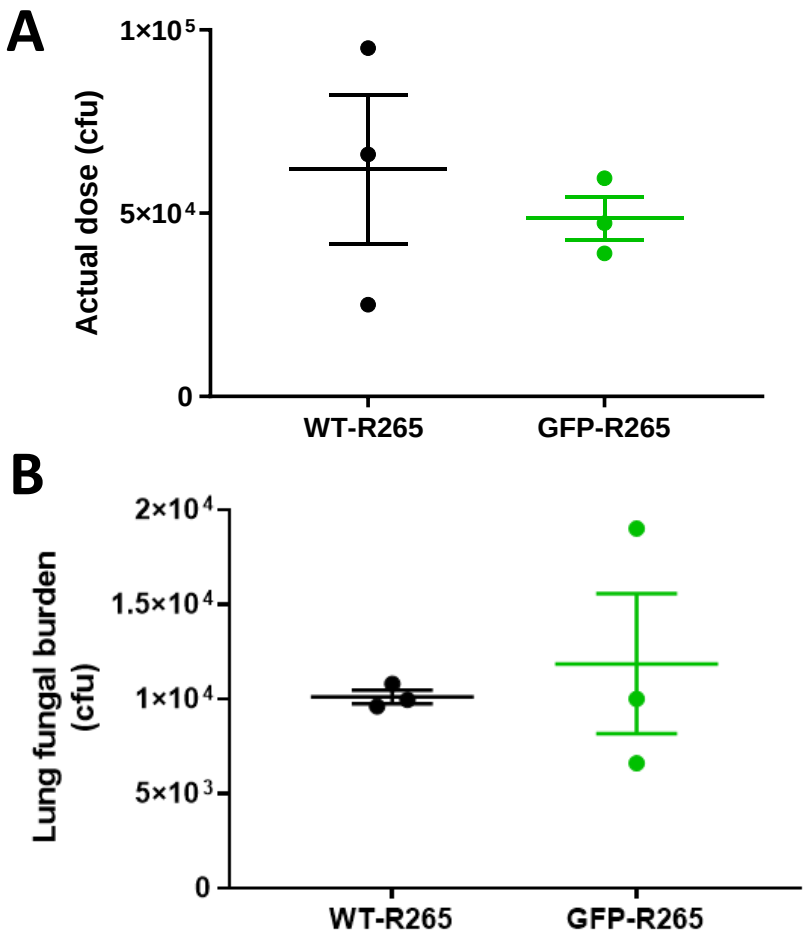

Figure 23 – Intranasal inocula of WT-R265 and GFP-R265 did not differ. Animals received the same size of inocula regardless of *C. gattii* strain, and approximately 20% of inocula could be recovered from the lungs *ex vivo*. (**A**) The inocula animal received did not differ between treatment groups (t=0.6327, df=4, p=0.5613). (**B**) Lung fungal burdens at 0dpi reveal that the efficiency of intranasal inoculation was equivalent for both strains of *C. gattii* (t=0.4709, df=4, p=0.6623). Inocula were compared using an unpaired t-test, whereas 0dpi lung fungal burdens were compared using a Welch's t-test. Data presented as mean ± SD. Each point represents a different animal.

4.2.2 – Pulmonary fungal burdens of GFP-R265 *C. gattii* were lower than those of WT-R265 *C. gattii* at 7dpi

Having established that mice could be successfully infected with *C. gattii*, early fungal growth in the lungs of infected mice were assessed by comparing pulmonary fungal burdens of WT-R265 and GFP-R265 *C. gattii* from mice culled at 1 and 7dpi (Figure 24). Interestingly, there was no change in pulmonary fungal burdens between 0 and 1dpi, with either strain of *C. gattii*. However, 7dpi fungal burdens of WT-R265 *C. gattii* were 100-fold higher than those at 0 or 1dpi. Pulmonary fungal burdens of GFP-R265 *C. gattii* at 7dpi also appeared to be higher than those at 0 and 1dpi, although this difference was not significant. In addition, 7dpi pulmonary fungal burdens of WT-R265 were ten times higher than those of GFP-R265, suggesting that GFP-R265 *C. gattii* was less well adapted to colonising the lungs of mice.

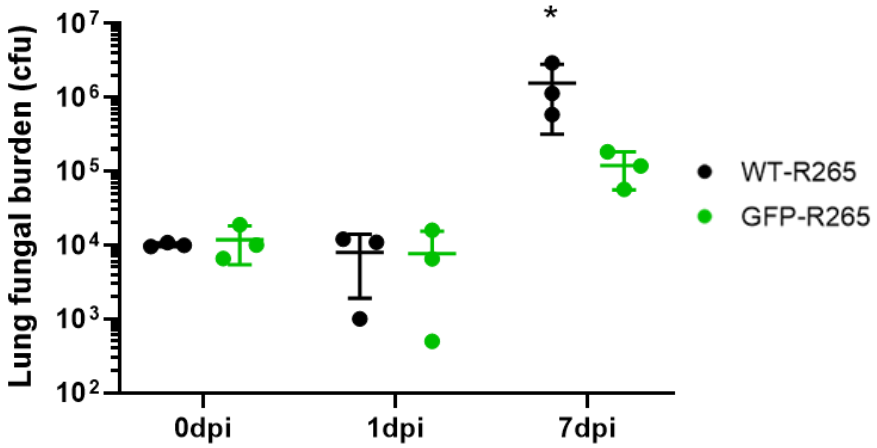

Figure 24 – Pulmonary GFP-R265 *C. gattii* fungal burdens are lower than those of WT-R265 *C. gattii* infection at 7dpi. *C. gattii* pulmonary fungal burdens of WT-R265 were significantly elevated at 7dpi compared to all other time points and conditions, which was not seen with GFP-R265 *C. gattii* infection at 7dpi. Interaction – F(2, 12)=4.038, p=0.0456. Time – F(2,12)=5.366, p=0.0216. Strain – F(1,12)=4.026, p=0.0679. Lung burdens were compared by two-way ANOVA with *post hoc* Tukey multiple comparisons. Data presented as mean ± SD. Each point represents a different animal. * - p<0.05

4.2.3 – Lungs from C57BL/6 mice infected with either WT-R265 or GFP-R265 *C. gattii* show no difference in lung pathology at 0, 1 and 7dpi

Aside from tissue fungal burden, the weight and appearance of infected lung tissue were also compared. At 0, 1 and 7dpi, no significant differences in tissue weight were found, regardless of strain or time post infection (Figure 25A). However, as early as 1dpi, lungs from mice infected with either WT-R265 or GFP-R265 *C. gattii* appeared discoloured (Figure 25B). At 7dpi, this discolouration was even more pronounced, and was coupled with the appearance of small masses on the tissue exterior.

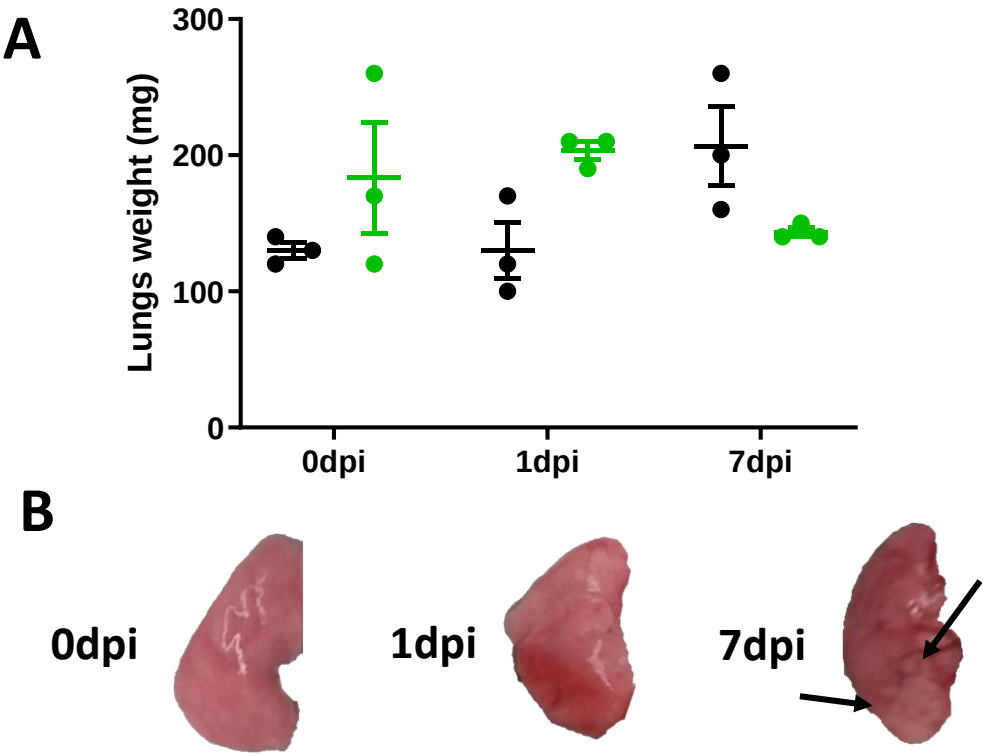

Figure 25 – Lung pathologies in C57BL/6 mice did not appear to differ at 7dpi with WT-R265 or GFP-R265 *C. gattii* infection. No significant differences in tissue weight or appearance could be observed, although lungs appeared more discoloured at 7dpi in the case of infection with either strain. (**A**) The weight of lungs infected with *C. gattii* showed a significant interaction of *C. gattii* strain and time post infection, although no specific differences could be determined. Interaction – $F(2,12)=5.369$, $p=0.0216$. Time – $F(2,12)=0.3321$, $p=0.7238$, Strain – $F(1,12)=1.318$, $p=0.2734$. (**B**) Representative images of WT-R265 *C. gattii* infected lungs at 0, 1 and 7dpi, showing how infected lung tissue becomes discoloured over time. Arrows indicate potential masses visible on the lung exterior at 7dpi. The appearance of GFP-R265 *C. gattii* infected lungs also appeared this way. Lung weights over time were compared by two-way ANOVA with *post hoc* Tukey multiple comparisons. Data presented as mean ± SD. Each point represents a different animal.

4.2.4 – Fungal burdens in the trachea, brain and spleen of infected C57BL/6 mice were identical at 0, 1 and 7dpi with WT-R265 and GFP-R265 *C. gattii* infection

Having examined the pulmonary infection phenotype, the involvement of other tissues was then examined. Fungal burdens in the spleen and brain were determined *ex vivo*, as these tissues are commonly associated with *Cryptococcus* infection in mouse models of cryptococcosis (Olszewski *et al.*, 2004). Tracheal fungal burdens were also examined to investigate if intranasal inoculation also resulted in significant infection of the upper airways.

At 0, 1 and 7dpi, no significant differences in dissemination or fungal burden were observed in these tissues in mice infected with either strain of *C. gattii* (Figure 4A, E). Tracheal fungal burdens changed significantly over time, although specific differences could not be identified between WT-R265 and GFP-R265 *C. gattii* infection (Figure 4C). Additionally, no significant differences in tissue weight were observed (Figure 4B, D, F).

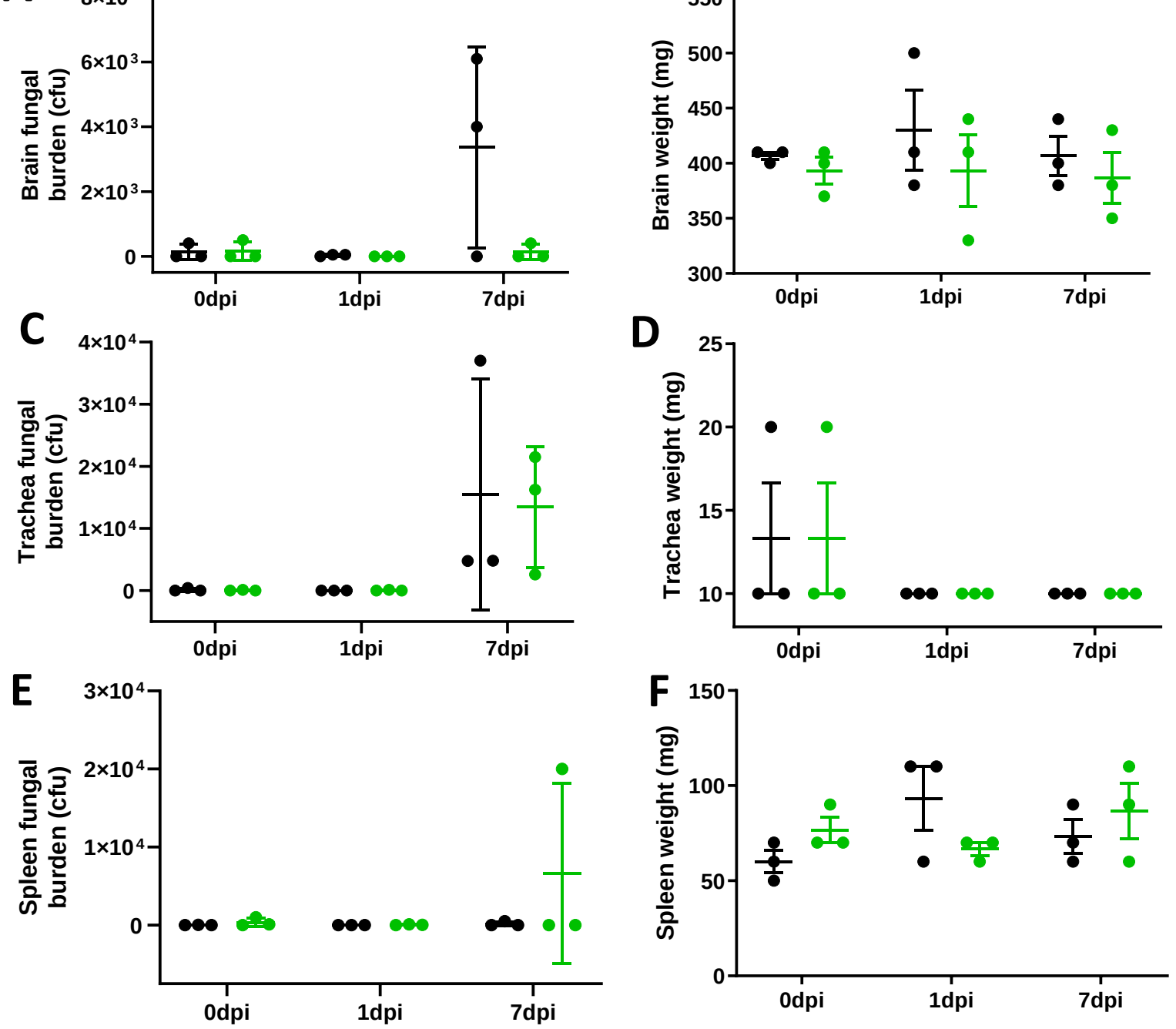
Brain fungal burden (cfu)
6×10³
4×10³
2×10³
0
0dpi
1dpi
7dpi
Brain weight (mg)
500
450
400
350
300
C
Trachea fungal burden (cfu)
4×10⁴
3×10⁴
2×10⁴
1×10⁴
0
D
Trachea weight (mg)
25
20
15
10
E
Spleen fungal burden (cfu)
3×10⁴
2×10⁴
1×10⁴
F
Spleen weight (mg)
150
100
50

Figure 26 – Fungal burdens and weights of C57BL/5 mice brain, trachea and spleen did not significantly differ between WT-R265 and GFP-R265 *C. gattii* infection at 0, 1 and 7dpi. While tracheal fungal burdens appear to be significantly higher at 7dpi, there was no difference between *C. gattii* infections in brain, trachea and spleen fungal burdens or weight. (**A**) There were no significant differences between brain fungal burdens of WT-R265 and GFP-R265 from infected animals over time. Interaction – $F(2, 12)=3.203$, $p=0.0768$. Time – $F(2,12)=3.420$, $p=0.0668$. Strain – $F(1,12)=3.202$, $p=0.0988$. (**B**) There were no significant differences in the weight of brain tissue of animals infected with either WT-R265 or GFP-R265 over time. Interaction – $F(2, 12)=0.1279$, $p=0.8812$. Time – $F(2, 12)=0.2197$, $p=0.8059$. Strain – $F(1,12)=1.446$, $p=0.2524$. (**C**) Tracheal fungal burdens were significantly affected by time post infection, but not by the strain of *C. gattii* mice were infected with, although specific differences could not be identified. Interaction – $F(2, 12)=0.02819$, $p=0.9723$. Time – $F(2, 12)=5.664$, $p=0.0185$. Strain – $F(1,12)=0.03093$, $p=0.8633$. (**D**) There were no significant differences in tracheal tissue weight of animals infected with either WT-R265 or GFP-R265 over time. Interaction – $F(2, 12)=0$, $p>0.9999$. Time –$F(2, 12)=2$, $p=0.178$. Strain – $F(1,12)=0$, $p>0.9999$. (**E**) There were no significant differences in spleen fungal burdens in animals infected with either WT-R265 or GFP-R265. Interaction – $F(2, 12)=0.8919$, $p=0.4354$. Time – $F(2, 12)=0.9841$, $p=0.4020$. Strain – $F(1,12)=1.068$, $p=0.3218$. (**F**) There were no significant differences in spleen tissue weight in animals infected with either WT-R265 or GFP-R265 over time. Interaction – $F(2, 12)=2.661$, $p=0.1105$. Time – $F(2, 12)=0.8305$, $p=0.4594$. Strain – $F(1,12)=0.01695$, $p=0.8986$. All comparisons were done by two-way ANOVA with *post hoc* Tukey comparisons. Data presented as mean ± SD. Each point represents a different animal. * - $p<0.05$.

4.2.5 – GFP-R265 *C. gattii* is avirulent over 23 days of infection

Although there were significant differences in pulmonary fungal burdens at 7dpi, it was yet to be seen if these differences in fungal burden correlated with differences in virulence, as no infected animals exhibited any clinical signs of infection during this period. Therefore, animals were subjected to survival analysis – briefly, mice were intranasally inoculated with either 50,000cfu WT-R265 or GFP-R265 *C. gattii* and monitored for up to 23 days. Animals were humanely euthanized if they reached pre-determined humane end points during this time – including behavioural changes or body weight losses approaching 20%, a commonly utilised marker of animal welfare during mouse infection studies (Morton and Griffiths, 1985).

During the examined period, all animals infected with WT-R265 *C. gattii* reached humane endpoints by 20dpi. However, all GFP-R265 inoculated animals survived until day 23

without showing any clinical signs of infection (Figure 27A). Additionally, WT-R265 *C. gattii* inoculated animals had sudden onsets of weight loss 2-4 days prior to being culled (6 out of 7; Figure 27B). Conversely, no animal infected with GFP-R265 *C. gattii* exhibited significant weight loss. However, one WT-R265 infected animal (Figure 27B, red arrow) did not show significant weight loss, yet had to be culled due to exhibiting clinical signs, suggesting that weight loss was not a universal symptom in terminally infected mice.

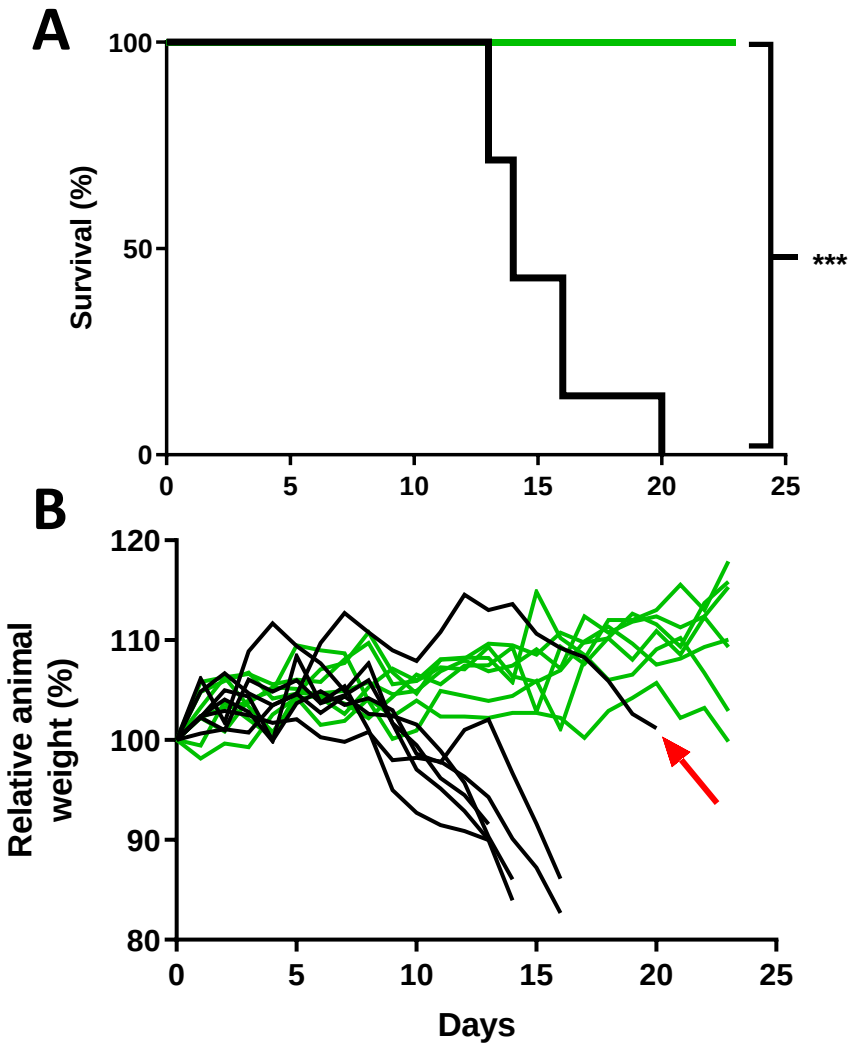

Figure 27 – GFP-R265 is avirulent in a pulmonary *C. gattii* infection mouse model of infection over 23 days. All mice intranasally inoculated with WT-R265 had to be culled due to clinical signs or significant weight loss, while animals infected with R265-GFP showed no mortality over 23 days. (**A**) GFP-R265 is avirulent compared to WT-R265 in C57BL/6 mice over 23 days in an intranasal infection model (chi square=14.23, df=1, p=0.0002). (**B**) Bodyweight changes in mice over 23 days of *C. gattii* infection. Red arrow highlights an animal that was culled due to clinical signs a bodyweight no lower than 100%. Survival curves were compared using a log-rank test. Each line on the survival curve is representative of seven animals. Each line in **B** represents a different animal. *** - p<0.001.

4.2.6 – Higher pulmonary fungal burdens of *C. gattii* in survival C57BL/6 mice were associated with mortality

As there was a clear different in the virulence of WT-R265 and GFP-R265 *C. gattii* over 23 days, the phenotypes of these terminal infections in C57BL/6 animals were investigated further. Therefore, lung tissue was taken for fungal burden analysis when an animal during the survival experiment was culled to determine whether fungal burdens significantly differed between treatment groups (Figure 28). WT-R265 infected animals, despite being culled earlier than GFP-R265 infected animals, were found to have significantly higher pulmonary fungal burdens (p=0.0138). It is also important to note that the pulmonary fungal burdens of both WT-R265 and GFP-R265 infected animals at the time of culling during the survival experiment were approximately ten times higher than those observed at 7dpi, suggesting further proliferation occurred.

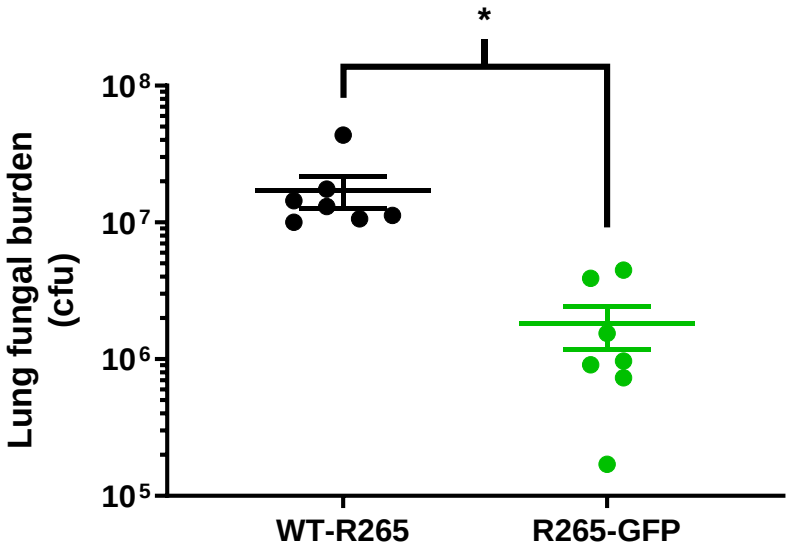

Figure 28 – WT-R265 infection resulted in higher pulmonary fungal burdens in terminal survival animals compared to GFP-R265 infected animals that survived 23 days. Pulmonary fungal burdens in WT-R265 inoculated animals that had to be culled due to clinical signs (14-20dpi) were significantly higher than those of GFP-R265 inoculated animals that were culled at 23dpi (t=3.394, df=6.239, p=0.0138). This is despite WT-R265 infected animals having to be culled prior to 21dpi. Lung fungal burdens were compared using an unpaired t-test. Data presented as mean ± SD. Each point represents a different animal. * - p<0.05.

4.2.7 – Lungs from terminal C57BL/6 mice infected with WT-R265 showed greater evidence of damage than those from GFP-R265 inoculated animals that survived for 23 days

The weight and appearance of infected lungs from survival experiment animals were also compared, to determine whether differences in mortality could be attributed to differences in lung pathology. The lungs of WT-R265 infected animals were significantly heavier than those from surviving animals infected with GFP-R265 (Figure 29A). This could have been the result of increased fibrosis, oedema or increased immune cell infiltration. However, although this cannot be confirmed in the absence of appropriate histopathology and Evans blue treatment of animals to determine oedema levels.

All *C. gattii* infected lungs from survival animals featured white patches visible on the exterior that may be evidence of granuloma formation or extreme fungal growth (Figure 29B). However, lung tissue from animals infected with different strains of *C. gattii* also varied in appearance (Figure 29B). More severe phenotypes were observed in WT-R265 infection – arbitrarily labelled here as ‘moderate’ or ‘severe’. These tissues also showed additional signs of visible tissue damage and even loss of structure. This level of tissue damage in WT-R265 inoculated animals can be hypothesised to have reduced tissue elasticity and made respiration increasingly difficult. Therefore, respiratory failure is a potential cause of death in these animals.

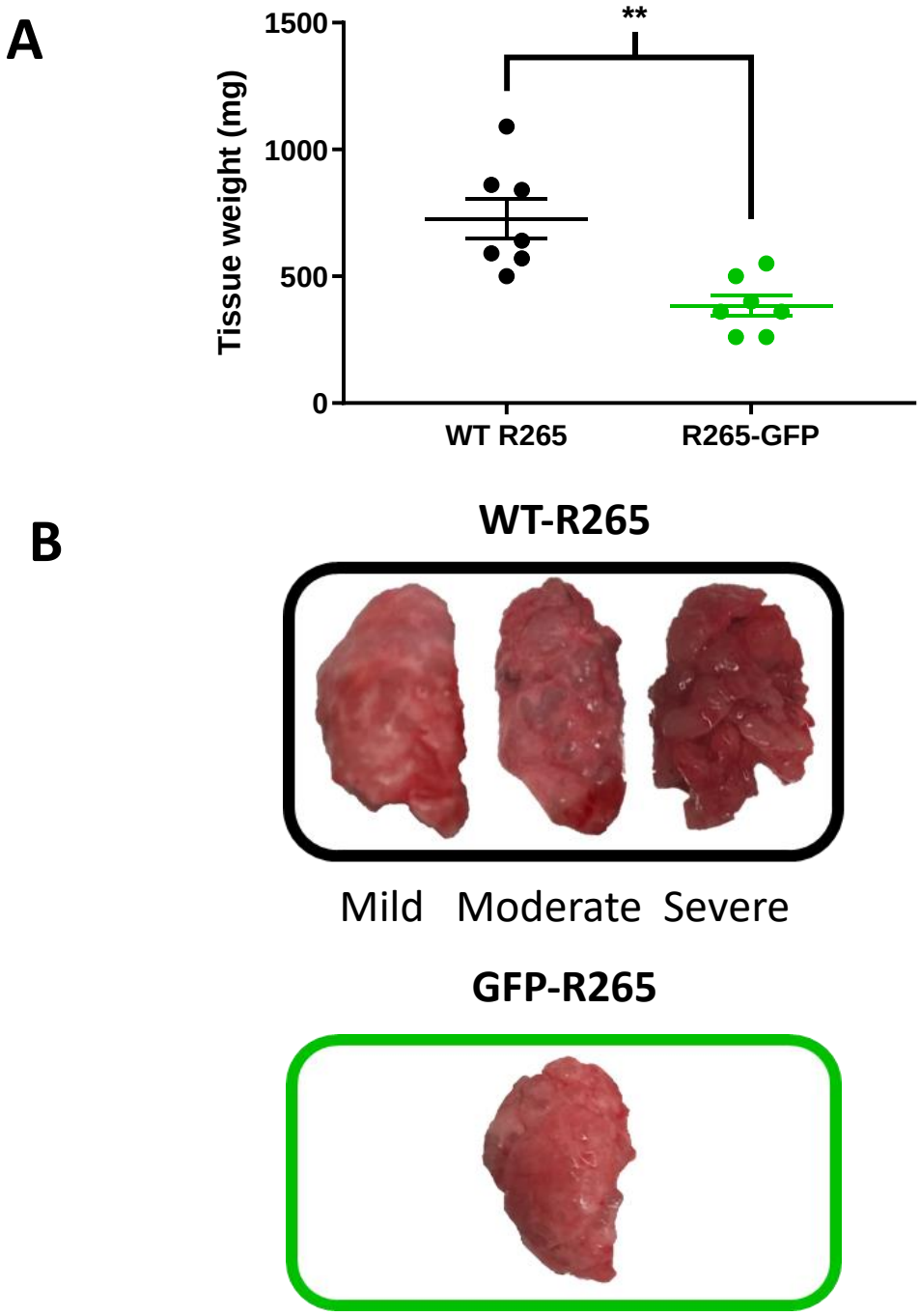

Figure 29 – C57BL/6 mouse lungs infected with WT-R265 *C. gattii* show evidence of greater levels of lung damage compared to those infected with GFP-R265. Lungs from mice infected with WT-R265 appeared more damaged than those infected with GFP-R265, although both infections appeared to cause damage. (**A**) Terminal survival animals infected with WT-R265 had significantly larger lungs than those from surviving animals infected with GFP-R265 (t=3.822, df=12, p=0.0024). (**B**) – Representative images of various lung phenotypes taken post mortem from WT-R265 and GFP-R265 infected animals. Tissue weights were compared using a Welch's t-test. Data presented as mean ± SD. Each point represents a different animal. ** - p<0.01.

4.2.8 – The dissemination of both WT-R265 and GFP-R265 *C. gattii* in C57BL/6 mice did not significantly differ

The dissemination of both WT-R265 and GFP-R265 to the spleen or brain of infected animals were compared, to establish if differences in mortality could also be attributed to differences in dissemination. However, WT-R265 *C. gattii* was not observed to have disseminated to other tissues more frequently than GFP-R265 infection ($p=0.2657$; Figure 30A-B). This provides further evidence that the lung pathology was the main cause of mortality in WT-R265 *C. gattii* infected mice.

Additionally, the weights and fungal burden of these other tissues were also compared to establish whether the growth of GFP-R265 in specific tissues was impaired. However, no differences in fungal burdens in the brain, trachea or spleen could be identified (Figure 30C, E, G), nor could any differences in tissue weight (Figure 30D, F, H).

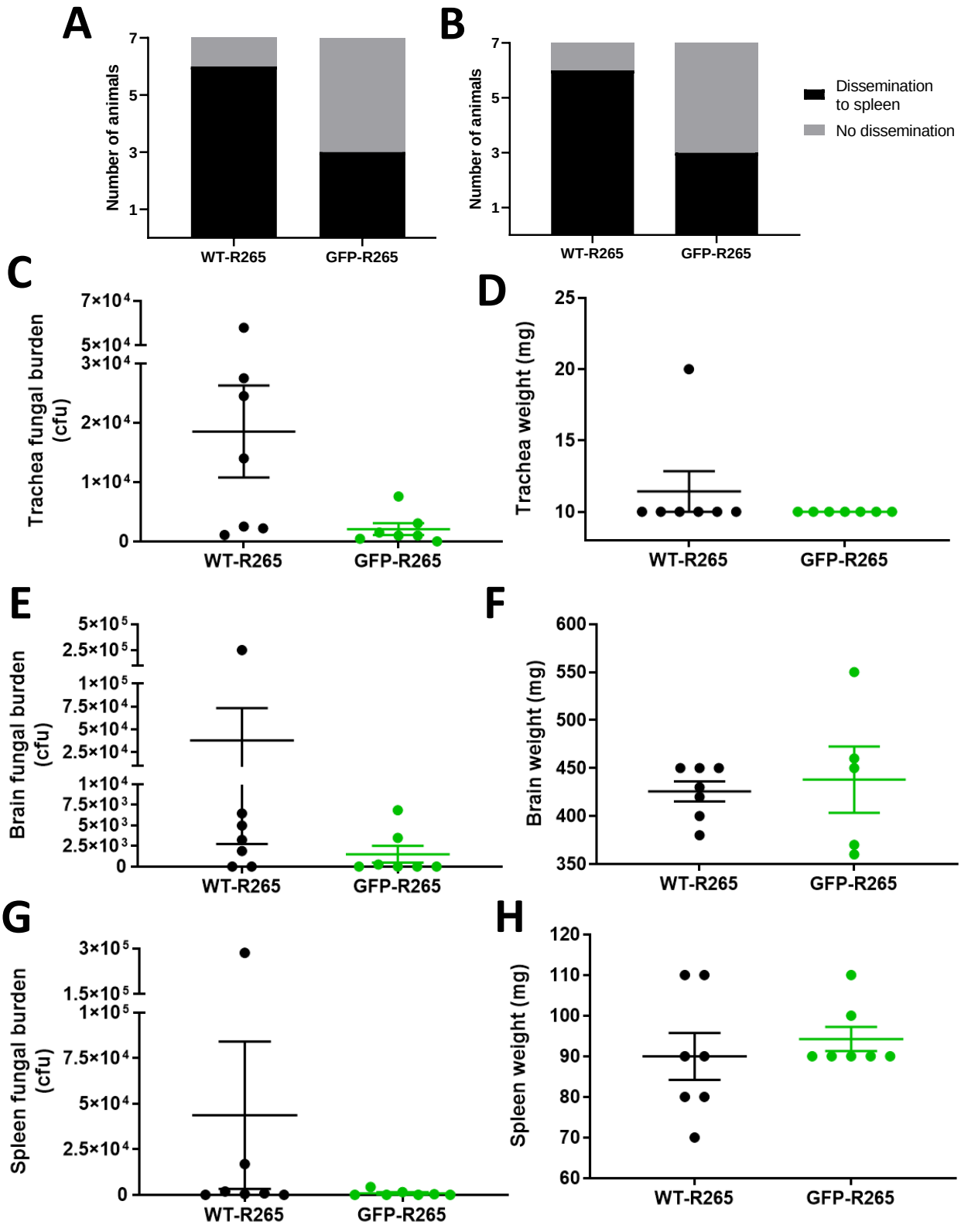
A
Number of animals
7
5
3
1
WT-R265
GFP-R265
B
Number of animals
7
5
3
1
WT-R265
GFP-R265
Dissemination to spleen
No dissemination
C
Trachea fungal burden (cfu)
7×10⁴
5×10⁴
3×10⁴
2×10⁴
1×10⁴
0
WT-R265
GFP-R265
D
Trachea weight (mg)
25
20
15
10
WT-R265
GFP-R265
E
Brain fungal burden (cfu)
5×10⁵
2.5×10⁵
1×10⁵
7.5×10⁴
5×10⁴
2.5×10⁴
1×10⁴
7.5×10³
5×10³
2.5×10³
0
WT-R265
GFP-R265
F
Brain weight (mg)
600
550
500
450
400
350
WT-R265
GFP-R265
G
Spleen fungal burden (cfu)
3×10⁵
1.5×10⁵
1×10⁵
7.5×10⁴
5×10⁴
2.5×10⁴
0
WT-R265
GFP-R265
H
Spleen weight (mg)
120
110
100
90
80
70
60
WT-R265
GFP-R265

Figure 30 – There were no significant differences in dissemination, fungal burden or weight in the spleen, brain and trachea of survival animals infected with either WT-R265 or GFP-R265 *C. gattii*. Although more animals infected with WT-R265 *C. gattii* had disseminated disease, this difference was not significant. Additionally, no significant differences in tissue weight or fungal burden could be identified in any examined tissue. WT-R265 infected animals were culled between 14-20dpi and GFP-R265 infected animals were culled at 23dpi. (**A**) There was no significant difference in the number of C57BL/6 mice that were positive for dissemination to the brain with WT-R265 and GFP-R265 infection (Chi-square=2.8, df=1, z=1.673, p=0.0943). (**B**) There was no significant difference in the number of C57BL/6 mice that were positive for dissemination to the spleen with WT-R265 and GFP-R265 infection (Chi-square=2.8, df=1, z=1.673, p=0.0943). (**C**) Brain fungal burdens were not significantly different in survival animals infected with different strains of *C. gattii* (t=1.577, df=5.097, p=0.1744). (**D**) Survival animal brain weight did not significantly differ due to infection with different strains of *C. gattii* (t=0.7026, df=12, p=0.4957). (**E**) Spleen fungal burdens were not significantly different in survival animals infected with different strains of *C. gattii* (t=1.059, df=6.003, p=0.3302). (**F**) Survival animal spleen weights did not significantly differ due to infection with different strains of *C. gattii* (t=0.6599, df=12, p=0.5218). (**G**) Tracheal fungal burdens were not significantly different in survival animals infected with different strains of *C. gattii* (t=2.107, df=6.195, p=0.0783). (**H**) Survival animal tracheal weight did not significantly differ due to infection with different strains of *C. gattii* (t=0.7026, df=12, p=0.4957). Rates of dissemination were compared using Chi-squared analysis. Brain weight and spleen weight were compared using an unpaired t-test, while brain fungal burden, trachea fungal burden, trachea weights and spleen fungal burden were compared using a Welch's t-test. Data presented as mean ± SD. Each point represents a different animal.

4.3 – Discussion

Here, I present an *in vivo* murine inhalation infection model of cryptococcosis that enables the virulence of *Cryptococcus* to be assessed and compared. In this instance, I used this model to characterise the progression of a fatal pulmonary infection with *C. gattii* and confirmed that the GFP-R265 strain of *C. gattii* is comparatively avirulent.

4.3.1 – The characteristics and utility of the mouse inhalation model of *Cryptococcus* infection

The presented inhalation mouse model of *Cryptococcus* infection recapitulates many important key elements of human infection. Firstly, the mortality rate in mice infected with virulent WT-R265 *C. gattii* correlates with the mortality observed in untreated cryptococcosis patients (Mwaba *et al.*, 2001). Additionally, virulent *C. gattii* infection was fatal despite the fact that the mice used are immunocompetent. While cryptococcosis is typically associated with immunocompromise, a feature of human *C. gattii* infection is the association of serious *C. gattii* infection with immunocompetent individuals (Mitchell *et al.*, 1995). Furthermore, in the case of fatal *C. gattii* infection, mouse infection progression was parallel to what is observed in human patients – mice remained asymptomatic followed by a rapid onset of serious symptoms (weight loss, lethargy) prior to animals having to be culled. In human cryptococcosis, patients typically only seek medical attention following a rapid onset of symptoms during late stage disease, where treatment is required rapidly (Baradkar *et al.*, 2009). Finally, the symptoms animals presented with were consistent with those of cryptococcosis due to *C. gattii*. Although cryptococcosis is most commonly associated with meningitis, where patient symptoms include ataxia, seizures and behavioural changes (Abassi, Boulware and Rhein, 2015; Rajasingham *et al.*, 2017), *C. gattii* infection is known to be commonly associated with a more severe pulmonary infection – in both human and mouse models (Harris *et al.*, 2011; Chen, Meyer and Sorrell, 2014). Consistent with this, terminal mice presented with crackling lungs and open mouth breathing, which are symptoms of pneumonia in mice. Additionally, the association of virulent WT-R265 infection with pneumonia, when coupled to higher pulmonary fungal burdens and signs of lung damage further asserts a lung-centric pathology in mice. These parallels between the intranasal model and the human clinical situation suggests there is a high level of translation in the results from this mouse model.

Although this model revealed differences in the virulence of WT-R265 and GFP-R265 *C. gattii*, this approach did have several limitations. One limitation was that the survival experiment was only 23 days long – while this was enough to confirm that GFP-R265 was less virulent than WT-R265, this was not long enough to confirm whether GFP-R265

was also avirulent. Pulmonary fungal burdens of GFP-R265 at 23dpi were ~100 times higher than fungal burdens at 0dpi, meaning that although less virulent, GFP-R265 likely continued to grow within the lungs of infected animals, albeit at a slower rate than the parental WT-R265. Therefore, it could have been that GFP-R265 *C. gattii* was still virulent, although mortality was delayed and would have occurred later than 23dpi. It is also possible that fungal burdens may have actually peaked between 8-22dpi before a change in either fungal replication or immunity resulted in lower fungal burdens which was observed at 23dpi. Confirming this would require establishing fungal burdens at additional time points. Another limitation may have been the lack of a negative control group (PBS treated) in this study, which is important for confirming whether the intranasal dosing methodology adversely affected animal health status. However, as the primary aim of this study was to compare the virulence of WT-R265 and GFP-R265 strains of *C. gattii*, the PBS control group would not have informed this comparison. Therefore this control group was consciously omitted, both to reduce the number of animals subjected to procedures and because the intranasal dosing methodology is well-established to have a low risk of adverse events (Turner *et al.*, 2011). Finally, this study also highlighted that there was a problem with relying exclusively on bodyweight loss as a marker of animal welfare. Although 6 out of 7 WT-R265 inoculated animals did show notable weight loss which informed the time point that these animals were culled, one animal had to be culled instead because of significant clinical signs, including crackling lungs, hunched appearance, piloerection and minimal exploratory behaviour – despite a bodyweight near 100%. Although all animals were monitored for this behaviour daily and no animal exceeded severity limits, the lungs of this animal showed the most severe tissue damage of all WT-R265 animals. This highlights the importance of examining trends in weight loss, and not just relying on bodyweight as a percentage of day 0 bodyweight.

4.3.2 – The dynamics of *C. gattii* pulmonary infection in mice early in infection

The intranasal mouse model of cryptococcosis revealed interestingly that pulmonary fungal burdens did not change between 0 and 1dpi with either WT-R265 or GFP-R265 infection. This could mean that despite animal inocula are likely to be significantly higher than expected human exposure to *Cryptococcus*, there is either host control of pulmonary infection during initial infection, or that *C. gattii* is initially quiescent upon being inhaled. This early infection phenotype requires further investigation, as if there is initial host control of inhaled fungal cells, understanding these mechanisms of host control may reveal new therapeutic opportunities to enhance fungal clearance in patients. However, it is worth noting that the technique used to quantify fungal burden, cfu plating, may not have been sensitive enough to detect any differences in fungal burden that existed. To examine this further, visualising host-pathogen interactions in infected mouse lung tissue

would allow for both the host immune response and fungal replication to be determined at these early points of infection.

Meanwhile, at 7dpi pulmonary fungal burdens of virulent WT-R265 *C. gattii* were significantly higher than those at 1dpi. This suggests that after 24 hours, fungal growth in the lung outcompetes any initial host control of *C. gattii*. However, as animal fungal burdens were not analysed between 1 and 7dpi, there could have been significant fluctuations in fungal burden during this time – although other *in vivo* studies of lung fungal burdens in mice have examined fungal burdens at 3dpi (Van Dyke *et al.*, 2017) which suggest that fungal burdens increase continuously between 1 and 7dpi. To confirm this, an intravital live imaging modality that allowed for fungal burdens of *C. gattii* to be quantified repeatedly over time, such as bioluminescent imaging (Vanherp *et al.*, 2019), is required.

4.3.3 – GFP-R265 *C. gattii* is less virulent than WT-R265 *C. gattii in vivo*

Most importantly, this study confirmed that the GFP-R265 *C. gattii* strain, that was avirulent in a zebrafish embryo model of infection, was also avirulent in mammals. The GFP-R265 strain was generated by biolistic transformation, meaning that the GFP construct was inserted in a largely random manner into the target cell genome. When first generated, the strain was characterised *in vitro*, with no defects in growth observed in various conditions, including high temperature, hypoxia, oxidative stress, nitrosative stress and hyperosmolar stress (Voelz *et al.*, 2010). In addition, the interactions of GFP-R265 with J774 cells in relation to intracellular growth and phagocytosis were also the same between strains. Subsequent whole genome sequencing of both WT-R265 and GFP-R265 strains revealed a 32kB deletion on chromosome 1 in the GFP-R265 strain (Farrer *et al.*, 2016; Bojarczuk, 2020). This region corresponds to the loss of six genes, described in detail by Bojarczuk (Bojarczuk, 2020).

Both the zebrafish and mouse study reveal that either one, some or all of these six genes are important for *C. gattii* virulence and/or *in vivo* host colonisation. However, the results of these studies alone are not sufficient to determine with confidence which of these genes are critical for virulence. For example, the significantly lower pulmonary fungal burdens of GFP-R265 in the lungs of mice at both 7 and 23dpi could be attributed to any number of mechanisms. These could include changes in metabolic processes that are important for growth in the lung, a susceptibility to the host immune response or a combination of both. However, this study does still provide important information regarding GFP-R265 infection that may inform future studies of this avirulent phenotype.

Firstly, as significant differences in fungal burden were only observed in the lungs with no differences in dissemination, it can be assumed that these genes are most important for pulmonary growth. However, as fungal burdens were equivalent at both 0 and 1dpi, it can also be determined that these genes are likely not critical for initial colonisation of the lung, but rather for infection progression. Interestingly, the results of this study provides evidence that in the case of *C. gattii* infection, dissemination occurs independently of lung fungal burdens. Instead, it may provide evidence that dissemination in instead host dependent. Of the mechanisms of dissemination proposed, 'Trojan horse' dissemination via macrophage phagocytosis would therefore the most likely mechanism of pathogen escape in this instance, although this needs further investigation (Santiago-Tirado *et al.*, 2017; Squizani *et al.*, 2018). Alternatively, it is also possible that the lack of a difference in dissemination between infections of the two strains were the result of low n numbers (Figure 30). Alternatively, a lack of dissemination may have been falsely attributed to animals where low fungal burdens were below the limits of detection (50cfu) for this assay – suggesting this should be confirmed by more sensitive methods, such as high-content imagine or PCR.

In order to determine which gene or combination of genes is important for virulence, ideally new transgenic variants of WT-R265 *C. gattii* would be generated with specific knockouts of each potential gene and combination thereof. However, this would require generating 62 additional transgenic strains, and subjecting each one to *in vivo* analysis, requiring significant time and resources. Alternatively, an RNA interference screen against the corresponding mRNA of these strains might provide a higher throughput method to screen for the avirulent phenotype. Additionally, *in silico* modelling methods may enable the structure of each gene product to be predicted so that inhibitors can be used to identify genes important for *in vivo* infection. Aside from confirming which genetic changes are critical for the changes in phenotype, determining the mechanism of avirulence is also important. Therefore, the susceptibility of this strain to the host immune response should also be assessed *in vitro*. The strain has already been observed to be well handled by J774 cells, suggesting that the macrophage response is not related to the virulence of this strain (Voelz *et al.*, 2010). Instead, the growth of GFP-R265 should be assessed in the presence other innate immune cells, such as DCs, NK cells and T cells – which may reveal significantly changed host-pathogen interactions that explain the reduced virulence *in vivo*. Also, as this defect in virulence appears to be associated with pulmonary infection, developing a suitable model to study the GFP-R265 within the lung environment, such as PCLS or microfluidics, would be the best models with which to screen and validate findings. Regardless, determining why R265-GFP is avirulent could have clinical significance, as modulators of these gene(s) and/or the associated proteins could be translated into therapy for patients.

In conclusion, this study was important for developing a mammalian model of cryptococcosis, where the pathology mimics that of prediction human infection, albeit with some differences. Most importantly, it enabled the avirulent GFP-R265 phenotype to be confirmed in a mammalian model that features lungs, a 37^{o}C body temperature and where the route of infection was more akin to the predicted human exposure. However, the progression of WT-R265 requires further characterisation by looking at additional time points, and genetic and proteomic methods should be approved to identify a mechanism responsible for the avirulence of R265-GFP.

Chapter 5 – IFNγ and IL-1β fail to protect mice from *C. neoformans* infection

5.1 – Introduction

5.1.1 – IFNγ and IL-1β in cryptococcosis *in vivo*

The Th1 cytokine IFNγ has received a lot of attention clinically and pre-clinically as a potential immunotherapeutic for cryptococcosis. This is because numerous *in vivo* studies in mice have observed that high levels of IFNγ are associated with protective immunity, and that treating infected animals with IFNγ improves survival in models of cryptococcosis (Fulton *et al.*, 2004; Wormley *et al.*, 2007; Zhou *et al.*, 2007; Mosser and Edwards, 2008; Davis *et al.*, 2015). This culminated in a small clinical trial which concluded that two doses of IFNγ adjuvant to antifungal therapy in HIV-positive cryptococcal meningitis patients enhanced fungal clearance (Jarvis *et al.*, 2012). Despite this overwhelmingly positive evidence of a benefit to patients, it is currently not understood by exactly what mechanism(s) IFNγ protects the host from cryptococcosis. To better understand this protective action, the *in vivo* effects of IFNγ on the initial innate immune response to *C. neoformans* were examined in our lab using a localised zebrafish embryo model of cryptococcosis (Kamuyango, 2017). In these experiments, IFNγ treatment at the time of infection improved host outcomes with protection correlated with increased macrophage fungistatic activity and IL-1β expression. However, when I attempted to confirm these fungistatic effects of IFNγ with a mammalian J774 macrophage *in vitro* model, it was instead observed that these cells when treated with IFNγ were no better or poorer at handling intracellular *Cryptococcosis neoformans* (see chapter 3). However, there was minimal evidence of improved *in vitro* control of *C. neoformans* by J774 cells with IL-1β treatment.

As described previously, macrophages feature prominently throughout the immune response to cryptococcosis – from resident alveolar macrophages being the first leukocytes to respond to inhaled fungal cells (Guillot *et al.*, 2008), through to late stage disease granuloma formation (Farnoud *et al.*, 2015) and immune responses of resident brain glial cells in cases of cryptococcal meningitis (Goldman *et al.*, 2001). However, this macrophage-centric immune response means that the disconnect between the therapeutic potential of IFNγ in *in vivo* models and the observation that IFNγ worsened J774 cell control of intracellular *C. neoformans in vitro* means there is a pressing need to confirm the benefit of IFNγ *in vivo* – so either the benefit of IFNγ can be confirmed or instances can be identified where IFNγ treatment may be ineffective or dangerous for patients to help inform clinical use of IFNγ.

5.1.2 – The detrimental effects of IFNγ during autoimmunity and infection

As stated previously, the detrimental effect of IFNγ observed on J774 cells *in vitro* was a controversial observation (see Chapter 3) – few studies have studied a pathological role for IFNγ and associated Th1 immune responses in cryptococcosis, and those that have, have focused on late stage infection (Eschke *et al.*, 2015; Neal *et al.*, 2017). In cryptococcal meningitis models, it has been observed that high levels of IFNγ in the CNS during *C. neoformans* infection correlated with increased mortality, despite increased fungal clearance (Neal *et al.*, 2017). However, there has yet to be a study that has observed a pathological role of IFNγ in the context of pulmonary cryptococcosis.

Pathological roles for IFNγ have been described in the context of other infections. In mouse models of bacterial meningitis (*Streptococcus pneumoniae*), high expression of IFNγ in the CNS is associated with increased mortality (Pettini *et al.*, 2015). And in the case of aseptic meningitis in children, IFNγ has also been correlated with fever (Minamishima *et al.*, 1991). IFNγ also has pathological roles in several autoimmune diseases. IFNγ heavily implicated in the development of systemic lupus erythematous, a systemic autoimmune disease associated with tissue damage (Prud'homme, Kono and Theofilopoulos, 1995). Additionally, autoimmune conditions of the CNS have also been correlated with high levels of IFNγ (Kulkarni, Ganesan and O'Donnell, 2016).

In relation to macrophage-specific effects, IFNγ increases NADPH activity and subsequently increases the capacity for macrophage respiratory burst and ROS production (Casbon *et al.*, 2012). Although this an antimicrobial mechanism utilised by macrophages, it is non-specific and results in cytotoxic ROS release into the local environment, which can result in tissue damage. In the context of pulmonary cryptococcosis, damage to the lung epithelium may contribute to the dissemination of *C. neoformans* (Barbosa *et al.*, 2006; Carnesecchi *et al.*, 2009). This is of particular concern, as if macrophages are skewed towards a pro-inflammatory phenotype but are not significantly contributing to cryptococcal clearance, IFNγ treatment may only induce pathological inflammation and contribute to pathology and mortality. The potential for autoimmunity with IFNγ means it is critical to understand any mechanisms of protection to predict and understand potential side effects, and minimise toxicity in patients.

5.1.3 – Links between IL-1β and susceptibility to infection

Aside from the potential detrimental role of IFNγ, there is always evidence that IL-1β may be protective based on our observation in both zebrafish and J774 cells (see chapter 3; Kamuyango, 2017). However, these experiments only involved the exogenous

application of IL-1β, and did not examine whether pharmacological or genetic inhibition of IL-1β signalling significantly affected the antifungal activity or host susceptibility.

As mentioned previously, the role of IL-1β has not been widely studied in the context of cryptococcosis. Only a single case study to date has associated defects in IL-1β to incidences of disseminated cryptococcosis – and this only described a single patient with multiple immune defects (Marroni *et al.*, 2007). Additionally, one study in mice that lack the IL-1β receptor, IL-1RI, were less protected from pulmonary infection with 52D *C. neoformans* (Shourian *et al.*, 2018). Again, however, the results of this study cannot be attributed solely to the contribution of IL-1β, as IL-1α also signals via the IL-1RI receptor and therefore it may be this signal that is important for host protection. The only other evidence for a protective role of IL-1β has been incidental findings associating cytokine levels with protection. Examples include high expression of IL-1β in mouse granulomas – which are hypothesised to be protective structures in mice (Farnoud *et al.*, 2015), and has also been observed in the CNS of surviving animals (Maffei *et al.*, 2004). *In vitro*, the NLRP3 inflammasome, a post translational protein complex required for IL-1β production, is observed to be activated in macrophages by acapsular strains of *C. neoformans* and cryptococcal cell components (Guo *et al.*, 2014). As acapsular *C. neoformans* is avirulent and the cryptococcal capsule abrogates IL-1β production, this also provides evidence of a relationship between IL-1β and host susceptibility. However, no single study has specifically addressed whether IL-1β is critical for host protection in the case of highly virulent *C. neoformans* infection.

It is therefore examining the evidence for IL-1β being protective for immunity to other infections. For example, *Candida albicans* and other invasive fungal infections are known to be susceptible to Th17 immune responses (Puel *et al.*, 2011). These responses require IL-1β to skew Th cells towards this phenotype, with defects in production associated with susceptibility to these infections (Mailer *et al.*, 2015). Furthermore, IL-1β has been shown to be important for infections where neutrophils have a critical role, such as *Staphylococcus aureus* infection (Pires and Parker, 2018). However, IL-1β has also been shown to be important infections that are more chronic, similar to cryptococcosis, such as *Mycobacterium marinum*, where IL-1β is also reported to have a protective role (Ogryzko *et al.*, 2019).

Therefore, there is evidence that IFNγ may not always be beneficial in the case of pulmonary cryptococcosis, and that and it had yet to be determined whether IL-1β significantly contributes to host protection, or the action of IFNγ. Therefore, in order to test these hypotheses, the inhalation model developed in chapter 4 was used in combination with transgenic and pharmacological manipulation to determine if and how IFNγ and IL-1β contribute to host protection in a mammalian *in vivo* model.

5.2 – Results

5.2.1 – A single dose of IFNγ at the time of infection, or the absence of IL-1β, does not significantly affect the survival of C57BL/6 mice infected with high inocula KN99α GFP *C. neoformans*

IFNγ treatment had been observed to have a beneficial role in an *in vivo* zebrafish model and a detrimental role in an *in vitro* J774 cell model of *C. neoformans* infection (see Chapter 3; Kamuyango, 2017). Therefore, the effects of IFNγ were examined in a mouse model of infection with highly virulent KN99α GFP infection. Additionally, the mice used in these experiments were transgenic wild-type(IL1β$^{tm1c(EUCOMM)}$) and IL-1β KO(*pgk2-Cre-IL1β^{tm1d}*) mice generated on a C57BL/6 backgrounded (see 2.2), so that the role of IL-1β in host protection could also be established. Mice were subjected to survival analysis for up to 40 days, using the same monitoring protocol and humane endpoints as were used in chapter 4. Mice were then culled either after 40 days, or having reached a humane endpoint, and lung and brain tissue was taken for fungal burden analysis.

Firstly, the effects of a single dose of 2.5μg IFNγ or PBS when given intranasally at the time of infection were examined in mice that either did or didn't produce IL-1β. This concentration of 2.5μg was chosen based on 5μg/ml that was found to be sufficient for protection in zebrafish experiments (Kamuyango, 2017) and was akin to dosing regimens used in previous *in vivo* studies of IFNγ in mice. Although the dose in these experiments was ten times larger, this dose was chosen based on the observed low efficiency of intranasal dosing observed in Chapter 4 experiments (~20%). Additionally, the intranasal route was selected in order to replicate the zebrafish experiments, where IFNγ was administered directly to the site of infection, in order to stimulate local cells.

Unlike what was observed in zebrafish embryo experiments, a single dose of IFNγ was not protective in the mouse survival model. Instead, mouse mortality was not observed to be significantly changed by treatment (Figure 31). Additionally, there was no effect of mouse IL-1β status, with or without IFNγ treatment. Interestingly, the only treatment group with surviving mice were wild-type(IL1β$^{tm1c(EUCOMM)}$) animals treated with PBS. Bodyweight changes over time for each animal are shown in Appendix A.

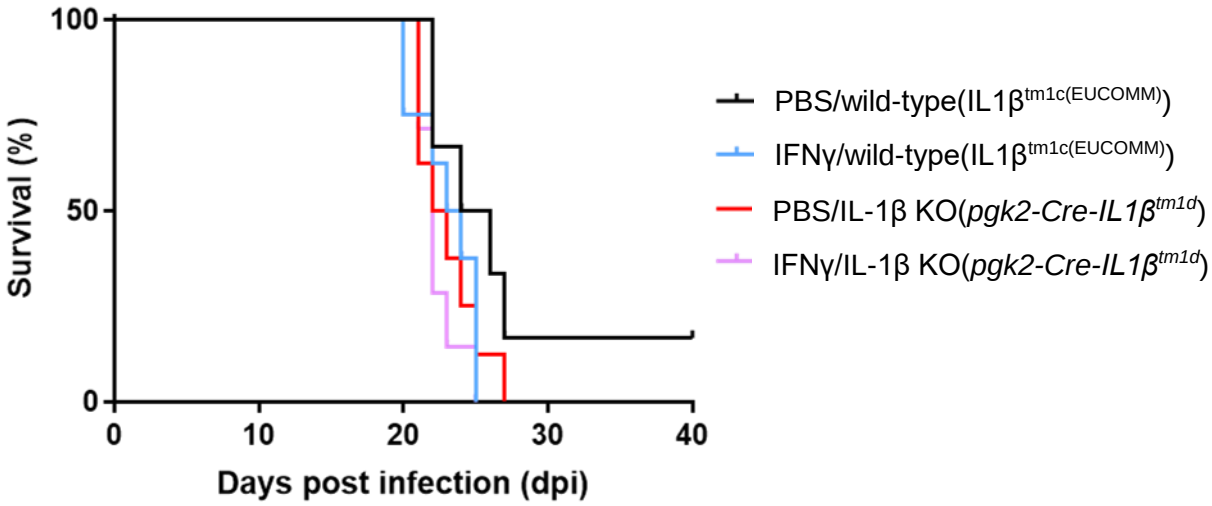

Figure 31 – Neither a single dose of IFNγ at the time of infection or the absence of IL-1β significantly affected mouse survival due to infection with KN99α GFP *C. neoformans*. Mice unable to produce functional IL-1β or treated with IFNγ at the time of KN99α GFP *C. neoformans* showed comparable survival. Additionally, there was no significant effect of a combination of both treatments (chi square=2.002, df=1, p=0.1571). Survival curves were compared using a log-rank test. PBS/wild-type(IL1β$^{tm1c(EUCOMM)}$) – n=6, IFNγ/wild-type(IL1β$^{tm1c(EUCOMM)}$) – n=8, PBS/IL-1β KO(*pgk2-Cre-IL1β^{tm1d}*) - n=8, IFNγ/IL-1β KO(*pgk2-Cre-IL1β^{tm1d}*) - n=8.

5.2.2 – A single dose of IFNγ at the time of KN99α GFP *C. neoformans* infection or ablating IL-1β signalling induced significant weight loss in infected animals

While no examined treatment significantly affected mouse survival, it was noted that the progression of infection was different. While all infected PBS/wild-type(IL1β$^{tm1c(EUCOMM)}$) animals had to be culled due to clinical signs of infection (open mouth breathing, ataxia), all other animals that either received treatment with IFNγ, lacked IL-1β or both, instead had to be culled due to significant weight loss.

Therefore, the bodyweights of animals at the time of culling, culled prior to 40dpi, were compared (Figure 32). While weight loss was largely absent in the PBS/wild-type(IL1β$^{tm1c(EUCOMM)}$) group, all IFNγ treated and IL-1β$^{-/-}$ knockout animals showed significant lower bodyweights at the time of culling – confirming that the infection phenotype was significantly changed in these groups.

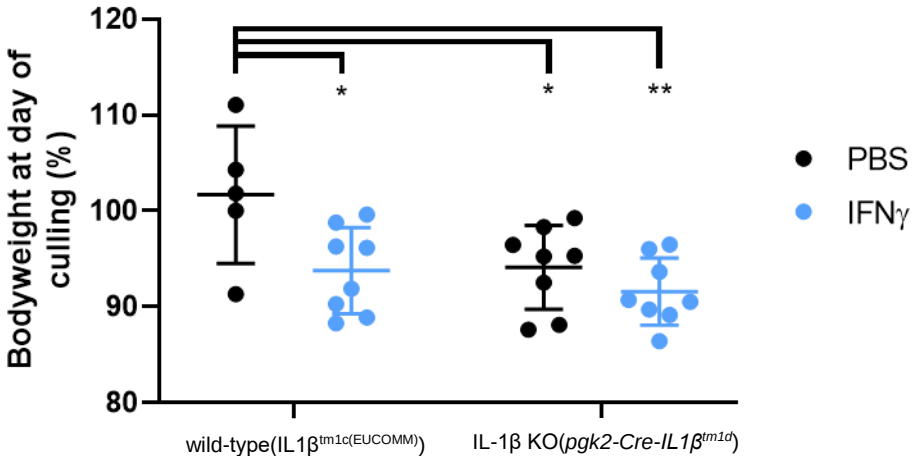

Figure 32 – Both IFNγ at the time of infection or ablating IL-1β resulted in significant weight loss in mice terminally infected with KN99α GFP *C. neoformans*. While wild-type(IL1β$^{tm1c(EUCOMM)}$) mice treated with PBS that had to be culled during survival experiments were culled due to clinical signs, all animals that either received IFNγ at the time of infection or that lacked IL-1β were culled due to significant weight loss. Interaction – $F(1,26)=3.676$, $p=0.0663$. Genotype – $F(1,26)=9.684$, $p=0.0045$. Treatment – $F(1,26)=10.82$, $p=0.0029$. From left to right, significant p values from multiple comparisons were 0.0346, 0.0451 and 0.0052. Bodyweights were compared using a two-way ANOVA with *post hoc* Tukey comparisons. Data presented as mean ± SD. Each point represents a different animal: PBS/wild-type(IL1β$^{tm1c(EUCOMM)}$) – n=5, IFNγ/wild-type(IL1β$^{tm1c(EUCOMM)}$) – n=8, PBS/IL-1β KO(*pgk2-Cre-IL1β^{tm1d}*) - n=8, IFNγ/IL-1β KO(*pgk2-Cre-IL1β^{tm1d}*) - n=8. * - $p<0.05$, ** - $p<0.01$. All animals were culled between 20-27dpi.

5.2.3 – Infected mouse tissue fungal burdens were unaffected by treatment with a single dose of IFNγ or the absence of IL-1β

Having established that the phenotype of KN99α GFP infection was significantly affected by IFNγ treatment and IL-1β status, fungal burdens in the lung and brain from infected animals were therefore compared to establish if fungal clearance was also affected.

Interestingly, no significant differences were observed regardless of treatment group (Figure 33A). In terms of dissemination, infection of the brain was observed in all animals, regardless of treatment group. Additionally, fungal burdens in the brain of infected animals did not significantly differ (Figure 33B).

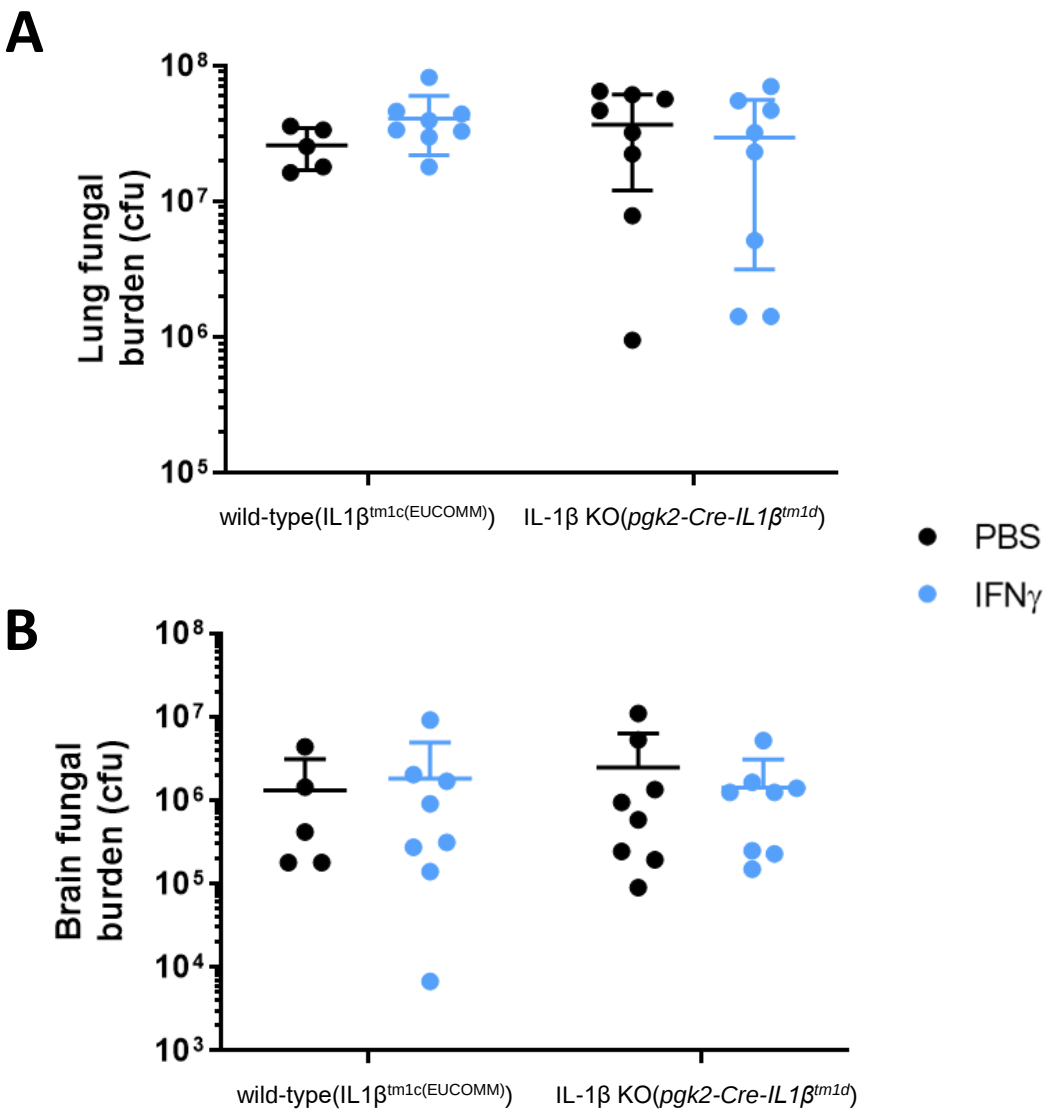

Figure 33 – Neither ablating IL-1β or IFNγ treatment in mice significantly affected tissue fungal burdens in animals infected with KN99α GFP *C. neoformans*. Despite significant differences in the bodyweight, no treatment of survival animals significantly affected the fungal burden in the lung or the brain. (**A**) Pulmonary fungal burdens of KN99α GFP were unaffected by IL-1β status or IFNγ treatment. Interaction – $F(1,25)=1.791$, $p=0.1929$. Genotype – $F(1,25)=0.0008968$, $p=0.9763$. Treatment – $F(1,25)=0.2231$, $p=0.6408$. (**B**) Brain fungal burdens of KN99α GFP were unaffected by IL-1β status or IFNγ treatment. Interaction – $F(1,25)=0.5146$, $p=0.4798$. Genotype – $F(1,25)=0.1196$, $p=0.7323$. Treatment – $F(1,25)=0.06298$, $p=0.8039$. Pulmonary and brain fungal burdens were compared using a two-way ANOVA. Data presented as mean ± SD. Each point represents a different animal (n≥5): PBS/wild-type(IL1β$^{tm1c(EUCOMM)}$) – n=5, IFNγ/wild-type(IL1β$^{tm1c(EUCOMM)}$) – n=8, PBS/IL-1β KO(*pgk2-Cre-IL1β^{tm1d}*) - n=8, IFNγ/IL-1β KO(*pgk2-Cre-IL1β^{tm1d}*) - n=8. All data presented is from animals culled between 20-27dpi.

5.2.4 – Mice infected with the H99α IFNγ strain of *C. neoformans* succumb to infection significantly faster than those infected with the parental H99α WT strain

Unlike with previous zebrafish embryo experiments, no benefit of a single dose of IFNγ on host outcomes was observed. However, the inoculum of *C. neoformans* mice received was higher than what zebrafish embryo received, with experiments also lasting eight times longer (Kamuyango, 2017). Therefore, it was hypothesised that a single dose of IFNγ was not sufficient for host protection, and so the effect of a continuous IFNγ signal was investigated. This continuous signal was provided by infecting wild-type(IL1β$^{tm1c(EUCOMM)}$) and IL-1β$^{-/-}$ animals with the transgenic H99α IFNγ strain of *C. neoformans*, as fungal cells of this strain constitutively produces murine IFNγ and export it out into the surrounding milieu. As a negative control, animals were infected with the parental H99α WT *C. neoformans* strain, which does not produce IFNγ.

In contrast to previous observations of mouse infections using this strain, infections of mice with H99α IFNγ *C. neoformans* in this model resulted in significantly accelerated mortality compared to H99α WT infection (Figure 34). However, neither strain showed differential virulence in the absence of IL-1β.

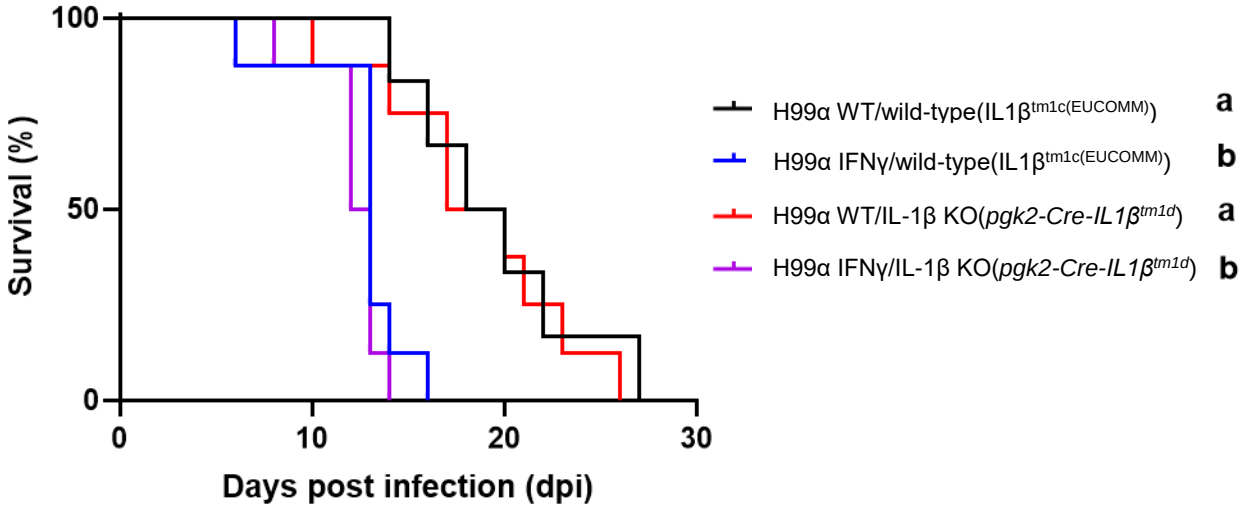

Figure 34 – H99α IFNγ infection results in significantly accelerated mortality in mice compared to H99α WT infection. Wild-type(IL1β$^{tm1c(EUCOMM)}$) and IL-1β$^{-/-}$ mice intranasally inoculated with H99α IFNγ had to be culled significantly sooner than animals inoculated with H99α WT (Chi square=21.62, df=3, p<0.0001). H99α WT/wild-type(IL1β$^{tm1c(EUCOMM)}$) compared to H99α IFNγ/wild-type(IL1β$^{tm1c(EUCOMM)}$) (Chi square=9.421, df=1, adjusted p value=0.0126). H99α WT/wild-type(IL1β$^{tm1c(EUCOMM)}$) compared to H99α IFNγ/IL-1β KO(*pgk2-Cre-IL1β^{tm1d}*) (Chi square=10.09, df=1, adjusted p value=0.0042). H99α WT/IL-1β KO(*pgk2-Cre-IL1β^{tm1d}*) compared to H99α IFNγ/IL-1β KO(*pgk2-Cre-IL1β^{tm1d}*) (Chi square=9.367, df=1, adjusted p value=0.0132). H99α WT/IL-1β KO(*pgk2-Cre-IL1β^{tm1d}*) compared to H99α IFNγ/wild-type(IL1β$^{tm1c(EUCOMM)}$) (Chi square=8.703, df=1, adjusted p value=0.0192). Other differences were non-significant. Survival curves were compared by a log-rank test, followed by *post hoc* multiple log rank comparisons, corrected to account for multiple comparisons. Survival curves with a different letter were significantly different. Data is presented as mean ± SD. Each point represents a different animal: H99α WT/wild-type(IL1β$^{tm1c(EUCOMM)}$) – n=6, H99α IFNγ/wild-type(IL1β$^{tm1c(EUCOMM)}$) – n=8, H99α WT/IL-1β KO(*pgk2-Cre-IL1β^{tm1d}*) - n=8, H99α IFNγ/IL-1β KO(*pgk2-Cre-IL1β^{tm1d}*) - n=8. * - p<0.05, ** - p<0.01.

5.2.5 – *C. neoformans* strain, but not IL-1β status, significantly affects mouse weight loss due to infection with H99α *C. neoformans*

Because there was a large difference in the survival times of animals infected with H99α IFNγ *C. neoformans*, significant differences in infection phenotype were anticipated, particularly as significant weight loss was observed with just a single dose of IFNγ. Therefore, changes in the bodyweight of terminal mice were compared.

H99α WT infection of wild-type(IL1β$^{tm1c(EUCOMM)}$) mice, as with KN99α GFP infection, only resulted in one terminal animal exhibiting significant weight loss on the day of culling (Figure 35). In the case of H99α IFNγ infection, however, significant weight loss was observed in terminal wild-type(IL1β$^{tm1c(EUCOMM)}$) and IL-1β KO(*pgk2-Cre-IL1β^{tm1d}*) mice, as was observed with a single dose of IFNγ (Figure 32). This weight loss was also the reason these animals had to be culled. Bodyweight changes over time for each animal are shown in Appendix B.

Interestingly, unlike what was observed with KN99α GFP infection (Figure 32), the absence of IL-1β did not result in significant weight loss with H99α WT infection. This suggests that KN99α GFP and H99α WT infections have differential relationships with IL-1β with regard to mouse anorexia responses.

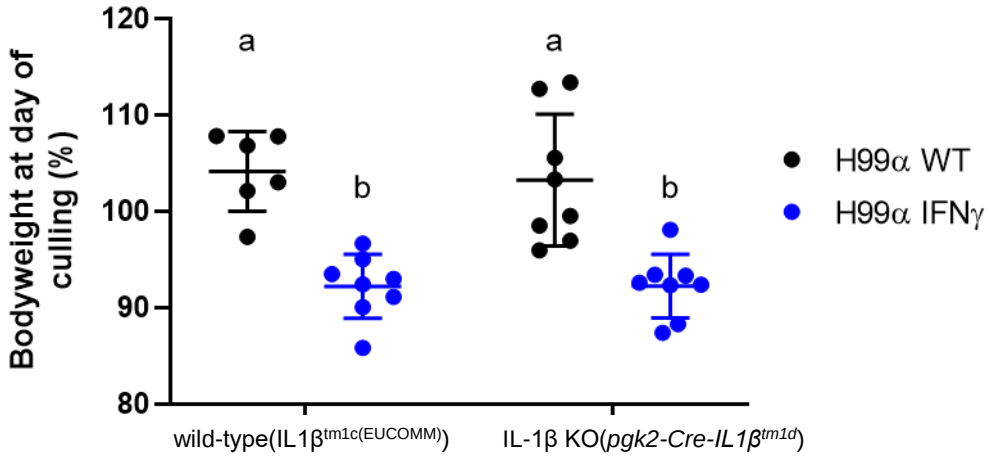

Figure 35 – *C. neoformans* strain, not IL-1β status, significantly affected bodyweight loss in terminally infected mice. While H99α IFNγ infection resulted in significant weight loss, the absence of IL-1β did not in the case of H99α WT infection. Interaction – F(1,26)=0.07573, p=0.7854. Genotype – F(1,26)=44.84, p<0.0001. Infection – F(1,26)=0.06617, p=0.7990. H99α WT/wild-type(IL1β$^{tm1c(EUCOMM)}$) compared to H99α IFNγ/wild-type(IL1β$^{tm1c(EUCOMM)}$) (adjusted p value=0.0004). H99α WT/wild-type(IL1β$^{tm1c(EUCOMM)}$) compared to H99α IFNγ/IL-1β KO(*pgk2-Cre-IL1β^{tm1d}*) (adjusted p value=0.0004). H99α WT/IL-1β KO(*pgk2-Cre-IL1β^{tm1d}*) compared to H99α IFNγ/IL-1β KO(*pgk2-Cre-IL1β^{tm1d}*) (adjusted p value=0.0004). H99α WT/IL-1β KO(*pgk2-Cre-IL1β^{tm1d}*) compared to H99α IFNγ/wild-type(IL1β$^{tm1c(EUCOMM)}$) (adjusted p value=0.0004). Other comparisons were non-significant. Bodyweight changes were compared using a two-way ANOVA with *post hoc* Tukey multiple comparisons. Datasets labelled with different letters significantly differ. Data presented as mean ± SD. Each point represents a different animal: H99α WT/wild-type(IL1β$^{tm1c(EUCOMM)}$) – n=6, H99α IFNγ/wild-type(IL1β$^{tm1c(EUCOMM)}$) – n=8, H99α WT/IL-

5.2.6 – Intranasal infection of mice with H99α IFNγ *C. neoformans* results in significantly higher pulmonary fungal burdens compared to H99α WT *C. neoformans* infection

Having determined that H99α IFNγ *C. neoformans* infection resulted in significant weight loss, pulmonary fungal burdens in terminal animals infected with H99α WT or H99α IFNγ were then compared. Interestingly, pulmonary fungal burdens of H99α IFNγ *C. neoformans* were approximately double those observed with H99α WT infection (Figure 36). Additionally, as with weight loss, there was no significant effect of ablating IL-1β signalling on pulmonary fungal burdens in wild-type(IL1β$^{tm1c(EUCOMM)}$) or IL-1β$^{-/-}$ animals. From this, it can be inferred that IL-1β does not have an important role in the host mediated clearance of H99α strains of *C. neoformans* from the lungs.

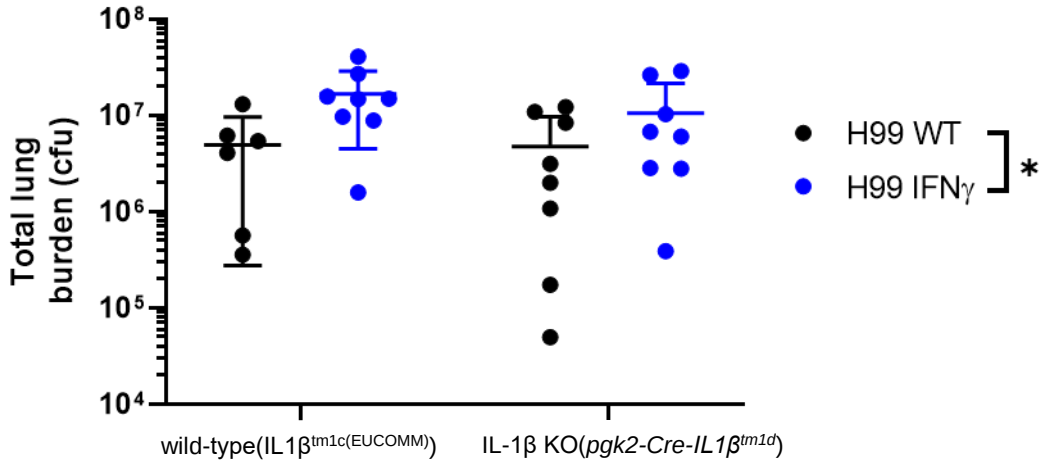

Figure 36 – Pulmonary fungal burdens in mice infected with H99α IFNγ *C. neoformans* are significantly higher than those due to H99α WT *C. neoformans* infection. As was observed with animal survival and the weight loss response, the absence of IL-1β did not significantly affect pulmonary fungal burdens, although burdens of H99α IFNγ *C. neoformans* were significantly higher. Interaction – $F(1,26)=0.7742$, $p=0.3870$. Genotype – $F(1,26)=0.8879$, $p=0.3547$. Infection – $F(1,26)=6.822$, $p=0.0148$. No specific significant differences were identified with multiple comparisons. Pulmonary fungal burdens were compared using a two-way ANOVA with *post hoc* Tukey multiple comparisons. Data presented as mean ± SD. Each point represents a different animal: H99α WT/wild-type(IL1β$^{tm1c(EUCOMM)}$) – n=6, H99α IFNγ/wild-type(IL1β$^{tm1c(EUCOMM)}$) – n=8, H99α WT/IL-1β KO(*pgk2-Cre-IL1β^{tm1d}*) - n=8, H99α IFNγ/IL-1β KO(*pgk2-Cre-IL1β^{tm1d}*) - n=8. * - $p<0.05$. H99α WT infected animals were culled between 10-27dpi, while H99α IFNγ infected animals were culled between 6-16dpi

5.2.7 – Lower numbers of H99α IFNγ *C. neoformans* cells were found in the brain of terminal survival C57BL/6 mice compared to with H99α WT infection

The tissue burdens in the CNS of terminal infected animals were also examined alongside burdens in the lungs (Figure 37). However, despite the association of *C. neoformans* with meningitis, dissemination to the CNS was not observed in terminal animals infected with H99α WT, despite animals having to be culled due to clinical signs of infection (Figure 35). Even though dissemination to the CNS was observed in all H99α IFNγ infected animals, no significant difference in occurrence between H99α WT and H99α IFNγ infection was observed (Figure 37A). Controversially, however, when the fungal burdens in the CNS of animals that were positive for meningitis were compared, H99α IFNγ infection actually resulted in significantly smaller fungal burdens than those infected with H99α WT (Figure 37B), although again IL-1β status did not significantly affect this.

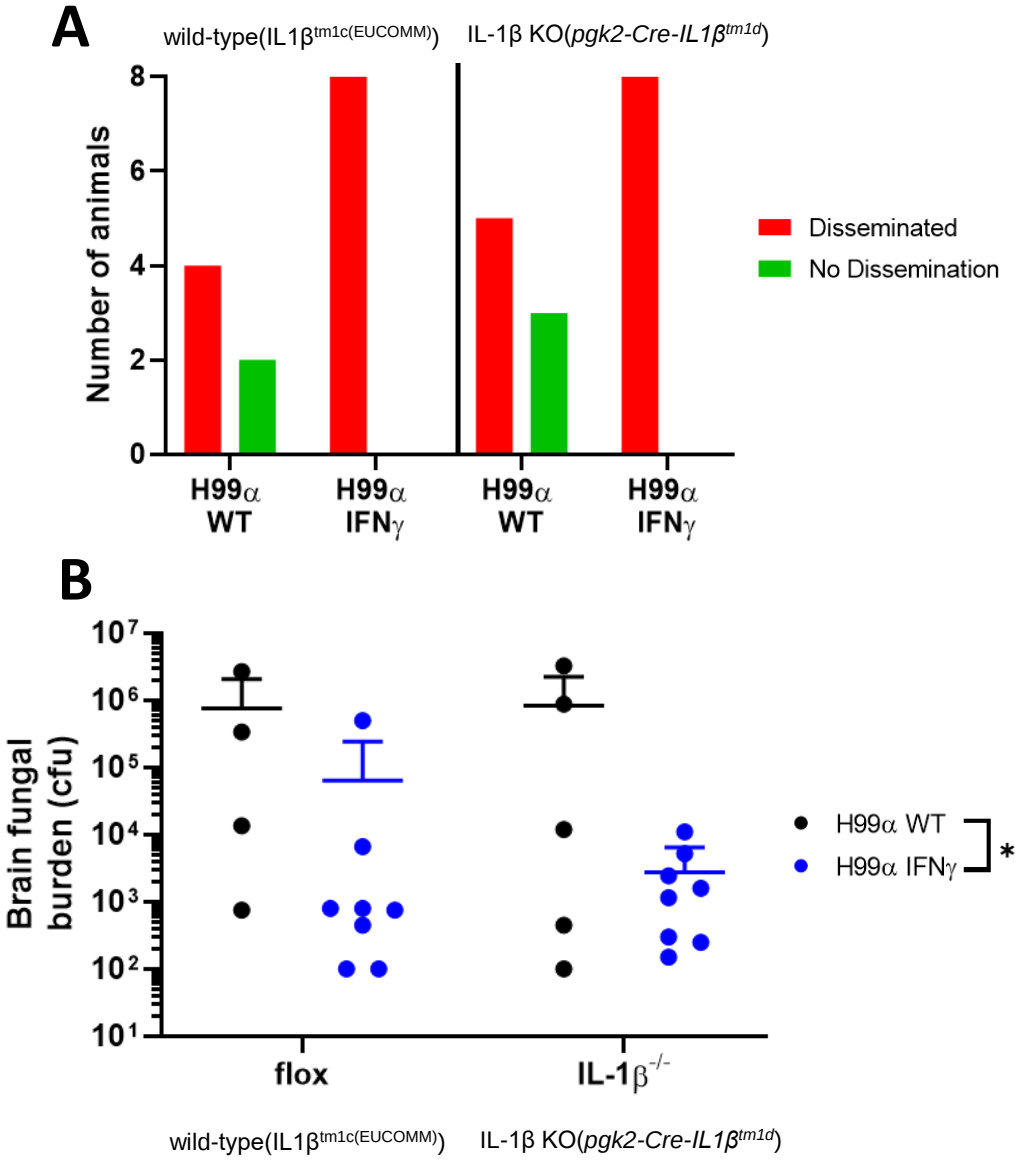

Figure 37 – H99α IFNγ *C. neoformans* disseminated to the CNS of mice more than H99α WT *C. neoformans*, although results in lower CNS fungal burdens. Despite universal dissemination in mice, CNS fungal burdens of H99α IFNγ *C. neoformans* were significantly lower compared to H99α WT infection. (**A**) Meningitis was confirmed in all H99α IFNγ infected mice, but not in those infected with H99α WT – although this difference was not found to be significant (Chi-square=6.9, df=3, p=0.0752). (**B**) Brain fungal burdens of H99α WT in infected animals positive for meningitis were significantly higher than those with H99α IFNγ infection. Interaction – F(1,21)=0.04013, p=0.8432. Genotype – F(1,21)=0.0002526, p=0.9875. Infection – F(1,21)=5.269, p=0.0321. Incidences of dissemination were analysed by a Chi-squared test and CNS fungal burdens were compared by a two-way ANOVA. Data presented as mean ± SD. Each point in **B** represents a different animal: H99α WT/wild-type(IL1β$^{tm1c(EUCOMM)}$) – n=6, H99α IFNγ/wild-type(IL1β$^{tm1c(EUCOMM)}$) – n=8, H99α WT/IL-1β KO(*pgk2-Cre-IL1β^{tm1d}*) - n=8, H99α IFNγ/IL-1β KO(*pgk2-Cre-IL1β^{tm1d}*) - n=8. * - p<0.05. H99α WT infected animals were culled between 10-27dpi, while H99α IFNγ infected animals were culled between 6-16dpi

5.3 – Discussion

By utilising the *in vivo* mouse intranasal infection model developed in Chapter 4, I was able to assess the efficacy of IFNγ in affecting mouse survival – both as a single dose and as a continuous infusion. Additionally, the contribution of IL-1β to both host survival and the action of IFNγ during *C. neoformans* infection. Controversially, a single dose of IFNγ at the time of infection offered no benefit to mice and even accelerated mortality in the case of H99α IFNγ infection. Additionally, no contribution of IL-1β was found with regard to animal survival or IFNγ action. However, both increased IFNγ and ablation of IL-1β resulted in significant weight loss during KN99α GFP infection, while only IFNγ affected weight loss due to H99α WT infection.

5.3.1 – IFNγ enhanced the virulence of *C. neoformans* infection *in vivo*

While a single dose of IFNγ had no significant effect on KN99α GFP *C. neoformans* infection outcomes, intranasal infection with the IFNγ producing H99α IFNγ *C. neoformans* strain resulted in significantly accelerated mortality. These observations contradict previous *in vivo* experiments with H99α IFNγ, where this strain has been reported instead to be avirulent compared to H99α WT infection in both BALB/c and C57BL/6 mice (Wormley *et al.*, 2007; Castro-Lopez *et al.*, 2018). Interestingly, it should be noted that although BALB/c mice are less resistant to H99α WT *C. neoformans* infection compared to C57BL/6 mice (Nielsen *et al.*, 2005), infection with H99α IFNγ is

relatively more virulent in C57BL/6 mice (Castro-Lopez *et al.*, 2018). Even then, H99α IFNγ infection only resulted in a mortality rate of 60% in C57BL/6 mice, while H99α WT infection at the same dose resulted in 100% mortality. This means that the accelerated mortality observed with H99α IFNγ infection in my experiments is not explained solely by the choice of mouse strain. Instead, the biggest differences in methodology between these studies was the size of the inoculum animals received. Previous H99α IFNγ experiments used an inoculum of $1x10^4$ cfu – five times smaller than the inocula used here (Wormley *et al.*, 2007; Castro-Lopez *et al.*, 2018). This higher inocula will not only have resulted in higher fungal burdens, but also would have increased the amount of IFNγ present in the system, which may have resulted in toxicity.

Examining the mechanisms that explain the differences in increased virulence of H99α IFNγ in survival experiments, it was observed that meningitis occurred in all animals infected with H99α IFNγ. However, H99α IFNγ CNS fungal burdens were significantly lower compared to H99α WT infection. This could be assumed to be due to a reduced ability to grow on CNS tissue. However, *C. neoformans* is a relatively immunologically quiescent pathogen, as evidenced by the immunosuppressive roles of secreted GXM (Decote-Ricardo *et al.*, 2019), the existence of latent infection (Pan *et al.*, 2021) and the largely asymptomatic nature of infection in patients prior to the onset of meningitis (Neal *et al.*, 2017). Therefore, the IFNγ production associated with H99α IFNγ likely increased the immunogenicity of fungal cells in the CNS. The enhanced recruitment and function of immune cells may have resulted in higher levels of dangerous neuroinflammation than was observed with parental H99α WT strain infection. Additionally, IFNγ is indirectly neurotoxic by stimulating microglia to produce TNFα and IL-1β. As IL-1β has been associated with neuronal damage and death in mice, IFNγ may have indirectly resulted in neuronal cell death in the CNS of infected mice (Brás et al., 2020). Furthermore, increased immune responses to *C. neoformans* in the CNS of mice have been reported to be a source of mortality (Neal *et al.*, 2017). Although fungal burdens of *C. neoformans* are observed to peak in the CNS weeks prior to maximal immune cell infiltration, it has been the latter that correlates with mortality (Neal *et al.*, 2017). In IFNγ treated animals, higher numbers of pro-inflammatory cells would be anticipated, in particular IFNγ producing T cells which and specifically associated with mortality (Neal *et al.*, 2017). However, these experiments were not sufficient to confirm that neuroinflammation in this model resulted in an anorexia response. In order to confirm this hypothesis, additional experiments would be required. Firstly, immune phenotyping of the CNS of terminally infected animals would be required, using flow cytometry, to confirm that IFNγ increased immune cell infiltration into the CNS. This could suggest that the cause of death in H99α IFNγ infection was neuroinflammation.

It should also be confirmed if there is another explanation for lower CNS burdens of H99α IFNγ. Both H99α WT and H99α IFNγ should be cultured in CSF to confirm that the growth of H99α IFNγ was not changed in this environment. It is also possible that lower CNS fungal burdens of H99α IFNγ were just the result of H99α IFNγ animals having to be culled sooner – affording H99α IFNγ cells a smaller window of time to replicate within the CNS. However, this would require characterising CNS fungal burdens at additional time points.

One other potential explanation is that elevated IFNγ resulted in an excessive anorexia response in infected mice. IFNγ is already an approved treatment in other conditions, currently indicated for chronic granulomatous disease and severe malignant osteoporosis (NICE, 2021). This means that toxicity due to this treatment is well characterised, with reported side effects of high dose treatment including lethargy, chills and anorexia (Sriskandan *et al.*, 1986) – many of which are also symptoms of terminal cryptococcosis in mice. Therefore, a combination of *C. neoformans* infection and higher concentrations of IFNγ may have been additive. The specific effect of H99α IFNγ infection exacerbating anorexia responses in mice, however, is evidence that this may have the major contributing mechanism of mortality in IFNγ treated animals. Weight loss is a common symptom during infections, hypothesised to have evolved as a mechanism of host defence by host organisms to reduce pathogen access to host-derived nutrients. In mouse models, however, this weight loss can be excessive, leading to cachexia and eventually death (Murray and Murray, 1979). This is why bodyweight is a common predictor of mortality in many *in vivo* infection models (Krarup *et al.*, 1999; Trammell and Toth, 2011). However, perturbations in any physiological system can result in weight loss. Of particular relevance to these experiments is that anorexia is associated with various proinflammatory cytokines, and in particularly IFNγ (Mccarthy, 2000). Mechanistically, psychoneuroimmunological studies have identified neuropeptide α-MSH as an endogenous appetite suppressant that acts via the hypothalamus and is associated with anorexia in mice (Lawrence and Rothwell, 2001; Fetissov *et al.*, 2002). In the case of CNS infection, the rodent-borne virus lymphocytic choriomeningitis was found to result in elevated levels of both IFNγ and α-MSH. This mechanism may have contributed to the significant anorexia response that occurred in my experiments (Kamperschroer and Quinn, 2002).

However, it is important to note that in these survival experiments, weight loss was sudden onset, suggesting it was associated with a specific pathological event such as dissemination or infiltration of leukocytes into the CNS. In mouse models, intranasal infection results in dissemination to the CNS as early as 1dpi, suggesting that dissemination could be correlated with anorexia responses (Coelho *et al.*, 2019).

Alternatively, Additionally, infecting mice lacking the IFNγ receptor would help to confirm the specificity of the anorexia response, and confirm whether it was the result of IFNγ or other neuroinflammatory mediators. Finally, characterising CNS burdens at other time points of infection would confirm whether anorexia was the result of dissemination or not.

Alternatively, IFNγ may have accelerated mortality by inadvertently enhancing the virulence of *C. neoformans* cells. As described previously, IFNγ treatment is reported to enhance the antimicrobial action of macrophages (Voelz, Lammas and May, 2009; Jarvis *et al.*, 2012). However, as was observed *in vitro* (chapter 3), intracellular *C. neoformans* cells are highly resistant to macrophage antifungal activity. Therefore in survival experiments, IFNγ may have generated more pro-inflammatory macrophages (low pH, increased ROS) which rather than increase fungal clearance may have stimulated a more rapid adaptation of *C. neoformans* cells to the macrophage intracellular environment. Several *C. neoformans* virulence factors, such as Plb1, are known to have optimal activity at low pH. IFNγ may have therefore stimulated capsular growth within the lungs, in turn have increasing the virulence of individual *C. neoformans* cells *in vivo* (Wright *et al.*, 2007), without stimulating sufficient fungal clearance. Additionally, the resulting adaptations may have better protected fungal cells from the antifungal activity of potentially more fungicidal cells such as DCs, NK cells and $CD4^+$ cells (Ma *et al.*, 2004; Evans *et al.*, 2015; Specht *et al.*, 2015; Seoane *et al.*, 2020). Higher pulmonary fungal burdens in survival experiments with H99α IFNγ could be evidence of either suppressed immunity and/or more adaptation of *C. neoformans* cells to the host environment. To confirm this theory, intravital imaging of *C. neoformans* cells interacting with macrophages *in vivo* in the lung would allow for host-pathogen interactions to be assayed to determine what effect IFNγ had on inhaled *C. neoformans* cells.

Another potential explanation related to the intranasal dosing methodology. Intranasal inocula are distributed throughout the lungs (see Chapter 6). This may have resulted in multiple localised areas within foci of infection, leading to chemotactic 'confusion' whereby immune cells were inappropriately recruited to sterile regions of the lung positive for IFNγ stimulation or ablating chemotactic gradients at infection foci. This may have reduced numbers of leukocytes at foci of pulmonary infection (Murphy *et al.*, 2008). To investigate this further, immune cell recruitment should be assessed using both flow cytometry to compare absolute numbers, and intravital imaging and PCLS to assess the spatial distribution of immune cells and pathogens within the lungs in the case of IFNγ treatment.

There is also the possibility that the high levels of IFNγ created an IRIS like phenotype (Chang *et al.*, 2013) – a complication in cryptococcosis patients characterised by excessive and dangerous activation of the immune system. In the case of H99α IFNγ

infection, the concentration of IFNγ in mice may have been high enough to induce an IRIS like phenotype and result in systemic autoimmunity. Paradoxically, however, IFNγ has also been successfully used to treat incidences of IRIS, and so quantification of serum cytokine levels in infected animals should be done, to confirm if animals were in an IRIS-like state and if IFNγ was detrimental in these incidences (Perfect *et al.*, 2010). Finally, there is also the potential that the H99α IFNγ strain used in these experiments had significantly mutated since it was first characterised, and therefore had different virulence and behaviour *in vivo,* as discussed in chapter 3.

5.3.2 – IL-1β has a minimal role in host protection during cryptococcosis

Compared to the effects of IFNγ, IL-1β was found to have a comparatively subtle impact on infection outcomes and fungal burdens in these experiments. The absence of IL-1β did not significantly affect mouse survival, fungal burdens or dissemination in all survival experiments, regardless of the strain of *C. neoformans* animals were infected with. This implies that IL-1β is not critical for host survival in the case of cryptococcosis.

However, one interesting observation in the case of KN99α GFP infection was that animals lacking IL-1β had to be culled due to significant bodyweight loss, similarly to IFNγ treated animals. However, this weight loss phenotype was not observed with H99α WT infection in the absence of IL-1β. The differential dependence of anorexia responses with different but related strains of *C. neoformans* warrants further investigation, with specific reference to the role of IL-1β. Interestingly, it indicated that there is a difference in both the pathology and host immune response to these two strains.

A mechanism that explains the weight loss observed with KN99α GFP infection in the absence of IL-1β is not clear from these experiments. The weight loss in IL-1β knockout mice suggests that IL-1β reduces or prevents anorexia. However, IL-1β is strongly associated with anorexia (Layé *et al.*, 2000; Lawrence and Rothwell, 2001; Kamperschroer and Quinn, 2002; Gonzalez *et al.*, 2006; Rao *et al.*, 2017). This suggests that in these survival experiments, weight loss occurred by a different mechanism. It may be that in cryptococcosis IL-1β plays an important regulatory role, and loss of this signal results in excessive production of other inflammatory cytokines or mediators that stimulate anorexia, such as IL-6 or TNFα (Kamperschroer and Quinn, 2002). However, in order to better understand the differences in KN99α and H99α infection, these mechanisms of weight loss should be investigated, examining additional readouts such as CNS cytokine production and α-MSH levels, before attempting to generate the same anorexia phenotype using cytokine treatment both without *C. neoformans* infection and with H99α WT infection.

Importantly these survival experiments revealed that there was also no apparent interaction or dependence of IFNγ treatment on IL-1β. This provides evidence that the elevated IL-1β levels in zebrafish embryo experiments were not critical to the action of IFNγ, and was instead just a marker of IFNγ signalling – such as M1 polarised macrophages (Arango Duque and Descoteaux, 2014; Kamuyango, 2017). It is possible that IL-1β is important for the protective action of IFNγ in the case of zebrafish embryo experiments and that this contribution is species dependent. To this end, in mice it is possible that the IFNγ/IL-1β axis has a level of redundancy and different cytokines in mammals can compensate for the absence of IL-1β. The most likely candidate is IL-18, another IL-1 family cytokine shown to be important in mouse models of cryptococcosis and closely associated with the action of IFNγ (Kawakami *et al.*, 1997). As IL-18 is not present in zebrafish, this redundancy of IL-1β may not exist, and therefore play a more critical role in this organism (Huising *et al.*, 2004). In order to confirm this, production of IL-1β should be inhibited in the zebrafish embryo model to examine how this impacted host outcomes.

5.3.3 – Limits of translation with mouse survival experiments of IFNγ and IL-1β

Although these experiments provided important data regarding the importance of the host immune response and the contribution of cytokines to host protection, there were also limitations.

One limitation was the use of strains of two different backgrounds, KN99α and H99α, which during this study were revealed to significantly different in terms of their infection phenotype in mice. Both of these strains are of serotype A – the most frequently observed serotype clinically (Casadevall and Perfect, 1998) – and are comparably virulent *in vivo* (Nielsen *et al.*, 2003, 2005). The pathology of infection in mice with both strains are also the same – pulmonary infection of mice resulted in an initially asymptomatic infection followed by a rapid deterioration in animal health status with infection with either strain resulting in nearly 100% mortality in untreated animals (Mwaba *et al.*, 2001) – mirroring the human clinic situation. In addition, symptoms of late stage human infection were recapitulated with infection of either strain, causing symptoms such as breathlessness and ataxia.

Important differences between these strains include their different origins – H99α was originally isolated from a patient in 1978 (Perfect, Lang and Durack, 1980), while KN99α was generated experimentally *in vitro* by crossing a rare clinical *C. neoformans* isolate of the **a** mating type with H99α (Nielsen *et al.*, 2003). This means that both strains have different genotypes, which may significantly affect virulence. Additionally, the genotype of KN99α was fully characterised during its inception, meaning genotypes between

studies can be confirmed prior to starting work. However, the historic origin of the H99α strain means that the strain used today has been retrospectively determined to different from the original strain, due to mutations over time (Arras *et al.*, 2017). This limits the comparisons that can be drawn between studies of H99α. Finally, although both strains show comparable virulence *in vivo*, it is important to note when mice were co-infected with both H99α and KN99α, H99α was observed to disseminate to the CNS preferentially (Nielsen *et al.*, 2005). These differences in H99α and KN99α must be taken into account when comparing the two, and limits the direct comparisons that can be drawn between KN99α GFP and H99α WT experiments.

Additionally, the size of inocula used for mouse survival experiments was $5x10^4$ cfu was chosen because this inoculum resulted in approximately one cryptococcal cell per alveoli (chapter 6). However, as human exposure is thought to be no more than a few fungal cells or spores at a time, these inocula of different magnitudes significantly affects translatability of findings in survival experiments as method of administration and inocula received are not akin to natural human exposure. It is also possible that the inocula animals received may have been too high with which to study the contributions of IFNγ or IL-1β. Repeating these studies using inocula five times smaller, as was used in previous H99α IFNγ *in vivo* experiments may reveal significant contributions of these cytokines that were lost due to the high fungal burden (Wormley *et al.*, 2007; Castro-Lopez *et al.*, 2018). However, this does suggest that there is an upper limit to the fungal burden which the mouse immune system can handle, even if treated with immune enhancing therapy – an important observation that may inform clinical guidelines regarding the use of IFNγ in cryptococcal meningitis patients.

Finally, these experiments did lack certain readouts that would also help to inform the mechanisms of accelerated mortality. For example, one useful readout would have been histological examination of lung tissue, using hematoxylin and eosin staining (Fischer *et al.*, 2008). This histological analysis allows for tissue damage and immune cell recruitment to be determined, which would inform how much inflammation IFNγ induced and if this correlated with the accelerated mortality observed. Additionally, as with Chapter 4, Evans blue treatment of mice would enable oedema to be assessed as well.

In conclusion, these results support the *in vitro* observations in Chapter 3 and provide evidence that IFNγ does not universally improve host outcomes in cryptococcosis. Most significantly, IFNγ may actually worsen immunocompetent patient outcomes, particularly in high burden infection. Furthermore, I established that while IL-1β may protect mice from anorexia due to KN99α GFP infection, this cytokine is not critical for host survival or the action of IFNγ.

Chapter 6 – Developing a precision cut lung slice model of cryptococcosis to study the initial innate response to inhaled *Cryptococcus neoformans* in mice

6.1 – Introduction

6.1.1 – The difficulty in studying opportunistic infections

Opportunistic infections are a growing global healthcare burden, due to both increasing numbers of patients receiving long-term immunosuppressive therapy and increasing incidences of antimicrobial resistance (Wiederhold, 2017). Therefore, there is a clear need for alternative classes of antimicrobial therapy that pathogens are less likely to develop resistance to. Immunotherapy is one alternative class of treatment currently being investigated for a number of infections that works by enhancing the host immune response to better fight infection (Ramamurthy *et al.*, 2021). As these treatments do not directly target pathogens, and as the immune system has multiple antimicrobial mechanisms, resistance is less likely and slower to develop.

However, the immune response is complex and, if inappropriately stimulated, can result in off-target immune suppression or autoimmunity. In addition, 'ideal' immune responses are pathogen-specific, so enhancing the immune response to one pathogen may result in a patient being more susceptible to another. This means that before any immunotherapeutic can be developed, a thorough understanding of the healthy immune response to a pathogen is required in order to provide as detailed a blueprint as possible for the development of any new therapy.

Ideally, this understanding of the immune response to opportunistic pathogens should be informed by clinical data from resolving infections in immunocompetent patients. However, because these infections are typically cleared subclinically without intervention, and there are numerous ethical issues with deliberately infecting healthy individuals, this data is scarce. Therefore, experimental models are critical for advancing our understanding of immune mediated host protection to opportunistic pathogens. Even though there are a multitude of model systems available for the study of host-pathogen interactions, each approach has issues that greatly limit the translation of findings using these approached into patients. For example, *in vitro* monoculture systems, even when using human primary cells, lack the cellular diversity found in tissues or *in vivo* systems, and therefore are missing a multitude of factors that can significantly impact host responses. Mammalian *in vivo* models (mice, rats, non-human primates) offer a high level of biological similarity to humans and feature the complex, multicellular environment

often absent in *in vitro* systems. However, *in vivo* studies in these species typically rely on a limited number of biomarkers that can be obtained from limited live samples, or rely on post-mortem analysis which prevents repeated sampling and greatly increases animal use. More specifically, when examining host-pathogen interactions, phenomena should be directly visualised *in vivo* using intravital imaging methods – examples of which include bioluminescence or surgical window approaches (Looney and Bhattacharya, 2014; Vanherp *et al.*, 2019). However, these methodologies require very high levels of surgical expertise and/or highly specialist equipment, limiting their availability to the scientific community. In addition, bioluminescent imaging is currently too low resolution to visualise events at the cellular level, while surgical windows only allow for hours, not days, of imaging at a time. More recently, groups such as ours have championed the use of alternative animal species, such as the zebrafish (Bojarczuk *et al.*, 2016; Davis *et al.*, 2016). Transparent embryos and relatively high breeding rates with this species enables high-powered studies to prepared relatively quickly, that are compatible with high contrast, non-invasive intravital imaging methods. However, the greater evolutionary distance between humans and these species means that there is ofen significantly different anatomy and immunology, which greatly limits the translatability of findings in these models – particularly in the context of pulmonary pathogens.

Therefore, there is a need for a model that enables host-pathogen interactions within the lung to be visualised for days at a time, at a resolution high enough to study immune responses at the cellular level, but without the requirement for highly specialist equipment or invasive surgery.

6.1.2 – Precision cut lung slices as a model approach to study host-pathogen interactions

The precision cut lung slices (PCLS) methodology is an approach that fulfils all these criteria, and is described briefly in Figure 38. Briefly, the method involves instilling the lungs of a recently humanely culled mouse with a low percentage (1-4%) low-melting-point agarose gel. Once set, the lungs are excised from the animal and slices (usually 100-1000μm) of inflated lung tissue are prepared on a vibratome. Resulting PCLS have preserved lung structure and immune cells, yet are thin enough to be compatible with a wide array of high content imaging modalities. In addition, PCLS can be kept viable for days, allowing for immune responses within PCLS to be studied over time. Despite the advent of this technique in 1987 and the use of PCLS in the fields of lung anatomy (Akram *et al.*, 2019), allergy (Patel *et al.*, 2019) and viral infection (Ebsen *et al.*, 2002), they have yet to be properly utilised to study opportunistic fungal infections (Placke and Fisher, 1987).

C. neoformans is an example of an often-fatal opportunistic fungal pathogen for which successful immunity is still poorly understood. Although it is estimated that as many as ~70% of people in urban environments are exposed to *C. neoformans* before the age of 21 (Goldman *et al.*, 2001), it is not understood how these individuals clear infection. Infection is thought to start in the lungs, but cryptococcosis patients typically only become symptomatic in the later stages of infection after fungal cells have disseminated to the CNS. This means experimental and clinical research is focussed on these later elements of infection (Jarvis *et al.*, 2012; M. Zhang *et al.*, 2016; Neal *et al.*, 2017; Seoane *et al.*, 2020). This means that this initial infection is the least well understood phase of cryptococcosis clinically due to the difficulty in studying this phenomenon in patients. Therefore, cryptococcosis is an ideal candidate disease for which there is still a need to understand immunocompetent clearance and the host-pathogen interactions that occur in the lungs (Goldman *et al.*, 2001; Posch *et al.*, 2017). I therefore sought to develop a PCLS model of cryptococcosis so that immunity to this pathogen could be directly visualised in the lungs, with a specific focus on the initial immune response following inhalation of *C. neoformans*. All imaging of *ex vivo* bead experiments, as well as all animal procedures were done by Dr Leo Carlin.

6.2 – Results

6.2.1 – Infected precision cut lung slices exhibit high structural and cellular fidelity

Initially the compatibility of infected PCLS with high content microscopy was confirmed, and the anatomy of the lung was found to be preserved. Low magnification widefield differential interference contrast (DIC) imaging (2x) of PCLS showed that major anatomical features of the lung were preserved, with evidence of both smaller and larger airways (Figure 39A). Imaging of PCLS at a higher magnification (20x) revealed that individual alveolar air spaces were also clearly visible (Figure 39B).

As the PCLS methodology would be applied to different animals, variability in tissue appearance was anticipated due to both individual differences between animals and the depth of tissue at which PCLS were prepared. Therefore, the number of alveoli per 20x widefield frame of KN99α GFP *C. neoformans* and 6μm bead inoculated PCLS were quantified. The number of alveoli was found to be consistent for PCLS prepared at 0 hours post inoculation (HPI; Figure 39C) and at 24HPI (Figure 39D).

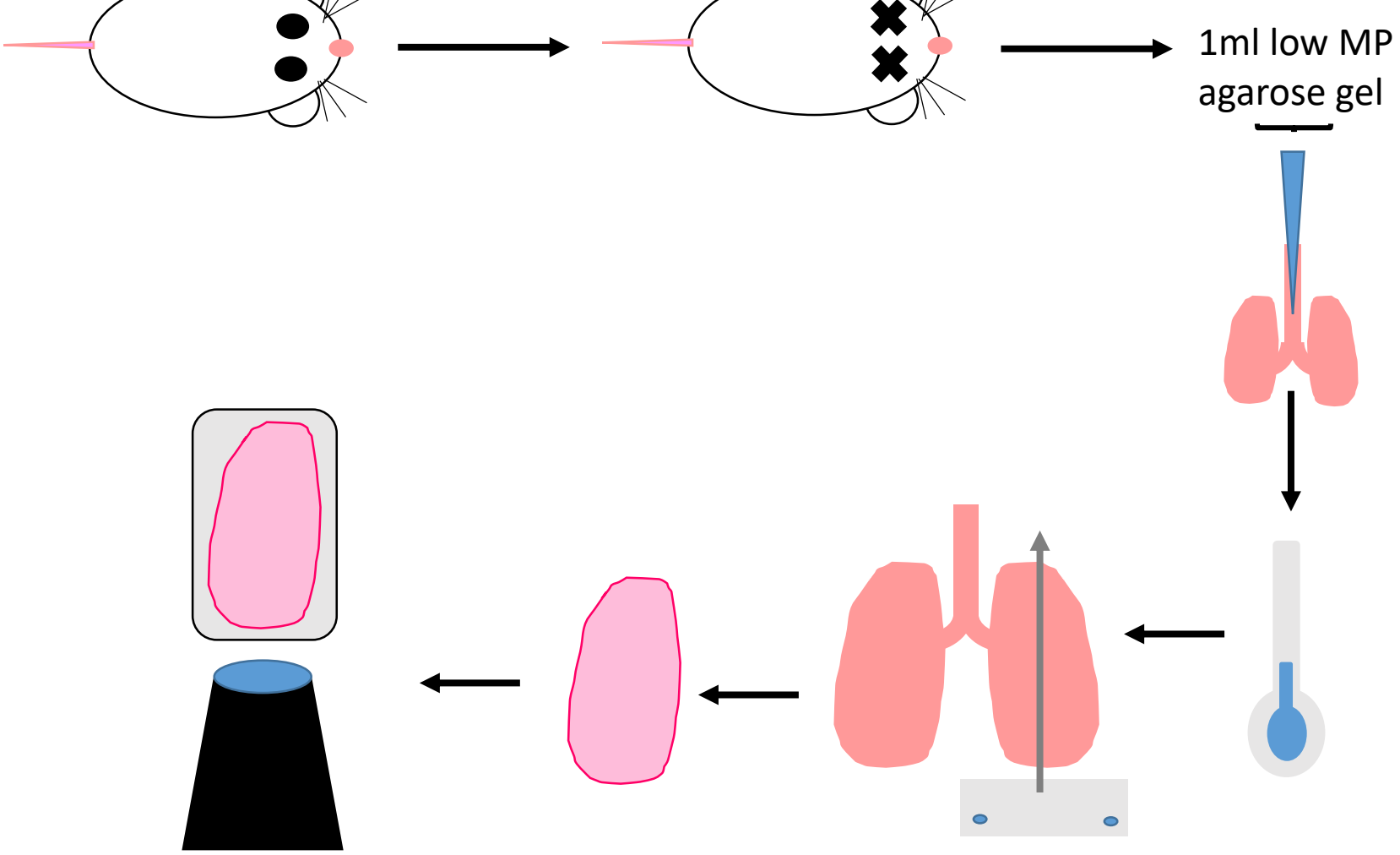

Figure 38 – Summary of PCLS process. A diagram showing the main steps involved in the preparation of murine PCLS. A mouse is humane m (~40°C) trachea. The mo ow the gel aver, and the sing k slices of Finally, slices o croscopy g.

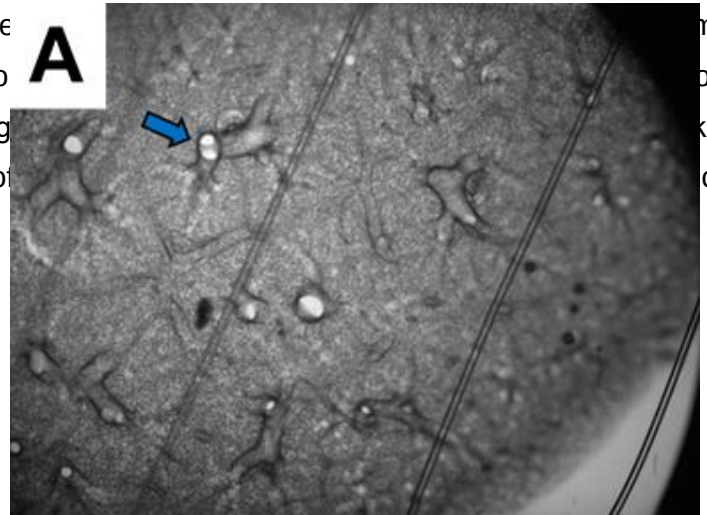

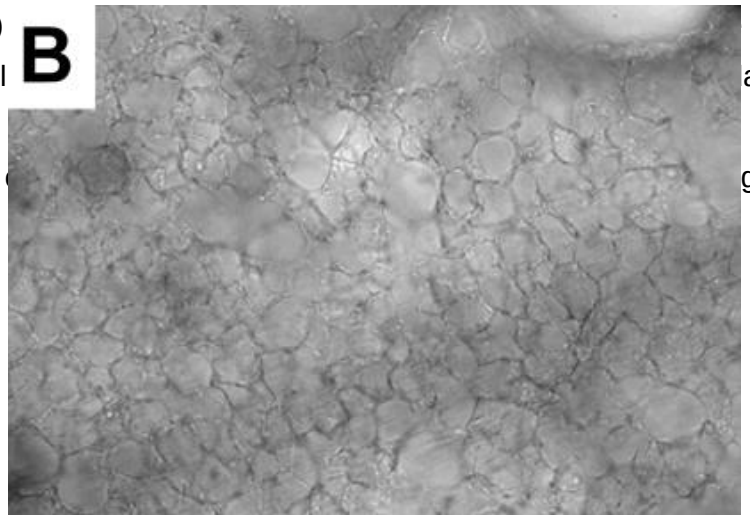

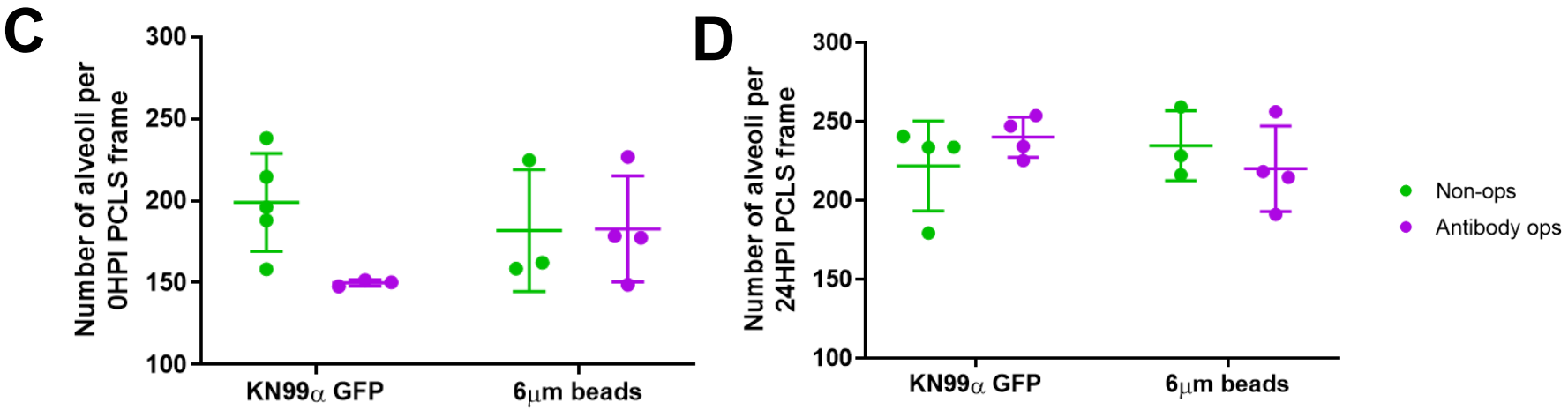
C
Number of alveoli per 0HPI PCLS frame
300
250
200
150
100
KN99α GFP
6μm beads
D
Number of alveoli per 24HPI PCLS frame
300
250
200
150
100
KN99α GFP
6μm beads
Non-ops
Antibody ops

Figure 39 – PCLS have conserved anatomical features and are consistent in appearance between animals. PCLS exhibit preserved anatomical features of the lungs and no significant differences in the number of alveoli per frame were observed with different treatments between animal treatment groups (**A**) Representative 2x widefield image of PCLS reveals that larger airways are visible (blue arrow – large airway; scale bar – 1000μm). (**B**) Representative 20x widefield image of PCLS showing individual alveoli can be seen (scale bar – 100μm). (**C**) Regardless of the treatment mice received, the number of alveoli per 20x widefield frame in 0HPI PCLS did not significantly vary. Interaction – F(1,11)=2.607, p=0.1347. Inoculum – F(1,11)=0.2608, p=0.6197. Opsonin – F(1,11)=2.406, p=0.1491. (**D**) Regardless of the inoculum animals received, the number of alveoli per 20x widefield frame in 24HPI PCLS did not significantly vary. Interaction – F(1,11)=1.805, p=0.2062. Inoculum – F(1,11)=0.08635, p=0.7743. Opsonin - F(1,11)=0.02281, p=0.8827. Alveolar numbers were compared by two-way ANOVA. Data presented as mean ± SD. Each point represents the mean value of a different animal based on at least one field of view: 0HPI non-ops KN99α GFP – n=5, 0HPI antibody ops KN99α GFP – n=3, 0HPI non-ops 6μm beads – n=3, 0HPI antibody ops 6μm beads – n=4, 24HPI non-ops KN99α GFP – n=4, 24HPI antibody ops KN99α GFP – n=4, 24HPI non-ops 6μm beads – n=3, 24HPI antibody ops 6μm beads – n=4.

6.2.2 – The pulmonary innate cellular immune system is preserved in PCLS

Next the immunology of PCLS was characterised as this was critical for the model to be suitable to study host-pathogen interactions. At 0HPI, the most abundant cells resident in the healthy lungs at the time of infection are expected to be AMs (Martin and Frevert, 2005). To determine if these immune cells were present in PCLS, mice were inoculated with $1x10^8$ 10μm beads *ex vivo* prior to the preparation of PCLS. PCLS were then treated with isolectin GS-IB_4 conjugated to Alexa Fluor 647. Isolectin GS-IB_4 is a glycoprotein that acts as a dye in tissue by binding to a-D-galactosyl residues – which are found at a high density on both AMs and the lung endothelium (Sorokin and Hoyt, 1992). This was therefore used to identify the presence and localisation of AMs within PCLS.

Rounded isolectin GS-IB_4^+ cells were observed in 0HPI PCLS, typically found in proximity to the endothelium (Figure 40A). These cells were found at a density of less than one macrophage per alveolus – consistent with previous observations regarding AMs (Bhattacharya and Westphalen, 2016). To have a greater level of confidence that rounded isolectin GS-IB_4^+ cells were alveolar macrophages, PCLS were also co-stained with a primary antibody conjugate against CD11c – a surface marker for AMs (Misharin *et al.*, 2013) – to better identify these cells (Figure 40B) .

At later time points of infection, circulating myeloid cells including monocyte derived macrophages (MDMs), DCs and neutrophils (neuts) were also anticipated to be recruited into the lungs and present in PCLS prepared at later time points. As these cell types are difficult to differentiate based on DIC morphology alone, a panel of primary antibody conjugates was utilised to differentiate these cell populations (Table 5, Figure 8; Lyons-Cohen et al., 2017). All three cell types could be successfully identified by 20x widefield imaging of 24HPI PCLS following inoculation of mice with $5x10^4$ 6µm beads (Figure 40C).

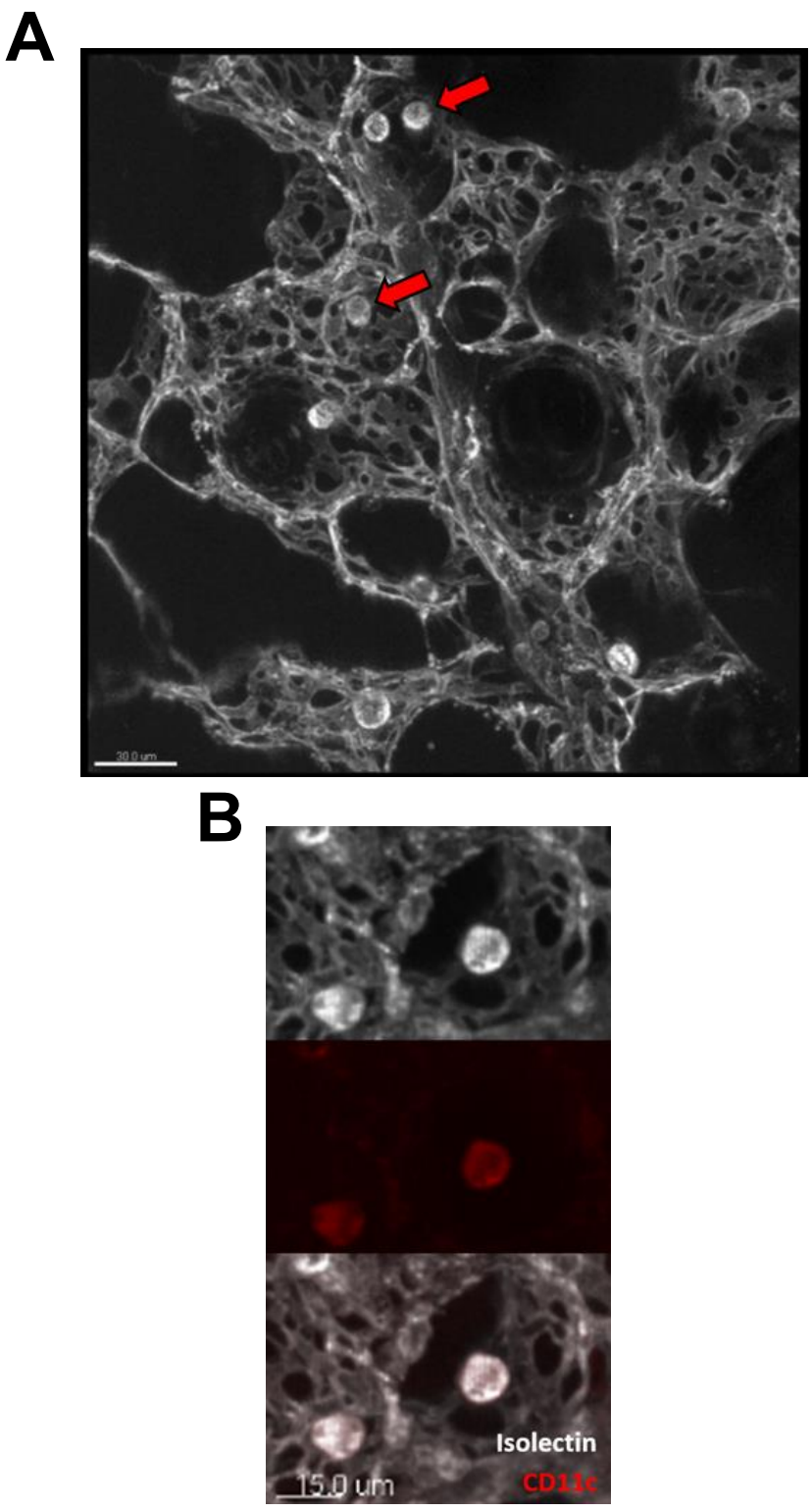

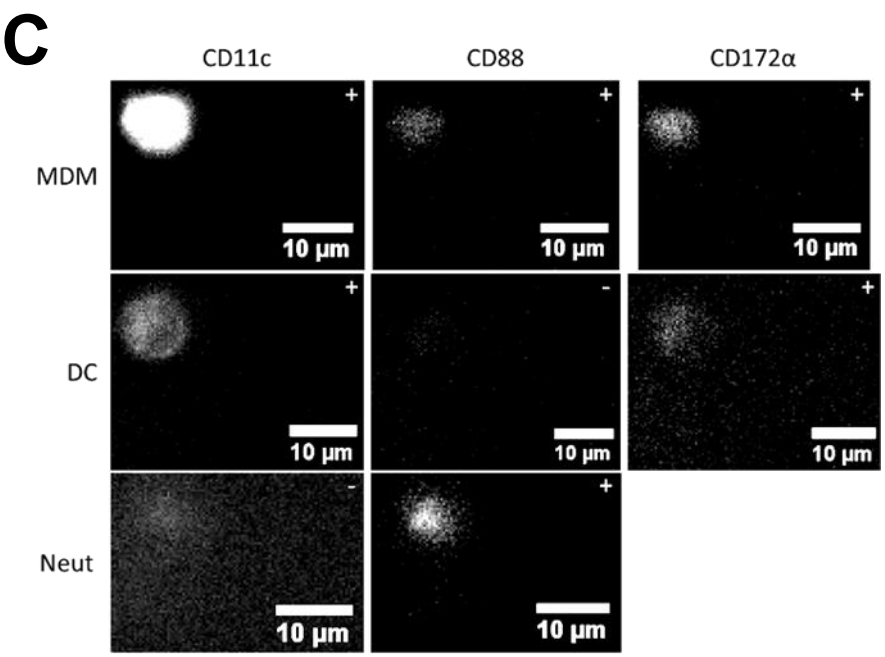

Figure 40 – Innate immune cells are present in infected PCLS. All examined immune cells were found to be present in PCLS. (**A**) Representative 20x confocal image of PCLS stained with isolectin GS-IB_4 revealed that pulmonary vascular networks are preserved. Also, round isolectin GS-IB_4^+ cells were observed in proximity to alveolar boundaries, consistent with AMs (red arrow; scale bar – 30µm). (**B**) Representative 20x confocal images of rounded GS-IB_4^+/$CD11c^+$ cells – consistent with AMs (scale bar – 15µm). (**C**) Representative widefield images of MDMs, DCs and neuts based on surface marker expression.

6.2.3 – Phagocytosis by macrophages within PCLS appears to be dependent on target size

Given that AMs are the most abundant cells in the healthy lung prior to infection, it was next determined whether the functions of these cells were preserved in PCLS *ex vivo*. One of the most common responses of macrophages to pathogens is phagocytosis (Vance, Isberg and Portnoy, 2009). Additionally, previous *in vitro* studies by other groups have identified that the size of a target particle significantly affects the occurrence of phagocytosis by immune cells (Pratten and Lloyd, 1986; Koval *et al.*, 1998). Given that *C. neoformans* is known to undergo drastic size changes during the course of infection, it was imperative to confirm that this relationship was conserved in PCLS (Bojarczuk *et al.*, 2016). Therefore, large inocula of 1µm (10^9) and 10µm (10^8) sized beads were instilled at high concentrations into mice *ex vivo*, and the number of intracellular beads within AMs was assessed in PCLS.

In the case of 1µm beads, most beads were observed to have been phagocytosed before PCLS could be imaged, although additional phagocytosis was still observed *ex vivo* (Figure 40A-B). This confirmed that phagocytosis readily occurred *ex vivo* in PCLS, and so a single animal was deemed to be sufficient as an appropriate positive control, with no need to use or cull additional animals. However, when 10µm beads were instilled *ex vivo*, only a single 10µm bead was observed to have been phagocytosed in PCLS prepared from three different animals despite the high inoculum (Figure 41A, 41C). No additional phagocytosis of 10µm beads was observed in PCLS. To confirm this discrepancy, 1µm ($5x10^8$) and 10µm ($5x10^7$) beads were instilled together *ex vivo* into a culled mouse. Again, 1µm beads were observed to be readily phagocytosed while all 10µm beads remained extracellular (Figure 41D-E). However, AMs were still observed to interact with 10µm beads (Figure 41E).

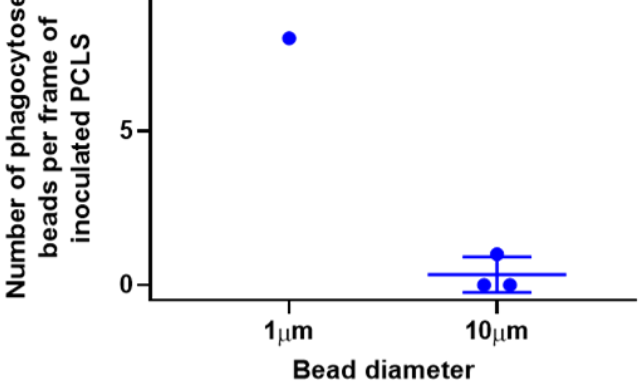
Number of phagocytosed beads per frame of inoculated PCLS
5
0
1μm
10μm
Bead diameter

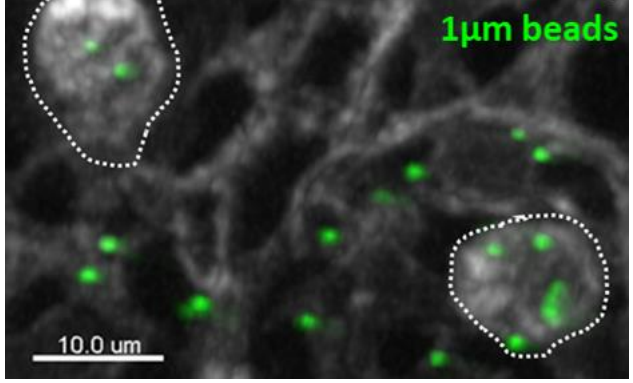
1μm beads
10.0 um

C

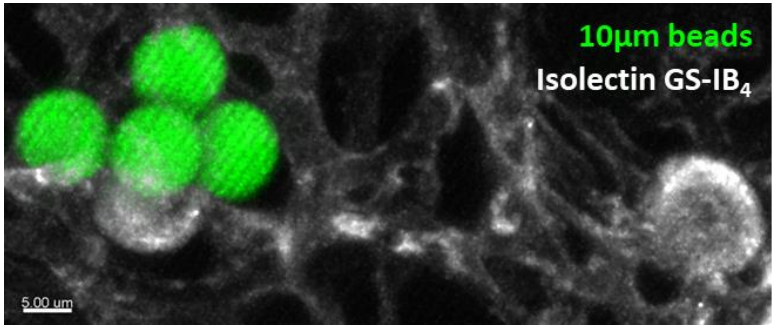
10μm beads
Isolectin GS-IB4
5.00 um

D

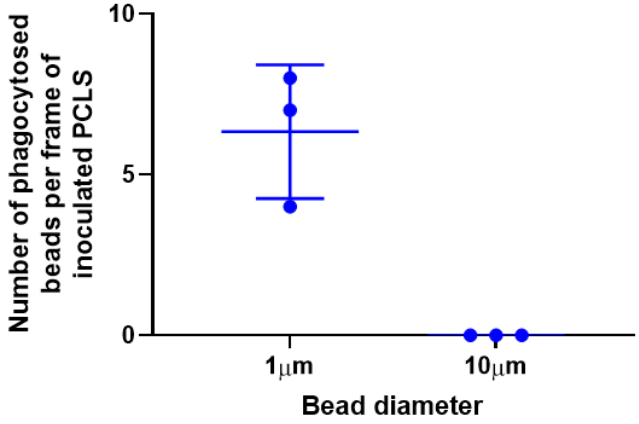
Number of phagocytosed beads per frame of inoculated PCLS
10
5
0
1μm
10μm
Bead diameter

E

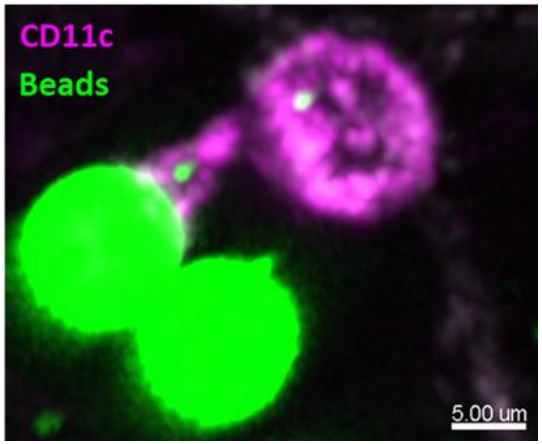
CD11c
Beads
5.00 um

Figure 41 – Macrophage phagocytosis of beads in PCLS is affected by target size. Instilling different sized beads *ex vivo* into the lungs of mice revealed that phagocytosis was size dependent. (**A**) 1µm beads were confirmed to be readily phagocytosed by macrophages *ex vivo*, whereas only one incidence of phagocytosis was observed with 10µm beads. Each point represents a different animal: 1µm – n=1, 10µm – n=3. (**B**) Representative confocal image (20x) of 1µm beads phagocytosed by AMs in PCLS (dotted lines). (**C**) Representative confocal image (20x) of 10µm beads failing to be phagocytosed by a AM in PCLS. (**D**) When instilled together *ex vivo*, 1µm beads were readily phagocytosed by AMs while 10µm beads were not. Each point represents the number of phagocytosed beads per frame of PCLS. Each point represents one field of view from PCLS prepared from a single animal. (**E**) Representative confocal image (20x) of (**D**), showing two phagocytosed 1µm beads and an AM failing to phagocytose a 10µm bead. Data presented as mean ± SD.

6.2.4 – Foci of 6µm beads appear larger in 24HPI PCLS compared to 0HPI

Having confirmed that immune responses to inoculated particles could be studied using PCLS prepared from mice, immunity to intranasally inoculated 6µm beads was examined. This was chosen as a size matched negative control for *C. neoformans* infection, with the aim of determining a baseline PCLS immune response to inhaled particles. Firstly, the distribution of 6µm beads in PCLS was assessed immediately after animals received either a higher (~$2x10^5$ beads) or lower ($5x10^4$ beads) intranasal inoculum to inform dose selection.

Importantly, a strong correlation was observed between the intranasal inocula animals received and the number of beads observed per bead-containing widefield frame (20x) of PCLS (R^2=0.82; Figure 42A). It was also confirmed using low magnification (2x) widefield imaging that inoculated 6µm beads were distributed throughout PCLS (Figure 42B).

The lower inoculum was chosen for all subsequent experiments, as this inoculum resulted in typically no more than one bead per alveolus, which is predicted to be akin to predicted human environmental exposure (Figure 42C). Subsequently, the distribution of 6µm beads was assessed in PCLS this time prepared at 24HPI from mice that had been inoculated with the lower inoculum ($5x10^4$). Interestingly, foci of beads in low magnification (2x) widefield images appeared to be larger (Figure 42D). This was confirmed by higher magnification imaging, with more 6µm beads observed per bead containing frame of 24HPI PCLS compared to 0HPI PCLS (Figure 42E-F). This suggests that 6µm beads inoculated into mice became more clustered in the first 24 hours of infection.

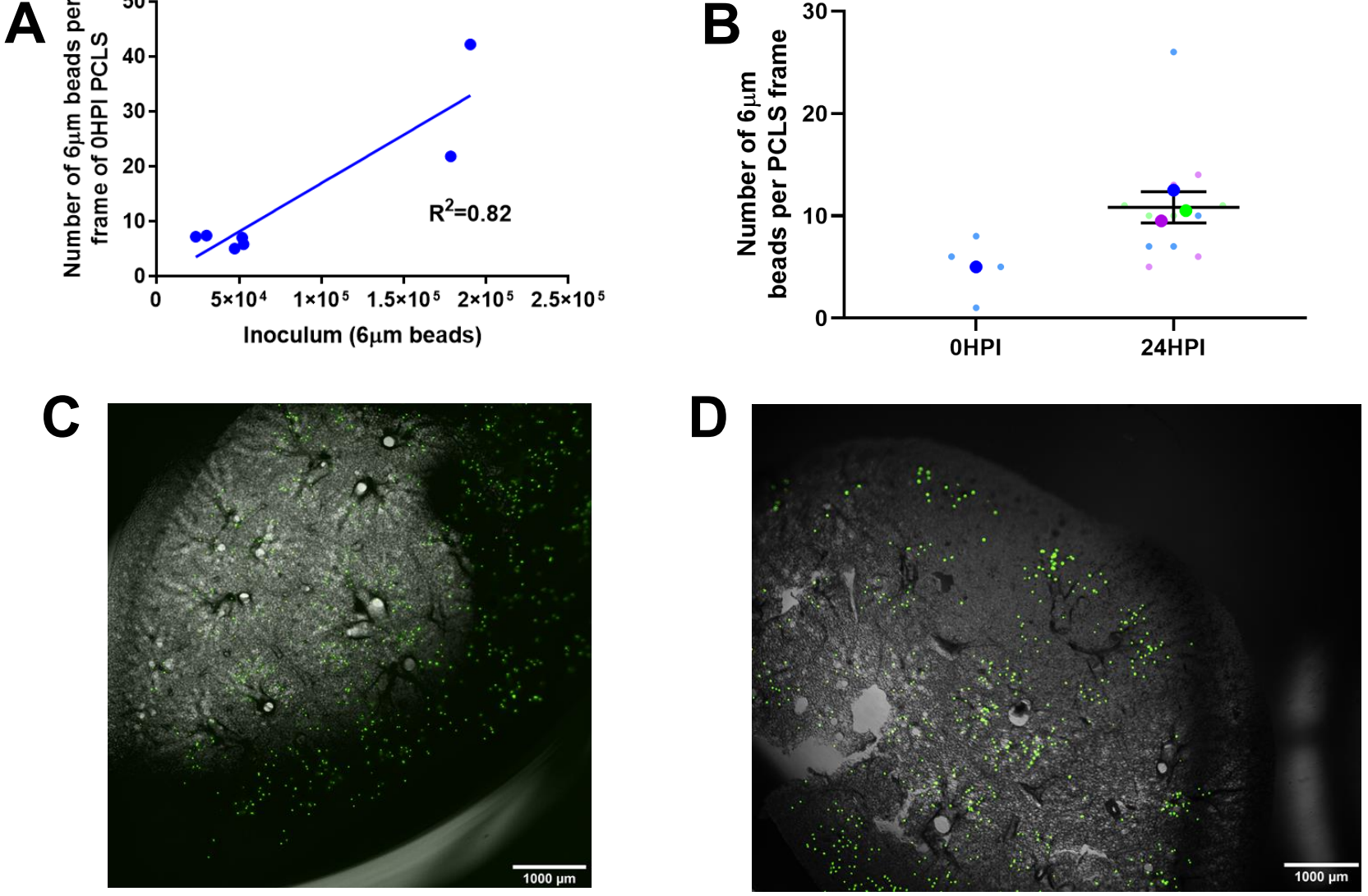
A
Number of 6µm beads per frame of 0HPI PCLS
50
40
30
20
10
0
0
5×10⁴
1×10⁵
1.5×10⁵
2×10⁵
2.5×10⁵
Inoculum (6µm beads)
R²=0.82
B
Number of 6µm beads per PCLS frame
30
20
10
0
0HPI
24HPI
C
1000 µm
D
1000 µm

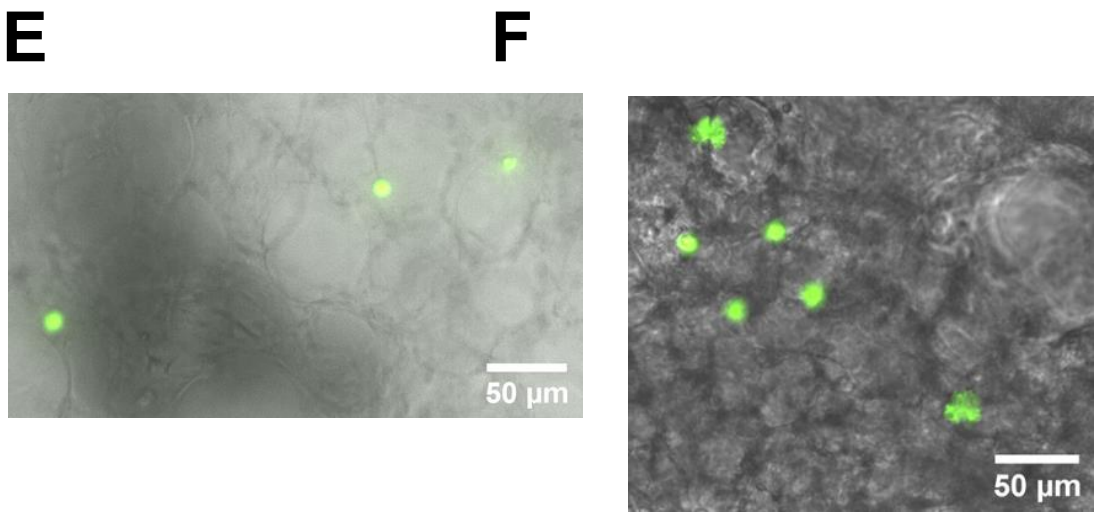

Figure 42 – Foci of 6µm beads appear larger in 24HPI PCLS than 0HPI PCLS. 6µm beads appeared more clustered in PCLS prepared 24 hours following inoculation. (**A**) The number of 6µm beads intranasally inoculated into mice *in vivo* correlated with the number of beads observed per 20x widefield frame of 0HPI PCLS that contained beads (R^2=0.82, p=0.005). Each point represents a different animal (n=6). (**B**) More 6µm beads were observed in 24HPI 20x widefield frames of PCLS containing beads compared to at 0HPI. (**C**) Representative 2x widefield image of 6µm beads in 0HPI PCLS. (**D**) Representative 2x widefield image of 6µm beads in 24HPI PCLS. (**E**) Representative 20x widefield image of 6µm beads in 0HPI PCLS. (**F**) Representative 20x widefield image of 6µm beads in 24HPI PCLS. Correlations between bead numbers in 0HPI PCLS and inocula were analysed by Pearson correlation coefficients. Data in **B** presented as mean ± SD. Each large point represents the mean of a different animal (0HPI – n=1, 24HPI – n=3), while each small point represents a different frame of PCLS. * - p<0.05

6.2.5 – Mice intranasally inoculated with 6µm beads are asymptomatic

As beads were observed to both persist and cluster in the lungs of animals at 24HPI (Figure 42F), inoculated animal health status was monitored to confirm whether intranasally inoculating animals with 6µm beads resulted in symptoms. No symptoms of a pulmonary injury were observed in inoculated animals. Additionally, no weight loss was observed (Figure 43).

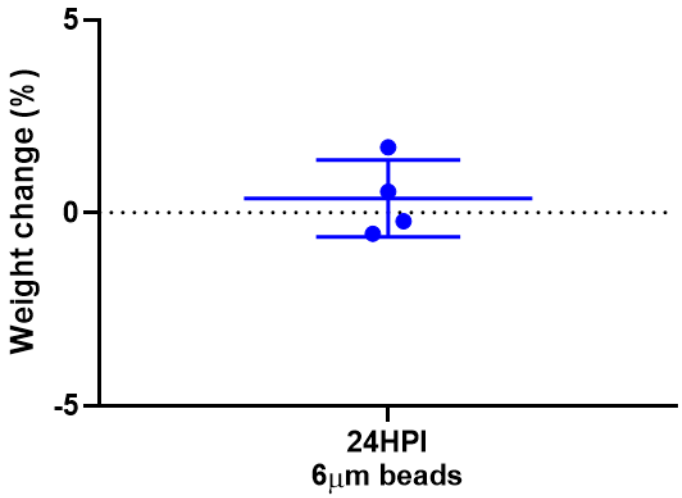

Figure 43 – Mice inoculated with 6μm beads exhibit no weight loss or symptoms at 24HPI. Inoculating mice with 6μm beads is asymptomatic. Additionally, no significantly weight loss was observed in 24HPI animals (dotted line – no weight change). Data presented as mean ± SD. Each point represents a different animal (n=4).

6.2.6 – Immune responses to 6μm beads in PCLS are macrophage centric

The immune response to intranasally inoculated 6μm beads in PCLS was also characterised. As was observed with PCLS containing 10μm beads, there was no significant immune response to 6μm beads in 0HPI PCLS – isolectin GS-IB_4^+ cells remained dispersed throughout PCLS at a low density (Figure 44A).

In 24HPI PCLS, $CD11c^+$ cells were observed to 'cluster' in the vicinity of 6μm beads (Figure 44B), suggesting that an immune response had taken place. However, when the number of rounded isolectin GS-IB_4^+ cells (0HPI) was compared to the number of $CD11c^+$ cells (24HPI) per bead containing frame of PCLS, no significant increase in cell number was found (Figure 44C). Additionally, very low numbers of MDMs, neutrophils or DCs were observed in 24HPI PCLS – and those that were present were not found in the immediate vicinity of 6μm beads (Figure 44E).

Because there was a change in the distribution of macrophages in 24HPI PCLS, but not total numbers, the 'cluster' behaviour was described to quantify this change. A 'cluster' was defined as ≥3 macrophages within 10μm of either an inoculated particle or another 'cluster' macrophage. When this behaviour was examined, it was found to be absent in 0HPI PCLS, but approximately one cluster was typically observed per bead containing frame of 24HPI PCLS (Figure 44D) – indicative of a macrophage response.

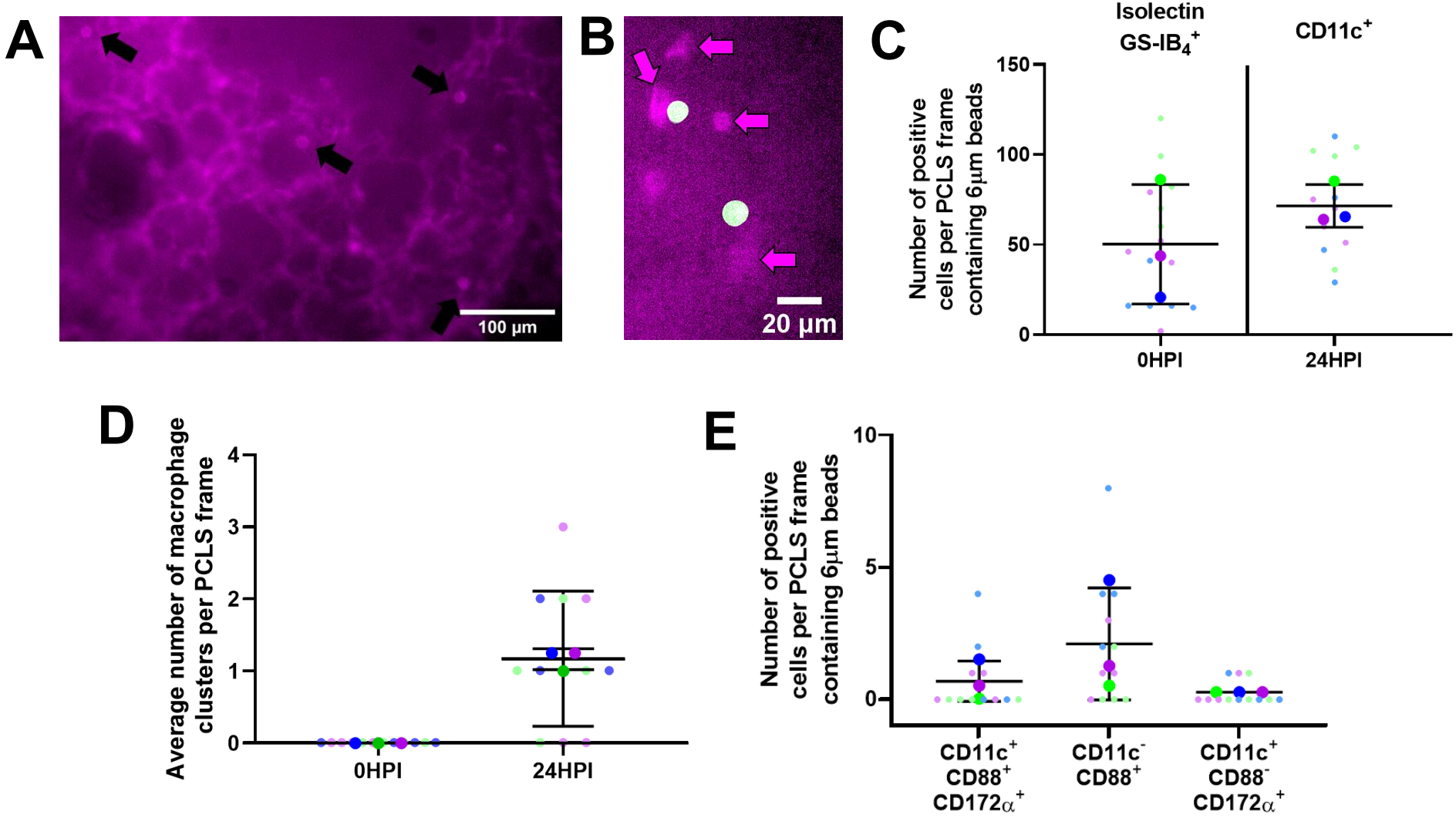
A
100 µm
B
20 µm
C
Isolectin
GS-IB4+
CD11c+
Number of positive cells per PCLS frame containing 6µm beads
150
100
50
0
0HPI
24HPI
D
Average number of macrophage clusters per PCLS frame
4
3
2
1
0
0HPI
24HPI
E
Number of positive cells per PCLS frame containing 6µm beads
10
5
0
CD11c+ CD88+ CD172α+
CD11c- CD88+
CD11c+ CD88- CD172α+

Figure 44 – **There is a macrophage centric immune response to 6µm beads in 24HPI PCLS.** Although macrophages showed no obvious response to inoculated 6µm beads in 0HPI PCLS, macrophages were observed to 'cluster' around beads in 24HPI PCLS. (**A**) Representative widefield image (20x) of the sparse distribution of macrophages in 0HPI PCLS, despite 6µm beads being inoculated (black arrow – macrophage). (**B**) Representative widefield image (20x) of macrophages within 10µm of 6µm beads in 24HPI PCLS (pink arrow – macrophages within 10µm of a 6µm bead). The top three macrophages could be considered a 'cluster'. (**C**) The total number of macrophages per bead containing frame in 0HPI and 24HPI PCLS did not significantly differ (t=1.048, df=4, p=0.3538). (**D**) A mean of one macrophage cluster per frame was observed in 24HPI PCLS, while no clusters were observed in 0HPI PCLS. (**E**) Low numbers of MDMs, neuts and DCs were observed in 24HPI PCLS inoculated with 6µm beads. Cell numbers in 0 and 24HPI PCLS were compared using an unpaired t-test. Data presented as mean ± SD. Each large point represents a different animal (n=3), while each small point represents a different frame of PCLS.

6.2.7 – The phagocytosis of 6µm beads only occurs *in vivo,* but not at 0HPI

Having observed AMs respond to 6µm beads, although only in 24HPI PCLS, phagocytosis was then quantified in 0HPI and 24HPI PCLS. Despite phagocytosis being a signature response of macrophages to infectious particles (Vance, Isberg and Portnoy, 2009), no phagocytosis of 6µm beads was observed in 0HPI PCLS. Phagocytosis of 6µm beads was observed to have occurred in 24HPI PCLS, although this occurred prior to PCLS imaging. Then 0HPI and 24HPI PCLS were imaged *ex vivo* for 24 hours, with extracellular *C. neoformans* cells tracked over this period. No phagocytosis occurred in any PCLS condition – no *C. neoformans* cells were observed to become intracellular over 24 hours *ex vivo* in either 0HPI or 24HPI PCLS. This suggests a difference in the occurrence of this behaviour *in vivo* and *ex vivo*, and that phagocytosis does not occur in the PCLS model (Figure 45A). Additionally, although phagocytosis was observed in 24HPI PCLS, phagocytosis was rare and variable (Figure 45B-C).

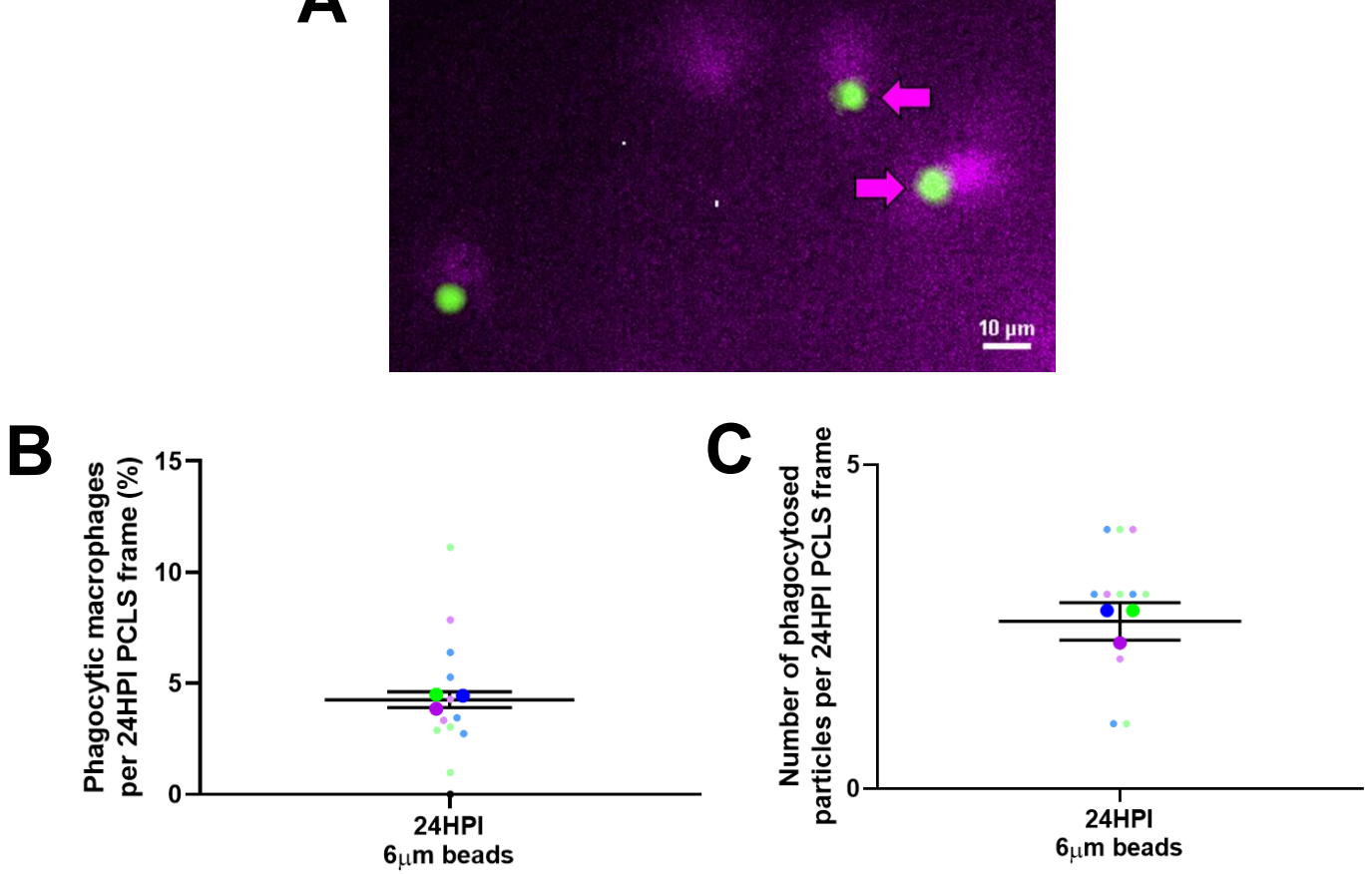

Figure 45 – The phagocytosis of 6µm beads is rare and variable in 24HPI PCLS. In 0HPI PCLS, no phagocytosed 6µm beads were observed, even after 24 hours of culture *ex vivo*. Phagocytosis was observed to have occurred in 24HPI PCLS *in vivo*, but not *ex vivo*. (**A**) Representative widefield image (20x) of two 6µm beads that have been phagocytosed by $CD11c^+$ cells in 24HPI PCLS (pink arrow – intracellular 6µm beads, scale bar – 10µm). (**B**) Only a small number of 6µm beads were observed to have been phagocytosed in 24HPI PCLS. (**C**) The proportion of $CD11c^+$ cells per frame of 24HPI PCLS that phagocytosed 6µm beads was low. Data presented as mean ± SD. Each large point represents a different animal (n=3), while small points represent different frames of PCLS.

6.2.8 – Pulmonary fungal burdens of KN99α GFP *C. neoformans* do not change in the first 24 hours of infection

The initial immune responses to inhaled *C. neoformans* were next compared and contrasted with responses to 6μm beads at 0 and 24HPI. These time points were chosen as these are the least well understood clinically. Firstly, the fungal burdens in the multilobe lung of intranasally inoculated mice at 0HPI and 24HPI were compared. As was observed previously (see Chapter 4), there was no difference in fungal burdens at these time points (Figure 46A). Additionally, it was confirmed that there was no difference in the inocula animals at both time points received (Figure 46B). Animal health status was also monitored in infected animals, with *C. neoformans* intranasal infection resulting in no symptoms of infection or large weight loss, as with bead inoculation (Figure 46C).

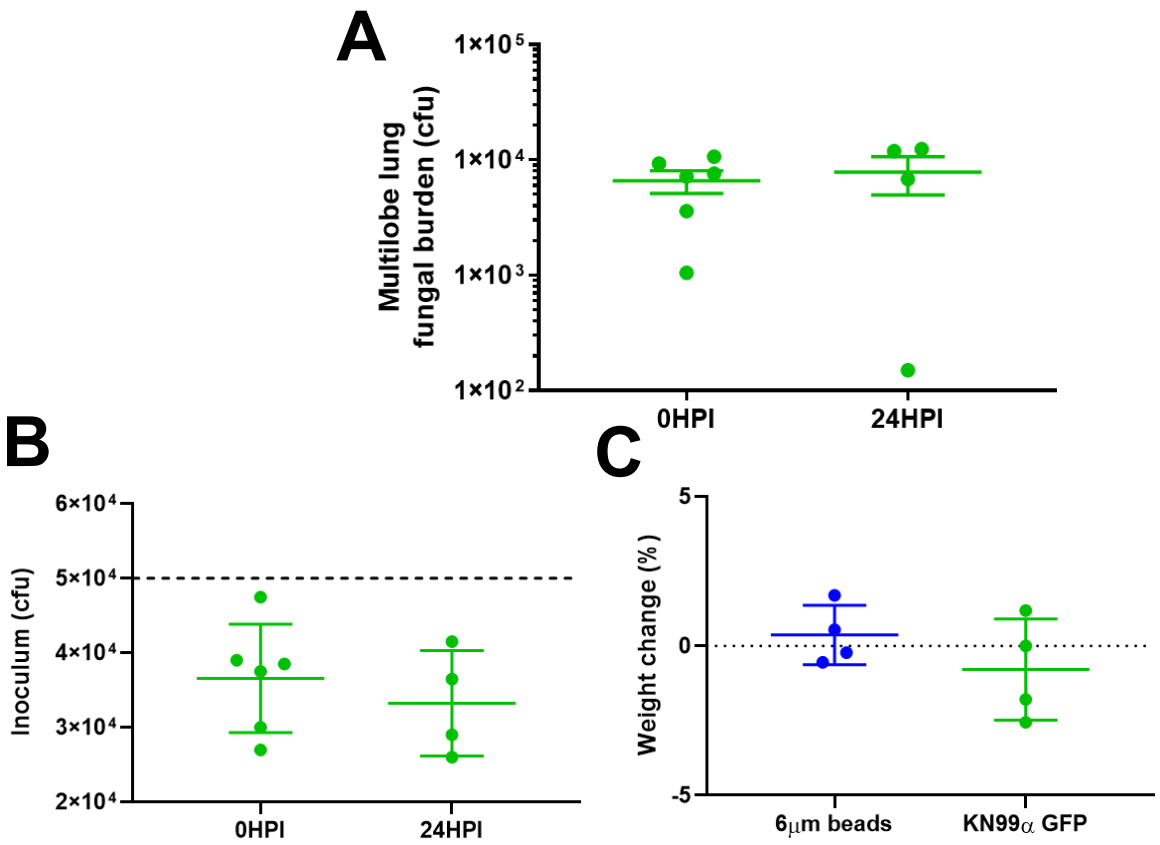

Figure 46 – **Pulmonary fungal burdens of KN99α GFP *C. neoformans* do not change in the first 24 hours of infection.** Intranasal inoculation of mice with KN99α GFP *C. neoformans* results in an asymptomatic infection with no change in fungal burdens between 0HPI and 24HPI. (**A**) Pulmonary fungal burdens of KN99α GFP were the same at 0HPI and 24HPI (t=0.425, df=8, p=0.682). Each point represents a different animal (0HPI – n=6, 24HPI – n=4). (**B**) KN99α GFP Inocula that animals received at 0HPI and 24HPI did not significantly differ (dotted line – calculated inoculum; t=0.7179, df=8, p=0.4933). Each point represents a different animal (0HPI – n=6, 24HPI – n=4). (**C**) 24HPI animals inoculated with either 6μm beads or KN99α GFP showed no significant differences in bodyweight (dotted line – no weight change; t=1.176, df=6, p=0.2841). Each point represents a different animal (n=4). Pulmonary fungal burdens, inocula and bodyweight changes were compared using unpaired t-tests. Data presented as mean ± SD.

6.2.9 – Foci of *C. neoformans* KN99α GFP infection in PCLS are larger at 24HPI

Because tissue fungal burdens did not change in the first 24 hours of infection, it suggests that initially there is no significant fungal replication or clearance. However, as 6μm bead foci were larger in 24HPI PCLS (Figure 42B), it was examined whether the same occurred with KN99α GFP *C. neoformans* infection.

Unlike 6μm beads in 0HPI PCLS, KN99α GFP *C. neoformans* cells were not visible in in low magnification (2x) widefield images of 0HPI PCLS (Figure 47A). However, in low magnification (2x) widefield images of 24HPI PCLS, foci of KN99α GFP infection were visible, suggesting foci of infection were larger at 24HPI (Figure 47B). When infected PCLS at 0HPI were examined at a higher magnification (20x), no more than one fungal cell was observed per alveolus (Figure 47C), although the number of KN99α GFP cells per infected widefield frame (20x) of 24HPI PCLS was significantly higher than at 0HPI (Figure 47D-E).

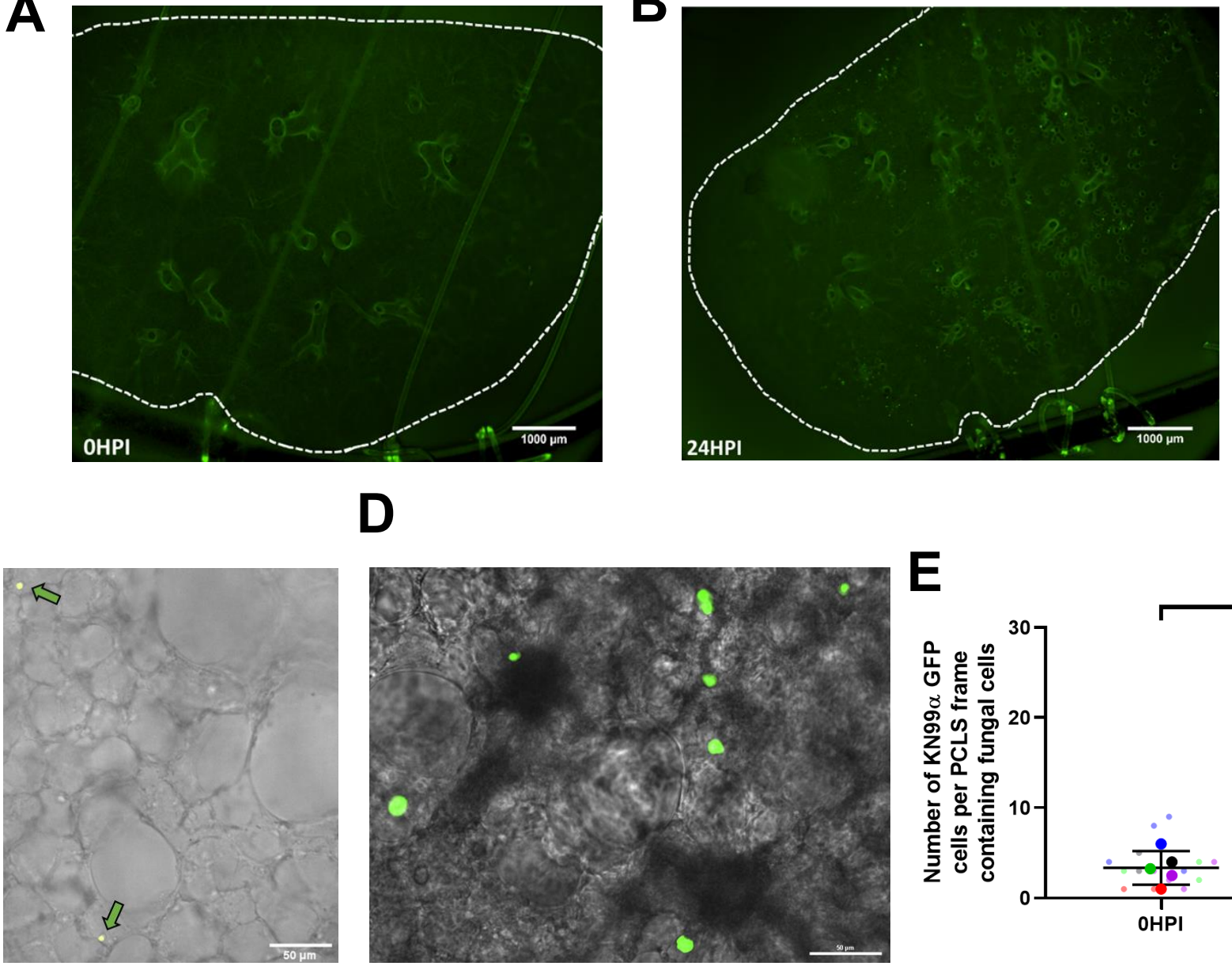
A
0HPI
1000 µm
B
24HPI
1000 µm
C
50 µm
D
E
**
Number of KN99α GFP cells per PCLS frame containing fungal cells
30
20
10
0
0HPI
24HPI

Figure 47 – Foci of KN99α GFP *C. neoformans* infection in 24HPI PCLS are larger than in 0HPI PCLS. As was observed with 6μm beads, more KN99α GFP *C. neoformans* cells were found in 24HPI PCLS foci of infection. (**A**) Representative widefield image (2x) of PCLS at 0HPI, showing that foci of infection are not visible (dotted line – PCLS boundary). (**B**) Representative widefield image (2x) of PCLS at 24HPI, showing that foci of infection are large enough to be visible (dotted line – PCLS boundary). The green signal in the bottom right of the image is autofluorescence from the fishing wire used to weigh the tissue down. (**C**) Representative widefield image (20x) of 0HPI PCLS showing the distribution of fungal cells at foci of infection. (**D**) Representative widefield image (20x) of 24HPI PCLS showing the distribution of fungal cells at larger foci of infection (scale bar – 50μm). (**E**) Significantly more KN99α GFP cells were observed per infected frame of 24HPI PCLS compared to 0HPI PCLS (t=3.931, df=7, p=0.0057). KN99α GFP cell numbers in PCLS were compared using an unpaired t-test. Data presented as mean ± SD. Each large point represents a different animal (0HPI – n=5, 24HPI – n=4), while each small point represents a different PCLS frame. ** - p<0.01

6.2.10 – The cellular immune response to KN99α GFP *C. neoformans* is identical to the response to 6μm beads in both 0HPI and 24HPI PCLS

Although the distribution of 6μm beads and KN99α GFP *C. neoformans* cells was the same in 0HPI and 24HPI PCLS, it was next determined whether immune responses were also the same. High magnification (20x) widefield imaging of 0HPI PCLS revealed no 'clustering' of isolectin GS-IB_4^+ cells to KN99α GFP *C. neoformans* cells as was observed with 6μm beads (Figure 48A, 47C). In infected 24HPI PCLS, $CD11c^+$ cell 'clusters' were observed at foci of KN99α GFP infection (Figure 48B-C), although the number of 'clusters' was the same as was observed in response to 6μm beads (Figure 48D). Additionally, the mean number of isolectin GS-IB_4^+ cells and $CD11c^+$ cells per infected frame of 0 and 24HPI PCLS were the same, regardless of inocula animals received (Figure 48E).

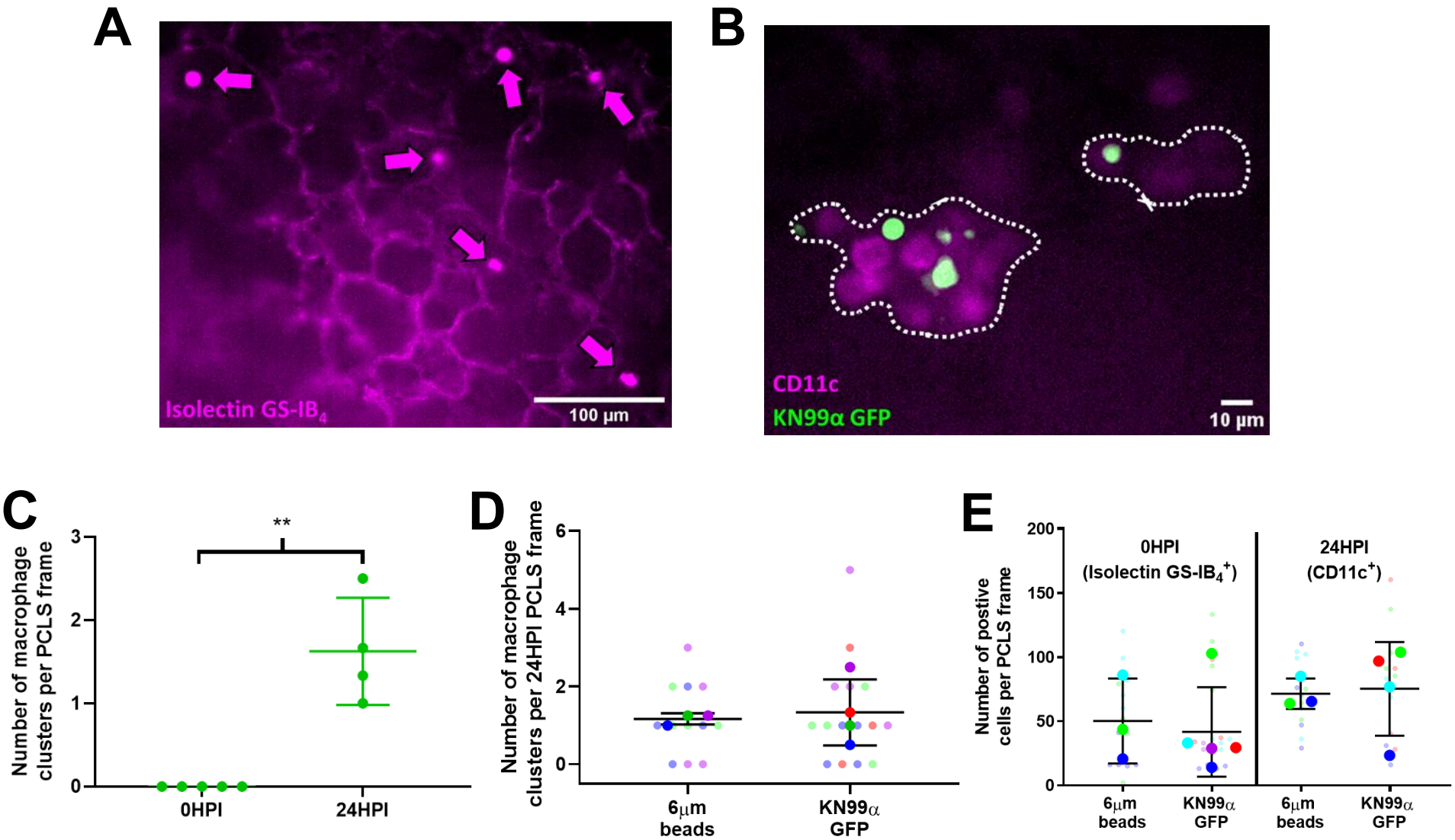
A
Isolectin GS-IB4
100 µm
B
CD11c
KN99α GFP
10 µm
C
Number of macrophage clusters per PCLS frame
**
0HPI
24HPI
D
Number of macrophage clusters per 24HPI PCLS frame
6µm beads
KN99α GFP
E
Number of postive cells per PCLS frame
0HPI (Isolectin GS-IB4+)
24HPI (CD11c+)
6µm beads
KN99α GFP
6µm beads
KN99α GFP

Figure 48 – The response of macrophages to KN99α GFP *C. neoformans* in 0HPI and 24HPI PCLS is the same as it is to 6μm beads. At both 0HPI and 24HPI, the response of macrophages to KN99α GFP *C. neoformans* was the same as it was to 6μm beads. (**A**) Representative widefield image (20x) of 0HPI PCLS showing that isolectin GS-IB_4^+ cells remain at a low density despite KN99α GFP infection (pink arrows – isolectin GS-IB_4^+ cells). (**B**) Representative widefield image (20x) of a macrophage 'cluster' in response to KN99α GFP in 24HPI PCLS. (**C**) – Macrophage 'clusters' were only observed in response to KN99α GFP *C. neoformans* in 24HPI PCLS (Mann-Whitney U=0, p=0.0079). Each point represents a different animal (6μm beads – n=3, KN99α GFP – n=4). (**D**) The number of macrophage 'clusters' observed in 24HPI PCLS were the same regardless of if animals were inoculated with 6μm beads or KN99α GFP cells (t=0.3284, df=5, p=0.7559). Each large point represents a different animal (0HPI – n=5, 24HPI – n=4), while each small point represents a different field of view. (**E**) – The number of cells in infected PCLS prepared at both 0HPI and 24HPI were the same, regardless of if mice were inoculated with 6μm beads or KN99α GFP *C. neoformans*. Interaction – F(1,10)=0.04956, p=0.8283. Time post infection – F(1,10)=2.381, p=0.1538. Inoculum – F(1,10)=0.04956, p=0.8283. Each large point represents a different animal: 0HPI 6μm beads – n=3, 0HPI KN99α GFP – n=5, 24HPI 6μm beads – n=3, 24HPI KN99α GFP – n=4. Each small point represents a different field of view. Number of macrophage 'clusters' between 0 and 24HPI were compared using a Mann Whitney test, numbers of 'clusters' at 24HPI were compared using an unpaired t-test and positive cells were compared using a two-way ANOVA. Data presented as mean ± SD. ** - $p<0.01$

6.2.11 – Minimal evidence of myeloid cells recruitment was observed in 24HPI PCLS in response to KN99α GFP *C. neoformans* infection

As with 6μm bead inoculated 24HPI PCLS, the number of MDMs, neuts and DCs in KN99α GFP infected frames of 24HPI PCLS were quantified. There was significantly more variation in MDM numbers in 24HPI PCLS due to KN99α GFP infection compared to 6μm beads, with 0 to 20 cells observed per infected frame (Figure 49A). On the other hand, neut and DC cell numbers were consistently low (Figure 49B-C). In all cases, numbers of all investigated myeloid cell types per infected frame of 24HPI PCLS were found to not significantly differ, regardless of what animals were inoculated with (Figure 49A-C). Additionally, all myeloid cells in 24HPI PCLS were not observed to interact with KN99α GFP *C. neoformans* cells.

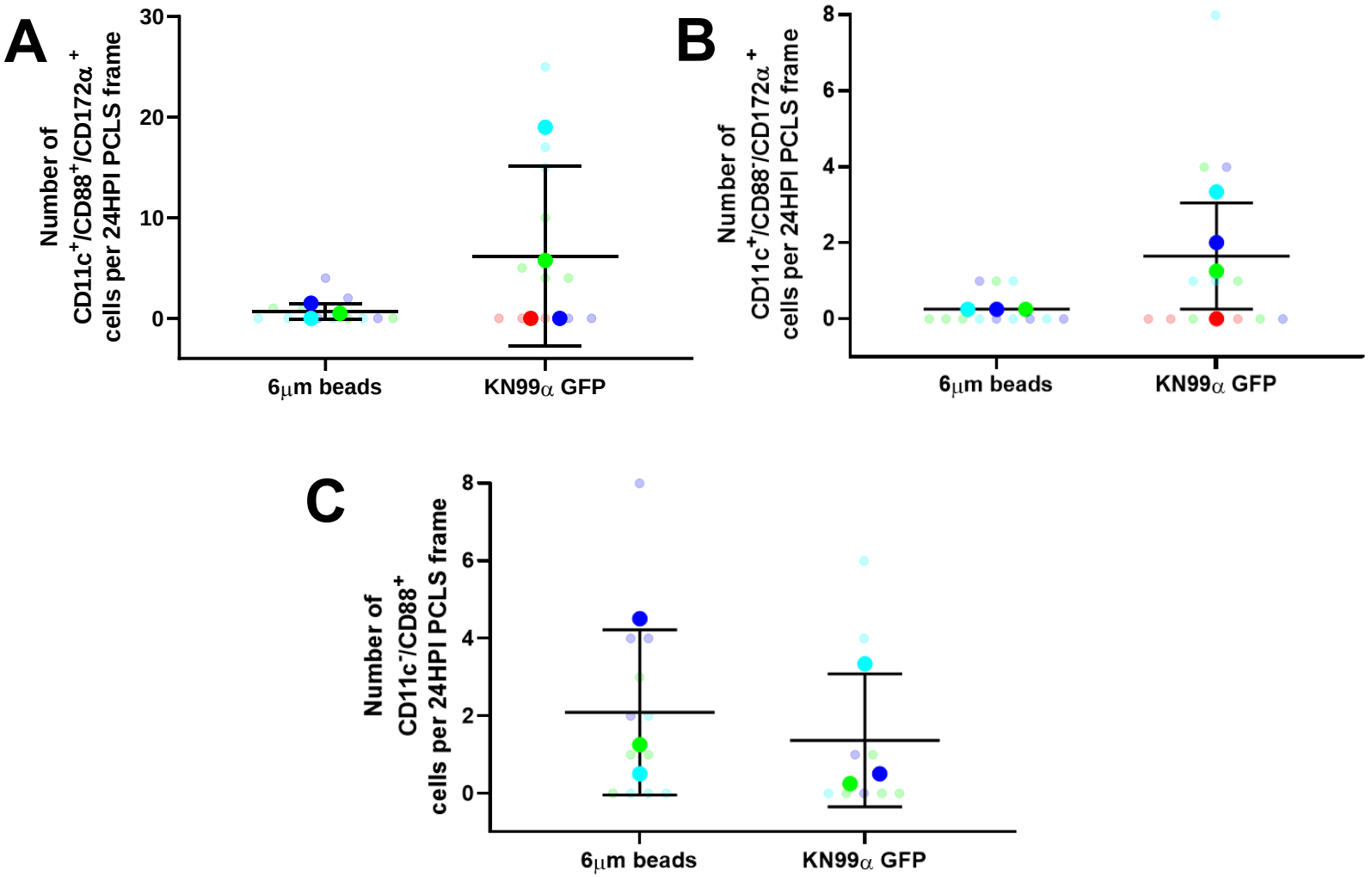
A
Number of CD11c+/CD88+/CD172α+ cells per 24HPI PCLS frame
30
20
10
0
6μm beads
KN99α GFP
B
Number of CD11c+/CD88-/CD172α+ cells per 24HPI PCLS frame
8
6
4
2
0
6μm beads
KN99α GFP
C
Number of CD11c-/CD88+ cells per 24HPI PCLS frame
8
6
4
2
0
6μm beads
KN99α GFP

Figure 49 – Minimal myeloid cell recruitment was observed to have occured in 24HPI PCLS in response to KN99α GFP *C. neoformans* infection. The recruitment of myeloid cells to 24HPI PCLS was minimal, as in response to inert 6μm beads. (**A**) Numbers of MDM cells were more variable in KN99α GFP infected 24HPI PCLS at 24HPI than with 6μm beads (F=137.7, DFn =3, p=0.0144), although numbers were not significantly different (t=1.226, df=3.058, p=0.3061). Each large point represents a different animal (6μm beads – n=3, KN99α GFP – n=4), while each small point represents a different field of view. (**B**) Neut numbers were equally low in 24HPI PCLS in response to either 6μm beads or KN99α GFP (t=0.9867, df=5, p=0.3691). Each large point represents a different animal (n=3), while each small point represents a different field of view. (**C**) DC numbers were more variable in 24HPI PCLS infected with KN99α GFP than with 6μm beads (F=∞, DFn=3, p>0.0001), although numbers were not significantly different (t=2.001, df=3, p=0.1392). Each large point represents a different animal (6μm beads – n=3, KN99α GFP – n=4), while each small point represents a different field of view. MDM and DC numbers were compared using an unpaired t-test with Welch's correction, while neut numbers were compared using an unpaired t-test. Data presented as mean ± SD.

6.2.12 – The early phagocytosis of KN99α GFP *C. neoformans* was limited and variable

At this point, it has been established that the initial immune response to both 6μm beads and KN99α GFP *C. neoformans* cells was macrophage centric, with minimal recruitment of myeloid cells to sites of infection. Therefore, the nature of the host-pathogen interactions between responding macrophages and KN99α GFP *C. neoformans* cells were compared to those observed with 6μm beads – specifically phagocytosis. In 0HPI PCLS, as with 6μm beads, no phagocytosis of KN99α GFP cells was observed, even when PCLS were cultured for 24 hours *ex vivo*. Phagocytosis was observed to have occurred in 24HPI PCLS (Figure 50A). However, phagocytosis of KN99α GFP cells was equally low in occurrence as it was with 6μm beads, although the phagocytosis of *C. neoformans* was significantly more variable (Figure 50B-C). Additionally, no additional phagocytosis was observed when either 0 and 24HPI PCLS were cultured *ex vivo* for 24 hours.

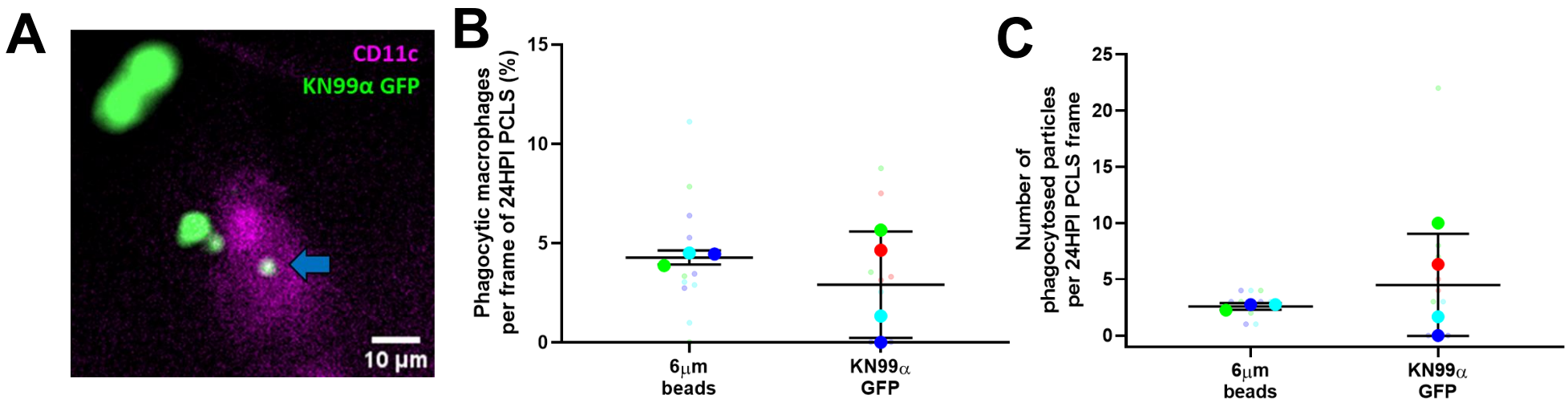

Figure 50 - The phagocytosis of KN99α GFP *C. neoformans* in the lung was limited and variable. Compared to 6μm beads, the phagocytosis of KN99α GFP in PCLS was equally low, although significantly more variable. (**A**) Representative widefield image (20x) of phagocytosed and extracellular KN99α GFP cells in 24HPI PCLS (blue arrow – phagocytosed fungal cell). (**B**) The phagocytosis of KN99α GFP cells and 6μm beads in 24HPI PCLS was equally low (t=0.8417, df=3.032, p=0.4612). (**C**) The number of phagocytic macrophages in 24HPI PCLS in response to KN99α GFP infection was no different to the number of phagocytic macrophages in response to 6μm beads (Mann-Whitney U=6, p>0.9999). Phagocytosed particles were compared using an unpaired t-test with Welch's correction, while phagocytic macrophages were compared using a Mann-Whitney test. Data presented as mean ± SD. Each large point represents a different animal (6μm beads – n=3, KN99α GFP – n=4), while each small point represents a different PCLS frame.

6.2.13 – Extracellular KN99α GFP *C. neoformans* cells grow significantly larger in the lungs of mice over 24 hours of infection

Because phagocytosis was rare, potential bottlenecks to this process were investigated using the PCLS model. Firstly, the relationship between phagocytosis and fungal cell size was examined as *C. neoformans* cell size is known to be an important pathological feature *in vivo* (Kress, Feldmesser and Casadevall, 2001; Bojarczuk *et al.*, 2016), and a relationship between target size and phagocytosis had already been confirmed in the PCLS model using different sized of beads (Figure 41). Therefore, the sizes of extracellular and intracellular fungal cells in 0HPI and 24HPI PCLS were compared (Figure 51A). A significant increase in the mean size of extracellular KN99α GFP *C. neoformans* cells was observed in 24HPI PCLS (5.151μm) compared to in 0HPI PCLS (3.152μm). Although intracellular KN99α GFP *C. neoformans* cells in 24HPI PCLS on mean also appeared larger (4.235μm), this difference was not found to be significantly elevated. This provided evidence that the size of cryptococcal cells was related to their phagocytosis by macrophages.

It is also interesting to note that in 24HPI PCLS some KN99α GFP cell diameters were large enough to be considered titan cells (>10μm; Figure 51B-C), implying that this phenotypic shift in *C. neoformans* cells may occur in the first 24 hours of infection (Dambuza *et al.*, 2018) – although other titan cell characteristics in these cells could not be confirmed.

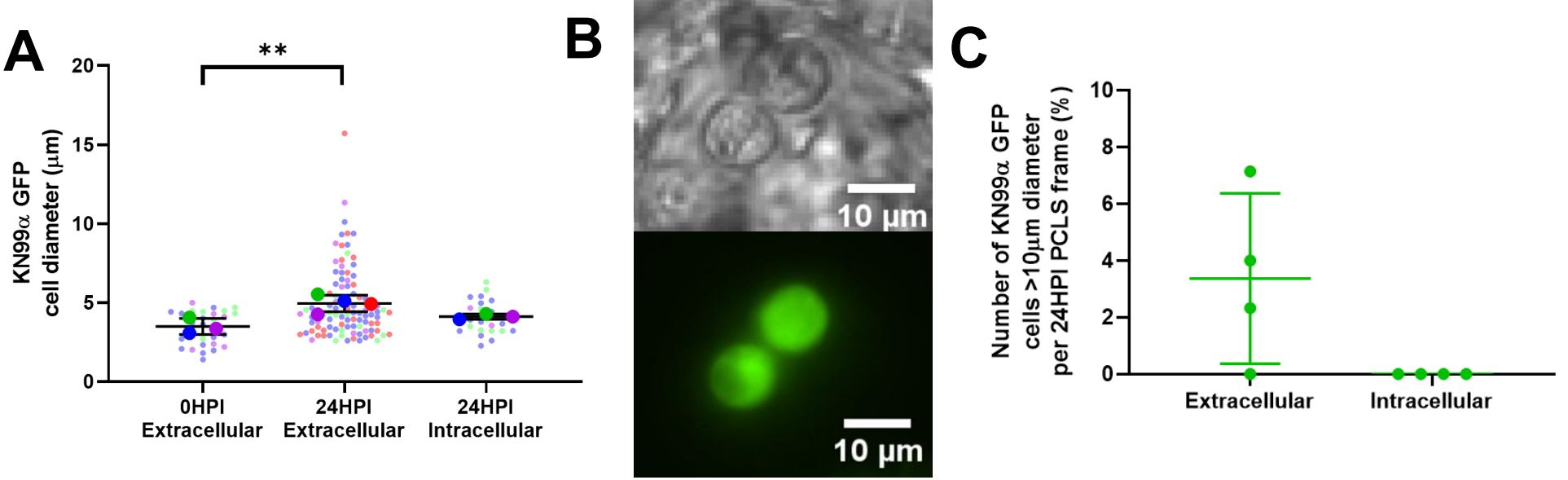

Figure 51 – The size of KN99α GFP *C. neoformans* cells is associated with phagocytosis in 24HPI PCLS. Compared to the size of fungal cells sizes in 0HPI PCLS, extracellular, but not intracellular KN99α GFP *C. neoformans* cells were significantly larger in 24HPI PCLS. (**A**) There was a significant difference in KN99α GFP cell size in PCLS prepared at 0HPI and 24HPI ($F=9.193$, $p=0.011$). Extracellular ($p=0.0094$), but not intracellular ($p=0.2745$) KN99α GFP cells were significantly larger in 24HPI PCLS compared to extracellular fungal cells in 0HPI PCLS. Each large point represents a different animal: 0HPI Extracellular – n=3, 24HPI Extracellular – n=4, 24HPI Intracellular – n=3, while each small point represents a different field of view. (**B**) Representative widefield images (20x) of KN99α GFP cells in 24HPI PCLS that are larger than 10μm in diameter (grey – DIC, green – GFP). (**C**) Only extracellular KN99α GFP *C. neoformans* cells in 24HPI PCLS were observed to be larger than 10μm in diameter, although not in all instances. Each point represents a different animal (n=4). KN99α GFP cell sizes were compared by a one-way ANOVA with *post hoc* Tukey comparisons. * - $p<0.05$, ** - $p<0.01$

6.2.14 – 6μm beads and KN99α GFP *C. neoformans* can be IgG opsonised

Having established that phagocytosis of *C. neoformans* cells was rare and variable, it was next determined whether phagocytosis could be enhanced – and if this affected pulmonary fungal burdens or host-pathogen interactions. Specifically, if macrophages were important for fungal clearance in the lung early in infection, increased phagocytosis would result in lower pulmonary fungal burdens. As antibodies are the best studied class of opsonin in the context of cryptococcosis, KN99α GFP *C. neoformans* cells and 6μm beads were opsonised with IgG antibodies prior to being inoculated into mice. The antibody used against *C. neoformans* was 18B7 (Casadevall *et al.*, 1998) – an anti-capsular IgG antibody well characterised to bind to *C. neoformans in vitro* and enhance phagocytosis (Mukherjee, Feldmesser and Casadevall, 1996) – and 6μm beads were coated with BSA and subsequently opsonised with anti-BSA IgG (Zheleznyak and Brown, 1992). This was investigated instead of *C. gattii* infection as the interest was in *C. neoformans* infection, which is associated with immunocompromise.

Firstly, the opsonin status of IgG labelled KN99α GFP *C. neoformans* and 6μm beads was confirmed by fluorescent microscopy. A secondary anti-Fc IgG conjugate was applied to opsonised particles, so opsonised particles would fluoresce. Both 6μm beads and KN99α GFP both were positive for the presence of the secondary antibody conjugate, indicating that both inocula were successfully IgG opsonised prior to administration to animals (Figure 52).

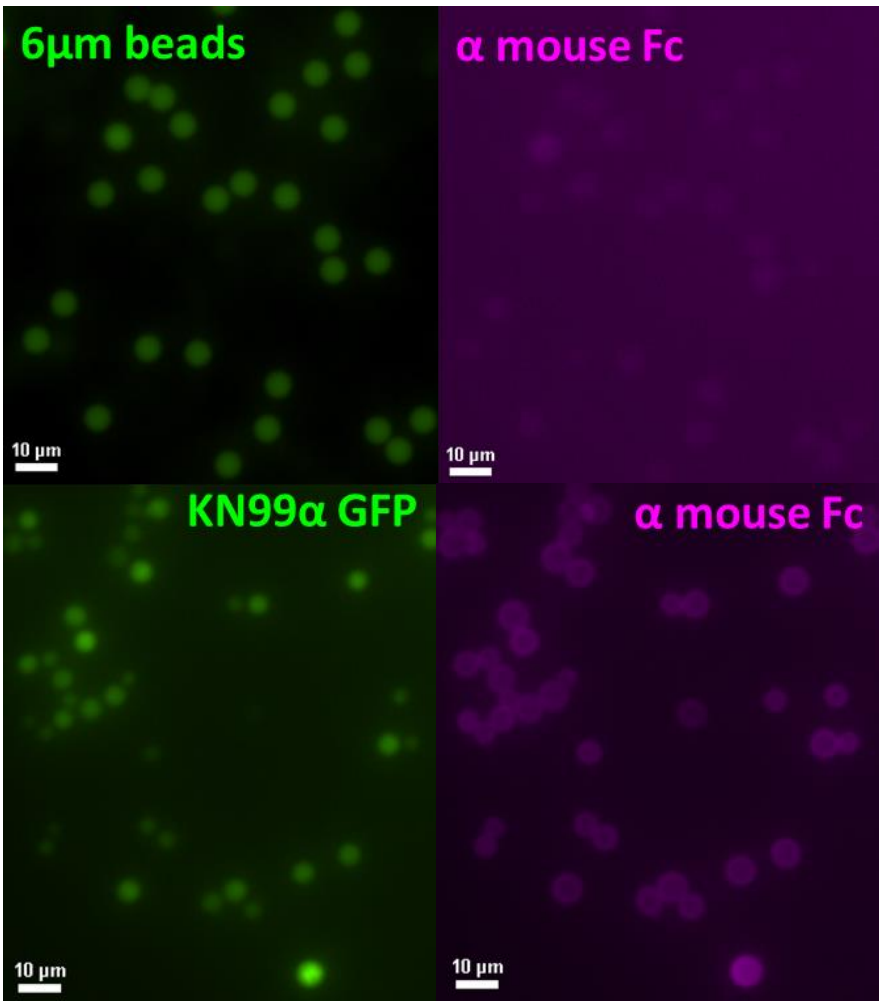

Figure 52 – KN99α GFP *C. neoformans* and 6µm beads can both be opsonised with IgG. Representative 20x widefield images of IgG opsonised KN99α GFP *C. neoformans* and 6µm beads successfully labelled with an anti-Fc fluorescent conjugate. IgG opsonisation appeared less clear with 6µm beads.

6.2.15 – Antibody opsonising inocula did not affect pulmonary fungal burdens, PCLS foci size or infection pathology in the first 24 hours of infection in mice

Mice were intranasally inoculated with KN99α GFP *C. neoformans* or 6μm beads that had been opsonised with IgG *in vitro* to determine if this enhanced fungal clearance and host-pathogen interactions.

Firstly, fungal burdens in the multi-lobe lungs of KN99α GFP inoculated animals were compared at both 0HPI and 24HPI, with and without an antibody opsonin. Pulmonary fungal burdens at both time points were found to be unaffected by *C. neoformans* opsonin status (Figure 53A). It was confirmed that there were no significant differences in the size of inocula animals received (Figure 53B). Additionally, opsonised *C. neoformans* infection also was asymptomatic with no significant changes in bodyweight – as was observed with non-opsonised *C. neoformans* infection (Figure 53C).

Then infected PCLS were compared. There was also no change in the number of KN99α GFP cells per infected frame (20x) in 0HPI PCLS and 24HPI PCLS due to opsonin status – although foci of KN99α GFP infection were still found to be significantly larger in 24HPI PCLS (Figure 53D). Furthermore, the numbers of 6μm beads and KN99α GFP cells observed per frame (20x) of 24HPI PCLS were compared, with and without IgG opsonin. No effect of different inocula or antibody opsonin was observed (Figure 53E).

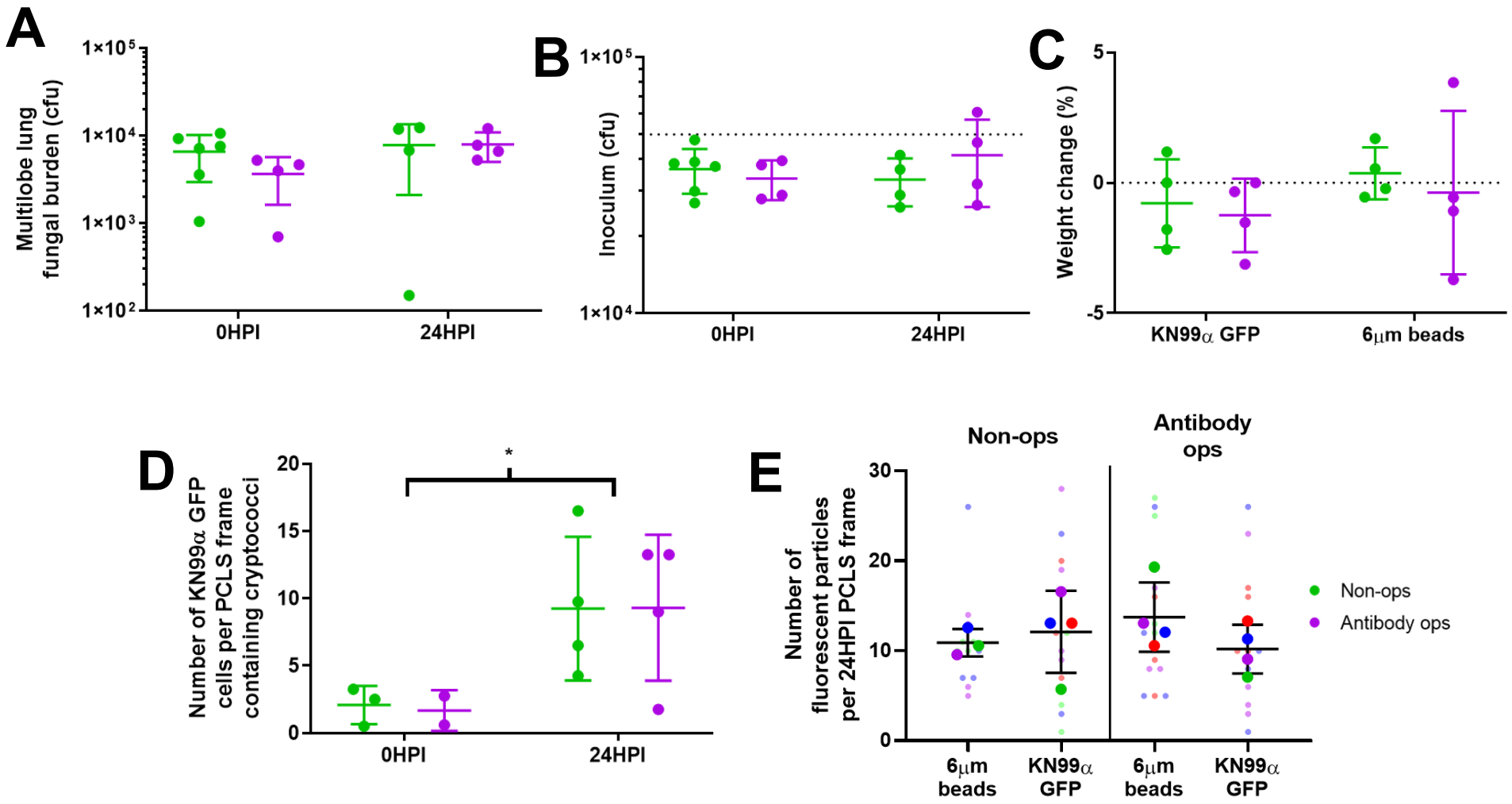
A
Multilobe lung fungal burden (cfu)
1×10^5
1×10^4
1×10^3
1×10^2
0HPI
24HPI
B
Inoculum (cfu)
1×10^5
1×10^4
0HPI
24HPI
C
Weight change (%)
5
0
-5
KN99α GFP
6μm beads
D
Number of KN99α GFP cells per PCLS frame containing cryptococci
*
20
15
10
5
0
0HPI
24HPI
E
Non-ops
Antibody ops
Number of fluorescent particles per 24HPI PCLS frame
30
20
10
0
6μm beads
KN99α GFP
6μm beads
KN99α GFP
Non-ops
Antibody ops

Figure 53 – **IgG opsonising KN99α GFP *C. neoformans* does not affect pulmonary fungal burdens or the size of foci of infection in the first 24 hours of infection.** Opsonising *C. neoformans* cells with IgG did not improve mouse control of infection in the first 24 hours. (**A**) Fungal burdens at 0 and 24HPI were not affected by *C. neoformans* opsonin status. Interaction – $F(1,14)=0.7178$, $p=0.4111$. Time post infection – $F(1,14)=2.338$, $p=0.1485$. Opsonin status – $F(1,14)=0.5741$, $p=0.4612$. (**B**) Inocula of KN99α GFP that animals received did not differ. Interaction – $F(1, 14)=1.546$, $p=0.2342$. Time post infection – $F(1,14)=0.2538$, $p=0.6222$. Opsonin status – $F(1,14)=0.3446$, $p=0.5665$. (**C**) Inoculation of mice with either 6μm beads or KN99α GFP did not induce significant weight loss, regardless of opsonin status. Interaction – $F(1,12)=0.02049$, $p=0.8886$. Inoculum – $F(1,12)=1.049$, $p=0.3259$. Opsonin – $F(1,12)=0.368$, $p=0.5554$. (**D**) The number of KN99α GFP cells per infected frame of 0HPI and 24HPI PCLS were significantly different, but unaffected by opsonin status. Interaction – $F(1,9)=0.008312$, $p=0.9294$. Time post infection – $F(1,9)=8.217$, $p=0.0186$. Opsonin status – $F(1,9)=0.004484$, $p=0.9481$. (**E**) The number of KN99α GFP cells and 6μm beads at foci of infection in 24HPI PCLS were the same, regardless of opsonin status. Interaction – $F(1,11)=1.731$, $p=0.215$. Inoculum – $F(1,11)=0.4215$, $p=0.5295$. Opsonin status – $F(1,11)=0.06685$, $p=0.8008$. All comparisons were done using a two-way ANOVA. Data presented as mean ± SD. Each large point represents a different animal ($n\geq2$), while each small point represents a different PCLS frame. * - $p<0.05$

6.2.16 – The pulmonary cellular immune responses to KN99α GFP *C. neoformans* cells and 6μm beads are unaffected by IgG opsonin

Although tissue burdens and foci of infection were unaffected by IgG status, it was still hypothesised that an opsonin would increase the immunogenicity of inoculated cells, affecting the number of innate cells recruited to sites of infection. Therefore, the numbers of immune cells in both 0HPI PCLS and 24HPI PCLS were examined. Numbers of isolectin GS-IB_4^+ (0HPI) and $CD11c^+$ (24HPI) cells were not found to be significantly affected by opsonin status – both with KN99α GFP cells and 6μm beads (Figure 54A-B). Additionally, the number of macrophage 'clusters' per frame were also found to be unaffected (Figure 54C). Finally, cell numbers of recruited MDMs, neuts and DCs were all observed to be identical, regardless of inocula and opsonin status (Figure 54D-F).

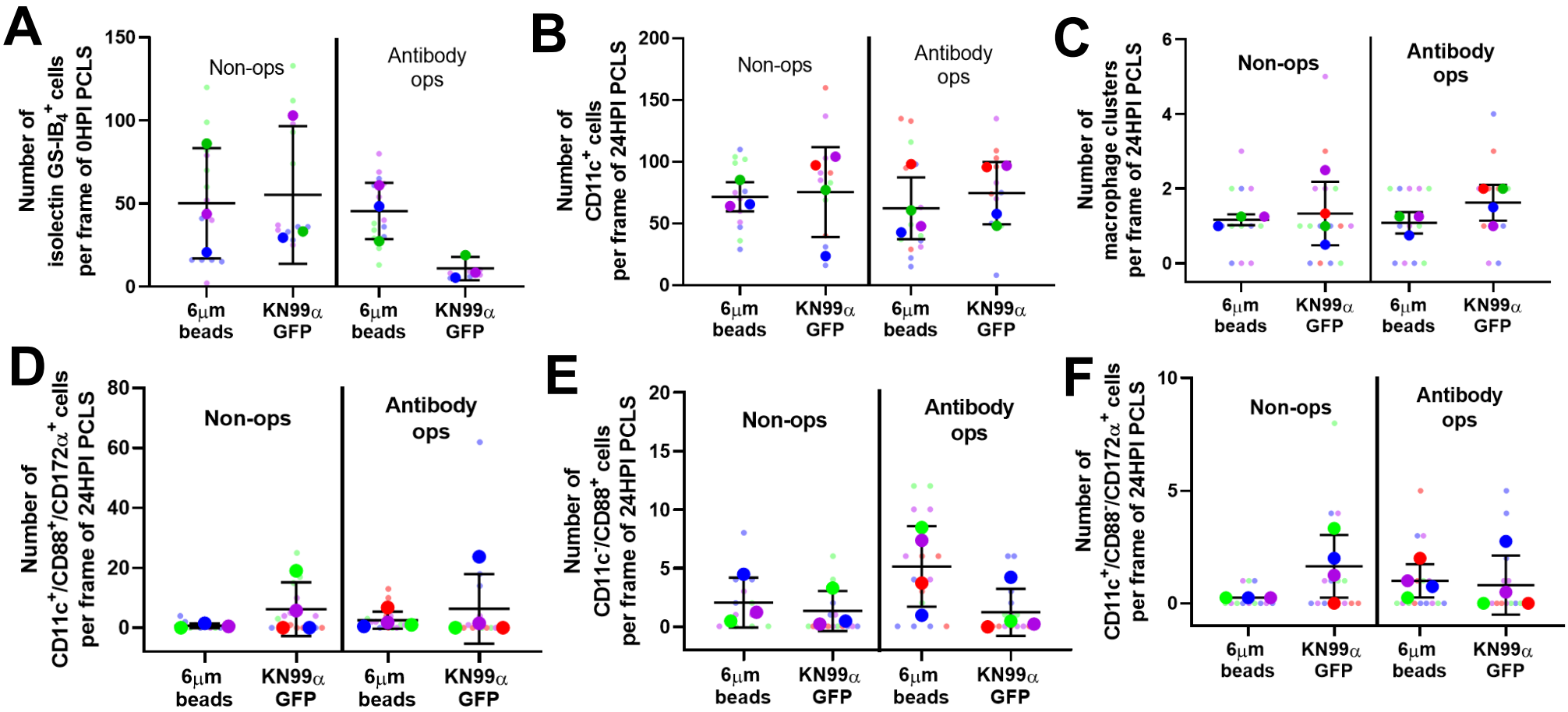
A
Number of isolectin GS-IB4+ cells per frame of 0HPI PCLS
150
100
50
0
Non-ops
Antibody ops
6μm beads
KN99α GFP
6μm beads
KN99α GFP
B
Number of CD11c+ cells per frame of 24HPI PCLS
200
150
100
50
0
Non-ops
Antibody ops
6μm beads
KN99α GFP
6μm beads
KN99α GFP
C
Number of macrophage clusters per frame of 24HPI PCLS
6
4
2
0
Non-ops
Antibody ops
6μm beads
KN99α GFP
6μm beads
KN99α GFP
D
Number of CD11c+/CD88+/CD172α+ cells per frame of 24HPI PCLS
80
60
40
20
0
Non-ops
Antibody ops
6μm beads
KN99α GFP
6μm beads
KN99α GFP
E
Number of CD11c-/CD88+ cells per frame of 24HPI PCLS
20
15
10
5
0
Non-ops
Antibody ops
6μm beads
KN99α GFP
6μm beads
KN99α GFP
F
Number of CD11c+/CD88-/CD172α+ cells per frame of 24HPI PCLS
10
5
0
Non-ops
Antibody ops
6μm beads
KN99α GFP
6μm beads
KN99α GFP

Figure 54 – IgG opsonising KN99α GFP *C. neoformans* cells and 6µm beads did not affect immune cell numbers in 0HPI PCLS and 24HPI PCLS. For all investigated cell types, opsonin status was not found to significantly affect their number in 0HPI or 24HPI PCLS. (**A**) The number of rounded isolectin GS-IB_4^+ cells per infected frame in 0HPI PCLS was not significantly affected by IgG opsonisation. Interaction – $F(1,8)=1.491$, $p=0.2568$. Inoculum – $F(1,8)=0.8347$, $p=0.3876$. Opsonin – $F(1,8)=2.277$, $p=0.1697$. (**B**) The number of $CD11c^+$ cells per infected frame in 24HPI PCLS was not significantly affected by IgG opsonisation. Interaction – $F(1,11)=0.08996$, $p=0.7698$. Inoculum – $F(1,11)=0.324$, $p=0.5806$. Opsonin – $F(1,11)=0.1311$, $p=0.7241$. (**C**) The number of macrophage 'clusters' observed per infected frame in 24HPI PCLS was not significantly affected by IgG opsonisation. Interaction – $F(1,10)=0.3936$, $p=0.5445$. Inoculum – $F(1,10)=1.404$, $p=0.2634$. Opsonin – $F(1,10)=0.1215$, $p=0.7347$. (**D**) The number of MDMs per infected frame in 24HPI PCLS was not significantly affected by IgG opsonisation. Interaction – $F(1,11)=0.04462$, $p=0.8366$. Inoculum – $F(1,11)=1.309$, $p=0.2768$. Opsonin – $F(1,11)=0.05853$, $p=0.8133$ (**E**) The number of neuts per infected frame in 24HPI PCLS was not significantly affected by IgG opsonisation. Interaction – $F(1,10)=1.396$, $p=0.2648$. Inoculum – $F(1,10)=2.946$, $p=0.1169$. Opsonin status – $F(1,10)=1.208$, $p=0.2975$. (**F**) The number of DCs per infected frame in 24HPI PCLS was not significantly affected by IgG opsonisation. Interaction – $F(1,11)=2.015$, $p=0.1835$. Inoculum – $F(1,11)=1.173$, $p=0.3019$. Opsonin – $F(1,11)=0.0055581$, $p=0.9418$. All comparisons were done using a two-way ANOVA. Data presented as mean ± SD. Each larger point represents a different animal ($n\geq3$), while each smaller point represents a different PCLS frame.

6.2.17 – IgG opsonin does not enhance macrophage phagocytosis of 6μm beads or KN99α GFP *C. neoformans* within the lung or PCLS in the first 24 hours of infection

18B7 IgG is well characterised to enhance the phagocytosis of *C. neoformans* by macrophages in *in vitro* models of cryptococcosis (Mukherjee, Feldmesser and Casadevall, 1996; Casadevall *et al.*, 1998). Additionally, it has been observed to increase the phagocytosis of KN99α GFP *C. neoformans* by J774 cells (see Chapter 3). Therefore, it was confirmed if the same occurred in the lungs of mice during the first 24 hours of infection. Controversially, however, it was observed that IgG opsonised 6μm beads and KN99α GFP *C. neoformans* were not differentially phagocytosed in 0 and 24HPI PCLS. As was observed with non-opsonised inocula, no phagocytosis of IgG opsonised 6μm beads of KN99α GFP was observed in 0HPI PCLS – even when PCLS were cultured for 24 hours *ex vivo*. While phagocytosis was observed in 24HPI PCLS, incidences of phagocytosis were found to be equally low with both IgG opsonised 6μm beads and KN99α GFP cells (Figure 55A-B). It is worth noting though that the 18B7 antibody did appear to reduce the variability in incidence of phagocytosis observed in 24HPI PCLS infected with KN99α GFP (Figure 55A). Again though, no additional phagocytosis was observed when 24HPI PCLS were cultured *ex vivo* for 24 hours.

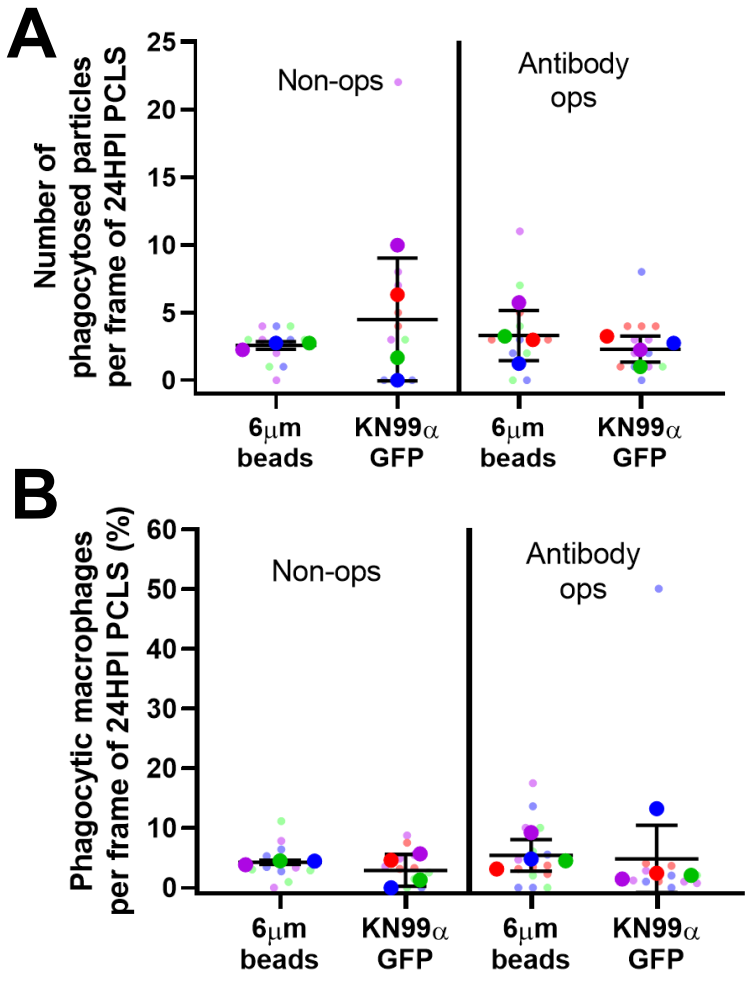

Figure 55 – IgG opsonising KN99α GFP *C. neoformans* and 6μm beads did not affect phagocytosis *in vivo* or *ex vivo* at 0HPI and 24HPI. Despite being well established to enhance phagocytosis *in vitro*, IgG opsonins did not enhance the phagocytosis of 6μm beads or KN99α GFP in the lungs of mice in the first 24 hours of infection. (**A**) The number of KN99α GFP cells and 6μm beads phagocytosed by macrophages in 24HPI PCLS was unaffected by IgG opsonin status. Interaction – $F(1,11)=1.149$, $p=0.3066$. Inoculum – $F(1,11)=0.1135$, $p=0.7425$. Opsonin status – $F(1,11)=0.2874$, $p=0.6026$. (**B**) The proportion of macrophages in 24HPI PCLS that phagocytosed KN99α GFP or 6μm beads were unaffected by IgG opsonin status. Non-ops 6μm beads vs Antibody ops 6μm beads – Mann-Whitney $U=3$, $p>0.9999$. Non-ops KN99α GFP vs Antibody ops KN99α GFP – Mann-Whitney $U=6$, $p>0.9999$. Antibody ops 6μm beads vs Antibody ops KN99α GFP – Mann-Whitney $U=6$, $p>0.9999$. Phagocytosed fungal cells were assessed using a two-way ANOVA, while phagocytic macrophage proportions were compared using multiple Mann-Whitney U tests, with p values adjusted for multiple comparisons (multiplied by 3). Data presented as mean ± SD. Each larger point represents a different animal: Non-ops 6μm beads – n=3, non-ops KN99α GFP – n=4, antibody ops 6μm beads – n=4, antibody ops KN99α GFP – n=4. Each smaller point represents a different PCLS frame.

6.2.18 – Opsonisation of KN99α GFP *C. neoformans* cells with 18B7 IgG does not affect fungal cell size

Aside from being more likely to be phagocytosed, the binding of anti-capsular IgG to *C. neoformans* cells is reported to affect the architecture of the cryptococcal capsule (Feldmesser *et al.*, 2000; Cordero *et al.*, 2013). As the size of *C. neoformans* cells is significantly affected by the capsule – and size is known to significantly affect phagocytosis – the size of IgG opsonised KN99α GFP *C. neoformans* cells in 0HPI PCLS and 24HPI PCLS was examined. No differences PCLS fungal cell sizes were observed as a result of 18B7 IgG binding at either time point (Figure 56A-B). Additionally, the proportion of KN99α GFP cells greater than 10μm in diameter was also unaffected by IgG opsonin in 24HPI PCLS (Figure 56C).

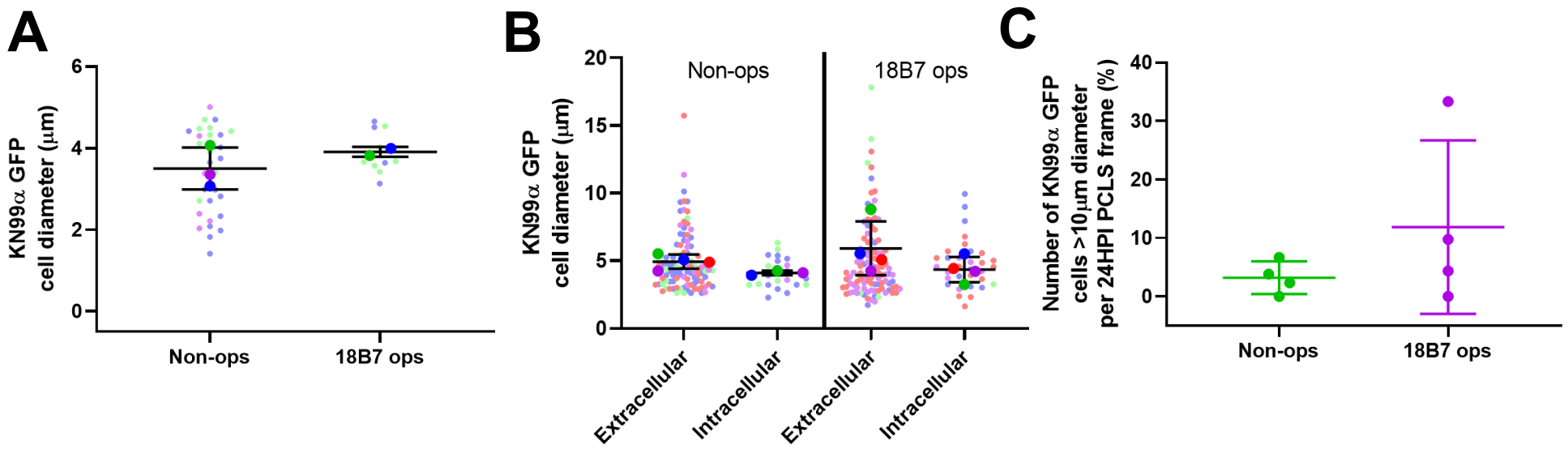

Figure 56 – IgG opsonin did not significantly affect the size of KN99α GFP *C. neoformans* cells in PCLS at 0HPI or 24HPI. Neither cell size, nor the proportion of KN99α GFP *C. neoformans* cells greater than 10μm in diameter, were affected by IgG opsonin PCLS. (**A**) The size of KN99α GFP cells in 0HPI PCLS was not affected by IgG opsonin (t=1.052, df=3, p=0.3701). Non-ops – n=3, 18B7 ops – n=2. (**B**) The size of extracellular and intracellular KN99α GFP cells in 24HPI PCLS was not affected by IgG opsonin status. Interaction – F(1,11)=0.3512, p=0.5654. Location – F(1,11)=3.79, p=0.0775. Opsonin status – F(1,11)=0.9995, p=0.3389. Extracellular non-ops – n=4, intracellular non-ops – n=3, extracellular ops – n=4, intracellular ops – n=4. (**C**) IgG opsonin did not affect the proportion of KN99α GFP cells greater than 10μm in diameter in 24HPI PCLS (Mann-Whitney U=4.5, p=0.3714), n=4. 0HPI KN99α GFP cell diameters were compared using an unpaired t-test, 24HPI PCLS KN99α GFP cell diameters were compared using a two-way ANOVA and the proportion of KN99α GFP cells with a diameter >10μm were compared using Mann-Whitney U test. Data presented as mean ± SD. Each larger point represents a different animal, while each smaller point represents a different *C. neoformans* cell.

6.2.19 – The replication of KN99α GFP *C. neoformans* cells is unaffected by phagocytosis

Another signature pathological feature of *C. neoformans* cells is the ability to parasitise macrophages – a behaviour has been observed both *in vitro,* and in the zebrafish embryo *in vivo* (Mukherjee, Feldmesser and Casadevall, 1996; Bojarczuk *et al.*, 2016). However, this has yet to be observed in live lung tissue. Therefore, the dynamics of *C. neoformans* replication was assessed in PCLS to confirm the suitability of the model for studying this phenomenon in the future, and determine the antifungal activity of pulmonary macrophages. Therefore, PCLS prepared at both 0HPI and 24HPI were cultured *ex vivo* and imaged over 24 hours.

In infected PCLS prepared at both 0HPI and 24HPI, extracellular KN99α GFP cell budding was observed (Figure 57A), while in 24HPI PCLS, phagocytosed KN99α GFP cells were observed to replicate intracellularly (Figure 57B). This makes this the first reported observation of intracellular replication by *C. neoformans* in live lung tissue.

Although fungal replication could be observed in PCLS, it was important to establish whether the replication of KN99α GFP cells *ex vivo* in PCLS correlated with KN99α GFP fungal cell replication in the lungs of mice *in vivo*. Therefore, the number of KN99α GFP cells per infected frame after 0HPI PCLS were cultured for 24 hours *ex vivo* was compared to the number of KN99α GFP cells observed in 24HPI PCLS. Interestingly, KN99α GFP cell numbers were not found to significantly differ (Figure 57C), suggesting that the change in KN99α GFP cell numbers over 24 hours *ex vivo* in 0HPI PCLS is the same as occurs *in vivo* over the first 24 hours of infection. This means that *ex vivo* culture of PCLS could replace subjecting animals to procedures *in vivo*.

A more controversial observation, however, was that the doubling times of extracellular and intracellular KN99α GFP cells in 24HPI PCLS were indistinguishable (Figure 57D). This finding calls into question the host protective role of pulmonary macrophages during early cryptococcosis, and indicates that any early clearance of KN99α GFP cells is likely not mediated by AMs.

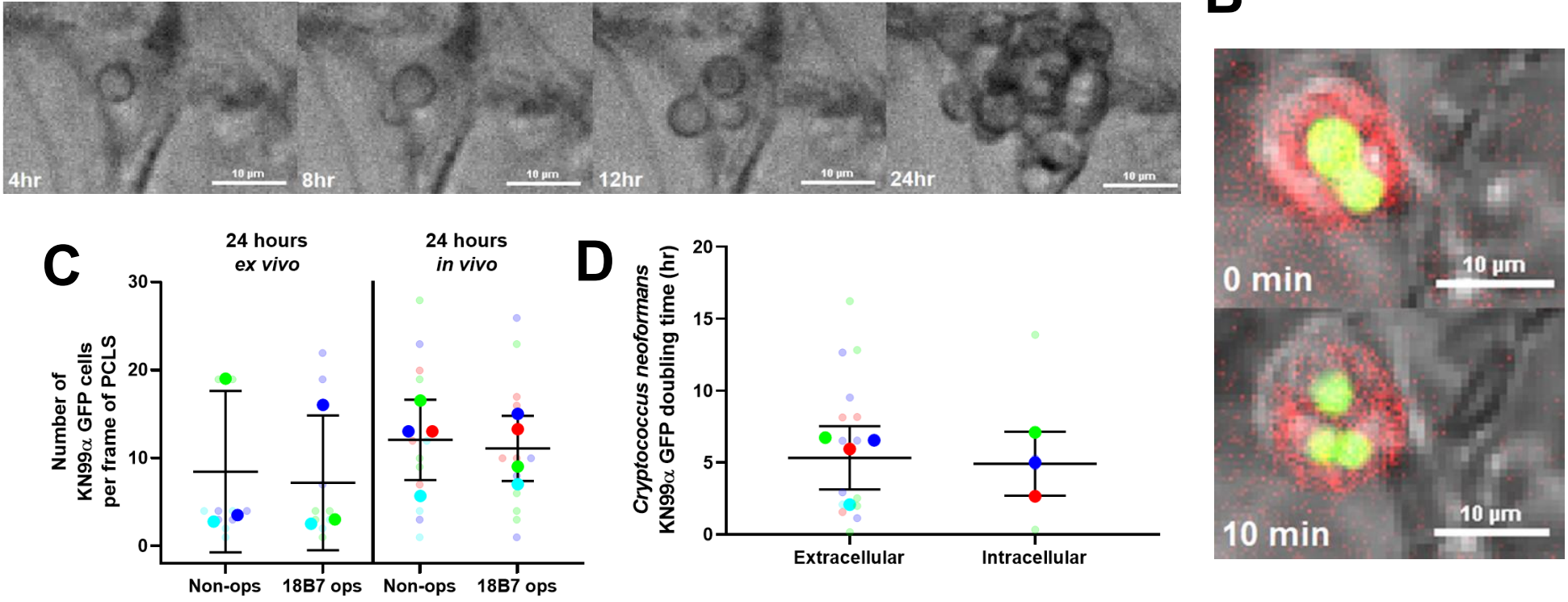

Figure 57 – Phagocytosis of KN99α GFP *C. neoformans* cells did not affect fungal replication. Although it was observed that KN99α GFP *C. neoformans* cells replicate within AMs in live lung tissue, this was found not to significantly affect fungal replication. (**A**) Representative widefield images (20x) of extracellular KN99α GFP *C. neoformans* cell replication in 24HPI PCLS (scale bar – 10µm). (**B**) Representative widefield images (20x) of intracellular KN99α GFP *C. neoformans* cells replicating inside a macrophage. (**C**) The numbers of KN99α GFP cells per infected frame of 0HPI PCLS after 24 hours of *ex vivo* culture are no different from the number of KN99α GFP cells per infected frame of 24HPI PCLS, regardless of opsonin status. Interaction – $F(1,10)=0.001617$, $p=0.9687$. *Ex vivo* or *in vivo* – $F(1,10)=1.247$, $p=0.7475$. Opsonin status – $F(1,10)=0.1095$, $p=0.7475$. (**D**) The doubling times of extracellular and intracellular KN99α GFP cells in 24HPI PCLS did not differ significantly ($t=0.2423$, $df=5$, $p=0.8182$). KN99α GFP cell numbers in PCLS *ex vivo* and *in vivo* were compared using a two-way ANOVA, while KN99α GFP cell doubling times were compared using an unpaired t-test. Data presented as mean ± SD. Each larger point represents a different animal ($n\geq3$), while each smaller point represents a different PCLS frame.

6.2.20 – The proportion of KN99α GFP *C. neoformans* cells that replicate *ex vivo* in PCLS is not significantly affected by IgG opsonin status

Although the dynamics of fungal replication were unaffected by phagocytosis, effect of IgG opsonin on replicating proportions of KN99α GFP *C. neoformans* cells in PCLS was assessed. There was no significant difference in the proportion of KN99α GFP cells that replicated in 0HPI PCLS and 24HPI PCLS (Figure 58A). However, the low numbers of KN99α GFP cells per infected frame of 0HPI PCLS (1-4 cells) resulted in high variance that makes statistical comparisons difficult. However, IgG opsonin was found not to significantly affect the proportion of KN99α GFP cells that replicated *ex vivo* in 0HPI PCLS (Figure 58B).

Then the proportion of replicating KN99α GFP cells in 24HPI PCLS was compared. Interestingly, the proportion of 18B7 opsonised fungal cells that replicated in 24HPI PCLS appeared larger than was observed with non-opsonised KN99α GFP cells (Figure 58C). This was examined more closely, by comparing the replicating proportions of intracellular and extracellular KN99α GFP cells in 24HPI PCLS. However, no significant effect of opsonin status was observed, although intracellular fungal replication was highly variable due to the low numbers of phagocytosed KN99α GFP cells (Figure 58D).

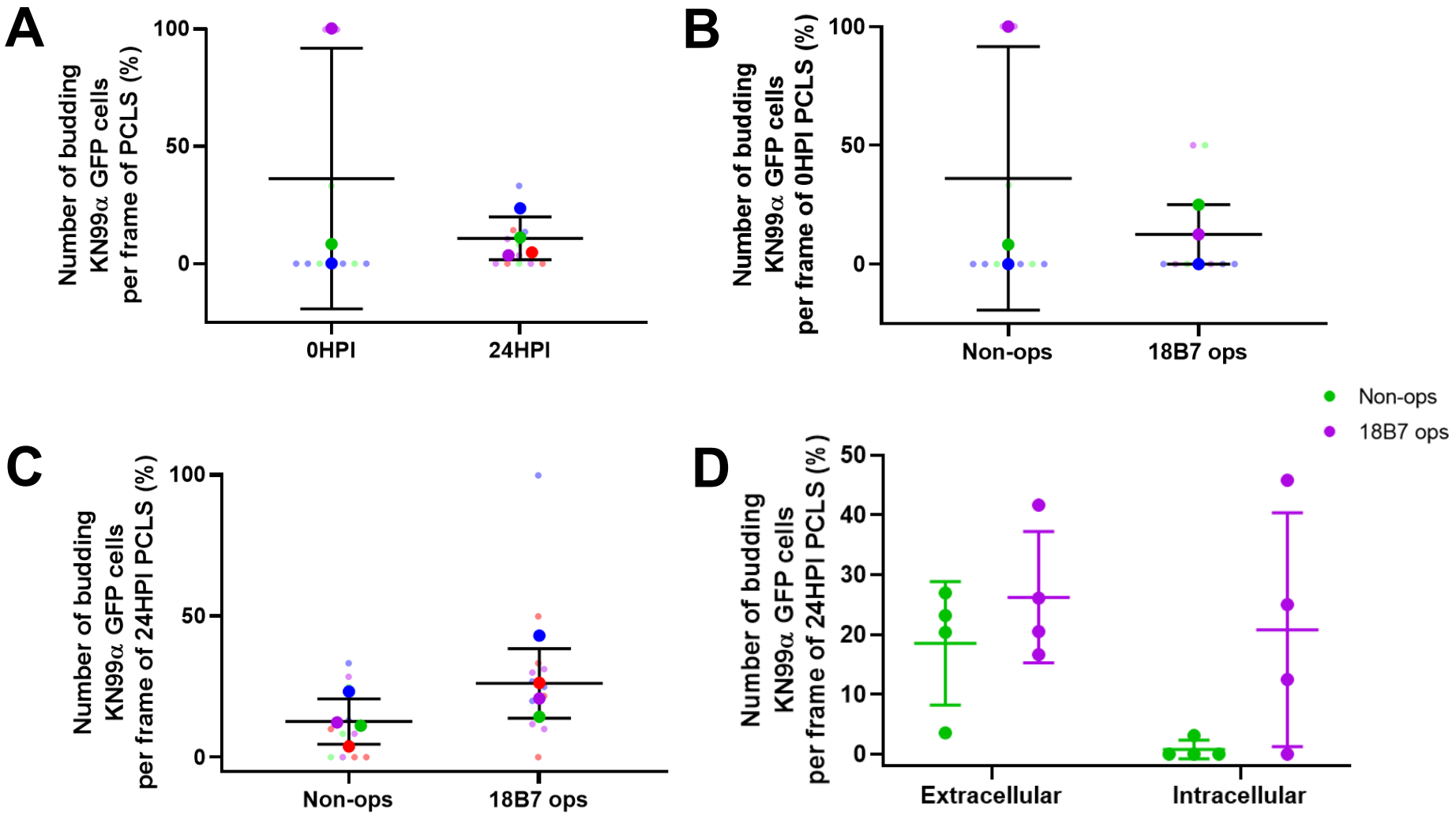
A
Number of budding KN99α GFP cells per frame of PCLS (%)
100
50
0
0HPI
24HPI
B
Number of budding KN99α GFP cells per frame of 0HPI PCLS (%)
100
50
0
Non-ops
18B7 ops
C
Number of budding KN99α GFP cells per frame of 24HPI PCLS (%)
100
50
0
Non-ops
18B7 ops
D
Number of budding KN99α GFP cells per frame of 24HPI PCLS (%)
50
40
30
20
10
0
Extracellular
Intracellular
Non-ops
18B7 ops

Figure 58 – The proportion of KN99α GFP cells that replicate *ex vivo* in PCLS is not significantly affected by IgG opsonin. While there was no effect of time post infection on replicating proportions of KN99α GFP cells in PCLS *ex vivo*, a significant effect of IgG opsonin was observed in 24HPI PCLS. (**A**) The proportion of KN99α GFP cells that replicated *ex vivo* in 0HPI PCLS was not significantly different from replication proportions in 24HPI PCLS (Mann-Whitney U=6, p>0.9999). (**B**) The proportion of KN99α GFP cells that bud in 0HPI PCLS are not affected by IgG opsonisation (Mann-Whitney U=4.5, p>0.9999). (**C**) The proportion of 18B7 IgG opsonised KN99α GFP cells that replicated in 24HPI PCLS appeared higher than with non-opsonised fungal cells, although this was not significant (Mann-Whitney U=2, p=0.1143). (**D**) The proportions of extracellular and intracellular KN99α GFP cells that replicated in 24HPI PCLS was not significantly affected by opsonin status. Non-ops extracellular vs Non-ops intracellular – Mann-Whitney U=0, adjusted p value=0.1144. Antibody-ops extracellular vs Antibody-ops intracellular – Mann-Whitney U=6, adjusted p value>0.9999. Non-ops extracellular vs Antibody-ops extracellular – Mann-Whitney U=6, adjusted p value>0.9999. Non-ops intracellular vs Antibody-ops intracellular – Mann-Whitney U=6, adjusted p value=0.5716. KN99α GFP replicating proportions in **A** and **B** were compared using a Mann Whitney test, in **C** using an unpaired t-test and in **D** multiple Mann-Whitney U tests adjusted p value=0.5716. Data presented as mean ± SD. Each larger point represents a different animal (n≥3), while each smaller point represents a different PCLS frame.

6.2.21 – Intranasal infection of mice with avirulent *plb1* H99α GFP results in lower fungal burdens and smaller foci of infection in 24HPI PCLS

At this point, it had been determined that the highly virulent reference strain of *C. neoformans*, KN99α GFP, was unaffected by phagocytosis, indicating that there was no protective role for AMs during initial *C. neoformans* infection in mice. However, this may also have been an artefact of the PCLS methodology which perturbed macrophages *ex vivo*. To confirm that macrophage antimicrobial activity was preserved, animals were inoculated with an avirulent strain of *C. neoformans* that is reported to be unable to replicate intracellularly inside macrophages – *plb1* H99α GFP. This strain is a transgenic variant of the highly virulent H99α GFP strain, characterised by the loss of the cryptococcal virulence factor, *plb1* (Evans *et al.*, 2019). *plb1* has several functions that aid the pathology of *C. neoformans* infection (see 1.4.2.3), but most importantly has also been shown to be indispensable for intracellular survival within macrophages *in vitro* (Evans *et al.*, 2015). This strain was also investigated to better understand the role of

the macrophage in *C. neoformans* infection, which is associated with immunocompromise, rather than *C. gattii* infection which is associated with inflammatory immune responses.

Therefore, to confirm the antimicrobial activity of macrophages was preserved in the PCLS model, 24HPI PCLS were prepared at from animals inoculated intranasally with *plb1* H99α GFP. Firstly, the fungal burden of the multi-lobe lung at 24HPI was compared between KN99α GFP and *plb1* H99α GFP infection. Fungal burdens of *plb1* H99α GFP appeared to be lower (Figure 59A), although this difference was not significant. This could be due to insufficient statistical power or due to the highly variable fungal burdens reported due to KN99α GFP infection. However, it also could have been because inocula of *plb1* H99α GFP were significantly smaller than inocula of KN99α GFP (Figure 59B).

Even though *plb1* H99α GFP inocula were approximately half as large as those of KN99α GFP, inocula of *plb1* H99α GFP were still of the same magnitude as KN99α GFP inocula (10^4). To establish whether this is likely to have affected mouse pulmonary fungal burdens or the number of fungal cells observed per infected frame of PCLS, correlations were examined between KN99α GFP inocula (opsonised and non-opsonised) and both multi-lobe fungal burdens at 24HPI (Figure 59C) and the number of KN99α GFP cells per infected frame of 24HPI PCLS (Figure 59D). There was no significant correlation in both instances, providing evidence that smaller inocula of *plb1* H99α GFP should not have significantly affected 24HPI fungal burdens or the number of cells observed in 24HPI PCLS. Finally, the numbers of *plb1* H99α GFP cells was compared with numbers of KN99α GFP cells in infected frames of 24HPI PCLS. Again, *plb1* H99α GFP cells numbers appeared lower, although not significantly (Figure 59E).

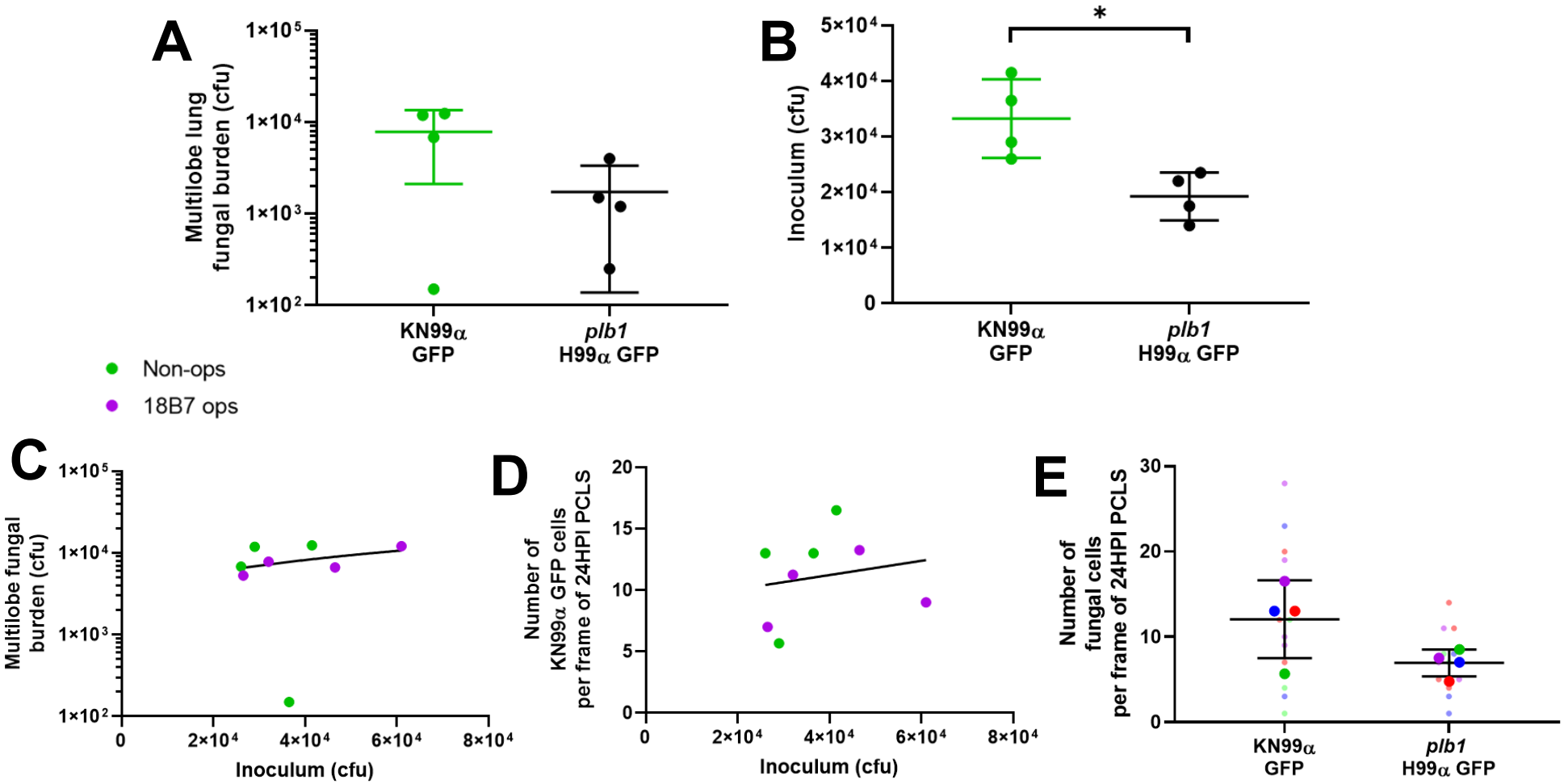
A
Multilobe lung fungal burden (cfu)
1×10⁵
1×10⁴
1×10³
1×10²
KN99α GFP
plb1 H99α GFP
B
Inoculum (cfu)
5×10⁴
4×10⁴
3×10⁴
2×10⁴
1×10⁴
0
*
KN99α GFP
plb1 H99α GFP
Non-ops
18B7 ops
C
Multilobe fungal burden (cfu)
1×10⁵
1×10⁴
1×10³
1×10²
0
2×10⁴
4×10⁴
6×10⁴
8×10⁴
Inoculum (cfu)
D
Number of KN99α GFP cells per frame of 24HPI PCLS
20
15
10
5
0
2×10⁴
4×10⁴
6×10⁴
8×10⁴
Inoculum (cfu)
E
Number of fungal cells per frame of 24HPI PCLS
30
20
10
0
KN99α GFP
plb1 H99α GFP

Figure 59 – **Avirulent *plb1* H99α GFP infection does not result in lower pulmonary fungal burdens and smaller foci of infection.** Although not significant, infection of mice with avirulent *plb1* H99α GFP resulted in lower fungal burdens and fewer fungal cells per infected frame of 24HPI PCLS. (**A**) Multi-lobe lung fungal burdens of *plb1* H99α GFP were lower than those observed with KN99α GFP infection, although not significantly (t=2.052, df=6, p=0.086). (**B**) Inocula of *plb1* H99α GFP that animals received were significantly smaller than the inocula of KN99α GFP (t=3.383, df=6, 0.0148). (**C**) The inocula of non-opsonised and antibody opsonised KN99α GFP that animals received did not significantly correlate with multi-lobe fungal burdens at 24HPI (R^2=0.1173, p=0.4062). (**D**) The inocula of non-opsonised and antibody opsonised KN99α GFP that animals received did not significantly correlate with the number of KN99α GFP cells that were observed per infected frame of 24HPI PCLS (R^2=0.03681, p=0.649). (**E**) The number of *plb1* H99α GFP cells per infected frame of 24HPI PCLS was lower than the number of KN99α GFP cells, although this difference was not significantly different (t=2.115, df=6, p=0.0788). **A**, **B** and **E** were compared using an unpaired t-test, while correlations were assessed using Pearson correlation coefficients. Data in **A**, **B**, and **E** presented as mean ± SD. Each larger point represents a different animal (n=4), while each smaller point represents a different PCLS frame. * - $p<0.05$

6.2.22 - *plb1* H99α GFP infection of mice does not affected immune cell numbers in 24HPI PCLS compared to KN99α GFP infection

Having observed both potentially lower fungal burdens and potential lower numbers of fungal cells per infected PCLS frame, the immune cells present in 24HPI PCLS were compared between *plb1* H99α GFP and KN99α GFP infection. However, observed numbers of $CD11c^+$ cells (Figure 60A), MDMs (Figure 60B), neuts (Figure 60C) and DCs (Figure 60D) were not significantly different, suggesting these infections did not results in differential immune cell numbers.

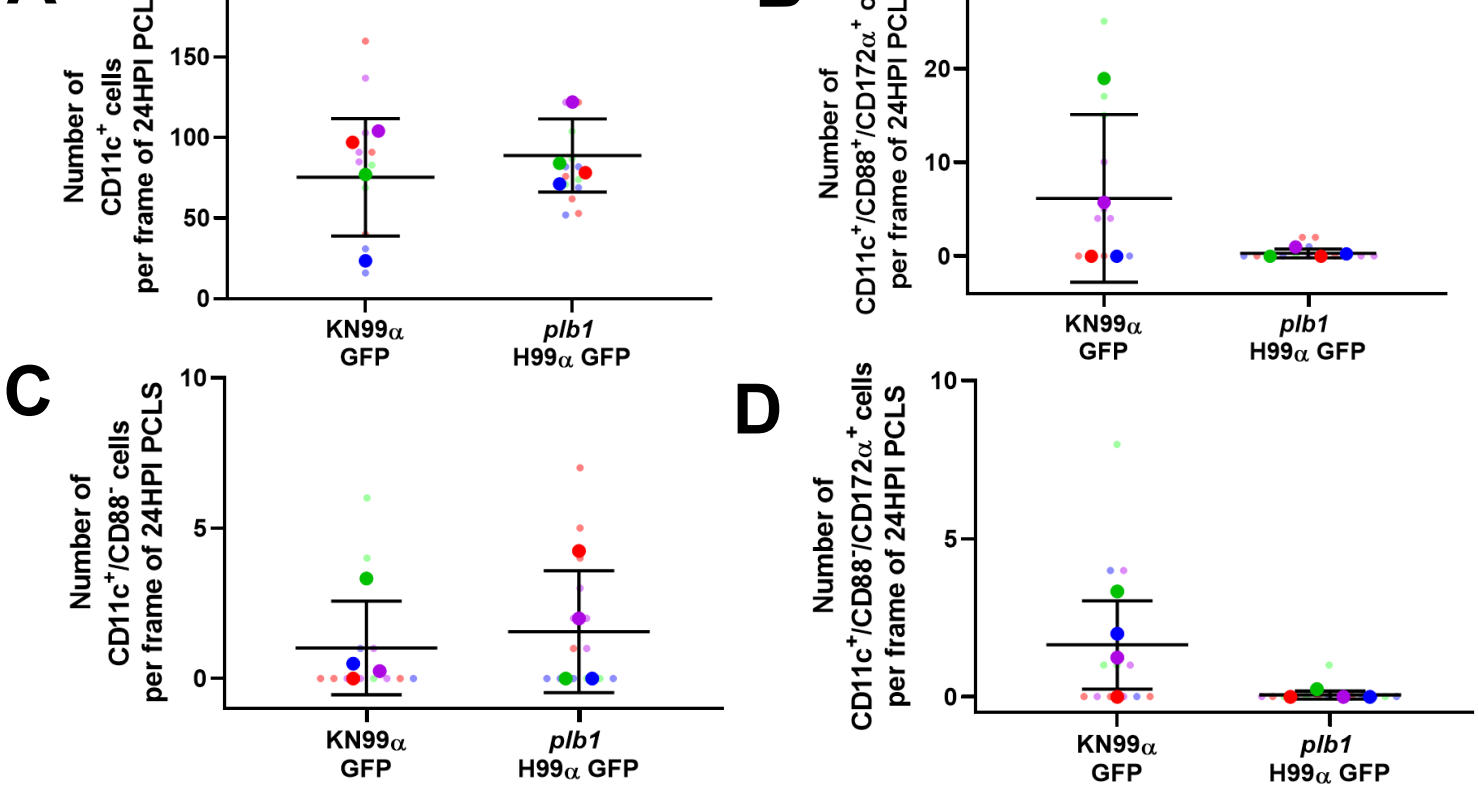

Figure 60 – The immune responses to *plb1* H99α GFP and KN99α GFP infection in 24HPI PCLS are equivalent. Despite evidence of different fungal burdens, immune cell numbers in 24HPI PCLS were the same with *plb1* H99α GFP and KN99α GFP infection. (**A**) $CD11c^+$ cell numbers per infected frame of 24HPI PCLS were the same (t=0.6291, df=6, p=0.5524). (**B**) The number of MDMs per infected frame of 24HPI PCLS were the same (t=1.309, df=3.017, p=0.2812), although more variable in number in PCLS with KN99α GFP infection (F=358.6, df=3, p=0.0005). (**C**) The number of neut cells per infected frame of 24HPI PCLS were the same (t=0.4244, df=6, p=0.6861). (**D**) The number of DCs per infected frame of 24HPI PCLS were the same (t=2.261, df=3.048, p=0.1074), although DC numbers in PCLS due to KN99α GFP infection were significantly more variable (F=124.6, DFn=3, p=0.0024). $CD11c^+$ and neut numbers were compared by an unpaired t-test, whereas MDM and DC numbers were compared by an unpaired t-test with Welch's correction. Data presented as mean ± SD. Each large point represents a different animal (n=4), while each smaller point represents a different PCLS frame.

6.2.23 – *plb1* H99α GFP cells are not phagocytosed within the lungs of mice in the first 24 hours of infection

Although murine pulmonary immune responses to *plb1* H99α GFP and KN99α GFP in 24HPI PCLS were of the same magnitude, the differences were hypothesised to be the response of macrophages to these cells – specifically in terms of phagocytosis and inhibiting intracellular replication. Therefore, the response of PCLS macrophages to infection were analysed in 24HPI PCLS. Firstly, number of macrophage 'clusters' were compared. Although no significant differences were found, there appeared to be fewer macrophage clusters in response to *plb1* H99α GFP infection (Figure 61A). However, of most significance was that no intracellular *plb1* H99α GFP cells were observed in 24HPI PCLS, even after 24 hours of *ex vivo* culture (Figure 61B-C). This suggests that *plb1* H99α GFP cells are more resistant to phagocytosis, which implies greater virulence.

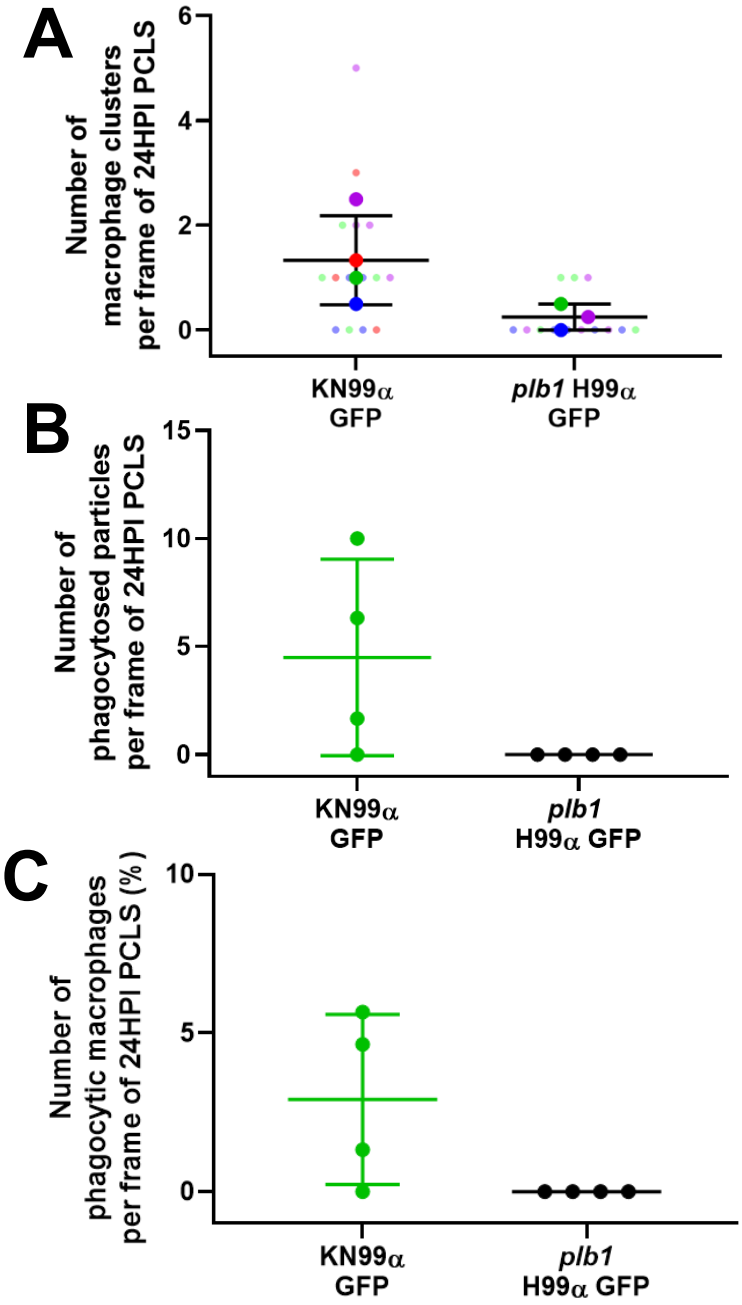

Figure 61 – *plb1* H99α GFP *C. neoformans* cells were not phagocytosed in the lungs of mice during the first 24 hours of infection. Despite being avirulent, *plb1* H99α GFP is highly resistant to phagocytosis in PCLS prepared at 24HPI. (**A**) The number of macrophage 'clusters' in 24HPI PCLS infected with *plb1* H99α GFP appeared lower than those infected with KN99α GFP, although this difference was not significant (Mann-Whitney U=0.5, p=0.0857). (**B**) No intracellular *plb1* H99α GFP cells were observed in 24HPI PCLS. (**C**) No macrophages were observed to have phagocytosed *plb1* H99α GFP in 24HPI. Macrophage cluster numbers were compared using a Mann-Whitney U test. Data presented as mean ± SD. Each large point represents a different animal (n≥3), while each smaller point represents a different PCLS frame.

6.2.24 – *plb1* H99α GFP *C. neoformans* cells are larger than KN99α GFP cells in 24HPI PCLS

The lack of phagocytosed *plb1* H99α GFP within 24HPI PCLS was a controversial observation as this strain is both avirulent in mouse models (Noverr *et al.*, 2003) and more susceptible to macrophage antifungal activity *in vitro* (Evans *et al.*, 2015). Therefore, factors that may explain this discrepancy were investigated. As size was previously observed to be an important factor in the PCLS model affecting the phagocytosis of both KN99α GFP cells (see 6.2.13) and different sizes of beads (see 6.2.3). Additionally, *plb1* is reported to be an important factor for regulating cryptococcal cell size (Evans *et al.*, 2015). Therefore, the size of *plb1* H99α GFP cells in 24HPI PCLS was examined. Importantly, *plb1* H99α GFP cells were found to be significantly larger than KN99α GFP cells in 24HPI PCLS (Figure 62A).

Therefore, the growth of *plb1* H99α GFP cells was examined further, and the growth of both KN99α GFP and *plb1* H99α GFP cells over 24 hours of *ex vivo* culture were compared. Ten fungal cells per infected PCLS frame were sampled every four hours and their cell size recorded. Strikingly, while the mean size of KN99α GFP cells remained constant during this time period, *plb1* H99α GFP cells were observed to significantly increase in size over time – as early as 4 hours post infection (Figure 62B). However, there wasn't a greater proportion of *plb1* H99α GFP cells with a diameter ≥10μm in 24HPI PCLS (Figure 62C-D).

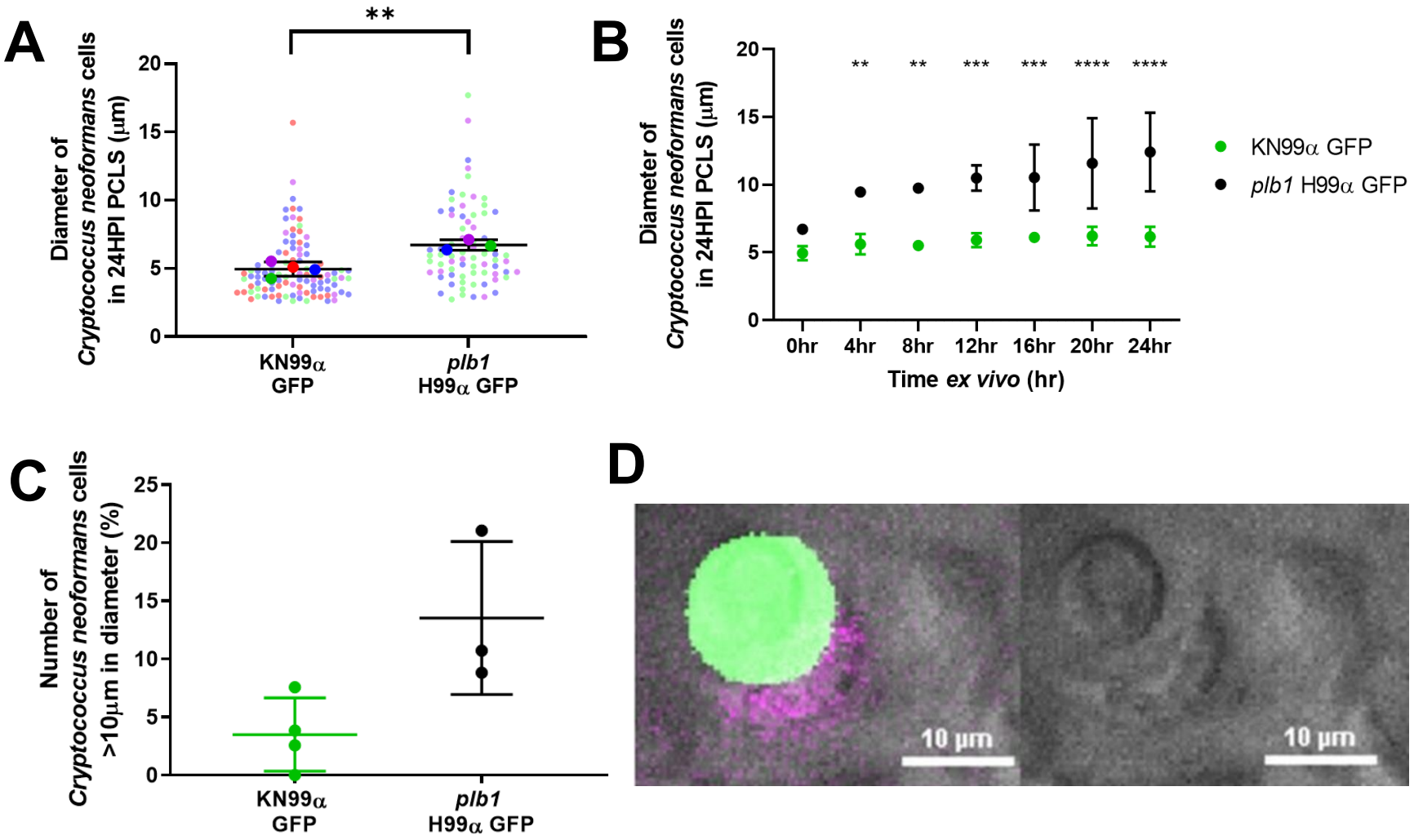
A
**
Diameter of Cryptococcus neoformans cells in 24HPI PCLS (μm)
20
15
10
5
0
KN99α GFP
plb1 H99α GFP
B
Diameter of Cryptococcus neoformans cells in 24HPI PCLS (μm)
**
**
***
***
****
****
0hr
4hr
8hr
12hr
16hr
20hr
24hr
Time ex vivo (hr)
KN99α GFP
plb1 H99α GFP
C
Number of Cryptococcus neoformans cells >10μm in diameter (%)
25
20
15
10
5
0
KN99α GFP
plb1 H99α GFP
D
10 μm
10 μm

Figure 62 – *plb1* H99α GFP *C. neoformans* cells are larger and grow significantly more than KN99α GFP *C. neoformans* cells in 24HPI PCLS . The size of *plb1* H99α GFP cells was significantly greater than that of KN99α GFP cells, and these cells continued to grow significantly more over time. (**A**) *plb1* H99α GFP cells are larger than KN99α GFP cells in 24HPI PCLS (t=4.865, df=5, p=0.0046). (**B**) *plb1* H99α GFP cells grow significantly within 24HPI PCLS over 24 hours *ex vivo* compared to KN99α GFP cells. Interaction – F(6, 30)=2.734, p=0.0307. Time – F(6,30)=4.739, p=0.0017. Strain – F(1,5)=44.31, p=0.0012. Subject – F(5,30)=4.296, p=0.0046. (**C**) A greater proportion of *plb1* H99α GFP cells were larger than 10μm in diameter, although this was not significant (Mann-Whitney U=0, p-value=0.0571). (**D**) Representative 20x widefield images of a *plb1* H99α GFP cell failing to be phagocytosed by a $CD11c^+$ cell (green – *plb1* H99α GFP cell, purple – $CD11c^+$ cell). **A** was compared using an unpaired t-test, while the growth of *C. neoformans* cells over 24 hours was compared using a one-way ANOVA with repeated measures and post hoc Sidak multiple comparisons at each time point. **C** was compared using a Mann-Whitney U test. Data presented as mean ± SD. Each point in C represents an mean size of up to 10 randomly sampled *plb1* H99α GFP and KN99α GFP cells over time from ≥3 different animals. Each large point in **A** and **B** represents a different animal (n≥3), while each small point represents a different *C. neoformans* cell. * - p<0.05, ** - p<0.01, *** - p<0.001, **** - p<0.0001

6.2.25 – The proportions of *plb1* H99α GFP and KN99α GFP *C. neoformans* cells that replicate extracellularly in 24HPI PCLS are equivalent

Although *plb1* H99α GFP pulmonary burdens and cell numbers were lower than those observed with KN99α GFP infection, *plb1* H99α GFP cells were significantly larger and completely resistant to phagocytosis in the first 24 hours of pulmonary infection. Therefore, the extracellular replication of *plb1* H99α GFP cells was examined to determine if fungal replication was lower with this strain, which would explain the lower fungal burdens observed in 24HPI PCLS. However, replicating proportions of both strains were found to be equivalent in 24HPI PCLS (Figure 63). Meanwhile, the low numbers of replication events in 24HPI PCLS prevented the growth dynamics of both strains over 24 hours of *ex vivo* culture could not be compared. However, this does provide evidence that initial fungal clearance in the lungs of mice infected with *C. neoformans* is likely not the result of macrophages, despite their abundance within the lungs.

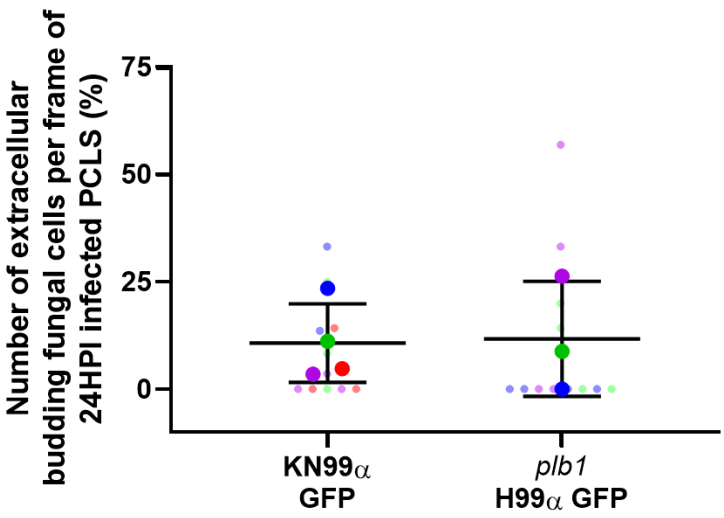

Figure 63 – The proportion of extracellular *plb1* H99α GFP and KN99α GFP *C. neoformans* cells that replicate in 24HPI PCLS over 24 hours *ex vivo* are equivalent. The proportion of extracellular cells in 24HPI PCLS that replicated over 24 hours *ex vivo* was the same with *plb1* H99α GFP and KN99α GFP infection (Mann-Whitney U=5, p=0.8571). Replicating proportions of *C. neoformans* were compared using a Mann-Whitney U test. Data presented as mean ± SD. Each larger point represents the mean of a different animal (n≥3), while each smaller point represents a different PCLS frame.

6.3 – Discussion

Here, I present the first reported PCLS model of cryptococcosis and use it to examine pulmonary host-pathogen interactions that occur in the first 24 hours of intranasal *C. neoformans* infection in mice (Sanderson, 2011). By combining both traditional *in vivo* and novel *ex vivo* approaches, I show that pulmonary burdens of *C. neoformans* remain unchanged in the first 24 hours of infection – this provides important evidence that there are equal rates of fungal replication and fungal clearance during this time. Therefore, understanding these processes may provide novel targets for immunotherapy. However, imaging of infected PCLS revealed that the initial response is AM centric, although the response of these cells to *C. neoformans* appears to be insufficient (Rudman, Evans and Johnston, 2019). This insufficiency was determined by limited AM phagocytosis of fungal cells at foci of infection and equal rates of fungal replication extracellularly and intracellularly – indicating negligible antimicrobial activity. While fungal cell size was a significant factor in the phagocytosis of *C. neoformans* by AMs, controversially it was observed that opsonising *C. neoformans* with the well characterised 18B7 IgG antibody *in vivo* did not enhance phagocytosis at early time points of infection (Casadevall *et al.*, 1998). The PCLS model also enabled *C. neoformans* replication within pulmonary macrophages to be observed in live lung tissue for the first time *ex vivo*. Additionally, the

PCLS model revealed that other myeloid cell types are not recruited to foci of infection in significant numbers during initial infection. There was also evidence of early titan cell formation in the first 24 hours of pulmonary infection. Finally, pulmonary infection with the avirulent *plb1* H99α GFP strain of *C. neoformans* resulted in lower burdens and fewer fungal cells at foci of infection. However, fungal cells of this avirulent strain was found to be significantly larger within PCLS and completely resistant to phagocytosis in the first 24 hours of infection. Combined, this suggests that initial clearance of *C. neoformans* from the lung during initial infection is likely not mediated by AMs, but rather is the result of either immune cells not investigated during this study or non-cellular antifungal mechanisms.

6.3.1 – The utility of the PCLS model

The most important impact of this work is the successful showcasing of the utility of the PCLS model to study pulmonary infection. The biggest advantage of the PCLS model is that it greatly increases the number and types of experimental measures possible during *in vivo* studies, while reducing the need to subject animals to procedures. The preparation of PCLS is a relatively simple methodology compared to intravital imaging methods, associated with lower initial costs and fewer requirements for expertise. This means it is possible for most laboratories to adopt this technique – important for reducing animal use. Furthermore, PCLS are easy to maintain and have been reported to remain viable for up to 7 days, allowing for long term investigation (Sanderson, 2011). In addition, the PCLS model is highly flexible and can be modified for purpose – although this study focussed on high-resolution time-lapse imaging, PCLS can be combined with other techniques such as –omics (Niehof *et al.*, 2017) and high throughput screening (Hess *et al.*, 2016). Because multiple slices can be obtained from the same animal, PCLS can be assessed in multiple ways in the same experiment. The PCLS model is also not just exclusive for modelling cryptococcosis – PCLS are compatible with any number of pulmonary pathogens that are suitable to be inoculated into mice (Danov *et al.*, 2019; Molina-Torres *et al.*, 2020). The premise of PCLS is also not restricted to the lungs, with the basic methodology of PCLS able to be expanded out to different organs such as the liver (Paish *et al.*, 2019) and the brain (Rosenfeld *et al.*, 2017).

Despite numerous advantages, there are limitations to the PCLS model. Although most physiological processes are preserved in PCLS *ex vivo*, such as immunity and airway contraction (Bergner *et al.*, 2006), both blood flow and respiratory cyclic stretch are absent (Sanderson, 2011). This may limit the phenomena that PCLS are appropriate for modelling. These may also greatly affect studies of infectious disease. In the case of *C. neoformans*, both dissemination of fungal cells out of the lung and the extravasation of

circulating immune cells into the lung cannot be studied using PCLS alone. Instead, observations in PCLS can be correlated with traditional *in vivo* measures and/or short-term intravital imaging. Finally, it also important to note that the additional recruitment of immune cells cannot occur in PCLS once slices have been prepared. While this prevents single PCLS being used to study the development of immune responses over time, this may be of benefit when interrogating immune responses at specific time points – providing a snapshot of the live immune response at that time point.

6.3.2 – *C. neoformans* infection of PCLS reveals growth of foci of infection over 24 hours *in vivo* and is likely host mediated

In this study, the PCLS model was used to characterise the initial cellular immune response to *C. neoformans* infection. This time point was chosen as clinical data surrounding *C. neoformans* cell inhalation is limited.

First and foremost, there was no change in pulmonary fungal burdens observed at 0 and 24HPI. This lack of a change in fungal burden is a controversial observation – a previous *in vivo* study of *C. gattii* infection observed that mice inoculated with 10^7 cfu by intratracheal instillation had pulmonary fungal burdens 100 fold lower 24 hours later (Carvalho Costa *et al.*, 2016). However, it is important to note that in this study the pulmonary fungal burden at 0hpi was not determined. Even though intratracheal instillation is the most direct route of inoculation, it is possible that dosing efficiency was lower than anticipated – either the whole inocula was not retained within the lung, inocula had lower viability than expected or clearance in the lungs of mice is fungal burden dependent. However, this does highlight the importance of determining inoculation efficiency, so that subsequent changes in fungal burden can be appropriately attributed to either biological mechanisms or artefacts of the experimental procedure.

Aside from fungal burdens, the size of infection foci in the lungs of mice could also be examined with the PCLS model. The size of infection foci was observed to increase between 0HPI and 24HPI with KN99α GFP infection, suggesting fungal cells replicated. Interestingly, however, larger foci were also observed with 6μm beads. This suggests that focal growth is not the result of fungal replication. Instead, it implies that inhaled *C. neoformans* cells are initially quiescent. Paradoxically though, this also means that there is no significant fungal clearance, although the larger foci of infection observed in 24HPI PCLS are the result of host activity, as neither beads of *C. neoformans* cells are known to be motile. This therefore implies that inhaled particles may have been taken up by immune cells between 0HPI and 24HPI *in vivo*, and deposited together to intentionally create larger foci of infection. However, the mechanism by which this may have occurred remains unknown.

AMs were the most abundant cells in 0HPI PCLS, and therefore would be assumed to be responsible for this transport of inhaled particles. Additionally, clustering of macrophages may be evidence of this, bringing phagocytosed fungal cells together. However, in 24HPI PCLS, even when cultured *ex vivo* for 24 hours, AMs were not observed to be motile. Additionally, limited phagocytosis by AMs was observed. It is possible that AMs phagocytosed and migrated to create larger foci of infection between 0HPI and 24HPI. It is also then possible that many phagocytosed *C. neoformans* cells then were able to escape from phagocytic AMs via vomocytosis – explaining the low intracellular fungal burden observed in 24HPI PCLS. To determine if this was the case, PCLS would need to be prepared at various time points between 0 and 24HPI to examine whether the increase in *C. neoformans* cells at foci of infection preceded macrophage clustering, or vice versa. Additionally, mice should be treated with a known inhibitor of vomocytosis, such as the Arp2/3 activator jasplakinolide (Johnston and May, 2010), to determine whether this increased the number of phagocytosed *C. neoformans* cells observed in 24HPI PCLS.

If this behaviour was not AM mediated, it may have been that this was mediated by other innate immune cells. However, low number of neutrophils, MDMs and DCs were observed, and none of these cell types were observed to be in proximity to inhaled beads or *C. neoformans*. One potential explanation is that this was mediated by neutrophils between 0 and 24HPI. Neutrophils are highly motile cells (de Oliveira, Rosowski and Huttenlocher, 2016) yet are also relatively short lived (Hidalgo *et al.*, 2019). This may have meant that there was an initial neutrophil response between 0HPI and 24HPI, where these cells mediated focal growth through phagocytosis and migration, followed by efferocytosis by AMs which resolved prior to the preparation of 24HPI PCLS (Herold, Mayer and Lohmeyer, 2011). However, as neutrophil disorders are not associated with incidences of cryptococcosis (Gibson and Johnston, 2015), it suggests that this process is not an important determinant of host outcomes, if this is the case.

Regardless of the mechanism, the purpose of focal growth is also an interesting host mechanism. It is possible that this is the earliest stage of granuloma formation – immune structures consisting of macrophages and lymphocytes that serve to contain pathogens, restrict dissemination and increase the concentration of antimicrobial mediators within an area (Ulrichs and Kaufmann, 2006; Farnoud *et al.*, 2015). Therefore, although higher numbers of fungal cells in a given area may be indicative of disease progression, this may be the early stages of a protective response by the host, with an aim to increase antifungal activity.

However, additional study of this phenomenon is required – PCLS would need to be prepared at later time points of infection (7dpi, 14dpi) to confirm whether granuloma

formation occurs and confirm their host protective role. Additionally, earlier time points should also be investigated to examine focal growth. The effects of inhibiting both AM and neutrophil chemotaxis, as well as ablating AMs and neutrophil numbers, on 24HPI PCLS and foci of infection should also be determined – in both incidences, smaller foci of infection would be anticipated as a result. It is important to note that inhibiting macrophage chemotaxis is likely difficult, as the specific signal responsible for this movement, if it occurs, is unknown.

6.3.3 – The role of macrophages in the early immune response to *C. neoformans* in the lung of mice

The macrophage-centric response to *C. neoformans* observed in the PCLS model has long been hypothesised, based on multiple clinical observations in late stage cryptococcosis patients (Wang *et al.*, 2014), increased mortality observed *in vivo* when macrophages are ablated (Osterholzer, Milam, *et al.*, 2009) and the association of macrophages with clearance in various experimental systems (Bojarczuk *et al.*, 2016). Here, I present the first visual evidence that macrophages are the most abundant immune cells in the initial pulmonary immune response to *C. neoformans* infection in live tissue. However, I also present evidence of macrophage insufficiency in this period.

The ineffective nature of macrophages observed in this model is not a new idea – there is mounting evidence that macrophages can be inadvertent allies to *C. neoformans* (Alvarez *et al.*, 2009; Charlier *et al.*, 2009; Sabiiti *et al.*, 2014; Rudman, Evans and Johnston, 2019). The most highly documented potential pathological role for macrophages is in cryptococcal meningitis, where macrophages are hypothesised to be important mediators of Trojan Horse dissemination of *C. neoformans* cells into the CNS (Santiago-Tirado *et al.*, 2017). In the case of early infection, however, macrophages may inadvertently provide an intracellular niche that 'shelters' phagocytosed cryptococci from more potent fungicidal mechanisms such as more fungicidal immune cells, extracellular mediators or antifungal therapy. In the case of initial colonisation of the lung, this might be particularly significant for colonising the lung before *C. neoformans* cells can form protective biofilms – which take 48 hours to form *in vitro* (Martinez and Casadevall, 2007) – or before high densities of cryptococcal cells can be established to dilute the antifungal activity of any extracellular mediators present in lung between 0HPI and 24HPI. Observing this for the first time *ex vivo* within live lung tissue provides further evidence that intracellular survival within macrophages is probably important for human infection too.

Although *C. neoformans* adaptation to the macrophage intracellular environment was observed in infected PCLS, there was no evidence of macrophage fungicidal/static

activity. It is also worth noting that macrophage killing of *C. neoformans* has yet to be reliably observed *in vitro,* despite having been reported in previous *in vitro* and *in vivo* studies (Wager *et al.*, 2015; Bojarczuk *et al.*, 2016). Many *in vitro* studies that have previously reported that macrophages can kill *C. neoformans in vitro* have relied on lysing infected macrophages and plating surviving intracellular *C. neoformans* cells to determine changes in cfu counts (Flesch, Schwamberger and Kaufmann, 1989; Wager *et al.*, 2015; De Leon-Rodriguez, Rossi, *et al.*, 2018). However, these studies aren't compatible with repeated sampling of the same infected macrophages and can be confounded by other host-pathogen interactions that can influence intracellular fungal cell numbers, such as vomocytosis. Macrophage antifungal activity has also been assessed by live imaging of macrophages, although in these studies only reductions in intracellular fungal replication are observed, rather than fungal cell killing (Voelz, Lammas and May, 2009). However, these studies are also limited as the fluorophores typically utilised to visualise *C. neoformans* cells (GFP, calcofluor white) all of which don't report cryptococcal cell viability. Therefore, in the absence of a suitable live/dead stain for *C. neoformans* compatible with live imaging, the antifungal activity of macrophages has still yet to be properly described *in vitro*.

Another possibility is that by only imaging fields of view that contained *C. neoformans* cells, only macrophages with low antifungal activity were observed. A previous study examining the murine pulmonary immune response to *C. neoformans* in the first 48 hours of infection identified two distinct populations of AMs: Those positive for CXCL2, and those not (Xu-Vanpala *et al.*, 2020). These two populations were observed to have differential gene expression patterns and antifungal activity, with $CXCL2^{+}$ AMs also observed to have a greater phagocytic capacity and a more M1-like phenotype. It is therefore possible that only $CXCL2^{-}$ AMs were imaged during this study, which were previously observed to account for ~50% of all observable AMs. Therefore, in the future examining CXCL2 status in PCLS AMs using transgenic mice may correlate the non-responding phenotype to this population of AMs.

There are other explanations for the lack of antifungal activity observed in this model. One reason may have been that AMs only show significant antifungal activity later in infection, after adaptive immune cells (Th cells) and adaptive cytokines are present to augment AM antimicrobial activity (Huffnagle *et al.*, 1994; Abe *et al.*, 2000; Arora *et al.*, 2005; Voelz, Lammas and May, 2009). Alternatively, it is possible that macrophage antifungal activity was inadvertently perturbed by the PCLS methodology. One antimicrobial mechanism utilised by macrophages is nutrient restriction to 'starve' phagocytosed pathogens within the phagolysosome (Uribe-Quero and Rosales, 2017). However, PCLS were maintained in a relatively glucose rich media (low-glucose DMEM),

which may have prevented the low nutrient phagolysosome from being maintained (Watkins, King and Johnston, 2017). Additional work is therefore needed to characterise macrophage function within PCLS to confirm whether their function is preserved and in what contexts the model is appropriate to study cryptococcosis host-pathogen interactions. Finally, it may also be that AMs in early infection are not primarily antifungal effectors, but rather supportive cells through antigen presentation and leukocyte recruitment (Vecchiarelli *et al.*, 1994). Again, characterising the immune response in PCLS at additional time points will be important to better understand the role of macrophages during initial pulmonary infection.

It is also important to note that differentiating between infiltrating and resident macrophages is notoriously difficult (Hashimoto *et al.*, 2013). Although several studies have suggested surface markers that differentiate the two, there is still a level of uncertainty with these approaches. Therefore, in future PCLS studies, our immunofluorescence approach should be supplemented with alternative methodologies, such as lineage mapping, single cell RNA sequencing and flow cytometric analysis, so that cell populations can be identified with a greater level of confidence (Misharin *et al.*, 2013; Lyons-Cohen *et al.*, 2017).

6.3.4 – Phagocytosis of *C. neoformans* is rare and not enhanced with anti-capsular IgG

An important finding of this study regarding macrophages was that the phagocytosis of *C. neoformans* cells in PCLS immediately following inoculation was completely absent, and only occurred at low levels in 24HPI PCLS. This was shown not to be an artefact of the PCLS methodology, as the *ex vivo* instillation of 1µm beads was confirmed to result in high levels of rapid phagocytosis. The limited phagocytosis of *C. neoformans* by macrophages has been previously observed *in vitro* (Mukherjee, Feldmesser and Casadevall, 1996). However, this study is the first to observe a relationship between fungal cell size and phagocytosis in live lung tissue.

Another important observation was that phagocytosis of 6µm beads and *C. neoformans* was not observed *ex vivo* in the PCLS model. However, *ex vivo* phagocytosis was observed with 1µm beads. Therefore, this suggests that one of the factors preventing the occurrence of phagocytosis in the PCLS model is the size of the target size. Mechanistically, this could be explained by the presence of the agarose gel in PCLS. By surrounding immune cells with a gel, this would create an additional force pressing against leukocyte membrane, meaning a greater force would need to generated for successful phagocytosis. With larger targets, an even larger force is required, so the presence of the agarose may have raised the threshold force required for successful

phagocytosis to a value too high for phagocytosis to occur (Jaumouillé and Waterman, 2020). Alternatively, the gel may have provided a physical obstruction of antigenic components of cells and bead, reducing receptor engagement and reducing successful phagocytosis.

The relationship between size and phagocytosis has been previously suggested based on *in vitro* bead studies (Champion, Walker and Mitragotri, 2008). Additionally, *C. neoformans* cell geometry is known to be an important factor that can limit phagocytosis (Johnston and May, 2013; Bojarczuk *et al.*, 2016). In this PCLS study, significant differences in the size of intracellular and extracellular *C. neoformans* cells was found in 24HPI. However, it cannot be concluded from this study alone whether the smaller size of intracellular fungal cells made cells more susceptible to phagocytosis, or the growth of these cells was the result of having been phagocytosed. Phagocytosed *C. neoformans* cells have been observed to increase their production of capsule in response to conditions within the macrophage phagolysosome (Bahn *et al.*, 2006), suggesting that phagocytosis would induce significantly more growth. However, capsular GXM is also known to be released into the phagolysosome, potentially to scavenge RONS within the environment or to buffer phagolysosomal pH (De Leon-Rodriguez, Fu, *et al.*, 2018). The cost of this may be less capsular associated GXM, which may have also reduced the size of intracellular cells. Therefore, fungal cell size should be assessed at various times post infection to better understand this relationship.

It should also be noted that the majority of cryptococci in PCLS, extracellular or intracellular, were 3-6μm in diameter. Therefore, the significant difference in size may be the result of the positively skewed cell size distribution – with a subset of extracellular cells significantly greater than 10μm in diameter. As this behaviour only occurred in extracellular cells in PCLS, this may have led to the false assumption that extracellular cells on average were larger, when instead cells were typically of the same size except for a few larger outlier cells that were only observed in the extracellular compartment.

However, it is worth noting that the proportion of *C. neoformans* cells in 24HPI PCLS that fit the size criteria to be classed as titan cells (~4%) is much lower than are generated using the *in vitro* protocol, and is observed in the lungs of mice at 7 and 14dpi (~50%; Dambuza et al., 2018; García-Barbazán et al., 2016). Additionally, it cannot be confirmed that cells >10μm in diameter were actually titan cells, as the this study did not determine the capsule:cell body ratio of cells, nor whether cells were polyploid. Regardless, this increased *C. neoformans* cell size is likely to be an important mechanism by which *C. neoformans* resists phagocytosis To determine the significance of this phenotypic shift early in infection, mice should be infected with titan cells generated *in vitro*, and PCLS

should be prepared so that the significance of this morphology during early infection can be determined (Dambuza *et al.*, 2018).

Another controversial observation was that the well characterised 18B7 IgG antibody opsonin did not enhance phagocytosis in PCLS (Casadevall *et al.*, 1998). Many *in vitro* studies have observed that opsonising *C. neoformans* with the 18B7 antibody robustly increases phagocytosis by macrophages *in vitro*. This is supported by *in vivo* observations in other mouse models and has even led to clinical trials of 18B7 (Casadevall *et al.*, 1998). However, a potential explanation of this lack of efficacy of 18B7 during early infection may be the density of AMs in the lungs of mice prior to infection. *In vitro* studies of macrophage-*Cryptococcus* interactions typically employ a high density of macrophages for *in vitro* assays (Voelz *et al.*, 2010), guaranteeing interactions between cryptococci and macrophages. Therefore, opsonising fungal cells with the 18B7 antibody increases the chance of an interaction resulting in phagocytosis, which translates into increased phagocytosis. However, in the lung where the density of AMs is low (less than one macrophage per alveolus), although an interaction between an AM and an opsonised fungal cell is more likely to result in phagocytosis, these interactions are too rare at early time points of infection for this to translate into significant increases in phagocytosis. This would explain why other *in vivo* studies have found significant effects of this opsonin, which typically have looked later in infection, where the density of immune cells is higher (Casadevall *et al.*, 1998). This may mean that the 18B7 antibody only influences host immune responses late in infection when greater numbers of immune cells have been recruited.

Alternatively, macrophage expression of the Fc receptor early in infection may be low – the receptor that recognises IgG opsonin. However, previous studies have observed relatively high Fc receptor expression by pulmonary macrophages (Berger *et al.*, 1994). Instead, it is possible that *C. neoformans* manipulates expression of the Fc receptor, as is reported to occur in the case of other infections (Hunegnaw *et al.*, 2019). In the case of cryptococcosis, Fc receptor signalling may be inhibited by both exogenous GXM competitively binding to the Fc receptor, or through rearrangement of capsular GXM to obscure the Fc region of bound IgG molecules (Netski and Kozel, 2002). To explore this further, AM Fc receptor expression should be assessed through either RNAseq or immunofluorescence. Furthermore, a different opsonin such as complement should be used as a comparator to see if the lack of enhanced phagocytosis was opsonin specific (Zaragoza, Taborda and Casadevall, 2003). However, this study does emphasise the issues with exclusively modelling phenomena *in vitro*, which do not always recapitulate the *in vivo*/*ex vivo* environment.

6.3.5 – The lack of a role of recruited myeloid cells in the initial pulmonary immune response to *C. neoformans* infection

It was also observed at these early time points of infection that there was a lack of infiltrating leukocytes observed in 0HPI and 24HPI PCLS – suggesting that these cells do not mediate early control and clearance of *C. neoformans* from the lung that may have occurred in this model.

The lack of neutrophilic infiltration is not unexpected, as there are no known clinical associations between incidences of cryptococcosis and neutropenic disorders (Gibson and Johnston, 2015), although previous studies have identified a peak in pulmonary neutrophils in response to *C. neoformans* infection at 24hpi (Xu-Vanpala *et al.*, 2020). However, this was in response to an inoculum 100 times greater, and therefore may have crossed an immunogenic threshold that resulted in greater neutrophil recruitment into the lungs. However, DCs are resident in the lung and are reported to have cryptocidal activity (Wozniak and Levitz, 2008; Nelson, Hawkins and Wozniak, 2020), making their minimal appearance in early pulmonary responses to cryptococcosis in the PCLS model surprising. In the case of MDMs, although significant numbers of these cells were observed, none of these cells were found proximal to *C. neoformans* cells, despite the association of macrophages with cryptococcosis. Previous *in vivo* studies have observed that MDM cell numbers peak at 3 days post infection in mouse models of cryptococcosis, which may explain the variable numbers of MDMs observed in 24HPI PCLS, and suggest that these cells play a significant role later in infection (Heung and Hohl, 2019). It is also possible that there may have been recruitment and subsequently resolution of myeloid cell recruitment between 0 and 24HPI. Therefore, characterising immune responses in PCLS prepared between these two time points is required to establish a more comprehensive timeline of the sequence of events that occurs during the mouse pulmonary immune response to *C. neoformans*.

6.3.6 – Potential non-cellular mechanisms of immunity yet to be investigated in PCLS

Even though there was no evidence of cell-mediated killing of *C. neoformans* within PCLS, there may be a non-cellular mechanisms of antifungal activity. Lung surfactant – the protein rich solution that primarily functions to maintain surface tension within the lungs – although components of this solution are also observed to have antimicrobial activity (Schelenz *et al.*, 1995; Holmer *et al.*, 2014). However, the antifungal activity of these components is not clear with regard to *C. neoformans* infection. Both SP-A and SP-D have been reported to significantly affect pulmonary immunity to *C. neoformans*. However, although both SP-A and SP-D are reported to bind to capsular *Cryptococcus*

(Schelenz *et al.*, 1995), the result of this binding appears to be largely detrimental for host outcomes. Specifically, SP-A is reported to negate the opsonising effect of IgG, which may have contributed to the lack of an effect with 18B7 IgG opsonised samples in 24HPI PCLS (Giles *et al.*, 2007). SP-D meanwhile is reported to protect phagocytosed *C. neoformans* fungal cells from macrophage ROS (Gross *et al.*, 1998; Van De Wetering *et al.*, 2004) – this protective effect may have contributed to the high rates of intracellular replication and survival that were observed in PCLS. Combined, this suggests that while SP-A and SP-D likely do not mediate any significantly early clearance of *Cryptococcus*, they may contribute significantly to the virulence of early *Cryptococcus* infection. This is supported by *in vivo* studies in transgenic mice that do not express SP-D, which show increased survival compared to wild-type animals when infected with *C. neoformans* (Geunes-Boyer *et al.*, 2012). However, in the PCLS model, it has yet to be confirmed whether surfactant is still present in mice – both the cessation of respiration and the instilling of agarose may have perturbed this system. However, the potential significance of these components means that establishing their presence in PCLS is important for future cryptococcosis modelling.

The other non-cellular mechanism that was not investigated during these experiments was the complement system. As described previously, the complement system has multiple roles in immunity to infection, including opsonising pathogens and directly antimicrobial functions (see 1.4.1.1.2, Ehlenberger and Nussenzweig, 1977; Guo and Ward, 2005; Tegla et al., 2011). In the context of cryptococcosis, there is evidence that this system is critical for host protection, with the alternative complement pathway known to be activated by *Cryptococcus in vitro* (Kozel, Wilson and Murphy, 1991; Young and Kozel, 1993) and genetic ablation of C5 observed to greatly increase mouse mortality that results from experimental cryptococcosis (Dromer *et al.*, 1989). In particular, C5 is associated with formation of the membrane attack complex, a pore forming structure that binds to pathogens and results in the leakage of cytoplasmic contents and eventual cell death. In the context of the initial immune response, this complex may be critical for early fungal clearance and may also have been perturbed by the PCLS methodology. Therefore, complement signalling within PCLS needs to be confirmed, as does the inherent susceptibility of *C. neoformans* to the membrane attack complex *in vitro* and *in vivo*.

6.3.7 – *plb1* H99α GFP cells may be better at resisting macrophage phagocytosis in 24HPI PCLS despite being avirulent *in vivo*

plb1 H99α mutant strains have been studied for many years due to the multifaceted role of *plb1* as a virulence factor in *Cryptococcus*. Features of *C. neoformans* cells in the

absence of *plb1* include larger cells (Evans *et al.*, 2015), an inability to replicate within macrophages (Evans *et al.*, 2015) and no dissemination to the CNS in mouse infection models (Noverr *et al.*, 2003). In these experiments where early lung infection with *plb1* H99α GFP was examined using PCLS, fungal burdens and foci of infection were observed to be same. However, no phagocytosed *plb1* H99α GFP cells were observed in PCLS prepared at either 0HPI or 24HPI. This provides further evidence that any early fungal clearance of *C. neoformans* in the first 24 hours of infection is likely not to have been the result of macrophage activity. However, it is also possible that there was phagocytosis of *plb1* H99α GFP cells prior to 24HPI, and that these cells were cleared prior to imaging at 24HPI, with foci of infection may have started to resolve prior to 24HPI.

Additionally, the significantly larger size of *plb1* H99α GFP cells was confirmed in PCLS (Trevijano-Contador *et al.*, 2018). Having established a significant relationship between fungal cell size and phagocytosis with KN99α GFP infection in PCLS, the increased size of *plb1* H99α GFP cells strain may have contributed to the lack of phagocytosis. However, this strain is also reported not to disseminate to the CNS in mouse models of infection (Noverr *et al.*, 2003). Therefore, this may provide indirect evidence of a pathological role for macrophages in cryptococcal dissemination, as a strain of *C. neoformans* that is significantly larger is not taken up as well during initial infection by macrophages, and may therefore be less able to disseminate by Trojan horse mechanisms. Taken together, these studies suggest that resisting phagocytosis and evading immune responses is actually detrimental for cryptococcal dissemination, and highlights that the macrophage intracellular niche may be important for the pathology of *C. neoformans* infection. To confirm this, PCLS prepared at later time points of *plb1* H99α GFP infection need to be examined, with phagocytosis and macrophage responses in these PCLS correlated with fungal burdens in the brain and lungs.

To conclude, this study provides the first visual account of the initial pulmonary immune response to the opportunistic pathogen *C. neoformans* in live mammalian lung tissue. During the first 24 hours of infection, AMs were identified to be the major cell type present at foci of infection in PCLS, although the response of these cells appeared to be insufficient to clear or control infection. The PCLS model also reveals that fungal cells increase their size during early infection, and provides the first recorded proof of intracellular *C. neoformans* replication within lung tissue. As a result, I believe this approach is highly tractable and should be widely adopted in future studies of pulmonary infection and immunity, as well as used to better understand immunity to cryptococcosis.

Chapter 7 – Final Discussion

7.1 – Findings of the thesis

In this thesis, I have used *in vitro, in vivo* and *ex vivo* models to study the pulmonary immune response to inhaled *C. neoformans*. Specifically, using a well characterised J774 cell *in vitro* model of infection, I demonstrated that IFNγ treatment significantly worsened macrophage handling of *C. neoformans* infection, while IL-1β appeared to have little to no role. I then established a mouse model of intranasal *C. neoformans* infection, using this model to confirm that a transgenic GFP expressing strain of *C. gattii* was avirulent in mammals, indicating that this phenotype likely is important for human infection. Having established this mouse model, I then used it to challenge the notion that IFNγ is always beneficial in the context of cryptococcosis. Instead, I observed increased mouse mortality in response to IFNγ at the time of infection, with transgenic ablation of IL-1β found to be largely insignificant with regard to host outcomes. Finally, to overcome limitations associated with mouse models of infection, I developed a novel PCLS model of cryptococcosis, that enables host-pathogen interactions to be visualised in live mammalian lung tissue. This model was then used to characterise the initial immune response to *C. neoformans*, where it was observed that although fungal burdens remain constant, there is host-mediated growth of foci of infection and an insufficiency in the response of macrophages to *C. neoformans* infection. Below, these key findings and their potential impact are discussed.

7.1.1 – IFNγ as an immunotherapy for cryptococcosis patients

Widespread antimicrobial resistance (Aslam *et al.*, 2018) and increasing numbers of patients receiving chronic immunosuppressive therapy (Lerner, Jeremias and Matthias, 2015) means that there is a desperate need for alternative treatments for infection. One possible approach to treatment is immunotherapy – enhancing the patient immune system to better control and clear infections. This is particularly attractive to researchers in the case of opportunistic infections, as incidences of these diseases are associated with compromised immunity and/or immune dysfunction. Additionally, because the immune system employs multiple antimicrobial mechanisms in response to pathogens, resistance should be less likely or slower to develop to these therapies. The rationale is that pathogens would be required to adapt to multiple antimicrobial pathways at once, greatly reducing the emergence of resistance in the case of immune augmentation. However, this multifaceted nature of the immune system also makes target selection and therapeutic design extremely complex, as manipulating any immunological pathway will

have a multitude of different effects that range from autoimmunity to susceptibility to other infections. Additionally, 'ideal' immune responses are pathogen specific. Therefore, a thorough understanding of the host-pathogen interactions of a pathogen are first required so that the specific elements of the immune system critical for clearance can be targeted while allowing for side effects to be predicted and/or avoided.

In the case of cryptococcosis, incidences and deaths due to this infection are actually estimated to have decreased in the past 10 years (Park *et al.*, 2009; Rajasingham *et al.*, 2017). However, this is thought to be the result of improved management of HIV/AIDS – increasing the availability of highly active antiretroviral therapy resulting in a smaller population that are susceptible to cryptococcosis. Therefore, even though fewer cryptococcosis deaths are reported, the case fatality rate in cryptococcosis has remained consistent. Even in the most developed regions of the world, mortality rates due to cryptococcal meningitis remain as high as 40-60%.

This statistic highlights that the current 'gold standard' therapies are plagued with issues – limited availability (Miot *et al.*, 2021), high levels of resistance (Stone *et al.*, 2019) and toxicity (Meiring *et al.*, 2016). Combined with the fact that no new therapies indicated for cryptococcosis have been approved since the 1990s, and cryptococcosis has a global distribution, the development of new therapies is very much needed (Santos-Gandelman *et al.*, 2019). However, host-pathogen interactions in cryptococcosis are both unique and complex, and include parasitising macrophages (Bojarczuk *et al.*, 2016), significant changes in fungal cell size (Dambuza *et al.*, 2018), vomocytosis (Smith, Dixon and May, 2015) and the ability to utilise host immune cells to cross the blood brain barrier (Santiago-Tirado *et al.*, 2017). Additionally, clinically cryptococcosis has been observed to affect multiple physiological systems. Combined, this means that immunity to cryptococcosis is still poorly understood and identifying potential targets for augmentation is difficult (Maziarz and Perfect, 2016).

That said, it is well-established that there is a correlation between incidences of cryptococcosis and uncontrolled HIV/AIDS. This means that $CD4^+$ T cells have received extensive attention with regard to immunotherapy – specifically the cytokine IFNγ as its production is highly associated with $CD4^+$ T cells (Yoshimoto *et al.*, 1998). Therefore, IFNγ treatment has been observed to improve outcomes for *C. neoformans* infected mice (Wormley *et al.*, 2007). Most significantly, however, IFNγ treatment reduced patient fungal burdens when two doses of IFNγ were given adjunctive to gold standard antifungal therapy in a small clinical trial of HIV positive cryptococcal meningitis patients (Jarvis *et al.*, 2012).

Despite this success, however, progress into the clinic has been limited at the time of writing (Spadari *et al.*, 2020) – most likely as the mechanism by which IFNγ mediates improved host outcomes is still not clear. There is, however, strong evidence that the protective effects of IFNγ are at least partially dependent on enhanced macrophage antifungal activity (Leopold Wager *et al.*, 2018). As macrophages feature throughout the immune response to cryptococcosis, understanding the specific contributions of IFNγ to the antifungal activity of these cells is critical for it to be utilised as a mainstay therapy. Therefore, our lab has previously investigated both macrophage immunity and IFNγ in the context of a zebrafish embryo model of localised infection (Kamuyango, 2017). In this model, it was also observed that a single dose of IFNγ administered at the time of infection also improved host outcomes. This enhanced protection was dependent on macrophages, which exhibited increased fungistatic activity in response to IFNγ treatment. In addition to improved host outcomes, elevated IL-1β was also observed in infected zebrafish treated with IFNγ. While the significance of this signal was not determined, it is possible that IL-1β is a an important effector of IFNγ mediated host protection, particularly as IL-1β action is closely associated with pro-inflammatory macrophages (Qiao *et al.*, 2013). Therefore, I investigated the significance of both IFNγ treatment and IL-1β in the context of mammalian models of cryptococcosis. Initially, I examined the effect of these cytokines on macrophage host-pathogen interactions *in vitro* using the J774 cell model, so that the macrophage specific effects of treatments could be determined. However, treatment of these cells with IFNγ, IL-1β or a combination of both either had no effect or worsened macrophage handling of *C. neoformans* infection *in vitro*. This result was controversial, particularly as IFNγ treatment has been previously observed to improve macrophage handling of *C. neoformans* (Mukherjee, Feldmesser and Casadevall, 1996; Voelz, Lammas and May, 2009).

Therefore, I examined the contribution of IFNγ treatment and IL-1β again, this time using an *in vivo* model, in case the *in vitro* results observed were specific to the J774 cell model. Again, however, a single dose of IFNγ at the time of infection did not improve mouse survival due to intranasal *C. neoformans* infection, nor reduce fungal burdens in the lungs and brain. More strikingly, when IFNγ treatment was given continuously via infection with a transgenic strain of *C. neoformans* that constitutively produces murine IFNγ, H99α IFNγ infection resulted in animals reaching humane endpoints twice as fast as wild-type controls.

Combined, this suggests that treatment with IFNγ alone is actually detrimental to the host. As described before, however, there are numerous studies that have recorded benefits with IFNγ treatment in multiple model systems. Aside from the previous clinical trial of IFNγ (Jarvis *et al.*, 2012) and previous *in vivo* studies with H99α IFNγ (Wormley

et al., 2007; Castro-Lopez *et al.*, 2018), there are a plethora of *in vitro* studies that have identified specific effects of IFNγ on macrophages that skew macrophages towards a pro-inflammatory phenotype which is associated with *C. neoformans* clearance. These includes increased expression of iNOS (MacMicking, Xie and Nathan, 1997), $gp67^{phox}$ (Gupta *et al.*, 1992), $gp91^{phox}$ (Cassatella *et al.*, 1990), FcRγI (Erbe *et al.*, 1990), C2 (Strunk *et al.*, 1985), C4 (Vincent *et al.*, 1993), complement receptor 3 (Drevets, Leenen and Campbell, 1996), TNFα receptor (Tsujimoto, Yip and Vilcek, 1986), caspase 1 (Chin *et al.*, 1997) and NF-κB (De Wit *et al.*, 1996). Even in the survival studies presented here, CNS fungal burdens of H99α IFNγ were lower than with wild type *C. neoformans* infection, indicative of improved fungal clearance – although this may simply be the product of fungal cells having less time to replicate before animals had to be culled.

Despite this overwhelming majority of studies observing a benefit with IFNγ treatment in the context of cryptococcosis, there are also studies that have suggested potentially detrimental or dangerous side effects with IFNγ. As was concluded here, and previously postulated, *in vivo* observations show that while high levels of IFNγ and IFNγ-producing immune cells are associated with fungal clearance, they are also associated with dangerous levels of neuroinflammation that reduce animal survival (Eschke *et al.*, 2015; Neal *et al.*, 2017). Additionally, other *in vitro* studies have also found that IFNγ treatment alone is not sufficient to significantly reduce the replication of intracellular *C. neoformans* cells within macrophages (Voelz, Lammas and May, 2009). Together, this suggests that in certain scenarios IFNγ therapy alone may not be sufficient to improve host outcomes – giving birth to the idea of the double edged sword of IFNγ. Although IFNγ can improve fungal clearance and host outcomes, this sometimes is not enough for sufficient antifungal activity, resulting in no benefit as well as the associated inflammation – which may accelerate mortality.

Therefore, this thesis helps to identify situations in which IFNγ treatment alone may benefit patients, and when additional antifungal therapy is required. As IFNγ treatment alone in mice has improved host survival in low inocula infection models (Wormley *et al.*, 2007; Kamuyango, 2017; Castro-Lopez *et al.*, 2018), my work reveals that the same benefit to the host with early IFNγ monotherapy is not observed in the context of high burden *C. neoformans* pulmonary infection. This is particularly important, as with recent improvements in diagnostics, it may be that that screening programs for at-risk populations for cryptococcosis may soon be viable (Rajasingham *et al.*, 2019) and patients may be diagnosed prior to the onset of cryptococcal meningitis. If IFNγ treatment alone was appropriate, this could be a suitable first line therapy that would not require hospitalisation – as is required with antifungal therapy currently. This would reduce healthcare burdens by reducing and preventing hospitalisation due to *C. neoformans*

infection, increasing the viability of such a scheme in low income regions of the world, where disease burdens are highest. This would also minimise the development of antifungal resistance, which would allow gold standard antifungal therapies to be reserved only for acute, life-threatening incidences of cryptococcal meningitis. However, if IFNγ is only beneficial for patients if given adjunctive to traditional antimicrobial therapy, this will limit the utility and uptake of IFNγ into the clinic globally, as the increased cost of treatment may potentially not outweigh the survival benefit seen in patients.

However, although potential clinical benefit of adjunctive IFNγ has been shown in HIV/AIDS patients, the results of this thesis indicate that this same treatment in non-HIV associated cryptococcosis may be ineffective or more dangerous. It is important to note this study utilised immunocompetent mice and did not recapitulate the HIV-positive host where IFNγ has been previously shown to improve fungal clearance clinically (Jarvis *et al.*, 2012). Therefore, the results of my study in immunocompetent mice suggests that immunocompetent patients with normal $CD4^+$ cell function may see no benefit of exogenous IFNγ treatment as sufficient production already occurs. Instead, this may just result in toxicity (G. Wu *et al.*, 2020).

However, IFNγ may also have a pathological role in HIV-positive patients too. While low IFNγ is a predictor for IRIS in HIV patients (Chang *et al.*, 2013) – suggesting that IFNγ is protective – IRIS is characterised by cytokine storm and significantly elevated IFNγ (Wiesner and Boulware, 2011). Therefore, while IFNγ is likely protective, treatment must be timed appropriately to avoid IRIS or IRIS-like symptoms in patients. The same is seen in sepsis patients, where IFNγ during acute sepsis is associated with pathology and inflammation (Romero *et al.*, 2010), but in the subsequent immune dampening that follows sepsis, IFNγ has been successfully trialled in improving immunosuppression and reducing infection following sepsis (Payen *et al.*, 2019).

Regardless, this double edged nature of IFNγ and lack of clear guidance highlights how a greater understanding of the cryptococcosis immune response is required so that specific treatment guidelines can accompany any large-scale clinical uptake. Therefore, for IFNγ to be made more widely available to cryptococcosis patients, more work is needed to ascertain exactly which patients IFNγ treatment is suitable for and in what situations – particularly as current guidelines are vague (Abassi, Boulware and Rhein, 2015).

Finally, no significant protective role for IL-1β was observed either *in vitro* or *in vivo* in any of my experiments. This suggests that although IL-1β may be associated with improved host outcomes *in vivo*, it is likely only indicative of a pro-inflammatory phenotype rather than actively mediating significant host protective effects.

Functionally, IL-1β is more closely associated with Th17 immune responses (Lasiglië *et al.*, 2011) – a response of less clear benefit in cryptococcosis. Additionally, functional effects of IL-1β with regard to infection primarily revolve around neutrophil recruitment, such as chemokine and adhesion expression (Gershenwald *et al.*, 1990; Rosenwasser, 1998). These effects are beneficial in infections with a defined host-protective role of neutrophils such as *Mycobacterium marinum* infection, where IL-1β is observed to increase neutrophil number and antimicrobial activity leading to smaller bacterial burdens (Ogryzko *et al.*, 2019). However, as host protection during cryptococcosis is currently not associated with neutrophils, it is not surprising that the IL-1β$^{-/-}$ mice used in this thesis did not have changed survival due to *C. neoformans* infection. However, IL-1β is also known to significantly influence adaptive immune responses – synergising with IL-6 to increase IL-2 receptor expression (Vannier and Dinarello, 1994) and induce IL-4 expression for B cell activation (Vannier, Miller and Dinarello, 1992). Even though both B and T cells are thought to be important in cryptococcosis, the studies presented here instead suggest that the contribution of IL-1β to these processes is either minimal or redundant. Therefore, when developing immunotherapy, it can be concluded that inhibiting IL-1β will likely not adversely affect cryptococcosis patients.

7.1.2 – Virulence of *C. gattii*

Transgenic pathogens that express GFP are important research tools. Not only does GFP expression aid their identification in biological samples, but it also enables the subcellular localisation of tagged proteins to be determined – all of which are important when studying pathogen virulence. However, despite advances in molecular biology and the wide range of methods available to researchers, mutagenesis protocols are still not 100% predictable. Therefore, insertion of GFP gene insertion can have significant off-target effects – either as a result of the large GFP protein (~27kDa) significantly affecting the expression and function of conjugated proteins (Snapp, 2005), or as a result of inadvertently altering pathogen genomes.

However, while these unintended changes in genomics can significantly affect experiments, if these unintended changes in phenotype can be successfully attributed to changes in genotype, they can reveal a great deal about mechanisms of virulence. For my thesis, the GFP expressing R265 strain of *C. gattii* used was originally generated by biolistic transformation (Voelz *et al.*, 2010). This method has been utilised to efficiently generate many other transgenic strains of *C. gattii* and *C. neoformans*. In the case of GFP-R265, a six-gene deletion on chromosome 1 was identified when the GFP strains was compared to the parental strain (Bojarczuk, 2020). This highlights the importance of sequencing transgenic strains when they are generated as an important control.

Particularly as in the case of the GFP-R265 strain, the strain was instead subjected to extensive *in vitro* characterisation where no defects in growth were observed (Voelz *et al.*, 2010) – avirulence was only apparent once the strain was inoculated into zebrafish embryos.

The six genes identified to be absent in the GFP strain of *C. gattii* appear to have metabolic functions (Bojarczuk, 2020). This type of function helps to explain the results of the GFP-R265 experiments presented in this thesis. First and foremost, it suggests that the GFP-R265 strain was not completely avirulent. As fungal burdens were observed to increase in the lungs of mice between 7 and 23dpi, this suggests that the growth of this strain was slowed rather than abated. If the survival study period had been longer, it can be hypothesised that there would have been eventual mortality. Importantly though, this does show that the growth of this strain is significantly reduced in the lungs of mice, and that the defect in growth involved a substrate present in lung tissue. If identified, this lead to multiple therapeutic strategies – an inhibitor of the protein/s absent in GFP-R265 may be a useful antifungal treatment, while identification of the host substrate required for this protein may enable the identification of susceptible patients.

However, it should be noted that the results from the mouse study suggests that dissemination of GFP-R265 was unaffected compared to the parental strain. Interestingly, this suggests that dissemination of GFP-R265 occurs independently of growth in the lungs, and that the substrates utilised by *C. gattii* in the brain are different to those in the lung. However, as *C. gattii* infection is more commonly associated with aggressive pulmonary infection rather than disseminated disease, the relevance of this finding to *C. gattii* virulence should be confirmed (Krockenberger *et al.*, 2010).

7.1.3 – The initial pulmonary immune response to *C. neoformans*

The majority of *in vivo* studies of cryptococcosis use mice – their widespread use makes studies highly comparable while their relatively small size and short gestation times make for convenient husbandry (Vandamme, 2014). Combined with physiological similarity and a well characterised genome, mice are an attractive model organism to researchers. However, they are not a perfect model of human disease. One of the biggest issues is that high content imaging of the immune system in live animals over days is currently not possible (Pittet and Weissleder, 2011). This makes determining the spatial distribution of immune cells within tissues – and understanding host-pathogen interactions – difficult. While intravital imaging methods are available, these are also associated with significant limitations. Bioluminescent (Vanherp *et al.*, 2019) methodologies are currently not high resolution enough to examine events at the cellular level, while surgical window based methods only allow for a few hours of imaging at a time (Alieva *et al.*, 2014). Instead,

most studies utilise *ex vivo* readouts such as flow cytometry and histology. All of these methods require the destruction or fixing of tissue, or removing the cells from the context of tissue – preventing live interactions between cells from being examined *in situ*. Additionally, in an effort to improve animal welfare within research, there is a global push to find alternative model animal species to mammals where possible (*The 3Rs* | *NC3Rs*). Aside from the ethical advantages to using species such as flies and zebrafish, their smaller size and thinner skin does enable long term intravital imaging of host-pathogen interactions. However, the greater evolutionary distance between these species and humans means that many biological pathways and anatomical features are not conserved, greatly limiting the translation of findings in these models.

Therefore, finding a model that offers the translatability of the mammal that is compatible with live, high content imaging of host-pathogen interactions in live tissue while reducing the need to subject animals to procedures *in vivo* is a high priority to the scientific community. The *ex vivo* PCLS model of cryptococcosis presented here provides a solution – the lung tissue is kept viable for days at a time, is compatible with high content imaging and be repeatedly sampled (Sanderson, 2011). PCLS have been successfully used in the past to study various phenomena such as lung development (Akram *et al.*, 2019), viral infection (Ebsen *et al.*, 2002) and allergy (Patel *et al.*, 2019), but have yet to be realised as a model for studying fungal infection. Using *C. neoformans* infection as a model pathogen, I examined the initial pulmonary immune response using high content time lapse imaging. Although this study focused on high-content imaging, PCLS can also be compatible with many analytical methods, such as '-omics' or electron microscopy.

A surprising observation was that although foci of infection during the first 24 hours of infection appear to get larger *in vivo*, this does not appear to be the result of fungal replication. This suggests that focal growth is instead a host-mediated process. This observation may not only be a potentially important mechanism of host defence in multiple infections, but is also a phenomenon that would not have been identified without the PCLS model. Therefore, the ability to visualise responses afforded by PCLS makes modelling and understanding host-pathogen interactions possible, and highlights the utility of the model.

In this study, PCLS revealed that the initial immune response to *C. neoformans* is macrophage centric*,* as has been previously hypothesised (Shao *et al.*, 2005). Additionally, macrophage clustering was also observed, another phenomena that has been reported previously in models of cryptococcosis (Bojarczuk *et al.*, 2016). However, most of the clinical attention on such behaviour is focussed on late stage macrophage-centric structures described as granulomas (Williams and Williams, 1983). Granulomas are defined as masses of immune cells, primarily macrophages, that contain pathogens

that cannot be cleared (*C. neoformans, Mycobacterium tuberculosis*). Functionally, these structures are thought to exist to contain pathogen growth and prevent dissemination (Shibuya *et al.*, 2005). However, they are also reported to be pathological by becoming inadvertent pathogen 'reservoirs' in chronic infection that provide a protective niche to pathogens (*Mycobacterium tuberculosis;* James, 2000; Ramakrishnan, 2012). In the case of cryptococcosis, these structures are hypothesised to be largely protective (Ristow and Davis, 2021), although their study has been limited as it has been previously reported that granulomas do not form in mice unless specific transgenic strains of *C. neoformans* are used (Farnoud *et al.*, 2015) – the reason for this has been hypothesised to be a feature of mouse infection. Yet in this study, clusters of macrophages that may be indicative of early granuloma formation were observed – this could indicate that granulomas actually do occur in the lungs of mice infected with *C. neoformans*, but require the PCLS methodology in order to be studied since they have not been successfully studied by other methods.

In the case of early infection, the clustering of macrophages and pathogens in a smaller space may be of benefit to the host. Because AMs are at an inherently low density in the lung prior to infection (Bhattacharya and Westphalen, 2016), the chance of an interaction between an inhaled pathogen and an AM is low. This low density may also explain the lack of an opsonising effect observed with 18B7 IgG in this study. Therefore, by establishing larger foci of infection, cell densities may be great enough for increased phagocytosis, higher concentrations of antimicrobial mediations and early granuloma formation.

On the other hand, *C. neoformans* in 24HPI PCLS appeared to be more pathogenic than those in 0HPI PCLS – fungal cells were larger and more incidences of fungal replication were observed. It is known that *C. neoformans* has many virulence factors which have optimal activity at 37^{o}C – such as once inoculated into an animal (Bloom *et al.*, 2019). However, activation and increased expression of these factors likely takes time – time potentially afforded by early macrophage insufficiency. If this is the case, then focal growth may instead enable cryptococcal adaptation and establishment of infection. Confirming whether foci size is indicative of *Cryptococcus* pathology or host protection is important for identifying factors critical for host clearance, and therefore, potential targets for immunotherapy.

The final important conclusion from the PCLS study is that AMs during early infection are unable to control initial *C. neoformans* infection in the lungs of mice. Although clustering was observed, phagocytosis was rare and when it did occur, did not inhibit fungal replication. Although initially troubling, this finding is in agreement with the current understanding of cryptococcosis pathology – the initial immune response is macrophage

centric, although the recruitment of adaptive immune cells is required to enhance the activity of macrophages enough for fungal clearance and the resolution of infection. This is supported by the high incidences of cryptococcal meningitis in patients with uncontrolled HIV/AIDS (Rajasingham *et al.*, 2017), and the hypothesised benefit of Th1 cytokines, such as IFNγ (Jarvis *et al.*, 2012). However, as described previously, IFNγ treatment in HIV positive cryptococcal meningitis patients has only trialled adjunctive to fungicidal therapy (Jarvis *et al.*, 2012). When supported by this thesis where no benefit of IFNγ treatment alone was observed in mouse survival experiments, this implies that IFNγ only stimulates macrophages fungistatic activity or minimal fungicidal activity – not enough to rescue the host from high burden infection. However, this would still explain the absence of any macrophage antifungal activity observed in this model, as the time points examined were prior to the recruitment of a significant number of IFNγ producing adaptive cells.

7.2 – Future Plans

7.2.1 – Cryptococcosis immunotherapy

One of the biggest gaps in knowledge revealed by this work is that it has yet to be established in exactly which contexts IFNγ therapy to beneficial in cryptococcosis, and when treatment may be dangerous for patients. Previous low inoculum experiments in zebrafish embryos in our lab have shown that a single dose of IFNγ at the time of treatment was sufficient to improve host outcomes (Kamuyango, 2017). This implies that this treatment may be of benefit when given prophylactically to patients who either lack or have dysfunctional adaptive immunity. However, this study should be repeated in a mammalian model with a size matched inoculum to confirm the benefit of prophylactic IFNγ therapy.

Additionally, low inoculum acute infection of mice with H99α IFNγ also revealed a benefit of continuous IFNγ treatment (Wormley *et al.*, 2007; Castro-Lopez *et al.*, 2018). This therefore suggests that in patients with asymptomatic but established pulmonary cryptococcosis, multiple doses of IFNγ alone may be sufficient to improve infection outcomes without the need for antifungal therapy – akin to at-risk patients who were diagnosed with cryptococcosis as a result of regular antigen screening. However, these experiments used immunocompetent mice, and therefore did not establish whether this same benefit would be observed in immunosuppressed animals. Therefore, low inoculum H99α IFNγ infection experiments should be repeated in mice either infected with HIV, or who have their $CD4^+$ cells depleted, as a model of HIV/AIDS patients. However, a model using HIV infection would be better from a translational point of view,

as HIV infection has a myriad of other immunological consequences, including low level inflammation and changed macrophage biology (Ieong *et al.*, 2000; Deeks, Tracy and Douek, 2013; Seoane *et al.*, 2020). For additional translation, this should also be repeated in mice receiving immunosuppressive therapy regiments akin to solid organ transplant patients should also be investigated.

The survival experiments I conducted as part of this thesis involved a high inoculum pulmonary infection of mice, similar to original experiments in mice using H99α IFNγ infection. This experiment was designed to mimic the clinical situation of patients that may present to the clinic due to the non-specific symptoms of pulmonary cryptococcosis. Unlike in low inoculum experiments, a single dose of IFNγ did not significantly affect animal survival, while continuous IFNγ actually worsened host outcomes. Again, however, this study only utilised immunocompetent mice – IL-1β$^{-/-}$ were utilised, although it was observed that this phenotype did not affect mouse survival. Therefore, these experiments should be repeated with immunosuppressed mice as described previously, where lower levels of IFNγ would be observed. Additionally, this experiment should also be repeated in mice that receive antifungal therapy alone, or in combination with IFNγ – to establish if IFNγ would offer any benefit to patients over existing therapies. Finally, to better understand the benefit of adjunctive IFNγ observed in clinical trials, IFNγ should be administered to mice with established cryptococcal meningitis in two different experiments. Firstly, immunocompetent mice should receive IFNγ treatment adjunctive to antifungal therapy to determine if the benefit of IFNγ is likely to be exclusive to immunosuppressed patients. Then, immunocompromised mice with established cryptococcal meningitis should be treated with IFNγ alone to confirm whether existing antifungal therapy is still required (Jarvis *et al.*, 2012).

The results of all of these studies would then provide a more thorough understanding of the treatment and management of cryptococcosis, and the amount of associated treatment that is required (Figure 64). These results could then inform clinical practice and clinical trial design with regard to IFNγ treatment – helping to ensure treatment is only administered where there is clear evidence of a benefit with a better understanding of the potential risks of any treatment, IFNγ or otherwise. This is important, particularly as this thesis has shown that IFNγ may potentially accelerate mortality in certain patients.

Additionally, there is further research still required to understand the mechanisms of action of IFNγ in cryptococcosis. Although there is a clear role of IFNγ in cryptococcosis, this cytokine has a central immunological role and a broad spectrum of activity – therefore meaning a wide range of side effects. This relatively non-specific action might

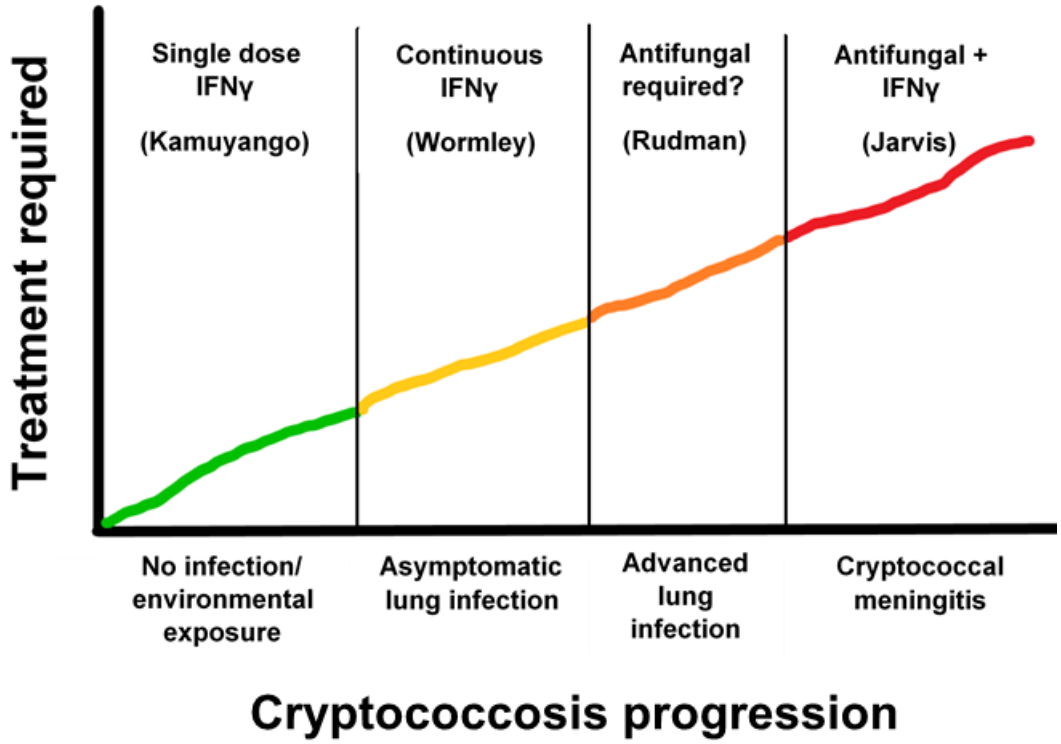

Figure 64 – Schematic linking the limits of IFNγ treatment at various clinical stages of cryptococcosis. Picture showcasing various clinical presentations of cryptococcosis of differing severity, and our current understanding of in which contexts IFNγ can improve host outcomes. A single dose of IFNγ has been shown to be protective in zebrafish embryos that have been infected with very small inocula of C. neoformans, whereas H99α IFNγ experiments revealed that continuous IFNγ was of benefit to mice, although inocula were significantly larger (Wormley et al., 2007; Kamuyango, 2017). On the other hand, in late stage cryptococcal meningitis, IFNγ has only been shown to be beneficial when given adjunctive to antifungal therapy – while the survival experiments presented in this thesis suggest that IFNγ treatment alone cannot protect mice from high fungal burden pulmonary cryptococcosis (Jarvis et al., 2012). Each of these scenarios, however, require addition modelling.

explain the mortality observed in survival experiment animals. In humans, side effects of IFNγ treatment include chills, diarrhoea, nausea and leukopenia (International Chronic Granulomatous Disease Cooperative Study Group, 1991; Miller, Maher and Young, 2009). In mouse models, chills may be misinterpreted as signs of neurodegeneration associated with meningitis. Additionally, gastric symptoms in humans may translate into reduced appetite in mice, resulting weight loss observed in these models. Finally, the leukopenia may have resulted in inflammation and tissue damage. In support of this theory, mice treated with IL-18 and IL-12 concurrently – which induces significant levels of IFNγ – are observed to exhibit significant weight loss and symptoms akin to those in LPS-induced sepsis, a condition associated with excessive inflammation (Nakamura *et al.*, 2000). Therefore, even though IFNγ may increase antifungal activity, the associated inflammation – and in particular neuroinflammation – may mean that IFNγ is not an appropriate therapy (Neal *et al.*, 2017). Instead, IFNγ may be an important 'signpost', indicating that a number of associated IFNγ pathways are beneficial for antifungal clearance. Additional work to identify and characterise these pathways may reveal opportunities to develop more specific immune enhancing therapies that more selectively activate these pathways and reduce IFNγ associated side effects.

There were also some important limitations to the mouse model used in this thesis. Due to their less aggressive behaviour and easier husbandry, all *in vivo* experiments in this thesis used exclusively female mice. However, cryptococcosis is observed to affect more men than women at a ratio of at least 2:1 (Edwards, Sutherland and Tyrer, 1970; Mitchell *et al.*, 1995), which has been shown not to be a results of differences in exposure to *Cryptococcus* (Davis *et al.*, 2007). The risk of death for hospitalised males has also been observed to be higher (McClelland *et al.*, 2013). Mechanistically, oestrogen – a female sex hormone – has been observed to inhibit the replication of *C. neoformans* cells *in vitro* (Mohr *et al.*, 1972). When macrophages from human patients were compared, male macrophages were observed to have a comparatively lower level of antifungal activity and lower phagocytic capacity (McClelland *et al.*, 2013). In the case of *C. gattii* infection, *in vivo* studies in mice observed that females had delayed mortality, as well as increased neutrophil recruitment and lower fungal burdens as early as 24hpi (Carvalho Costa *et al.*, 2020). This improved fungal handling was not observed with ovariectomised mice. This potential protective role for oestrogen in cryptococcosis means that any mechanisms explored here may be significantly different in male and female mice. Therefore, repeating these studies in male mice would not only increase confidence that these mechanisms are universal, but if different may help to explain mechanisms for sex-differences in cryptococcosis incidence and severity.

To date, it has been determined that STAT1 signalling is critical for IFNγ mediated protection in cryptococcosis *in vivo* (Leopold Wager *et al.*, 2014). Specifically, this pathway has been found to be critical for stimulating macrophage antifungal activity (Leopold Wager *et al.*, 2018). Therefore, fully characterising the STAT1 pathways may reveal a more specific approach to immunotherapy that offers host protection with fewer side effects in the case of a STAT1 activator. Alternatively, STAT1 signalling is negatively regulated by STAT3, which is in turn induced by IL-10 (Dallagi *et al.*, 2015). STAT3 inhibitors have been developed for cancer treatment, where inhibiting STAT3 reduces the immunosuppressive activity of tumours (Zou *et al.*, 2020). However, it has also been shown to be dangerous in a sepsis model, whereby STAT3 inhibition exacerbates dangerous inflammation (Williamson *et al.*, 2019) – similar to what is observed with IFNγ in cryptococcosis models (Neal *et al.*, 2017). Therefore, determining the downstream target genes of the IFNγ/STAT1 pathway will maybe enable the targeting of more specific IFNγ related pathways that can be modulated with safer safety profiles.

Finally, cost-benefit projections for IFNγ therapy in cryptococcosis are required. Currently, there is clinical evidence that adjunctive IFNγ may be of benefit to HIV positive cryptococcal meningitis patients (Jarvis *et al.*, 2012), and therefore should be more widely investigated in clinical practice, particularly in more economically developed regions where mortality is still as high as 40-60% (Rajasingham *et al.*, 2017). However, the burden of cryptococcal meningitis is highest in resource limited settings, such as sub-Saharan Africa. This means any new treatments, aside from being efficacious, need to be readily available, affordable and reduce hospitalisation times. IFNγ is already an approved medication, currently indicated for use in chronic granulomatous disease and severe malignant osteoporosis (NICE, 2021). The cost of two doses of 100μg IFNγ in 1997 was approximately $280 (Stadtmauer and Cunningham-Rundles, 1997), while the cost of one week of antifungal therapy is $1861, while two weeks of treatment cost $2285 (Chen *et al.*, 2019). Depending on how the price of IFNγ has changed over time, the addition of IFNγ as an adjunctive therapy would still cost less than a two-week treatment regimen. Furthermore, one of the highest costs of treating cryptococcal meningitis is the hospital time and bedside care required due to both the raised ICP and risk of renal toxicity with amphotericin B treatment (Rajasingham *et al.*, 2012). Therefore, if IFNγ treatment reduces time for which bedside treatment is required, IFNγ in HIV positive patients may be economically viable. Additional studies in other patients in different states of immunocompromise may allow for the use of IFNγ to then be expanded and enable this potentially life and cost saving therapy to be available to as many patients as possible. However, cost-benefit projections should be expanded to both screening programmes and prophylactic IFNγ treatment. By examining the cost of such programs and establishing how many cases of cryptococcal meningitis they could prevent or

reduce the severity of, such programs may be viable, even in less economically regions. Even in the absence of prophylactic IFNγ treatment, the benefit of screening at-risk patients with either the *Cryptococcus* antigen lateral flow assay (Lourens *et al.*, 2014) or (1->3)-β-D-glucan (BDG) assay (Rhein, Boulware and Bahr, 2015) may allow for better patient stratification – which may be required for IFNγ treatment.

7.2.2 – Understanding the virulence of *C. gattii*

Although it was confirmed that GFP-R265 was comparatively less virulent, the study time was too short to confirm whether the GFP-R265 *C. gattii* strain is completely avirulent or instead results in delayed mortality. Therefore, survival analysis should be repeated, but the examined period should be extended out further (90 days). Additional fungal burden analysis should also take place between 7 and 23dpi and after 23dpi to confirm the dynamics of GFP-R265 infection in mice. If GFP-R265 infection results in persistent pulmonary fungal burdens without mortality, this strain may provide a model of latent infection.

Most importantly, the mechanism of GFP-R265 hypovirulence should be determined. However, six genes, or any combination thereof, may potentially be responsible for this phenotype. Therefore, identifying which genes fully contribute to this hypovirulence would require generating 61 knockout strains of WT-R265 – a missing a different gene/combination of genes. Instead, siRNA based approaches should be examined as a method to more rapidly screen for knockout strains that recapitulate the avirulence phenotype. Additionally, avirulent phenotypes could be screened for in zebrafish embryo models of infection, as this species is more compatible with high-throughput screening methods. However, this would first require confirming whether siRNA treatment of *C. gattii* cells is possible (Skowyra and Doering, 2012).

Once the specific genes responsible for the phenotype have been determined, stable transgenic *C. gattii* WT-R265 lines should be generated and subjected to metabolic screening. Briefly, the strain/s should be cultured in the presence of different substrates that utilise different metabolic processes, to confirm which of these pathways are abrogated by the mutation. This metabolic screen should include substrates found in the zebrafish embryo and in murine tissues, including lung, brain and serum. Finally, growth of this strain in the presence of macrophages should also be assessed, to determine whether the strain is differentially susceptible to the host immune response.

7.2.3 – Modelling and understanding the immune response to *C. neoformans*

One of the most striking observations within the PCLS model was the focal growth that occurs between 0 and 24HPI that appeared to be independent of fungal replication – a

process which has not been described previously in cryptococcosis. Although the mechanism of focal growth could be not determined, macrophages were the most abundant cells at foci of infection. Although it was not confirmed whether these cells are responsible for focal enlargement, the most likely explanation currently is that focal enlargement is the result of phagocytosis, migration and subsequent vomocytosis. However, incidences of phagocytosis were absent in 0HPI PCLS, no significant migration of AMs was observed *ex vivo* and neither were incidences vomocytosis.

It is also possible that focal enlargement was due to the activity of other immune cell types. Neutrophils are highly motile immune cells that can be rapidly recruited to sites of inflammation. It is therefore feasible that neutrophils could have been recruited to sites of infection where they phagocytosed *C. neoformans* cells before migrating to other foci of infection. Once there, neutrophils may have been subsequently cleared by reverse migration and/or efferocytosis (Greenlee-Wacker, 2016; Grégoire *et al.*, 2018; Snarr *et al.*, 2020). However, the lack of a clinical association between neutrophil disorders and incidences of cryptococcosis suggests neutrophils are not responsible (Gibson and Johnston, 2015). However, it may also be that associations of neutropenia with cryptococcosis have been not been identified because of the small window in which neutrophils have a significant role in infection. Cryptococcosis is reported to remain latent for years following initial host control of infection (Alanio, 2020). As exposure to *C. neoformans* is estimated to occur in most individuals before the age of 21 (Goldman *et al.*, 2001), it suggests that this initial role for neutrophils will have likely concluded by the time of reactivation, and so incidences of clinical infection are not associated with their absence or dysfunction. Counter to this, Kamuyango showed in the zebrafish embryo that neutrophils are not important for early fungal clearance (Kamuyango, 2017). However, no resident macrophages have been identified in the zebrafish embryo to date, meaning that all macrophages were migratory, unlike in the lung (Lin, Wen and Xu, 2019) – therefore the role of neutrophils in initial mammalian infection may be less redundant. It is also possible that MDMs can fulfil this role, as these cells are migratory and also recruited early in infection (Cui *et al.*, 2018). Therefore, PCLS should be prepared at various time points between 0HPI and 24HPI so the timeline of focal enlargement can be established. Additionally, resident macrophages, neutrophils and MDMs should be ablated in the lungs of mice prior to infection to determine how this affects focal enlargement and early changes in pulmonary fungal burden. Efferocytosis should also be inhibited in AMs to help confirm whether this process is significant in focal growth.

It was also observed that phagocytosis by macrophages did not inhibit fungal growth *ex vivo*. This suggests that any fungal clearance that may have occurred in the lungs was not the result of macrophages. However, none of the other investigated cell types were

observed proximal to foci of infection. This may have been an artefact of the PCLS methodology. The frames of PCLS that were examined were chosen because *C. neoformans* cells were visible at those sites. However, this means that these fungal cells were likely to be those that had evaded immune mediated clearance, and therefore these fungal cells may have been more resistant to macrophage antifungal activity. Therefore, examining PCLS prepared prior to 24HPI may instead reveal foci of infection with different properties that are also more fungicidal or fungi static. Additionally, NK cells should also be examined in this model – these innate cells are reported to be cryptocidal (Li *et al.*, 2013) and are associated with innate immunity (Culley, 2009). Therefore, it should be examined whether these cells are present in 24HPI PCLS and whether they interact with *C. neoformans* cells – potentially using a fluorescent conjugated antibody against NKp46 (Tomasello *et al.*, 2012).

The PCLS model should also be utilised to study the later elements of the immune response in cryptococcosis. In particular, the PCLS model may have particular utility in studying the processes of antigen presentation and adaptive immunity. Typically, the most efficient antigen presenting cells are assumed to be DCs (Wozniak, 2018). However, only low numbers of these cells were observed in 24HPI PCLS, and were not observed to interact with *C. neoformans* cells. However, as adaptive immune responses take days to generate, the role of DCs may only be apparent in PCLS prepared at later time points. However, it's also possible that antigen presentation is mediated by macrophages – a function these cells have been observed to do both *in vitro* and *in vivo* (Vecchiarelli *et al.*, 1994). Therefore, the interactions of DCs and macrophages with *C. neoformans* cells in PCLS prepared later in infection should be examined. Additionally, the effect of depleting these cell populations on T cell numbers should be established.

In terms of adaptive immunity, one of the hypothesised functions of this response is granuloma formation. However, granulomas have been previously reported not to occur in mouse models of infection without using specific transgenic strains of *C. neoformans* (Farnoud *et al.*, 2015) – limiting our understanding of these phenomena. However, preliminary experiments using PCLS prepared at 7dpi and 14dpi from wild-type(IL1β$^{tm1c(EUCOMM)}$) and IL-1β KO(*pgk2-Cre-IL1β^{tm1d}*) mice infected with KN99α GFP *C. neoformans* have revealed the presence of large macrophage centric structures surrounding *C. neoformans* cells – believed to be granulomas (Appendix 3). This has important implications for future *in vivo* cryptococcosis studies, as the PCLS model may allow for granuloma formation, function and antifungal activity to be assessed with any number of reference *C. neoformans* strains. Aside from high-content imaging of these structures using PCLS, concurrent genomic and proteomic analysis will also enable

factors to be identified that are associated with granuloma responses, and for their contribution to host protective nature to be better determined.

Conditions in PCLS that correlate with dissemination to the CNS should also be investigated – although the outcome of infection in the lungs is thought to determine if cryptococcosis results in asymptomatic clearance or fatal infection, it is still not understood how *Cryptococcus* cells actually escape from this tissue (Denham and Brown, 2018). Epithelial cell uptake of *Cryptococcus* has been observed *in vitro*, which has been associated with epithelial cell death (Barbosa *et al.*, 2006) – however, this has yet to be observed in live tissue due to the limitations of traditional *in vivo* cryptococcosis mouse models. Additionally, cryopreservation techniques associated with lung histology can inadvertently result in tissue damage that may significantly affect results (Taqi *et al.*, 2018). Therefore, PCLS treated with an epithelial cell marker (CD324) should be used in combination with a live/dead stain to correlate *Cryptococcus*-epithelial cell interactions with the occurrence of dissemination *in vivo* (Heyen *et al.*, 2016). It is important to note that for these experiments, inocula should be administered intratracheally, as intranasal inoculation results in rapid dissemination of *C. neoformans* to the CNS by other routes (Coelho *et al.*, 2019).

It should be noted that n numbers for this section of the thesis was very low, particularly for how variable some of the readouts were, with some treatment groups only having an n of 1. The reason n numbers were not increased was due to resource and financial limitations, particularly as mice had to be ordered in and were not bred on site. In the future, with increased resources these n numbers should be increased to enable sufficient statistical power for appropriate statistical comparison.

The PCLS methodology should also be applied to other species such as rats and guinea pigs (Ressmeyer *et al.*, 2006; Huang *et al.*, 2019). In the case of cryptococcosis, these species are invaluable pre-clinical models, with infections in these animals recapitulating more elements of human disease than mice (Kirkpatrick *et al.*, 2007; Krockenberger *et al.*, 2010). For example, infection with *C. neoformans* in mice is ordinarily fatal, unlike with humans (Zaragoza *et al.*, 2007). However, both rats and guinea pigs have been used to model latent infection and a need for immunocompromised animals for significant mortality to occur. Therefore, the PCLS approach should be applied to these species and observations compared to those in mice to determine whether immune responses are any different. Additionally, the effects of IFNγ in models of prophylaxis (Kamuyango, 2017), low fungal burden (Wormley *et al.*, 2007), high fungal burden and late-stage cryptococcal meningitis (Jarvis *et al.*, 2012) should be investigated to confirm findings in a more translatable model system.

Alternatively, the PCLS model may afford the opportunity to refine the mouse cryptococcosis model. Almost all mouse *in vivo* studies of *Cryptococcus* use inocula in the order of magnitude of 10^3 cfu and above – far greater than anticipated environmental exposure (Zaragoza *et al.*, 2007; Walsh *et al.*, 2019). However, experiments using smaller inocula are not widely used as these experiments take longer, which makes study design difficult, expensive and more time consuming. Additionally, phenotypes are likely less obvious and therefore more difficult to examine. However, the PCLS model may allow for the study of host-pathogen interactions using very low inocula of fungal cells that can still be visualised – allowing for PCLS conditions to be correlated with more 'real world' infection *in vivo*. However, this approach requires refinement and validation to determine inocula that still result in visible *Cryptococcus* cells.

Finally, the utility of the PCLS model should be expanded to examine additional immunological phenomena. For example, PCLS conditions in response to *Cryptococcus* infection should be compared between mouse strains to explore why these mice have a differential susceptibility (Nielsen *et al.*, 2005; Zaragoza *et al.*, 2007). By comparing PCLS prepared at different time points and using –omics methods, important differences may be revealed between strains. Not only would this refine the design and interpretation of mouse studies, it may also reveal host factors which are important for *C. neoformans* clearance that are relevant to human infection. Additionally, the PCLS infection model also has utility outside of the field of cryptococcosis. The PCLS approach should be applied to study the pulmonary immune responses to other extracellular pathogens, such as bacteria and other fungi. Finally, comparing the observations of immune responses to various pathogens in PCLS may reveal conserved immunological mechanisms that may help inform our general understanding of the immune system, but also reveal new possibilities for these to be exploited therapeutically to benefit the greatest number of people.

7.2.3 – Thesis Summary

To conclude, this project has resulted in the establishing of an intranasal mouse model of cryptococcosis that enables fungal virulence to be determined. More specifically, it has enabled the avirulence of a GFP construct of *C. gattii* to be confirmed in a mammalian model. Using this model and an *in vitro* macrophage model, IFNγ is controversially shown to be detrimental for host outcomes and host-pathogen interactions in certain contexts. This has provided important evidence that IFNγ monotherapy is not sufficient for treating patients in the later stages of infection, and highlights further study of IFNγ therapy is required for safe and effective treatment of patients. Finally, I present a novel *ex vivo* PCLS model of cryptococcosis that is compatible with *in vivo* methods and can be used to study pulmonary immune responses

in live lung tissue *ex vivo*. Using this approach, the initial mammalian immune response to *C. neoformans* is visualised in the lung for the first time, revealing that early macrophage responses in cryptococcosis are insufficient to control fungal infection in the first 24 hours of infection.

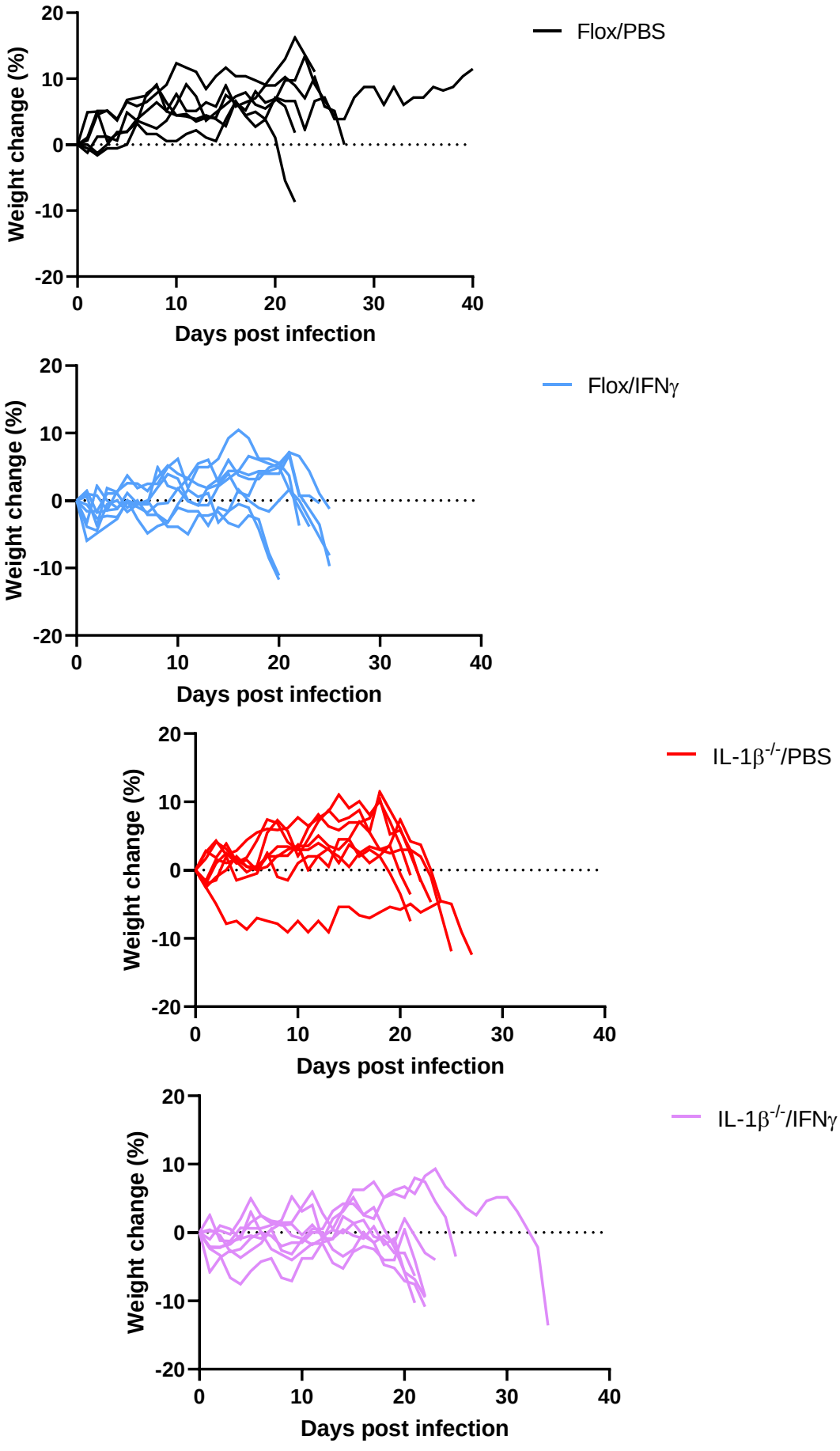
Flox/PBS
Weight change (%)
Days post infection
Flox/IFNγ
Weight change (%)
Days post infection
IL-1β-/-/PBS
Weight change (%)
Days post infection
IL-1β-/-/IFNγ
Weight change (%)
Days post infection

Figure 65 – Bodyweight traces from single dose IFNγ survival experiment. Graphs showing the bodyweight changes of mice infected with KN99α GFP over the course of a survival experiment. Figure shows that the majority of wild-type(IL1β$^{tm1c(EUCOMM)}$)/PBS mice did not show significant weight loss in the days prior to being culled, while all other treatment groups showed weight loss prior to being culled. Each line represents a different animal: wild-type(IL1β$^{tm1c(EUCOMM)}$)/PBS – n=6, wild-type(IL1β$^{tm1c(EUCOMM)}$)/IFNγ – n=8, IL-1β$^{-/-}$/PBS – n=8, IL-1β$^{-/-}$/IFNγ – n=8.

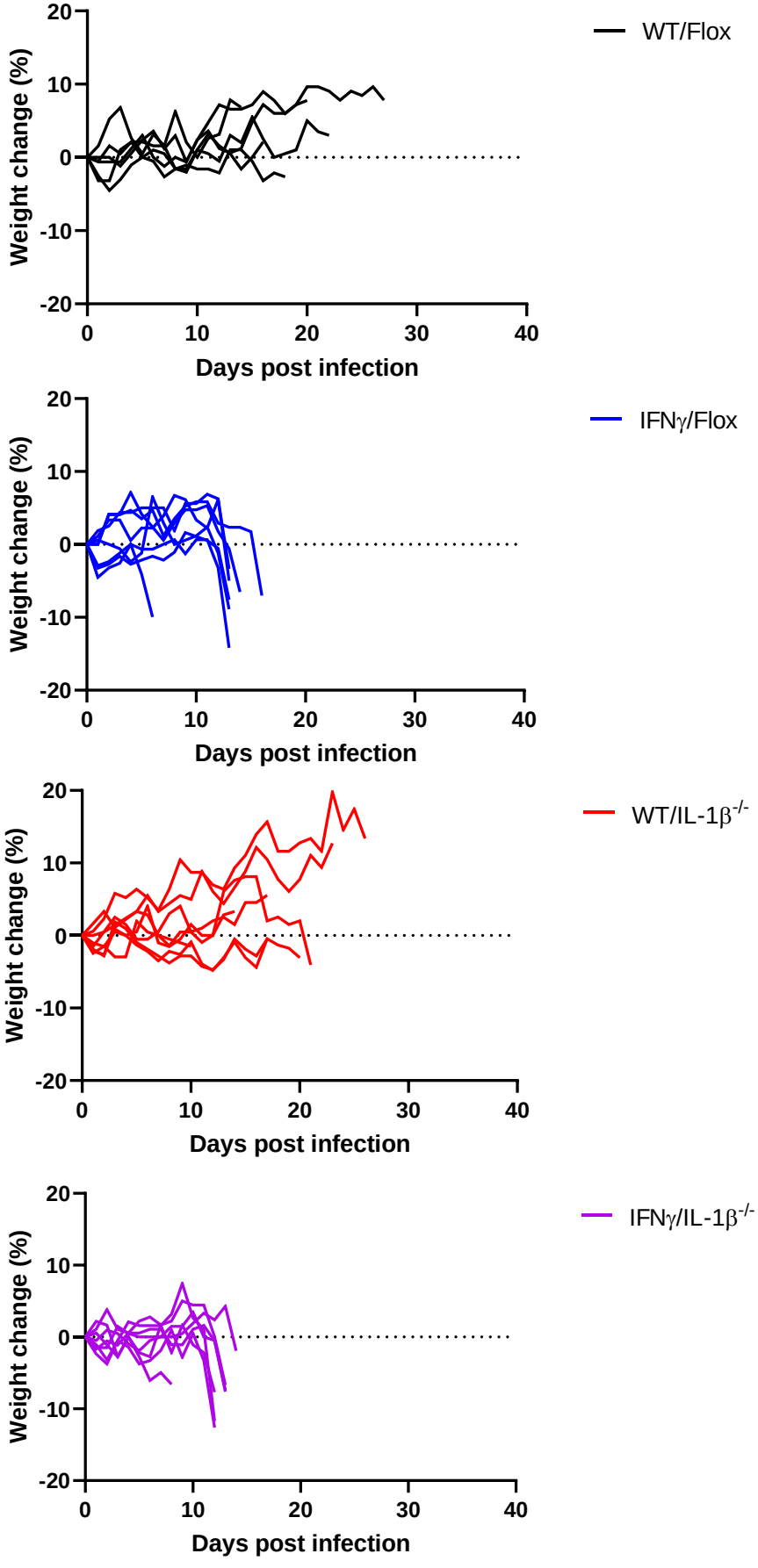
WT/Flox
IFNγ/Flox
WT/IL-1β-/-
IFNγ/IL-1β-/-
Weight change (%)
Days post infection
20
10
0
-10
-20
0
10
20
30
40

Figure 66 – Bodyweight traces from H99α IFNγ survival experiment. Graphs showing the bodyweight changes of mice infected with either H99α WT or H99α IFNγ over the course of a survival experiment. Figure shows that the majority of WT/*wild-type(IL1β$^{tm1c(EUCOMM)}$)* and WT/IL-1β$^{-/-}$ mice did not show significant weight loss in the days prior to being culled, while all other treatment groups showed weight loss prior to being culled. Each line represents a different animal: WT/*wild-type(IL1β$^{tm1c(EUCOMM)}$)* – n=6, WT/IFNγ – n=8, IL-1β$^{-/-}$/WT – n=8, IL-1β$^{-/-}$/IFNγ – n=8.

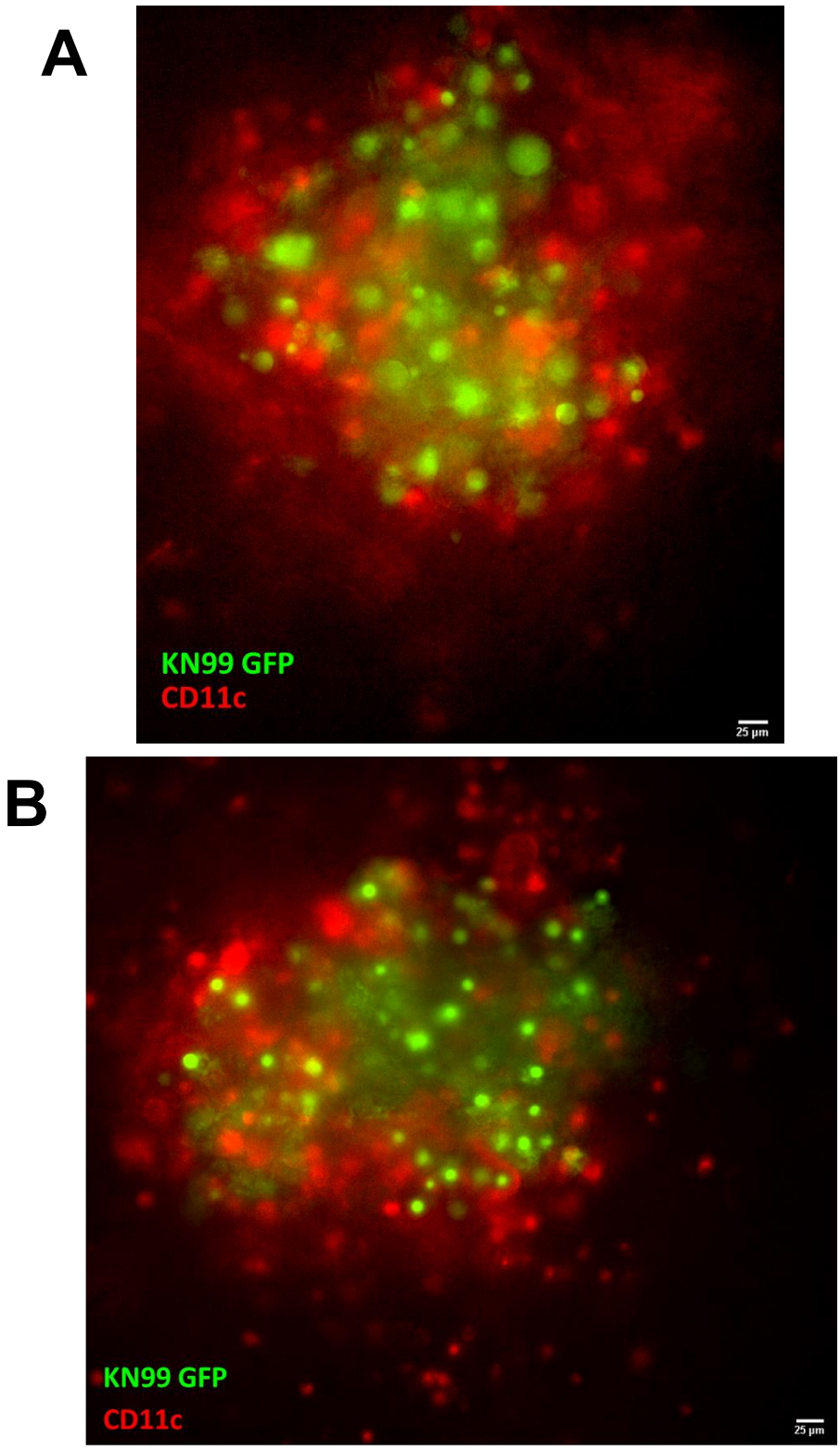

Figure 67 – **PCLS prepared at 7dpi and 14dpi reveal granuloma-like structures in the lungs of infected mice.** At later time points of infection, multicellular granuloma like structures could be observed in PCLS prepared at (**A**) 7dpi and (**B**) 14dpi from *wild-type(IL1β$^{tm1c(EUCOMM)}$)* mice infected with KN99α GFP *C. neoformans*. Representative widefield images (20x; scale bar - 25µm)

Experiment sources

Chapter 3

1 experiment (3.2.2-3.2.8)

1 experiment (3.2.9-3.2.14)

Chapter 4

1 experiment (4.2.2-4.2.4)

1 experiment (4.2.5-4.2.8)

Chapter 5

1 experiment (5.2.1-5.2.3)

1 experiment (5.2.4-5.2.7)

Chapter 6

Ex vivo bead experiment (1 experiment)

All *in vivo* 0hpi (1 experiment)

All *in vivo* 24hpi (1 experiment)

All Plb1 (1 experiment)

Chapter 9 – Bibliography

Abassi, M., Boulware, D.R. and Rhein, J. (2015) 'Cryptococcal Meningitis: Diagnosis and Management Update', *Current Tropical Medicine Reports*, 2(2), 90–99.

Abe, K., Kadota, J.I., Ishimatsu, Y., Iwashita, T., Tomono, K., Kawakami, K. and Kohno, S. (2000) 'Th1-Th2 cytokine kinetics in the bronchoalveolar lavage fluid of mice infected with Cryptococcus neoformans of different virulences', *Microbiology and Immunology*, 44(10), 849–855.

Ben Abid, F., Abdel Rahman Al Soub, H.S., Al Maslamani, M., Hamad Ibrahim, W., Ghazouani, H., Al-Khal, A. and Taj-Aldeen, S. (2020) 'Incidence and clinical outcome of Cryptococcosis in a nation with advanced HIV surveillance program', *The Aging Male*, 23(5), 1125–1130.

Adams, D.O. and Hamilton, T.A. (1984) 'The cell biology of macrophage activation.', *Annual Review of Immunology*, 2, 283–318.

Adner, M., Canning, B.J., Meurs, H., Ford, W., Ramírez, P.R., van den Berg, M.P.M., Birrell, M.A., Stoffels, E., Lundblad, L.K.A., Nilsson, G.P., Olsson, H.K., Belvisi, M.G. and Dahlén, S.E. (2020) 'Back to the future: Re-establishing Guinea pig in vivo asthma models', *Clinical Science*, 134(11), 1219–1242.

Adriouch, S., Dox, C., Welge, V., Seman, M., Koch-Nolte, F. and Haag, F. (2002) 'Cutting Edge: A Natural P451L Mutation in the Cytoplasmic Domain Impairs the Function of the Mouse P2X7 Receptor', *The Journal of Immunology*, 169(8), 4108–4112.

Aghaei Gharehbolagh, S., Nasimi, M., Agha Kuchak Afshari, S., Ghasemi, Z. and Rezaie, sassan (2017) 'First case of superficial infection due to Naganishia albida (formerly Cryptococcus albidus) in Iran: A review of the literature', *Current Medical Mycology*, 3(2), 33–37.

Aguirre, K. and Miller, S. (2002) 'MHC class II-positive perivascular microglial cells mediate resistance to Cryptococcus neoformans brain infection', *Glia*, 39(2), 184–188.

Aguirre, K.M., Gibson, G.W. and Johnson, L.L. (1998) 'Decreased resistance to primary intravenous Cryptococcus neoformans infection in aged mice despite adequate resistance to intravenous rechallenge', *Infection and Immunity*, 66(9), 4018–4024.

Akram, K.M., Yates, L.L., Mongey, R., Rothery, S., Gaboriau, D.C.A., Sanderson, J., Hind, M., Griffiths, M. and Dean, C.H. (2019) 'Live imaging of alveologenesis in precision-cut lung slices reveals dynamic epithelial cell behaviour', *Nature*

Communications, 10(1), 1–16.

Alanio, A. (2020) 'Dormancy in cryptococcus neoformans: 60 years of accumulating evidence', *Journal of Clinical Investigation*, 130(7), 3353–3360.

Ali, R.A., Wuescher, L.M., Dona, K.R. and Worth, R.G. (2017) 'Platelets Mediate Host Defense against Staphylococcus aureus through Direct Bactericidal Activity and by Enhancing Macrophage Activities', *The Journal of Immunology*, 198(1), 344–351.

Alieva, M., Ritsma, L., Giedt, R.J., Weissleder, R. and Van Rheenen, J. (2014) 'Imaging windows for long-term intravital imaging: General overview and technical insights', *IntraVital*, 3(2), e29917.

Alvarez, M., Burn, T., Luo, Y., Pirofski, L. and Casadevall, A. (2009) 'The outcome of Cryptococcus neoformans intracellular pathogenesis in human monocytes.', *BMC Microbiology*, 9, 51.

Alvarez, M. and Casadevall, A. (2006) 'Phagosome Extrusion and Host-Cell Survival after Cryptococcus neoformans Phagocytosis by Macrophages', *Current Biology*, 16(21), 2161–2165.

Anas, A., Poll, T. V.D. and de Vos, A.F. (2010) 'Role of CD14 in lung inflammation and infection', *Critical Care*, 14(2), 209.

Anderson, L.C. (1987) 'Guinea pig husbandry and medicine', *Veterinary Clinics of North America - Small Animal Practice*, 17(5), 1045–1060.

Andersson, J., Samarina, A., Fink, J., Rahman, S. and Grundström, S. (2007) 'Impaired expression of perforin and granulysin in CD8+ T cells at the site of infection in human chronic pulmonary tuberculosis', *Infection and Immunity*, 75(11), 5210–5222.

Apfeld, J. and Alper, S. (2018) 'What can we learn about human disease from the nematode C. Elegans?', in *Methods in Molecular Biology*. Humana Press Inc., 53–75.

Apidianakis, Y., Rahme, L.G., Heitman, J., Ausubel, F.M., Calderwood, S.B. and Mylonakis, E. (2004) 'Challenge of Drosophila melanogaster with Cryptococcus neoformans and role of the innate immune response', *Eukaryotic Cell*, 3(2), 413–419.

Arango Duque, G. and Descoteaux, A. (2014) 'Macrophage cytokines: involvement in immunity and infectious diseases.', *Frontiers in Immunology*, 5, 491.

Aratani, Y., Kura, F., Watanabe, H., Akagawa, H., Takano, Y., Ishida-Okawara, A., Suzuki, K., Maeda, N. and Koyama, H. (2006) 'Contribution of the myeloperoxidase-dependent oxidative system to host defence against Cryptococcus neoformans', *Journal of Medical Microbiology*, 55, 1291–1299.

Arora, S., Hernandez, Y., Erb-Downward, J.R., McDonald, R.A., Toews, G.B. and Huffnagle, G.B. (2005) 'Role of IFN-gamma in regulating T2 immunity and the development of alternatively activated macrophages during allergic bronchopulmonary mycosis.', *Journal of Immunology*, 174(10), 6346–56.

Arora, S., McDonald, R.A., Toews, G.B. and Huffnagle, G.B. (2006) 'Effect of a CD4-depleting antibody on the development of Cryptococcus neoformans-induced allergic bronchopulmonary mycosis in mice', *Infection and Immunity*, 74(7), 4339–4348.

Arora, S., Olszewski, M.A., Tsang, T.M., McDonald, R.A., Toews, G.B. and Huffnagle, G.B. (2011) 'Effect of Cytokine Interplay on Macrophage Polarization during Chronic Pulmonary Infection with Cryptococcus neoformans', *Infection and Immunity*, 79(5), 1915–1926.

Arras, S.D.M., Ormerod, K.L., Erpf, P.E., Espinosa, M.I., Carpenter, A.C., Blundell, R.D., Stowasser, S.R., Schulz, B.L., Tanurdzic, M. and Fraser, J.A. (2017) 'Convergent microevolution of Cryptococcus neoformans hypervirulence in the laboratory and the clinic', *Scientific Reports*, 7(1), 17918.

Aslam, B., Wang, W., Arshad, M.I., Khurshid, M., Muzammil, S., Rasool, M.H., Nisar, M.A., Alvi, R.F., Aslam, M.A., Qamar, M.U., Salamat, M.K.F. and Baloch, Z. (2018) 'Antibiotic resistance: a rundown of a global crisis', *Infection and Drug Resistance*, 11, 1645–1658.

Autissier, P., Soulas, C., Burdo, T.H. and Williams, K.C. (2010) 'Evaluation of a 12-color flow cytometry panel to study lymphocyte, monocyte, and dendritic cell subsets in humans', *Cytometry A*, 77(5), 410–419.

Aye, C., Henderson, A., Yu, H. and Norton, R. (2016) 'Cryptococcosis—the impact of delay to diagnosis', *Clinical Microbiology and Infection*, 22(7), 632–635.

Bahn, Y.S., Kojima, K., Cox, G.M. and Heitman, J. (2006) 'A unique fungal two-component system regulates stress responses, drug sensitivity, sexual development, and virulence of Cryptococcus neoformans', *Molecular Biology of the Cell*, 17(7), 3122–3135.

Baradkar, V., Mathur, M., De, A., Kumar, S. and Rathi, M. (2009) 'Prevalence and clinical presentation of Cryptococcal meningitis among HIV seropositive patients', *Indian Journal of Sexually Transmitted Diseases and AIDS*, 30(1), 19.

Barbosa, F.M., Fonseca, F.L., Figueiredo, R.T., Bozza, M.T., Casadevall, A., Nimrichter, L. and Rodrigues, M.L. (2007) 'Binding of glucuronoxylomannan to the CD14 receptor in human A549 alveolar cells induces interleukin-8 production', *Clinical*

and Vaccine Immunology, 14(1), 94–98.

Barbosa, F.M., Fonseca, F.L., Holandino, C., Alviano, C.S., Nimrichter, L. and Rodrigues, M.L. (2006) 'Glucuronoxylomannan-mediated interaction of Cryptococcus neoformans with human alveolar cells results in fungal internalization and host cell damage', *Microbes and Infection*, 8(2), 493–502.

Barcenas-Morales, G., Cortes-Acevedo, P. and Doffinger, R. (2019) 'Anticytokine autoantibodies leading to infection: early recognition, diagnosis and treatment options', *Current Opinion in Infectious Diseases*, 32(4), 330–336.

Barnett, J.A. (2010) 'A history of research on yeasts 14: medical yeasts part 2, Cryptococcus neoformans', *Yeast*, 27(11), 875–904.

Bauler, T.J., Starr, T., Nagy, T.A., Sridhar, S., Scott, D., Winkler, C.W., Steele-Mortimer, O., Detweiler, C.S. and Peterson, K.E. (2017) 'Salmonella Meningitis Associated with Monocyte Infiltration in Mice', *American Journal of Pathology*, 187(1), 187–199.

Bauman, S.K., Huffnagle, G.B. and Murphy, J.W. (2003) 'Effects of tumor necrosis factor alpha on dendritic cell accumulation in lymph nodes draining the immunization site and the impact on the anticryptococcal cell-mediated immune response', *Infection and Immunity*, 71(1), 68–74.

Bauman, S.K., Nichols, K.L. and Murphy, J.W. (2000) 'Dendritic cells in the induction of protective and nonprotective anticryptococcal cell-mediated immune responses.', *Journal of Immunology*, 165(1), 158–67.

Bava, A.J., Iovannitti, C. and Negroni, R. (1989) 'Comparative study of four antifungal drugs in an experimental model of murine cryptococcosis', *Mycopathologia*, 108(2), 81–88.

Baxter, E.W., Graham, A.E., Re, N.A., Carr, I.M., Robinson, J.I., Mackie, S.L. and Morgan, A.W. (2020) 'Standardized protocols for differentiation of THP-1 cells to macrophages with distinct M(IFNγ+LPS), M(IL-4) and M(IL-10) phenotypes', *Journal of Immunological Methods*, 478.

Ben-Abdalleh, M., Sturny-Leclere, A., Avé, P., Louise, A., Moyrand, F., Weih, F., Janbon, G. and Mémet, S. (2012) 'Fungal-Induced Cell Cycle Impairment, Chromosome Instability and Apoptosis via Differential Activation of NF-κB', *PLoS Pathogens*, 8(3), e1002555.

Berger, M., Norvell, T.M., Tosi, M.F., Emancipator, S.N., Konstan, M.W. and Schreiber, J.R. (1994) 'Tissue-specific fc γ and complement receptor expression by alveolar

macrophages determines relative importance of igg and complement in promoting phagocytosis of pseudomonas aeruginosa', *Pediatric Research*, 35(1), 68–77.

Berges, C., Naujokat, C., Tinapp, S., Wieczorek, H., Höh, A., Sadeghi, M., Opelz, G. and Daniel, V. (2005) 'A cell line model for the differentiation of human dendritic cells', *Biochemical and Biophysical Research Communications*, 333(3), 896–907.

Bergner, A., Kellner, J., Silva, A.K. da, Gamarra, F. and Huber, R.M. (2006) 'Ca2+-signaling in airway smooth muscle cells is altered in T-bet knock-out mice.', *Respiratory research*, 7(1), 33.

Bermas, A. and Geddes-McAlister, J. (2020) 'Combatting the evolution of antifungal resistance in Cryptococcus neoformans', *Molecular Microbiology*, 114(5), 721–734.

Bewley, M.A., Preston, J.A., Mohasin, M., Marriott, H.M., Budd, R.C., Swales, J., Collini, P., Greaves, D.R., Craig, R.W., Brightling, C.E., Donnelly, L.E., Barnes, P.J., Singh, D., Shapiro, S.D., Whyte, M. and Dockrell, D.H. (2017) 'Impaired Mitochondrial Microbicidal Responses in Chronic Obstructive Pulmonary Disease Macrophages', *American Journal of Respiratory and Critical Care Medicine*, 196(7), 845–855.

Bhattacharya, J. and Westphalen, K. (2016) 'Macrophage-epithelial interactions in pulmonary alveoli', *Seminars in Immunopathology*, 38(4), 461–469.

Blanchette, J., Jaramillo, M. and Olivier, M. (2003) 'Signalling events involved in interferon-γ-inducible macrophage nitric oxide generation', *Immunology*, 108(4), 513.

Bloom, A.L.M., Jin, R.M., Leipheimer, J., Bard, J.E., Yergeau, D., Wohlfert, E.A. and Panepinto, J.C. (2019) 'Thermotolerance in the pathogen Cryptococcus neoformans is linked to antigen masking via mRNA decay-dependent reprogramming', *Nature Communications*, 10(1), 1–13.

Bojarczuk, A. (2020) *Insights into the opportunistic fungal pathogen Cryptococcus and neutrophilic inflammation using zebrafish models*. The University of Sheffield.

Bojarczuk, A., Miller, K.A., Hotham, R., Lewis, A., Ogryzko, N. V., Kamuyango, A.A., Frost, H., Gibson, R.H., Stillman, E., May, R.C., Renshaw, S.A. and Johnston, S.A. (2016) 'Cryptococcus neoformans Intracellular Proliferation and Capsule Size Determines Early Macrophage Control of Infection', *Scientific Reports*, 6(1), 21489.

Boneh, A., Mandla, S. and Tenenhouse, H.S. (1989) 'Phorbol myristate acetate activates protein kinase C, stimulates the phosphorylation of endogenous proteins and inhibits phosphate transport in mouse renal tubules', *BBA - Molecular Cell Research*, 1012(3), 308–316.

Borges, M.A.S.B., de Araújo Filho, J.A., Oliveira, B. de J.S., Moreira, I.S., de Paula, V.V., de Bastos, A.L., Soares, R. de B.A. and Turchi, M.D. (2019) 'Prospective cohort of AIDS patients screened for cryptococcal antigenaemia, pre-emptively treated and followed in Brazil', *PLOS ONE*, 14(7), e0219928.

Bose, I., Reese, A.J., Ory, J.J., Janbon, G. and Doering, T.L. (2003) 'A yeast under cover: the capsule of Cryptococcus neoformans.', *Eukaryotic cell*, 2(4), 655–63.

Bouklas, T., Diago-Navarro, E., Wang, X., Fenster, M. and Fries, B.C. (2015) 'Characterization of the virulence of Cryptococcus neoformans strains in an insect model', *Virulence*, 6(8), 809–813.

Bouzani, M., Ok, M., McCormick, A., Ebel, F., Kurzai, O., Morton, C.O., Einsele, H. and Loeffler, J. (2011) ' Human NK Cells Display Important Antifungal Activity against Aspergillus fumigatus , Which Is Directly Mediated by IFN-γ Release ', *The Journal of Immunology*, 187(3), 1369–1376.

Boyer-Chammard, T., Temfack, E., Alanio, A., Jarvis, J.N., Harrison, T.S. and Lortholary, O. (2019) 'Recent advances in managing HIV-associated cryptococcal meningitis', *F1000Res*, 8, 743.

Bradley, L.M., Dalton, D.K. and Croft, M. (1996) 'A direct role for IFN-gamma in regulation of Th1 cell development.', *The Journal of Immunology*, 157(4).

Brandt, M.E., Bragg, S.L. and Pinner, R.W. (1993) 'Multilocus enzyme typing of Cryptococcus neoformans', *Journal of Clinical Microbiology*. J Clin Microbiol, 2819–2823.

Brás, J.P., Bravo, J., Freitas, J., Barbosa, M.A., Santos, S.G., Summavielle, T. and Almeida, M.I. (2020) 'TNF-alpha-induced microglia activation requires miR-342: impact on NF-kB signaling and neurotoxicity', *Cell Death and Disease*, 11(6), 1–15.

Bratton, E.W., El Husseini, N., Chastain, C.A., Lee, M.S., Poole, C., Stürmer, T., Juliano, J.J., Weber, D.J. and Perfect, J.R. (2012) 'Comparison and temporal trends of three groups with cryptococcosis: HIV-infected, solid organ transplant, and HIV-negative/non-transplant', *PLoS ONE*, 7(8).

Brown, E.J., Berger, M., Joiner, K.A. and Frank, M.M. (1983) 'Classical Complement Pathway Activation by Antipneumococcal Antibodies Leads to Covalent Binding of C3b to Antibody Molecules', *Infection and Immunity*, 42(2), 594–598.

Buchanan, K.L. and Doyle, H.A. (2000) 'Requirement for CD4+ T lymphocytes in host resistance against Cryptococcus neoformans in the central nervous system of immunized mice', *Infection and Immunity*, 68(2), 456–462.

Bueno, O.F., Brandt, E.B., Rothenberg, M.E. and Molkentin, J.D. (2002) 'Defective T cell development and function in calcineurin Aβ-deficient mice', *Proceedings of the National Academy of Sciences of the United States of America*, 99(14), 9398–9403.

Buitrago, S., Martin, T.E., Tetens-Woodring, J., Belicha-Villanueva, A. and Wilding, G.E. (2008) 'Safety and efficacy of various combinations of injectable anesthetics in BALB/c mice', *Journal of the American Association for Laboratory Animal Science*, 47(1), 11–17.

Bulmer, G.S. and Tacker, J.R. (1975) 'Phagocytosis of Cryptococcus neoformans by Alveolar Macrophages', *Infection and Immunity*, 11(1), 73–79.

Bunting, L.A., Neilson, J.B. and Bulmer, G.S. (1979) 'Cryptococcus neoformans: Gastronomic delight of a soil ameba', *Medical Mycology*, 17(3), 225–232.

Bürgel, P.H., Marina, C.L., Saavedra, P.H.V., Albuquerque, P., De Oliveira, S.A.M., Veloso Janior, P.H. de H., Castro, R.A. de, Heyman, H.M., Coelho, C., Cordero, R.J.B., Casadevall, A., Nosanchuk, J.D., Nakayasu, E.S., May, R.C., Tavares, A.H. and Bocca, A.L. (2020) 'Cryptococcus neoformans Secretes Small Molecules That Inhibit IL-1 β Inflammasome-Dependent Secretion', *Mediators of Inflammation*, 2020.

Burke, J.E. and Dennis, E.A. (2009) 'Phospholipase A2 structure/function, mechanism, and signaling', *Journal of Lipid Research*. American Society for Biochemistry and Molecular Biology, S237–S242.

Busse, O. (1894) 'Uber parasitare Zelleinschlusse und ihre Zuchtung', *Centrabl. Bakt. Parasit.*, 16.

Byrne, A.J., Mathie, S.A., Gregory, L.G. and Lloyd, C.M. (2015) 'Pulmonary macrophages: Key players in the innate defence of the airways', *Thorax*, 70(12), 1189–1196.

Canteros, C.E., Rodero, L., Rivas, M.C. and Davel, G. (1996) 'A rapid urease test for presumptive identification of Cryptococcus neoformans', *Mycopathologia*, 136(1), 21–23.

Carnesecchi, S., Deffert, C., Pagano, A., Garrido-Urbani, S., Métrailler-Ruchonnet, I., Schäppi, M., Donati, Y., Matthay, M.A., Krause, K.H. and Argiroffo, C.B. (2009) 'NADPH oxidase-1 plays a crucial role in hyperoxia-induced acute lung injury in mice', *American Journal of Respiratory and Critical Care Medicine*, 180(10), 972–981.

Carnovale, D.E., Fukuda, A., Underhill, D.C., Laffan, J.J. and Breuel, K.F. (2001) 'Aspirin dose dependently inhibits the interleukin-1 beta-stimulated increase in inducible nitric oxide synthase, nitric oxide, and prostaglandin E(2) production in rat

ovarian dispersates cultured in vitro.', *Fertility and Sterility*, 75(4), 778–84.

Caron, J., Loredo-Osti, J.C., Laroche, L., Skamene, E., Morgan, K. and Malo, D. (2002) 'Identification of genetic loci controlling bacterial clearance in experimental Salmonella enteritidis infection: an unexpected role of Nramp1 (Slc11a1) in the persistence of infection in mice', *Genes and Immunity*, 3(4), 196–204.

Carroll, S.F., Lafferty, E.I., Flaczyk, A., Fujiwara, T.M., Homer, R., Morgan, K., Loredo-Osti, J.C. and Qureshi, S.T. (2012) 'Susceptibility to progressive Cryptococcus neoformans pulmonary infection is regulated by loci on mouse chromosomes 1 and 9', *Infection and Immunity*, 80(12), 4167–4176.

Carson, M.J., Doose, J.M., Melchior, B., Schmid, C.D. and Ploix, C.C. (2006) 'CNS immune privilege: Hiding in plain sight', *Immunological Reviews*, 213(1), 48–65.

Carvalho Costa, M., Fernandes, H.B., Goncalves, G.K.N., Santos, A.P.N., Ferreira, G.F., Freitas, G.J.C., Carmo, P.H.F., Hubner, J., Emidio, E.C.P., Santos, J.R.A., Santos, J.L., Reis, A.M., Fagundes, C.T., Silva, A.M. and Santos, D.A. (2020) '17-β-Estradiol increases macrophage activity through activation of the G-protein-coupled estrogen receptor and improves the response of female mice to Cryptococcus gattii', *Cellular Microbiology*, 22(6), e13179.

Carvalho Costa, M., Ribeiro, J., Santos, A., Juliana, M., Ribeiro, A., Cota De Freitas, G.J., Bastos, R.W., Ferreira, G.F., Miranda, A.S., Duque, R., Arifa, N., Santos, P.C., Dos, F., Martins, S., Alves Paixão, T., Lúcio Teixeira, A., Souza, D.G. and Santos, D.A. (2016) 'The absence of microbiota delays the inflammatory response to Cryptococcus gattii', *International Journal of Medical Microbiology*, 306, 187–195.

Casadevall, A. (2008) 'Evolution of intracellular pathogens', *Annual Review of Microbiology*, 62, 19–33.

Casadevall, A. (2010) 'Cryptococci at the brain gate: Break and enter or use a Trojan horse?', *Journal of Clinical Investigation*, 120(5), 1389–1392.

Casadevall, A., Cleare, W., Feldmesser, M., Glatman-Freedman, A., Goldman, D.L., Kozel, T.R., Lendvai, N., Mukherjee, J., Pirofski, L.A., Rivera, J., Rosas, A.L., Scharff, M.D., Valadon, P., Westin, K. and Zhong, Z. (1998) 'Characterization of a murine monoclonal antibody to Cryptococcus neoformans polysaccharide that is a candidate for human therapeutic studies.', *Antimicrobial agents and chemotherapy*, 42(6), 1437–46.

Casadevall, A., Coelho, C. and Alanio, A. (2018) 'Mechanisms of Cryptococcus neoformans-mediated host damage', *Frontiers in Immunology*, 30(9), 855.

Casadevall, A., Coelho, C., Cordero, R.J.B., Dragotakes, Q., Jung, E., Vij, R. and Wear, M.P. (2019) 'The capsule of Cryptococcus neoformans', *Virulence*, 10(1), 822–831.

Casadevall, A. and Perfect, J.R. (1998) 'Cryptococcus neoformans', in *Cryptococcus neoformans*. 1st edn. Washington, DC, USA: ASM Press, 41–70.

Casadevall, A., Rosas, A.L. and Nosanchuk, J.D. (2000) 'Melanin and virulence in Cryptococcus neoformans', *Current Opinion in Microbiology*, 3(4), 354–358.

Casbon, A., Long, M.E., Dunn, K.W., Allen, L.H. and Dinauer, M.C. (2012) 'Effects of IFN-γ on intracellular trafficking and activity of macrophage NADPH oxidase flavocytochrome b 558', *Journal of Leukocyte Biology*, 92(4), 869–882.

Cassatella, M.A., Bazzoni, F., Flynn, R.M., Dusi, S., Trinchieri, G. and Rossi, F. (1990) 'Molecular basis of interferon-γ and lipopolysaccharide enhancement of phagocyte respiratory burst capability. Studies on the gene expression of several NADPH oxidase components', *Journal of Biological Chemistry*, 265(33), 20241–20246.

Cassim, N., Schnippel, K., Coetzee, L.M. and Glencross, D.K. (2017) 'Establishing a cost-per-result of laboratory-based, reflex Cryptococcal antigenaemia screening (CrAg) in HIV+ patients with CD4 counts less than 100 cells/μl using a Lateral Flow Assay (LFA) at a typical busy CD4 laboratory in South Africa', *PLOS ONE*, 12(2), e0171675.

Castro-Lopez, N., Campuzano, A., Hole, C., Leopold Wager, C.M., Wozniak, K.L. and Wormley, F.L. (2018) 'Requirement of CXCL11 chemokine production for induction of protection against pulmonary cryptococcosis', *The Journal of Immunology*, 200(1 Supplement), 52.31.

CDC (1981) 'Kaposi's sarcoma and Pneumocystis pneumonia among homosexual men--New York City and California', *MMWR Morb Mortal Wkly Rep.*, 30(25), 305–308.

Cellier, M.F., Courville, P. and Campion, C. (2007) 'Nramp1 phagocyte intracellular metal withdrawal defense', *Microbes and Infection*, 9(14–15), 1662–1670.

Champion, J.A., Walker, A. and Mitragotri, S. (2008) 'Role of particle size in phagocytosis of polymeric microspheres', *Pharmaceutical Research*, 25(8), 1815–1821.

Chang, C.C., Lim, A., Omarjee, S., Levitz, S.M., Gosnell, B.I., Spelman, T., Elliott, J.H., Carr, W.H., Moosa, M.Y.S., Ndung'U, T., Lewin, S.R. and French, M.A. (2013) 'Cryptococcosis-IRIS is associated with lower cryptococcus-specific IFN-γ responses before antiretroviral therapy but not higher T-cell responses during therapy', *Journal of Infectious Diseases*, 208(6), 898–906.

Chang, Y.C. and Kwon-Chung, K.J. (1994) ‘Complementation of a capsule-deficient mutation of Cryptococcus neoformans restores its virulence.’, *Molecular and Cellular Biology*, 14(7), 4912–9.

Chang, Y.C., Stins, M.F., McCaffery, M.J., Miller, G.F., Pare, D.R., Dam, T., Paul-Satyasee, M., Kim, K.S., Kwon-Chung, K.J. and Paul-Satyasee, Maneesh (2004) ‘Cryptococcal Yeast Cells Invade the Central Nervous System via Transcellular Penetration of the Blood-Brain Barrier’, *Infection and Immunity*, 72(9), 4985–4995.

Charlier, C., Nielsen, K., Daou, S., Brigitte, M., Chretien, F. and Dromer, F. (2009) ‘Evidence of a role for monocytes in dissemination and brain invasion by Cryptococcus neoformans’, *Infection and Immunity*, 77(1), 120–127.

Chayakulkeeree, M., Johnston, S.A., Oei, J.B., Lev, S., Williamson, P.R., Wilson, C.F., Zuo, X., Leal, A.L., Vainstein, M.H., Meyer, W., Sorrell, T.C., May, R.C. and Djordjevic, J.T. (2011) ‘SEC14 is a specific requirement for secretion of phospholipase B1 and pathogenicity of Cryptococcus neoformans’, *Molecular Microbiology*, 80(4), 1088–1101.

Chayakulkeeree, M., Sorrell, T.C., Siafakas, A.R., Wilson, C.F., Pantarat, N., Gerik, K.J., Boadle, R. and Djordjevic, J.T. (2008) ‘Role and mechanism of phosphatidylinositol-specific phospholipase C in survival and virulence of Cryptococcus neoformans’, *Molecular Microbiology*, 69(4), 809–826.

Chen, G.H., McDonald, R.A., Wells, J.C., Huffnagle, G.B., Lukacs, N.W. and Toews, G.B. (2005) ‘The gamma interferon receptor is required for the protective pulmonary inflammatory response to Cryptococcus neoformans’, *Infection and Immunity*, 73(3), 1788–1796.

Chen, J., Varma, A., Diaz, M.R., Litvintseva, A.P., Wollenberg, K.K. and Kwon-Chung, K.J. (2008) ‘Cryptococcus neoformans Strains and Infection in Apparently Immunocompetent Patients, China’, *Emerging Infectious Diseases*, 14(5), 755–762.

Chen, M., Xing, Y., Lu, A., Fang, W., Sun, B., Chen, C., Liao, W. and Meng, G. (2015) ‘Internalized Cryptococcus neoformans Activates the Canonical Caspase-1 and the Noncanonical Caspase-8 Inflammasomes’, *The Journal of Immunology*, 195(10), 4962–4972.

Chen, S.C.A., Meyer, W. and Sorrell, T.C. (2014) ‘Cryptococcus gattii infections’, *Clinical Microbiology Reviews*, 27(4), 980–1024.

Chen, S.C.A., Wright, L.C., Golding, J.C. and Sorrell, T.C. (2000) ‘Purification and characterization of secretory phospholipase B, lysophospholipase and lysophospholipase/transacylase from a virulent strain of the pathogenic fungus

Cryptococcus neoformans', *Biochemical Journal*, 347(2), 431–439.

Chen, T., Mwenge, L., Lakhi, S., Chanda, D., Mwaba, P., Molloy, S.F., Gheorghe, A., Griffiths, U.K., Heyderman, R.S., Kanyama, C., Kouanfack, C., Mfinanga, S., Chan, A.K., Temfack, E., Kivuyo, S., Hosseinipour, M.C., Lortholary, O., Loyse, A., Jaffar, S. *et al.* (2019) 'Healthcare Costs and Life-years Gained From Treatments Within the Advancing Cryptococcal Meningitis Treatment for Africa (ACTA) Trial on Cryptococcal Meningitis: A Comparison of Antifungal Induction Strategies in Sub-Saharan Africa', *Clinical Infectious Diseases*, 69(4), 588–595.

Chen, Y.L., Lehman, V.N., Lewit, Y., Averette, A.F. and Heitman, J. (2013) 'Calcineurin governs thermotolerance and virulence of cryptococcus gattii', *G3: Genes, Genomes, Genetics*, 3(3), 527–539.

Chiapello, L.S., Aoki, M.P., Rubinstein, H.R. and Masih, D.T. (2003) 'Apoptosis induction by glucuronoxylomannan of Cryptococcus neoformans', *Medical Mycology*, 41(4), 347–353.

Chin, Y.E., Kitagawa, M., Kuida, K., Flavell, R.A. and Fu, X.Y. (1997) 'Activation of the STAT signaling pathway can cause expression of caspase 1 and apoptosis.', *Molecular and Cellular Biology*, 17(9), 5328–5337.

Chleboun, J. and Nade, S. (1977) 'Skeletal cryptococcosis', *J Bone Joint Surg Am*, 59(4), 509–514.

Chow, E.W.L., Clancey, S.A., Billmyre, R.B., Averette, A.F., Granek, J.A., Mieczkowski, P., Cardenas, M.E. and Heitman, J. (2017) 'Elucidation of the calcineurin-Crz1 stress response transcriptional network in the human fungal pathogen Cryptococcus neoformans', *PLOS Genetics*, 13(4), e1006667.

Chrétien, F., Lortholary, O., Kansau, I., Neuville, S., Gray, F. and Dromer, F. (2002) 'Pathogenesis of Cerebral *Cryptococcus neoformans* Infection after Fungemia', *The Journal of Infectious Diseases*, 186(4), 522–530.

Chrisman, C.J., Alvarez, M. and Casadevall, A. (2010) 'Phagocytosis of cryptococcus neoformans by, and nonlytic exocytosis from, Acanthamoeba castellanii', *Applied and Environmental Microbiology*, 76(18), 6056–6062.

Chun, C.D., Liu, O.W. and Madhani, H.D. (2007) 'A link between virulence and homeostatic responses to hypoxia during infection by the human fungal pathogen Cryptococcus neoformans', *PLoS Pathogens*, 3(2), 225–238.

Chun, F.Z., Ling, L.M., Jones, G.J., Gill, M.J., Krensky, A.M., Kubes, P. and Mody, C.H. (2007) 'Cytotoxic CD4+ T cells use granulysin to kill Cryptococcus neoformans, and

activation of this pathway is defective in HIV patients', *Blood*, 109(5), 2049–2057.

Cleare, W. and Casadevall, A. (1998) 'The different binding patterns of two immunoglobulin M monoclonal antibodies to Cryptococcus neoformans serotype A and D strains correlate with serotype classification and differences in functional assays', *Clinical and Diagnostic Laboratory Immunology*, 5(2), 125–129.

Coelho, C., Camacho, E., Salas, A., Alanio, A. and Casadevall, A. (2019) ' Intranasal Inoculation of Cryptococcus neoformans in Mice Produces Nasal Infection with Rapid Brain Dissemination ', *mSphere*, 4(4).

Cogliati, M. (2013) 'Global Molecular Epidemiology of Cryptococcus neoformans and Cryptococcus gattii: An Atlas of the Molecular Types.', *Scientifica*, 2013, 675213.

Cogliati, M., D'Amicis, R., Zani, A., Montagna, M.T., Caggiano, G., De Giglio, O., Balbino, S., De Donno, A., Serio, F., Susever, S., Ergin, C., Velegraki, A., Ellabib, M.S., Nardoni, S., Macci, C., Oliveri, S., Trovato, L., Dipineto, L., Rickerts, V. *et al.* (2016) 'Environmental distribution of Cryptococcus neoformans and C. Gattii around the Mediterranean basin', *FEMS Yeast Research*, 16(4), 1–12.

Collins, H.L. and Bancroft, G.J. (1992) 'Cytokine enhancement of complement-dependent phagocytosis by macrophages: synergy of tumor necrosis factor-α and granulocyte-macrophage colony-stimulating factor for phagocytosis of Cryptococcus neoformans', *European Journal of Immunology*, 22(6), 1447–1454.

Collins, L.C., Roberts, A.M., Robinson, T.W. and Joshua, I.G. (1996) 'Direct Effects of Meconium on Rat Tracheal Smooth Muscle Tension in Vitro', *Pediatric Research*, 40, 587–591.

Cordero, R.J.B., Pontes, B., Frases, S., Nakouzi, A.S., Nimrichter, L., Rodrigues, M.L., Viana, N.B. and Casadevall, A. (2013) 'Antibody Binding to Cryptococcus neoformans Impairs Budding by Altering Capsular Mechanical Properties', *The Journal of Immunology*, 190(1), 317–323.

Corr, M., Boyle, D.L., Ronacher, L.M., Lew, B.R., van Baarsen, L.G., Tak, P.P. and Firestein, G.S. (2011) 'Interleukin 1 receptor antagonist mediates the beneficial effects of systemic interferon beta in mice: implications for rheumatoid arthritis.', *Annals of the Rheumatic Diseases*, 70(5), 858–63.

Cox, G.M., McDade, H.C., Chen, S.C., Tucker, S.C., Gottfredsson, M., Wright, L.C., Sorrell, T.C., Leidich, S.D., Casadevall, A., Ghannoum, M.A. and Perfect, J.R. (2001) 'Extracellular phospholipase activity is a virulence factor for Cryptococcus neoformans.', *Molecular Microbiology*, 39(1), 166–75.

Cox, G.M., Mukherjee, J., Cole, G.T., Casadevall, A. and Perfect, J.R. (2000) 'Urease as a virulence factor in experimental cryptococcosis', *Infection and Immunity*, 68(2), 443–448.

Crabtree, J.N., Okagaki, L.H., Wiesner, D.L., Strain, A.K., Nielsen, J.N. and Nielsen, K. (2012) 'Titan Cell Production Enhances the Virulence of Cryptococcus neoformans', *Infection and Immunity*, 80(11), 3776–3785.

Crosby, L., Casey, W., Morgan, K., Ni, H., Yoon, L., Easton, M., Misukonis, M., Burleson, G. and Ghosh, D.K. (2010) 'Murine J774 macrophages recognize LPS/IFN-g, non-CpG DNA or two-CpG DNA-containing sequences as immunologically distinct', *Nitric Oxide*, 22(3), 242–257.

Cross, C.E. and Bancroft, G.J. (1995) 'Ingestion of acapsular Cryptococcus neoformans occurs via mannose and beta-glucan receptors, resulting in cytokine production and increased phagocytosis of the encapsulated form.', *Infection and Immunity*, 63(7), 2604–11.

Crowhurst, M.O., Layton, J.E. and Lieschke, G.J. (2002) 'Developmental biology of zebrafish myeloid cells', *Int J Dev Biol*, 46(4), 483–492.

Cui, G. (2019) 'TH9, TH17, and TH22 Cell Subsets and Their Main Cytokine Products in the Pathogenesis of Colorectal Cancer', *Frontiers in Oncology*, 9, 1002.

Cui, K., Ardell, C.L., Podolnikova, N.P. and Yakubenko, V.P. (2018) 'Distinct Migratory Properties of M1, M2, and Resident Macrophages Are Regulated by αDβ2 and αMβ2 Integrin-Mediated Adhesion', *Frontiers in Immunology*, 9, 2650.

Culley, F.J. (2009) 'Natural killer cells in infection and inflammation of the lung', *Immunology*, 128(2), 151–163.

Curtis, F. (1896) 'Contribution à l'étude de la saccharomycose humaine', *Ann Inst Pasteur*, 10, 449–468.

Daëron, M. (1997) 'Fc receptor biology', *Annual Review of Immunology*, 15, 203–234.

Dallagi, A., Girouard, J., Hamelin-Morrissette, J., Dadzie, R., Laurent, L., Vaillancourt, C., Lafond, J., Carrier, C. and Reyes-Moreno, C. (2015) 'The activating effect of IFN-γ on monocytes/macrophages is regulated by the LIF-trophoblast-IL-10 axis via Stat1 inhibition and Stat3 activation', *Cellular and Molecular Immunology*, 12(3), 326–341.

Dambuza, I.M., Drake, T., Chapuis, A., Zhou, X., Correia, J., Taylor-Smith, L., LeGrave, N., Rasmussen, T., Fisher, M.C., Bicanic, T., Harrison, T.S., Jaspars, M., May, R.C., Brown, G.D., Yuecel, R., MacCallum, D.M. and Ballou, E.R. (2018) 'The

Cryptococcus neoformans Titan cell is an inducible and regulated morphotype underlying pathogenesis', *PLoS Pathogens*, 14(5), e1006978.

Damsker, J.M., Hansen, A.M. and Caspi, R.R. (2010) 'Th1 and Th17 cells: adversaries and collaborators.', *Annals of the New York Academy of Sciences*, 1183, 211–21.

Danov, O., Martin, G., Greif, A., Bailly, B., Braubach, P., Jonigk, D.D., Warnecke, G., von Itzstein, M., Sewald, K., Wronski, S. and Braun, A. (2019) 'Enhanced Tissue Damage Following H1N1 Infection in Human Precision-Cut Lung Slices (PCLS)', in *American Thoracic Society International Conference Meetings Abstracts American Thoracic Society International Conference Meetings Abstracts*. American Thoracic Society, A5742–A5742.

Das, S., MacDonald, K., Chang, H.-Y.S. and Mitzner, W. (2013) 'A Simple Method of Mouse Lung Intubation', *JoVE*, (73), 50318.

Datta, K., Bartlett, K.H., Baer, R., Byrnes, E., Galanis, E., Heitman, J., Hoang, L., Leslie, M.J., MacDougall, L., Magill, S.S., Morshed, M.G., Marr, K.A. and Northwest, for the C. gattii W.G. of the P. (2009) 'Spread of Cryptococcus gattii into Pacific Northwest Region of the United States', *Emerging Infectious Diseases*, 15(8), 1185–1191.

Davidson, A.J. and Zon, L.I. (2004) 'The "definitive" (and 'primitive') guide to zebrafish hematopoiesis', *Oncogene*, 23(6), 7233–7246.

Davis, J., Zheng, W.Y., Glatman-Freedman, A., Ng, J.A.N., Pagcatipunan, M.R., Lessin, H., Casadevall, A. and Goldman, D.L. (2007) 'Serologic evidence for regional differences in pediatric cryptococcal infection', *Pediatric Infectious Disease Journal*, 26(6), 549–551.

Davis, J.M., Huang, M., Botts, M.R., Hull, C.M. and Huttenlocher, A. (2016) 'A zebrafish model of cryptococcal infection reveals roles for macrophages, endothelial cells, and neutrophils in the establishment and control of sustained fungemia', *Infection and Immunity*, 84(10), 3047–3062.

Davis, M.J., Eastman, A.J., Qiu, Y., Gregorka, B., Kozel, T.R., Osterholzer, J.J., Curtis, J.L., Swanson, J.A. and Olszewski, M.A. (2015) '*Cryptococcus neoformans*– Induced Macrophage Lysosome Damage Crucially Contributes to Fungal Virulence', *The Journal of Immunology*, 194(5), 2219–2231.

DeBess, E., Lockhart, S.R., Iqbal, N. and Cieslak, P.R. (2014) 'Isolation of Cryptococcus gattii from Oregon soil and tree bark, 2010-2011', *BMC Microbiology*, 14(1), 323.

Decken, K., Köhler, G., Palmer-Lehmann, K., Wunderlin, A., Mattner, F., Magram, J., Gately, M.K. and Alber, G. (1998) 'Interleukin-12 is essential for a protective Th1 response in mice infected with Cryptococcus neoformans', *Infection and Immunity*, 66(10), 4994–5000.

Decote-Ricardo, D., LaRocque-de-Freitas, I.F., Rocha, J.D.B., Nascimento, D.O., Nunes, M.P., Morrot, A., Freire-de-Lima, L., Previato, J.O., Mendonça-Previato, L. and Freire-de-Lima, C.G. (2019) 'Immunomodulatory Role of Capsular Polysaccharides Constituents of Cryptococcus neoformans', *Frontiers in Medicine*, 6, 129.

DeDiego, M.L., Martinez-Sobrido, L. and Topham, D.J. (2019) 'Novel Functions of IFI44L as a Feedback Regulator of Host Antiviral Responses', *Journal of Virology*, 93(21).

Deeks, S.G., Tracy, R. and Douek, D.C. (2013) 'Systemic Effects of Inflammation on Health during Chronic HIV Infection', *Immunity*, 39(4), 633.

Denham, S.T. and Brown, J.C.S. (2018) 'Mechanisms of pulmonary escape and dissemination by cryptococcus neoformans', *Journal of Fungi*, 4(1), 25.

Denning, D.W., Stevens, D.A. and Hamilton, J.R. (1990) 'Comparison of Guizotia abyssinica seed extract (birdseed) agar with conventional media for selective identification or Cryptococcus neoformans in patients with acquired immunodeficiency syndrome', *Journal of Clinical Microbiology*, 28(11), 2565–2567.

Denton, M.D., Geehan, C.S., Alexander, S.I., Sayegh, M.H. and Briscoe, D.M. (1999) 'Endothelial cells modify the costimulatory capacity of transmigrating leukocytes and promote CD28-mediated CD4+ T cell alloactivation', *Journal of Experimental Medicine*, 190(4), 555–566.

Diamond, R.D. and Bennett, J.E. (1974) 'Prognostic factors in cryptococcal meningitis. A study in 111 cases', *Annals of Internal Medicine*, 80(2), 176–181.

Ding, A.H., Nathan, C.F. and Stuehr, D.J. (1988) 'Release of reactive nitrogen intermediates and reactive oxygen intermediates from mouse peritoneal macrophages. Comparison of activating cytokines and evidence for independent production', *J Immunol*, 141(7), 2407–2412.

Dockrell, D.H., Lee, M., Lynch, D.H. and Read, R.C. (2001) 'Immune-Mediated Phagocytosis and Killing of *Streptococcus pneumoniae* Are Associated with Direct and Bystander Macrophage Apoptosis', *The Journal of Infectious Diseases*, 184(6), 713–722.

Domev, H., Milkov, I., Itskovitz-Eldor, J. and Dar, A. (2014) 'Immunoevasive Pericytes

From Human Pluripotent Stem Cells Preferentially Modulate Induction of Allogeneic Regulatory T Cells', *Stem Cells Translational Medicine*, 3(10), 1169–1181.

Dragotakes, Q., Fu, M.S. and Casadevall, A. (2019) 'Dragotcytosis: Elucidation of the Mechanism for *Cryptococcus neoformans* Macrophage-to-Macrophage Transfer', *The Journal of Immunology*, 202(9), 2661–2670.

Drevets, D.A., Leenen, P.J.M. and Campbell, P.A. (1996) 'Complement receptor type 3 mediates phagocytosis and killing of Listeria monocytogenes by a TNF-α- and IFN-γ-stimulated macrophage precursor hybrid', *Cellular Immunology*, 169(1), 1–6.

Dromer, F., Moulignier, A., Dupont, B., Guého, E., Baudrimont, M., Improvisi, L., Provost, F. and Gonzalez-Canali, G. (1995) 'Myeloradiculitis due to Cryptococcus curvatus in AIDS', *AIDS*, 9(4), 395–396.

Dromer, F., Perronne, C., Barge, J., Vilde, J.L. and Yeni, P. (1989) 'Role of IgG and complement component C5 in the initial course of experimental cryptococcosis', *Clinical & Experimental Immunology*, 78(3), 412–417.

Dufaud, C., Rivera, J., Rohatgi, S. and Pirofski, L.A. (2018) 'Naïve B cells reduce fungal dissemination in cryptococcus neoformans infected Rag1-/- mice', *Virulence*, 9(1), 173–184.

Van Dyke, M.C.C., Chaturvedi, A.K., Hardison, S.E., Leopold Wager, C.M., Castro-Lopez, N., Hole, C.R., Wozniak, K.L. and Wormley, F.L. (2017) 'Induction of broad-spectrum protective immunity against disparate Cryptococcus serotypes', *Frontiers in Immunology*, 8, 1359.

Ebsen, M., Mogilevski, G., Anhenn, O., Maiworm, V., Theegarten, D., Schwarze, J. and Morgenroth, K. (2002) 'Infection of murine precision cut lung slices (PCLS) with respiratory syncytial virus (RSV) and chlamydophila pneumoniae using the Krumdieck technique', *Pathology Research and Practice*, 198(11), 747–753.

Edwards, V.E., Sutherland, J.M. and Tyrer, J.H. (1970) 'Cryptococcosis of the central nervous system. Epidemiological, clinical, and therapeutic features', *J Neurol Neurosurg Psychiatry*, 33(4), 415–425.

Ehlenberger, A.G. and Nussenzweig, V. (1977) 'The role of membrane receptors for C3b and C3d in phagocytosis.', *The Journal of Experimental Medicine*, 145(2), 357–71.

Eisenman, H.C., Mues, M., Weber, S.E., Frases, S., Chaskes, S., Gerfen, G. and Casadevall, A. (2007) 'Cryptococcus neoformans laccase catalyses melanin synthesis from both D- and L-DOPA', *Microbiology*, 153(12), 3954–3962.

Ellerbroek, P.M., Ulfman, L.H., Hoepelman, A.I. and Coenjaerts, F.E.J. (2004) 'Cryptococcal glucuronoxylomannan interferes with neutrophil rolling on the endothelium', *Cellular Microbiology*, 6(6), 581–592.

Ellis, D.H. (1987) 'Cryptococcus neoformans var. gattii in Australia', *Journal of Clinical Microbiology*, 25(2), 430–431.

Engelborghs, S., Niemantsverdriet, E., Struyfs, H., Blennow, K., Brouns, R., Comabella, M., Dujmovic, I., van der Flier, W., Frölich, L., Galimberti, D., Gnanapavan, S., Hemmer, B., Hoff, E., Hort, J., Iacobaeus, E., Ingelsson, M., Jan de Jong, F., Jonsson, M., Khalil, M. *et al.* (2017) 'Consensus guidelines for lumbar puncture in patients with neurological diseases', *Alzheimer's and Dementia: Diagnosis, Assessment and Disease Monitoring*, 8, 111–126.

Erbe, D. V., Collins, J.E., Shen, L., Graziano, R.F. and Fanger, M.W. (1990) 'The effect of cytokines on the expression and function of Fc receptors for IgG on human myeloid cells', *Molecular Immunology*, 27(1), 57–67.

Eschke, M., Piehler, D., Schulze, B., Richter, T., Grahnert, A., Protschka, M., Müller, U., Köhler, G., Höfling, C., Rossner, S. and Alber, G. (2015) 'A novel experimental model of Cryptococcus neoformans-related immune reconstitution inflammatory syndrome (IRIS) provides insights into pathogenesis', *European Journal of Immunology*, 45(12), 3339–3350.

Evans, R.J., Li, Z., Hughes, W.S., Djordjevic, J.T., Nielsen, K. and May, R.C. (2015) 'Cryptococcal phospholipase B1 is required for intracellular proliferation and control of titan cell morphology during macrophage infection.', *Infection and Immunity*, 83(4), 1296–304.

Evans, R.J., Pline, K., Loynes, C.A., Needs, S., Aldrovandi, M., Tiefenbach, J., Bielska, E., Rubino, R.E., Nicol, C.J., May, R.C., Krause, H.M., O'Donnell, V.B., Renshaw, S.A. and Johnston, S.A. (2019) '15-keto-prostaglandin E2 activates host peroxisome proliferator-activated receptor gamma (PPAR-γ) to promote Cryptococcus neoformans growth during infection', *PLOS Pathogens*, 15(3), e1007597.

Fa, Z., Xie, Q., Fang, W., Zhang, Haibing, Zhang, Haiwei, Xu, Jintao, Pan, W., Xu, Jinhua, Olszewski, M.A., Deng, X. and Liao, W. (2017) 'RIPK3/Fas-associated death domain axis regulates pulmonary immunopathology to cryptococcal infection independent of necroptosis', *Frontiers in Immunology*, 8(SEP), 1055.

Fan, X., Patera, A.C., Pong-Kennedy, A., Deno, G., Gonsiorek, W., Manfra, D.J., Vassileva, G., Zeng, M., Jackson, C., Sullivan, L., Sharif-Rodriguez, W., Opdenakker, G., Van Damme, J., Hedrick, J.A., Lundell, D., Lira, S.A. and Hipkin, R.W. (2007)

‘Murine CXCR1 is a functional receptor for GCP-2/CXCL6 and interleukin-8/CXCL8’, *Journal of Biological Chemistry*, 282(16), 11658–11666.

Farnoud, A.M., Bryan, A.M., Kechichian, T., Luberto, C. and Del Poeta, M. (2015) ‘The Granuloma Response Controlling Cryptococcosis in Mice Depends on the Sphingosine Kinase 1-Sphingosine 1-Phosphate Pathway.’, *Infection and Immunity*, 83(7), 2705–13.

Farrar, M.A. and Schreiber, R.D. (1993) ‘The Molecular Cell Biology of Interferon-gamma and its Receptor’, *Annual Review of Immunology*, 11(1), 571–611.

Farrer, R.A., Voelz, K., Henk, D.A., Johnston, S.A., Fisher, M.C., May, R.C. and Cuomo, C.A. (2016) ‘Microevolutionary traits and comparative population genomics of the emerging pathogenic fungus *Cryptococcus gattii*’, *Philosophical Transactions of the Royal Society B: Biological Sciences*, 371(1709), 20160021.

Feldmesser, M., Casadevall, A., Kress, Y., Spira, G. and Orlofsky, A. (1997) ‘Eosinophil-Cryptococcus neoformans interactions in vivo and in vitro’, *Infection and Immunity*, 65(5), 1899–1907.

Feldmesser, M., Kress, Y., Novikoff, P. and Casadevall, A. (2000) ‘Cryptococcus neoformans is a facultative intracellular pathogen in murine pulmonary infection.’, *Infection and Immunity*, 68(7), 4225–37.

Fetissov, S.O., Hallman, J., Oreland, L., Klinteberg, B. af, Grenbäck, E., Hulting, A.L. and Hökfelt, T. (2002) ‘Autoantibodies against α-MSH, ACTH, and LHRH in anorexia and bulimia nervosa patients’, *Proceedings of the National Academy of Sciences of the United States of America*, 99(26), 17155–17160.

Fischer, A.H., Jacobson, K.A., Rose, J. and Zeller, R. (2008) ‘Hematoxylin and eosin staining of tissue and cell sections’, *CSH Protocols*, 2008.

Fisher, R.A. (1918) ‘The Correlation Between Relatives on the Supposition of Mendelian Inheritance.’, *Philosophical Transactions of the Royal Society of Edinburgh*, 52, 399–433.

Flaczyk, A., Duerr, C.U., Shourian, M., Lafferty, E.I., Fritz, J.H. and Qureshi, S.T. (2013) ‘ IL-33 Signaling Regulates Innate and Adaptive Immunity to Cryptococcus neoformans ’, *The Journal of Immunology*, 191(5), 2503–2513.

Flesch, I.E.A., Schwamberger, G. and Kaufmann, S.H. (1989) ‘Fungicidal activity of IFN-gamma-activated macrophages. Extracellular killing of Cryptococcus neoformans’, *Journal of Immunology*, 142(9), 3219–3224.

Frazão, S. de O., de Sousa, H.R., da Silva, L.G., Folha, J.D.S., Gorgonha, K.C. de M.,

de Oliveira, G.P., Felipe, M.S.S., Silva-Pereira, I., Casadevall, A., Nicola, A.M. and Albuquerque, P. (2020) 'Laccase affects the rate of cryptococcus neoformans nonlytic exocytosis from macrophages', *mBio*, 11(5), 1–6.

Freskgård, P.O. and Urich, E. (2017) 'Antibody therapies in CNS diseases', *Neuropharmacology*, 120, 38–55.

Fu, M.S., Coelho, C., De Leon-Rodriguez, C.M., Rossi, D.C.P., Camacho, E., Jung, E.H., Kulkarni, M. and Casadevall, A. (2018) 'Cryptococcus neoformans urease affects the outcome of intracellular pathogenesis by modulating phagolysosomal pH', *PLoS Pathogens*, 14(6), e1007144.

Fulton, S.A., Reba, S.M., Pai, R.K., Pennini, M., Torres, M., Harding, C. V and Boom, W.H. (2004) 'Inhibition of major histocompatibility complex II expression and antigen processing in murine alveolar macrophages by Mycobacterium bovis BCG and the 19-kilodalton mycobacterial lipoprotein.', *Infection and Immunity*, 72(4), 2101–10.

Gago, S., Esteban, C., Valero, C., Zaragoza, Ó., De La Bellacasa, J.P. and Buitrago, M.J. (2014) 'A multiplex real-time PCR assay for identification of pneumocystis jirovecii, histoplasma capsulatum,and cryptococcus neoformans/cryptococcus gattii in samples from AIDS patients with opportunistic pneumonia', *Journal of Clinical Microbiology*, 52(4), 1168–1176.

Gál, P., Dobó, J., Beinrohr, L., Pál, G. and Závodszky, P. (2013) 'Inhibition of the serine proteases of the complement system.', *Advances in Experimental Medicine and Biology*, 735, 23–40.

Galanis, E. and MacDougall, L. (2010) 'Epidemiology of Cryptococcus gattii, British Columbia, Canada, 1999-2007', *Emerging Infectious Diseases*, 16(2), 251–257.

García-Barbazán, I., Trevijano-Contador, N., Rueda, C., de Andrés, B., Pérez-Tavárez, R., Herrero-Fernández, I., Gaspar, M.L. and Zaragoza, O. (2016) 'The formation of titan cells in *Cryptococcus neoformans* depends on the mouse strain and correlates with induction of Th2-type responses', *Cellular Microbiology*, 18(1), 111–124.

Garro, A.P., Chiapello, L.S., Baronetti, J.L. and Masih, D.T. (2011) 'Rat eosinophils stimulate the expansion of Cryptococcus neoformans-specific CD4+ and CD8+ T cells with a T-helper 1 profile', *Immunology*, 132(2), 174–187.

Gasse, P., Mary, C., Guenon, I., Noulin, N., Charron, S., Schnyder-Candrian, S., Schnyder, B., Akira, S., Quesniaux, V.F.J., Lagente, V., Ryffel, B. and Couillin, I. (2007) 'IL-1R1/MyD88 signaling and the inflammasome are essential in pulmonary inflammation and fibrosis in mice', *Journal of Clinical Investigation*, 117(12), 3786–99.

Gazzoni, A.F., Severo, C.B., Salles, E.F. and Severo, L.C. (2009) 'Histopathology, serology and cultures in the diagnosis of cryptococcosis', *Revista do Instituto de Medicina Tropical de Sao Paulo*, 51(5), 255–259.

Gershenwald, J.E., Fong, Y.M., Fahey 3rd, T.J., Calvano, S.E., Chizzonite, R., Kilian, P.L., Lowry, S.F. and Moldawer, L.L. (1990) 'Interleukin 1 receptor blockade attenuates the host inflammatory response', *Proc. Natl. Acad. Sci. USA*, 87(13), 4966–4970.

Gervais, F., Desforges, C. and Skamene, E. (1989) 'The C5-sufficient A/J congenic mouse strain. Inflammatory response and resistance to Listeria monocytogenes', *Journal of Immunology*, 142(6), 2057–2060.

Geunes-Boyer, S., Beers, M.F., Perfect, J.R., Heitman, J. and Wright, J.R. (2012) 'Surfactant protein D facilitates Cryptococcus neoformans infection', *Infection and Immunity*, 80(7), 2444–2453.

Geunes-Boyer, S., Oliver, T.N., Janbon, G., Lodge, J.K., Heitman, J., Perfect, J.R. and Wright, J.R. (2009) 'Surfactant protein D increases phagocytosis of hypocapsular Cryptococcus neoformans by murine macrophages and enhances fungal survival', *Infection and Immunity*, 77(7), 2783–2794.

Ghasemi, A. and Záhediasl, S. (2012) 'Normality Tests for Statistical Analysis: A Guide for Non-Statisticians', *International Journal of Endorinology Metabolism*, 10(2), 486–489.

Gibson, J.F. and Johnston, S.A. (2015) 'Immunity to Cryptococcus neoformans C. gattii during cryptococcosis', *Fungal Genetics and Biology*, 78, 76–86.

Gilbert, A.S. (2017) *Investigating the Molecular Mechanisms of Vomocytosis*. University of Birmingham.

Gilbert, A.S., Seoane, P.I., Sephton-Clark, P., Bojarczuk, A., Hotham, R., Giurisato, E., Sarhan, A.R., Hillen, A., Velde, G. Vande, Gray, N.S., Alessi, D.R., Cunningham, D.L., Tournier, C., Johnston, S.A. and May, R.C. (2017) 'Vomocytosis of live pathogens from macrophages is regulated by the atypical MAP kinase ERK5', *Science Advances*, 3(8), e1700898.

Giles, S.S., Zaas, A.K., Reidy, M.F., Perfect, J.R. and Wright, J.R. (2007) 'Cryptococcus neoformans is resistant to Surfactant protein A mediated host defense mechanisms', *PLoS ONE*, 2(12).

Goerke, J. (1998) 'Pulmonary surfactant: Functions and molecular composition', *Biochimica et Biophysica Acta - Molecular Basis of Disease*, 1408(2–3), 79–89.

Goldberg, M., Belkowski, L.S. and Bloom, B.R. (1990) 'Regulation of Macrophage Function by Interferon-y Somatic Cell Genetic Approaches in Murine Macrophage Cell Lines to Mechanisms of Growth Inhibition, the Oxidative Burst, and Expression of the Chronic Granulomatous Disease Gene', *Journal of Clinical Investigation*, 85, 563–569.

Goldberg, M., Nagata, Y. and Bloom, B.R. (1985) 'IFN alpha and IFN gamma inhibit the growth of macrophage cell lines and variants by different mechanisms', in *The Interferon System*. 1st edn. Springer-Verlag Wien, 349–353.

Goldman, D., Lee, S.C., Mednick, A.J., Montella, L. and Casadevall, A. (2000) *Persistent Cryptococcus neoformans Pulmonary Infection in the Rat Is Associated with Intracellular Parasitism, Decreased Inducible Nitric Oxide Synthase Expression, and Altered Antibody Responsiveness to Cryptococcal Polysaccharide*, *Infection and Immunity*.

Goldman, D., Song, X., Kitai, R., Casadevall, A., Zhao, M.L. and Lee, S.C. (2001) 'Cryptococcus neoformans induces macrophage inflammatory protein 1α (MIP-1α) and MIP-1β in human microglia: Role of specific antibody and soluble capsular polysaccharide', *Infection and Immunity*, 69(3), 1808–1815.

Goldman, Khine, Abadi, J., Lindenberg, D.J., Pirofski, L., Niang, R., Casadevall, A., Pirofski La, L., Niang, R. and Casadevall, A. (2001) 'Serologic Evidence for Cryptococcus neoformans Infection in Early Childhood', *Pediatrics*, 107(5), E66.

Gomes, M.C. and Mostowy, S. (2020) 'The Case for Modeling Human Infection in Zebrafish', *Trends in Microbiology*, 28, 10–18.

Gonzalez, P.V., Cragnolini, A.B., Schiöth, H.B. and Scimonelli, T.N. (2006) 'Interleukin-1β-induced anorexia is reversed by ghrelin', *Peptides*, 27(12), 3220–3225.

Gordon, M.A., Jack, D.L., Dockrell, D.H., Lee, M.E. and Read, R.C. (2005) 'Gamma interferon enhances internalization and early nonoxidative killing of Salmonella enterica serovar Typhimurium by human macrophages and modifies cytokine responses', *Infection and Immunity*, 73(6), 3445–3452.

Granger, D.L., Perfect, J.R. and Durack, D.T. (1986) 'Macrophage-mediated fungistasis in vitro: Requirements for intracellular and extracellular cytotoxicity', *The Journal of Immunology*, 136, 672–680.

Greenlee-Wacker, M.C. (2016) 'Clearance of apoptotic neutrophils and resolution of inflammation', *Immunological Reviews*, 273(1), 357–370.

Grégoire, M., Uhel, F., Lesouhaitier, M., Gacouin, A., Guirriec, M., Mourcin, F., Dumontet, E., Chalin, A., Samson, M., Berthelot, L.L., Tissot, A., Kerjouan, M.,

Jouneau, S., Le Tulzo, Y., Tarte, K., Zmijewski, J.W. and Tadié, J.M. (2018) 'Impaired efferocytosis and neutrophil extracellular trap clearance by macrophages in ARDS', *European Respiratory Journal*, 52(2).

Gross, N.T., Camner, P., Chinchilla, M. and Jarstrand, C. (1998) 'In vitro effect of lung surfactant on alveolar macrophage defence mechanisms against Cryptococcus neoformans', *Mycopathologia*, 144(1), 21–27.

Guillot, L., Carroll, S.F., Homer, R. and Qureshi, S.T. (2008) 'Enhanced innate immune responsiveness to pulmonary Cryptococcus neoformans infection is associated with resistance to progressive infection', *Infection and Immunity*, 76(10), 4745–4756.

Guo, C., Chen, M., Fa, Z., Lu, A., Fang, W., Sun, B., Chen, C., Liao, W. and Meng, G. (2014) 'Acapsular Cryptococcus neoformans activates the NLRP3 inflammasome', *Microbes and Infection*, 16(10), 845–854.

Guo, R. and Ward, P.A. (2005) 'Role of C5a in inflammatory responses', *Annual Review of Immunology*, 23(1), 821–852.

Gupta, J.W., Kubin, M., Hartman, L., Cassatella, M. and Trinchieri, G. (1992) 'Induction of Expression of Genes Encoding Components of the Respiratory Burst Oxidase during Differentiation of Human Myeloid Cell Lines Induced by Tumor Necrosis Factor and γ-Interferon', *Cancer Research*, 52(9), 2530–2537.

Gutteridge, J.M.C. (1989) 'Iron and Oxygen: A Biologically Damaging Mixture', *Acta Paediatrica*, 78(361), 78–85.

Gyetko, M.R., Chen, G.H., McDonald, R.A., Goodman, R., Huffnagle, G.B., Wilkinson, C.C., Fuller, J.A. and Toews, G.B. (1996) 'Urokinase is required for the pulmonary inflammatory response to Cryptococcus neoformans: A murine transgenic model', *Journal of Clinical Investigation*, 97(8), 1818–1826.

Haczku, A. (2008) 'Protective role of the lung collectins surfactant protein A and surfactant protein D in airway inflammation', *Journal of Allergy and Clinical Immunology*, 122(5), 861–879.

Haddow, L.J., Colebunders, R., Meintjes, G., Lawn, S.D., Elliott, J.H., Manabe, Y.C., Bohjanen, P.R., Sungkanuparph, S., Easterbrook, P.J., French, M.A. and Boulware, D.R. (2010) 'Cryptococcal immune reconstitution inflammatory syndrome in HIV-1-infected individuals: proposed clinical case definitions', *The Lancet Infectious Diseases*. NIH Public Access, 791–802.

Haddow, L.J., Easterbrook, P.J., Mosam, A., Khanyile, N.G., Parboosing, R., Moodley, P. and Moosa, M.Y.S. (2009) 'Defining immune reconstitution inflammatory syndrome:

Evaluation of expert opinion versus 2 case definitions in a south african cohort', *Clinical Infectious Diseases*, 49(9), 1424–1432.

Hagen, F., Khayhan, K., Theelen, B., Kolecka, A., Polacheck, I., Sionov, E., Falk, R., Parnmen, S., Lumbsch, H.T. and Boekhout, T. (2015) 'Recognition of seven species in the Cryptococcus gattii/Cryptococcus neoformans species complex', *Fungal Genetics and Biology*, 78, 16–48.

Hagen, F., Lumbsch, H.T., Arsic Arsenijevic, V., Badali, H., Bertout, S., Billmyre, R.B., Bragulat, M.R., Cabañes, F.J., Carbia, M., Chakrabarti, A., Chaturvedi, S., Chaturvedi, V., Chen, M., Chowdhary, A., Colom, M.-F., Cornely, O.A., Crous, P.W., Cuétara, M.S., Diaz, M.R. *et al.* (2017) 'Importance of Resolving Fungal Nomenclature: the Case of Multiple Pathogenic Species in the Cryptococcus Genus', *mSphere*, 2(4), 238–255.

Haley, P.J. (2003) 'Species differences in the structure and function of the immune system', *Toxicology*, 188(1), 49–71.

Hansakon, A., Ngamskulrungroj, P. and Angkasekwinai, P. (2020) 'Contribution of Laccase Expression to Immune Response against Cryptococcus gattii Infection', *Infection and Immunity*, 88(3).

Hardison, S.E., Ravi, S., Wozniak, K.L., Young, M.L., Olszewski, M.A. and Wormley, F.L. (2010) 'Pulmonary Infection with an Interferon-γ-Producing Cryptococcus neoformans Strain Results in Classical Macrophage Activation and Protection', *The American Journal of Pathology*, 176(2), 774–785.

Hardison, S.E., Wozniak, K.L., Kolls, J.K. and Wormley, F.L. (2010) 'Interleukin-17 is not required for classical macrophage activation in a pulmonary mouse model of Cryptococcus neoformans infection.', *Infection and Immunity*, 78(12), 5341–51.

Hardy, G.A.D., Sieg, S., Rodriguez, B., Anthony, D., Asaad, R., Jiang, W., Mudd, J., Schacker, T., Funderburg, N.T., Pilch-Cooper, H.A., Debernardo, R., Rabin, R.L., Lederman, M.M. and Harding, C. V. (2013) 'Interferon-α Is the Primary Plasma Type-I IFN in HIV-1 Infection and Correlates with Immune Activation and Disease Markers', *PLoS ONE*, 8(2).

Harris, J.R., Lockhart, S.R., Debess, E., Marsden-Haug, N., Goldoft, M., Wohrle, R., Lee, S., Smelser, C., Park, B. and Chiller, T. (2011) 'Cryptococcus gattii in the united states: Clinical aspects of infection with an emerging pathogen', *Clinical Infectious Diseases*, 53(12), 1188–1195.

Hartshorn, K.L., Crouch, E., White, M.R., Colamussi, M.L., Kakkanatt, A., Tauber, B., Shepherd, V. and Sastry, K.N. (1998) 'Pulmonary surfactant proteins A and D enhance

neutrophil uptake of bacteria', *American Journal of Physiology - Lung Cellular and Molecular Physiology*, 274(6 18-6).

Hashimoto, D., Chow, A., Noizat, C., Teo, P., Beasley, M.B., Leboeuf, M., Becker, C.D., See, P., Price, J., Lucas, D., Greter, M., Mortha, A., Boyer, S.W., Forsberg, E.C., Tanaka, M., van Rooijen, N., García-Sastre, A., Stanley, E.R., Ginhoux, F. *et al.* (2013) 'Tissue-Resident Macrophages Self-Maintain Locally throughout Adult Life with Minimal Contribution from Circulating Monocytes', *Immunity*, 38(4), 792–804.

Hassan, M., Blanc, P.J., Pareilleux, A. and Goma, G. (1995) 'Production of cocoa butter equivalents from prickly-pear juice fermentation by an unsaturated fatty acid auxotroph of Cryptococcus curvatus grown in batch culture', *Process Biochemistry*, 30(7), 629–634.

Hayashida, M.Z., Seque, C.A., Pasin, V.P., Enokihara, M.M.S. e. S. and Porro, A.M. (2017) 'Disseminated cryptococcosis with skin lesions: Report of a case series', *Anais Brasileiros de Dermatologia*, 92(5), 69–72.

Hedayati, M.T., Mayahi, S., Fakhar, M., Shokohi, T. and Majidi, M. (2011) 'Cryptococcus neoformans isolation from swallow (Hirundo rustica) excreta in Iran', *Revista do Instituto de Medicina Tropical de São Paulo*, 53(3), 125–127.

Helyes, Z., Tékus, V., Szentes, N., Pohóczky, K., Botz, B., Kiss, T., Kemény, Á., Környei, Z., Tóth, K., Lénárt, N., Ábrahám, H., Pinteaux, E., Francis, S., Sensi, S., Dénes, Á. and Goebel, A. (2019) 'Transfer of complex regional pain syndrome to mice via human autoantibodies is mediated by interleukin-1–induced mechanisms', *Proceedings of the National Academy of Sciences of the United States of America*, 116(26), 13067–13076.

Herndon, F.J. and Kayes, S.G. (1992) 'Depletion of eosinophils by anti-IL-5 monoclonal antibody treatment of mice infected with Trichinella spiralis does not alter parasite burden or immunologic resistance to reinfection', *Journal of Immunology*, 149(11), 3642–3647.

Herold, S., Mayer, K. and Lohmeyer, J. (2011) 'Acute Lung Injury: How Macrophages Orchestrate Resolution of Inflammation and Tissue Repair', *Frontiers in Immunology*, 2(NOV), 65.

Herring, A.C., Falkowski, N.R., Chen, G.-H., McDonald, R.A., Toews, G.B. and Huffnagle, G.B. (2005) 'Transient neutralization of tumor necrosis factor alpha can produce a chronic fungal infection in an immunocompetent host: potential role of immature dendritic cells.', *Infection and Immunity*, 73(1), 39–49.

Hess, A., Wang-Lauenstein, L., Braun, A., Kolle, S.N., Landsiedel, R., Liebsch, M., Ma-Hock, L., Pirow, R., Schneider, X., Steinfath, M., Vogel, S., Martin, C. and Sewald, K. (2016) 'Prevalidation of the ex-vivo model PCLS for prediction of respiratory toxicity', *Toxicology in Vitro*, 32, 347–361.

Heung, L.J. and Hohl, T.M. (2019) 'Inflammatory monocytes are detrimental to the host immune response during acute infection with cryptococcus neoformans', *PLoS Pathogens*, 15(3).

Heyen, L., Müller, U., Siegemund, S., Schulze, B., Protschka, M., Alber, G. and Piehler, D. (2016) 'Lung epithelium is the major source of IL-33 and is regulated by IL-33-dependent and IL-33-independent mechanisms in pulmonary cryptococcosis', *Pathogens and Disease*, 74(7), 86.

Hidalgo, A., Chilvers, E.R., Summers, C. and Koenderman, L. (2019) 'The Neutrophil Life Cycle', *Trends in Immunology*, 40(7), 584–597.

Hirai, Y., Ainoda, Y., Shoji, T., Fujita, T., Yoshinaga, K., Shiseki, M., Mori, N., Teramura, M., Totsuka, K. and Motoji, T. (2011) 'Disseminated Cryptococcosis in a Non-Hodgkin's Lymphoma Patient with Late-Onset Neutropenia Following Rituximab-CHOP Chemotherapy: A Case Report and Literature Review', *Mycopathologia*, 172(3), 227–232.

Hirano, S., Zhou, Q., Furuyama, A. and Kanno, S. (2017) 'Differential Regulation of IL-1β and IL-6 Release in Murine Macrophages', *Inflammation*, 40(6), 1933–1943.

Hoag, K.A., Lipscomb, M.F., Izzo, A.A. and Street, N.E. (1997) 'IL-12 and IFN-γ are required for initiating the protective Th1 response to pulmonary cryptococcosis in resistant C.B-17 Mice', *American Journal of Respiratory Cell and Molecular Biology*, 17(6), 733–739.

Hoag, K.A., Street, N.E., Huffnagle, G.B. and Lipscomb, M.F. (1995) 'Early cytokine production in pulmonary Cryptococcus neoformans infections distinguishes susceptible and resistant mice.', 13(4), 487–495.

Hobeika, A.C., Etienne, W., Torres, B.A., Johnson, H.M. and Subramaniam, P.S. (1999) 'IFN-γ induction of p21(WAF1) is required for cell cycle inhibition and suppression of apoptosis', *Journal of Interferon and Cytokine Research*, 19(12), 1351–1361.

Hoenderdos, K. and Condliffe, A. (2013) 'The neutrophil in chronic obstructive pulmonary disease: Too little, too late or too much, too soon?', *American Journal of Respiratory Cell and Molecular Biology*, 48(5), 531–539.

Hole, C.R., Bui, H., Wormley, F.L. and Wozniak, K.L. (2012) 'Mechanisms of dendritic cell lysosomal killing of cryptococcus', *Scientific Reports*, 2(1), 1–9.

Holladay, S.D. and Smialowicz, R.J. (2000) 'Development of the murine and human immune system: Differential effects of immunotoxicants depend on time of exposure', *Environmental Health Perspectives*, 108(SUPPL. 3), 463–473.

Holmer, S.M., Evans, K.S., Asfaw, Y.G., Saini, D., Schell, W.A., Ledford, J.G., Frothingham, R., Wright, J.R., Sempowski, G.D. and Perfect, J.R. (2014) 'Impact of surfactant protein D, interleukin-5, and eosinophilia on cryptococcosis', *Infection and Immunity*, 82(2), 683–693.

Hommel, B., Mukaremera, L., Cordero, R.J.B., Coelho, C., Desjardins, C.A., Sturny-Leclère, A., Janbon, G., Perfect, J.R., Fraser, J.A., Casadevall, A., Cuomo, C.A., Dromer, F., Nielsen, K. and Alanio, A. (2018) 'Titan cells formation in Cryptococcus neoformans is finely tuned by environmental conditions and modulated by positive and negative genetic regulators', *PLoS Pathogens*, 14(5), e1006982.

Hu, G., Hacham, M., Waterman, S.R., Panepinto, J., Shin, S., Liu, X., Gibbons, J., Valyi-Nagy, T., Obara, K., Jaffe, H.A., Ohsumi, Y. and Williamson, P.R. (2008) 'PI3K signaling of autophagy is required for starvation tolerance and virulence of Cryptococcus neoformans', *Journal of Clinical Investigation*, 118(3), 1186–1197.

Hu, Z., Xu, C., Liu, D., Meng, F., Chi, Y. and Chen, W. (2020) 'Pulmonary cryptococcal immune reconstitution syndrome in a person living with HIV: a case report', *International Journal of STD and AIDS*, 31(3), 280–284.

Huang, H.R., Li, F., Han, H., Xu, X., Li, N., Wang, S., Xu, J.F. and Jia, X.M. (2018) 'Dectin-3 recognizes glucuronoxylomannan of Cryptococcus neoformans serotype AD and Cryptococcus gattii serotype B to initiate host defense against cryptococcosis', *Frontiers in Immunology*, 9(AUG), 6.

Huang, L. and Appleton, J.A. (2016) 'Eosinophils in Helminth Infection: Defenders and Dupes', *Trends in Parasitology*, 32(10), 798–807.

Huang, X., Li, L., Ammar, R., Zhang, Y., Wang, Y., Ravi, K., Thompson, J. and Jarai, G. (2019) 'Molecular characterization of a precision-cut rat lung slice model for the evaluation of antifibrotic drugs', *American Journal of Physiology - Lung Cellular and Molecular Physiology*, 316(2), L348–L357.

Huffnagle, G.B., Lipscomb, M.F., Lovchik, J.A., Hoag, K.A. and Street, N.E. (1994) 'The role of CD4+ and CD8+ T cells in the protective inflammatory response to a pulmonary cryptococcal infection', *Journal of Leukocyte Biology*, 55(1), 35–42.

Huising, M.O., Stet, R.J.M., Savelkoul, H.F.J. and Verburg-Van Kemenade, B.M.L. (2004) 'The molecular evolution of the interleukin-1 family of cytokines; IL-18 in teleost fish', *Developmental and Comparative Immunology*, 28(5), 395–413.

Hunegnaw, R., Mushtaq, Z., Enyindah-Asonye, G., Hoang, T. and Robert-Guroff, M. (2019) 'Alveolar Macrophage Dysfunction and Increased PD-1 Expression During Chronic SIV Infection of Rhesus Macaques', *Frontiers in Immunology*, 10(JULY), 1537.

Husain, S., Wagener, M.M. and Singh, N. (2001) 'Cryptococcus neoformans infection in organ transplant recipients: variables influencing clinical characteristics and outcome.', *Emerging Infectious Diseases*, 7(3), 375–81.

Hussell, T. and Bell, T.J. (2014) 'Alveolar macrophages: Plasticity in a tissue-specific context', *Nature Reviews Immunology*, 14(2), 81–93.

Huston, S.M., Li, S.S., Stack, D., Timm-McCann, M., Jones, G.J., Islam, A., Berenger, B.M., Xiang, R.F., Colarusso, P. and Mody, C.H. (2013) ' Cryptococcus gattii Is Killed by Dendritic Cells, but Evades Adaptive Immunity by Failing To Induce Dendritic Cell Maturation ', *The Journal of Immunology*, 191(1), 249–261.

Ieong, M.H., Reardon, C.C., Levitz, S.M. and Kornfeld, H. (2000) 'Human Immunodeficiency Virus Type 1 Infection of Alveolar Macrophages Impairs Their Innate Fungicidal Activity', *American Journal of Respiratory and Critical Care Medicine*, 162(3), 966–970.

Ikeda, R., Sugita, T., Jacobson, E.S. and Shinoda, T. (2003) 'Effects of melanin upon susceptibility of Cryptococcus to antifungals', *Microbiology and Immunology*, 47(4), 271–277.

INTERFERON GAMMA-1B | Drug | BNF content published by NICE (2021). Available at: https://bnf.nice.org.uk/drug/interferon-gamma-1b.html (Accessed: 7 April 2021).

International Chronic Granulomatous Disease Cooperative Study Group (1991) 'A Controlled Trial of Interferon Gamma to Prevent Infection in Chronic Granulomatous Disease', *New England Journal of Medicine*, 324(8), 509–516.

Israël, N., Hazan, U., Alcami, J., Munier, A., Arenzana-Seisdedos, F., Bachelerie, F., Israël, A. and Virelizier, J.L. (1989) 'Tumor necrosis factor stimulates transcription of HIV-1 in human T lymphocytes, independently and synergistically with mitogens.', *Journal of Immunology*, 143(12), 3956–60.

James, D.G. (2000) 'A clinicopathological classification of granulomatous disorders', *Postgraduate Medical Journal*, 76(898), 457–465.

James, G. (2000) ‘A clinicopathological classification of granulomatous disorders’, *Postgraduate Medical Journal*, 76, 457–465.

Janbon, G., Ormerod, K.L., Paulet, D., Byrnes, E.J., Yadav, V., Chatterjee, G., Mullapudi, N., Hon, C.-C., Billmyre, R.B., Brunel, F., Bahn, Y.-S., Chen, W., Chen, Y., Chow, E.W.L., Coppée, J.-Y., Floyd-Averette, A., Gaillardin, C., Gerik, K.J., Goldberg, J. *et al.* (2014) ‘Analysis of the Genome and Transcriptome of Cryptococcus neoformans var. grubii Reveals Complex RNA Expression and Microevolution Leading to Virulence Attenuation’, *PLoS Genetics*, 10(4), e1004261.

Janeway Jr., C.A., Travers, P., Walport, M. and Shlomchik, M.J. (2001) ‘Janeway Immunobiology’, in Austin, P. and Lawrence, E. (eds) *Janeway Immunobiology*. 5th edn. New York: Garland Publishing, 15–19.

Jarvis, J.N., Bicanic, T., Loyse, A., Namarika, D., Jackson, A., Nussbaum, J.C., Longley, N., Muzoora, C., Phulusa, J., Taseera, K., Kanyembe, C., Wilson, D., Hosseinipour, M.C., Brouwer, A.E., Limmathurotsakul, D., White, N., van der Horst, C., Wood, R., Meintjes, G. *et al.* (2014) ‘Determinants of Mortality in a Combined Cohort of 501 Patients With HIV-Associated Cryptococcal Meningitis: Implications for Improving Outcomes’, *Clinical Infectious Diseases*, 58(5), 736–745.

Jarvis, J.N., Casazza, J.P., Stone, H.H., Meintjes, G., Lawn, S.D., Levitz, S.M., Harrison, T.S. and Koup, R.A. (2013) ‘The phenotype of the cryptococcus-specific CD4+ memory T-cell response is associated with disease severity and outcome in HIV-associated cryptococcal meningitis’, *Journal of Infectious Diseases*, 207(12), 1817–1828.

Jarvis, J.N., Meintjes, G., Bicanic, T., Buffa, V., Hogan, L., Mo, S., Tomlinson, G., Kropf, P., Noursadeghi, M., Harrison, T.S. and Alspaugh, J.A. (2015) ‘Cerebrospinal Fluid Cytokine Profiles Predict Risk of Early Mortality and Immune Reconstitution Inflammatory Syndrome in HIV-Associated Cryptococcal Meningitis’, *PLoS Pathogens*, 11(4).

Jarvis, J.N., Meintjes, G., Rebe, K., Williams, G.N., Bicanic, T., Williams, A., Schutz, C., Bekker, L.-G., Wood, R. and Harrison, T.S. (2012) ‘Adjunctive interferon-γ immunotherapy for the treatment of HIV-associated cryptococcal meningitis’, *AIDS*, 26(9), 1105–1113.

Jaumouillé, V. and Waterman, C.M. (2020) ‘Physical Constraints and Forces Involved in Phagocytosis’, *Frontiers in Immunology*, 11, 1097.

Jayaraman, P., Sada-Ovalle, I., Nishimura, T., Anderson, A.C., Kuchroo, V.K., Remold, H.G. and Behar, S.M. (2013) ‘IL-1β Promotes Antimicrobial Immunity in Macrophages

by Regulating TNFR Signaling and Caspase-3 Activation', *The Journal of Immunology*, 190(8), 4196–4204.

Jeans, A., Ustianowski, A., Vilar, J. and Wilkins, E. (2011) 'Voriconazole treatment of cryptococcal meningitis', *Journal of Infection*, 63(6), e76.

Jennings, B.H. (2011) 'Drosophila-a versatile model in biology & medicine', *Materials Today*, 14(5), 190–195.

Johnston, S.A. and May, R.C. (2010) 'The human fungal pathogen Cryptococcus neoformans escapes macrophages by a phagosome emptying mechanism that is inhibited by Arp2/3 complex-mediated actin polymerisation.', *PLoS pathogens*, 6(8), e1001041.

Johnston, S.A. and May, R.C. (2013) '*Cryptococcus* interactions with macrophages: evasion and manipulation of the phagosome by a fungal pathogen', *Cellular Microbiology*, 15(3), 403–411.

Jones, G.J., Wiseman, J.C.D., Marr, K.J., Wei, S., Djeu, J.Y. and Mody, C.H. (2009) 'In contrast to anti-tumor activity, YT cell and primary NK cell cytotoxicity for Cryptococcus neoformans bypasses LFA-1', *International Immunology*, 21(4), 423–432.

Jung, K.W., Strain, A.K., Nielsen, K., Jung, K.H. and Bahn, Y.S. (2012) 'Two cation transporters Ena1 and Nha1 cooperatively modulate ion homeostasis, antifungal drug resistance, and virulence of Cryptococcus neoformans via the HOG pathway', *Fungal Genetics and Biology*, 49(4), 332–345.

Kahlenberg, J.M. and Dubyak, G.R. (2004) 'Differing caspase-1 activation states in monocyte versus macrophage models of IL-1β processing and release', *Journal of Leukocyte Biology*, 76(3), 676–684.

Kaiko, G.E., Horvat, J.C., Beagley, K.W. and Hansbro, P.M. (2008) 'Immunological decision-making: How does the immune system decide to mount a helper T-cell response?', *Immunology*, 123(3), 326–338.

Kambugu, A., Meya, D.B., Rhein, J., O'Brien, M., Janoff, E.N., Ronald, A.R., Kamya, M.R., Mayanja-Kizza, H., Sande, M.A., Bohjanen, P.R. and Boulware, D.R. (2008) 'Outcomes of cryptococcal meningitis in Uganda before and after the availability of highly active antiretroviral therapy', *Clinical Infectious Diseases*, 46(11), 1694–1701.

Kamiński, D.M. (2014) 'Recent progress in the study of the interactions of amphotericin B with cholesterol and ergosterol in lipid environments', *European Biophysics Journal*, 43(10–11), 453–467.

Kammalac Ngouana, T., Dongtsa, J., Kouanfack, C., Tonfack, C., Fomena, S., Mallié, M., Delaporte, E., Boyom, F.F. and Bertout, S. (2015) 'Cryptoccocal meningitis in Yaoundé (Cameroon) HIV infected patients: Diagnosis, frequency and Cryptococcus neoformans isolates susceptibility study to fluconazole', *Journal de Mycologie Medicale*, 25(1), 11–16.

Kamperschroer, C. and Quinn, D.G. (2002) 'The Role of Proinflammatory Cytokines in Wasting Disease During Lymphocytic Choriomeningitis Virus Infection', *The Journal of Immunology*, 169(1), 340–349.

Kamuyango, A.A. (2017) *Stimulation of innate immunity leads to clearance of C. neoformans infection in zebrafish*. The University of Sheffield.

Kang, T.J., Lee, G.S., Kim, S.K., Jin, S.H. and Chae, G.T. (2010) 'Comparison of two mice strains, A/J and C57BL/6, in caspase-1 activity and IL-1β secretion of macrophage to Mycobacterium leprae infection', *Mediators of Inflammation*, 2010.

Katchanov, J., von Kleist, M., Arastéh, K. and Stocker, H. (2014) '"Time-to-amphotericin B" in cryptococcal meningitis in a European low-prevalence setting: analysis of diagnostic delays', *QJM: An International Journal of Medicine*, 107(10), 799–803.

Kavanagh, K. and Fallon, J.P. (2010) 'Galleria mellonella larvae as models for studying fungal virulence', *Fungal Biology Reviews*, 24, 79–83.

Kawakami, K., Koguchi, Y., Qureshi, M.H., Miyazato, A., Yara, S., Kinjo, Y., Iwakura, Y., Takeda, K., Akira, S., Kurimoto, M. and Saito, A. (2000) ' IL-18 Contributes to Host Resistance Against Infection with Cryptococcus neoformans in Mice with Defective IL-12 Synthesis Through Induction of IFN-γ Production by NK Cells ', *The Journal of Immunology*, 165(2), 941–947.

Kawakami, K., Koguchi, Y., Qureshi, M.H., Yara, S., Kinjo, Y., Uezu, K. and Saito, A. (2000) 'NK cells eliminate Cryptococcus neoformans by potentiating the fungicidal activity of macrophages rather than by directly killing them upon stimulation with IL-12 and IL-18', *Microbiology and Immunology*, 44(12), 1043–1050.

Kawakami, K., Qifeng, X., Tohyama, M., Qureshi, M.H. and Saito, A. (1996) 'Contribution of tumour necrosis factor-alpha (TNF-alpha) in host defence mechanism against Cryptococcus neoformans.', *Clinical and Experimental Immunology*, 106(3), 468–74.

Kawakami, K., Qureshi, M.H., Koguchi, Y., Nakajima, K. and Saito, A. (1999) 'Differential effect of Cryptococcus neoformans on the production of IL-12p40 and IL-10

by murine macrophages stimulated with lipopolysaccharide and gamma interferon', *FEMS Microbiology Letters*, 175, 87–94.

Kawakami, K., Qureshi, M.H., Zhang, T., Okamura, H., Kurimoto, M. and Saito, A. (1997) 'IL-18 protects mice against pulmonary and disseminated infection with Cryptococcus neoformans by inducing IFN-gamma production', *Journal of Immunology*, 159(11), 5528–5534.

Kawasaki, T. and Kawai, T. (2014) 'Toll-Like Receptor Signaling Pathways', *Frontiers in Immunology*, 5(SEP), 461.

Kechichian, T.B., Shea, J. and Del Poeta, M. (2007) 'Depletion of alveolar macrophages decreases the dissemination of a glucosylceramide-deficient mutant of Cryptococcus neoformans in immunodeficient mice', *Infection and Immunity*, 75(10), 4792–4798.

Keller, P.J. (2013) 'In vivo imaging of zebrafish embryogenesis', *Methods*, 62(3), 268–278.

Kelly, R.M., Chen, J., Yauch, L.E. and Levitz, S.M. (2005) 'Opsonic requirements for dendritic cell-mediated responses to Cryptococcus neoformans', *Infection and Immunity*, 73(1), 592–598.

Kendall, L. V., Owiny, J.R., Dohm, E.D., Knapek, K.J., Lee, E.S., Kopanke, J.H., Fink, M., Hansen, S.A. and Ayers, J.D. (2018) 'Replacement, Refinement, and Reduction in Animal Studies With Biohazardous Agents', *ILAR Journal*, 59(2), 177–194.

Kestelyn, P., Taelman, H., Bogaerts, J., Kagame, A., Aziz, M.A., Batungwanayo, J., Stevens, A.M. and Van de Perre, P. (1993) 'Ophthalmic manifestations of infections with Cryptococcus neoformans in patients with the acquired immunodeficiency syndrome', *American Journal of Ophthalmology*, 116(6), 721–727.

Kidd, S.E., Hagen, F., Tscharke, R.L., Huynh, M., Bartlett, K.H., Fyfe, M., MacDougall, L., Boekhout, T., Kwon-Chung, K.J. and Meyer, W. (2004) 'A rare genotype of Cryptococcus gattii caused the cryptococcosis outbreak on Vancouver Island (British Columbia, Canada)', *Proceedings of the National Academy of Sciences of the United States of America*, 101(49), 17258–17263.

Kim, J., Koo, B. and Knoblich, J. (2020) 'Human organoids: model systems for human biology and medicine', *Nature Reviews Molecular Cell Biology*, 21, 571–584.

Kimmel, C.B., Ballard, W.W., Kimmel, S.R., Ullmann, B. and Schilling, T.F. (1995) *Stages of Embryonic Development of the Zebrafish*.

King, D.P. and Jones, P.P. (1983) ‘Induction of Ia and H-2 antigens on a macrophage cell line by immune interferon’, *J Immunol*, 131(1), 315–318.

Kirkpatrick, W.R., Najvar, L.K., Bocanegra, R., Patterson, T.F. and Graybill, J.R. (2007) ‘New guinea pig model of cryptococcal meningitis’, *Antimicrobial Agents and Chemotherapy*, 51(8), 3011–3013.

Klein, K.R., Hall, L., Deml, S.M., Rysavy, J.M., Wohlfiel, S.L. and Wengenack, N.L. (2009) ‘Identification of Cryptococcus gattii by use of L-canavanine glycine bromothymol blue medium and DNA sequencing’, *Journal of Clinical Microbiology*, 47(11), 3669–3672.

Kmoníčková, E., Melkusová, P., Farghali, H., Holý, A. and Zídek, Z. (2007) ‘Nitric oxide production in mouse and rat macrophages: A rapid and efficient assay for screening of drugs immunostimulatory effects in human cells’, *Nitric Oxide*, 17(3–4), 160–169.

Kneale, M., Bartholomew, J.S., Davies, E. and Denning, D.W. (2016) ‘Global access to antifungal therapy and its variable cost’, *Journal of Antimicrobial Chemotherapy*, 71(12), 3599–3606.

Ko, Y.J., Yu, Y.M., Kim, G.B., Lee, G.W., Maeng, P.J., Kim, S., Floyd, A., Heitman, J. and Bahn, Y.S. (2009) ‘Remodeling of global transcription patterns of Cryptococcus neoformans genes mediated by the stress-activated HOG signaling pathways’, *Eukaryotic Cell*, 8(8), 1197–1217.

Koguchi, Y. and Kawakami, K. (2002) ‘Cryptococcal infection and Th1-Th2 cytokine balance’, *International Reviews of Immunology*, 21(4–5), 423–428.

Koo, G.C., Blake, J.T., Talento, A., Nguyen, M., Lin, S., Sirotina, A., Shah, K., Mulvany, K., Hora, D., Cunningham, P., Wunderler, D.L., McManus, O.B., Slaughter, R., Bugianesi, R., Felix, J., Garcia, M., Williamson, J., Kaczorowski, G., Sigal, N.H. *et al.* (1997) ‘Blockade of the voltage-gated potassium channel Kv1.3 inhibits immune responses in vivo.’, *The Journal of Immunology*, 158(11).

Koval, M., Preiter, K., Adles, C., Stahl, P.D. and Steinberg, T.H. (1998) ‘Size of IgG-opsonized particles determines macrophage response during internalization’, *Experimental Cell Research*, 242(1), 265–273.

Kozel, T.R., Wilson, M.A. and Murphy, J.W. (1991) ‘Early events in initiation of alternative complement pathway activation by the capsule of Cryptococcus neoformans.’, *Infection and Immunity*, 59(9), 3101–10.

Krarup, A., Chattopadhyay, P., Bhattacharjee, A.K., Burge, J.R. and Ruble, G.R. (1999) ‘Evaluation of surrogate markers of impending death in the galactosamine-sensitized

murine model of bacterial endotoxemia', *Lab Anim Sci*, 49(5), 545–550.

Kraus, P.R., Boily, M.-J., Giles, S.S., Stajich, J.E., Allen, A., Cox, G.M., Dietrich, F.S., Perfect, J.R. and Heitman, J. (2004) 'Identification of Cryptococcus neoformans temperature-regulated genes with a genomic-DNA microarray.', *Eukaryotic cell*, 3(5), 1249–60.

Kress, Y., Feldmesser, M. and Casadevall, A. (2001) 'Dynamic changes in the morphology of Cryptococcus neoformans during murine pulmonary infection', *Microbiology*, 147(8), 2355–2365.

Krismer, B., Weidenmaier, C., Zipperer, A. and Peschel, A. (2017) 'The commensal lifestyle of Staphylococcus aureus and its interactions with the nasal microbiota', *Nature*, 15, 675–687.

Krockenberger, M.B., Malik, R., Ngamskulrungroj, P., Trilles, L., Escandon, P., Dowd, S., Allen, C., Himmelreich, U., Canfield, P.J., Sorrell, T.C. and Meyer, W. (2010) 'Pathogenesis of Pulmonary Cryptococcus gattii Infection: A Rat Model', *Mycopathologia*, 170(5), 315–330.

Krysan, D.J. (2015) 'Toward improved anti-cryptococcal drugs: Novel molecules and repurposed drugs', *Fungal Genetics and Biology*, 78, 93–98.

Kulkarni, A., Ganesan, P. and O'Donnell, L.A. (2016) 'Interferon gamma: Influence on neural stem cell function in neurodegenerative and neuroinflammatory disease', *Clinical Medicine Insights: Pathology*, 2016(Suppl 1), 9–19.

Kumari, S., Verma, R.K., Singh, D.P. and Yadav, R. (2016) 'Comparison of antigen detection and nested PCR in CSF samples of HIV positive and negative patients with suspected cryptococcal meningitis in a tertiary care hospital', *Journal of Clinical and Diagnostic Research*, 10(4), DC12–DC15.

Kwon-Chung, K.J. and Bennett, J.E. (1978) 'Distribution of α and α mating types of Cryptococcus neoformans among natural and clinical isolates', *American Journal of Epidemiology*, 108(4), 337–340.

Kwon-Chung, K.J. and Bennett, J.E. (1984) 'Epidemiologic differences between the two varieties of Cryptococcus neoformans', *American Journal of Epidemiology*, 120(1), 123–130.

Kwon-Chung, K.J., Bennett, J.E., Wickes, B.L., Meyer, W., Cuomo, C.A., Wollenburg, K.R., Bicanic, T.A., Castañeda, E., Chang, Y.C., Chen, J., Cogliati, M., Dromer, F., Ellis, D., Filler, S.G., Fisher, M.C., Harrison, T.S., Holland, S.M., Kohno, S., Kronstad, J.W. *et al.* (2017) 'The Case for Adopting the "Species Complex" Nomenclature for the

Etiologic Agents of Cryptococcosis', *mSphere*, 2(1).

Kwon-Chung, K.J., Boekhout, T., Fell, J.W. and Diaz, M. (2002) '(1557) Proposal to conserve the name Cryptococcus gattii against C. hondurianus and C. bacillisporus (Basidiomycota, Hymenomycetes, Tremellomycetidae)', *Taxon*, 51(4), 804–806.

Kwon-Chung, K.J. and Varma, A. (2006) 'Do major species concepts support one, two or more species within Cryptococcus neoformans?', *FEMS Yeast Research*, 6(4), 574–587.

Kyei, S.K., Ogbomo, H., Li, S., Timm-McCann, M., Xiang, R.F., Huston, S.M., Ganguly, A., Colarusso, P., Gill, M.J. and Mody, C.H. (2016) 'Mechanisms by which interleukin-12 corrects defective NK cell anticryptococcal activity in HIV-infected patients', *mBio*, 7(4).

Lachmann, P.J. and Halbwachs, L. (1975) 'The influence of C3b inactivator (KAF) concentration on the ability of serum to support complement activation.', *Clinical and Experimental Immunology*, 21(1), 109–14.

Lai, Y.H. and Mosmann, T.R. (1999) 'Mouse IL-13 enhances antibody production in vivo and acts directly on B cells in vitro to increase survival and hence antibody production', *J Immunol*, 162(1), 78–87.

Lam, J., Herant, M., Dembo, M. and Heinrich, V. (2009) 'Baseline mechanical characterization of J774 macrophages.', *Biophysical Journal*, 96(1), 248–54.

Lam, S.H., Chua, H.L., Gong, Z., Lam, T.J. and Sin, Y.M. (2004) 'Development and maturation of the immune system in zebrafish, Danio rerio: A gene expression profiling, in situ hybridization and immunological study', *Developmental and Comparative Immunology*, 28(1), 9–28.

Langford, D.J., Bailey, A.L., Chanda, M.L., Clarke, S.E., Drummond, T.E., Echols, S., Glick, S., Ingrao, J., Klassen-Ross, T., Lacroix-Fralish, M.L., Matsumiya, L., Sorge, R.E., Sotocinal, S.G., Tabaka, J.M., Wong, D., Van Den Maagdenberg, A.M.J.M., Ferrari, M.D., Craig, K.D. and Mogil, J.S. (2010) 'Coding of facial expressions of pain in the laboratory mouse', *Nature Methods*, 7(6), 447–449.

Laniado-Laborín, R. and Cabrales-Vargas, M.N. (2009) 'Amphotericin B: side effects and toxicity', *Revista Iberoamericana de Micologia*, 26(4), 223–227.

Lappin, D.F., Guc, D., Hill, A., McShane, T. and Whaley, K. (1992) 'Effect of interferon-gamma on complement gene expression in different cell types.', *The Biochemical Journal*, 281, 437–42.

Larsen, R.A., Pappas, P.G., Perfect, J., Aberg, J.A., Casadevall, A., Cloud, G.A., James, R., Filler, S. and Dismukes, W.E. (2005) 'Phase I evaluation of the safety and pharmacokinetics of murine-derived anticryptococcal antibody 18B7 in subjects with treated cryptococcal meningitis', *Antimicrobial Agents and Chemotherapy*, 49(3), 952–958.

Lasigliè, D., Traggiai, E., Federici, S., Alessio, M., Buoncompagni, A., Accogli, A., Chiesa, S., Penco, F., Martini, A. and Gattorno, M. (2011) 'Role of IL-1 beta in the development of human TH17 cells: Lesson from NLPR3 mutated patients', *PLoS ONE*, 6(5).

Law, S.K. and Levine, R.P. (1977) 'Interaction between the third complement protein and cell surface macromolecules.', *Proceedings of the National Academy of Sciences of the United States of America*, 74(7), 2701–5.

Lawrence, C.B. and Rothwell, N.J. (2001) 'Anorexic but not pyrogenic actions of interleukin-1 are modulated by central melanocortin-3/4 receptors in the rat', *Journal of Neuroendocrinology*, 13(6), 490–495.

Layé, S., Gheusi, G., Cremona, S., Combe, C., Kelley, K., Dantzer, R. and Parnet, P. (2000) 'Endogenous brain IL-1 mediates LPS-induced anorexia and hypothalamic cytokine expression', *American Journal of Physiology - Regulatory Integrative and Comparative Physiology*, 279(1 48-1).

Lee, A., Toffaletti, D.L., Tenor, J., Soderblom, E.J., Thompson, J.W., Moseley, M.A., Price, M. and Perfect, J.R. (2010) 'Survival defects of Cryptococcus neoformans mutants exposed to human cerebrospinal fluid result in attenuated virulence in an experimental model of meningitis', *Infection and Immunity*, 78(10), 4213–4225.

Lee, A.J., Chen, B., Chew, M. V., Barra, N.G., Shenouda, M.M., Nham, T., van Rooijen, N., Jordana, M., Mossman, K.L., Schreiber, R.D., Mack, M. and Ashkar, A.A. (2017) 'Inflammatory monocytes require type I interferon receptor signaling to activate NK cells via IL-18 during a mucosal viral infection', *Journal of Experimental Medicine*, 214(4), 1153–1167.

Lee, K.D., Nir, S. and Papahadjopoulos, D. (1993) 'Quantitative analysis of liposome-cell interactions in vitro: Rate constants of binding and endocytosis with suspension and adherent J774 cells and human monocytes', *Biochemistry*, 32(3), 889–899.

Lee, S.C., Kress, Y., Dickson, D.W. and Casadevall, A. (1995) 'Human microglia mediate anti-Cryptococcus neoformans activity in the presence of specific antibody', *Journal of Neuroimmunology*, 62(1), 43–52.

Lemon, J.K., Miller, M.R. and Weiser, J.N. (2015) ‘Sensing of interleukin-1 cytokines during Streptococcus pneumoniae colonization contributes to macrophage recruitment and bacterial clearance’, *Infection and Immunity*, 83(8), 3204–3212.

De Leon-Rodriguez, C.M., Fu, M.S., Çorbali, M.O., Cordero, R.J.B. and Casadevall, A. (2018) ‘The Capsule of Cryptococcus neoformans Modulates Phagosomal pH through Its Acid-Base Properties’, *mSphere*, 3(5).

De Leon-Rodriguez, C.M., Rossi, D.C.P., Fu, M.S., Dragotakes, Q., Coelho, C., Guerrero Ros, I., Caballero, B., Nolan, S.J. and Casadevall, A. (2018) ‘The Outcome of the Cryptococcus neoformans– Macrophage Interaction Depends on Phagolysosomal Membrane Integrity’, *The Journal of Immunology*, 201(2), 583–603.

Leopold Wager, C.M., Hole, C.R., Campuzano, A., Castro-Lopez, N., Cai, H., Caballero Van Dyke, M.C., Wozniak, K.L., Wang, Y. and Wormley, F.L. (2018) ‘IFN-γ immune priming of macrophages in vivo induces prolonged STAT1 binding and protection against Cryptococcus neoformans’, *PLOS Pathogens*, 14(10), e1007358.

Leopold Wager, C.M., Hole, C.R., Wozniak, K.L., Olszewski, M.A. and Wormley, F.L. (2014) ‘ STAT1 Signaling Is Essential for Protection against Cryptococcus neoformans Infection in Mice ’, *The Journal of Immunology*, 193(8), 4060–4071.

Lerner, A., Jeremias, P. and Matthias, T. (2015) ‘The World Incidence and Prevalence of Autoimmune Diseases is Increasing’, *International Journal of Celiac Disease*, 3(4), 151–155.

Levitz, S.M. and DiBenedetto, D.J. (1989) ‘Paradoxical role of capsule in murine bronchoalveolar macrophage-mediated killing of Cryptococcus neoformans’, *Journal of Immunology*, 142(2), 659–665.

Levitz, S.M., Harrison, T.S., Tabuni, A. and Liu, X. (1997) ‘Chloroquine induces human mononuclear phagocytes to inhibit and kill Cryptococcus neoformans by a mechanism independent of iron deprivation.’, *The Journal of Clinical Investigation*, 100(6), 1640–6.

Levitz, S.M., Nong, S.H., Seetoo, K.F., Harrison, T.S., Speizer, R.A. and Simons, E.R. (1999) ‘Cryptococcus neoformans resides in an acidic phagolysosome of human macrophages’, *Infection and Immunity*, 67(2), 885–890.

Li, H., Li, Y., Sun, T., Du, W., Li, C., Suo, C., Meng, Y., Liang, Q., Lan, T., Zhong, M., Yang, S., Niu, C., Li, D. and Ding, C. (2019) ‘Unveil the transcriptional landscape at the Cryptococcus-host axis in mice and nonhuman primates’, *PLoS Neglected Tropical Diseases*, 13(7).

Li, H., Zhou, X., Huang, Y., Liao, B., Cheng, L. and Ren, B. (2021) ‘Reactive Oxygen

Species in Pathogen Clearance: The Killing Mechanisms, the Adaption Response, and the Side Effects', *Frontiers in Microbiology*, 11, 3610.

Li, S.S., Kyei, S.K., Timm-Mccann, M., Ogbomo, H., Jones, G.J., Shi, M., Xiang, R.F., Oykhman, P., Huston, S.M., Islam, A., Gill, M.J., Robbins, S.M. and Mody, C.H. (2013) 'The NK receptor NKp30 mediates direct fungal recognition and killing and is diminished in NK cells from HIV-infected patients', *Cell Host and Microbe*, 14(4), 387–397.

Liao, T.-L., Chen, Y.-M. and Chen, D.-Y. (2016) 'Risk factors for cryptococcal infection among patients with rheumatoid arthritis receiving different immunosuppressive medications', *Clinical Microbiology and Infection*, 22(9), 815.e1-815.e3.

Lin, L. and Hu, K. (2017) 'Tissue-type plasminogen activator modulates macrophage M2 to M1 phenotypic change through annexin A2-mediated NF-κB pathway', *Oncotarget*, 8(50), 88094–88103.

Lin, X., Wen, Z. and Xu, J. (2019) 'Tissue-resident macrophages: from zebrafish to mouse', *Blood Science*, 1(1), 57–60.

Lin, Y.Y., Shiau, S. and Fang, C.T. (2015) 'Risk factors for invasive Cryptococcus neoformans diseases: A case-control study', *PLoS ONE*, 10(3).

Lindell, D.M., Moore, T.A., McDonald, R.A., Toews, G.B. and Huffnagle, G.B. (2005) ' Generation of Antifungal Effector CD8 + T Cells in the Absence of CD4 + T Cells during Cryptococcus neoformans Infection ', *The Journal of Immunology*, 174(12), 7920–7928.

Lindemann, A. and Mertelsmann, R. (1995) 'Interleukin-3 and its receptor.', *Cancer Treatment and Research*, 80, 107–142.

Lionakis, M.S. and Kontoyiannis, D.P. (2003) 'Glucocorticoids and invasive fungal infections', *The Lancet*, 362, 1828–1838.

Litman, G.W., Hawke, N.A. and Yoder, J.A. (2001) 'Novel immune-type receptor genes', *Immunological Reviews*, 181(1), 250–259.

Littman, M.L. and Zimmerman, L.E. (1956) *Cryptococcosis-Torulosis*.

Litvintseva, A.P., Carbone, I., Rossouw, J., Thakur, R., Govender, N.P. and Mitchell, T.G. (2011) 'Evidence that the Human Pathogenic Fungus Cryptococcus neoformans var. grubii May Have Evolved in Africa', *PLoS ONE*, 6(5), e19688.

Lodish, H., Berk, A., Zipursky, S.L., Matsudaira, P., Baltimore, D. and Darnell, J. (2000) *Molecular Cell Biology*. New York: Freeman and Company.

Van Loo, P.L.P., Van de Weerd, H.A., Van Zutphen, L.F.M. and Baumans, V. (2003) 'Preference for social contact versus environmental enrichment in male laboratory mice', *Laboratory Animals*, 38, 178–188.

Looney, M.R. and Bhattacharya, J. (2014) 'Live imaging of the lung', *Annual Review of Physiology*, 76, 431–445.

Lortholary, O., Fontanet, A., Mémain, N., Martin, A., Sitbon, K. and Dromer, F. (2005) 'Incidence and risk factors of immune reconstitution inflammatory syndrome complicating HIV-associated cryptococcosis in France', *AIDS*, 19(10), 1043–1049.

Lortholary, O., Improvisi, M.N., Nicolas, M., Provost, F., Dupont, B. and Dromer, F. (1999) 'Fungemia during murine cryptococcosis sheds some light on pathophysiology', *Medical Mycology*, 37(3), 169–174.

Lourens, A., Jarvis, J.N., Meintjes, G. and Samuel, C.M. (2014) 'Rapid diagnosis of cryptococcal meningitis by use of lateral flow assay on cerebrospinal fluid samples: Influence of the high-dose "hook" effect', *Journal of Clinical Microbiology*, 52(12), 4172–4175.

Loyse, A., Wainwright, H., Jarvis, J.N., Bicanic, T., Rebe, K., Meintjes, G. and Harrison, T.S. (2010) 'Histopathology of the arachnoid granulations and brain in HIV-associated cryptococcal meningitis: Correlation with cerebrospinal fluid pressure', *AIDS*, 24(3), 405–410.

Luberto, C., Martinez-Mariño, B., Taraskiewicz, D., Bolaños, B., Chitano, P., Toffaletti, D.L., Cox, G.M., Perfect, J.R., Hannun, Y.A., Balish, E. and Del Poeta, M. (2003) 'Identification of App1 as a regulator of phagocytosis and virulence of Cryptococcus neoformans.', *The Journal of Clinical Investigation*, 112(7), 1080–94.

Lyons-Cohen, M.R., Thomas, S.Y., Cook, D.N. and Nakano, H. (2017) 'Precision-cut Mouse Lung Slices to Visualize Live Pulmonary Dendritic Cells', *JoVE*, 2017(122).

Ma, H., Croudace, J.E., Lammas, D.A. and May, R.C. (2006) 'Expulsion of Live Pathogenic Yeast by Macrophages', *Current Biology*, 16(21), 2156–2160.

Ma, H., Croudace, J.E., Lammas, D.A. and May, R.C. (2007) 'Direct cell-to-cell spread of a pathogenic yeast', *BMC Immunology*, 8(1).

Ma, L.L., Spurrell, J.C.L., Wang, J.F., Neely, G.G., Epelman, S., Krensky, A.M. and Mody, C.H. (2002) ' CD8 T Cell-Mediated Killing of Cryptococcus neoformans Requires Granulysin and Is Dependent on CD4 T Cells and IL-15 ', *The Journal of Immunology*, 169(10), 5787–5795.

Ma, L.L., Wang, C.L.C., Neely, G.G., Epelman, S., Krensky, A.M. and Mody, C.H. (2004) 'NK Cells Use Perforin Rather than Granulysin for Anticryptococcal Activity', *The Journal of Immunology*, 173(5), 3357–3365.

MacMicking, J., Xie, Q.W. and Nathan, C. (1997) 'Nitric oxide and macrophage function', *Annual Review of Immunology*, 15, 323–350.

Maffei, C.M.L., Mirels, L.F., Sobel, R.A., Clemons, K. V. and Stevens, D.A. (2004) 'Cytokine and Inducible Nitric Oxide Synthase mRNA Expression during Experimental Murine Cryptococcal Meningoencephalitis', *Infection and Immunity*, 72(4), 2338–2349.

Mailer, R.K.W., Joly, A.L., Liu, S., Elias, S., Tegner, J. and Andersson, J. (2015) 'IL-1β promotes Th17 differentiation by inducing alternative splicing of FOXP3', *Scientific Reports*, 5(1), 14674.

Mambula, S.S., Simons, E.R., Hastey, R., Selsted, M.E. and Levitz, S.M. (2000) 'Human neutrophil-mediated nonoxidative antifungal activity against Cryptococcus neoformans', *Infection and Immunity*, 68(11), 6257–6264.

Mandal, P., Roy, T.S., Das, T.K., Banerjee, U., Xess, I. and Nosanchuk, J.D. (2007) 'Differences in the cell wall architecture of melanin lacking and melanin producing Cryptococcus neoformans clinical isolates from India: An electron microscopic study', *Brazilian Journal of Microbiology*, 38(4), 662–666.

Manfredi, R., Pieri, F., Pileri, S. and Chiodo, F. (2000) 'The changing face of AIDS-related opportunism: Cryptococcosis in the highly active antiretroviral therapy (HAART) era. Case reports and literature review', *Mycopathologia*, 148(2), 73–78.

Mansour, M.K., Latz, E. and Levitz, S.M. (2006) 'Cryptococcus neoformans glycoantigens are captured by multiple lectin receptors and presented by dendritic cells', *Journal of Immunology*, 176(5), 3053–3061.

Mansour, M.K., Reedy, J.L., Tam, J.M. and Vyas, J.M. (2014) 'Macrophage-Cryptococcus interactions: An update', *Current Fungal Infection Reports*, 8(1), 109–115.

Marchetti, M., Monier, M.-N., Fradagrada, A., Mitchell, K., Baychelier, F., Eid, P., Johannes, L. and Lamaze, C. (2006) 'Stat-mediated Signaling Induced by Type I and Type II Interferons (IFNs) Is Differentially Controlled through Lipid Microdomain Association and Clathrin-dependent Endocytosis of IFN Receptors', *Molecular Biology of the Cell*, 17(7), 2896–2909.

Marroni, M., Pericolini, E., Cenci, E., Bistoni, F. and Vecchiarelli, A. (2007) 'Functional defect of natural immune system in an apparent immunocompetent patient with

pulmonary cryptococcosis', *Journal of Infection*, 54(1).

Martin, R.M. and Lew, A.M. (1998) 'Is IgG2a a good Th1 marker in mice?', *Immunology today*, 19(1), 49.

Martin, T.R. and Frevert, C.W. (2005) 'Innate Immunity in the Lungs', *Proc Am Thorac Soc*, 2, 403–411.

Martinez, L.R. and Casadevall, A. (2007) 'Cryptococcus neoformans biofilm formation depends on surface support and carbon source and reduces fungal cell susceptibility to heat, cold, and UV light', *Applied and Environmental Microbiology*, 73(14), 4592–4601.

Martins, R.R., Ellis, P.S., MacDonald, R.B., Richardson, R.J. and Henriques, C.M. (2019) 'Resident Immunity in Tissue Repair and Maintenance: The Zebrafish Model Coming of Age', *Frontiers in Cell and Developmental Biology*, 7, 12.

Mattner, F., Magram, J., Ferrante, J., Launois, P., Padova, K. Di, Behin, R., Gately, M.K., Louis, J.A. and Alber, G. (1996) 'Genetically resistant mice lacking interleukin-12 are susceptible to infection with Leishmania major and mount a polarized Th2 cell response', *European Journal of Immunology*, 26(7), 1553–1559.

Maus, U.A., Janzen, S., Wall, G., Srivastava, M., Blackwell, T.S., Christman, J.W., Seeger, W., Welte, T. and Lohmeyer, J. (2006) 'Resident alveolar macrophages are replaced by recruited monocytes in response to endotoxin-induced lung inflammation', *American Journal of Respiratory Cell and Molecular Biology*, 35(2), 227–235.

May, R.C., Stone, N.R.H., Wiesner, D.L., Bicanic, T. and Nielsen, K. (2016) 'Cryptococcus: From environmental saprophyte to global pathogen', *Nature Reviews Microbiology*, 14(2), 106–117.

Mayer, A., Lilly, F. and Duran-Reynals, M.L. (1980) 'Genetically dominant resistance in mice to 3-methylcholanthrene-induced lymphoma', *Proceedings of the National Academy of Sciences of the United States of America*, 77(5), 2960–2963.

Maziarz, E.K. and Perfect, J.R. (2016) 'Cryptococcosis', *Infectious Disease Clinics of North America*, 30(1), 179–206.

McBurney, M.W., Staines, W.A., Boekelheide, K., Parry, D., Jardine, K. and Pickavance, L. (1994) 'Murine PGK-1 promoter drives widespread but not uniform expression in transgenic mice', *Developmental Dynamics*, 200(4), 278–293.

Mccarthy, D.O. (2000) 'Cytokines and the Anorexia of Infection: Potential Mechanisms and Treatments', *Biological Research For Nursing*, 1(4), 287–298.

McClelland, E.E., Hobbs, L.M., Rivera, J., Casadevall, A., Potts, W.K., Smith, J.M. and

Ory, J.J. (2013) ‘The role of host gender in the pathogenesis of Cryptococcus neoformans infections.’, *PloS one*, 8(5), e63632.

McDade, H.C. and Cox, G.M. (2001) ‘A new dominant selectable marker for use in Cryptococcus neoformans’, *Medical Mycology*, 39(1), 151–154.

McKenney, J., Smith, R.M., Chiller, T.M., Detels, R., French, A., Margolick, J. and Klausner, J.D. (2014) ‘Prevalence and Correlates of Cryptococcal Antigen Positivity Among AIDS Patients—United States, 1986–2012’, *Pediatric Infectious Disease Journal*, 33(12), 1269.

McLean, G.R., Torres, M., Elguezabal, N., Nakouzi, A. and Casadevall, A. (2002) ‘Isotype Can Affect the Fine Specificity of an Antibody for a Polysaccharide Antigen’, *The Journal of Immunology*, 169(3), 1379–1386.

McQuiston, T.J. and Williamson, P.R. (2012) ‘Paradoxical roles of alveolar macrophages in the host response to Cryptococcus neoformans’, *Journal of Infection and Chemotherapy*, 18(1), 1–9.

McTaggart, L.R., Lei, E., Richardson, S.E., Hoang, L., Fothergill, A. and Zhang, S.X. (2011) ‘Rapid identification of Cryptococcus neoformans and Cryptococcus gattii by matrix-assisted laser desorption ionization-time of flight mass spectrometry’, *Journal of Clinical Microbiology*, 49(8), 3050–3053.

Mednick, A.J.J., Feldmesser, M., Rivera, J. and Casadevall, A. (2003) ‘Neutropenia alters lung cytokine production in mice and reduces their susceptibility to pulmonary cryptococcosis’, *European Journal of Immunology*, 33(6), 1744–1753.

Meier-Kriesche, H.U., Friedman, G., Jacobs, M., Mulgaonkar, S., Vaghela, M. and Kaplan, B. (1999) ‘Infectious complications in geriatric renal transplant patients: comparison of two immunosuppressive protocols.’, *Transplantation*, 68(10), 1496–502.

Meijer, A.H., Gabby Krens, S.F., Medina Rodriguez, I.A., He, S., Bitter, W., Snaar-Jagalska, B.E. and Spaink, H.P. (2004) ‘Expression analysis of the Toll-like receptor and TIR domain adaptor families of zebrafish’, *Molecular Immunology*, 40(11), 773–783.

Meiring, S., Fortuin-de Smidt, M., Kularatne, R., Dawood, H. and Govender, N.P. (2016) ‘Prevalence and Hospital Management of Amphotericin B Deoxycholate-Related Toxicities during Treatment of HIV-Associated Cryptococcal Meningitis in South Africa’, *PLoS Neglected Tropical Diseases*, 10(7).

Merry, M. and Boulware, D.R. (2016) ‘Cryptococcal Meningitis Treatment Strategies Affected by the Explosive Cost of Flucytosine in the United States: A Cost-

effectiveness Analysis', *Clinical Infectious Diseases*, 62(12), 1564–1568.

Mershon-Shier, K.L., Vasuthasawat, A., Takahashi, K., Morrison, S.L. and Beenhouwer, D.O. (2011) 'In vitro C3 deposition on Cryptococcus capsule occurs via multiple complement activation pathways', *Molecular Immunology*, 48(15–16), 2009–2018.

Mershon, K.L., Vasuthasawat, A., Lawson, G.W., Morrison, S.L. and Beenhouwer, D.O. (2009) 'Role of complement in protection against cryptococcus gattii infection', *Infection and Immunity*, 77(3), 1061–1070.

Milam, J.E., Herring-Palmer, A.C., Pandrangi, R., McDonald, R.A., Huffnagle, G.B. and Toews, G.B. (2007) 'Modulation of the pulmonary type 2 T-cell response to Cryptococcus neoformans by intratracheal delivery of a tumor necrosis factor alpha-expressing adenoviral vector', *Infection and Immunity*, 75(10), 4951–4958.

Miljkovic, D. and Trajkovic, V. (2004) 'Inducible nitric oxide synthase activation by interleukin-17', *Cytokine and Growth Factor Reviews*, 15(1), 21–32.

Miller, C.H.T., Maher, S.G. and Young, H.A. (2009) 'Clinical use of interferon-γ', in *Annals of the New York Academy of Sciences*, 69–79.

Min, K.H. and Kwon-Chung, K.J. (1986) 'The biochemical basis for the distinction between the two cryptococcus neoformans varieties with CGB medium', *Zentralblatt fur Bakteriologie Mikrobiologie und Hygiene - Abt. 1 Orig. A*, 261(4), 471–480.

Minamishima, I., Ohga, S., Ishii, E., Miyazaki, C., Hamada, K., Akazawa, K. and Ueda, K. (1991) 'Aseptic meningitis in children: Correlation between fever and interferon-gamma level', *European Journal of Pediatrics*, 150(10), 722–725.

Minutti, C.M., García-Fojeda, B., Sáenz, A., de las Casas-Engel, M., Guillamat-Prats, R., de Lorenzo, A., Serrano-Mollar, A., Corbí, Á.L. and Casals, C. (2016) 'Surfactant Protein A Prevents IFN-γ/IFN-γ Receptor Interaction and Attenuates Classical Activation of Human Alveolar Macrophages', *The Journal of Immunology*, 197(2), 590–598.

Miot, J., Leong, T., Takuva, S., Parrish, A. and Dawood, H. (2021) 'Cost-effectiveness analysis of flucytosine as induction therapy in the treatment of cryptococcal meningitis in HIV-infected adults in South Africa', *BMC Health Services Research*, 21(1).

Misharin, A. V., Morales-Nebreda, L., Mutlu, G.M., Scott Budinger, G.R., Perlman, H., Budinger, G.R.S. and Perlman, H. (2013) 'Major Technical Advances Flow Cytometric Analysis of Macrophages and Dendritic Cell Subsets in the Mouse Lung', *American Journal of Respiratory and Critical Care Medicine*, 49(4), 503–510.

Mitchell, D.H., Sorrell, T.C., Allworth, A.M., Heath, C.H., Mcgregor, A.R., Papanaoum, K., Richards, M.J. and Gottlieb, T. (1995) 'Cryptococcal Disease of the CNS in Immunocompetent Hosts: Influence of Cryptococcal Variety on Clinical Manifestations and Outcome', *Clinical Infectious Diseases*, 21(1).

Mitchell, T.G. and Friedman, L. (1972) 'In Vitro Phagocytosis and Intracellular Fate of Variously Encapsulated Strains of Cryptococcus neoformans', *Infection and Immunity*, 5(4), 491–498.

Mitchell, T.G. and Perfect, J.R. (1995) 'Cryptococcosis in the era of AIDS--100 years after the discovery of Cryptococcus neoformans.', *Clinical Microbiology Reviews*, 8(4), 515–48.

Miyakawa, Y., Kagaya, K., Watanabe, K. and Fukazawa, Y. (1989) 'Characteristics of Macrophage Activation by Gamma Interferon for Tumor Cytotoxicity in Peritoneal Macrophages and Macrophage Cell Line J774. 1', *Microbiology and Immunology*, 33(12), 1027–1038.

Mody, C.H., Toews, G.B. and Lipscomb, M.F. (1988) 'Cyclosporin A inhibits the growth of Cryptococcus neoformans in a murine model', *Infection and Immunity*, 56(1), 7–12.

Mohr, J.A., Long, H., McKown, B.A. and Muchmore, H.G. (1972) 'In vitro susceptibility of Cryptococcus neoformans to steroids', *Sabouraudia*, 10(2), 171–172.

Molina-Torres, C.A., Flores-Castillo, O.N., Carranza-Torres, I.E., Guzmán-Delgado, N.E., Viveros-Valdez, E., Vera-Cabrera, L., Ocampo-Candiani, J., Verde-Star, J., Castro-Garza, J. and Carranza-Rosales, P. (2020) 'Ex vivo infection of murine precision-cut lung tissue slices with Mycobacterium abscessus: a model to study antimycobacterial agents', *Annals of Clinical Microbiology and Antimicrobials*, 19(1), 52.

Monick, M.M., Carter, A.B., Gudmundsson, G., Geist, L.J. and Hunninghake, G.W. (1998) 'Changes in PKC isoforms in human alveolar macrophages compared with blood monocytes', *American Journal of Physiology - Lung Cellular and Molecular Physiology*, 275(2 19-2).

Monteiro, R.C. and Van De Winkel, J.G.J. (2003) 'IgA Fc receptors', *Annual Review of Immunology*, 21, 177–204.

Morris, L. V. (2017) *The effect of Macrophage Activation and Apoptosis in the Immune Response to Respiratory Pathogens*. The University of Sheffield.

Mosser, D.M. and Edwards, J.P. (2008) 'Exploring the full spectrum of macrophage activation', *Nature Reviews Immunology*, 8(12), 958–969.

Mukherjee, J., Pirofski, L.A., Scharff, M.D. and Casadevall, A. (1993) 'Antibody-mediated protection in mice with lethal intracerebral Cryptococcus neoformans infection', *Proceedings of the National Academy of Sciences of the United States of America*, 90(8), 3636–3640.

Mukherjee, J., Zuckier, L.S., Scharff,' And, M.D. and Casadevall, A. (1994) 'Therapeutic Efficacy of Monoclonal Antibodies to Cryptococcus neoformans Glucuronoxylomannan Alone and in Combination with Amphotericin B', *Antimicrobial Agents and Chemotherapy*, 38(3), 580–587.

Mukherjee, S., Feldmesser, M. and Casadevall, A. (1996) 'J774 Murine Macrophage-like Cell Interactions with Cryptococcus neoformans in the Presence and Absence of Opsonins', *The Journal of Infectious Diseases*, 173(5), 1222–1231.

Mukherjee, S., Lee, S.C. and Casadevall, A. (1995) 'Antibodies to Cryptococcus neoformans Glucuronoxylomannan Enhance Antifungal Activity of Murine Macrophages', *Infection and Immunity*, 63(2), 573–579.

Mulero, V. and Brock, J.H. (1999) 'Regulation of iron metabolism in murine J774 macrophages: Role of nitric oxide-dependent and -independent pathways following activation with gamma interferon and lipopolysaccharide', *Blood*, 94(7), 2383–2389.

Müller, E., Christopoulos, P.F., Halder, S., Lunde, A., Beraki, K., Speth, M., Øynebråten, I. and Corthay, A. (2017) 'Toll-Like Receptor Ligands and Interferon-γ Synergize for Induction of Antitumor M1 Macrophages', *Frontiers in Immunology*, 8(OCT), 1383.

Murdock, B.J., Huffnagle, G.B., Olszewski, M.A. and Osterholzer, J.J. (2014) 'Interleukin-17A Enhances Host Defense against Cryptococcal Lung Infection through Effects Mediated by Leukocyte Recruitment, Activation, and Gamma Interferon Production', *Infection and Immunity*, 82(3), 937–948.

Murphy, J., Summer, R., Wilson, A.A., Kotton, D.N. and Fine, A. (2008) 'The Prolonged Life-Span of Alveolar Macrophages', *American Journal of Respiratory Cell and Molecular Biology*, 38(4), 380.

Murray, M.J. and Murray, A.B. (1979) 'Anorexia of infection as a mechanism of host defense', *The American Journal of Clinical Nutrition*, 32(3), 593–596.

Murray, P.D., McGavern, D.B., Pease, L.R. and Rodriguez, M. (2002) 'Cellular sources and targets of IFN-γ-mediated protection against viral demyelination and neurological deficits', *European Journal of Immunology*, 32(3), 606–615.

Musubire, K.B., Meya, B.D., Mayanja-Kizza, H., Lukande, R., Wiesner, L.D., Bohjanen,

P. and Boulware, R.D.R. (2012) ‘Challenges in diagnosis and management of cryptococcal immune reconstitution inflammatory syndrome (IRIS) in resource limited settings’, *African Health Sciences*, 12(2), 226–230.

Mwaba, P., Mwansa, J., Chintu, C., Pobee, J., Scarborough, M., Portsmouth, S. and Zumla, A. (2001) ‘Clinical presentation, natural history, and cumulative death rates of 230 adults with primary cryptococcal meningitis in Zambian AIDS patients treated under local conditions’, *Postgraduate Medical Journal*, 77(914), 769–773.

Mylonakis, E., Ausubel, F.M., Perfect, J.R., Heitman, J. and Calderwood, S.B. (2002) ‘Killing of Caenorhabditis elegans by Cryptococcus neoformans as a model of yeast pathogenesis’, *Proceedings of the National Academy of Sciences of the United States of America*, 99(24), 15675–15680.

Mylonakis, E., Moreno, R., El Khoury, J.B., Idnurm, A., Heitman, J., Calderwood, S.B., Ausubel, F.M. and Diener, A. (2005) ‘Galleria mellonella as a model system to study Cryptococcus neoformans pathogenesis’, *Infection and Immunity*, 73(7), 3842–3850.

Naicker, S.D., Mpembe, R.S., Maphanga, T.G., Zulu, T.G., Desanto, D., Wadula, J., Mvelase, N., Maluleka, C., Reddy, K., Dawood, H., Maloba, M. and Govender, N.P. (2020) ‘Decreasing fluconazole susceptibility of clinical South African Cryptococcus neoformans isolates over a decade’, *PLOS Neglected Tropical Diseases*, 14(3), e0008137.

Nakamura, K., Miyazato, A., Xiao, G., Hatta, M., Inden, K., Aoyagi, T., Shiratori, K., Takeda, K., Akira, S., Saijo, S., Iwakura, Y., Adachi, Y., Ohno, N., Suzuki, K., Fujita, J., Kaku, M. and Kawakami, K. (2008) ‘Deoxynucleic Acids from Cryptococcus neoformans Activate Myeloid Dendritic Cells via a TLR9-Dependent Pathway’, *The Journal of Immunology*, 180(6), 4067–4074.

Nakamura, S., Otani, T., Ijiri, Y., Motoda, R., Kurimoto, M. and Orita, K. (2000) ‘IFN-γ-Dependent and -Independent Mechanisms in Adverse Effects Caused by Concomitant Administration of IL-18 and IL-12’, *The Journal of Immunology*, 164(6), 3330–3336.

Naslund, P.K., Miller, W.C. and Granger, D.L. (1995) ‘Cryptococcus neoformans fails to induce nitric oxide synthase in primed murine macrophage-like cells.’, *Infection and Immunity*, 63(4), 1298–304.

Nathan, C.F., Murray, H.W., Wlebe, I.E. and Rubin, B.Y. (1983) ‘Identification of interferon-γ, as the lymphokine that activates human macrophage oxidative metabolism and antimicrobial activity’, *Journal of Experimental Medicine*, 158(3), 670–689.

Neal, L.M., Xing, E., Xu, J., Kolbe, J.L., Osterholzer, J.J., Segal, B.M., Williamson, P.R.

and Olszewski, M.A. (2017) ‘CD4+ T Cells Orchestrate Lethal Immune Pathology despite Fungal Clearance during Cryptococcus neoformans Meningoencephalitis.’, *mBio*, 8(6).

Nelson, B.N., Hawkins, A.N. and Wozniak, K.L. (2020) ‘Pulmonary Macrophage and Dendritic Cell Responses to Cryptococcus neoformans’, *Frontiers in Cellular and Infection Microbiology*, 10, 37.

Netski, D. and Kozel, T.R. (2002) ‘Fc-dependent and Fc-independent opsonization of Cryptococcus neoformans by anticapsular monoclonal antibodies: Importance of epitope specificity’, *Infection and Immunity*, 70(6), 2812–2819.

Neumann, J., Henneberg, S., von Kenne, S., Nolte, N., Müller, A.J., Schraven, B., Görtler, M.W., Reymann, K.G., Gunzer, M. and Riek-Burchardt, M. (2018) ‘Beware the intruder: Real time observation of infiltrated neutrophils and neutrophil—Microglia interaction during stroke in vivo’, *PLOS ONE*, 13(3), e0193970.

Niehof, M., Hildebrandt, T., Danov, O., Arndt, K., Koschmann, J., Dahlmann, F., Hansen, T. and Sewald, K. (2017) ‘RNA isolation from precision-cut lung slices (PCLS) from different species’, *BMC Research Notes*, 10(1), 121.

Nielsen, K., Cox, G.M., Litvintseva, A.P., Mylonakis, E., Malliaris, S.D., Benjamin, D.K., Giles, S.S., Mitchell, T.G., Casadevall, A., Perfect, J.R. and Heitman, J. (2005) ‘Cryptococcus neoformans α strains preferentially disseminate to the central nervous system during coinfection’, *Infection and Immunity*, 73(8), 4922–4933.

Nielsen, K., Cox, G.M., Wang, P., Toffaletti, D.L., Perfect, J.R. and Heitman, J. (2003) ‘Sexual cycle of Cryptococcus neoformans var. grubii and virulence of congenic a and alpha isolates.’, *Infection and Immunity*, 71(9), 4831–41.

Nielsen, T.B., Yan, J., Luna, B. and Spellberg, B. (2018) ‘Murine oropharyngeal aspiration model of ventilator-associated and hospital-acquired bacterial pneumonia’, *JoVE*, 2018(136), 57672.

Noris, M. and Remuzzi, G. (2013) ‘Overview of complement activation and regulation.’, *Seminars in Nephrology*, 33(6), 479–92.

Nosanchuk, J.D., Rosas, A.L. and Casadevall, A. (1998) ‘The Antibody Response to Fungal Melanin in Mice’, *The Journal of Immunology*, 160(12), 6026–6031.

Noverr, M.C., Cox, G.M., Perfect, J.R. and Huffnagle, G.B. (2003) ‘Role of PLB1 in pulmonary inflammation and cryptococcal eicosanoid production.’, *Infection and Immunity*, 71(3), 1538–47.

Nowicki, B., Singhal, J., Fang, L.I., Nowicki, S. and Yallampalli, C. (1999) 'Inverse relationship between severity of experimental pyelonephritis and nitric oxide production in C3H/HeJ mice', *Infection and Immunity*, 67(5), 2421–2427.

Nunes, S., Sa-Leao, R., Carrico, J., Alves, C.R., Mato, R., Avo, A.B., Saldanha, J., Almeida, J.S., Sanches, I.S. and de Lencastre, H. (2005) 'Trends in Drug Resistance, Serotypes, and Molecular Types of Streptococcus pneumoniae Colonizing Preschool-Age Children Attending Day Care Centers in Lisbon, Portugal: a Summary of 4 Years of Annual Surveillance', *Journal of Clinical Microbiology*, 43(3), 1285–1293.

O'Brien, A.D., Rosenstreich, D.L. and Taylor, B.A. (1980) 'Control of natural resistance to salmonella typhimurium and leishmania donovani in mice by closely linked but distinct genetic loci', *Nature*, 287(5781), 440–442.

Obernier, J.A. and Baldwin, R.L. (2006) 'Establishing an Appropriate Period of Acclimatization Following Transportation of Laboratory Animals', *ILAR Journal*, 47(4), 364–369.

Odom, A., Muir, S., Lim, E., LToffaletti, D., Perfect, J., Heitman, J. and And, C. (1997) 'Calcineurin is required for virulence of Cryptococcus neoformans factors have been identified (including capsule production, mating type, prototrophy, phenoloxidase activity and man', *The EMBO Journal*, 16(10), 2576–2589.

Ogryzko, N. V., Lewis, A., Wilson, H.L., Meijer, A.H., Renshaw, S.A. and Elks, P.M. (2019) 'Hif-1α–Induced Expression of Il-1β Protects against Mycobacterial Infection in Zebrafish', *The Journal of Immunology*, 202(2), 494–502.

Okagaki, L.H. and Nielsen, K. (2012) 'Titan cells confer protection from phagocytosis in Cryptococcus neoformans infections', *Eukaryotic Cell*, 11(6), 820–826.

Okagaki, L.H., Strain, A.K., Nielsen, J.N., Charlier, C., Baltes, N.J., Chrétien, F., Heitman, J., Dromer, F. and Nielsen, K. (2010) 'Cryptococcal Cell Morphology Affects Host Cell Interactions and Pathogenicity', *PLoS Pathogens*, 6(6), e1000953.

de Oliveira, S., Rosowski, E.E. and Huttenlocher, A. (2016) 'Neutrophil migration in infection and wound repair: going forward in reverse', *Nature Reviews Immunology*, 16(6), 378–391.

Olszewski, M.A., Noverr, M.C., Chen, G.H., Toews, G.B., Cox, G.M., Perfect, J.R. and Huffnagle, G.B. (2004) 'Urease Expression by Cryptococcus neoformans Promotes Microvascular Sequestration, Thereby Enhancing Central Nervous System Invasion', *American Journal of Pathology*, 164(5), 1761–1771.

Onishi, R.M. and Gaffen, S.L. (2010) 'Interleukin-17 and its target genes: mechanisms

of interleukin-17 function in disease.', *Immunology*, 129(3), 311–21.

Osterholzer, J.J., Chen, G.-H., Olszewski, M.A., Curtis, J.L., Huffnagle, G.B. and Toews, G.B. (2009) ' Accumulation of CD11b + Lung Dendritic Cells in Response to Fungal Infection Results from the CCR2-Mediated Recruitment and Differentiation of Ly-6C high Monocytes ', *The Journal of Immunology*, 183(12), 8044–8053.

Osterholzer, J.J., Curtis, J.L., Polak, T., Ames, T., Chen, G.-H., McDonald, R., Huffnagle, G.B. and Toews, G.B. (2008) ' CCR2 Mediates Conventional Dendritic Cell Recruitment and the Formation of Bronchovascular Mononuclear Cell Infiltrates in the Lungs of Mice Infected with Cryptococcus neoformans ', *The Journal of Immunology*, 181(1), 610–620.

Osterholzer, J.J., Milam, J.E., Chen, G.-H.H., Toews, G.B., Huffnagle, G.B. and Olszewski, M.A. (2009) 'Role of dendritic cells and alveolar macrophages in regulating early host defense against pulmonary infection with Cryptococcus neoformans.', *Infection and Immunity*, 77(9), 3749–58.

Osterholzer, J.J., Surana, R., Milam, J.E., Montano, G.T., Chen, G.H., Sonstein, J., Curtis, J.L., Huffnagle, G.B., Toews, G.B. and Olszewskiz, M.A. (2009) 'Cryptococcal urease promotes the accumulation of immature dendritic cells and a non-protective T2 immune response within the lung', *American Journal of Pathology*, 174(3), 932–943.

Paish, H.L., Reed, L.H., Brown, H., Bryan, M.C., Govaere, O., Leslie, J., Barksby, B.S., Garcia Macia, M., Watson, A., Xu, X., Zaki, M.Y.W., Greaves, L., Whitehall, J., French, J., White, S.A., Manas, D.M., Robinson, S.M., Spoletini, G., Griffiths, C. *et al.* (2019) 'A Bioreactor Technology for Modeling Fibrosis in Human and Rodent Precision-Cut Liver Slices', *Hepatology*, 70(4), 1377–1391.

Pan, H., Deutsch, G.H. and Wert, S.E. (2019) 'Comprehensive anatomic ontologies for lung development: A comparison of alveolar formation and maturation within mouse and human lung', *Journal of Biomedical Semantics*, 10(1), 18.

Pan, W.G., Chen, B.C., Li, Y.F., Wu, R.X. and Wang, C.H. (2021) 'An unusual case of reactivated latent pulmonary cryptococcal infection in a patient after short-term steroid and azathioprine therapy: a case report', *BMC Pulmonary Medicine*, 21(1), 76.

Panackal, A.A., Wuest, S.C., Lin, Y.-C., Wu, T., Zhang, N., Kosa, P., Komori, M., Blake, A., Browne, S.K., Rosen, L.B., Hagen, F., Meis, J., Levitz, S.M., Quezado, M., Hammoud, D., Bennett, J.E., Bielekova, B. and Williamson, P.R. (2015) 'Paradoxical Immune Responses in Non-HIV Cryptococcal Meningitis', *PLOS Pathogens*, 11(5), e1004884.

Panepinto, J., Liu, L., Ramos, J., Zhu, X., Valyi-Nagy, T., Eksi, S., Fu, J., Jaffe, H.A., Wickes, B. and Williamson, P.R. (2005) 'The DEAD-box RNA helicase Vad1 regulates multiple virulence-associated genes in Cryptococcus neoformans', *Journal of Clinical Investigation*, 115(3), 632–641.

Pappas, P.G. (2013) 'Cryptococcal infections in non-HIV-infected patients.', *Transactions of the American Clinical and Climatological Association*, 124, 61–79.

Parikh, V., Tucci, V. and Galwankar, S. (2012) 'Infections of the nervous system', *International Journal of Critical Illness and Injury Science*, 2(2), 82–97.

Park, B.J., Wannemuehler, K.A., Marston, B.J., Govender, N., Pappas, P.G. and Chiller, T.M. (2009) 'Estimation of the current global burden of cryptococcal meningitis among persons living with HIV/AIDS', *AIDS*, 23(4), 525–530.

Park, Y.D., Shin, S., Panepinto, J., Ramos, J., Qiu, J., Frases, S., Albuquerque, P., Cordero, R.J.B., Zhang, N., Himmelreich, U., Beenhouwer, D., Bennett, J.E., Casadevall, A. and Williamson, P.R. (2014) 'A Role for LHC1 in Higher Order Structure and Complement Binding of the Cryptococcus neoformans Capsule', *PLoS Pathogens*, 10(5).

Patel, D.F., Peiró, T., Bruno, N., Vuononvirta, J., Akthar, S., Puttur, F., Pyle, C.J., Suveizdyte, K., Walker, S.A., Singanayagam, A., Carlin, L.M., Gregory, L.G., Lloyd, C.M. and Snelgrove, R.J. (2019) 'Neutrophils restrain allergic airway inflammation by limiting ILC2 function and monocyte-dendritic cell antigen presentation', *Science Immunology*, 4(41), 7006.

Payen, D., Faivre, V., Miatello, J., Leentjens, J., Brumpt, C., Tissières, P., Dupuis, C., Pickkers, P. and Lukaszewicz, A.C. (2019) 'Multicentric experience with interferon gamma therapy in sepsis induced immunosuppression. A case series', *BMC Infectious Diseases 2019 19:1*, 19(1), 1–10.

Perfect, J.R. and Bicanic, T. (2015) 'Cryptococcosis diagnosis and treatment: What do we know now', *Fungal Genetics and Biology*, 78, 49–54.

Perfect, J.R., Dismukes, W.E., Dromer, F., Goldman, D.L., Graybill, J.R., Hamill, R.J., Harrison, T.S., Larsen, R.A., Lortholary, O., Nguyen, M.H., Pappas, P.G., Powderly, W.G., Singh, N., Sobel, J.D. and Sorrell, T.C. (2010) 'Clinical practice guidelines for the management of cryptococcal disease: 2010 update by the infectious diseases society of America', *Clinical Infectious Diseases*, 291–322.

Perfect, J.R., Lang, S.D.R. and Durack, D.T. (1980) 'Chronic cryptococcal meningitis. A new experimental model in rabbits', *American Journal of Pathology*, 101(1), 177–193.

Person, A.K., Kontoyiannis, D.P. and Alexander, B.D. (2010) 'Fungal Infections in Transplant and Oncology Patients', *Infectious Disease Clinics of North America*, 24(2), 439.

Pettini, E., Fiorino, F., Cuppone, A.M., Iannelli, F., Medaglini, D. and Pozzi, G. (2015) 'Interferon-γ from brain leukocytes enhances meningitis by type 4 Streptococcus pneumoniae', *Frontiers in Microbiology*, 6(DEC).

Piaszyk-Borychowska, A., Széles, L., Csermely, A., Chiang, H.-C., Wesoły, J., Lee, C.-K., Nagy, L. and Bluyssen, H.A.R. (2019) 'Signal Integration of IFN-I and IFN-II With TLR4 Involves Sequential Recruitment of STAT1-Complexes and NFκB to Enhance Pro-inflammatory Transcription', *Frontiers in Immunology*, 10(JUN), 1253.

Pikaar, J.C., Voorhout, W.F., Van Golde, L.M.G., Verhoef, J., Van Strijp, J.A.G. and Van Iwaarden, J.F. (1995) 'Opsonic activities of surfactant proteins A and D in phagocytosis of gram-negative bacteria by alveolar macrophages', *Journal of Infectious Diseases*, 172(2), 481–489.

Pinteaux, E., Abdulaal, W.H., Mufazalov, I.A., Humphreys, N.E., Simonsen-Jackson, M., Francis, S., Müller, W. and Waisman, A. (2020) 'Cell-specific conditional deletion of interleukin-1 (IL-1) ligands and its receptors: a new toolbox to study the role of IL-1 in health and disease', *Journal of Molecular Medicine*, 98(7), 923–930.

Pires, S. and Parker, D. (2018) 'IL-1β activation in response to Staphylococcus aureus lung infection requires inflammasome-dependent and independent mechanisms', *European Journal of Immunology*, 48(10), 1707–1716.

Pirofski, L. anne (2001) 'Polysaccharides, mimotopes and vaccines for fungal and encapsulated pathogens', *Trends in Microbiology*, 9(9), 445–451.

Pittet, M.J. and Weissleder, R. (2011) 'Intravital imaging', *Cell*, 147(5), 983–991.

Placke, M.E. and Fisher, G.L. (1987) 'Adult Peripheral Lung Organ Culture - A Model for Respiratory Tract Toxicology', *Toxicology and Applied Pharmacology*, 90, 284–298.

Plested, J.S., Ferry, B.L., Coull, P.A., Makepeace, K., Lehmann, A.K., MacKinnon, F.G., Griffiths, H.G., Herbert, M.A., Richards, J.C. and Richard Moxon, E. (2001) 'Functional opsonic activity of human serum antibodies to inner core lipopolysaccharide (galE) of serogroup B meningococci measured by flow cytometry', *Infection and Immunity*, 69(5), 3203–3213.

Pline, K. (2019) *Investigating the role of Cryptococcus neoformans-macrophage interactions on the outcome of cryptococcal infection*. The University of Sheffield.

Poltorak, A., He, X., Smirnova, I., Liu, M.Y., Van Huffel, C., Du, X., Birdwell, D., Alejos, E., Silva, M., Galanos, C., Freudenberg, M., Ricciardi-Castagnoli, P., Layton, B. and Beutler, B. (1998) 'Defective LPS signaling in C3H/HeJ and C57BL/10ScCr mice: Mutations in Tlr4 gene', *Science*, 282(5396), 2085–2088.

Popgeorgiev, N., Bonneau, B., Prudent, J. and Gillet, G. (2018) 'Control of Programmed Cell Death During Zebrafish Embryonic Development', in *Recent Advances in Zebrafish Researches*. InTech.

Posas, F., Takekawa, M. and Saito, H. (1998) 'Signal transduction by MAP kinase cascades in budding yeast', *Current Opinion in Microbiology*, 1(2), 175–182.

Posch, W., Steger, M., Wilflingseder, D. and Lass-Flörl, C. (2017) 'Promising immunotherapy against fungal diseases', *Expert Opinion on Biological Therapy*, 17(7), 861–870.

Pratten, M.K. and Lloyd, J.B. (1986) 'Pinocytosis and phagocytosis: the effect of size of a particulate substrate on its mode of capture by rat peritoneal macrophages cultured in vitro', *BBA*, 881(3), 307–313.

Del Prete, G., De Carli, M., Almerigogna, F., Giudizi, M.G., Biagiotti, R. and Romagnani, S. (1993) 'Human IL-10 is produced by both type 1 helper (Th1) and type 2 helper (Th2) T cell clones and inhibits their antigen-specific proliferation and cytokine production.', *The Journal of Immunology*, 150(2).

Prud'homme, G.J., Kono, D.H. and Theofilopoulos, A.N. (1995) 'Quantitative polymerase chain reaction analysis reveals marked overexpression of interleukin-1β, interleukin-10 and interferon-γ mRNA in the lymph nodes of lupus-prone mice', *Molecular Immunology*, 32(7), 495–503.

Puel, A., Cypowyj, S., Bustamante, J., Wright, J.F., Liu, L., Lim, H.K., Migaud, M., Israel, L., Chrabieh, M., Audry, M., Gumbleton, M., Toulon, A., Bodemer, C., El-Baghdadi, J., Whitters, M., Paradis, T., Brooks, J., Collins, M., Wolfman, N.M. *et al.* (2011) 'Chronic mucocutaneous candidiasis in humans with inborn errors of interleukin-17 immunity', *Science*, 332(6025), 65–68.

Qiao, H. and May, J.M. (2009) 'Macrophage differentiation increases expression of the ascorbate transporter (SVCT2)', *Free Radical Biology and Medicine*, 46(8), 1221–1232.

Qiao, Y., Giannopoulou, E.G., Chan, C.H., Park, S. ho, Gong, S., Chen, J., Hu, X., Elemento, O. and Ivashkiv, L.B. (2013) 'Synergistic activation of inflammatory cytokine genes by interferon-γ-induced chromatin remodeling and toll-like receptor signaling', *Immunity*, 39(3), 454–469.

Quiniou, S.M.A., Boudinot, P. and Bengtén, E. (2013) 'Comprehensive survey and genomic characterization of Toll-like receptors (TLRs) in channel catfish, Ictalurus punctatus : identification of novel fish TLRs', *Immunogenetics*, 65(7), 511–530.

Rajasingham, R., Rolfes, M.A., Birkenkamp, K.E., Meya, D.B. and Boulware, D.R. (2012) 'Cryptococcal Meningitis Treatment Strategies in Resource-Limited Settings: A Cost-Effectiveness Analysis', *PLoS Medicine*, 9(9), e1001316.

Rajasingham, R., Smith, R.M., Park, B.J., Jarvis, J.N., Govender, N.P., Chiller, T.M., Denning, D.W., Loyse, A. and Boulware, D.R. (2017) 'Global burden of disease of HIV-associated cryptococcal meningitis: an updated analysis', *The Lancet Infectious Diseases*, 17(8), 873–881.

Rajasingham, R., Wake, R.M., Beyene, T., Katende, A., Letang, E. and Boulware, D.R. (2019) 'Cryptococcal meningitis diagnostics and screening in the era of point-of-care laboratory testing', *Journal of Clinical Microbiology*, 57(1), e01238-18.

Ralph, P., Moore, M.A.S. and Nilsson, K. (1976) 'Lysozyme Synthesis by Established Human and Murine Histiocytic Lymphoma Cell Lines', *The Journal of Experimental Medicine*, 143, 1528–1533.

Ralph, P. and Nakoinz, I. (1975) 'Phagocytosis and cytolysis by a macrophage tumour and its cloned cell line', *Nature*, 257(5525), 393–394.

Ramakrishnan, L. (2012) 'Revisiting the role of the granuloma in tuberculosis', *Nature Reviews Immunology*, 12(5), 352–366.

Ramamurthy, D., Nundalall, T., Cingo, S., Mungra, N., Karaan, M., Naran, K. and Barth, S. (2021) 'Recent advances in immunotherapies against infectious diseases', *Immunotherapy Advances*, 1(1), 1–16.

Randhawa, H.S., Kowshik, T., Chowdhary, A., Preeti Sinha, K., Khan, Z.U., Sun, S. and Xu, J. (2008) 'The expanding host tree species spectrum of *Cryptococcus gattii* and *Cryptococcus neoformans* and their isolations from surrounding soil in India', *Medical Mycology*, 46(8), 823–833.

Rao, S., Schieber, A.M.P., O'connor, C.P., Leblanc, M., Michel, D. and Ayres Correspondence, J.S. (2017) 'Pathogen-Mediated Inhibition of Anorexia Promotes Host Survival and Transmission', *Cell*, 168, 503–516.

Rayhane, N., Lortholary, O., Fitting, C., Callebert, J., Huerre, M., Dromer, F. and Cavaillon, J.-M. (1999) 'Enhanced Sensitivity of Tumor Necrosis Factor/Lymphotoxin-a–Deficient Mice to Cryptococcus neoformans Infection despite Increased Levels of Nitrite/Nitrate, Interferon-y, and Interleukin-12', *The Journal of Infectious Diseases*,

180, 1637–1647.

Reddi, K., Phagoo, S.B., Anderson, K.D. and Warburton, D. (2003) ‘Burkholderia cepacia-Induced IL-8 Gene Expression in an Alveolar Epithelial Cell Line: Signaling Through CD14 and Mitogen-Activated Protein Kinase’, *Pediatric Research*, 54, 297–305.

Reisfeld-Zadok, S., Elis, A., Szyper-Kravitz, M., Chowers, M. and Lishner, M. (2009) ‘Cryptococcal Meningitis in Chronic Lymphocytic Leukemia Patients’, *IMAJ*, 11, 437–439.

Ressmeyer, A.R., Larsson, A.K., Vollmer, E., Dahlèn, S.E., Uhlig, S. and Martin, C. (2006) ‘Characterisation of guinea pig precision-cut lung slices: Comparison with human tissues’, *European Respiratory Journal*, 28(3), 603–611.

Retini, C., Vecchiarelli, A., Monari, C., Tascini, C., Bistoni, F. and Kozel, T.R. (1996) ‘Capsular polysaccharide of Cryptococcus neoformans induces proinflammatory cytokine release by human neutrophils.’, *Infection and Immunity*, 64(8), 2897–903.

Rhein, J., Boulware, D.R. and Bahr, N.C. (2015) ‘1,3-β-D-glucan in cryptococcal meningitis’, *The Lancet Infectious Diseases*, 15(10), 1136–1137.

Ristow, L.C. and Davis, J.M. (2021) ‘The granuloma in cryptococcal disease’, *PLOS Pathogens*, 17(3), e1009342.

Rock, R.B., Gekker, G., Hu, S., Sheng, W.S., Cheeran, M., Lokensgard, J.R. and Peterson, P.K. (2004) ‘Role of microglia in central nervous system infections’, *Clinical Microbiology Reviews*, 17(4), 942–964.

Roddie, H.G., Armitage, E.L., Coates, J.A., Johnston, S.A. and Evans, I.R. (2019) ‘Simu-dependent clearance of dying cells regulates macrophage function and inflammation resolution’, *PLoS Biology*, 17(5), e2006741.

Rodrigues, M.L., Nakayasu, E.S., Oliveira, D.L., Nimrichter, L., Nosanchuk, J.D., Almeida, I.C. and Casadevall, A. (2008) ‘Extracellular vesicles produced by Cryptococcus neoformans contain protein components associated with virulence’, *Eukaryotic Cell*, 7(1), 58–67.

Rohatgi, S., Gohil, S., Kuniholm, M.H., Schultz, H., Dufaud, C., Armour, K.L., Badri, S., Mailliard, R.B. and Pirofski, L.A. (2013) ‘Fc gamma receptor 3A polymorphism and risk for HIV-associated cryptococcal disease’, *mBio*, 4(5).

Rohatgi, S. and Pirofski, L. (2012) ‘Molecular Characterization of the Early B Cell Response to Pulmonary Cryptococcus neoformans Infection’, *The Journal of*

Immunology, 189(12), 5820–5830.

Romero, C., Herzig, D., Etogo, A., Nunez, J., Mahmoudizad, R., Fang, G., Murphey, E.D., Toliver-Kinsky, T.E. and Sherwood, E.R. (2010) 'The role of interferon-γ in the pathogenesis of acute intra-abdominal sepsis', *Journal of Leukocyte Biology*, 88(4), 725–735.

Rosales, C. (2018) 'Neutrophil: A cell with many roles in inflammation or several cell types?', *Frontiers in Physiology*, 9(FEB), 113.

Rosenfeld, A.B., Doobin, D.J., Warren, A.L., Racaniello, V.R. and Vallee, R.B. (2017) 'Replication of early and recent Zika virus isolates throughout mouse brain development', *Proceedings of the National Academy of Sciences of the United States of America*, 114(46), 12273–12278.

Rosenwasser, L.J. (1998) 'Biologic activities of IL-1 and its role in human disease', *Journal of Allergy and Clinical Immunology*, 102(3), 344–350.

Rosowski, E.E., Knox, B.P., Archambault, L.S., Huttenlocher, A., Keller, N.P., Wheeler, R.T. and Davis, J.M. (2018) 'The zebrafish as a model host for invasive fungal infections', *Journal of Fungi*, 4(4), 136.

Rudman, J., Evans, R.J. and Johnston, S.A. (2019) 'Are macrophages the heroes or villains during cryptococcosis?', *Fungal Genetics and Biology*, 132, 103261.

Rudziak, P., Ellis, C.G. and Kowalewska, P.M. (2019) 'Role and molecular mechanisms of pericytes in regulation of leukocyte diapedesis in inflamed tissues', *Mediators of Inflammation*, 2019.

Ruiz, A., Neilson, J.B. and Bulmer, G.S. (1982) 'Control of Cryptococcus neoformans in nature by biotic factors', *Sabouraudia*, 20(1), 21–29.

Rush, D. (2013) 'The impact of calcineurin inhibitors on graft survival', *Transplantation Reviews*, 27(3), 93–95.

Ruxton, G.D. (2006) 'The unequal variance t-test is an underused alternative to Student's t-test and the Mann–Whitney U test', *Behavioural Ecology*, 17(4), 688–690.

Sabiiti, W., May, R.C. and Pursall, E.R. (2012) 'Experimental models of cryptococcosis', *International Journal of Microbiology*, 2012.

Sabiiti, W., Robertson, E., Beale, M.A., Johnston, S.A., Brouwer, A.E., Loyse, A., Jarvis, J.N., Gilbert, A.S., Fisher, M.C., Harrison, T.S., May, R.C. and Bicanic, T. (2014) 'Efficient phagocytosis and laccase activity affect the outcome of HIV-associated cryptococcosis', *Journal of Clinical Investigation*, 124(5), 2000–2008.

Salas, S.D., Bennett, J.E., Kwon-Chung, K.J., Perfect, J.R. and Williamson, P.R. (1996) ‘Effect of the laccase gene, CNLAC1, on virulence of Cryptococcus neoformans’, *Journal of Experimental Medicine*, 184(2), 377–386.

Salim, T., Sershen, C.L. and May, E.E. (2016) ‘Investigating the role of TNF-α and IFN-γ activation on the dynamics of iNOS gene expression in lps stimulated macrophages’, *PLoS ONE*, 11(6).

Sanderson, M.J. (2011) ‘Exploring lung physiology in health and disease with lung slices’, *Pulmonary Pharmacology & Therapeutics*, 24(5), 452–465.

Santiago-Tirado, F.H., Onken, M.D., Cooper, J.A., Klein, R.S. and Doering, T.L. (2017) ‘Trojan horse transit contributes to blood-brain barrier crossing of a eukaryotic pathogen’, *mBio*, 8(1), e02183-16.

Santos-Gandelman, J., Machado-Silva, A., Santos-Gandelman, J. and Machado-Silva, A. (2019) ‘Drug development for cryptococcosis treatment: what can patents tell us?’, *Memórias do Instituto Oswaldo Cruz*, 114(1), 1–8.

Sapey, E. and Stockley, R.A. (2019) ‘Getting stuck or choosing to stay Neutrophil transit times in the lung in acute inflammation and COPD’, *Thorax*, 74(7), 631–632.

Schelenz, S., Malhotra, R., Sim, R.B., Holmskov, U. and Bancroft, G.J. (1995) ‘Binding of host collectins to the pathogenic yeast Cryptococcus neoformans: human surfactant protein D acts as an agglutinin for acapsular yeast cells.’, *Infection and Immunity*, 63(9), 3360–6.

Schneemann, M. and Schoedon, G. (2002) ‘Species differences in macrophage NO production are important (multiple letters)’, *Nature Immunology*, 3(2), 102.

Schurch, S., Lee, M. and Gehr, P. (1992) ‘Pulmonary surfactant: Surface properties and function of alveolar and airway surfactant’, *Pure & Applied Chemistry*, 64(11), 1745–1750.

Scrimgeour, E.M. and Purohit, R.G. (1984) ‘Chronic pulmonary cryptococcosis in a Rattus rattus from Rabaul, Papua New Guinea’, *Transactions of the Royal Society of Tropical Medicine and Hygiene*, 78(6), 827–828.

Seoane, P.I., Taylor-Smith, L.M., Stirling, D., Bell, L.C.K., Noursadeghi, M., Bailey, D. and May, R.C. (2020) ‘Viral infection triggers interferon-induced expulsion of live Cryptococcus neoformans by macrophages’, *PLOS Pathogens*, 16(2), e1008240.

Sepulcre, M.P., Alcaraz-Pérez, F., López-Muñoz, A., Roca, F.J., Meseguer, J., Cayuela, M.L. and Mulero, V. (2009) ‘Evolution of Lipopolysaccharide (LPS)

Recognition and Signaling: Fish TLR4 Does Not Recognize LPS and Negatively Regulates NK-kB Activation', *The Journal of Immunology*, 182, 1836–1845.

Setianingrum, F., Rautemaa-Richardson, R. and Denning, D.W. (2019) 'Pulmonary cryptococcosis: A review of pathobiology and clinical aspects', *Medical Mycology*, 57(2), 133–150.

Shah, S.I., Bui, H., Velasco, N. and Rungta, S. (2017) 'Incidental finding of Cryptococcus on prostate biopsy for prostate adenocarcinoma following cardiac transplant: Case report and review of the literature', *American Journal of Case Reports*, 18, 1171–1180.

Shao, X., Mednick, A., Alvarez, M., van Rooijen, N., Casadevall, A. and Goldman, D.L. (2005) 'An innate immune system cell is a major determinant of species-related susceptibility differences to fungal pneumonia.', *Journal of Immunology*, 175(5), 3244–51.

Shi, Y., Liu, C.H., Roberts, A.I., Das, J., Xu, G., Ren, G., Zhang, Y., Zhang, L., Yuan, Z.R., Tan, H.S.W., Das, G. and Devadas, S. (2006) 'Granulocyte-macrophage colony-stimulating factor (GM-CSF) and T-cell responses: what we do and don't know', *Cell Research*, 16(2), 126–133.

Shibuya, K., Hirata, A., Omuta, J., Sugamata, M., Katori, S., Saito, N., Murata, N., Morita, A., Takahashi, K., Hasegawa, C., Mitsuda, A., Hatori, T. and Nonaka, H. (2005) 'Granuloma and cryptococcosis.', *Journal of Infection and Chemotherapy*, 11(3), 115–22.

Shirley, R.M. and Baddley, J.W. (2009) 'Cryptococcal lung disease', *Current Opinion in Pulmonary Medicine*, 15(3), 254–260.

Shourian, M., Ralph, B., Angers, I., Sheppard, D.C. and Qureshi, S.T. (2018) 'Contribution of IL-1RI Signaling to Protection against Cryptococcus neoformans 52D in a Mouse Model of Infection', *Frontiers in Immunology*, 8(JAN), 1987.

Siafakas, A.R., Sorrell, T.C., Wright, L.C., Wilson, C., Larsen, M., Boadle, R., Williamson, P.R. and Djordjevic, J.T. (2007) 'Cell wall-linked cryptococcal phospholipase B1 is a source of secreted enzyme and a determinant of cell wall integrity', *Journal of Biological Chemistry*, 282(52), 37508–37514.

Siddiqui, A.A., Brouwer, A.E., Wuthiekanun, V., Jaffar, S., Shattock, R., Irving, D., Sheldon, J., Chierakul, W., Peacock, S., Day, N., White, N.J. and Harrison, T.S. (2005) 'IFN-gamma at the site of infection determines rate of clearance of infection in cryptococcal meningitis', *Journal of Immunology*, 174(3), 1746–1750.

Simon, V., Ho, D.D. and Abdool Karim, Q. (2006) 'HIV/AIDS epidemiology, pathogenesis, prevention, and treatment', *Lancet*, 368(9534), 489–504.

Singh, N., Alexander, B.D., Lortholary, O., Dromer, F., Gupta, K.L., John, G.T., Del Busto, R., Klintmalm, G.B., Somani, J., Lyon, G.M., Pursell, K., Stosor, V., Muňoz, P., Limaye, A.P., Kalil, A.C., Pruett, T.L., Garcia-Diaz, J., Humar, A., Houston, S. *et al.* (2007) 'Cryptococcus neoformans in organ transplant recipients: Impact of calcineurin-inhibitor agents on mortality', *Journal of Infectious Diseases*, 195(5), 756–764.

Sionov, E., Mayer-Barber, K.D., Chang, Y.C., Kauffman, K.D., Eckhaus, M.A., Salazar, A.M., Barber, D.L. and Kwon-Chung, K.J. (2015) 'Type I IFN Induction via Poly-ICLC Protects Mice against Cryptococcosis', *PLoS Pathogens*, 11(8).

Skowyra, M.L. and Doering, T.L. (2012) 'RNA interference in cryptococcus neoformans', in *Methods in Molecular Biology*. Humana Press Inc., 165–186.

Smith, L.M., Dixon, E.F. and May, R.C. (2015) 'The fungal pathogen Cryptococcus neoformans manipulates macrophage phagosome maturation', *Cellular Microbiology*, 17(5), 702–713.

Snapp, E. (2005) 'Design and Use of Fluorescent Fusion Proteins in Cell Biology', *Current Protocols in Cell Biology*, 27(1).

Snarr, B.D., St-Pierre, G., Ralph, B., Lehoux, M., Sato, Y., Rancourt, A., Takazono, T., Baistrocchi, S.R., Corsini, R., Cheng, M.P., Sugrue, M., Baden, L.R., Izumikawa, K., Mukae, H., Wingard, J.R., King, I.L., Divangahi, M., Satoh, M.S., Yipp, B.G. *et al.* (2020) 'Galectin-3 enhances neutrophil motility and extravasation into the airways during Aspergillus fumigatus infection', *PLOS Pathogens*, 16(8), e1008741.

Sorokin, S.P. and Hoyt, R.F. (1992) 'Macrophage development: I. Rationale for using Griffonia simplicifolia isolectin B4 as a marker for the line', *The Anatomical Record*, 232(4), 520–526.

Spadari, C. de C., Wirth, F., Lopes, L.B. and Ishida, K. (2020) 'New approaches for cryptococcosis treatment', *Microorganisms*, 8(4).

Specht, C.A., Lee, C.K., Huang, H., Tipper, D.J., Shen, Z.T., Lodge, J.K., Leszyk, J., Ostroff, G.R. and Levitz, S.M. (2015) 'Protection against experimental cryptococcosis following vaccination with glucan particles containing cryptococcus alkaline extracts', *mBio*, 6(6), 1–11.

Spinelle-Jaegle, S., Devillier, P., Doucet, S., Millet, S., Banissi, C., Diu-Hercend, A. and Ruuth, E. (2001) 'Inflammatory cytokine production in interferon-gamma-primed mice, challenged with lipopolysaccharide. Inhibition by SK&F 86002 and interleukin-1 beta-

converting enzyme inhibitor', *Eur Cytokine Netw*, 12(2), 280–289.

Squizani, E.D., Oliveira, N.K., Reuwsaat, J.C.V., Marques, B.M., Lopes, W., Gerber, A.L., de Vasconcelos, A.T.R., Lev, S., Djordjevic, J.T., Schrank, A., Vainstein, M.H., Staats, C.C. and Kmetzsch, L. (2018) 'Cryptococcal dissemination to the central nervous system requires the vacuolar calcium transporter Pmc1', *Cellular Microbiology*, 20(2), e12803.

Sriskandan, K., Garner, P., Watkinson, J., Pettingale, K.W., Brinkley, D., Caiman, F.M.B. and Tee, D.E.H. (1986) 'A toxicity study of recombinant interferon-gamma given by intravenous infusion to patients with advanced cancer', *Cancer Chemother Pharmacol*, 18, 63–68.

Stadtmauer, G. and Cunningham-Rundles, C. (1997) 'Outcome analysis and cost assessment in immunologic disorders', *Journal of the American Medical Association*, 278(22), 2018–2023.

Staib, F. and Bethauser, G. (1968) 'Von Cryptococcus neoformans in Stab von einem Taubenschlag', *Mykosen*, 11, 619–624.

Staib, F., Seibold, M. and L'Age, M. (1990) 'Persistence of Cryptococcus neoformans in seminal fluid and urine under itraconazole treatment. The urogenital tract (prostate) as a niche for Cryptococcus neoformans', *Mycoses*, 33(7–8), 369–373.

Stamme, C., Walsh, E. and Wright, J.R. (2000) 'Surfactant protein A differentially regulates IFN-γ- and LPS-induced nitrite production by rat alveolar macrophages', *American Journal of Respiratory Cell and Molecular Biology*, 23(6), 772–779.

Stano, P., Williams, V., Villani, M., Cymbalyuk, E.S., Qureshi, A., Huang, Y., Morace, G., Luberto, C., Tomlinson, S. and Del Poeta, M. (2009) 'App1: an antiphagocytic protein that binds to complement receptors 3 and 2.', *Journal of Immunology*, 182(1), 84–91.

Steen, B.R., Zuyderduyn, S., Toffaletti, D.L., Marra, M., Jones, S.J.M., Perfect, J.R. and Kronstad, J. (2003) 'Cryptococcus neoformans Gene Expression during Experimental Cryptococcal Meningitis', *Eukaryotic Cell*, 2(6), 1336–1349.

Steenbergen, J.N., Nosanchuk, J.D., Malliaris, S.D. and Casadevall, A. (2003) 'Cryptococcus neoformans virulence is enhanced after growth in the genetically malleable host Dictyostelium discoideum', *Infection and Immunity*, 71(9), 4862–4872.

Steenbergen, J.N., Shuman, H.A. and Casadevall, A. (2001) 'Cryptococcus neoformans interactions with amoebae suggest an explanation for its virulence and intracellular pathogenic strategy in macrophages', *Proceedings of the National*

Academy of Sciences of the United States of America, 98(26), 15245–15250.

Stenger, S., Hanson, D.A., Teitelbaum, R., Dewan, P., Niazi, K.R., Froelich, C.J., Ganz, T., Thoma-Uszynski, S., Melián, A., Bogdan, C., Porcelli, S.A., Bloom, B.R., Krensky, A.M. and Modlin, R.L. (1998) 'An antimicrobial activity of cytolytic T cells mediated by granulysin', *Science*, 282(5386), 121–125.

Stephen, C., Lester, S., Black, W., Fyfe, M. and Raverty, S. (2002) 'Multispecies outbreak of cryptococcosis on southern Vancouver Island, British Columbia', *Canadian Veterinary Journal*, 43(10), 792–794.

Sternberg, N. and Hamilton, D. (1981) 'Bacteriophage P1 site-specific recombination. I. Recombination between loxP sites', *Journal of Molecular Biology*, 150(4), 467–486.

Stone, N.R.H., Rhodes, J., Fisher, M.C., Mfinanga, S., Kivuyo, S., Rugemalila, J., Segal, E.S., Needleman, L., Molloy, S.F., Kwon-Chung, J., Harrison, T.S., Hope, W., Berman, J. and Bicanic, T. (2019) 'Dynamic ploidy changes drive fluconazole resistance in human cryptococcal meningitis', *The Journal of Clinical Investigation*, 129(3), 999–1014.

Strasak, A.M., Zaman, Q., Marinell, G., Pfeiffer, K.P. and Ulmer, H. (2007) 'The Use of Statistics in Medical Research', *The American Statistician*, 61, 47–55.

Strunk, R.C., Cole, F.S., Perlmutter, D.H. and Colten, H.R. (1985) 'γ-Interferon increases expression of class III complement genes C2 and factor B in human monocytes and in murine fibroblasts transfected with human C2 and factor B genes', *Journal of Biological Chemistry*, 260(28), 15280–15285.

Stukes, S., Coelho, C., Rivera, J., Jedlicka, A.E., Hajjar, K.A. and Casadevall, A. (2016) ' The Membrane Phospholipid Binding Protein Annexin A2 Promotes Phagocytosis and Nonlytic Exocytosis of Cryptococcus neoformans and Impacts Survival in Fungal Infection ', *The Journal of Immunology*, 197(4), 1252–1261.

Subramaniam, K.S., Datta, K., Quintero, E., Manix, C., Marks, M.S. and Pirofski, L. (2010) ' The Absence of Serum IgM Enhances the Susceptibility of Mice to Pulmonary Challenge with Cryptococcus neoformans ', *The Journal of Immunology*, 184(10), 5755–5767.

Surawut, S., Ondee, T., Taratummarat, S., Palaga, T., Pisitkun, P., Chindamporn, A. and Leelahavanichkul, A. (2017) 'The role of macrophages in the susceptibility of Fc gamma receptor IIb deficient mice to Cryptococcus neoformans', *Scientific Reports*, 7(1), 1–14.

Swihart, K., Fruth, U., Messmer, N., Hug, K., Behin, R., Huang, S., Giudice, G. Del,

Aguet, M. and Louis, J.A. (1995) ‘Mice from a genetically resistant background lacking the interferon γ receptor are susceptible to infection with leishmania major but mount a polarized T helper cell 1-type CD4+ T cell response’, *Journal of Experimental Medicine*, 181(3), 961–971.

Szabó, C., Southan, G.J., Wood, E., Thiemermann, C. and Vane, J.R. (1994) ‘Inhibition by spermine of the induction of nitric oxide synthase in J774.2 macrophages: requirement of a serum factor’, *British Journal of Pharmacology*, 112(2), 355–356.

Szymczak, W.A., Sellers, R.S. and Pirofski, L. (2012) ‘IL-23 dampens the allergic response to Cryptococcus neoformans through IL-17-independent and -dependent mechanisms.’, *The American Journal of Pathology*, 180(4), 1547–59.

Tan, S.Y.S. and Krasnow, M.A. (2016) ‘Developmental origin of lung macrophage diversity’, *Development*, 143(8), 1318–1327.

Tang, B.M., Shojaei, M., Teoh, S., Meyers, A., Ho, J., Ball, T.B., Keynan, Y., Pisipati, A., Kumar, Aseem, Eisen, D.P., Lai, K., Gillett, M., Santram, R., Geffers, R., Schreiber, J., Mozhui, K., Huang, S., Parnell, G.P., Nalos, M. *et al.* (2019) ‘Neutrophils-related host factors associated with severe disease and fatality in patients with influenza infection’, *Nature Communications*, 10(1), 22.

Tanner, D.C., Weinstein, M.P., Fedorciw, B., Joho, K.L., Thorpe, J.J. and Reller, L. (1994) ‘Comparison of commercial kits for detection of cryptococcal antigen.’, *Journal of Clinical Microbiology*, 32(7).

Taqi, S.A., Sami, S.A., Sami, L.B. and Zaki, S.A. (2018) ‘A review of artifacts in histopathology’, *Journal of Oral and Maxillofacial Pathology*, 22(2), 279.

Teame, T., Zhang, Z., Ran, C., Zhang, H., Yang, Y., Ding, Q., Xie, M., Gao, C., Ye, Y., Duan, M. and Zhou, Z. (2019) ‘The use of zebrafish (Danio rerio) as biomedical models’, *Animal Frontiers*, 9(3), 68–77.

Tegla, C.A., Cudrici, C., Patel, S., Trippe, R., Rus, V., Niculescu, F. and Rus, H. (2011) ‘Membrane attack by complement: the assembly and biology of terminal complement complexes’, *Immunologic Research*, 51(1), 45–60.

The 3Rs | NC3Rs (no date). Available at: https://www.nc3rs.org.uk/the-3rs (Accessed: 3 May 2021).

The top 10 causes of death (2017) *World Health Organization*. World Health Organization.

Thompson, G.R., Albert, N., Hodge, G., Wilson, M.D., Sykes, J.E., Bays, D.J.,

Firacative, C., Meyer, W. and Kontoyiannis, D.P. (2014) 'Phenotypic differences of cryptococcus molecular types and their implications for virulence in a drosophila model of infection', *Infection and Immunity*, 82(7), 3058–3065.

Thuang, S.L., Murphy, J.W. and Cauley, L.K. (1980) 'Host-Etiological Agent Interactions in Intranasally and Intraperitoneally Induced Cryptococcosis in Mice', *Infection and Immunity*, 29(2), 633–641.

Tomasello, E., Yessaad, N., Gregoire, E., Hudspeth, K., Luci, C., Mavilio, D., Hardwigsen, J. and Vivier, E. (2012) 'Mapping of NKp46+ Cells in Healthy Human Lymphoid and Non-Lymphoid Tissues', *Frontiers in Immunology*, 0(NOV), 344.

Toubiana, J., Okada, S., Hiller, J., Oleastro, M., Gomez, M., Becerra, J., Ouachée-Chardin, M Fouyssac, F., Girisha, K., Etzioni, A., Van Montfrans, J., Camcioglu, Y., Kerns, L., Belohradsky, B., Blanche, S., Bousfiha, A., Rodriguez-Gallego, C Meyts, I., Kisand, K., Reichenbach, J., Renner, E. *et al.* (2016) 'Heterozygous STAT1 gain-of-function mutations underlie an unexpectedly broad clinical phenotype', *Blood*, 127(25), 3154–3164.

Trammell, R.A. and Toth, L.A. (2011) 'Markers for predicting death as an outcome for mice used in infectious disease research', *Comparative Medicine*, 61(6), 492–498.

Trede, N.S., Langenau, D.M., Traver, D., Look, A.T. and Zon, L.I. (2004) 'The use of zebrafish to understand immunity', *Immunity*, 20(4), 367–379.

Trevijano-Contador, N., de Oliveira, H.C., García-Rodas, R., Rossi, S.A., Llorente, I., Zaballos, Á., Janbon, G., Ariño, J. and Zaragoza, Ó. (2018) 'Cryptococcus neoformans can form titan-like cells in vitro in response to multiple signals', *PLOS Pathogens*, 14(5), e1007007.

Trevijano-Contador, N., Rossi, S.A., Alves, E., Landín-Ferreiroa, S. and Zaragoza, O. (2017) 'Capsule Enlargement in Cryptococcus neoformans Is Dependent on Mitochondrial Activity', *Frontiers in Microbiology*, 8(JUL), 1423.

True, D.G., Penmetcha, M. and Peckham, S.J. (2002) 'Disseminated cryptococcal infection in rheumatoid arthritis treated with methotrexate and infliximab.', *The Journal of Rheumatology*, 29(7), 1561–3.

Trzaska, W.J. (2019) *Developing novel approaches to treat trauma - associated fungal infections*. University of Birmingham.

Tsuchiya, S., Yamabe, M., Yamaguchi, Y., Kobayashi, Y., Konno, T. and Tada, K. (1980) 'Establishment and characterization of a human acute monocytic leukemia cell line (THP-1)', *International Journal of Cancer*, 26(2), 171–176.

Tsujimoto, M., Yip, Y.K. and Vilcek, J. (1986) 'Interferon-gamma enhances expression of cellular receptors for tumor necrosis factor.', *The Journal of Immunology*, 136(7).

Tsutsui, H., Kayagaki, N., Kuida, K., Nakano, H., Hayashi, N., Takeda, K., Matsui, K., Kashiwamura, S.I., Hada, T., Akira, S., Yagita, H., Okamura, H. and Nakanishi, K. (1999) 'Caspase-1-independent, Fas/Fas ligand-mediated IL-18 secretion from macrophages causes acute liver injury in mice', *Immunity*, 11(3), 359–367.

Tucker, S.C. and Casadevall, A. (2002) 'Replication of Cryptococcus neoformans in macrophages is accompanied by phagosomal permeabilization and accumulation of vesicles containing polysaccharide in the cytoplasm', *Proceedings of the National Academy of Sciences of the United States of America*, 99(5), 3165–3170.

Tulone, C., Tsang, J., Prokopowicz, Z., Grosvenor, N. and Chain, B. (2007) 'Natural cathepsin E deficiency in the immune system of C57BL/6J mice', *Immunogenetics*, 59(12), 927–935.

Tulotta, C., Lefley, D. V., Moore, C.K., Amariutei, A.E., Spicer-Hadlington, A.R., Quayle, L.A., Hughes, R.O., Ahmed, K., Cookson, V., Evans, C.A., Vadakekolathu, J., Heath, P., Francis, S., Pinteaux, E., Pockley, A.G. and Ottewell, P.D. (2021) 'IL-1B drives opposing innate immune responses in primary tumours and bone metastases, limiting treatment options in breast cancer', *njp Breast Cancer* [Preprint].

Turner, P. V, Brabb, T., Pekow, C. and Vasbinder, M.A. (2011) 'Administration of Substances to Laboratory Animals: Routes of Administration and Factors to Consider', *Journal of the American Association for Laboratory Animal Science*, 50(5), 600.

Uicker, W., McCracken, J.P. and Buchanan, K.L. (2006) 'Role of CD4+ T cells in a protective immune response against Cryptococcus neoformans in the central nervous system', *Medical Mycology*, 44(1), 1–11.

Ulrichs, T. and Kaufmann, S.H. (2006) 'New insights into the function of granulomas in human tuberculosis', *The Journal of Pathology*, 208(2), 261–269.

Upadhya, R., Kim, H., Jung, K.W., Park, G., Lam, W., Lodge, J.K. and Bahn, Y.S. (2013) 'Sulphiredoxin plays peroxiredoxin-dependent and -independent roles via the HOG signalling pathway in Cryptococcus neoformans and contributes to fungal virulence', *Molecular Microbiology*, 90(3), 630–648.

Uribe-Quero, E. and Rosales, C. (2017) 'Control of phagocytosis by microbial pathogens', *Frontiers in Immunology*, 8(OCT).

Valdez, P.A.A., Vithayathil, P.J.J., Janelsins, B.M.M., Shaffer, A.L.L., Williamson, P.R.R. and Datta, S.K.K. (2012) 'Prostaglandin E2 Suppresses Antifungal Immunity by

Inhibiting Interferon Regulatory Factor 4 Function and Interleukin-17 Expression in T Cells', *Immunity*, 36(4), 668–679.

Vanbreuseghem, R. and Takashio, M. (1970) 'An atypical strain of Cryptococcus neoformans (San Felice) Vuillemin 1894. II. Cryptococcus neoformans var. gattii var. nov', *Ann Soc Belges Med Trop Parasitol Mycol*, 50(6), 695–702.

Vance, R.E., Isberg, R.R. and Portnoy, D.A. (2009) 'Patterns of Pathogenesis: Discrimination of Pathogenic and Nonpathogenic Microbes by the Innate Immune System', *Cell Host and Microbe*, 6(1), 10–21.

Vandamme, T. (2014) 'Use of rodents as models of human diseases', *Journal of Pharmacy and Bioallied Sciences*, 6(1), 2–9.

Vanherp, L., Ristani, A., Poelmans, J., Hillen, A., Lagrou, K., Janbon, G., Brock, M., Himmelreich, U. and Velde, G. Vande (2019) 'Sensitive bioluminescence imaging of fungal dissemination to the brain in mouse models of cryptococcosis', *DMM Disease Models and Mechanisms*, 12(6).

Vannier, E. and Dinarello, C.A. (1994) 'Histamine enhances interleukin (IL)-1-induced IL-6 gene expression and protein synthesis via H2 receptors in peripheral blood mononuclear cells', *Journal of Biological Chemistry*, 269(13), 9952–9956.

Vannier, E., Miller, L.C. and Dinarello, C.A. (1992) 'Coordinated antiinflammatory effects of interleukin 4: Interleukin 4 suppresses interleukin 1 production but up-regulates gene expression and synthesis of interleukin 1 receptor antagonist', *Proceedings of the National Academy of Sciences of the United States of America*, 89(9), 4076–4080.

Vecchiarelli, A., Dottorini, M., Pietrella, D., Monari, C., Retini, C., Todisco, T. and Bistoni, F. (1994) 'Role of human alveolar macrophages as antigen-presenting cells in Cryptococcus neoformans infection.', *American Journal of Respiratory Cell and Molecular Biology*, 11(2), 130–137.

Vecchiarelli, A., Retini, C., Pietrella, D., Monari, C., Tascini, C., Beccari, T. and Kozel, T.R. (1995) 'Downregulation by cryptococcal polysaccharide of tumor necrosis factor alpha and interleukin-1β secretion from human monocytes', *Infection and Immunity*, 63(8), 2919–2923.

Velagapudi, R., Hsueh, Y.-P.P., Geunes-Boyer, S., Wright, J.R. and Heitman, J. (2009) 'Spores as infectious propagules of Cryptococcus neoformans.', *Infection and Immunity*, 77(10), 4345–55.

Vertut-Doï, A., Ishiwata, H. and Miyajima, K. (1996) 'Binding and uptake of liposomes

containing a poly(ethylene glycol) derivative of cholesterol (stealth liposomes) by the macrophage cell line J774: influence of PEG content and its molecular weight', *Biochimica et Biophysica Acta - Biomembranes*, 1278(1), 19–28.

Vincent, F., De La Salle, H., Bohbot, A., Bergerat, J.P., Hauptmann, G. and Oberling, F. (1993) 'Synthesis and Regulation of Complement Components by Human Monocytes/Macrophages and by Acute Monocytic Leukemia', *DNA and Cell Biology*, 12(5), 415–423.

Voelz, K., Johnston, S.A., Rutherford, J.C. and May, R.C. (2010) 'Automated analysis of cryptococcal macrophage parasitism using GFP-tagged cryptococci.', *PloS One*, 5(12), e15968.

Voelz, K., Lammas, D.A. and May, R.C. (2009) 'Cytokine Signaling Regulates the Outcome of Intracellular Macrophage Parasitism by Cryptococcus neoformans', *Infection and Immunity*, 77(8), 3450–3457.

Voigt, J., Hünniger, K., Bouzani, M., Jacobsen, I.D., Barz, D., Hube, B., Löffler, J. and Kurzai, O. (2014) 'Human natural killer cells acting as phagocytes against Candida albicans and mounting an inflammatory response that modulates neutrophil antifungal activity', *Journal of Infectious Diseases*, 209(4), 616–626.

Vonk, A.G., Netea, M.G., Van Krieken, J.H., Iwakura, Y., Van Der Meer, J.W.M. and Kullberg, B.J. (2006) 'Endogenous interleukin (IL)-1α and IL-1β are crucial for host defense against disseminated candidiasis', *Journal of Infectious Diseases*, 193(10), 1419–1426.

Vu, K., Eigenheer, R.A., Phinney, B.S. and Gelli, A. (2013) 'Cryptococcus neoformans promotes its transmigration into the central nervous system by inducing molecular and cellular changes in brain endothelial cells', *Infection and Immunity*, 81(9), 3139–3147.

Vu, K., Tham, R., Uhrig, J.P., Thompson, G.R., Na Pombejra, S., Jamklang, M., Bautos, J.M. and Gelli, A. (2014) 'Invasion of the Central Nervous System by Cryptococcus neoformans Requires a Secreted Fungal Metalloprotease', *mBio*, 5(3), e01101-14-e01101-14.

Wager, C.M.L., Hole, C.R., Wozniak, K.L., Olszewski, M.A., Mueller, M. and Wormley, F.L. (2015) 'STAT1 Signaling within Macrophages Is Required for Antifungal Activity against Cryptococcus neoformans', *Infection and Immunity*, 83(12), 4513–4527.

Walenkamp, A.M.E., Verheul, A.F.M., Scharringa, J. and Hoepelman, I.M. (1999) 'Pulmonary surfactant protein A binds to Cryptococcus neoformans without promoting phagocytosis', *European Journal of Clinical Investigation*, 29(1), 83–92.

Walsh, N.M., Botts, M.R., McDermott, A.J., Ortiz, S.C., Wüthrich, M., Klein, B. and Hull, C.M. (2019) 'Infectious particle identity determines dissemination and disease outcome for the inhaled human fungal pathogen Cryptococcus', *PLoS Pathogens*, 15(6), e1007777.

Wan, F., Hu, C. Bin, Ma, J.X., Gao, K., Xiang, L.X. and Shao, J.Z. (2017) 'Characterization of γδ T cells from zebrafish provides insights into their important role in adaptive humoral immunity', *Frontiers in Immunology*, 7(JAN), 9.

Wang, J.-M., Zhou, Q., Cai, H.-R., Zhuang, Y., Zhang, Y.-F., Xin, X.-Y., Meng, F.-Q. and Wang, Y.-P. (2014) 'Clinicopathological features of pulmonary cryptococcosis with cryptococcal titan cells: a comparative analysis of 27 cases.', *International Journal of Clinical and Experimental Pathology*, 7(8), 4837–46.

Wang, J.P., Lee, C.K., Akalin, A., Finberg, R.W. and Levitz, S.M. (2011) 'Contributions of the MyD88-Dependent Receptors IL-18R, IL-1R, and TLR9 to Host Defenses following Pulmonary Challenge with Cryptococcus neoformans', *PLoS ONE*, 6(10), e26232.

Wang, Y. and Casadevall, A. (1994) 'Decreased susceptibility of melanized Cryptococcus neoformans to UV light', *Applied and Environmental Microbiology*, 60(10), 3864–3866.

Wang, Z.A., Li, L.X. and Doering, T.L. (2018) 'Unraveling synthesis of the cryptococcal cell wall and capsule', *Glycobiology*, 28(10), 719.

Wanner, R.A. and Baird, J.D. (1974) 'Cryptococcosis in a cat', *New Zealand Veterinary Journal*, 22(5), 78–81.

Ward, P.P., Uribe-Luna, S. and Conneely, O.M. (2002) 'Lactoferrin and host defense', *Biochemistry and Cell Biology*, 80(1), 95–102.

Warton, D.I. and Hui, F.K.C. (2011) 'The arcsine is asinine: The analysis of proportions in ecology', *Ecology*, 92(1), 3–10.

Waterman, S.R., Park, Y.-D., Raja, M., Qiu, J., Hammoud, D.A., O'Halloran, T. V and Williamson, P.R. (2012) 'Role of CTR4 in the Virulence of Cryptococcus neoformans.', *mBio*, 3(5), e00285-12.

Waterston, R.H., Lindblad-Toh, K., Birney, E., Rogers, J., Abril, J.F., Agarwal, P., Agarwala, R., Ainscough, R., Alexandersson, M., An, P., Antonarakis, S.E., Attwood, J., Baertsch, R., Bailey, J., Barlow, K., Beck, S., Berry, E., Birren, B., Bloom, T. *et al.* (2002) 'Initial sequencing and comparative analysis of the mouse genome', *Nature*, 420(6915), 520–562.

Watkins, R., King, J. and Johnston, S. (2017) ‘Nutritional Requirements and Their Importance for Virulence of Pathogenic Cryptococcus Species’, *Microorganisms*, 5(4), 65.

Watkins, R.A., Andrews, A., Wynn, C., Barisch, C., King, J.S. and Johnston, S.A. (2018) ‘Cryptococcus neoformans escape from Dictyostelium amoeba by both WASH-mediated constitutive exocytosis and vomocytosis’, *Frontiers in Cellular and Infection Microbiology*, 8(APR), 108.

Wedi, J., Straede, J., Wieland, B. and Kapp, A. (1999) ‘Eosinophil apoptosis is mediated by stimulators of cellular oxidative metabolisms and inhibited by antioxidants: involvement of a thiol-sensitive redox regulation in eosinophil cell death’, *Blood*, 94(7), 2365–73.

Weibel, E.R. (1963) ‘Morphometry of the Human Lung’, in *Morphometry of the Human Lung*. First. New York: Academic Press Inc., 136–142.

Weisbroth, S.H. and Freimer, E.H. (1969) ‘Laboratory rats from commercial breeders as carriers of pathogenic pneumococci’, *Lab Anim Care*, 19(4), 473–478.

Weiss, G., Werner-Felmayer, G., Werner, E.R., Grünewald, K., Wachter, H. and Hentze, M.W. (1994) ‘Iron regulates nitric oxide synthase activity by controlling nuclear transcription’, *Journal of Experimental Medicine*, 180(3), 969–976.

Weissgerber, T.L., Garcia-Valencia, O., Garovic, V.D., Milic, N.M. and Winham, S.J. (2018) ‘Meta-Research: Why we need to report more than “Data were Analyzed by t-tests or ANOVA”’, *eLife*, 10.7554/eL.

Wellington, M., Koselny, K. and Krysan, D.J. (2013) ‘Candida albicans morphogenesis is not required for macrophage interleukin 1β production’, *mBio*, 4(1).

Van De Wetering, J.K., Coenjaerts, F.E.J., Vaandrager, A.B., Van Golde, L.M.G. and Batenburg, J.J. (2004) ‘Aggregation of Cryptococcus neoformans by Surfactant Protein D Is Inhibited by Its Capsular Component Glucuronoxylomannan’, *Infection and Immunity*, 72(1), 145–153.

Wiederhold, N.P. (2017) ‘Antifungal resistance: current trends and future strategies to combat.’, *Infection and Drug Resistance*, 10, 249–259.

Wiesner, D.L. and Boulware, D.R. (2011) ‘Cryptococcus-related Immune Reconstitution Inflammatory Syndrome (IRIS): Pathogenesis and its clinical implications’, *Current Fungal Infection Reports*, 5(4), 252–261.

Wiesner, D.L., Specht, C.A., Lee, C.K.C.G., Smith, K.D., Mukaremera, L., Lee, S.T.,

Lee, C.K.C.G., Elias, J.A., Nielsen, J.N., Boulware, D.R., Bohjanen, P.R., Jenkins, M.K., Levitz, S.M. and Nielsen, K. (2015) 'Chitin Recognition via Chitotriosidase Promotes Pathologic Type-2 Helper T Cell Responses to Cryptococcal Infection', *PLoS Pathogens*, 11(3), 1–28.

Williams, G.T. and Williams, W.J. (1983) 'Granulomatous inflammation - A review', *Journal of Clinical Pathology*, 36(7), 723–733.

Williams, V. and del Poeta, M. (2011) 'Role of Glucose in the Expression of Cryptococcus neoformans Antiphagocytic Protein 1, App1', *Eukaryotic Cell*, 10(3), 293–301.

Williamson, L., Ayalon, I., Shen, H. and Kaplan, J. (2019) 'Hepatic STAT3 inhibition amplifies the inflammatory response in obese mice during sepsis', *American Journal of Physiology - Endocrinology and Metabolism*, 316(2), E286–E292.

Wilson, D.E., Bennett, J.E. and Bailey, J.W. (1968) 'Serologic Grouping of Cryptococcus neoformans', *Proceedings of the Society for Experimental Biology and Medicine*, 127(3), 820–823.

Wilson, M., Hsu, E., Marcuz, A., Courtet, M., Du Pasquier, L. and Steinberg, C. (1992) 'What limits affinity maturation of antibodies in Xenopus - The rate of somatic mutation or the ability to select mutants?', *EMBO Journal*, 11(12), 4337–4347.

Wiseman, J.C.D., Ma, L.L., Marr, K.J., Jones, G.J. and Mody, C.H. (2007) 'Perforin-Dependent Cryptococcal Microbicidal Activity in NK Cells Requires PI3K-Dependent ERK1/2 Signaling', *The Journal of Immunology*, 178(10), 6456–6464.

De Wit, H., Hoogstraten, D., Halie, R.M. and Vellenga, E. (1996) 'Interferon-γ modulates the lipopolysaccharide-induced expression of AP-1 and NF-κB at the mRNA and protein level in human monocytes', *Experimental Hematology*, 24(2), 228–235.

Wormley, F.L., Perfect, J.R., Steele, C. and Cox, G.M. (2007) 'Protection against cryptococcosis by using a murine gamma interferon-producing Cryptococcus neoformans strain', *Infection and Immunity*, 75(3), 1453–1462.

Wozniak, K.L. (2018) 'Interactions of Cryptococcus with Dendritic Cells.', *Journal of Fungi*, 4(1), 36.

Wozniak, K.L., Hardison, S.E., Kolls, J.K. and Wormley, F.L. (2011) 'Role of IL-17A on Resolution of Pulmonary C. neoformans Infection', *PLoS ONE*, 6(2), 17204.

Wozniak, K.L. and Levitz, S.M. (2008) 'Cryptococcus neoformans enters the endolysosomal pathway of dendritic cells and is killed by lysosomal components.',

Infection and Immunity, 76(10), 4764–71.

Wozniak, K.L., Ravi, S., Macias, S., Young, M.L., Olszewski, M.A., Steele, C. and Wormley, F.L. (2009) 'Insights into the mechanisms of protective immunity against Cryptococcus neoformans infection using a mouse model of pulmonary cryptococcosis', *PLoS ONE*, 4(9), 6854.

Wright, L.C., Santangelo, R.M., Ganendren, R., Payne, J., Djordjevic, J.T. and Sorrell, T.C. (2007) 'Cryptococcal lipid metabolism: Phospholipase B1 is implicated in transcellular metabolism of macrophage-derived lipids', *Eukaryotic Cell*, 6(1), 37–47.

Wu, G., Guo, X., Wang, Y. and Hu, Z. (2020) 'Clinical and Radiographic Features of Cryptococcal Neoformans Meningitis-associated Immune Reconstitution Inflammatory Syndrome', *Scientific Reports*, 10(1), 1–7.

Wu, Q., Liu, J., Wang, X., Feng, L., Wu, J., Zhu, X., Wen, W. and Gong, X. (2020) 'Organ-on-a-chip: recent breakthroughs and future prospects', *Biomed Eng Online*, 19(9).

Xu-Vanpala, S., Deerhake, E., Wheaton, J.D., Parker, M.E., Juvvadi, P.R., MacIver, N., Ciofani, M. and Shinohara, M.L. (2020) 'Functional heterogeneity of alveolar macrophage population based on expression of CXCL2', *Science Immunology*, 5(50).

Xu, J., Zhao, J., Ivey, M., Lopez, R., McClellan, B., Do, S., Malepati, A., Kroon, S., Mysel, A. and Olszewski, M.A. (2020) 'The Function of Brain Th1-like regulatory T cells in Suppressing Lethal Immune Pathology and Neurological Deterioration during Cryptococcus neoformans Meningoencephalitis', *The Journal of Immunology*, 204(1 Supplement), 156.21.

Yauch, L.E., Lam, J.S. and Levitz, S.M. (2006) 'Direct Inhibition of T-Cell Responses by the Cryptococcus Capsular Polysaccharide Glucuronoxylomannan', *PLoS Pathogens*, 2(11), e120.

Yauch, L.E., Mansour, M.K., Shoham, S., Rottman, J.B. and Levitz, S.M. (2004) 'Involvement of CD14, toll-like receptors 2 and 4, and MyD88 in the host response to the fungal pathogen Cryptococcus neoformans in vivo.', *Infection and Immunity*, 72(9), 5373–82.

Yoshimoto, T., Takeda, K., Tanaka, T., Ohkusu, K., Kashiwamura, S.I., Okamura, H., Akira, S. and Nakanishi, K. (1998) 'IL-12 Up-Regulates IL-18 Receptor Expression on T Cells, Th1 Cells, and B Cells: Synergism with IL-18 for IFN-g Production', *The Journal of Immunology*, 161, 3400–3407.

Young, B.J. and Kozel, T.R. (1993) 'Effects of strain variation, serotype, and structural

modification on kinetics for activation and binding of C3 to Cryptococcus neoformans.', *Infection and Immunity*, 61(7).

Yu, T. and Zheng, X.D. (2007) 'An integrated strategy to control postharvest blue and grey mould rots of apple fruit by combining biocontrol yeast with gibberellic acid', *International Journal of Food Science & Technology*, 42(8), 977–984.

Zaragoza, O., Alvarez, M., Telzak, A., Rivera, J. and Casadevall, A. (2007) 'The relative susceptibility of mouse strains to pulmonary Cryptococcus neoformans infection is associated with pleiotropic differences in the immune response', *Infection and Immunity*, 75(6), 2729–2739.

Zaragoza, O., Chrisman, C.J., Castelli, M.V., Frases, S., Cuenca-Estrella, M., Rodríguez-Tudela, J.L. and Casadevall, A. (2008) 'Capsule enlargement in Cryptococcus neoformans confers resistance to oxidative stress suggesting a mechanism for intracellular survival', *Cellular Microbiology*, 10(10), 2043–2057.

Zaragoza, O., Taborda, C.P.P. and Casadevall, A. (2003) 'The efficacy of complement-mediated phagocytosis of Cryptococcus neoformans is dependent on the location of C3 in the polysaccharide capsule and involves both direct and indirect C3-mediated interactions', *European Journal of Immunology*, 33(7), 1957–1967.

Zhang, M., Sun, D., Liu, G., Wu, H., Zhou, H. and Shi, M. (2016) 'Real-time in vivo imaging reveals the ability of neutrophils to remove Cryptococcus neoformans directly from the brain vasculature', *Journal of Leukocyte Biology*, 99(3), 467–473.

Zhang, T., Kawakami, K., Qureshi, M.H., Okamura, H., Kurimoto, M. and Saito, A. (1997) 'Interleukin-12 (IL-12) and IL-18 synergistically induce the fungicidal activity of murine peritoneal exudate cells against Cryptococcus neoformans through production of gamma interferon by natural killer cells', *Infection and Immunity*, 65(9), 3594–3599.

Zhang, Y., Liu, H., Yao, J., Huang, Y., Qin, S., Sun, Z., Xu, Y., Wan, S., Cheng, H., Li, C., Zhang, X. and Ke, Y. (2016) 'Manipulating the air-filled zebrafish swim bladder as a neutrophilic inflammation model for acute lung injury', *Cell Death and Disease*, 7(11), e2470–e2470.

Zhang, Y., Wang, F., Tompkins, K.C., McNamara, A., Jain, A. V., Moore, B.B., Toews, G.B., Huffnagle, G.B. and Olszewski, M.A. (2009) 'Robust Th1 and Th17 Immunity Supports Pulmonary Clearance but Cannot Prevent Systemic Dissemination of Highly Virulent Cryptococcus neoformans H99', *The American Journal of Pathology*, 175(6), 2489–2500.

Zhang, Y., Wang, H., Ren, J., Tang, X., Jing, Y., Xing, D., Zhao, G., Yao, Z., Yang, X.

and Bai, H. (2012) ‘IL-17A synergizes with IFN-γ to upregulate iNOS and NO production and inhibit chlamydial growth’, *PLoS ONE*, 7(6), 39214.

Zheleznyak, A. and Brown, E.J. (1992) ‘Immunoglobulin-mediated Phagocytosis by Human Monocytes Requires Protein Kinase C Activation’, *The Journal of Biological Chemistry*, 267(17), 12042–12048.

Zhou, H.X., Lu, L., Chu, T., Wang, T., Cao, D., Li, F., Ning, G. and Feng, S. (2014) ‘Skeletal cryptococcosis from 1977 to 2013’, *Frontiers in Microbiology*, 5(DEC).

Zhou, Q., Gault, R.A., Kozel, T.R. and Murphy, W.J. (2007) ‘Protection from direct cerebral cryptococcus infection by interferon-gamma-dependent activation of microglial cells.’, *Journal of Immunology*, 178(9), 5753–61.

Zhu, L.P., Wu, J.Q., Xu, B., Ou, X.T., Zhang, Q.Q. and Weng, X.H. (2010) ‘Cryptococcal meningitis in non-HIV-infected patients in a Chinese tertiary care hospital, 1997-2007’, *Medical Mycology*, 48(4), 570–579.

Zhu, Y.J., Wen, H., Gu, J.L., Xu, H., Huang, X. and Zhao, J. (2007) ‘In vitro interaction of Cryptococcus neoformans and human lung epithelial cells’, *Chinese Journal of Microbiology and Immunology*, 27(1), 33–37.

Zicari, S., Sessa, L., Cotugno, N., Ruggiero, A., Morrocchi, E., Concato, C., Rocca, S., Zangari, P., Manno, E.C. and Palma, P. (2019) ‘Immune activation, inflammation, and non-AIDS co-morbidities in HIV-infected patients under long-term ART’, *Viruses*, 11(3), 200.

Zou, S., Tong, Q., Liu, B., Huang, W., Tian, Y. and Fu, X. (2020) ‘Targeting stat3 in cancer immunotherapy’, *Molecular Cancer*, 19(1), 1–19.

Zvezdanova, M.E., Arroyo, M.J., Méndez, G., Guinea, J., Mancera, L., Muñoz, P., Rodríguez-Sánchez, B. and Escribano, P. (2020) ‘Implementation of maldi-tof mass spectrometry and peak analysis: Application to the discrimination of cryptococcus neoformans species complex and their interspecies hybrids’, *Journal of Fungi*, 6(4), 1–12.